

PUBLICATIONS
OF
DEBRECEN
HELIO PHYSICAL OBSERVATORY
OF THE
HUNGARIAN ACADEMY OF SCIENCES

ПУБЛИКАЦИИ
ДЕБРЕЦЕНСКОЙ
ГЕЛИОФИЗИЧЕСКОЙ ОБСЕРВАТОРИИ
ВЕНГЕРСКОЙ АКАДЕМИИ НАУК

A MAGYAR TUDOMÁNYOS AKADÉMIA
DEBRECENI
NAPFIZIKAI OBSZERVÁTORIUMÁNAK
KÖZLEMÉNYEI

VOLUME 5, PART 1

11th Regional Consultation on Solar Physics
Debrecen, Hungary
1983

PUBLICATIONS
OF
DEBRECEN
HELIOPHYSICAL OBSERVATORY
OF THE
HUNGARIAN ACADEMY OF SCIENCES

ПУБЛИКАЦИИ
ДЕБРЕЦЕНСКОЙ
ГЕЛИОФИЗИЧЕСКОЙ ОБСЕРВАТОРИИ
ВЕНГЕРСКОЙ АКАДЕМИИ НАУК

A MAGYAR TUDOMÁNYOS AKADÉMIA
DEBRECENI
NAPFIZIKAI OBSZERVÁTORIUMÁNAK
KÖZLEMÉNYEI

VOLUME 5

Proceedings of the
11th Regional Consultation on Solar Physics
held in Debrecen, Hungary,
September 1983

EDITORS:

L.DEZSŐ and B.KÁLMÁN
Heliophysical Observatory
Hungarian Academy of Sciences
H-4010 D E B R E C E N
HUNGARY

EDITORIAL ACKNOWLEDGEMENT

Thanks are due to Á.Kovács and A.Ludmány
for invaluable editorial assistance in
preparation of this volume.

ISSN 0209-7567

(Publ.Debrecen Obs., Volume 5, pages 666)

CONTENTS

PART 1

	PAGE
PREFACE	15
LIST OF PARTICIPANTS AND NON-PARTICIPANT CO-AUTHORS	17
№.1. INVITED REVIEW PAPERS	23
<i>V. N. Obridko</i>	25
SOME TRENDS IN MODERN SOLAR PHYSICS	
<i>В.Н.Обридко</i>	
О НЕКОТОРЫХ СОВРЕМЕННЫХ ТЕНДЕНЦИЯХ В СОЛНЕЧНОЙ ФИЗИКЕ	
<i>В.Е.Степанов, В.В.Касинский</i>	31
КРАТКИЕ ИТОГИ ИССЛЕДОВАНИЯ ВСПЫШЕК В ПЕРИОД ГСМ	
<i>V. E. Stepanov, V. V. Kasinskij</i>	
A SHORT REVIEW OF THE INVESTIGATIONS OF SOLAR FLARES IN THE SMO	
<i>V. Bumba</i>	47
PROPER MOTIONS OBSERVED IN ACTIVE REGIONS	
<i>В.Бумба</i>	
СОВРЕМЕННЫЕ ДВИЖЕНИЯ НАБЛЮДАЕМЫЕ В АКТИВНЫХ ОБЛАСТЯХ	
№.2. PAPERS RELATED TO THE SOLAR MAXIMUM YEAR PROGRAMS	71
<i>I. M. Chertok, V. V. Fomichev, V. N. Ishkov, A. K. Markeev</i>	73
<i>G. S. Minasyants, S. O. Obashev</i>	
RELATIONSHIP OF THE DYNAMIC EVENTS IN OPTICAL AND RADIO RANGES DURING THE FLARES OF NOVEMBER 9 AND 10, 1979	
<i>И.М.Черток, В.В.Фомичев, В.Н.Ишков, А.К.Маркеев,</i>	
<i>Г.С.Минасянц, С.О.Обашев</i>	
СООТНОШЕНИЕ ДИНАМИЧЕСКИХ ЯВЛЕНИЙ В ОПТИЧЕСКОМ И РАДИОДИАПАЗОНАХ ВО ВРЕМЯ ВСПЫШЕК 9 И 10 НОЯБРЯ 1979 Г.	
<i>B. Sylwester, J. Sylwester, J. Jakimiec, R. Mewe, R. D. Bentley</i>	85
SMM FLAT CRYSTAL SPECTROMETER DATA ANALYSIS OF 7 APRIL 1980 FLARE	
<i>Б.Сильвестер, Я.Сильвестер, Я.Якимец, Р.Меве, Р.Д.Бентлей</i>	
АНАЛИЗ НАБЛЮДЕНИЙ ВСПЫШЕК ИЗ 7 АПРЕЛЯ 1980 Г ПОЛУЧЕННЫХ КРИСТАЛЛИЧЕСКИМ СПЕКТРОМЕТРОМ ИЗ БОРТА SMM	
<i>A. Antalová</i>	93
THE PHOTOSPHERIC DOPPLER SHIFT OBSERVED IN HALE ARS 16862 AND 16863 (MAY 22 AND 23, 1980)	
<i>А.Анталова</i>	
ФОТОСФЕРНЫЕ ЛУЧЕВЫЕ СКОРОСТИ НАБЛЮДАЕМЫЕ В АКТИВНЫХ ОБЛАСТЯХ ХЕЙЛА 16862 И 16863 (С 22 ПО 23 МАЯ 1980 Г.)	

	PAGE
(No. 2) <i>I. Nagy</i> SUNSPOT PROPER MOTIONS IN THE WESTERN PART OF HALE REGION 16864 (MAY 25 -29, 1980) <i>И.Надь</i> СОБСТВЕННЫЕ ДВИЖЕНИЯ СОЛНЕЧНЫХ ПЯТЕН В ЗАПАДНОЙ ЧАСТИ АКТИВНОЙ ОБЛАСТИ ХЕЙЛ № 16864 (25-29 МАЯ, 1980 Г)	107
<i>N. Seehafer</i> POSSIBLE MAGNETIC RECONNECTION IN THE SOLAR ACTIVITY COMPLEX OF MAY 1980 <i>Н.Зеехафер</i> ВОЗМОЖНОЕ МАГНИТНОЕ ПЕРЕСОЕДИНЕНИЕ В СОЛНЕЧНОМ АКТИВНОМ КОМПЛЕКСЕ МАЯ 1980 Г.	117
<i>J. Jakimiec, R. Mewe, J. Schrijver, J. Sylwester, B. Sylwester</i> TIME VARIATION OF THE DIFFERENTIAL EMISSION MEASURE OF HOT FLARE PLASMA <i>Я.Якимец, Р.Меве, Я.Шривер, Я.Сильвестер, Б.Сильвестер</i> ВРЕМЕННЫЕ ВАРИАЦИИ ДИФФЕРЕНЦИАЛЬНОЙ МЕРЫ ЭМИССИИ ГОРЯЧЕЙ ВСПЫШЕЧНОЙ ПЛАЗМЫ	127
<i>L. Gesztelyi, L. Kondás</i> THE DEVELOPMENT OF ACTIVITY IN HALE REGION 17098 (28 AUGUST - 8 SEPTEMBER 1980) <i>Л.Гестейи, Л.Кондаш</i> РАЗВИТИЕ АКТИВНОСТИ В ОБЛАСТИ ХЕЙЛ № 17098 (28 АВГУСТА - 8 СЕНТЯБРЯ 1980 Г.)	133
<i>P. Ambrož</i> LOCATION OF SOURCES OF SOLAR NOISE STORMS RELATIVE TO THE STRUCTURE OF EXTRAPOLATED CORONAL MAGNETIC FIELDS <i>П.Амброж</i> ПОЛОЖЕНИЕ ИСТОЧНИКОВ СОЛНЕЧНЫХ ШУМОВЫХ БУРЬ ОТНОСИТЕЛЬНО СТРУКТУРЫ ЭКСТРАПОЛИРОВАННЫХ КОРОНАЛЬНЫХ МАГНИТНЫХ ПОЛЕЙ	145
<i>V. F. Mel'nikov, V. P. Nefed'ev, T. S. Podstrigach, V. S. Prokudina,</i> <i>N. N. Potapov, G. Ya. Smol'kov</i> THE RADIO BURSTS OF 13 AND 16 MAY 1981 AND ASSOCIATED EVENTS IN THE RADIO BRIGHTNESS DISTRIBUTION ABOVE AN ACTIVITY COMPLEX <i>В.Ф.Мельников, В.П.Нефедьев, Т.С.Подстригач, В.С.Прокудина,</i> <i>Н.Н.Потапов, Г.Я.Смольков</i> ВСПЛЕСКИ РАДИОИЗЛУЧЕНИЯ 13 И 16 МАЯ 1981 Г. И СОПУТСТВУЮЩИЕ ИМ ЯВЛЕНИЯ В РАСПРЕДЕЛЕНИИ РАДИОКОСТИ НАД АКТИВНЫМ КОМПЛЕКСОМ	167
<i>K. V. Alikaeva, N. N. Kondrashova, P. N. Polupan, T. I. Redyuk</i> ФОТОСФЕРНЫЕ СЛОИ ВСПЫШЕК 14 И 15 МАЯ 1981 Г. В КОМПЛЕКСЕ АР 3106+3112 <i>К.В.Аликаева, Н.Н.Кондрашова, П.Н.Полупан, Т.И.Редюк</i> PHOTOSPHERIC LAYERS OF FLARES FOR MAY 14, 15, 1981 IN AR 3106+3112	177

	PAGE
(No. 2) <i>H. Aurass, A. Böhme, A. Krüger</i> THE RADIO EMISSION AND ACTIVE REGION DEVELOPMENT DURING THE PERIOD OF MAY 15- 25, 1981 <i>Х. Аукас, А. Бёме, А. Крюгер</i> РАДИО ЭМИССИЯ И РАЗВИТИЕ АКТИВНЫХ ОБЛАСТЕЙ В ПЕРИОД 15 - 25 МАЯ 1981 Г.	185
<i>V. N. Ishkov, A. K. Markeev, V. V. Fomichev, G. P. Chernov, I. M. Chertok,</i> <i>O. B. Likin, N. F. Pisarenko, B. Valnicek, M. Karlicky, A. Tlamicha,</i> <i>F. Fárnik, B. Kálmán</i> PECULIARITIES OF THE DEVELOPMENT OF FLARE ON MAY 16, 1981 AS OBSERVED IN OPTICAL, X-RAYS AND RADIO WAVES <i>В. Н. Ишков, А. К. Маркеев, В. В. Фомичев, Г. П. Чернов, И. М. Черток,</i> <i>О. Б. Ликин, Н. Ф. Писаренко, Б. Валничек, М. Карлицкий,</i> <i>А. Тламиха, Ф. Фарник, Б. Калман</i> ОСОБЕННОСТИ РАЗВИТИЯ ВСПЫШКИ 16 МАЯ 1981 Г. ПО НАБЛЮДЕНИЯМ В РЕНТГЕНОВСКОМ, ОПТИЧЕСКОМ И РАДИОДИАПАЗОНАХ	193
<i>B. Kálmán, I. Nagy</i> PROPER MOTIONS IN HALE REGION 17644 (MAY 1981) AND THE MAY 16 FLARE <i>Б. Калман, И. Надь</i> СОБСТВЕННЫЕ ДВИЖЕНИЯ В ОБЛАСТИ ХЕЙЛА 17644 (МАЯ 1981 Г.) И ВСПЫШКА 16 МАЯ	207
<i>K. V. Alikaeva, I. F. Nikulin, P. N. Polupan</i> ИЗМЕНЕНИЕ ПРОФИЛЕЙ $H\alpha$ И $H\beta$ В ПРОЦЕССЕ ВСПЫШКИ 16 МАЯ 1981 Г. <i>K. V. Alikaeva, I. F. Nikulin, P. N. Polupan</i> VARIATION OF $H\alpha$ AND $H\beta$ PROFILES DURING 16 MAY, 1981 FLARE	217
No. 3. PAPERS ON MASS MOTION AND MAGNETIC FIELDS IN SOLAR ACTIVE REGIONS	223
<i>N. N. Stepanyan</i> ФОНОВЫЕ МАГНИТНЫЕ ПОЛЯ И СОЛНЕЧНАЯ АКТИВНОСТЬ <i>N. N. Stepanyan</i> BACKGROUND MAGNETIC FIELDS AND ACTIVITY OF THE SUN	225
<i>A. N. Koval', N. N. Stepanyan</i> ИЗМЕНЕНИЕ МАГНИТНЫХ ПОЛЕЙ СОЛНЕЧНЫХ ПЯТЕН В СВЯЗИ СО ВСПЫШКАМИ <i>F. N. Koval', N. N. Stepanyan</i> VARIATIONS IN THE MAGNETIC FIELDS OF SUNSPOTS RELATED TO FLARES	235
<i>S. I. Gopasyuk, B. Kálmán, V. A. Romanov</i> CHANGES IN THE LARGE-SCALE CURRENT SYSTEMS IN THE COURSE OF THE EVOLUTION OF AN ACTIVE REGION <i>С. И. Гопасюк, Б. Калман, В. А. Романов</i> ЭВОЛЮЦИЯ КРУПНОМАСШТАБНЫХ ТОКОВЫХ СТРУКТУР ЗА ВРЕМЯ РАЗВИТИЯ АКТИВНОЙ ОБЛАСТИ	249

	PAGE
(No. 3) <i>R. B. Teplytskaya, I. P. Tyrova, G. V. Kuklin</i> THE STUDY OF THE DYNAMIC PROCESS OF UMBRAL FLASHES <i>Р.Б. Теплицкая, И.П. Тyroва, Г.В. Куклин</i> ИССЛЕДОВАНИЕ ДИНАМИЧЕСКОГО ПРОЦЕССА "ВСПЫШКИ В ТЕНИ"	267
<i>Z. B. Korobova</i> STUDIES OF KINEMATIC ELEMENTS IN TWO MULTICENTER SUNSPOT GROUPS <i>З.Б. Коробова</i> ИССЛЕДОВАНИЕ КИНЕМАТИЧЕСКИХ ЭЛЕМЕНТОВ В ДВУХ МНОГО- ЦЕНТРОВЫХ ГРУППАХ СОЛНЕЧНЫХ ПЯТЕН	285
<i>V. E. Merkulenko, L. E. Palamarchuk, V. I. Polyakov</i> PHASE-COHERENCE OF CHROMOSPHERIC OSCILLATIONS WITHIN AN ACTIVITY COMPLEX AND DYNAMIC PROCESSES IN A FILA- MENT DURING THE FLARES ON 6 OCTOBER 1979 <i>В.Е. Меркуленко, Л.Э. Паламарчук, В.И. Поляков</i> СИНФАЗНОСТЬ КОЛЕБАНИЙ ХРОМОСФЕРЫ В ПРЕДЕЛАХ КОМПЛЕКСА АКТИВНОСТИ И ДИНАМИЧЕСКИЕ ПРОЦЕССЫ В ВОЛОКНЕ ВО ВРЕМЯ ВСПЫШЕК 6 ОКТЯБРЯ 1979 Г.	293
<i>L. Dezső, Á. Kovács</i> A NOTE ON FLARE LOOPS <i>Л. Дежэ, А. Ковач</i> ЗАМЕТКА О ВСПЫШЕЧНЫХ ПЕТЛЯХ	317
<i>B. I. Ryabov, A. R. Spector</i> CORONAL MAGNETIC STRUCTURES RELATED TO SOLAR FLARES <i>Б.И. Рябов, А.Р. Спектор</i> МАГНИТНЫЕ СТРУКТУРЫ В СОЛНЕЧНОЙ КОРОНЕ СВЯЗАННЫЕ СО ВСПЫШКАМИ	323
<i>S. I. Avdyushin, M. M. Alibegov, A. F. Bogomolov, V. A. Burov,</i> <i>E. I. Zajtsev, S. P. Leonenko, V. A. Poperchenko</i> RADIOEMISSION OF WEAK SOURCES AND MAGNETIC FIELD STRUCTURE <i>С.И. Авдюшин, М.М. Алибегов, А.Ф. Богомалов, В.А. Буров,</i> <i>Е.И. Зайцев, С.П. Леоненко, В.А. Поперченко</i> РАДИОИЗЛУЧЕНИЕ СЛАБЫХ ИСТОЧНИКОВ И СТРУКТУРА МАГНИТНОГО ПОЛЯ	333
<i>I. Sattarov, Z. B. Korobova</i> ЭВОЛЮЦИЯ И ВСПЫШЕЧНАЯ АКТИВНОСТЬ БОЛЬШОЙ ГРУППЫ СОЛНЕЧНЫХ ПЯТЕН ИЮЛЯ 1982 Г. <i>I. Sattarov, Z. B. Korobova</i> DEVELOPMENT AND FLARE ACTIVITY IN THE LARGE SUNSPOT GROUP IN JULY 1982	341

	PAGE
(No. 3) <i>В.Н.Ишков, З.Б.Коробова, Э.И.Могилевский</i> ЭВОЛЮЦИЯ СТРУКТУРЫ, СОБСТВЕННЫХ ДВИЖЕНИЙ И НЕКОТОРЫЕ ОСОБЕННОСТИ БОЛЬШИХ ВСПЫШЕК В МОЩНОЙ ВСПЫШЕЧНО- АКТИВНОЙ ОБЛАСТИ ИЮНЯ-ИЮЛЯ 1982 Г. <i>V. N. Ishkov, Z. B. Korobova, E. I. Mogilevskij</i> EVOLUTION OF STRUCTURE, PROPER MOTIONS AND SOME PECU- LIARITIES OF LARGE FLARES IN THE ACTIVE REGION OF JUNE-JULY 1982	355
<i>G. Bachmann, A. Hofmann, J. Staude</i> RESULTS OF VECTOR MAGNETOGRAPHIC MEASUREMENTS IN THE ACTIVE REGION SD 228/229 ON 15 JULY 1982 <i>Г.Башманн, А.Хофманн, Й.Штауде</i> РЕЗУЛЬТАТЫ НАБЛЮДЕНИЙ ВЕКТОРА МАГНИТНОГО ПОЛЯ В АКТИВНОЙ ОБЛАСТИ С.Д.228/229 15 ИЮЛЯ 1982 Г.	369
<i>V. M. Grigor'ev, B. F. Osak, V. L. Selivanov</i> DETERMINATION OF THE ACTIVE REGION MAGNETIC FIELD STRUCTURE USING VECTOR-MAGNETOGRAPHIC MEASUREMENTS <i>В.М.Григорьев, Б.Ф.Осак, В.Л.Селиванов</i> ОПРЕДЕЛЕНИЕ СТРУКТУРЫ МАГНИТНОГО ПОЛЯ АКТИВНЫХ ОБЛАСТЕЙ ПО ИЗМЕРЕНИЯМ НА ВЕКТОР-МАГНИТОГРАФЕ	377
P A R T 2	
№.4. MISCELLANEOUS PAPERS ON THEORETICAL ASPECTS OF SOLAR ACTIVITY	387
<i>Г.В.Куклин, В.Е.Степанов</i> ЗОНАЛЬНЫЕ ТЕЧЕНИЯ В СОЛНЕЧНОЙ КОРОНЕ <i>G. V. Kuklin, V. E. Stepanov</i> THE ZONAL STREAMS IN THE SOLAR CORONA	389
<i>Э.И.Могилевский</i> ПРОБЛЕМА ПЕРВИЧНОГО ИСТОЧНИКА ЭНЕРГИИ И ВЕЩЕСТВА СОЛНЕЧНЫХ ВСПЫШЕК <i>E. I. Mogilevskij</i> THE PROBLEM OF THE PRINCIPAL SOURCE OF ENERGY AND MASS OF SOLAR FLARES	409
<i>В.А.Мазур, А.В.Степанов</i> ДИНАМИКА ЭНЕРГИЧНЫХ ПРОТОНОВ В СОЛНЕЧНЫХ МАГНИТНЫХ ПЕТЛЯХ ЭФФЕКТЫ ДИСПЕРСИИ АЛЬВЕНОВСКИХ ВОЛН <i>V. A. Mazur, A. V. Stepanov</i> DYNAMICS OF ENERGETIC PROTONS ON SOLAR MAGNETIC LOOPS ALFVEN WAVE DISPERSION EFFECTS	419

	PAGE
(No. 4) <i>N. Seehafer, J. Hildebrandt, A. Krüger, Sh. Ahmedov, G. V. Gel'frejkh</i> A COMPARISON BETWEEN HIGHLY RESOLVED S-COMPONENT OBSERVATIONS AND MODEL CALCULATIONS USING FORCE-FREE MAGNETIC FIELD EXTRAPOLATIONS <i>Н. Зеехафер, Й. Хильдебрандт, А. Крюгер, Ш. Ахмедов, Г. В. Гельфрейх</i> СРАВНЕНИЕ НАБЛЮДЕНИЙ С-КОМПОНЕНТА С ВЫСОКИМ РАЗРЕШЕНИЕМ С МОДЕЛЬНЫМИ РАСЧЕТАМИ, ИСПОЛЬЗУЮЩИМИ БЕССИЛОВЫЕ ЭКСТРА- ПОЛЯЦИИ МАГНИТНОГО ПОЛЯ	431
<i>V. P. Nefed'ev</i> VARIATION OF CIRCULAR AND LINEAR POLARIZATION IN BURST EMISSION AS A CONSEQUENCE OF DYNAMIC PROCESSES IN THE SOLAR ATMOSPHERE <i>В. П. Нефедьев</i> ИЗМЕНЕНИЕ КРУГОВОЙ И ЛИНЕЙНОЙ ПОЛЯРИЗАЦИИ В ИЗЛУЧЕНИИ ВСПЛЕСКОВ КАК СЛЕДСТВИЕ ДИНАМИЧЕСКИХ ПРОЦЕССОВ В АТМОСФЕРЕ СОЛНЦА	443
<i>Yu. D. Zhugzhda, J. Staude, V. Ločan</i> A MODEL OF THE OSCILLATIONS IN THE CHROMOSPHERE AND TRANSITION REGION ABOVE SUNSPOT UMBRAE <i>Ю. Д. Жугжда, Й. Штауде, В. Лоцанс</i> МОДЕЛЬ КОЛЕБАНИЙ В ХРОМОСФЕРЕ И ПЕРЕХОДНОМ СЛОЕ НАД ТЕНЬЮ СОЛНЕЧНЫХ ПЯТЕН	451
<i>V. E. Merkulenko, V. I. Polyakov</i> A POSSIBLE MODEL FOR GLOBAL OSCILLATIONS OF THE SUN ACCORDING TO HILL'S OBSERVATIONAL DATA <i>В. Е. Меркуленко, В. И. Поляков</i> ВОЗМОЖНАЯ МОДЕЛЬ ГЛОБАЛЬНЫХ КОЛЕБАНИЙ СОЛНЦА ПО ДАННЫМ НАБЛЮДЕНИЙ ХИЛЛА	463
<i>V. N. Dermendjiev</i> ON THE EFFECTS OF MAGNETIC ENERGY INCREASE IN THE SUNSPOT CHROMOSPHERE <i>В. Н. Дерменджиев</i> ОБ ЭФФЕКТАХ РОСТА МАГНИТНОЙ ЭНЕРГИИ В СОЛНЕЧНОЙ ХРОМОСФЕРЕ НАД ПЯТНАМИ	475
<i>Э. И. Могилевский</i> СИНЕРГИТИЧЕСКОЕ ПОНИМАНИЕ ЭВОЛЮЦИИ СТРУКТУР МАГНИТНЫХ ПОЛЕЙ НА СОЛНЦЕ <i>Е. И. Mogilevskij</i> SYNERGIC EXPLANATION OF THE EVOLUTION OF SOLAR MAGNETIC FIELD STRUCTURES	487
<i>I. K. Csada</i> NEW COMPUTATIONAL RESULTS FOR THE SOLAR DYNAMO <i>И. К. Чада</i> НЕКОТОРЫЕ ЧИСЛЕННЫЕ РЕЗУЛЬТАТЫ ДЛЯ СОЛНЕЧНОГО ДИНАМО	495

	PAGE
№.5. PAPERS ON VARIOUS OBSERVATIONAL METHODS AND RESULTS	501
<i>M.N.Gnevyshev, V.P.Mikhailutsa</i>	503
STABILITY OF THE PHOTOMETRIC OUT-OFF-ECLIPSE OBSERVATIONS OF THE SOLAR CORONA AND VARIATIONS OF ITS INTENSITY IN THE 21th SOLAR CYCLE	
<i>М.Н.Гневашев, В.П.Михайлуца</i>	
СТАБИЛЬНОСТЬ ФОТОМЕТРИЧЕСКОЙ СИСТЕМЫ ВНЕЗАТМЕННЫХ НАБЛЮДЕНИЙ СОЛНЕЧНОЙ КОРОНЫ И ВАРИАЦИИ ЕЕ ИНТЕНСИВНОСТИ В 21-м ЦИКЛЕ	
<i>M.Minarovjeh, V.Rušin, M.Rybanskij</i>	511
PERIODIC VARIATIONS OF 530.3 nm CORONAL LINE	
<i>М.Минаровех, В.Рушин, М.Рибанский</i>	
ПЕРИОДИЧЕСКИЕ ИЗМЕНЕНИЯ КОРОНАЛЬНОЙ ЛИНИИ $\lambda 530.3$ nm	
<i>A.B.Delone, E.A.Makarova, J.Sykora</i>	517
ASCENT MOTIONS IN THE MONOCHROMATIC CORONA DURING TOTAL SOLAR ECLIPSE OF JULY 31, 1981	
<i>А.Б.Делоне, Е.А.Макарова, Й.Сикора</i>	
ПОДНИМАЮЩИЕСЯ ДВИЖЕНИЯ В МОНОХРОМАТИЧЕСКОЙ КОРОНЕ ВО ВРЕМЯ ПОЛНОГО СОЛНЕЧНОГО ЗАТМЕНИЯ 31 ИЮЛЯ 1981 Г.	
<i>J.Sykora</i>	523
CORONAL HOLE AS A PROBABLE SOURCE OF THE HIGHEST GEOACTIVITY IN 1981	
<i>Й.Сикора</i>	
КОРОНАЛЬНАЯ ДЫРА, КАК ВОЗМОЖНЫЙ ИСТОЧНИК НАИБОЛЬШОЙ ГЕОЭФФЕКТИВНОСТИ В 1981 Г.	
<i>J.Paciorek, T.Ciurla, B.Rompolt</i>	531
OBSERVATIONS AND INTERPRETATION OF A SET OF LIMB EVENTS OF SEPTEMBER 2, 1979	
<i>Я.Пацюрек, Т.Цюрла, Б.Ромпoldt</i>	
ИССЛЕДОВАНИЯ КОМПЛЕКСА ЛИМБОВЫХ ЯВЛЕНИЙ НАБЛЮДЕННЫХ 2 СЕНТЯБРЯ 1979 ГОДА	
<i>I.N.Garczynska, P.Majer, B.Rompolt</i>	543
THE CARD INDEX OF EJECTIONS AT THE WROCLAW OBSERVATORY	
<i>И.Н.Гарчинска, П.Маер, Б.Ромпoldt</i>	
КАТАЛОГ ВЫБРОСНЫХ ПРОТУБЕРАНЦЕВ НАБЛЮДЕННЫХ ВО ВРОЦЛАВЕ	
<i>B.Růžičková-Topolová, L.Buřka</i>	545
FLARE GEOEFFICIENCY IN RELATION TO PHOTOSPHERIC MAGNETIC FIELD ORIENTATION OF ACTIVE REGIONS	
<i>Б.Ружичкова-Топалова, Л.Буřка</i>	
ГЕОЭФФЕКТИВНОСТЬ ВСПЫШЕК В СВЯЗИ С ОРИЕНТАЦИЕЙ ФОТОСФЕРИЧЕСКИХ МАГНИТНЫХ ПОЛЕЙ АКТИВНЫХ ОБЛАСТЕЙ	

	PAGE
(No. 5) <i>S. Knoška, L. Krivský</i> FLARES OF TYPE II AND IV RADIO BURSTS IN MAGNETIC TYPES OF SUNSPOT GROUPS <i>Ш. Knoшка, Л. Кривский</i> ВСПЫШКИ С РАДИОВСПЛЕСКАМИ ТИПА II И IV В ГРУППАХ СОЛНЕЧНЫХ ПЯТЕН РАЗЛИЧНЫХ МАГНИТНЫХ ТИПОВ	557
<i>V. P. Maksimov</i> THE POSITION OF FLARE SEATS OF SUNSPOT UMBRAE <i>В. П. Максимов</i> ПОЛОЖЕНИЕ ОЧАГОВ ВСПЫШЕК В ТЕНЯХ СОЛНЕЧНЫХ ПЯТЕН	567
<i>A. Ludmány</i> ASYMMETRY OF NON-SPLITTING SPECTRAL LINES IN SUNSPOTS <i>А. Лудмань</i> АСИММЕТРИЯ НЕРАСЩЕПЛЕННЫХ СПЕКТРАЛЬНЫХ ЛИНИЙ В СОЛНЕЧНЫХ ПЯТНАХ	575
<i>M. Sobotka</i> ОПРЕДЕЛЕНИЕ РАССЕЯННОГО СВЕТА В МАЛЫХ СОЛНЕЧНЫХ ПЯТНАХ <i>M. Sobotka</i> STRAY LIGHT DETERMINATION IN SMALL SUNSPOTS	581
<i>G. Bachmann, K. Pflug</i> MINIMUM INSTRUMENTAL POLARIZATION AT CELESTAT TELESCOPE <i>Г. Бахманн, К. Пфлу</i> МИНИМАЛЬНАЯ ИНСТРУМЕНТАЛЬНАЯ ПОЛЯРИЗАЦИЯ НА ЦЕЛОСТАТНОМ ТЕЛЕСКОПЕ	589
<i>T. Baranyi, A. Ludmány</i> SYNTHESIS OF $H\alpha$ -PROFILES FROM FILTER TRANSMISSION FUNCTIONS <i>Т. Барани, А. Лудмань</i> СИНТЕЗ ПРОФИЛЕЙ $H\alpha$ ИЗ ФУНКЦИЙ ПРОПУСКАНИЯ ФИЛЬТРА	595
<i>S. I. Avdyushin, M. M. Alibegov, A. F. Bogomolov, V. A. Burov,</i> <i>E. N. Zajtsev, S. P. Leonenko, B. A. Poperchenko</i> ACTIVE REGION CHARACTERISTICS FROM TWO-FREQUENCY MAPPING WITH A TELESCOPE TNA-1500 <i>С. И. Авдюшин, М. М. Алибегов, А. Ф. Богомолов, В. А. Буров,</i> <i>Е. И. Зайцев, С. П. Леоненко, Б. А. Поперченко</i> ХАРАКТЕРИСТИКИ АКТИВНЫХ ОБЛАСТЕЙ ПО ДАННЫМ ДВУХЧАСТОТНОГО КАРТОГРАФИРОВАНИЯ НА РАДИОТЕЛЕСКОПЕ TNA-1500	603

- (No. 5) *O. A. Golubchina, V. N. Ikhsanova* 611
 OBSERVATIONS OF RAPID VARIATIONS OF THE POLARIZED AND
 NON-POLARIZED RADIO EMISSION OF LOCAL SOURCES WITH
 THE RATAN-600 AT $\lambda=2.3$ AND 4.5 cm BY THE "RELAY-RACE"
 METHOD
О.А.Голубчина, В.Н.Ихсанова
 НАБЛЮДЕНИЯ БЫСТРЫХ ИЗМЕНЕНИЙ ПОЛЯРИЗОВАННОГО И НЕПОЛЯРИ-
 ЗОВАННОГО РАДИОИЗЛУЧЕНИЯ ЛОКАЛЬНЫХ ИСТОЧНИКОВ НА ВОЛНАХ
 2.3 И 4.5 см НА РАТАН-600 МЕТОДОМ "ЭСТАФЕТА"
- A. Krüger, F. Fürstenberg, J. Hildebrandt, Sh. B. Ahmedov,* 619
V. M. Bogod, A. N. Korzhavin
 ON THE HEIGHT SCALE OF MAGNETIC FIELDS ABOVE SUNSPOT
 DERIVED FROM RATAN-600 OBSERVATIONS AND MODEL CAL-
 CULATIONS
А.Крюгер, Ф.Ф.рстенберг, Й.Хильдебрандт, Ш.Б.Ахмедов,
В.М.Богод, А.Н.Коржавин
 О ШКАЛЕ ВЫСОТ НАД СОЛНЕЧНЫМИ ПЯТНАМИ, ПОЛУЧЕННОЙ ИЗ
 НАБЛЮДЕНИЙ НА РАТАН-600 И ИЗ МОДЕЛЬНЫХ РАСЧЕТОВ
- N. S. Kaverin, M. M. Kobrin, A. I. Korshunov, V. V. Shushunov, H. Aurass,* 631
F. Fürstenberg, J. Hildebrandt, A. Krüger, N. Seehafer
 ON THE RELATION BETWEEN SPECTRAL CHARACTERISTICS OF
 THE MICROWAVE EMISSION FROM SOLAR ACTIVE REGIONS AND
 PHYSICAL CONDITIONS OF THE SOLAR ATMOSPHERE
Н.С.Каверин, М.М.Кобрин, А.И.Коршунов, В.В.Шушунов,
Х.Аурас, Ф.Ф.рстенберг, Й.Хильдебрандт, А.Крюгер,
Н.Зеехафер
 ЗАВИСИМОСТЬ СПЕКТРАЛЬНЫХ ХАРАКТЕРИСТИК МИКРОВОЛНОВОГО
 ИЗЛУЧЕНИЯ СОЛНЕЧНЫХ АКТИВНЫХ ОБЛАСТЕЙ ОТ ФИЗИЧЕСКИХ
 УСЛОВИЙ В СОЛНЕЧНОЙ АТМОСФЕРЕ
- S. T. Akinyan, V. V. Fomichev, I. M. Chertok, H. Aurass, A. Krüger* 639
 EFFECTS CHARACTERIZING THE RELATIONSHIP OF RADIO
 BURSTS AND PROTON FLARES OF 1980
С.Т.Акинян, В.В.Фомичев, И.М.Черток, Х.Аурас, А.Крюгер
 ЭФФЕКТЫ ХАРАКТЕРИЗУЮЩИЕ СВЯЗЬ РАДИОВСПЛЕСКОВ И ПРОТОННЫХ
 ВСПЫШЕК 1980 Г.
- N. S. Kaverin, A. I. Korshunov, V. V. Shushunov, H. Aurass, H. Detlefs,* 653
H. Hartmann, A. Krüger, J. Kurths
 SPECTROGRAPHIC OBSERVATIONS OF SOLAR MICROWAVE
 BURSTS IN THE 5.3 - 7.4 GHz RANGE
Н.С.Каверин, А.И.Коршунов, В.В.Шушунов, Х.Аурас,
Н.Детлефс, Х.Хартманн, А.Крюгер, Й.Куртс
 СПЕКТРОГРАФИЧЕСКИЕ НАБЛЮДЕНИЯ СОЛНЕЧНЫХ МИКРОВОЛНОВЫХ
 ВСПЛЕСКОВ В ДИАПАЗОНЕ 5.3 - 7.4

	PAGE
ABBREVIATIONS USED IN REFERENCES	661
LIST OF CONSULTATION PAPERS NOT INCLUDED IN THIS VOLUME	662
AN ACCOUNT OF SOME EXTRA SESSIONS OF THE CONSULTATION	663
NAME INDEX (AUTHORS AND PARTICIPANTS)	664

PUBLICATIONS
OF
DEBRECEN
HELIOPHYSICAL OBSERVATORY
OF THE
HUNGARIAN ACADEMY OF SCIENCES

ПУБЛИКАЦИИ
ДЕБРЕЦЕНСКОЙ
ГЕЛИОФИЗИЧЕСКОЙ ОБСЕРВАТОРИИ
ВЕНГЕРСКОЙ АКАДЕМИИ НАУК

A MAGYAR TUDOMÁNYOS AKADÉMIA
DEBRECENI
NAPFIZIKAI OBSZERVÁTORIUMÁNAK
KÖZLEMÉNYEI

VOLUME 5

Nos. 1-3

Proceedings of the
11th Regional Consultation on Solar Physics

PART 1

DEBRECEN

1983

(Publ. Debrecen Obs., Vol. 5, Part 1, Nos. 1-3, pages 1-384)

P R E F A C E

The 11th Regional Consultation on Solar Physics was held in Debrecen, Hungary, from 12 to 16 September 1983, under the joint sponsorship of the Hungarian Academy of Sciences and its Debrecen Academy Committee, and organized by the Debrecen Heliophysical Observatory according to an agreement of the KAPG organization. (The KAPG acronym is the abbreviation for a joint committee of the Academies of Sciences of some socialist countries for multilateral investigations on interdisciplinary problems of "Planetary Geophysics".) The Consultation was organized within the framework of KAPG Project 4.

The 11th Regional Consultation on Solar Physics should be regarded as a member of the series of "Consultations", initiated by Czechoslovakian and Polish solar astronomers, which includes the regional solar meetings as follows:

<i>No.</i>	<i>Year</i>	<i>Place</i>	<i>Country</i>
1st	1961	Tatranská Lomnica	Czechoslovakia
2nd	1962	Kalatowki	Poland
3rd	1964	Tatranská Lomnica	Czechoslovakia
4th	1966	Sopot	Poland
5th	1968	Potsdam	GDR
6th	1971	Gyula	Hungary
7th	1973	Stary Smokovec	Czechoslovakia
8th	1976	Irkutsk	USSR
9th	1978	Wroclaw	Poland
10th	1980	Potsdam	GDR

The 5th and from the 8th onwards were all formally KAPG Consultations. The majority of the papers presented at these meetings have generally been collectively published by the organizers of the Consultations in one of their own publications.

- The principal topics of the 11th Consultation were:
- I. Results relating to the Solar Maximum Year Programs (SMY) in Socialist Countries,
 - II. Results of Investigations on Mass Motions and Magnetic Fields in Solar Active Regions.

All papers presented during the 11th Consultation, both the oral and poster contributions, which were submitted to the editors by the deadline can be found in the present volume of Consultation Proceedings, irrespective of whether the editors agreed with all the views expressed or not. Authors and titles of those papers that are not included in this issue may be found at the end of the volume where some additional information on other sessions of the Consultation are given.

The Consultation was held at the headquarters of the Debrecen Academy Committee; both the sessions as well as a poster exhibition took place there.

The Local Organizing Committee consisted of L.Dezső (chairman), Lidia Gesztelyi, B.Kálmán, Ágnes Kovács and Mrs.Katalin Sári (treasurer).

L.Dezső, B.Kálmán

An additional note

The Editors feel it necessary to remark the following. Authors generally declared in writing in Consultation Participation Form that their contributed "paper(s) has not yet been published" elsewhere.

11th Regional Consultation on Solar Physics

LIST OF PARTICIPANTS AND NON-PARTICIPANT CO-AUTHORS

(Names in italics indicate the non-participant co-authors and asterisks mark those participants who are not among the authors)

B U L G A R I A

National Astronomical Observatory,
Astronomy Department, Bulgarian Academy of Sciences
SOFIA

Dermendjiev V.N.

C Z E C H O S L O V A K I A

Astronomical Institute, Czechoslovak Academy of Sciences

ONDŘEJOV

Ambrož P.	Kopecký M.*	Sobotka M.
Boučková O.*	Křivský L.	Tlamicha A.
Bumba V.	Letfus V.*	Tomášek P.*
Fárník F.	Růzičková-Topolová B.	Valníček B.
Karlický M.		

Astronomical Institute, Slovak Academy of Sciences

TATRANSKÁ LOMNICA

Antalová A.	<i>Minarovjech M.</i>	Rybanský M.
<i>Knoška S.</i>	Rušin V.	Sýkora J.

SUAA Observatory

HURBANOVO

Lorenc M.*	Lukáč B.*	Pintér T.*
------------	-----------	------------

Astronomical Society

PRAHA

Buřka L.

E N G L A N D (U.K.)

Mullard Space Science Laboratory, University College London,
DORKING Department of Physics and Astronomy

Bentley R.D.

G E R M A N D.R.

Central Institute for Solar-Terrestrial Physics, GDR Academy of Sciences
(ZISTP)

Radioastronomy Dept. (HHI)

BERLIN-Adlershof

Aurass H.
Böhme A.
Detlefs H.

Fürstenberg F.
Hartmann H.
Hildebrandt J.

Krüger A.
Kurths J.

Einsteinturm Solar Observatory

POTSDAM

Bachmann G.
Hoffmann H.

Pflug K.
Seehafer N.

Stäude J.

H O L L A N D

Space Research Laboratory, Astronomical Institute of Utrecht University

UTRECHT

Mewe R.

Schrijver J.

H U N G A R Y

Astronomical Research Institute, Hungarian Academy of Sciences

Konkoly Observatory

BUDAPEST

Csada I.K.

Grandpierre A.*

Szeidl B.*

Heliophysical Observatory

DEBRECEN

Baranyi T.
Csepura Gy.*
Dezső L.
Gerlei O.*

Gesztelyi L.
Kálmán B.
Kondás L.

Kovács Á.
Ludmány A.
Nagy I.

GYULA

Győri L.*

Seres F.*

Astronomy Department, Eötvös University

BUDAPEST

Marik M.*

Pap J.*

P O L A N D

Astronomical Observatory, Wrocław University

WROCLAW

Ciurla T.

Garczyńska I.

Jakimiec J.

Jakimiec M.

Mayer P.

Paciorek J.

Rompolt B.

Space Research Center, Polish Academy of Sciences

WROCLAW

Sylwester B.

Sylwester J.

Institute of Theoretical Physics and Astrophysics, University of Gdansk

GDANSK

*Bielicz E.**

*Sikorski J.**

S O V I E T U N I O N

Astronomical Institute, Kazakh Academy of Sciences

ALMA-ATA

Minasyants G.S.

Obashev S.O.

Radiophysical Research Institute, Gorkij State University

(NIRFI)

GORKIJ

Kaverin N.S.

Kobrin M.M.

Korshunov A.I.

Mel'nikov V.F.

Podstrigach T.S.

Shushunov V.V.

Siberian Institute of Terrestrial Magnetism, Ionosphere and

Radiowave Propagation, USSR Academy of Sciences

(SibIZMIR)

IRKUTSK

Grigor'jev V.N.

Kasinskij V.V.

Kuklin G.B.

Maksimov V.P.

Mazur V.A.

Merkulenko V.E.

Nefed'ev V.P.

Osak B.F.

Palamarchuk L.E.

Polyakov V.I.

Potapov N.N.

Selivanov V.L.

Smol'kov G.Ya.

Stepanov A.V.

Stepanov V.E.

Teplitskaya R.B.

Turova I.P.

Main Astronomical Observatory, Ukrainian Academy of Sciences

KIEV

Alikaeva K.V.

Astronomical Observatory, Kiev State University

KIEV

Kondrashova N.N.

Polupan P.N.

Redyuk T.I.

Krasnoyarsk State University

KRASNOYARSK

Romanov V.A.

Main Astronomical Observatory, USSR Academy of Sciences

(Pulkovo Observatory)

LENINGRAD

Achmedov Sh.B.

Gel'freikh G.B.

Ikhsanova V.N.

Kislovodsk Station of the Pulkovo Observatory

KISLOVODSK

Gnevyshev M.N.

Mikhajlutsa V.P.

Special Astrophysical Observatory, USSR Academy of Sciences

(Leningrad Branch)

LENINGRAD

Bogod V.M.

Golubchina O.A.

Korzavin A.N.

Sternberg Astronomical Institute, Moscow State University

MOSCOW

Delone A.B.

Nikulin I.F.

Prokudina V.S.

Makarova E.A.

Institute of Space Research, USSR Academy of Sciences

MOSCOW

Likin O.B.

Pisarenko N.F.

Institute of Applied Geophysics

MOSCOW

Alibegov M.M.

Avdyushin S.I.

Burov V.A.

Moscow Power Institute

MOSCOW

Bogomolov A.F.
Leonenko S.P.

Poperechenko B.A.

Zajtsev E.I.

Crimean Astrophysical Observatory, USSR Academy of Sciences

NAUCHNYJ

Gopasyuk S.I.

Koval' A.N.

Stepanyan N.N.

Radioastrophysical Observatory, Latvian Academy of Sciences

RIGA

Locāns V.

Ryabov B.I.

Spektor A.R.

Astronomical Institute, Uzbek Academy of Sciences

TASHKENT

Korobova Z.B.

Sattarov I.

Institute of Terrestrial Magnetism, Ionosphere and

Radiowave Propagation, USSR Academy of Sciences

(IZMIRAN)

TROITSK (Moscow rgn.)

Akinyan S.T.

Chernov G.P.

Chertok I.N.

Fomichev V.V.

Ishkov V.N.

Markeev A.K.

Mogilevskij E.I.

Obridko V.N.

Zhugzhda Yu.D.

Publ. Debrecen Obs. Vol. 5

No. 1.

INVITED REVIEW PAPERS

SOME TRENDS IN MODERN SOLAR PHYSICS

V. N. O B R I D K O

IZMIRAN, Troitsk

Abstract:

Discussed are the main three trends in modern solar physics i.e., the study of solar plasmas as a set of discrete structural elements in time and space, the study of global organization of solar activity, and the closer relationships between solar and stellar investigations.

О НЕКОТОРЫХ СОВРЕМЕННЫХ ТЕНДЕНЦИЯХ В СОЛНЕЧНОЙ ФИЗИКЕ

В.Н. ОБРИДКО

ИЗМИРАН, Троицк

Абстракт:

Анализируются три основные тенденции в современной солнечной физике: изучение солнечной плазмы как набора дискретных в пространстве и времени структурных элементов, изучение глобальной организации солнечной активности и объединение солнечных и звездных исследований.

*

First of all, I must apologize for the specific character of this report. Unlike the reports you will be listening to and discussing in the following five days, this one is not the result of a particular piece of scientific research, but rather of some reflections on the main tendencies that have developed in solar physics. During a preliminary discussion of the program of this Consultation, I shared my ideas with Prof. M. Kopecký, the leader of our Project, who found them interesting enough to be set forth in the form of an opening lecture. Further consideration of the program and acquaintance with the papers submitted, both oral and poster, reinforced this still more, since all of them are, in some way or other, associated with the three main tendencies which I am going to talk about.

1. The discretization of time and space distribution of physical properties and phenomena

As shown by numerous recent observations, diffuse properties and phenomena on the Sun are quite rare. As a typical example, let us consider the sunspot. It is known to occur as a result of complicated interaction of different mechanisms: circulation and oscillatory convection, magnetic field, radiative transfer, MHD-waves, etc. The relative contribution of these mechanisms is different in distinct layers of the sunspot. It could be expected that the features with diffuse boundaries having a wide scope of dimensions, brightness and magnetic field values could be observed. In fact, the objects on the Sun, however, being sometimes very complicated in shape, always have quite definite boundaries; the sunspot brightness is practically independent of any other parameters, except the phase of the solar cycle; the magnetic field values lie within a narrow range, and the sunspot size distribution indicates the existence of certain stable states in which the sunspot dimensions are close to the dimensions of supergranules. The features with diffuse boundaries and characteristics not corresponding to the stable states are rather numerous, but short-lived and they either decay quickly, or change into sunspots with standard characteristics.

The same applies to many other features. The entire surface of the Sun consists of granules, mesogranules, supergranules and giant granules. The magnetic field is concentrated in ropes containing up to 99% magnetic flux. The whole corona, both over the active and undisturbed regions, consists of loops which may be followed to distances very great from the Sun.

The analysis of time sequences also indicates a great difference from uniform noise distributions. 5-minute and 160-minute oscillations are well pronounced, characteristic oscillation periods in sunspots are 3 minutes in the chromosphere and 20-40 minutes in the corona over an active region.

The height variation of temperature in the solar atmosphere also infers the existence of steady states - the plateaus cor-

responding to 10^4K , $2.5 \cdot 10^4\text{K}$ and 10^6K . These are extended height regions with small temperature variations separated by comparatively thin transition zones.

These discrete phenomena (both spatial and temporal) seem to be characteristic energy states, the transition between them is accompanied by energy release or absorption.

The origin of irregularities in solar plasmas is still not clear. Synergetics - a new developing science dealing with self-organization of complex non-linear systems is very promising in this respect.

The fact that irregularity is a fundamental property of solar plasmas and that all processes on the Sun lead to the occurrence of irregular stable states or transitions between them is of great methodical importance. Many authors are still proceeding from the a priori concept of uniform matter. It would be more convenient to take irregularity into account right away when discussing any mechanism, or at least to determine its importance in the given problem.

2. Global organization and interdependence of solar phenomena

The statement about close correlation between solar phenomena may seem rather commonplace and in any case not new. In practice, however, when studying one or other object or phenomenon, we usually abstract from its relation to global processes. Recent observations have shown that this correlation is much closer than was supposed before. For instance, it is very difficult now to discriminate between active and undisturbed regions. In fact, the active region is the place for higher concentration of the same magnetic flux ropes which determine the structure of undisturbed regions. The coronal heating is due to transformation of superpotential magnetic field energy into thermal energy and this mechanism is the same both in active and undisturbed regions. Moreover, as is now clear, the only difference between energy release processes in non-stationary flare-like events and in stationary corona consists in their velocity. Thus, the flare is a regular stage in the evolution

of the active region and is necessary for the release of extra energy.

On the other hand, many phenomena that have so far been considered characteristic of undisturbed regions, e.g., granulation of different kinds, are observed (though in a somewhat modified form) in active regions and sunspots.

Sunspots are one of the most important components of an active region and their physics cannot be understood without knowing the physics of the latter.

The time scale of this stage is several rotations of the Sun.

The next stage in the organization of solar phenomena is the complex of activity. It transpired that even the active regions spaced about a solar radius are connected with each other. This relationship was first inferred from the nonrandom distribution of active regions. It turned out that the active regions with abnormal occurrence of some Zürich classes are concentrated in the vicinity of large proton groups. Proton flares are rare in isolated active regions. Series of correlated flares may often be observed in the groups situated far from each other, but forming part of one and the same complex of activity. And finally, direct observations on Skylab have revealed the existence of very long arches and loops that connect distant active regions sometimes situated in different hemispheres.

The interaction of active regions is undoubtedly determined by a magnetic field, most likely by a subphotospheric one. As seen from the analysis of large-scale magnetograms, the complex is formed by active regions that belong to a single magnetic field system.

The time scale of this stage is in the order of 1-2 years.

The next stage of organization is active longitudes and their interaction with background fields and the general field of the Sun. The phenomenon of active longitudes has been known for the last 20 years; when the works by V. Bumba and R. Howard appeared, this phenomenon was associated with so called magnetic field streams that extend from one hemisphere to another and rotate as a solid body. This is where one can observe the

largest active regions and the most powerful complexes of activity in which proton events occur. They influence the distribution of the magnetic field far beyond the Sun and produce the IMF sector structure. It allows us to study the Sun by analyzing the characteristics of the heliosphere, which may, thus, be considered as the outer atmosphere of the Sun. The sector structure is due to interaction between local fields and the general field of the Sun, whose origin is not clear yet.

The time scale of this stage is in the order of a solar cycle.

Though the description of the latter stage of matter organization lies beyond the scope of our Consultation, we have however to mention it, not merely to make the picture complete. The fact is (and this should be taken into account) that we are not dealing with three independent hierarchical stages, but rather with a single system of matter organization. It becomes more and more clear that the properties of elements at the lower hierarchical stage are connected with situation at the higher stage.

This may be confirmed by three effects discovered recently with different degree of reliability: the variation of sunspot brightness with the solar cycle; the correlation between the total solar irradiance and solar activity data; and the correlation of neutrino flux with Wolf numbers. These results suggest that solar activity is associated not only with the processes in the solar atmosphere, but also with deeper layers, including probably the core of the Sun.

3. Solar-stellar astrophysics

In addition to the above stated, we should mention another important tendency which developed in recent years. This is the revival of solar-stellar astrophysics. For a long time, these two branches of astrophysics developed independently. Stellar physics was based on observations so much inferior in informativeness to the usual solar observations that the application of any fine effects of solar physics was impossible. For the same reason, solar physicists did not see how they could

benefit from comparison with stellar astrophysics. Now the situation has changed drastically, in particular as far as stellar chromospheres and coronas are concerned. For the first time, astrophysicists are able to use the procedure applied in other fields of physics, i.e., to study in detail one or other phenomenon and then to verify the general character of established regularities. Now we could say, paraphrasing Kipling's words: "What can they know of the Sun who only the Sun know". Listed below are some of the most important results of solar-stellar astrophysics, relevant to the topic of this Consultation.

1. Starspots have been discovered in many stellar atmospheres of later types than the Sun. They have a relative brightness of the same order as sunspots and a magnetic field of 2000-4000 G. But there is also a difference: some of the starspots occupy up to 40% (in the corona up to 70%) of the surface of the star.

2. A large number of stars were found to have activity cycles close to the solar cycle of 5-10 years.

3. The intensity of coronal X-ray emission proved to be proportional to the square equatorial rotation velocity of the star. This important result could not have been discovered by solar physics alone.

4. The coronal heating can not be explained by sound waves. MHD-waves and dissipation of current sheets should be involved.

To my mind, the above three tendencies, i.e., the study of solar plasmas as a set of discrete structural elements in time and space, the study of the global organization of solar activity, and the closer relationships between solar and stellar investigations, will predominate during the next 10-15 years.

КРАТКИЕ ИТОГИ ИССЛЕДОВАНИЯ ВСПЫШЕК В ПЕРИОД ГСМ

В.Е. СТЕПАНОВ, В.В. КАСИНСКИЙ

СибИЗМИР, Иркутск

Абстракт:

Дан краткий обзор предварительных результатов исследований, использовавших наблюдения во время международной программы Год Солнечного Максимума.

A SHORT REVIEW OF THE INVESTIGATIONS OF
SOLAR FLARES IN THE SMY

V.E. STEPANOV, V.V.KASINSKIJ

SibIZMIR, Irkutsk

Abstract:

A short review of the preliminary results of investigations carried out using the data of the observations obtained during the international project Solar Maximum Year is given.

Что нового получено в познании вспышечного процесса в период выполнения международной программы Года Максимума Солнца?

Как известно, эмиссия в рентгене появляется в результате тормозного излучения энергичными электронами или вследствие термического разогрева плазмы до температуры $>10^7$ К. Появление такой высокой температуры во вспышках с эмиссией X-лучей является основным фактором. Эмиссия в линиях водорода и других элементов холодной плазмы является следствием высокой температуры.

Главной фазой развития вспышки является импульсная фаза, когда появляется жесткий рентген и микроволновое излучение. Жесткий рентген в импульсной фазе зависит от плотности и спектра энергичных электронов. Тормозное излучение появляется, когда электроны с энергиями 10-100 кев (в основном >30 кев) {1} поглощаются в плотной плазме. А микроволновое излучение зависит от напряженности магнитного поля и также от спектра энергичных электронов, с энергиями преимущественно >100 кев.

Наблюдения на SMM и радиотелескопе VLA {2} показали, что жесткий рентген светится в торцах вспышечной петли, а микроволновое излучение, преимущественно в вершинах петель. В некоторых вспышечных петлях микроволновая эмиссия имела асимметричную форму, что видимо связано с асимметричной концентрацией магнитного поля в петле. Это пространственное разделение двух высокоэнергичных явлений, происходящих одновременно в пределах точности фиксации моментов времени весьма важно. Наблюдения на японском спутнике "Гинотори" подтвердили наблюдения на SMM освещении жесткого рентгена в торцах вспышечной петли. В последующих стадиях развития вспышки микроволновое излучение, по-видимому, имеет тепловую природу.

Ученых тревожил вопрос - откуда берется вещество от вспышки, когда во время этого процесса наблюдалось выпадение вещества в хромосферу (это же явление наблюдается и в активных областях). Еще задолго до проведения программы ГСМ Нейпертом {3} в 1968 году была выдвинута гипотеза об "испарении" хромосферного вещества.

Испарение вещества хромосферы зарегистрировал Актон и др. {4} во вспышке 7 мая 1980 года. Максимум мягкого рентгена наступил спустя 30 секунд после максимума жесткого рентгена. Одновременно в обсерватории Сакраменто-Пик регистрировались контуры линии $H\alpha$ в двух узлах вспышки. Перед первым всплеском жесткого рентгена области показывали движения как вверх, так и вниз со скоростями ≤ 5 км/с. Непосредственно после первого всплеска жесткого рентгена в течение нескольких минут наблюдался подъем вещества со скоростями до 20 км/с. После этого всплеска как подъем так и опускание газа с такими же скоростями. Кроме того в максимуме всплеска, в резонансной линии Fe XXV ($\lambda=1.85 \text{ \AA}$) и в мягком рентгене зарегистрировано движение вверх нагретого хромосферного вещества {5,6}. Новым результатом является также появление "голубого" компонента этой линии, это свидетельствовало о подъеме вещества со скоростью 400 км/с. Расчеты показывают, что испарение хромосферы доставляет достаточно массы для объяснения меры эмиссии во вспышке. Нагрев хромосферы и ее испарение могут быть вызваны энергичными электронами, теплопроводностью, волнами Альфвена, сжатием или связаны с электродинамическими процессами {1}. Видимо первые два процесса играют преобладающую роль.

Во вспышках 21 мая, 27 июня 1980 г. и 2 апреля 1981 г. зарегистрированы горячие источники во вспышках (узлы вспышек), в которых наблюдалось излучение как с жестким так и с мягким тепловым спектром. Температура в этих источниках превышала $3 \cdot 10^7$ К. Изображения, полученное на Хинотори показали, что они компактны. Что мы знаем о второй ступени ускорения во вспышках? Ранее о наличии высокоионизированных частиц от вспышек мы знали только из измерений вблизи орбиты Земли. Хундхаузен {7} предположил, что они ускоряются в солнечном ветре на фронте ударной волны в межпланетном пространстве, а, следовательно, это стадия ускорения должна значительно запаздывать от времени протекания импульсной фазы. В первые месяцы международной программы не было зарегистрировано второй ступени ускорения частиц. Затем возникли более мощные

вспышки и было зарегистрировано большое число наблюдений в γ -излучении {8,9}. Эти данные показали, что линии эмиссии γ -излучения генерируются в течение нескольких секунд в импульсной фазе вспышки. Бай и др.{10} нашли малое запаздывание между импульсной фазой (энергия электронов <100 кев) и появлением протонов и электронов высокой энергии. Следовательно, в импульсной фазе возникают ударные волны и механизм ускорения первой ступени инжектирует частицы, которые в короне ускоряются до высоких энергий на фронтах ударных волн {11}.

Теперь о мало изученных явлениях. Кейн и др.{12} обработали данные "стерео" наблюдений вспышки с двух спутников, находившихся соответственно на околоземной и дальней орбитах. Более мягкий спектр рентгена зарегистрирован при наблюдении на лимбе и жесткий рентген на диске Солнца, это свидетельствовало о малой генерации жесткого излучения (уровень короны), как мы указывали выше. Однако, последующие наблюдения с двумя приборами для жесткого рентгена (ISEE-3 и Пионер) {13} дали дополнительные данные о пространственном протяжении источников жесткого спектра. Эти наблюдения также подтверждены спутником Хинотори, который обнаружил источник нетепловой эмиссии над вспышкой на высоте >50000 км {1}. Имеются новые исследования, подтвердившие открытие Мандельштама С.Л. и его группы, что явление вспышек может проявиться в короне без участия холодной атмосферы Солнца. На SMM зарегистрирована необычайная последовательность вспышечно-подобных явлений. Регулярная серия явлений генерирует жесткий, мягкий рентген и ультрафиолет примерно в такой же пропорции, как во вспышках, но без эмиссии и $\text{H}\alpha$ {15}. Это свидетельствует о развитии плазменной неустойчивости в магнитных полях короны с обычными механизмами, ускорением частиц, нагревом, испарением и теплопроводностью, которые могут иметь место и без значительного вовлечения хромосферы. Эти явления чрезвычайно важны в свете объяснения подпитки солнечного ветра до больших скоростей, взрывов протуберанцев, питания энергией корональных транзиентов, а также возможно высокой температуры короны. Сравнительно мало изученными явля-

ются корональные транзиенты. Открытие корональных транзиентов было сделано на приборах "Скайлаба", а затем получены данные на спутниках SMM, P-78 и с Земли на К-коронOMETре. Они наблюдаются в белом свете, а также в отдельных линиях, причем в одном и том же транзиенте светится линия Fe XIV и линия H α . Мак Куин {16} по материалам "Скайлаба" сделал обзор явлений. Основные типы транзиентов - это движущиеся расширяющиеся петли или облака различной формы. Средняя скорость вспышечных транзиентов 775 м/с, а объектов, связанных с протуберанцами - 330 км/с. Эти образования двигаются ускоренно, в среднем до $2 R_{\odot}$. Кинетическая энергия порядка 10^{31} эрг. Однако, Вагнер и др. {17} 7-го апреля 1980 г. наблюдали огромный петельный транзиент с нерадиальным движением. Движущийся радиоисточник IV типа был локализован очень близко к локализации транзиента. Комбинирование оптических и радиоастрономических данных позволило оценить механическую и магнитную энергии. Получен ошеломляющий результат: механическая энергия транзиента более чем на порядок больше полной энергии излучения вспышки, а его магнитная энергия еще больше. Явления транзиентов происходят довольно часто - в среднем I транзиент появляется в течение 2 дней и появляются в широком диапазоне гелиоширот - от 5 до 80°.

В проекте GSM, проводившемся в СССР с 1 октября 1979 г. по 1 октября 1981 г., приняли участие 18 обсерваторий солнечного профиля и 3 физических института: Институт космических исследований, Физический институт АН и Научно-исследовательский институт радиофизики (г. Горький).

Изменение контуров фотосферных магниточувствительных во вспышках изучено Аликаевой и др. {18}. Касинский В.В. {19} рассматривает накопление магнитной энергии в модели "нейтрального волокна". На основании наблюдений на поляриметре Нефедьев В.Л. {20} показал, что перед импульсной фазой иногда наблюдается линейная поляризация в радиоизлучении. Кобриным М.М. и др. {21} обнаружено возрастание КПК пульсаций радиоизлучения перед мощными вспышками, а Быстровым и др. {22,23} показана связь

между долгопериодическими флюктуациями радиоизлучения Солнца и магнитного поля Земли перед протонными вспышками. Северным А.Б. и др. {24} дан обзор методов прогноза вспышек, Буровым В.А. и др. {25}, Авдюшиным и др. {26} применены методы распознавания образов для прогноза вспышек с использованием 16 параметров.

Особенностью наблюдений в 1979/80 г. было установление (Огирь М.Б.{27}) того факта, что вспышечная активность на всем диске Солнца проявляется в виде серий, возникающих в различных активных областях или симпатических и гомологических вспышек в отдельных комплексах (Иошпа Б.А. и др. {28} и Головки А.А. {29}). В связи с этим, вопросу о пространственновременных закономерностях вспышек было посвящено относительно большое число работ. Из 158 вспышек, происходивших в двух взаимодействующих близкорасположенных активных областях NR 16341, 16344, в октябре 1979 г. 40% было либо одновременными, либо симпатическими (Ишков В.Н. и др. {30}). В работе Б.А. Иошпы и др. {28} была прослежена эволюция сильно растянутого по широте и долготе, $20^\circ \times 24^\circ$, комплекса из трех групп в течение четырех кэррингтоновских оборотов. Показано, что 16% вспышек из 150 происходили одновременно, а 62% произошли с небольшими интервалами 1-20 минут в различных частях комплекса. Это позволило сформулировать концепцию, согласно которой в комплексе большой широтно-долготной протяженностью с ясно выраженной подфотосферной магнитной связью большие вспышки маловероятны и выделение энергии деконцентрируется по большой площади в виде слабых симпатических и гомологических вспышек. Важный вопрос о случаях гомологических вспышек в ядрах пятен {25,27} и 29 мая 1980 г. был рассмотрен в работе Н. С. Шиловой и др. {31}, в которой показано, что интегральная по времени (2 ч) энергия водородной эмиссии в них ³⁰ соответствует вспышкам балла 2. Феномен вспышечной эмиссии $\approx 10^{30}$ эрг в чисто продольном поле пятен указывает на необходимость поиска источника энергии, отличного от токовых слоев, а именно в подфотосферных слоях, откуда, по мнению Э.И. Могилевского {32}, могут выходить цуги уединенных нелинейных возмущений - МГД-солитоны. С этим тесно связан вопрос

о магнитных транзиентах, обнаруженных Г.Зириным {33}. Анализ спектра солнечной вспышки 26 июля 1981 г. со значительной эмиссией в линиях металлов показал, что "магнитные транзиенты" имеют яркостную, а не магнитную природу {34}. Кроме того магнитные транзиенты возникали в периоды близкие к максимуму вспышки и поэтому не могут быть источниками возникновения вспышки. Гомологичность и синхронность вспышек на большом расстоянии (май 1980 г.) 20° была отмечена А.А. Головкин и др. {29}. Авторы нашли, что "серии" симпатических вспышек приходятся на моменты выноса магнитного потока N-полярности и выравнивание дисбаланса потока "лидер-хвостовые пятна". Отмечены синхронные колебания N и S-потока в спокойные периоды. В.Е. Степановым и др. {35} установлен ряд новых фактов, имеющих значение для моделей вспышек: обнаружены нелинейные колебания в узлах вспышек всех компонент скоростей, амплитуда и частота которых возрастают к максимуму вспышки с периодами 480-180 с. Предполагается наличие изменений направления электрических токов во вспышечной петле.

Во время вспышки изменяются структуры контуров хромосферных линий. Это явление изучено в серии работ Е.А. Окса {36}, В.Г. Банина и др. {37}, Коваль А.Н. и др. {38}, что позволило разработать метод диагностики параметров плазмы по эффекту Штарка в турбулентных электрических полях с оценкой уровня как высокочастотной так и низкочастотной плазменной турбулентности. По поляризации измерения вспышек и эмиссионных выбросов А.Н. Бабиным и др. {39} обнаружено присутствие нетеплового источника. В серии работ Э.И. Бараковского {40}, Л. Н. Курочки и др. {41,42} построены модели вспышек для объяснения интенсивности и полуширины бальмеровских линий.

Исследования Ш.Б. Ахмедова и др. {43} на спектрально-поляризационном радио-комплексе РАТАН-600 29 апреля - 10 мая 1979 г. в диапазоне 2-4 см показали, что источник состоит из двух сильно поляризованных деталей в пятне и широкой слабой поляризацией между пятнами. Поле $H = 30$ гс на высоте 50000 км. Наблюдения всплесков радиоизлучения в августе и ноябре 1979 г. в сантиметровом и метровом диапазонах показали, что за 20-30

минут перед вспышками наблюдается заметное ослабление шумовых бурь, что можно связать с результатом М.Р. Кунду {44} об усилении и упорядочении магнитного поля перед вспышками. Сложный многокомпонентный характер микроволновых всплесков свидетельствует о длительном (десятки минут) характере выделения энергии во вспышках в дискретной форме {45}. К аналогичному выводу о времени энерговыделения порядка 50 мин пришли авторы В.Н. Ишков и др. {46}. Причем, радиоисточник формировался при постоянстве структуры магнитного поля. Случай, когда вспышка (29 марта 1980 г.) сочетала жесткое и значительное энерговыделение (рентген, радиоизлучение) без генерации ударных волн и выбросов плазмы, исследован в работе В.Н. Боровик и др. {47}. Предложена двухкомпонентная модель источника в виде слабополяризованной плазмы в замкнутой арке поля и источника с сильной поляризацией в районе ядер пятен. Спектральная плотность радиоизлучения на фоне распада пятен исследовалась С. И. Болдыревым и др. {48} на БПР (Пулково).

М.М. Кобриным и др. {49} рассмотрена модель АО с токовым слоем. Ряд тонкоструктурных образований в S-компоненте могут быть объяснены в рамках этой модели.

Приоритет и передовые научные идеи советских теоретиков нашли отражение в период подготовки проекта ГСМ благодаря работам С.И. Сыроватского и его школы. В течение ГСМ эти концепции получили еще большее развитие. В работе {50} Сомов Б.В. рассматривал распространение в корону нового магнитного поля развивающейся области и что взаимодействие со старыми корональными полями приводит в магнитному пересоединению и к появлению плотных корональных петель с энерговыделением, разрывом структуры поля и появлением транзientа. Быстрая реализация энергии в токовом слое приводит к ударной волне и ряду эффектов в неоднородной атмосфере. Рассмотрено явление "испарения хромосферы". Конденсационная мода тепловой неустойчивости токового слоя может играть роль триггера во вспышках. Работа Л.В. Брушлинского и др. {51} была посвящена кумуляции энергии в окрестности нулевой линии поля, стабилизации разрывной неустойчивости и токовым слоям в сдвиговых течения плазмы. Проявления

турбулентного Штарк-эффекта в различных моделях вспышек с использованием спектроскопического метода рассмотрены В.П. Максимовым и др. {52} и Е.А. Оксом {53}. Как указывалось ранее, разнообразие вспышек, глубинные и гомологические вспышки в ядрах пятен не исключают иных теоретических объяснений энерговыделения. Показана Л.А. Пустыльником {54} роль в перегреве турбулентного слоя бесстолкновительной волны "замещения", обеспечивающей уровень ионно-звуковой турбулентности. В. В. Булановым {55,56} рассмотрено ускорение заряженных частиц в окрестности нулевой линии магнитного поля в импульсных электрических полях при разрыве токового слоя. Выполнен цикл работ Г.Е. Кочаровым и др. {57}, Я. Г. Кочаровым {58} по интерпретации обогащения ^3He солнечных быстрых частиц. Предлагается модель вспышки богатой ^3He . Обогащение ^3He происходит вследствие возбуждения ионно-звуковой турбулентности.

А.В. Степановым и др. {59} показана связь пульсаций всплесков IV. типа с энергичными протонами. Модуляция излучения возникает при инъекции протонов во вспышечную петлю. Развита модель может обеспечить прогноз показателя спектра и потоков протонов у Земли. Разработан плзменный механизм излучения вспышечных петель {60}.

Г. Бахман, К. Пфлюг, А. Гофман {28} участвовали в большой комплексной работе (18 авторов) в рамках программы СЕРФ-ГСМ с 23 по 29 мая 1980 г. на основе магнитных карт, полученных в ЦИСЗФ (ГДР). По этим картам был произведен расчет поля в хромосфере и короне в потенциальном и бессиловом приближении (за 27 мая). Обращает на себя внимание смещение расчетных фокусов потенциального поля относительно некоторых крупных пятен. Сопоставление магнитограмм с тахограммами, полученными по $\text{H}\alpha$ в ИЗМИРАН, показало, что участки границы раздела направлений доплеровских скоростей лежат вблизи нейтральной линии, почти параллельно последней.

В работе Л. Дежё, Б. Калман, Л. Кондаш {62} (Венгрия) на основе большого материала исследовались три гомологические вспышки 5, 7 и 9 октября 1979 г., произошедшие в результате динамического взаимодействия старых и новых групп пятен. При

обработке использованы магнитограммы Иркутска и Маунт Вилсон, полученные в рамках ГСМ по обмену через МЦД. Рассмотрена морфология и кинематика групп пятен. Определены скорости узлов вспышек, достигающие до 10 км/с. Отмечен новый факт: в то время как ленты вспышек в целом движутся в направлении, перпендикулярном их длине, ряд индивидуальных узлов двигались вдоль волокон дуленточных вспышек.

В работе А. Ковач, И. Надь, Р. Буковинский {63} рассмотрена эволюция майского комплекса 1980 г. (SERF) на основе 256 фотогелиограмм в белом свете и 492 H α -снимков. Впервые измерены точные положения нейтрального волокна (H $_n$ =0) на протяжении всей эволюции группы. Согласно фотогелиограммам узел большой вспышки 28 мая совпал с тем местом лидера 21469, где 26 мая были отмечены первые признаки нового всплывающего магнитного потока.

Эруптивный протуберанец, тесно связанный с явлением коронального транзиента, наблюдался В. Рудзяком и Б. Вршняком {64} (обсерватория Хвар, Югославия) 18 августа 1980 г. Оценены скорости подъема, составившие от 20 км/с до 140 км/с на поздней стадии. Стадия резкого ускорения протуберанца началась спустя один час с начала медленного подъема. Ускорение составило 0.6 - 0.8g \odot . Интересно, что 20 августа, т.е. спустя 2 суток, над той же самой нейтральной линией магнитного поля образовалось новое волокно (на диске). Даны оценки энергии эрупции. Масса M \approx 3 \cdot 10¹⁵ г. При средней скорости подъема 50 км/с это дает E(кинетическую) \approx 4 \cdot 10²⁸ эрг. Наивысшая скорость эрупции соответствует сдерживающему магнитному полю ~20-30 Гс.

Б. Ромпольшом, Н. Шили, Л. Гаузе и др. подтверждается тесная связь протуберанцев с корональными транзиентами и ударными волнами в межпланетном пространстве. Ф. Крюгером {65} совместно с сотрудниками ИЗМИРАН проводилась количественная диагностика протонных вспышек в 1979 г. Проанализировано 16 вспышек, 6 из которых представляли собой "восточные" события. Возрастания потока протонов в этих событиях не наблюдалось, что свидетельствует о сильном гелиодолготном ослаблении частиц. Необычные вспышки наблюдались во второй половине августа 1979 г.

Диагностика на основе радиоизлучения указывает на протонность этих событий. Однако расчетные характеристики существенно отличаются от наблюдаемых. Это можно объяснить наличием на диске на большом долготном расстоянии ($\ell \sim 70^\circ$) двух областей Mc Math 16224 и 239, связанных общим магнитным полем, в котором имел место захват и существенное перераспределение протонов.

В работе X Аурацца, А. Бёме и А. Крюгера {66} анализировались шумовые бури, S-компонента и радиовсплески за 22-29 мая 1980 г. Характерной чертой шумовых бурь, связанных с майским комплексом была относительно высокая интенсивность в сантиметровом диапазоне. Такое поведение спектра типично для групп без протонных вспышек. Ими составлен также список всплесков IV типа за весь период ГСМ (всего 27 событий). Приведена информация о круговой поляризации на избранных частотах.

В работе Г. Бромбоша, Е. Якимец и др. (Польша), Обридко В. (СССР), Ф. Фюрстенберг и др. (ГДР) {67} дана рабочая модель солнечных пятен на разных высотах по данным рентгеновского УФ и радиодиапазонов. Она подытожила результаты дискуссии во Вроцлаве (1979 г.) по теме "Вроцлавская рабочая модель" большого пятна. Кроме модели пятна приводится также модель факела, его окружения и невозмущенной фотосферы. Указанная модель объясняет ряд новых фактов, полученных в ходе ГСМ. Среди них:

1. Напряженность магнитного поля ~ 1300 Гс при $T \sim 10^5$ (C IV линия, по наблюдениям UVSP на борту SMM) и поле 600-900 Гс при $T \sim 10^6$ К (VLA на 6 см, Лэнг К.Р.). Указанная "Вроцлавская модель пятна" непосредственно применима для расчетов S-компоненты радиоизлучения.

В июле 1982 г. был проведен советско-американский эксперимент по инициативе Гельфрейха (СССР) и Ланга (США), целью которого являлась исследование одних и тех же активных областей.

Таким образом, в настоящее время мы знаем, что реализация энергии происходит в петельных системах, выясняется роль комплекса А0. Однако нам совершенно неизвестен механизм накопления энергии, хотя процесс накопления массы известен. В США планируется в 22. цикле солнечной активности исследование про-

цессов в короне. Рентгеновский телескоп будет иметь разрешение $0''2$.

Л и т е р а т у р а

- {1} NASA, "The Pinhole/Occluder Facility", 1983
- {2} Kundu, M.R., Gergely, T.E., Kane, S.R., Positional characteristics of meter-decameter wavelength bursts associated with hard X-ray bursts *Solar Phys.*, 79, 107, 1982
- {3} Neupert, W.M., Comparison of solar X-ray line emission with microwave emission during flares, *Ap.J.*, 153, L59, 1968
- {4} Acton, L.W., Canfield, R.C., Gunkler, T.A., Hudson, H.S., Kiplinger, A.L., Leibacher, J.W., Chromospheric evaporation in a well-observed compact flare, *Ap.J.*, 263, 409, 1982
- {5} Feldman, W.C., Asbridge, J.R., Bame, S.I., Fenimore, E.E., Gosling, J.T., The solar origins of solar wind interstream flows: Near-equatorial coronal streamers, *JGR A*, 86, 5408, 1981
- {6} Antonucci, E., Gabriel, A.H., Acton, L.W., Culhane, J.L., Doyle, J.G., Leibacher, J.W., Machado, M.E., Orwig, L.E., Rapley, C.G., Impulsive phase of flares in soft X-ray emission, *Solar Phys.*, 78, 107, 1982
- {7} Hundhausen, A.J., *Coronal expansion and solar wind*, Springer-Verlag, Heidelberg, 1972
- {8} Gardner, B.M., Forrest, D.J., Zolcinski, M.C., Chupp, E.L., Rieger, E., Reppin, C., Kanbach, G., Share, G., A comparison of gamma ray line and X-ray bremsstrahlung time profiles in several flares, *Bull.AAS*, 13, 903, 1981
- {9} Альберн, Ф., Ведрен, Ж., Камбу, Ф., Кудрявцев, М.И., Ликин, О.Б., Мелиоранский, А.С., Назарова, Н.И., Панков, В.М., Писаренко, Н.Ф., Савенко, И.А., Талон, Р., Шамолин, В.М., Всплески гамма-излучения, наблюдавшиеся во время солнечных вспышек 2, 4 и 7 августа 1972 г. на станции "Прогноз-2", сб. *Проблемы солнечной активности и космическая система "Прогноз"*, с.30, Изд."Наука", Москва, 1977
- {10} Bai, T., Second-phase acceleration versus second-step acceleration in solar flares, in *Gamma ray transients and related astrophysical phenomena*, Proc. La Jolla Workshop 1981, (eds. Lingenfelter, R.E. et al.) *Amer. Inst. of Phys. Conf. Proc. No.77*, 1982
- {11} Gubchenko, V.M., Zaitsev, V.V., On proton and electron acceleration by shock waves during large solar flares, *Solar Phys.*, 63, 337, 1979
- {12} Kane, S.R., Raoult, A., Downward shift of the acceleration/injection region during solar flares, *Ap.J.*, 248, L77, 1981
- {13} Kane, S.R., Fenimore, E.E., Klebesadel, R.W., Laros, J.G., Spatial structure of ≥ 100 keV X-ray sources in solar flares, *Ap.J.* 254, L53, 1982
- {15} Švestka, Z., Stewart, R.T., Hoyng, P., Van Tend, W., Acton, L.W., Gabriel, A.H., Rapley, C.G., Boelee, A., Bruner, E.C., de Jager, C., Lafleur, H. Nelson, G., Simnett, G.M., Van Beek, H.F., Wagner, W.J., Observations of a post-flare radio-burst in X-rays, *Solar Phys.*, 75, 305, 1982

- {16} MacQueen, R.M., Coronal transients: a summary, *Phil. Trans. R. Soc. London*, A 297, 605, 1980
- {17} Wagner, W.J., Hildner, E., House, L.L., Sawyer, C., Sheridan, K.V., Dulk, G.A. Radio and visible light observations of matter ejected from the Sun, *Ap. J.* 244, L123, 1981
- {18} Alikaeva, K.V., Ghandga, S.I., Kondrashova, N.N., Polupan, P.N., Reduk, T.I. About variations in Fraunhofer lines related to flare activity (in Russ.) *IСM-SMY Crimean Workshop*, 2, 53, 1981
- {19} Kasinsky, V.V., in *Solar-Terrestrial Predictions Proceedings*, 3, 94, 1981
- {20} Nefed'ev, V.P., On the possibility to estimate physical conditions in the current sheet region during the development of a chromospheric flare, (in Russ.) *Письма в АЖ*, 5, 96, 1979
- {21} Kobrin, M.M., Korshunov, A.I., Arbutov, S.I., Pakhomov, V.V., Fridman, V.M., Tikhomirov, Yu.V., Manifestation of pulsation instability in solar radio emission preceding proton flares, *Solar Phys.*, 56, 359, 1978
- {22} Bystrov, M.V., Kobrin, M.M., Snegirev, S.D., Pulsations of the Earth magnetic field before solar proton flares (in Russ.) *Письма в АЖ*, 4, 143, 1978
- {23} Быстров, М.В., Кобрин, М.М., Снегирев, С.Д., Квазипериодические пульсации магнитного поля Земли с периодами 20-200 мин и их связь с аналогичными пульсациями в радиоизлучении Солнца перед протонными вспышками, *Геомагн. и аэрон.* 19, 306, 1979
- {24} Severny, A.B. et al., in *Solar-Terrestrial Predictions Proceedings*, 1, 72, 1979
- {25} Burov, V.A. et al., in *Solar-Terrestrial Predictions Proceedings*, 2, 209, 1980
- {26} Авдюшин, С.И., Бернштейн, П.Б., Вайнберг, Ю.Р., Краткосрочный прогноз протонных вспышек в активной области, *Докл. АН СССР*, 254, 1380, 1980
- {27} Ogir, M.B., Intercorrelation between active solar regions according to H α observations on may 25, 28 and 29, 1980 (in Russ.) *IСM-SMY Crimean Workshop*, 2, 197, 1981
- {28} Ioshpa, B.A., Ishkov, V.N., Mogilevsky, E.I., Nikolskaya, K.I., Starkova, L.I. Utrobin, V.G., Bulavina, V.I., Delone, A.B., Kiryuchina, A.I., Makarova, E.A., Mitropolskaya, O.N., Yakunina, G.V., Korobova, Z.B., Stepanyan, N.N., Koval, A.N., Bachmann, H., Pflug, K., Hoffmann, A., The evolution of the complex of the active regions HR 16862-16864 in may 1980, *IСM-SMY Crimean Workshop*, 2, 134, 1981
- {29} Golovko, A.A., Kasinsky, V.V., Klochek, N.V., Magnetic fields and general space and time characteristics of the evolution and flare activity in the 21-29 may complex, *IСM-SMY Crimean Workshop*, 2, 170, 1981
- {30} Ishkov, V.N., Obashev, S.O., Chromospheric observations of the flare event on october 6, 1979, *IСM-SMY Crimean Workshop*, 2, 85, 1981
- {31} Shilova, N.S., Babin, A.N., Delone, A.B., Kiryuchina, A.I., Makarova, E.A., Yakunina, G.V., Mamedov, S.G., Musaev, M.M., Orudjev, A.Sh., Seidov, A.G. H α umbral flares of the end of may 1980, (in Russ.), *IСM-SMY Crimean Workshop*, 2, 180, 1981

- {32} Mogilevsky, E.I., Homologous $H\alpha$ -flares in the umbra of AR complex MM-16862-3 in may 1980, (in Russ.) *ГСМ-СМУ Crimean Workshop*, 2, 151, 1981
- {33} Patterson, A., Zirin, H., Transient magnetic field changes in flares, *Ap.J.* 243, L99, 1981
- {34} Lozitskaya, N.I., Lozitskiy, V.G., Do "magnetic transients" in solar flares exist? (in Russ.), *Письма в АЖ*, 8, 500, 1982
- {35} Stepanov, V.E., Ermakova, L.V., Merkulenko, V.E., Palamarchuk, L.E., Polyakov, V.I., Klochek, N.V., Motion in flare knots and magnetic fields in the 6 october 1979 flare, (in Russ.), *Исслед. СибИЗМИР*, 56, 98, 1981
- {36} Oks, E.A., On the method of investigation of the mechanism of solar flares by hydrogen spectral lines, (in Russ.), *Письма в АЖ*, 4, 415, 1978
- {37} Banin, V.G., Maksimov, V.P., Tomozov, V.M., On diagnostics of flare plasma from Stark effect in turbulent fields, (in Russ.), *Исслед. СибИЗМИР*, 45, 54, 1979
- {38} Koval, A.N., Oks, E.A., Some results of the searching of low-frequency plasma turbulence in large chromospheric flares, (in Russ.) *Изв. КрАО*, 67, 90, 1983
- {39} Babin, A.N., Koval, A.N., Investigation of the linear polarization of some solar emission features, (in Russ.), *Изв. КрАО*, 66, 89, 1983
- {40} Baranovsky, E.A., Balmer lines in solar flares, (in Russ.), *Изв. КрАО*, 67, 84, 1983
- {41} Kurochka, L.N., Telnjuk-Adamchuk, V.V., Calculation of line profiles of inhomogeneous solar formations, *Solar Phys.*, 59, 11, 1978
- {42} Kurochka, L.N., Rossada, V.M., The energy of optical solar flares radiation, III, (in Russ.), *Солн. Данн.*, 1981, 7, 95
- {43} Akhmedov, Sh.B., Bogod, V.M., Gelfreikh, G.B., The results of the study of the local source of solar active region Mac Math 159740 on SМУ program using RATAN-600, (in Russ.), *ГСМ-СМУ Crimean Workshop*, 2, 45, 1981
- {44} Kundu, M.R., Solar flare observations at centimeter wavelengths using the VLA, *ГСМ-СМУ Crimean Workshop*, 1, 24, 1981
- {45} Gnezdilov, A.A., Kovalev, V.A., Markeev, A.K., Fomichev, V.V., Chernov, G.P., Chertok, I.M., The peculiarities of an energy release in the large flares by radio bursts data during august-november 1979, (in Russ.), *ГСМ-СМУ Crimean Workshop*, 2, 59, 1981
- {46} Ishkov, V.N., Kovalev, V.A., Mogilevsky, E.I., Plotnikov, V.M., Chernov, G.P., The complex analysis of solar flare on august 20, 1979. (in Russ.), *ГСМ-СМУ Crimean Workshop*, 2, 72, 1981
- {47} Borovik, V.N., Gelfreikh, G.B., High-resolution microwave observations of solar flare on march 29, 1980 accompanied by strong X-ray and γ -ray emission, (in Russ.), *ГСМ-СМУ Crimean Workshop*, 2, 108, 1981

- {48} Boldyrev, S.I., Peterova, N.G., The local source of the active region No.2469 observed with the large Pulkovo radiotelescope (may-june 1980), (in Russ.), *ГСМ-SMY Crimean Workshop*, 2, 127, 1981
- {49} Kobrin, M.M., Korshunov, A.I., Kaverin, N.S., Tikhomirov, Yu.V., Shushunov V.V., Losovsky, B.Ya., Aurass, H., Hildebrandt, J., Krüger, A., Investigation of the fine structure of the spectrum of the S-component for revealing current sheets and pre-flare processes in solar active regions, *Phys. Solariterr.* 16, 173, 1981
- {50} Somov, B.V., Magnetic reconnection and energetics of a solar flare, (in Russ.), *ГСМ-SMY Crimean Workshop*, 1, 155, 1981
- {51} Brushlinskii, K.V., Bulanov, S.V., Dogiel, V.A., Zaborov, A.M., Podgornii, A.I., Frank, A.G., Theoretical investigation, laboratory experiments and numerical simulation of the physical processes that are the basis of the solar flares, (in Russ.), *ГСМ-SMY Crimean Workshop*, 1, 177, 1981
- {52} Maksimov, V.P., Tomozov, V.M., On possible manifestations of the turbulent Stark effect in different flare models, (in Russ.) *ГСМ-SMY Crimean Workshop*, 1, 168, 1981
- {53} Oks, E.A., Spectroscopy of plasma with oscillating electric fields and their diagnostics in solar flares, (in Russ.), *ГСМ-SMY Crimean Workshop*, 1, 200, 1981
- {54} Pustil'nik, L.A., On the energetics of the current sheet of a flare, (in Russ.), *Астрон.Ж.*, 57, 601, 1980
- {55} Буланов, С.В., Сасоров, П.В., Сыроватский, С.И., Магнитное пересоединение и ускорение частиц, *11-й Ленингр. семинар по космофиз.*, 83, 1979
- {56} Bulanov, S.V., On energetic spectrum of particles accelerated near singular line of magnetic field (in Russ.) *Письма в АЖ*, 6, 372, 1980
- {57} Kocharov, G.E., Kocharov, L.G., Charikov, Yu.E., On ways of further investigation of solar flares enriched by the helium-3 (in Russ.) *Физ.-техн. ин-т АН СССР (Препр.)*, 680, 17, 1980
- {58} Кочаров, Л.Г., *Труды 17-го симпозиума по космическим лучам*, 190, 1980
- {59} Зайцев, В.В., Степанов, А.В., Чернов, Г.П., *Препринт СибИЗМИР*, 12, 1983
- {60} Зайцев, В.В., Степанов, А.В., *Препринт СибИЗМИР*, 5, 1982
- {62} Dezső, L., Kálmán, B., Kondás, L., Two-ribbon flares, observed in the period 5-9 october 1979, *ГСМ-SMY Crimean Workshop*, 2, 97, 1981
- {63} Kovács, Á., Nagy, I., Bukovinszki, R., A note on the activity in the SESC region 2470, *ГСМ-SMY Crimean Workshop*, 2, 232, 1981
- {64} Ruždjak, V., Vršnak, B., The eruptive prominence of august 18, 1980 *ГСМ-SMY Crimean Workshop*, 2, 256, 1981
- {65} Akinyan, S.T., Chertok, I.M., Krüger, A., Results of quantitative diagnosis of proton flares by radio bursts for SMY period, *ГСМ-SMY*, 2, 11
- {66} Aurass, H., Böhme, A., Krüger, A., Analyses of noise storm fluctuations, S-component, and radio bursts during the period may 22-29, 1980 and further events during the SMY, *ГСМ-SMY Crimean Workshop*, 2, 215

- {67} Bromboszcz,G.,Jakimiec,J.,Siarkowski,M.,Sylwester,B.,Sylwester,J.,
Obridko,V.N.,Fürstenberg,F.,Hildebrandt,J.,Krüger,A.,Staude,J.,
Outline of a working model of sunspot structure at different
height levels from observations in the X-, EUV-, optical and
radio ranges, *ICM-SMY Crimean Workshop*,1. 224, 1981

PROPER MOTIONS OBSERVED IN ACTIVE REGIONS

V. B U M B A

Astron. Inst., Ondřejov

Abstract:

We summarize our results obtained from the observations of proper motions visible during the growth of local magnetic fields of active regions and during the formation and further development of their sunspot groups. We not only stress that this process is a part of the dynamics of the solar background field evolution, but we also examine separately the motions and shape changes observable during the whole active region's field life-time, as well as several types of motions and form changes during the interactions and collisions of sunspots both between themselves as well as with the photosphere. The low efficiency of magnetic forces during the studied processes and, in contrast, the importance of hydrodynamic forces is demonstrated. The feedback action of the moving photosphere on the shape of magnetic field distribution and on the sunspot forms is shown too. Problems of physical interpretation of the data presented are discussed. The importance of further observations, in the first place of the velocity fields, is underlined.

СОБСТВЕННЫЕ ДВИЖЕНИЯ НАБЛЮДАЕМЫЕ В АКТИВНЫХ ОБЛАСТЯХ

В. БУМБА

Астрон. Инст., Ондřejов

Абстракт:

Резюмируются результаты полученные из наблюдений собственных движений, видимых как в течение роста локальных магнитных полей активных областей, так и в течение формирования и дальнейшего развития их групп солнечных пятен. Подчеркивается не только тот факт, что эти процессы являются составляющей частью динамики развития солнечных фоновых полей. Отдельно рассматриваются движения и изменения формы, видимые в течение всей жизни магнитного поля активной области, равно как и несколько типов движений и изменений формы в процессе взаимодействий и столкновений солнечных пятен как между собой, так и с фотосферой. Демонстрируется как малая эффективность магнитных сил в течение изучаемых процессов, так и, наоборот, большое значение гидродинамических сил для этих процессов. Показывается обратное влияние движущейся фотосферы на формы распределения локального магнитного поля и на формы солнечных пятен. Дискутируются проблемы связанные с интерпретацией представленных данных. Обращается внимание на необходимость получения дальнейших наблюдательных данных, касающихся прежде всего полей скоростей в активных областях.

1. Introduction

The importance of knowledge about the distribution of motions in an active region for understanding its magnetic field and activity development is obvious {2},{36},{37},{35}. In this paper we should like to summarize our results concerning the observations of proper motions visible during the growth of active region's magnetic field and during the formation and further development of its group of sunspots; the main reasons are still very rare observational data concerning the radial motions in active regions. This summary should be used as one of the first steps for future, more general study of the role of motions and their physical consequences for the process of a local magnetic field evolution.

At the beginning of this paper I would once again like to stress that the development of an individual local magnetic field or of an active region is, in the frame of the solar background magnetic field, a global quality of the entire system of solar magnetic fields {17},{27},{28},{11},{12},{14},{15}. This must be true in the case of the velocity fields too, and the more so since the process of the new magnetic flux formation is bound to the evolutionary dynamics of the gulfs formed from the curved boundaries of the background magnetic field sector structure influenced by differential rotation {11},{12},{14},{15}, simultaneously it is carried out by the whole hierarchy of the convective elements {7},{8},{9},{13},{1}. The actual situation in an active region development depends at the same time, of course, on the stage of the complex activity development in which it occurs. The evolutionary phase of this complex of activity is closely related to the situation in the mutual interaction of magnetic active longitudes, and their evolutionary stages {19},{31},{30},{10},{17}.

If we now want to study the observable proper motions accompanying the local magnetic field development, we have not only to follow the displacements and form changes of all the local systems of magnetic fields on our magnetic maps, but also the shifts and form transformations of individual sunspots

of various types - the local concentrations of field lines of the system - on our photographs of active region's sunspot groups. We have also to consider the feedback action of the solar atmosphere moving or flowing around the active region as a whole as well as around its individual sunspots and the mutual interaction of the growing local field with the convective, mostly supergranular network.

2. Motions and shape changes observed during a local magnetic field development

During the formation of a new active region's magnetic field several types of forces play different roles. The fact that the newly developed field pattern follows the outlines of the preexisting supergranular network indicates the simultaneous influence of convection on the process (Fig.1){20},{11},{26},{27},{28}. In the course of the very fast, first evolutionary stage of the active region's field formation it seems that the magnetic forces become dominant in the process, although their subordination to the convective network remains - the progression of the growing field is guided by the inter-supergranular space. Unfortunately, only few observations indicating large and fast changing radial motions, visible during this phase of local field evolution above all in the magnetically singular "center of activity", are to be found scattered in the literature {44},{42},{41}. When the continuous mutual interaction of the growing magnetic field, with the convective network cells, displayed through the dynamics of individual cell growth and forming transformations in which parts of cell peripheries of a higher scale order change their forms due to the disappearance of the old and appearance of the new convective elements of a lower scale order {18},{5},{6}, the shifted front of magnetic field boundary reaches them, showing the mutual interdependence of both factors, namely of the magnetic field and convection. The close interrelation of both factors is also supported by the "quantization" of magnetic fluxes and distances in sunspot groups given by the sizes of convective elements of different scale orders {4},{29},{32}(Fig.2).

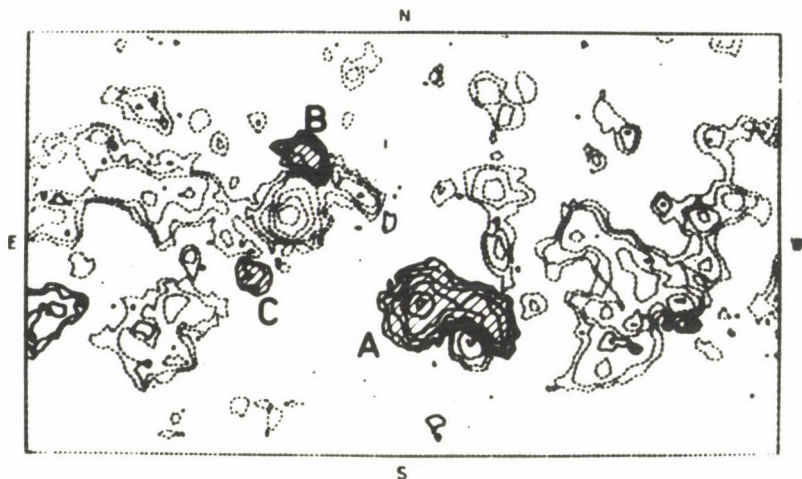


Fig.1. The Ondrejov Observatory magnetic map from 23 May, 1979 (7:15 to 9:30 UT) demonstrating the formation of a new positive polarity, indicated by A and B and C, (full lines) in an old negative polarity supergranular network.

Fig.2. Examples of drawings of sunspot dimensional types with indicated intervals of diameter values. The most frequent sizes are those with the unshortened diameter of the whole spot (umbra plus penumbra) of around 20000 km, 27000 km, 36000 km, 46000 km and 57000 km. The composition of greater spots from smaller types can often be observed.

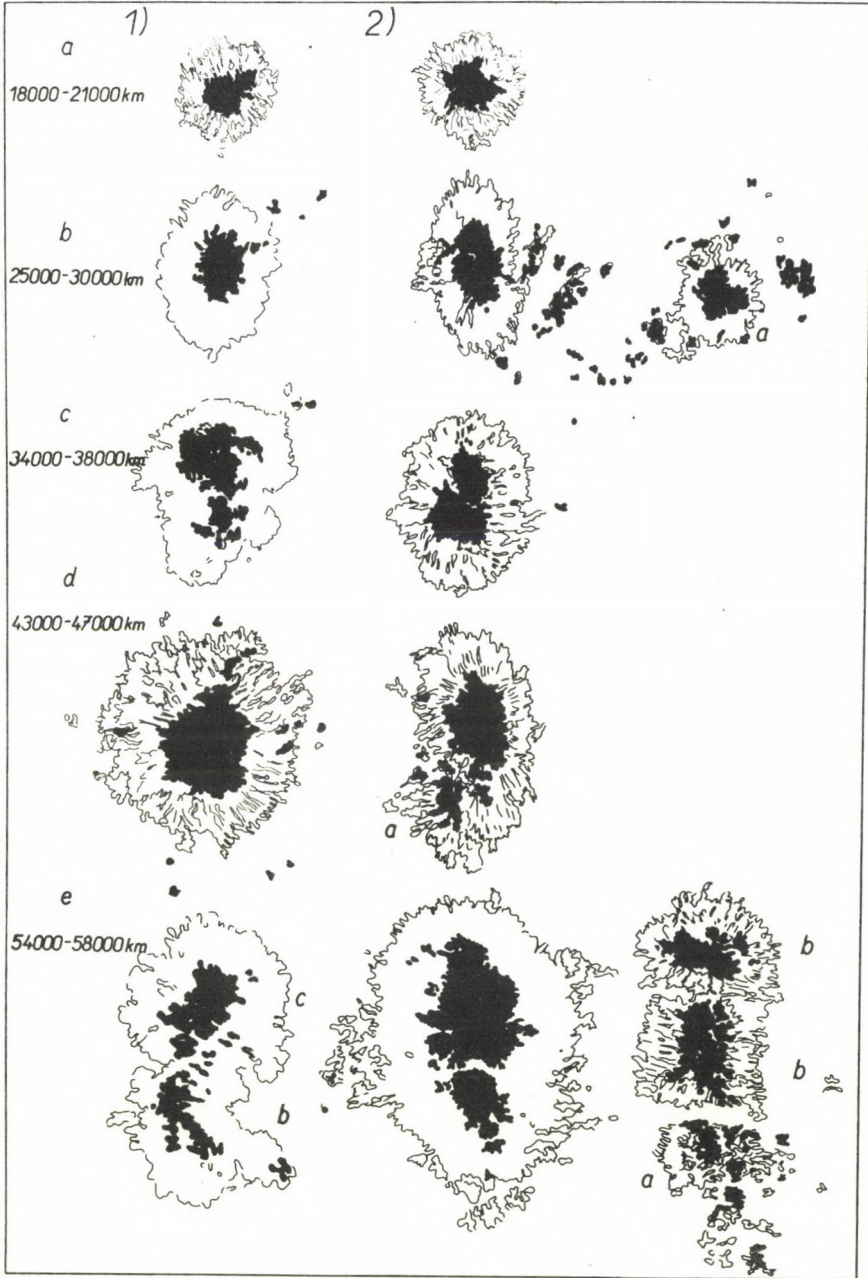


Fig.2.

During all phases of a local magnetic field development, i.e. also during its disintegration, we may observe a constant increase in the area occupied by the field as well as a continuous shift in its boundary at a constant velocity of about 50 m/sec in the photosphere (Fig.3){19},{20},{14} and of about 100 m/sec in the chromosphere, if observed in ionized Calcium line K, and about 200 m/sec in the Hydrogen line H α {19},{20},{14}. It goes without saying that in the chromosphere it is difficult to follow this boundary motion during the postmaximum evolutionary stage of the active region. This displacement of the magnetic field boundary indicating enlargement of space influenced by its magnetic field lines shows some characteristics of wave front propagation.

Another mode of magnetic field motions is represented by the morphological changes of the entire form of the active region's field during its development. Very often, at the beginning of a local magnetic field formation we observe its triangular form - two triangles are in close contact with their peaks - caused by the appearance and action of a "magnetic center" (Fig.4){11},{26},{24}. This triangular form of an active region's new magnetic field pattern is usually repeated in the chromospheric emission distribution {20}. Beginning with their development these two triangles are continuously transformed into two halves of an ellipse in such a way that the elliptical form of the whole active region is reached during the field's maximum stage of evolution. After that we observe the development of long field branches seeping out from this ellipse, at the ends of which, when they meet, a new secondary active region is often formed {27},{28},{29}. This transformation of the triangular into the elliptical shape seems to be related to the spiralling of both leading and following spots in the group during their premaximum stages in opposite directions {23},{24}, as will be mentioned later. The influence of supergranular patterns in the field distribution, especially during the long branches formation, is still easily observable.

If we investigate the shapes of local magnetic field dis-

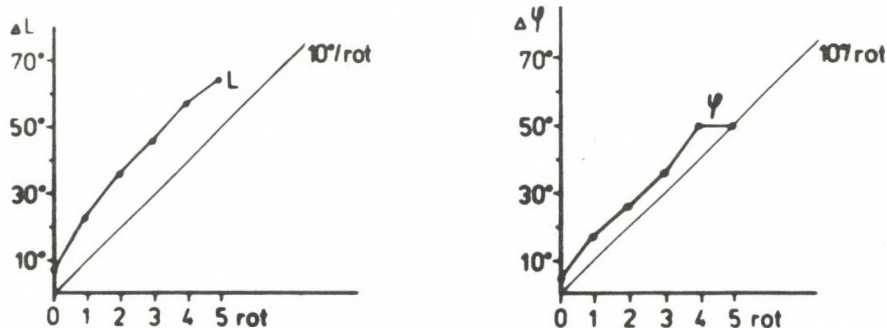


Fig. 3. The growth of the area of the active region's (McMath No 13736) magnetic field in heliogr.long L (to the left) and in heliogr.lat. φ (to the right).

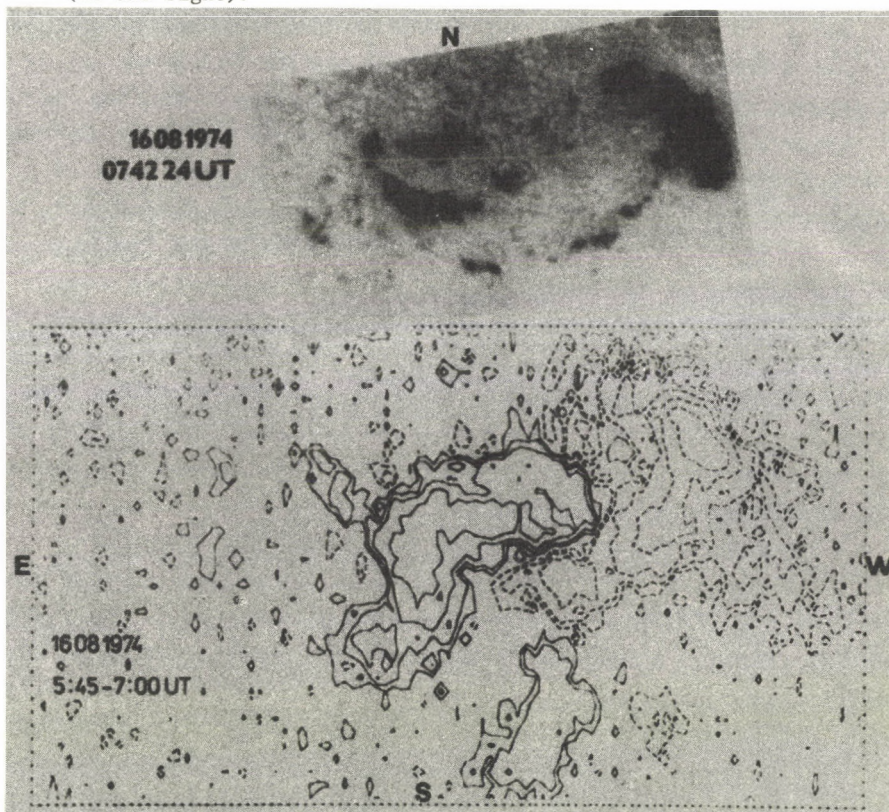


Fig. 4. Ondřejov Obs. photoelectric magnetic map of an August 1974 (CMP 14.6; $\varphi = 9.5^\circ$) active rgn., compared with an Ondřejov photograph of the same sunspot group, taken on the same day (7:42:24 UT). The linear scales of both pictures are the same. Two triangles of opposite polarity magnetic fields are in close contact forming a "magnetic center".

tribution carefully in their leading as well as following parts during its individual evolutionary stages, we may find the retro-influence of the moving photosphere flowing round it. Since in its second stage we see the action of the differential rotation determining its shape, we notice the first indications of an arrowhead form in both the leading as well as in the following portions, the extension and opening of which seems to depend on heliographic latitude. The observations demonstrating that the patterns of the following field differ slightly from those of the leading field, as though this difference were caused by the fact that the following field occurs in the "wake" of the leading field, indicate the possible influence of dynamic forces in the photosphere {14},{15},{16}. Similar results of dynamic forces action are observed during the fast motion of newly formed sunspots through the granular field, as will be mentioned later in more detail {22}. These forces probably act as a result of the solar material streaming round the obstacle of the system of the local magnetic field and active region's plasma re-influencing the system. The process may be caused by different depths of individual fields and their concentrations, above all by a deeper rooted field of the leading spot. The role of these dynamic forces and of differential rotation seems to increase slightly with the ageing of active regions and with the shallowing of their magnetic fields.

3. Motions observed during the sunspot formations

The process of the formation of a prot umbra of the main leading and following spots in the group of several "quantized" nuclei having a diameter of about 3"-5", recognizable in the umbra during practically the whole life-time of the spot, is very characteristic {34},{23},{24},{25},{41},{43}. The nuclei of what is practically the same area join to form the proto-umbra (Fig.5). During this process of joining, they move vortically in the leading portion in studied groups in the counterclockwise direction (Figs.6 and 7). The number of individual joining nuclei varies from a few to several. In one case, in which the penumbra did not develop at all {23}, we had only

one nucleus and some rudimentary spots or pores, in another case {24}, there were six or seven nuclei. In all cases the nuclei rotated in the leading part counterclockwise round the main one, which became the darkest one with the highest field intensity value, wrapping or slipping round it {23},{24},{25}. The process looks as if the impacts of individual more shallow nuclei coming from the "magnetic center" and joining the main darkest and deepest nucleus carry along impulses and deliver them to the whole system of nuclei to cause its vortical motion round the main nucleus. Action of the Coriolis force has also to be considered. The idea of impulses transfer is supported by observation of later change of the rotational direction of the main leading spot and of the direction of pieces of umbra outflowing from it into the opposite one - which means clockwise. This situation was observed during the post-maximum stage of the group development {25}.

The rotational motions observed during the formation of both leading and following main spots act in our observational material in opposite directions: counterclockwise in the leader and clockwise in the follower (Figs.5 and 7). In this way, the developed spiral forms of small spots and nuclei distribution probably lead to the successive transformation of active region's field shape from its early triangular to the later elliptical form - as already mentioned.

The well-known divergence of the leading and following spots during the first evolutionary stages of the group development {44} and later reduction of their distance as well as other observed regularities in sunspot proper motions {3} have also to be taken into account during attempts to interpret the observed proper spot motions. The changes in spot configuration in the group under the influence of large-scale photospheric streams visible, for example, as a distortion of their originally elliptical distribution into flattened irregular features {29} have to be considered too (Fig.8).

During the process of penumbra formation no real proper motions of penumbral details seem to be observed. Instead of

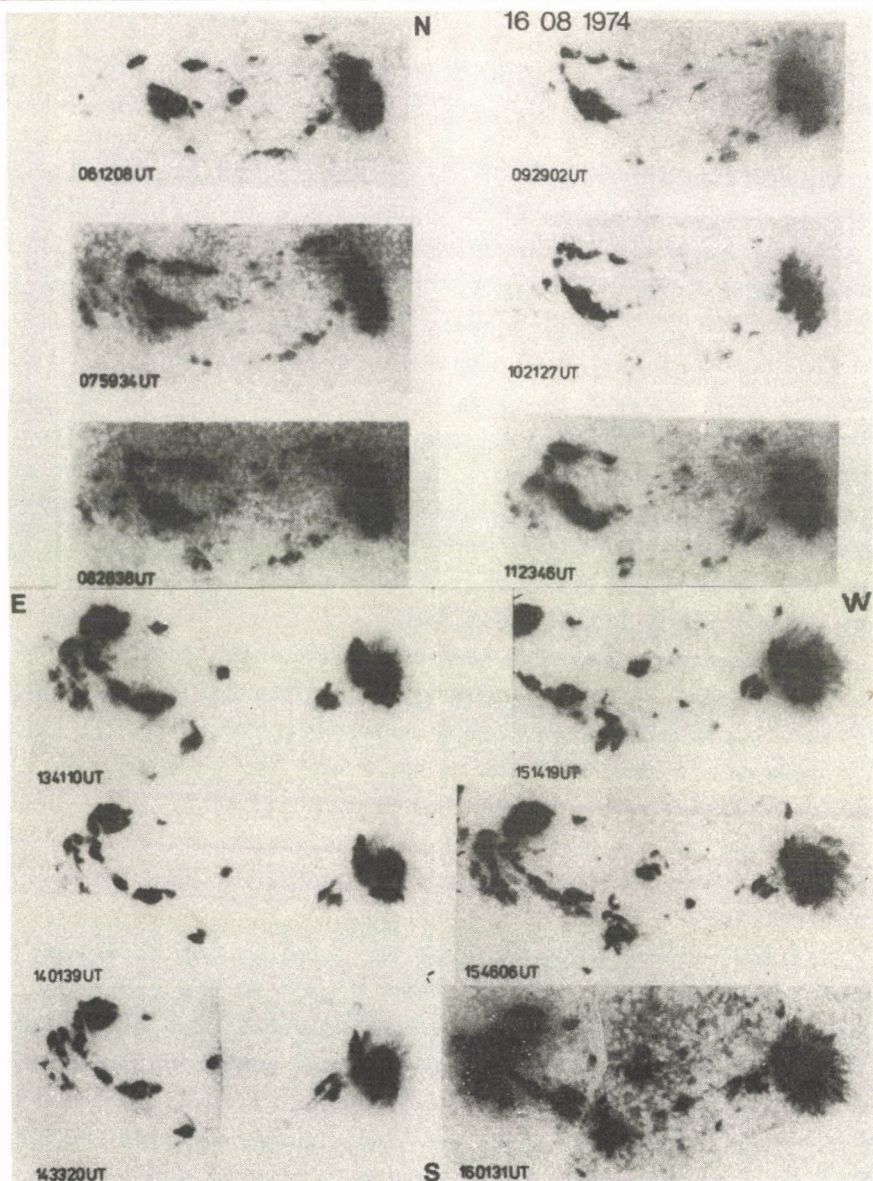


Fig. 5. A series of photographs of the same sunspot group as in Fig. 4 obtained during August 16 and 17, 1974. The umbral nuclei join to form the protumbra and they move vortically in both portions of the group: in the leading portion in the counterclockwise direction and clockwise in the following portion. The process of gradual penumbra formation may be followed as well as the characteristic mode of small spots and pores development and motion.

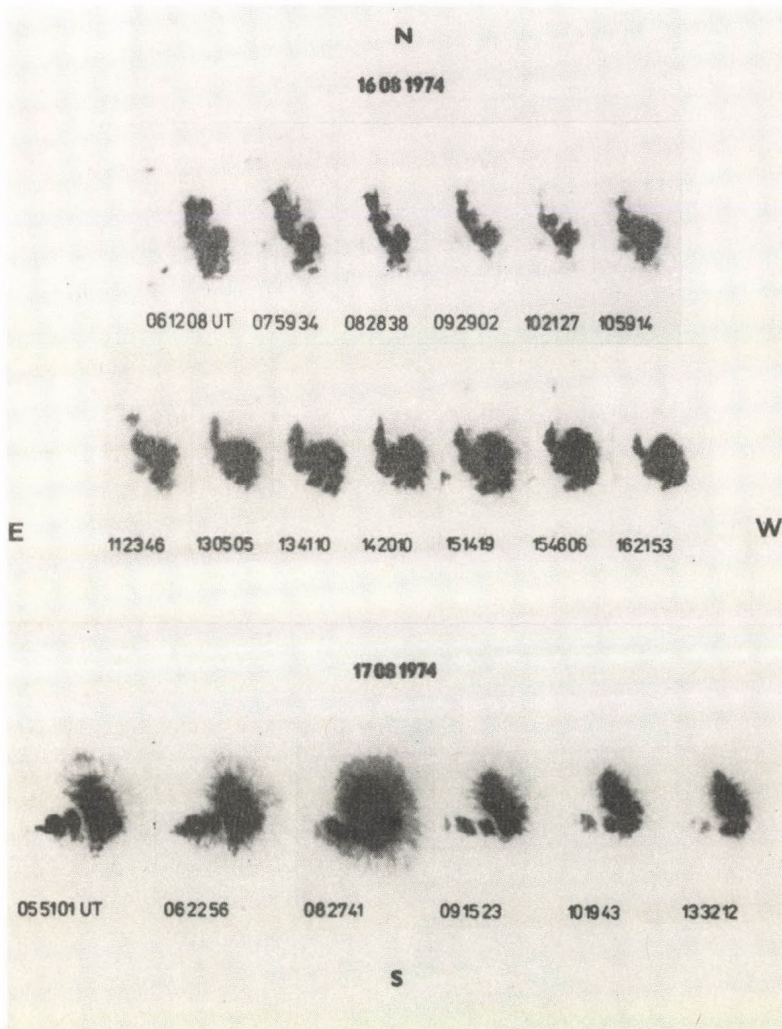


Fig. 6. A series of photographs of the leading spot of the same sunspot group as in Fig.4 and 5 during August 16 and 17, 1974. The formation of the proto-umbra and its rotation may clearly be seen.

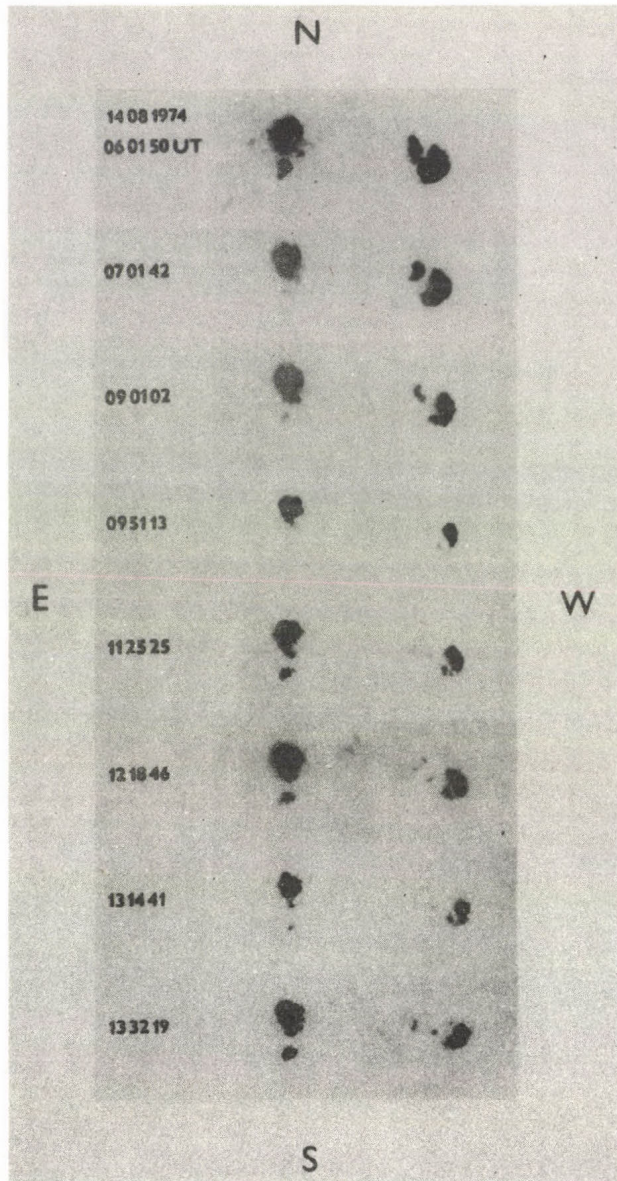


Fig. 7. A series of photographs of a small sunspot group from August 1974 ($L = 357^\circ, \phi = -11^\circ$). The rotation of the leading spot as well as the process of its desintegration may be followed. The "point of instability" in its southern corner is also visible.

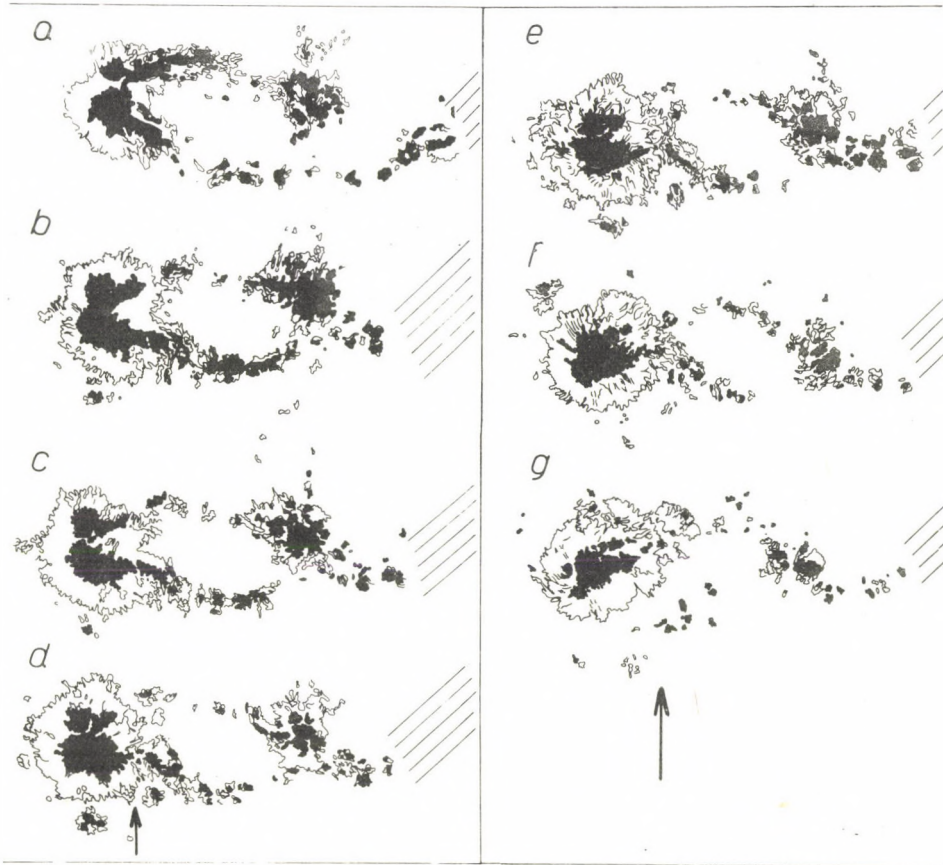


Fig. 8. Relative motions of spot nuclei in large sunspot group from June 1963. The elliptical feature is probably influenced by some large-scale photospheric organized motion acting on its SW region (see the arrow).

them we see a slow, continuous reorganization of area of granular field around the main spot protoumbra in strong dependence on the magnetic field topology taking place gradually around the umbra in its parts surrounded by opposite polarity (Figs.5 and 4). The process may stop or be reversed for a while and then continue again. As a basic step which may run in both directions we observe the formation of a row of bright photospheric granules which is transformed into a bright penumbral fibril, separated from other fibrils by aligned intergranular space, or, vice-versa, we may observe disintegration of this row into a field of irregularly distributed photospheric granules {4},{24},{25}.

The disappearance of sunspots seems to be characterized by two modes of the process {23},{24},{25}. One is usually connected with very small pores or pieces of dark elongated and curved intergranular material which often escapes in the form of a narrow rope from the disintegrating spot in a "Point of instability" at the spot's rim (Fig.7). It is represented mainly by migration and the increase of distances between the individual dark knots of the rope, i.e. by the divergence of dark material and the loss of contrast of its individual dark knots. The second one seems to have the form of an invasion of bright granular grains into the dark, more stable remnants of the umbra - this time already without penumbra. The possible reversal of the process sometimes visible as the evacuation or repeated reduction of contrast of the new invading granular grains at the periphery of the rest of spot seems to be quite remarkable. Both modes of spot disintegration may act on the same spot. The transformation of strips of the photosphere into the spot light-bridges and vice-versa has already been described several times {22}.

4. Motions in colliding sunspot groups

Another type of proper motions of sunspots has recently been investigated: {22},{14}. We studied the influence of collisions of large magnetic systems formed from parts of large active regions (August 1972 and June-July 1974 proton-flare

regions), including several field line concentrations in the form of large sunspot umbrae. The result of this research seems to be highly interesting: during this collision of large magnetic blocks we do not observe the consequences of interaction of large magnetic forces, but rather the dynamic or hydrodynamic effects caused by magnetically almost neutral sunspot systems floating in the photosphere. It looks as though the striking blocks or spot systems had a certain degree of elasticity and also during the motion of kinetic energy and inertia much greater than the magnetic forces. The colliding systems temporarily join together to produce very complicated structures, but as soon as the dynamic forces causing their interaction disappear, the complicated magnetic patterns quickly disintegrate again.

In the case of sunspots of the same polarity impacting the striking spot, if large enough, may not only press several other spots together, create several light-bridges in between their umbrae, but it is also able to push forward several smaller spots in front of itself, change the amount and direction of motion of another spot, flatten itself if it hits an obstacle, etc. In the case of a collision of spots of unlike polarities we observed a tangential collision resulting in the inclination and stretching of magnetic lines of force interconnecting the striking umbrae visible as penumbral fibrils of the penumbra-like light-bridge closed in between them. During the direct collisions both countermoving spots stop each other or the pushing spot slides around the obstacle. One exceptional strike seems to result in "magnetic annihilation" of colliding umbrae of opposite polarities - both umbrae disappeared. And we may speculate about the conversion of energy of this process into the white-light flare which almost occurred simultaneously.

5. The backward action of the photosphere
on the form of fast moving spots

Several times we have described the characteristic mode of small spots and pores development and motion {8},{9},{21},

{23}, {24}, {25}: dark bands of variously strengthened and darkened intergranular space gradually surround and then overflow parts of the granular field forcing its individual granules to darken - with the exception of their middle parts. As a result, they broaden, form elongated, differently curved dark features which finally roll up to constitute the "quantized" (3" -5" in diameter), almost round, small umbrae (Fig.5). During this process, they continue to penetrate between the stems of individual granules, successively reducing the brightness of their centra, or on the contrary, they evacuate the area, leaving the emerging granular field without any observable trace of the preceding invasion, both as far as the granular organization, structure and the brightness distribution are concerned {40}, {21}. These small systems of cooler plasma and magnetic lines of force imbedded in it behave like bunches of rubber tubes keeping their dark cool material isolated from their surrounding.

The form of these small dark umbrae - when shifted fast enough through the photosphere - seems to depend on the velocity and direction of their motion {22}. Already in the course of their establishment, it is possible to estimate from observations the direction of their motion. The influence of motion is even more visible on completed single nuclei, because their round form is transformed into a drop shape, the head of which seems to penetrate more easily into the granular field. In the photosphere it is sometimes possible to see, in front of the head of the drop, the formation of a sharp front of more compressed photospheric granules opposing the nucleus motion. The front part of the drop is also darker as the field is more concentrated in this part. On the other side, the drop's tail is considerably less dark going directly into the pieces of small umbrae, rudimentary penumbra and intergranular space, sometimes distributed in such a way that we may see the indications of the existence of turbulent whirls developing in the "wake" behind the umbra moving through the granular field.

6. How best to interpret the observed phenomena?

For the interpretation of all observed motions, but in the first place of proper motions in active regions, the majority of authors apply the conception of emerging flux tubes of magnetic field lines and magnetic forces only. Parker {36},{37} demonstrated theoretically that for the solution of certain motions and for explanation of development of large umbrae from smaller nuclei the aerodynamic or hydrodynamic interaction among different magnetic features also has to be taken into account. Of course, this action is again connected with the emergence of the flux tubes, this explains the mutual hydrodynamic attraction of the rising flux tube - two rising tubes attract each other, as a consequence of the wake of the leading tube when one is moving behind the other, and as a consequence of the Bernoulli effect when they are rising side by side {36}.

Recently, Unno et al. {41} using complex modern French and Japanese observational data, have tried to bring their observations into agreement with the ideas of Parker quoted. Although they demonstrated the consistency of observations with the hydrodynamic interpretation, they claim that the observations provide supporting evidence for the aerodynamic interactions, but not the proof. Moreover, they come to the same conclusion as we did {26},{11},{14}: The photosphere is not just a passive layer through which magnetic tubes come out from the convection zone into the chromosphere and the corona, but it is an active layer, where the magnetic field is reformed. There are other results to be considered in relation to this. For example, Sakurai and Levine {39} admit that the agitation by the flux emergence and by convective motion in the upper photosphere will drag field lines and induce an excess magnetic field.

We think that our summarized observations of proper motions give clear evidence that the hydrodynamic forces, which must not be always necessarily connected with emerging flux-tubes, play a much more important role in the local magnetic field and their sunspots evolution and motions than it has so

far been accepted and that their influence is greater than the action of magnetic forces. In our best quality observations we did not find any confirmation, or even any indication of a process morphologically resembling a flux tube emergence or its consequences. It is really hard to explain the observed motions as well as other phenomena by this convectional model only. We, therefore, also believe that the observed photospheric magnetic fields are not passive objects of variously acting forces and motions only, but rather that they more often actively respond to the processes, trying to change them and that they not only weaken due to these processes, but in many cases they strengthen, or even new local magnetic fields are generated. Probably this "local" generation of new magnetic flux is bound to the magnetic field singularity in a "center of magnetic activity" due to large and changing radial motions interacting with sheared magnetic field, influenced by differential rotation, vortical motions, streams flowing in the photosphere and other physical processes we still have to study more systematically and carefully. Motions in all layers of the solar atmosphere mutually interconnected not only through the field lines but also through several types of matter progression have to be considered too.

We still have another argument in favour of a "local dynamo", although it is not directly related to the topics discussed in this paper. It is the very difficult explanation with the use of the conventional model of emerging flux-tubes only of the simultaneous development of several active regions not only on both (eastern and western) sides, i.e. their leading on one side and their following parts on the other side, of one "unipolar" sector of the background field but also belonging to different solar hemispheres and even to different cycles of activity, not recalling the dynamics of new flux appearance, connected with the specific distortion of sector boundaries and the necessary presence of old magnetic fields {26},{11},{14}.

The observational data concerning the "floating" of solar magnetic fields in the photosphere are also very difficult to

interpret. Although we have to take the penetration of their field lines into the upper layers of the solar atmosphere into account and therefore the various modes of mutual coupling of the atmosphere's different layers interconnected in this way, the fact that the changes of umbral forms, their light-bridges and other structural details during the motion and collision of sunspots take place without any time delay, immediately after the collision, leads us again to the conclusion of the relative shallowness of the studied processes and relatively small thickness of the layer in which the observed activity plays the main role. We are also led to the same conclusion about the shallowness by observations of behaviours of small quantized pieces of umbra, the embryos of future components of larger umbrae, both during their formation, and during their specific mode of motion through the granular fields.

Since it seems that it is, as yet, practically impossible to interpret physically all the observed phenomena mentioned completely with the use of present theoretical conceptions, let us summarize our results in the following form: we may classify the observed motions following the forces causing them - if we know them - and in the future we have to try to obtain even more detailed and complex observational results enabling us to find finally, a physical explanation for their major part.

The concentration of magnetic field lines into the convectional intercellular space, accepted by many theoreticians (for example, {35}, {38}) also results most probably in the closest relation of the new magnetic flux appearance to the network of convectional elements. We see this relation not only in the faster displacement of new as well as old fields in the intercellular space as though in a conductor, in the bulging out of their field lines into the chromosphere in such a way that they join the supergranular peripheries, but also in the large stability of fields and of the phenomena connected with them as soon as they are bound to the whole set of convectional elements: sunspots filling in just one or more

supergranular cells {4},{32}, regular organization of individual sunspots depending on the supergranular network in a standard sunspot group and the quantized areas and distances of sunspots {29}, etc. The process of penumbra formation is closely related to the network {6}. Even the embryos of future components of umbral nuclei in all their evolutionary stages occupy the area of a given number of photospheric granules, having 3" - 5" in diameter. During the dissipation of large spots, the "point of instability" through which the greatest part of dark umbral material is seeping out from the spot into the intercellular space is again related to the morphology of the convectional network. This close relation of unstable magnetic fields to the convectional intercellular space and of stable field configurations to the insides of cells may be one of the reasons for the relatively small effectiveness of magnetic forces of fields bound to the network. Some magnetic field energy must be consumed during the orientation of fine structure elements in all layers of the solar atmosphere. Thus the only magnetic force the influence of which we observe, with the exception of the above mentioned cases, is the estimated and continuously acting trend for the simplification of complex fields into bipolar ones as well as with motions connected to this process, moreover, changes of group axis orientations and forms of entire magnetic patterns.

The main type of forces of which the action seems to us not only to be the best realized but also to play the principal role in the observed proper motions is represented by the hydrodynamic forces, which until now have seldom been considered for the interpretation of processes visible in active regions. We may briefly summarize their manifestation once more: processes during the interaction and collision of spots (elasticity, kinetic energy, inertia), vortical motions during the joining of smaller nuclei to form the main umbrae (probable transfer of impulses), influence of photospheric streams (changes of form of spot organization in the group), possible divergence and later reduction of distances of leading and

following spots, divergence of small spots during their disappearance, feedback action of streaming photosphere on the shape of entire local fields, interaction of moving umbrae with the surrounding granular fields (front ahead, drop-shape, wake), etc.

The only conclusion we can draw in this summary is that we still need more systematic and complex observations of the most simple processes visible during the most common active regions development, but before all we must pay more attention to better measurements of their velocity fields.

R e f e r e n c e s

- {1} Ambrož,P., Bumba,V., Howard,J., Sýkora,J., Opposite polarities in the development of some regularities in the distribution of large-scale magnetic fields, *IAU Symp.*43. 696, 1971
- {2} Beckers,J.M., Dynamics of the solar photosphere, *The Sun as a star*, (ed.Jordan, S.) *CNRS Paris, NASA SP-450 Washington,D.C.*,11, 1981
- {3} Bumba,V., Relative motions of sunspots in sunspot groups, *Prace Wrocławskiego Towarzystwa Naukowego, Seria B*, 112, 31, 1964
- {4} Bumba,V., Short note on the connections between the facular network and sunspots, *IAU Symp.*22, 192, 1965
- {5} Bumba,V., Hierarchy of solar magnetic field distribution (in Russ.) *PHD-thesis, Moscow*, 1967
- {6} Bumba,V., Observations of solar magnetic and velocity fields, *Rendiconti della Scuola Internazionale di Fisica "E.Fermi"*,39, 77, 1967
- {7} Bumba,V., Concerning the formation of giant regular structures in the solar atmosphere, *Solar Phys.*, 14, 80, 1970
- {8} Bumba,V., Large-scale solar magnetic fields, *IAU Symp.*71, 47, 1976
- {9} Bumba,V., Dynamics of sunspots development (in Russ.) *Trudy 8.consult. tom 3.*, 123, 1976
- {10} Bumba,V., August 1972 proton-flare region and different phases of its background magnetic field development, *BAC*, 31, 351, 1980
- {11} Bumba,V., Beginning stages of local magnetic field formation, *BAC*, 32, 129, 1981
- {12} Bumba,V., Solar magnetic fields and activity, *Compendium in Astronomy*, (eds. Mariolopoulos,E.G. et al.) *Reidel Dordrecht*, p.81, 1982
- {13} Bumba,V., Development of solar energetic particle sources within the background magnetic fields, *Space Sci.Rev.*, 32, 229, 1982
- {14} Bumba,V., Observable physical effects during new solar active regions formations, *A.N.*, 304, 7, 1983

- {15} Bumba,V., Observational facts concerning the local magnetic field generation, *Phys.Solariterr.*, (in press) 1983
- {16} Bumba,V., How does the magnetic field of an usual active region develop, *BAC*, 34, 219, 1983
- {17} Bumba,V., Hejna,L., June-July 1974 proton flare region. I. Individual stages of its background and local magnetic field development, *BAC*, 32, 349, 1981
- {18} Bumba,V., Howard,R., On the fine-scale distribution of solar magnetic fields, *Publ. Ondrejov*, 51, 24, 1964
- {19} Bumba,V., Howard,R., Large-scale distribution of solar magnetic fields *Ap.J.*, 141, 1502, 1965
- {20} Bumba,V., Howard,R., A study of the development of active regions, *Ap.J.*, 141, 1492, 1965
- {21} Bumba,V., Suda,J., Internal structure of sunspot umbrae, *BAC*,31,101,1980
- {22} Bumba,V., Suda,J., Development of sunspots in the colliding magnetic fields of the June-July 1974 proton-flare group, *BAC*,34, 29, 1983
- {23} Bumba,V., Suda,J., Processes observable in the photosphere during the formation of an active region. I. Development of a very small, secondary active region, *BAC*, 35, (in press) 1984
- {24} Bumba,V., Suda,J., Processes observable in the photosphere during the formation of an active region. II. Development of an usual active region, growth of a spot penumbra, *BAC*,35, (in press) 1984
- {25} Bumba,V., Suda,J., Processes observable in the photosphere during the formation of an active region. III. First stages of development of an usual active region at the edge of an older bipolar magnetic field, *BAC*, 35, (in press) 1984
- {26} Bumba,V., Tomášek,P., Initial phases of active region's photospheric magnetic field development, (in Russ.), *Phys.Solariterr.*13, 35, 1980
- {27} Bumba,V., Hejna,L., Le Bach Yen, June-July 1974 proton-flare region. II. Regularities in the magnetic field area and related sunspot and flare-activity development, *BAC*, 33, 160, 1982
- {28} Bumba,V., Klvaňa,M., Tomášek,P., Magnetic field development in an isolated active region (McMath No.13736), *BAC*, 33, 321, 1982
- {29} Bumba,V., Ranzinger,P., Suda,J., Photospheric convective network as a determining factor in sunspot and group development and stabilization, *BAC*, 24, 22, 1973
- {30} Gaizauskas,V., Harvey,K.L., Harvey,J.W., Zwaan,C., Large-scale patterns formed by solar active regions during the ascending phase of cycle 21, *Ap.J.*, 265, 1056, 1983
- {31} Howard,R., Švestka,Z., Development of a complex of activity in the solar corona, *Solar Phys.*,54, 65, 1977
- {32} Knoška,S., "Quantisation" of sunspot magnetic fields, *Publ. Debrecen Obs.* 2, 81, 1971

- {33} Martres, M.-J., Rayrole, J., Semd, M., Soru-Escout, I., Tanaka, K., Makita, M., Moriyama, F., Unno, W., Magnetic and velocity fields of emerging flux regions on the Sun, *Publ. Astron. Soc. Japan*, 34, 299, 1982
- {34} McIntosh, P.S., The birth and evolution of sunspots: observations, in *The physics of sunspots*, *Sac. Peak Obs. Conf. Proc.*, 7, 1981
- {35} Meyer, F., Schmidt, H.U., Weiss, N.O., Wilson, P.R., The growth and decay of sunspots, *M.N.*, 169, 35, 1974
- {36} Parker, E.N., The mutual attraction of magnetic knots, *Ap.J.* 222, 357, 1978
- {37} Parker, E.N., Sunspots and the physics of magnetic flux tubes.
I. The general nature of the sunspots, *Ap.J.*, 230, 905, 1979
- {38} Priest, E.R., *Solar magnetohydrodynamics*, Reidel, Dordrecht, 285, 1982
- {39} Sakurai, T., Levine, R.H., Generation of coronal electric currents due to convective motions on the photosphere, *Ap.J.*, 248, 817, 1981
- {40} Suda, J., The granulation in sunspot umbrae, *Trudy 8. consult. tom 3*,* 42, 1976 (in Russ.)
- {41} Unno, W., Tanaka, K., Semel, M., Hydrodynamical and electrodynamic interactions between magnetic features in the active-region photosphere, *Publ. Astron. Soc. Japan*, 33, 495, 1981
- {42} Vasilyeva, G.Y., On the distribution of radial velocities and brightness in the solar photosphere, (in Russ.) *Izv. GAO Pulkovo*, 22, No. 169, 39, 1961
- {43} Vrabec, D., Streaming magnetic features near sunspots, *IAU Symp.* 56, 201, 1974
- {44} Waldmeier, M., *Ergebnisse und Probleme der Sonnenforschung* 2. Ausg. Leipzig, 1955

* Физика солнечных пятен. Сопещения Академий Наук Социалистических Стран по Физике Солнца, АН СССР, СИБИЗМИР, Изд. "Наука" Москва 1976

Publ. Debrecen Obs. Vol. 5

No. 2.

PAPERS RELATED TO THE SOLAR MAXIMUM YEAR PROGRAMS

RELATIONSHIP OF THE DYNAMIC EVENTS IN OPTICAL AND RADIO RANGES
DURING THE FLARES OF NOVEMBER 9 AND 10, 1979

I.M. CHERTOK, V.V. FOMICHEV,
V.N. ISHKOV, A.K. MARKEEV
IZMIRAN, Troitsk
G.S. MINASYANTS, S.O. OBASHEV
Astrophys. Inst., Alma-Ata

СООТНОШЕНИЕ ДИНАМИЧЕСКИХ ЯВЛЕНИЙ В ОПТИЧЕСКОМ И РАДИОДИАПАЗОНАХ
ВО ВРЕМЯ ВСПЫШЕК 9 И 10 НОЯБРЯ 1979 Г.

И.М. ЧЕРТОК, В.В. ФОМИЧЕВ, В.Н. ИШКОВ, А.К. МАРКЕЕВ
ИЗМИРАН, Троицк
Г.С. МИНАСЯНЦ, С.О. ОБАШЕВ
Астрофиз. Инст., Алма-Ата

Abstract:

The results of simultaneous optical and radio observations of the solar flares on November 9 and 10, 1979 are presented. It was revealed that the both flares had a number of common features both in optical and in radio ranges: location of the flares in the same place of active region, the similar configuration of the flare ribbons, rather hard spectrum of impulsive microwave bursts, the unusual fine structure of type V radio burst on November 9 and of type II radio burst on November 10 in the form of narrow band elements. Such fine structure of radio emission is supposed to be connected with the existence of an orderly system of large scale loops in the corona.

The differences between these flares consisted in its dynamics. The flare on November 9 had a relatively quiet evolution, while the flare on November 10 was accompanied by a two-component mass ejection. This ejection was followed by two shock waves in the corona which resulted in the generation of type II radio burst.

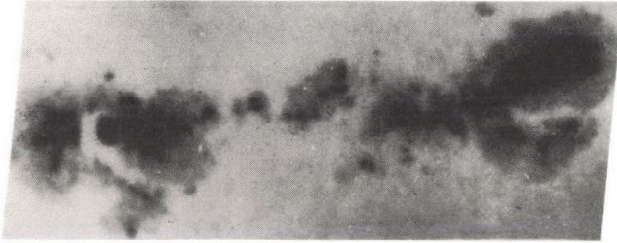
The purpose of this paper is an analysis of the features of optical and radio emission from two flares on November 9 (~06:02 UT) and 10 (~06:42 UT) 1979, which took place in active region HR 16413. The analysis is based on the observations carried out with a big $H\alpha$ coronagraph of the Astrophysical Institute of the Academy of Science of Kaz.SSR and with IZMIRAN's radiometers (204, 3000 MHz) and spectrographs in frequency ranges of 45-90, 130-180 MHz. With such cooperation it proved possible to compare the optical characteristics of the flares and its evolutions with time profiles, dynamic and frequency spectra and the unusual fine structure of the radio bursts. Information on propagation of coronal disturbances from these flares, as well as some data on a structure of the corona above the active region is obtained.

Flare of November 9

According to *Solar Geophysical Data* this flare began as one of importance 1N with maximum at 05:48 UT and then almost continuously turned into flare of importance 1B/M6 with maximum at 06:02 UT. From the very beginning the flare developed as a two ribboned one (Fig.1). At radio waves the first flare maximum was accompanied by a group of type III bursts and type V burst with overall duration of about 3 min as well as by relatively weak microwave burst with a peak flux density $F \sim 38$ s.f.u. at $f \sim 9$ GHz.

The following stage of the flare evolution was characterized by the formation and development of new flare knots of S-polarity near the border of the penumbra of the leading spot. The main dynamic processes of this stage in optics were: a) penetration of the S-polarity flare ribbon into the penumbra of the leading spot (06:00:35 - 06:04:05 UT); b) propagation of the emission along a neutral line and formation of a thin arc-like continuation of the S-polarity ribbon. At centimetre range the flare maximum had a form of intensive impulsive burst whose frequency spectrum was rather hard with maximum at $f \sim 17$ GHz (Fig.2).

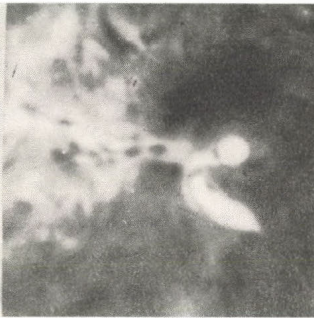
At metre waves, complex type III and V bursts were ob-



04:15 UT



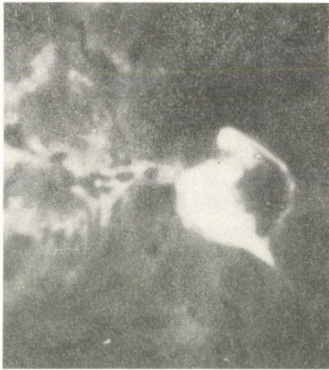
05:45:55 UT



06:00:35 UT



06:04:30 UT



06:07:55 UT



06:14:00 UT

Fig.1. Photospheric picture of the active region and evolution of the H α -flare of November 9, 1979.

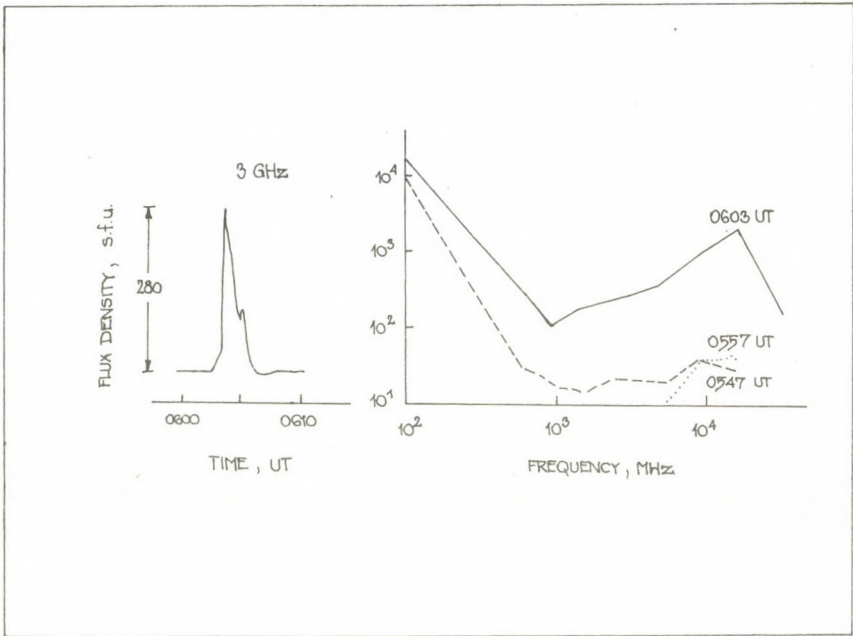


Fig. 2. Time profile and frequency spectrum of the radio burst of November 9, 1979.

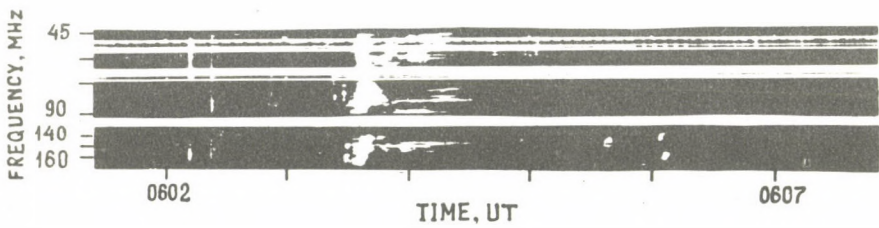


Fig. 3. Dynamic spectrum of the radio burst of November 9, 1979.

served at this time (Fig.3). An important peculiarity of dynamic spectrum of the type V burst was the presence of a system of numerous narrow-band ($\Delta f \sim 1-2$ MHz) elements with a duration of up to some tenths of a second. The frequency drift of the majority of these elements was in general small or absent. At 06:05:30 - 06:06 UT one can also see a faint manifestation of a type II burst in the range of 130-175 MHz.

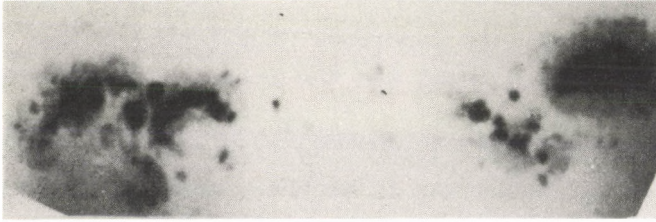
Flare of November 10

In this event three centres of enhanced brightness in $H\alpha$ were observed during the preflare stage, one of them being connected with a newly appeared region of N -polarity (Fig.4).

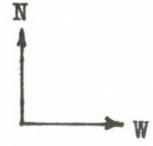
With the beginning of the flare of 2B/1X importance at 06:31 UT the emission knots sharply increased its brightness and the process of formation of the flare ribbons continued up to 06:37 UT. The sought N -polarity knot did not change its size practically, and was localized in the same place as in the flare of November 9. Its configuration and localization did not change during all the flare either, and this knot was a centre around which the following events developed. The flare S -polarity ribbon had a strongly curved S-like shape and surrounded both N -polarity regions.

A strong explosion in the west part of the flare at 06:41:30 UT was accompanied by a powerful mass ejection and by a fast (less than 5 min) disruption of the west flare knot. This phenomenon began with an ejection of a faint shining diffuse cloud having a velocity $V \sim 3000$ km s⁻¹ in the sky plane, as well as with an expansion of the flare S -polarity knots into the penumbra of the leader spot ($V \sim 100$ km s⁻¹) and the west N -polarity knot expansion in the direction of the diffuse cloud ($V \sim 300$ km s⁻¹). It should be noted that the east flare border was stable and coincided with the light bridge between the two small spots.

At 06:42:10 UT the details of the second component of mass ejection with a velocity $V \sim 1500$ km s⁻¹ became visible. It is essential that both ejection components developed approximately in the same direction (to the south-west from the



04:54 UT



1 arc min



06:30:20 UT



06:39:23 UT



06:42:00 UT



06:42:20 UT



06:42:35 UT



06:44:18 UT



06:59:30 UT

Fig.4.

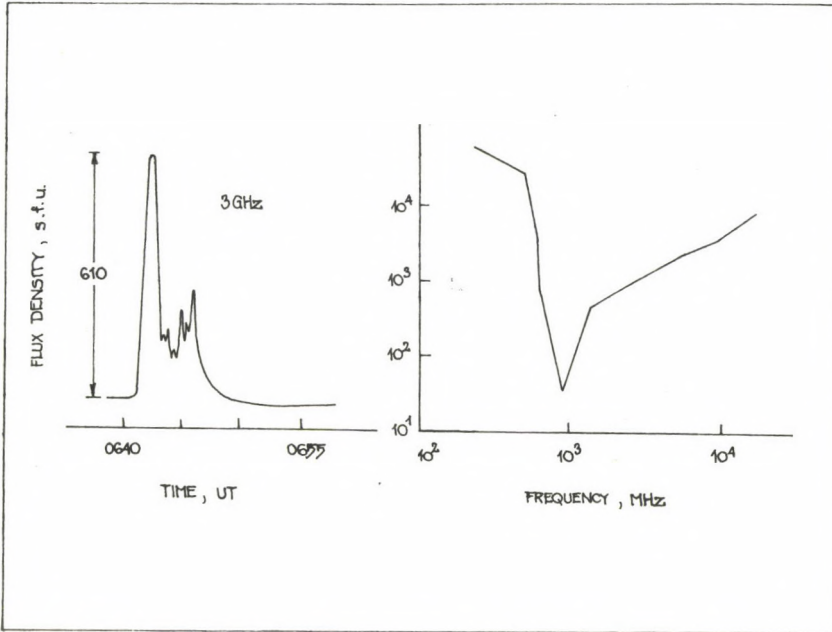


Fig.5. Time profile and frequency spectrum of the radio burst of November 10, 1979.

Fig.4. Photospheric picture of the active region and development of the H α -flare of November 10, 1979. The diffuse cloud at 06:42:00 UT marked by the arrow is the first visible component of the ejection. Evolution of the second main component of ejection can be seen beginning from 06:42:20 UT.

flare) and propagated in a relatively narrow cone $\sim 40^\circ$.

Impulsive microwave burst accompanying this flare was more powerful than one in the flare of November 9, and its frequency spectrum had a U-like shape with a minimum at $f=950$ MHz, and the increasing of flux density to high frequencies up to $f\sim 17$ GHz (Fig.5).

At metre range of the dynamic spectrum a type II burst predominated. It consisted of a number bands with a duration above 20 min. The bands in interval 06:43 - 06:49 UT are harmonical type II bursts with band splitting. A distinctive peculiarity of this event is the presence of a new variety of the type II burst fine structure, visible as bright discrete strips analogous to the elements of the fine structure in the type V burst of November 9 (see {1}). The strips have an instantaneous bandwidth $\Delta f\sim 1$ MHz and overall duration of up to 30-40 s. The shape of single strips is various: arch-like, without drift or with small negative frequency drift. Simultaneously more than 10 strips can be observed.

Analysis and discussion

The data described above show that the flares of November 9 and 10, 1979 have a number of common and very interesting features. In particular both flares had analogous structure in $H\alpha$ with the S-like form of the emission elements. Besides, both flares took place in the same part of the active region in the direct neighbourhood of the large leading spot. The close localization of $H\alpha$ -emission sites to spots corresponds to the hard frequency spectra of the microwave bursts observed in both cases (see {2}).

The most important differences between the flares under consideration (besides the intensity) consist in their dynamics. In the November 9 flare visible ejection was not observed. In this event the most of the flare energy was realized in the form of accelerated particles. Accordingly, the type III and V bursts predominated. The fragmentary type II burst was most probably initiated by faint explosive (non piston) shock wave, whose origin may be connected with the

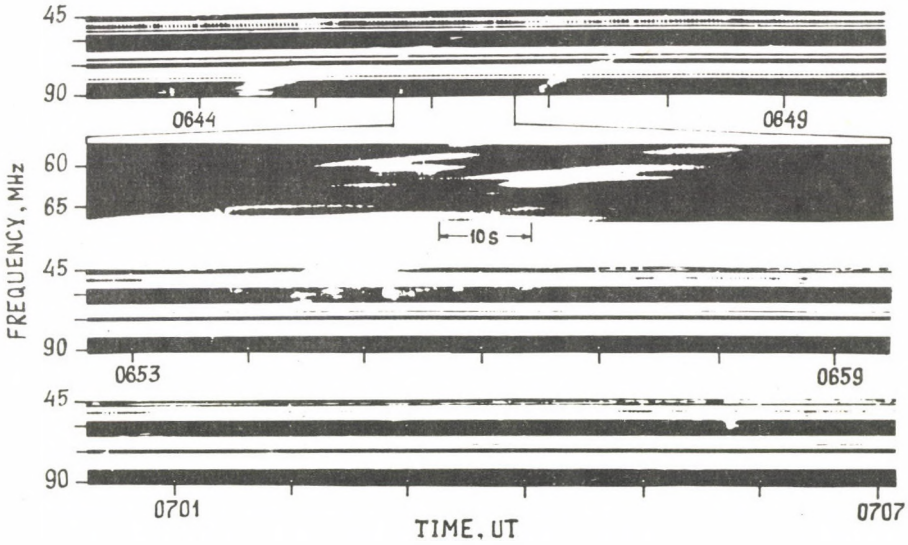


Fig.6. Dynamic spectrum of the radio burst of November 10, 1979.

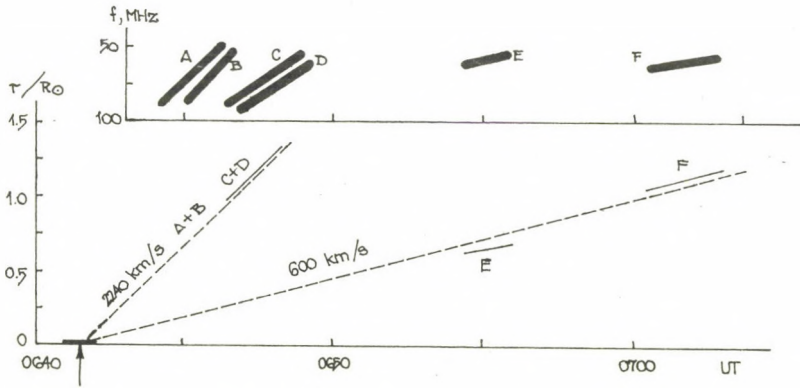


Fig.7. Schematic dynamic spectrum of the type II burst of November 10, 1979 (top) and "altitude-time" diagram showing the trajectories of two shock waves (bottom). Solid section on the time axis corresponds to the increasing phase of the microwave burst, the arrow marks the moment of the two-component ejection.

penetration of the $H\alpha$ emission into the penumbra of the leading spot.

On the other hand, the main dynamic process in the November 10 flare was the powerful high velocity two-component ejection. The generation of the complex and long type II burst was initiated by this ejection. Using the $2 \times$ Newkirk model for electron density distribution and observed burst structure (bands $A + B$, E are the fundamental, bands $C + D$, F are the harmonic) the trajectories of the corresponding disturbances on the "altitude - time" plane can be calculated. This diagram shows that in this event two shock waves with the velocities along the density gradient $V_{||} \sim 2200$ and 600 km s^{-1} have been initiated during the flash phase of the flare (Fig.7). It seems that each of these shock waves corresponded to one or two components of the ejection observed in optics.

As far as the fine structure of the metre-wave bursts is concerned it should be noted that the analogous structure in a form of discrete narrow band elements has been observed in the bursts of a different nature - in the November 9 type V burst and in the November 10 type II burst. That means that the origin of such a structure was not caused by the peculiarities of the generation mechanism of these bursts but by the specific physical conditions above the active region. The assumption of the ordered large scale structures of loop-like type that exist in the corona is the most natural. Then an injection of accelerated electrons in a number of such loops, following formation of radio emission sources near its tops in accordance with the model proposed by Zheleznyakov and Zaitsev [4], can show up the discrete emission strips on the dynamic spectrum of the type V burst. Because the band width Δf of every strip in frame of such a model is determined by the scatter of the electron density in the loop top, the observed values $\Delta f \sim 1-2 \text{ MHz}$ give an estimation for a transverse scale of the loop $\Delta r \sim 5 \cdot 10^8 - 10^9 \text{ cm}$.

The interpretation in frames of this scheme of the fine structure in the November 10 Type II burst is reduced to a

propagation of a shock wave through the system of the thin loops mentioned above. It is only necessary that the condition of the radio emission generation (Mach number M should exceed a critical value M_{CR}) should be satisfied inside these loops alone. Estimations of Mach number by the observed values of band splitting give $M \sim 1.2 - 1.1$ and $M \sim 1.4 - 1.2$ for perpendicular and parallel shock waves, respectively. These values are very close to the critical ones $M_{CR} \sim 1.1 - 1.15$. It follows that radio emission will be generated inside loops if a ratio $H/N^{\frac{1}{2}}$ (where H is a magnetic field strength, N is an electron density) is at least 10% less compared to the space between the loops. One possible version for this is the higher density of the loops as regards the surrounding corona.

In dependence on the mutual orientation of the shock front and loop, the generation of the strips with different frequency drift, including the strips with direct drift, without drift or of arch-like shape, can occur. The observed duration of the elements without visible drift $\tau \sim 20-30$ s and the shock wave velocity $V_{H1} \sim 2200$ km s⁻¹ allow the estimation of an extent for a typical loop near its top $l \sim 6 \cdot 10^9$ cm to be obtained.

Thus the analysis of two flares, which are different in intensity but look alike in many respects, points to the conclusion that physical conditions in the chromosphere and the corona above the given active region were unchanged for at least twenty four hours. These identical conditions resulted in the analogous configuration of the flares in optics and in the specific fine structure of the metre radio bursts.

References

- {1} Gnezdilov, A.A., Kovalev, V.A., Markeev, A.K., Fomichev, V.V., Chernov, G.P., Chertok, I.M., The peculiarities of an energy release in the large flares by radio bursts data during Aug.-Nov.1979, (in Russ.) *ICM-SMY Crimean Workshop 2*, 59,299, 1981
- {2} Hagen, J.P., Neidig, D.F.Jr., Identification of two distinctive types of centimeter radio bursts with flare location, *Solar Phys.*, 18,305,1971
- {3} *Solar-Geophysical Data, 1970-1981*
- {4} Zheleznyakov, V.V., Zaitsev, V.V., On the origin of type V solar radio bursts, (in Russ.) *Astron.zh.*, 45, 19, 1968

SMM FLAT CRYSTAL SPECTROMETER DATA ANALYSIS OF

7 APRIL 1980 FLARE

B. SYLWESTER, J. SYLWESTER

Space Res.Center, Wrocław

J. JAKIMIEC

Astron.Observatory, Wrocław

R. MEWE,

R.D. BENTLEY

Space Res.Lab., Utrecht

Mullard Space Sci.Lab., Dorking

Abstract:

We have analysed soft X-ray images of the 1B/M4 flare of 7 April 1980 (start at 00:50 UT) recorded by Flat Crystal Spectrometer aboard Solar Maximum Mission satellite. The X-ray flare consisted of two patches about 1 arcmin apart. Comparison with magnetograms and white light images indicates that the two soft X-ray patches originate from two different loops or systems of loops. Systematic displacements of the brightest points of the patches are clearly seen during the flare development. For two selected resolution elements of the X-ray pictures (one element in each patch) detailed differential emission measure analysis has been carried out and time evolution of the mean electron density and thermal energy content has been investigated.

АНАЛИЗ НАБЛЮДЕНИЙ ВСПЫШКИ ИЗ 7 АПРЕЛЯ 1980 Г

ПОЛУЧЕННЫХ КРИСТАЛЛИЧЕСКИМ СПЕКТРОМЕТРОМ ИЗ БОРТА SMM

Б. СИЛЬВЕСТЕР, Я. СИЛЬВЕСТЕР, Я. ЯКИМЕЦ,

ЦНИ, Вроцлав

Астрон.Обс., Вроцлав

Р. МЕВЕ,

Р.Д. БЕНТЛЕЙ

Носм.Лаб., Утрехт

Маллард Носм.Лаб., Доркинг

Абстракт:

В работе проведен анализ рентгеновских изображений солнечной вспышки балла 1B/M4 которая произошла 7 апреля 1980 г около 00:50 UT. Эти изображения были получены с помощью спектрометра с плоским кристаллом помещенного на борту спутника SMM. Рентгеновское изображение вспышки состоит из двух областей, находящихся на расстоянии 1 минуты дуги друг от друга. Сравнение этих изображений с магнитограммами и снимками фотосферы в белом свете показывает, что каждая излучающая область возникает в отдельной системе петель. Во время вспышки наблюдается перемещение центров рентгеновского излучения. Детальный анализ дифференциальной меры эмиссии был проведен для двух избранных элементов изображения размерами 15"×15". Рассматривались также временные изменения электронной плотности и тепловой энергии плазмы в этих элементах.

The analysed solar flare on 7 April 1980 at 00:50 UT was classified as $M4$ in soft X-rays and as $1B$ in $H\alpha$ radiation. It was of long duration (start at 00:48 UT, maximum phase at 01:10 UT, the end at 01:50 UT according *Solar-Geophysical Data, 1980*) and occurred in the magnetically complex AR 2372 located near the center of the solar disc.

This flare was extensively observed by means of the instruments placed aboard the Solar Maximum Mission satellite (SMM). In the present paper we will analyse in detail the data obtained by means of Flat Crystal Spectrometer (FCS) instrument. For the description of this instrument see Acton et al. (1). The flare, as seen in the soft X-ray FCS images, consists of one or two patches depending on the temperature range and/or the time of the observations. In Fig.1 the isophotes of the flare at 00:57 UT in channels 1, 5 and 7 are shown respectively. The emission is extended in EW direction in the lower temperature lines (OVIII, SXV), and only one patch is seen in the hottest temperatures (FeXXV image). Overlying the X-ray images with the magnetogram indicates that the X-ray structure are originally placed over the neutral line of the photospheric magnetic field. Comparing this with white light images we infer that the emission of the two patches may originate from the tops of two systems of loops overlying the complicated neutral line. During the development of the flare both soft X-ray patches change their positions. The mean velocities corresponding to these displacements are 5 and 10 km s⁻¹ for the brighter and the fainter patch respectively. At present it is not clear whether the observed displacements of the X-ray emission are connected with a real motion of the plasma. It is possible that these displacements represent either the motion of a triggering agent (which switches on the subsequent loops in the arcade) or the energy flow. To distinguish between these mechanisms it is important to analyse the changes of the differential emission measure and the energy content for each element (pixel) of the image. As an example, in the present paper, we have performed a multi-temperature analysis

for two pixels (A and B) which were the brightest in each of the X-ray patches at 01:11 UT.

It is very convenient to describe the analysis of the temperature structure of the plasma in terms of the differential emission measure distributions $\phi(T)$ as a function of the temperatures T :

$$\phi(T)dT = N_e^2 dV \quad (1)$$

Here N_e is the electron density, V is the emitting volume. The distribution $\phi(T)$ we will call the model of the emitting region. $\phi(T)$ were calculated in the temperature range 2-30 10^6 K using the iterative procedure (see {7},{8}) and the fluxes in 6 FCS channels as input data. In Fig.2 and 3 examples of the models calculated for pixels A and B for various moments are presented. The scale on the vertical axis is logarithmic. The numbers indicate times when the nearby bars correspond to $\log \phi(T) = 42$. From the figures the evolutionary changes are seen, as well as the differences between the models for pixels A and B. It is seen that during the whole evolution of the flare the temperature distribution of the plasma has two components in both pixels. The mean temperatures of the low (l) and high (h) temperature components change with the time in a different way for pixels A and B. The mean temperatures are somewhat lower for pixel B than for pixel A. From the models one can calculate the values of the emission measure in the temperature intervals from $2 \cdot 10^6$ K to T_{\min} and from T_{\min} to $30 \cdot 10^6$ K as:

$$\Sigma = \int \phi(T) dT \quad (2)$$

where T_{\min} correspond to the temperature of the local minimum of $\phi(T)$. The changes of the calculated emission measure in pixel B are smaller than in pixel A.

Assuming that \bar{N}_e is a mean plasma density within the emitting volume one can obtain from Eq.(1):

$$3k \int_T \phi(T) T dT = 3k \int_V N_e^2 T dV = E_{th} \bar{N}_e \quad (3)$$

where k is Boltzmann constant and E_{th} is the thermal energy

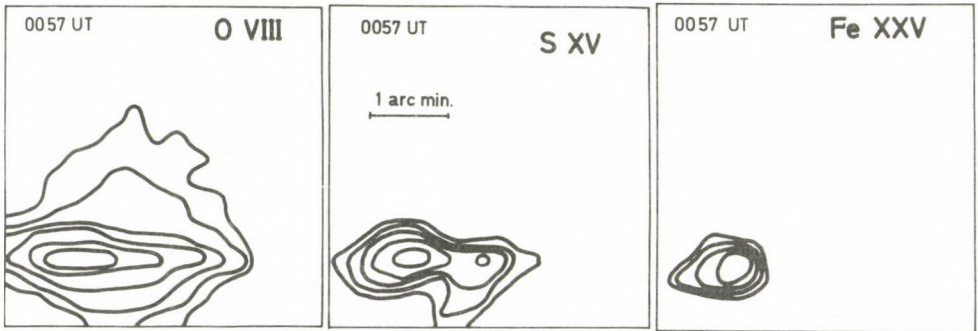
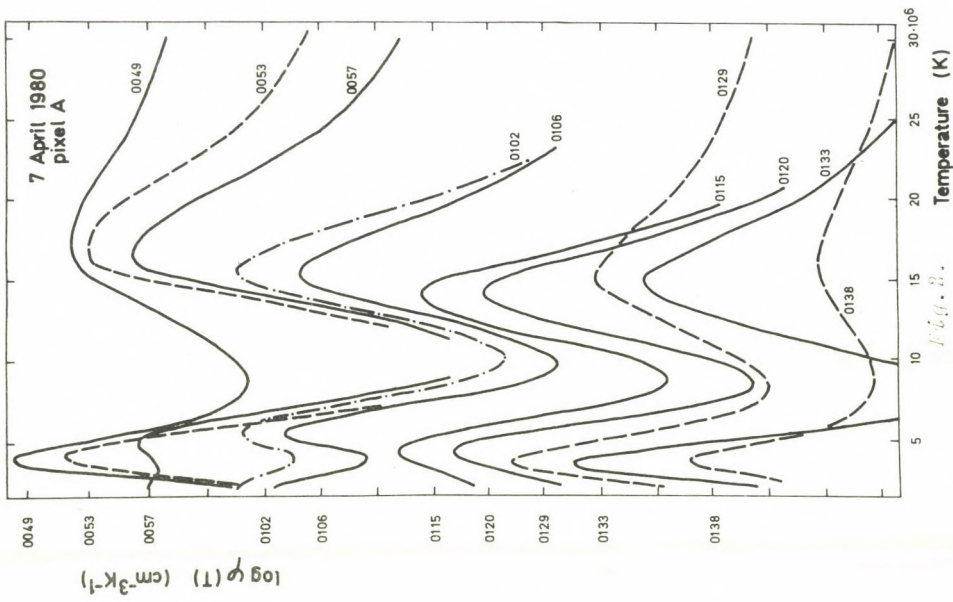
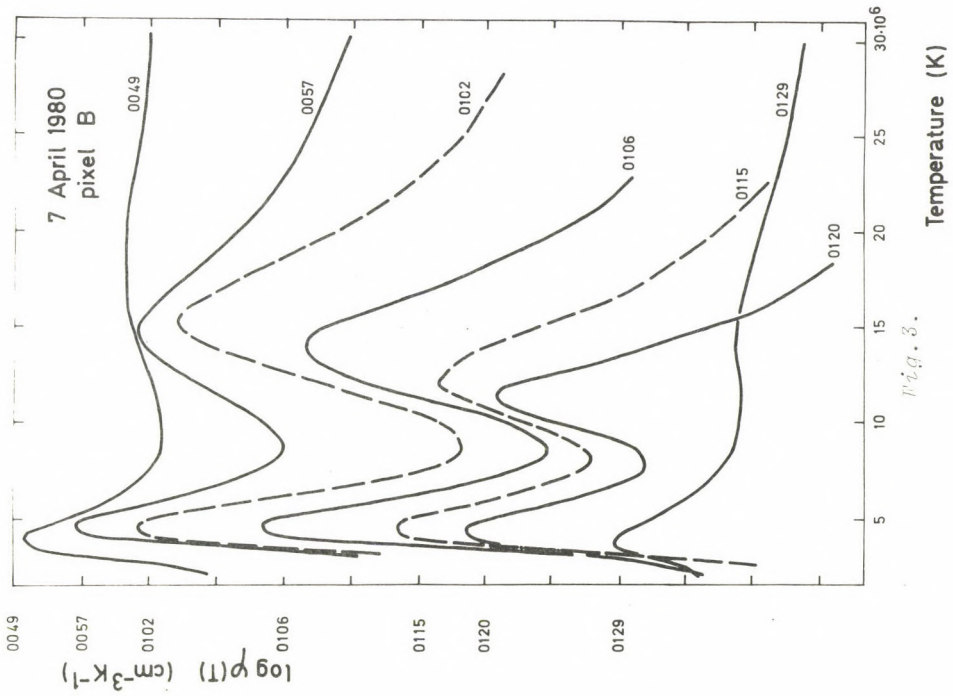


Fig. 1. The isophotes of the images obtained at 0057 UT by FCS instrument in the O VIII line ($T \sim 2.5 \cdot 10^6 \text{K}$), the S XV ($T \sim 15.5 \cdot 10^6 \text{K}$), and in the Fe XXV line ($T \sim 30 \cdot 10^6 \text{K}$). The isophotes correspond to levels of 3σ , 6σ , 12σ , ..., where 1σ is the r.m.s. fluctuation of the background level.

Fig. 2. Calculated models of the differential emission measure distribution for pixel A. The calculations were performed in the temperature range $2 \cdot 10^6 \text{K} - 30 \cdot 10^6 \text{K}$ for several times corresponding to the rise, maximum, and decay phase of the event. The vertical scale is logarithmic, and the numbers indicate times when the near by bars correspond to $\log \Phi(T) = 42$.

Fig. 3. Same as in Fig. 2 but for pixel B.



T A B L E 1

The mean electron densities
for both components of pixels A and B

Time UT	A		B	
	$(N_e)_l$	$(N_e)_h$	$(N_e)_l$	$(N_e)_h$
	cm^{-3}		cm^{-3}	
00:49	$6.3 \cdot 10^{10}$	$6.5 \cdot 10^{10}$	$3.0 \cdot 10^{10}$	$2.0 \cdot 10^{10}$
00:57	$1.0 \cdot 10^{11}$	$1.4 \cdot 10^{11}$	$3.5 \cdot 10^{10}$	$2.5 \cdot 10^{10}$
01:06	$1.6 \cdot 10^{11}$	$1.3 \cdot 10^{11}$	$4.6 \cdot 10^{10}$	$3.5 \cdot 10^{10}$
01:20	$1.2 \cdot 10^{11}$	$8.7 \cdot 10^{10}$	$4.8 \cdot 10^{10}$	$3.5 \cdot 10^{10}$
01:29	$9.9 \cdot 10^{10}$	$4.4 \cdot 10^{10}$	$4.5 \cdot 10^{10}$	$1.5 \cdot 10^{10}$

T A B L E 2

The thermal energy contents
for both components of both pixels

Time UT	A		B	
	$(E_{th})_l$	$(E_{th})_h$	$(E_{th})_l$	$(E_{th})_h$
	<i>ergs</i>		<i>ergs</i>	
00:49	$4.1 \cdot 10^{28}$	$1.4 \cdot 10^{29}$	$6.1 \cdot 10^{28}$	$1.5 \cdot 10^{29}$
00:57	$7.0 \cdot 10^{28}$	$2.8 \cdot 10^{29}$	$6.9 \cdot 10^{28}$	$1.4 \cdot 10^{29}$
01:06	$1.0 \cdot 10^{29}$	$2.3 \cdot 10^{29}$	$1.0 \cdot 10^{29}$	$1.8 \cdot 10^{29}$
01:20	$8.2 \cdot 10^{28}$	$1.4 \cdot 10^{29}$	$9.8 \cdot 10^{28}$	$1.4 \cdot 10^{29}$
01:29	$6.0 \cdot 10^{28}$	$8.0 \cdot 10^{28}$	$8.7 \cdot 10^{28}$	$5.2 \cdot 10^{28}$

content of the plasma investigated. The left-hand part of Eq. (3) can be calculated directly from the distributions $\varphi(T)$ for the low and high temperature components independently. Consequently we have the products $E_{th} \bar{N}_e$. In order to extract the values of the thermal energy content alone one should have appropriate estimates of the mean electron density \bar{N}_e of the emitting plasma. It can be derived from the emission measure as:

$$\bar{N}_e = \left(\frac{\epsilon}{V} \right)^{1/2} \quad (4)$$

if the volumes V of the segments of the loops contained within pixels A and B are known. These volumes have been estimated as $V = d^2 \times s$ ($s = 15''$ corresponds to the size of the FCS pixel and d being the estimates of the loop width). For the loop width d we have included the FWHM value of the intensity profiles across the loops (corrected for the instrumental FWHM) in the calculations. The OVIII and MgXI images were used in order to estimate the values of d for the lower temperature plasma component and the SXV images for the higher temperature component. The resulting mean electron densities \bar{N}_e and the values of thermal energy content E_{th} for low (l) and high (h) temperature plasma components in pixels A and B are given in Table 1 and 2 for different times during the flare. It is seen from Table 1 that the estimated mean electron densities \bar{N}_e change by factor 2-3 for pixel A, and less than 2 for pixel B, and that the density in pixel A is about three times higher than in pixel B.

It is worth noting that the values of \bar{N}_e should be considered as the lower estimate for the plasma density, because the filling factor may be smaller than unity. Therefore the corresponding values of E_{th} represent upper estimates of the thermal energy content.

The obtained results are in good agreement with the earlier estimates of these quantities derived in other ways for the flares as a whole. (See {3}, {5}, {2}, {4}.)

Acknowledgements

The authors wish to thank Dr Béla Kálmán from the Debre-

cen Heliophysical Observatory, Hungary, for supplying white light photosphere images. Dr Mona Hagyard provided MSFC magnetograms. The SMM-XRP experiment has been developed jointly by the University College London Mullard Space Science Laboratory (Prof. J.L.Culhane), Lockheed Palo Alto Research Laboratory (Prof. L.A.Acton) and the SERC Rutherford and Appleton Laboratory (Prof. A.H.Gabriel).

References

- {1} Acton, L.W., Culhane, J.L., Gabriel, A.H., and many others, The soft X-ray polychromator for the Solar Maximum Mission, *Solar Phys.* 65. 53, 1980
- {2} Kahler, S.W., Petrasso, R.D., The quantitative properties of three soft X-ray flare kernels observed with the AS&E X-ray telescope on Skylab, *Solar Phys.* 50. 179, 1976
- {3} McKenzie, D.L., Broussard, R.M., Landecker, P.B., Rugge, H.R., Young, R.M., Doschek, G.A., Feldman, U., Electron densities in a solar flare derived from X-ray spectra, *Ap.J.* 238. L43, 1980
- {4} Pallavicini, R., Vaiana, G.S., Spatial structure and temporal development of a solar X-ray flare observed from Skylab on June 15, 1973 *Solar Phys.* 45. 411, 1975
- {5} Smith, J.B.Jr., Wilson, R.M., Henze, W.Jr., Morphology and physical parameters of a solar flare, *Ap.J.* 216. L79, 1977
- {6} *Solar Geophysical Data*, No. 434. Part II. 1980
- {7} Sylwester, J., *Thesis*, Wrocław University, 1977
- {8} Sylwester, J., Schrijver, J., Mewe, R., Multitemperature analysis of solar X-ray line emission, *Solar Phys.* 67. 285, 1980

THE PHOTOSPHERIC DOPPLER SHIFT OBSERVED
IN HALE ARs 16862 AND 16863 (MAY 22 AND 23, 1980)

A. A N T A L O V Á

Astron.Inst., Tatranská Lomnica

Abstract:

The detail spatial structure analysis (1.2×2.0 arcseconds) of the four Meudon photoelectric charts of the photospheric Doppler shift (magneto-sensitive line FeI 630.25 nm) was done for Hale ARs 16862 and 16863 on May 22 and 23, 1980. It was found that at the very beginning of the appearance of the new sunspots, temporary (lasting only a few hours), small dimensional, upward, photospheric motions, with an amplitude larger than 900 m s^{-1} were observed. The result is valid for small new sunspots, which appeared in the penumbras of the large spots (16863p and 16862f). The umbra of the 16863p spot had complex velocity and structural patterns from May 21 to 23.

ФОТОСФЕРНЫЕ ЛУЧЕВЫЕ СКОРОСТИ НАБЛЮДАЕМЫЕ В АКТИВНЫХ ОБЛАСТЯХ
ХЕЙЛА 16862 И 16863 (С 22 ДО 23 МАЯ 1980 Г.)

А. Анталова

Астрон.Инст., Татранска Ломница

Абстракт:

Детальный пространственный анализ (1.2×2.0 дуговых секунд) четырех фотоэлектрических карт фотосферных лучевых скоростей (магнито-чувствительной линии нейтрального железа 630.25 нм) был сделан для активных областей Хейла 16862 и 16863 с 22 до 23 мая 1980 г. Было найдено, что с самого начала возникновения новых солнечных пятен, в течении нескольких часов, возможно наблюдать на малом участке площади, фотосферные движения кверху, с амплитудой больше чем 900 м с^{-1} . Результат был получен для маленьких пятен, которые возникли в полутени больших пятен (16863в и 16862с.) Тень ведущего пятна 16863 имела с 21 до 23 мая сложный структурный и скоростной характер.

1. Introduction

The photospheric velocity field can be divided into the umbral, penumbral and near-spots velocity patterns. During the evolution of the active regions, horizontal motions are predominantly observed in the photosphere. Observations of the umbral line shifts with an absolute wavelength reference {3}, {1} show no vertical motions in umbrae, exceeding 25 m s^{-1} . The best resolved umbral photospheric motions are umbral oscillations with a period from 3 to 5 minutes and an amplitude of speed $100\text{-}500 \text{ m s}^{-1}$ {4}.

The penumbra is the site of the most pronounced photospheric velocity feature "Evershed effect". Since it is impossible to review the evolution of this topic here, I will simply point out the current situation as based on the review by Beckers {4}. In the lower levels of the penumbra, along the dark penumbral filaments, the matter flows, nearly horizontally, out of the penumbra towards the surrounding photosphere with average velocities approaching a few kilometers per second. In the great majority of cases, the observations of the velocity concerned the regular large spots, which naturally belong to a late phase of sunspot development.

Some indications of the higher radial velocity values in the photosphere, namely in small and young sunspots were shown on the spectrographic measurements {8}, {9}, {12}.

2. The photospheric Doppler shift measurements

The Doppler shifts of the photospheric magneto-sensitive line Fe I 630.25 nm were measured with the new photoelectric magnetograph operating in Meudon Observatory since April 1980. Using the Newton-Gregory telescope (equivalent focal length 23 m), two reticon diode arrays, microcomputer TEXAS 990/4 and IBM 3740 "floppy disk", the maps of the radial velocity with the space resolution of 1.2×2.0 arcseconds can be obtained for AR in approximately six minutes {19}. The measurements of the Doppler shifts of line 630.25 nm were done in Hale ARs 16862 and 16863 for May 22, 1980 at 10:25, 14:41, 15:10 UT and May 23, 1980 at 08:21 UT.

3. The characterization of the AR 16862 and 16863

As is well known, the Hale ARs 16862, 16863 and 16864 (NOAA-SESC 2466, 2469, 2470) were selected during SMY as an FBS target of the second interval from 22 to 29 May 1980. Gaizauskas {11} has completed the data on the flare activity and global development in this complex of the three sunspot groups. The characteristics of this complex were studied in many articles (see {15}). In fact, the large flare activity occurred in this complex on May 28 and 29. The most attractive flare location was outside the western edge of the penumbra of the leading spot AR 16864, where new sunspots appeared. In this article attention is only concentrated on May 22 and 23, when Doppler shifts of the spots 16863_p and 16862_f were measured.

S p o t 16863_p. The large umbra of the preceding spot, Hale 16863 (NOAA-SESC 2466), was the preferred location of the umbral flares throughout the entire FBS Interval ({2}, Tab.3). On days May 21-23 the umbra of 16863_p was characterized by a fast increase in the area and also by changes in the mutual orientation of the main parts of the umbra {2}. Ioshpa et al. {14} found that the preceding spot of Hale AR 16863 on May 21 had an umbra of a fragmentary origin and consisted of 7 components of the same negative magnetic polarity (S), divided by faint bridges. On May 22-23, umbra 16863_p became more compact. This complex structure of the umbra 16863_p is probably related to the remarkably large occurrence of the umbral flares (the largest 1B umbral flare was observed on May 25, 05:54 UT).

S p o t 16862_f. The following spot of AR 16862 (NOAA-SESC 2469) had positive magnetic polarity and its umbra had a drop-like shape. On May 22 the new small sunspots were observed on the south-western edge of the penumbra of 16862_f spot.

4. Analysis of the Doppler shift maps

This article does not attempt to present the complete quantitative analysis of the Doppler shifts obtained during May 22 and 23 in Hale ARs 16862 and 16863. This will be published in the another article submitted to *Bull.Astron.Inst.*

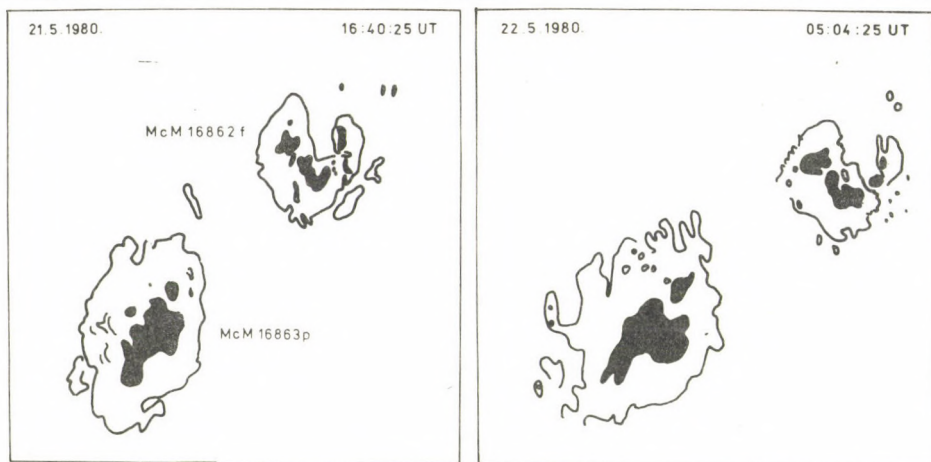


Fig. 1a.

Fig. 1b.

Fig. 1a. The photospheric images of the following spot McM 16862f and the leader of McM 16863p, observed on May 21, 1980 at 16:40:25 UT.

Fig. 1b. The same spots as on Fig. 1a, observed on May 22, 1980 at 05:04:25 UT. All white light (Fig. 1a-Fig. 5a) photospheric observations were taken in the Heliophysical Observatory Debrecen (Tab. 1).

Fig. 2a. White light observation of the spots 16862f and 16863p on May 22, 1980 at 10:30:16 UT. Note the new small spot, labeled by letter A, located on the southern edge of the penumbra 16862f. Spot A was not observed at 05:04 UT; it was seen as a faint spot at 08:50:55 UT (Tokyo).

Fig. 2b. The part of the Meudon Doppler shift map for 16862f spot measured on May 22, 1980 at 10:25:18 UT. The dashed line shows the neutral line $V_L = 0$. The dashed-point line shows the region with V_L^+ (toward the observer) larger than 400 m s^{-1} and cross-hatched region has V_L^+ larger than 800 m s^{-1} . The full line shows the region with downward V_L^- larger than 400 m s^{-1} and diagonally hatched region has V_L^- larger than 800 m s^{-1} . The site of the new spot is labeled by the letter A. The contours of umbra and penumbra are shown by a broader full line.

Fig. 2c. The part of the Meudon Doppler shift map for the 16863p spot. The meaning of the lines is the same as in Fig. 2b. The large areas in the penumbra 16863p with V_L larger than 800 m s^{-1} response to "the Evershed effect". Note the complex velocity pattern in the umbra of 16863p.

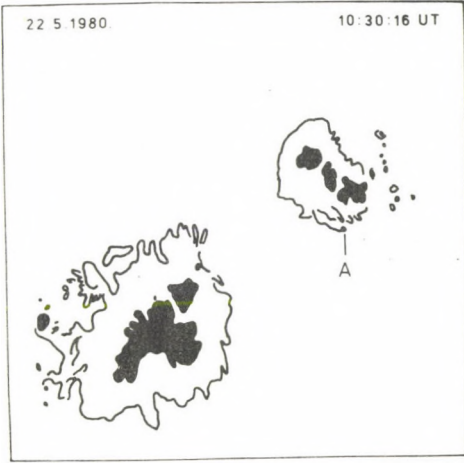


Fig. 2a.

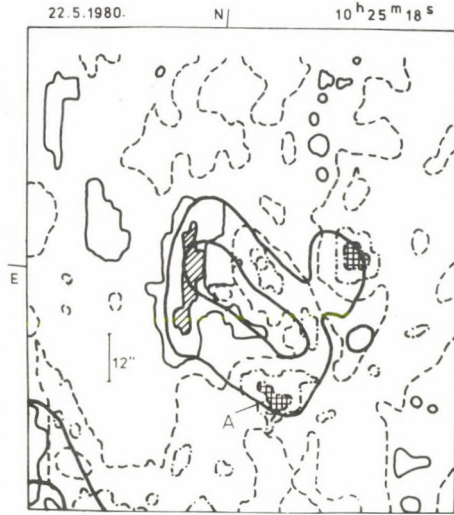


Fig. 2b.

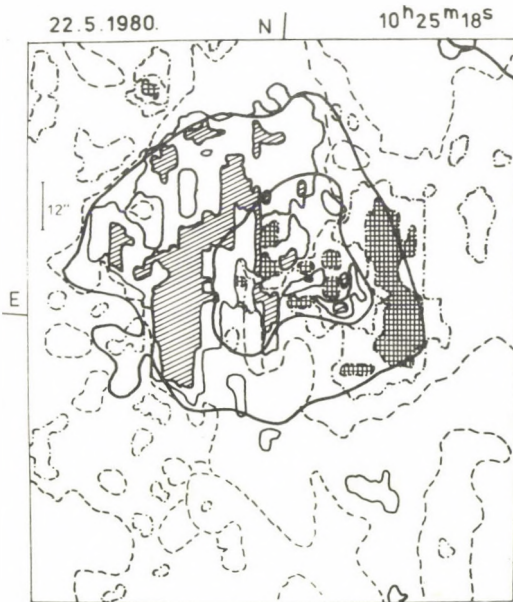


Fig. 2c.

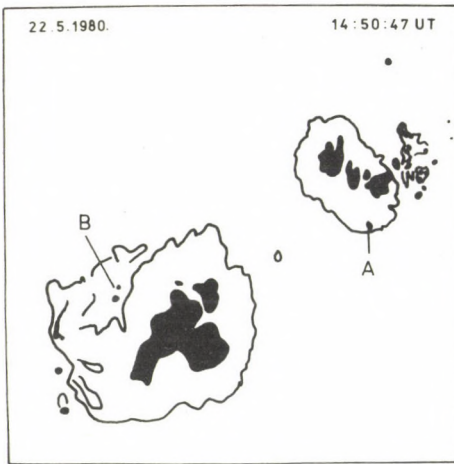


Fig. 3a.

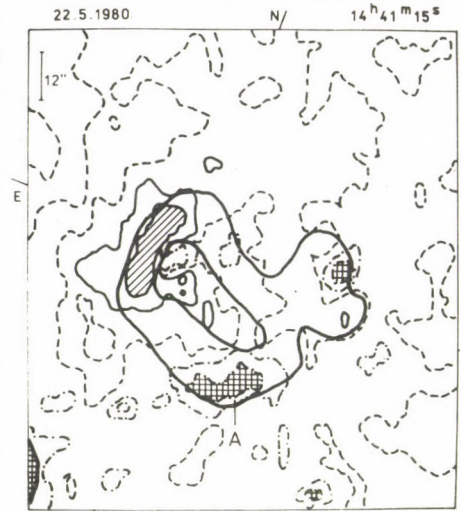


Fig. 3b.

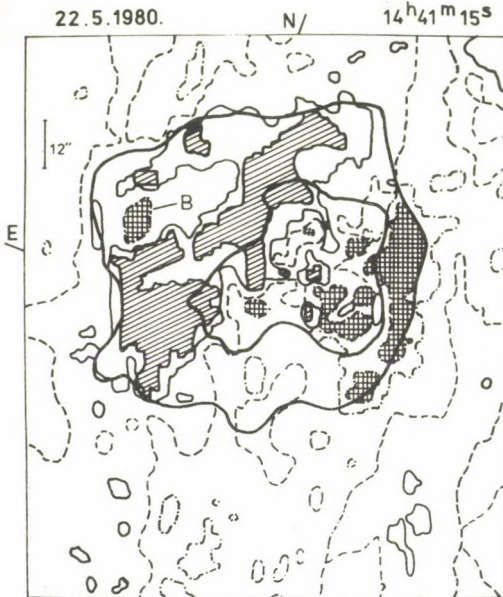


Fig. 3c.

Fig. 3c. The part of the Meudon Doppler shift map taken on May 22, 1980 at 14:41:15 UT for spot 16863p. Note that in the eastern part of the penumbra 16863p, where downward Evershed effect is expected, there is observed upward velocity region, labeled B.

Fig. 3a. The photospheric situation on May 22 at 14:50:47 UT. The spot labeled A became larger. On the north-eastern side of umbra 16863p new spots, labeled B, are observed. These spots were not seen at 10:30 UT in Debrecen photographs.

Fig. 3b. The part of the Meudon Doppler shift map for spot 16862f, taken on May 22 at 14:41:15 UT. The area with V_L^+ larger than 800 ms^{-1} related to new spot A, increased in value as compared to Fig. 2b.

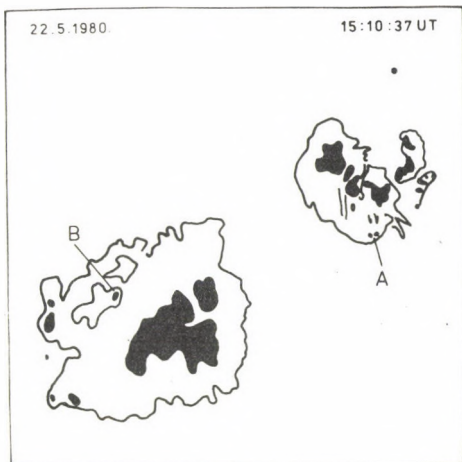


Fig. 4a.

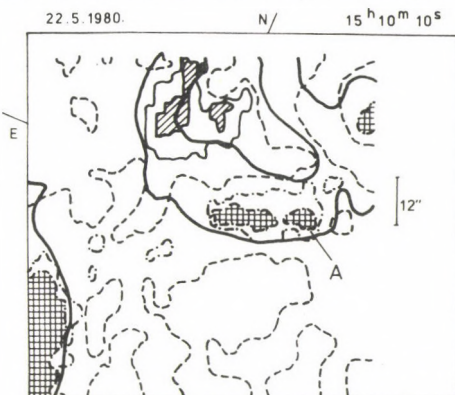


Fig. 4b.

Fig. 4a. The photospheric white light observations on May 22 at 15:10:37 UT. Difference if compare to Fig. 3a, is occurrence of the second spot in the location labeled A.

Fig. 4b. The part of the Meudon Doppler shift map for 16862f, observed on May 22, 1980, at 15:10:10 UT. Note the separation of two upward velocity areas, labeled by letter A and related to two spots in Fig. 4a.

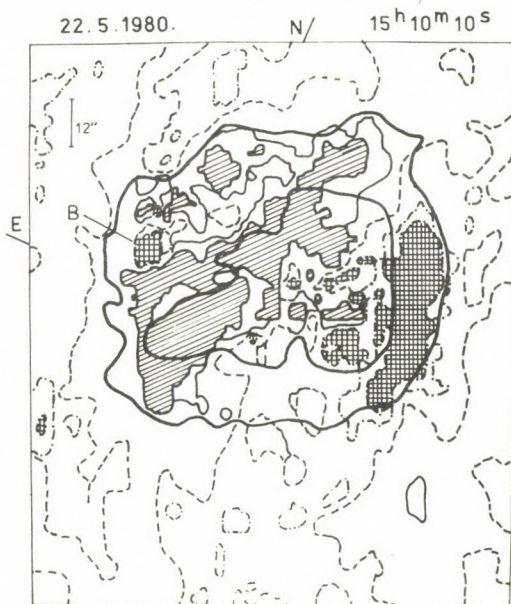


Fig. 4c.

Fig. 4c. The 16863p part of the Meudon Doppler shift map, for May 22, at 15:10:10 UT. The high upward V_L is observed in the site B.

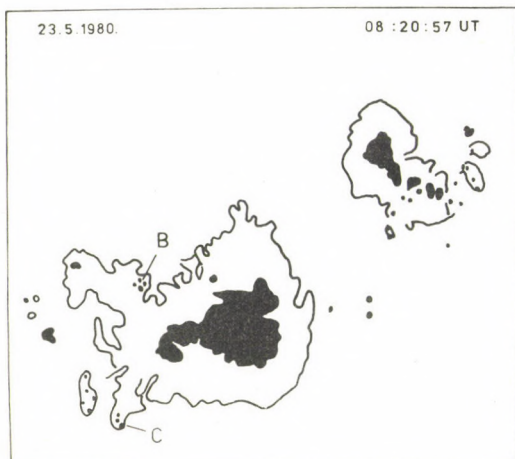


Fig. 5a.

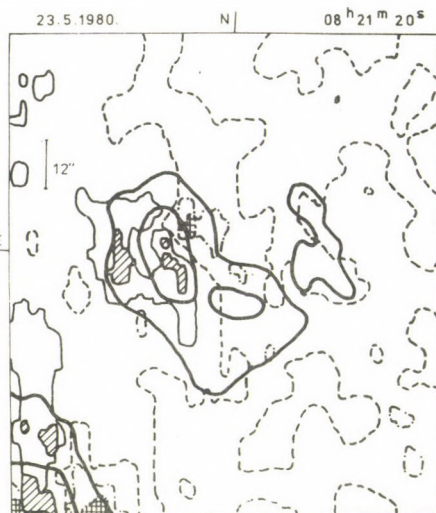


Fig. 5b.

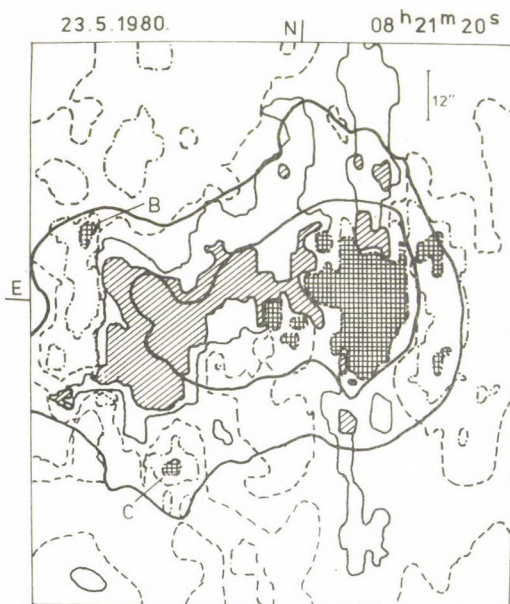


Fig. 5c.

Fig. 5a. The photospheric situation on May 23 at 08:20:57 UT. A new spot on the SE edge of the penumbra 16863p is labeled by letter C, the spot was already seen at 06:00 UT in Debrecen.

Fig. 5b. The 16862f part of the Meudon Doppler shift map, taken on May 23, 1980 at 08:21:20 UT. Note the absence of the high amplitude upward V_L velocity pattern.

Fig. 5c. The 16863p part of the Meudon Doppler shift map, observed on May 23, 1980, at 08:21:20 UT. The high upward V_L is observed in the sites B and C.

Czechosl. The focus in this article will be directed the enlargement of the vertical upward component of the velocity vector in different parts of the umbrae 16863p and 16862f and its relationship to the evolutionary properties in these sunspot groups.

The major observational problem, from this point of view, is to have good simultaneous photospheric white light and radial velocity observations. The sequence of the white light photospheric observations from May 21, 16:00 UT to May 23, 17:27 UT contains 19 white light observations, mainly from the Heliophysical Observatory Debrecen (10), Tokyo Astronomical Observatory (5), Ottawa River Observatory (2) and Skalnaté Pleso Observatory (2). Part of this white light sequence is given together with the data of the Meudon Doppler shift measurements in Table 1. From available temporal resolution of the observations, it is only possible to analyze sufficiently slowly-passing events, which continue for some hours.

The right-handed system of rectangular axes, where the xy-plane tangent to the solar surface, with the x-axis pointing in the direction of solar rotation, the y-axis tangent to a meridian to the Sun's north pole and z-axis pointing radially outwards, gives the opportunity to calculate the u , v , w components of the photospheric velocity V along these axes. When the heliographic coordinates of the sunspot are known, then the measured sight-line or longitudinal component V_L of the velocity vector V can be calculated using the formula

$$(1) \quad V_L = V(\sin\psi \cos\varphi \sin\alpha + \cos\psi \cos\alpha)$$

where α is angular heliographic distance of the spot from the centre of solar disk, ψ is angle measured between direction of the velocity vector V and the z-axis directed normally to the solar surface. φ is angle in xy-plane measured between Sun's equator parallel x (from the W to the N) to the horizontal component of the velocity vector V . From the equation (1) for the longitudinal component V_L it is possible by the least squares method to find rectangular components u , v , w of the velocity {18},{16},{17},{20}.

T A B L E 1

White light (WL) and Doppler shift (DS) photospheric observations

Date	WL		DS		Location	
	UT		UT		16862 ^f	16863 ^p
1980						
May 22	08:51	T				
	10:20	D	10:25	M	S08 E41	S12 E46
	10:30	D				
	14:51	D	14:41	M	S08 E39	S12 E44
	15:11	D	15:10	M		
May 23	04:34	SP				
	06:00	D				
	08:21	D	08:21	M	S08 E30	S12 E34

D - Heliophysical Observatory, Debrecen

M - L'Observatoire de Paris, Meudon

OR- Ottawa River Observatory

SP- Skalnaté Pleso Observatory

T - Tokyo Astronomical Observatory

T A B L E 2

Upward vertical component of velocity V^+ (m s^{-1}) of the new spots

Date	UT	A	A	B	C
		eastern spot	western spot		
1980					
May	22	10:25	1360		
		14:41	1300	1170	1550
		15:10	1430	1170	1550
	23	08:21			1220 990

In this article the analysis is only concentrated on the clear deviations of the expected behaviour of the "Evershed effect" in the penumbrae of the large spots. On May 22 and 23 the measured spots (see Table 1) are localized on the eastern side of the central meridian, in a position very favourable (45°) for measurement of the "Evershed effect".

For a simple model of the "Evershed effect" {6} it has been demonstrated on the basis of the observations of the photospheric lines that regular changes in the both radial velocities in the direction towards the observer (V_r^+) and from the observer (V_r^-) as the function of the angular distance of the spot from the solar disk center follow the relations

$$(2) \quad V_r^+ \approx 2v \sin \alpha \quad V_r^- \approx v(\sin \alpha + \cos \alpha) \quad \text{where } v = 1 \text{ km s}^{-1}.$$

These expected zones of V_r^+ and V_r^- in the photospheric penumbra of the large spots {7},{8},{13} are clearly seen on Meudon maps for spots 16864p and 16863p.

5. Results

1. From the analysis of the photospheric Doppler shifts in the umbra of 16863p spot it follows that upward V^+ and downward V^- component areas with amplitude larger than 1100 m s^{-1} during May 22, 1980 changed. The percentual distribution of the areas normalized to the area of the whole umbra as the unity were as follows

Date	V^+ larger than 1100 m s^{-1}	V^- larger than 1100 m s^{-1}
May 22, 10:25 UT	8.2%	11.4%
14:41	12.0	11.8
15:10	9.4	37.5

This large difference in the umbral downward motion at 15:10 UT is very interesting from the point of view of the occurrence of the subflare, observed in AR 16863 at 14:48 UT. With the connection of the complex umbral structure of the 16863p spot, I am reminded of the result of Seehafer et al.'s article (Proceedings of this Consultation), that the force free model was not suitable for this spot.

2. As is demonstrated in Figs. 2a-5c, at the SE edge of the penumbra of 16862 f spot, the appearance of the new small spot was observed on May 22 at 08:50 UT. Photospheric upward motion with maximal amplitude 1400 m s⁻¹ is seen from the Doppler shift measured at 10:25 UT (Table 2). The narrow connection of the upward motion and the appearance of the new spot is emphasized by the fact that when the second spot (Figs. 4a and 4b, labeled by letter A) appeared, the double structure was also clearly seen on the Doppler shift measurement (Fig. 4b).
3. The new spots, which occurred in the penumbra of 16863 p , labeled by letters B and C in Figs. 3a, 3c, 4a, 4c, 5a, 5c show the same correlation with upward motion as in point 2 (see Table 2).
4. The observed photospheric upward motions were only connected with the early phase of the appearance of the spots. As in all cases, upward component only of the velocity was observed, it is very unlikely that oscillatory motion is observed.

Acknowledgement

The author would like to thank Dr. J. Rayrole and Dr. Z. Mouradian from Meudon Observatory for Doppler shift measurements. Thanks are due to Dr. L. Dezső from the Helio-physical Observatory Debrecen, Dr. E. Hiei from Tokyo Astronomical Observatory and Dr. V. Gaizauskas from Herzberg Institute of Astrophysics for white light observations. I also wish to thank P. Bendik for preparing the figures.

R e f e r e n c e s

- {1} Adam, M.G., *M.N.* 188. 819, 1979
- {2} Antalová, A., *BAC*, 34. 96, 1983
- {3} Beckers, J.M., *Ap.J.* 213. 900, 1977
- {4} Beckers, J.M., *The Sun as a Star* (Jordan, S. ed.), *NASA SP-450*, p.11. 1981
- {5} Bhatnagar, A., *Kodaikanal Obs. Bull. Series A*, No. 180. 1967
- {6} Bumba, V., *Izv. KrAO*. 23. 253, 1960
- {7} Bumba, V., *BAC*, 14. 1, 1963

- {8} Bumba,V., in *The solar spectrum* (de Jager,C.ed.) p.266. D Reidel,1965
- {9} Bumba,V., *BAC*, 18. 238, 1967
- {10} Bumba,V., Suda,J., *BAC*, 34. 155, 1983
- {11} Gaizauskas,V., *Adv.Space Res.2. No.11.* 11, 1983
- {12} Gopasyuk,S.I., *Izv.KrAO.35.* 1967
- {13} Gopasyuk,S.I., *Izv.KrAO.66.* 77, 1983
- {14} Ioshpa,B.A., Ishkov,V.N., Mogilevsky,E.I., Nikolskaja,K.I., Starkova, L.I., Utrobin,B.G., Bulavina,V.I., Delone,A.B., Kirjuchina,A.I., Makarova,E.A., Mitropolskaja,O.N., Jakunina,G.V., Korobova,Z.B., Stepanjan,N.N., Koval,A.N., Bachmann,G., Pflug,K., Hoffmann,A., *FCM-SMY Crimean Workshop, 2.* 134, 1981
- {15} Ishkov,V.N., Kulcar,L., *BAC*, 34. 277, 1983
- {16} Kinman.T.D., *M.N.112.* 425, 1952
- {17} Kinman,T.D., *M.N.113.* 613, 1953
- {18} Plaskett,H.H.,*M.N.112.*414, 1952
- {19} Rayrole,J., in *Proceedings of the Japan-France seminar on Solar Physics* (Moriyama,F., Héroux,J.C.,eds.) 258, 1981
- {20} Servajean,R., *Ann.Astrophys.24.* 1, 1961

SUNSPOT PROPER MOTIONS
IN THE WESTERN PART OF HALE REGION 16864
(MAY 25 - 29, 1980)

I. N A G Y
Heliophysical Observatory, Debrecen

СОБСТВЕННЫЕ ДВИЖЕНИЯ СОЛНЕЧНЫХ ПЯТЕН
В ЗАПАДНОЙ ЧАСТИ АКТИВНОЙ ОБЛАСТИ ХЕЙЛ № 16864
(25 - 29 МАЯ, 1980 Г)

И. НАДЬ
Гелиофиз.Обс., Дебрецен

In Hale region 16864, on 26 May a new activity started close NW to the large old main p spot of Mount Wilson group No 21469 and two days later a series of important flares occurred there. Earlier on the basis of 14 white-light photo-heliograms a short note has been published {1} on the spot developments and motions of this small but active flare region. Some of our preliminary results have already been quoted in a review paper by V.Gaizauskas {2}. Since then I have studied once again the spot motions of this interesting flare region in more detail using 128 heliograms, taken with the 6" photo-heliograph at our observing station in Gyula.

Exact position measurements by means of an Ascorecord measuring instrument were made on the available photographic material of observations on which the solar diameter is about 10 cm. All umbrae and pores marked in Figs.1 and 2 were measured and their heliographic coordinates (B,L) determined (as usually

we do it in Debrecen, cf. e.g. {3}).

During May 25-29 the large p spot (Fig.1) moved in the Carrington coordinate network only 0.2° to E and 0.1° to S, with the average velocity of 0.03 km s^{-1} . Therefore all velocities, along solar parallels and meridians, relative to this large stable nucleus of umbra (I) of the main p spot of Mt.W. group 21469 are calculated (i.e. in the Figs. L-L_I and B-B_I data are given).

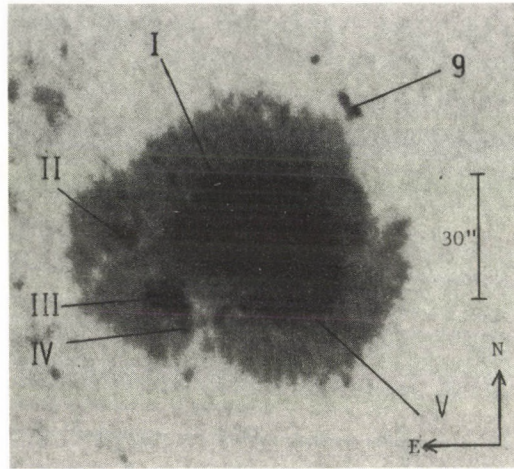


Fig.1. The main p spot of sunspot group Mt.W. No 12469 on May 25, 1980 (at 8:18 UT)

Fig.2. The region of new spot emergence close to the NW limb of penumbra of the large spot shown in Fig.1, during a period of 4 days. In the drawings only those spots are marked which could be identified and followed with absolute certainty for a reasonable period on successive heliograms. (Wherever possible the same designations are used as in {1}. This Figure supersedes Fig.2 in {1}.)

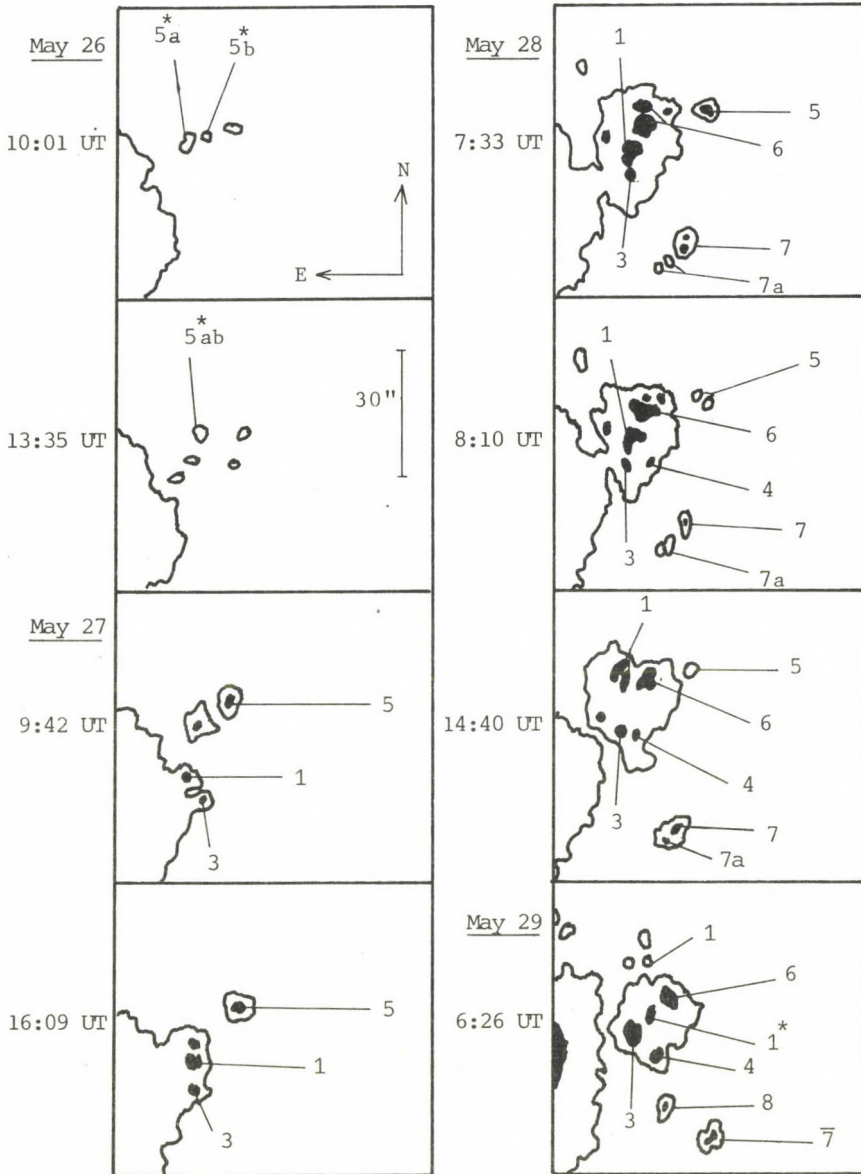
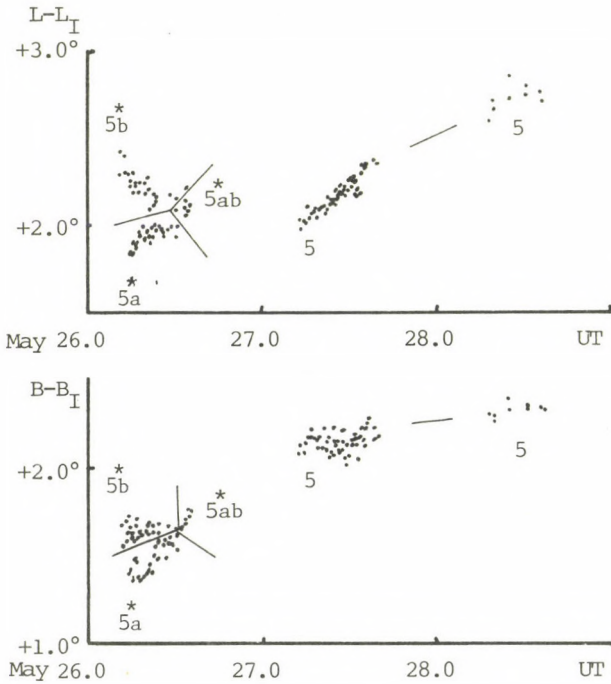
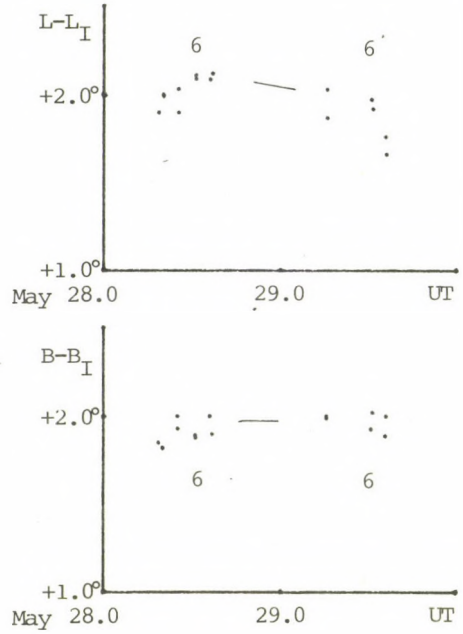


Fig.2.

Fig. 3. Heliographic coordinates relative to umbra I versus time of the f polarity spots 5, (5*) and 6.

(Here the magnetic polarity is N, i.e. +)



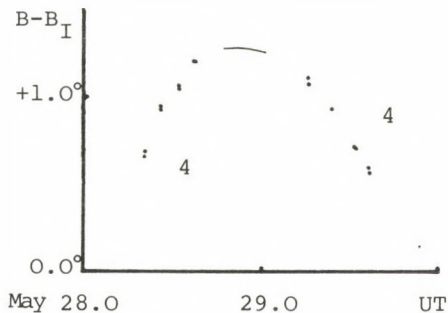
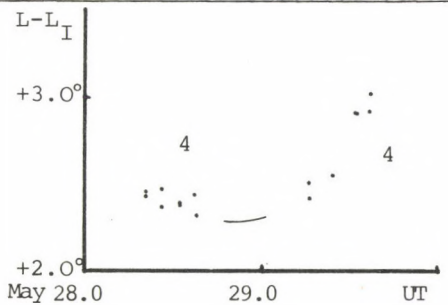


Fig.4. Heliographic coordinates relative to umbra I versus time of the p polarity spots 4, 7, and 8.

(Here the magnetic polarity is S, i.e. -)

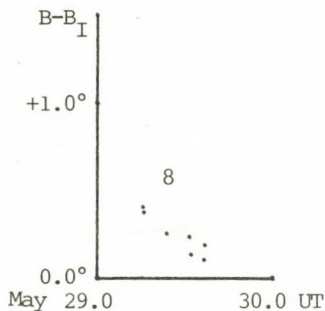
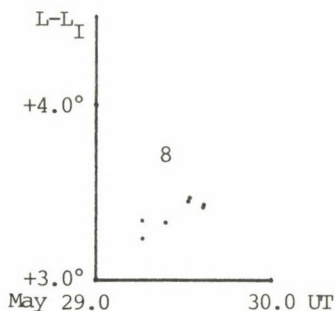
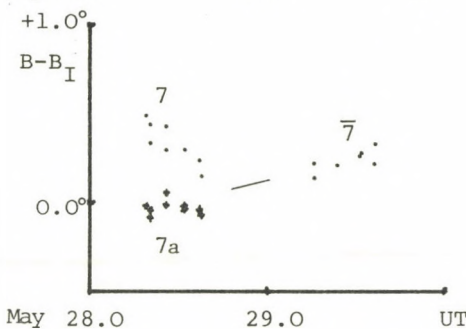
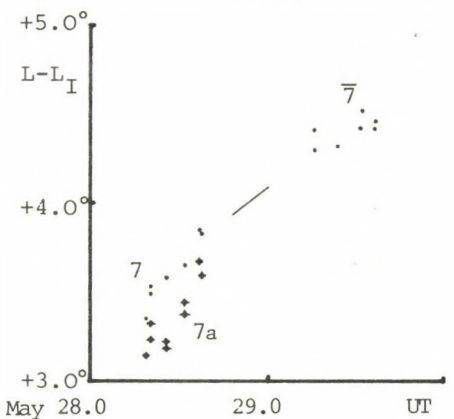
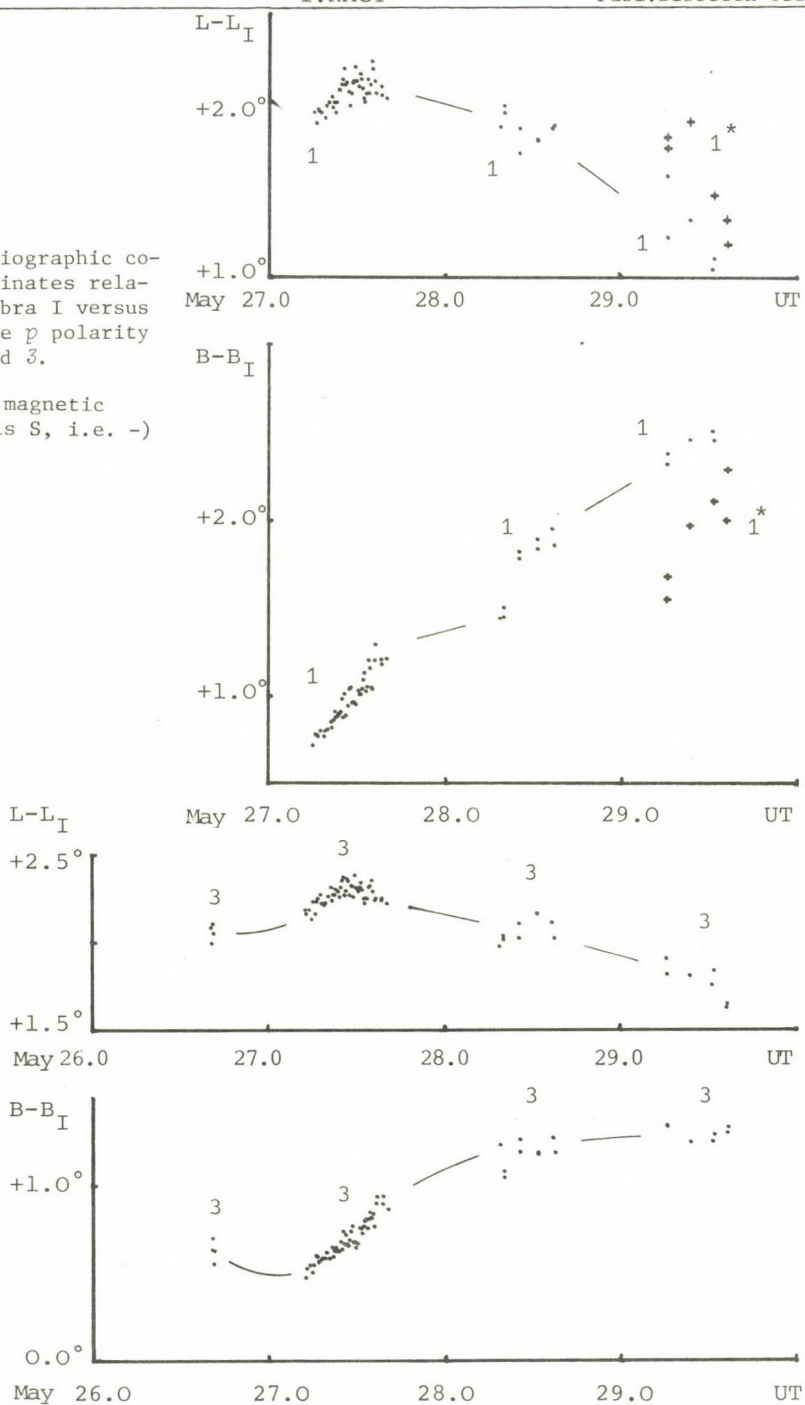


Fig. 5. Heliographic coordinates relative to umbra I versus time of the p polarity spots 1 and 3.

(Here the magnetic polarity is S, i.e. -)



T A B L E 1

Average velocities over 2 days, concerning the motion of two umbrae, within the penumbra of the old *p* spot Mt.W. No 16864, and that of spot 9 of *N* polarity (cf.Fig.6).

May	25	26	27	28
Umbra		$km\ s^{-1}$	$km\ s^{-1}$	$km\ s^{-1}$
III		0.05	0.04	0.03
IV		0.05	0.06	0.13
9		0.14	0.09	
n		61	100	58

T A B L E 2

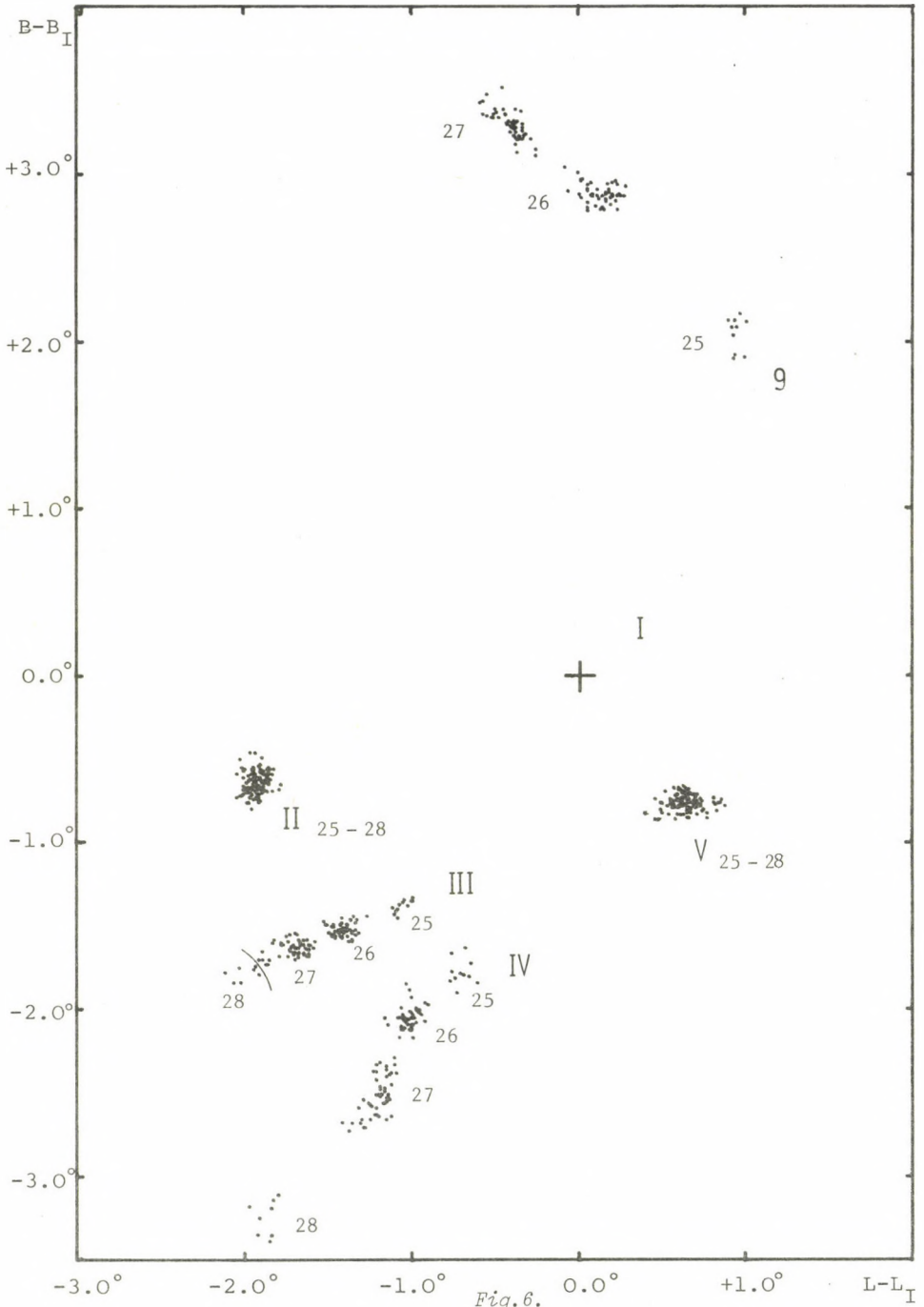
Velocities of daily motion of the small *S* polarity spots of the new spot group.

May	28	toward	n	29	toward	n
Spot	$km\ s^{-1}$			$km\ s^{-1}$		
4	0.24	<i>N</i>	8	0.29	<i>SW</i>	7
7a	0.18	<i>W</i>	9	0.06	<i>W</i>	7
7	0.20	<i>SW</i>	8			
8				0.20	<i>SW</i>	8

T A B L E 3

Velocities of spot motion within the common penumbra of new formation, on May 28-29.

May 27		28		29		
(5:11-16:11 UT)		(7:32-14:59 UT)		(6:22-14:41 UT)		
Spot polarity	no	$\frac{dB}{dt}$	$\frac{dL}{dt}$	$\frac{dB}{dt}$	$\frac{dL}{dt}$	
		$km\ s^{-1}$	$km\ s^{-1}$	$km\ s^{-1}$	$km\ s^{-1}$	
		(n)	(n)	(n)	(n)	
		$km\ s^{-1}$	$km\ s^{-1}$	$km\ s^{-1}$	$km\ s^{-1}$	
<i>S</i>	1	+0.16	+0.20	+0.07	-0.17	Detached parts of the old <i>p</i> spot
	1*	+0.06 (44)	-0.06 (9)	+0.21	-0.21 (6)	
<i>N</i>	5	+0.01	+0.11 (50)			Spots of the new group
	6		+0.04	-0.02	-0.07 (6)	



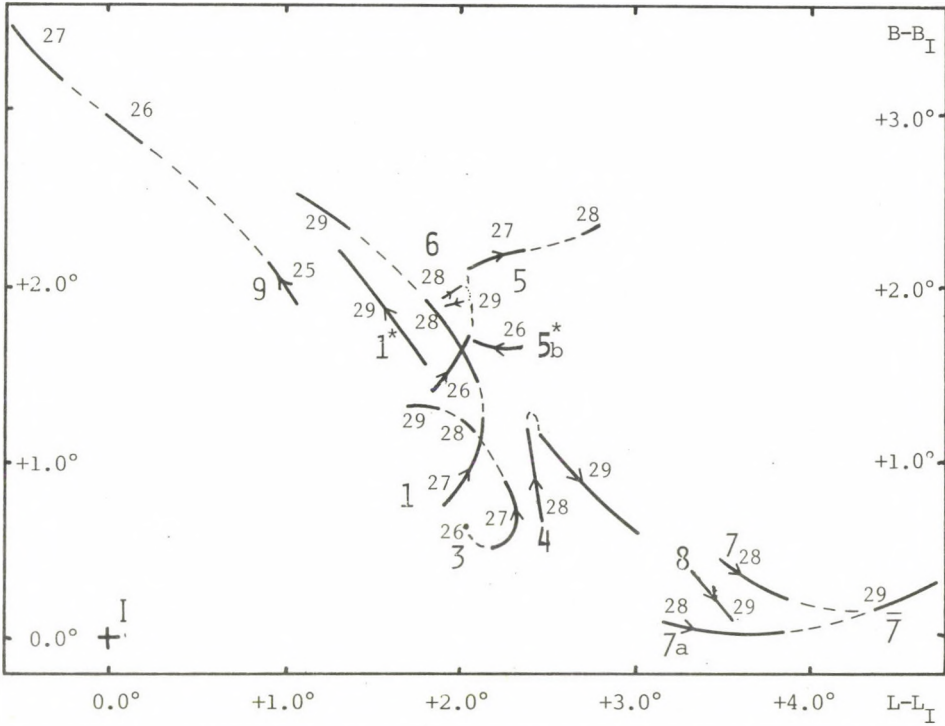


Fig.7. The typical trajectories of the average principal spot motions NW to umbra I in the period 25 - 29 May. (+ shows the center of gravity of umbra I. The zero point of the heliographic coordinate network is at +.)

Next to each trajectory the large number shows the designation of the spot according to Fig.2, while the days of observation are given by small numbers.

(This Fig. supersedes Fig.3. in {1}, and Fig.18 in {2}.)

Fig.6. Positions of umbrae II-V and that of spot 9 relative to the large stable nucleus of umbra I (+) in the period May 25 - 28. (The differences in heliographic coordinates are shown.)

Examining the Figs.3-6 it is possible to follow the rough outline of the whole rapid development in the photospheric level of the solar active region in question. The first pores of the new spot group NW to the old p spot were first observed at 6:01 UT on 26 May ($5a^*$, etc. in Fig.2). This time these pores did not show any special motion but later on and the following day some new umbrae appeared. A new umbra (6) was born between umbrae 1 and 5 overnight May 27- 28.

The most important development was during the morning of May 28. Umbra 1 had a large motion already on May 27 and on the 28th it was moving close to umbra 6 , of opposite polarity, forming a δ -configuration. Before the important series of homologous flares the velocity of approach of umbra 1 and umbra 6 was 0.21 km s^{-1} . Around the end of our observations (14:59 UT) the distance between these umbrae were only about $3 \cdot 10^3 \text{ km}$.

The spot velocities given in Tables 1-3 were determined by linear fits and also their standard deviations were calculated if the number of observations were high enough, i.e. in Table 1 and in the first column of Table 3. In all these cases the value of the standard deviations is 0.01 km s^{-1} . The error of all other velocities given may be estimated $\pm 0.03 \text{ km s}^{-1}$. (n - is the number of observations used for the velocity calculation in Tables 1-3.)

Fig.7 summarize the most important spot motions which were undoubtedly precursors of the great flare event of May 28, 1980.

Thanks are due to Prof.L.Dezső for suggesting this work and for his help.

R e f e r e n c e s

- {1} A.Kovács, I.Nagy, R.Bukovinszki, A note on the activity in the SESC Region 2470. *IMC-SMY Crimean Workshop 2*, 232, 1981
- {2} V.Gaizauskas, The relation of solar flares to the evolution and proper motions of magnetic fields, *Adv.Space Res. 2*, No.11, 11, 1982
- {3} I.Nagy, A.Ludmány, The birth and development of a regular bipolar sunspot group, *Publ.Debrecen Obs. 4*, 3, 1980.

POSSIBLE MAGNETIC RECONNECTION
IN THE SOLAR ACTIVITY COMPLEX OF MAY 1980

N. S E E H A F E R

"Einsteinurm" Solar Obs., Potsdam

Abstract:

Flare observations in the activity complex HR 16862, 16863, 16864 at the end of May 1980 are compared with the structure of force-free magnetic fields calculated from photospheric magnetograph measurements. The calculations suggest that a series of homologous flares connected with a δ -configuration in the NW of the leading spot of HR 16864 is caused by a magnetic neutral sheet. A second series of homologous flares, observed in the umbra of the leading spot of 16863 and in the trailing spot of 16862, seems to be produced by magnetic restructuring due to non-evolutionarity of the field.

ВОЗМОЖНОЕ МАГНИТНОЕ ПЕРЕСОЕДИНЕНИЕ
В СОЛНЕЧНОМ АКТИВНОМ КОМПЛЕКСЕ МАЯ 1980 Г.

Н. ЗЕЕХАФЕР

Солн.Обс. "Эйнштейнтурм", Потсдам

Абстракт:

Наблюдения вспышек в комплексе активных областей HR 16862, 16863, 16864 в конце мая 1980 г. сравнили с структурой бессимметричных магнитных полей, определенных из фотосферных магнетографических измерений. Результаты вычислений указывают на существование магнитного нейтрального слоя, который причинял серию гомологичных вспышек связанные с δ -конфигурацией в северо-западе лидера группы 16864. Причиной второй серии гомологичных вспышек наблюдаемые в ядре лидера группы 16863 и в хвостовом пятне группы 16862 вероятно является изменение структуры магнитного поля вследствие не-эволюционности магнитного поля.

1. Introduction

It is generally assumed that the energy released in a solar flare is stored in the magnetic field of the active region prior to the flare onset. The conversion of the magnetic energy into heat and directed particle energy is accomplished by magnetic reconnection in most models. Such models have been developed with reconnection at neutral current sheets between oppositely directed magnetic fields which are convected toward each other {13},{5} or inside loop structures {18}.

Now the mere fact that magnetic energy is dissipated does not imply that regions with finite electrical conductivity must be present. Mass motions can be explained by the action of Lorenz forces, heating by adiabatic compression, and the acceleration of charged particles by inductive electric fields due to rapidly changing magnetic fields.

There is, however, some indirect theoretical evidence that the slow passive evolution of the active region magnetic field can lead to situations in which reconnection necessarily develops. Because of the dominance of the magnetic pressure over the gas pressure an equilibrium magnetic field must be force-free. Two-dimensional studies of series of force-free equilibria show the occurrence of critical points at which different solution branches with different topological properties merge and/or beyond which equilibrium solutions do not exist {10},{8},{1},{14},{6}. One may take the view that a flare is triggered when a magnetic configuration which evolves quasi-statically in response to changing photospheric boundary conditions reaches such a critical point. During the transition from one equilibrium configuration to another with different topology reconnection will occur.

The present study compares flare observations in the activity complex HR 16862, 16863, 16864 at the end of May 1980 with the structure of three-dimensional force-free magnetic fields calculated from photospheric magnetograms. The calculations suggest that a series of strong homologous flares connected with a delta configuration in HR 16864 is caused by a

magnetic neutral sheet. A series of homologous umbral flares in HR 16862 and 16863 seems to be produced by magnetic restructuring due to non-evolutionarity of the above described type.

2. Observations

The complex HR 16862, 16863, 16864 was one of the targets of the FBS program of the Solar Maximum Year and is very well studied {2},{3},{7},{12},{11},{4},{17}. This consists of three bipolar active regions (Fig.1). Flare activity was observed at many places. Two of these are considered here:

- a) In the N-W of the large leading spot of HR 16864 a small positive magnetic feature surrounded by negative magnetic fields is situated (Fig.1). It began to emerge on 26 May and formed a delta configuration on 27 May. On 28 and 29 May a series of highly localized homologous flares erupted here. The main $H\alpha$ flaring was over the delta and over the penumbra of the main spot.
- b) Between 25 and 29 May a series of homologous flares in the umbra of the (negative) leading spot of HR 16863 was observed, with synchronous flaring in the (positive) trailing spot of HR 16862. The two flare sites were connected by arch filament systems.

3. Calculated three-dimensional magnetic structure

Using the method of Seehafer {15}, three-dimensional force-free magnetic fields with constant α (of the equation $\nabla \times B = \alpha B$) have been calculated with the magnetogram of Fig.1 as boundary data. Fig.2 shows lines of force calculated for three values of the parameter α . Comparison with $H\alpha$ photographs indicates that α is positive and its absolute value between 0.005 and 0.01 arcsec⁻¹ (Figs.2b and 2c). The three bipolar regions are magnetically connected with each other.

The vertical scaling of the field is given in Fig.3; the magnetic energy content of the region in dependence on the parameter α (with the vertical field component fixed at the photosphere) in Fig.4.

. At the places of the two series of homologous flares the

field calculations yield interesting results:

- a) Fig.5 shows field lines starting from a relatively fine mesh of foot points in rectangular photospheric area containing the positive island in the N-W of the leading spot of 16864 together with somewhat of its negative surrounding. There is a clear difference between the eastern and the western parts of the quasi-circular zero line. In contrast to the eastern part, the western part is not bridged by field lines. Except for some very short field lines crossing the northern boundary, all field lines starting from inside the island run east to the main spot. Field lines starting from foot points west of the island run to the western boundary of the active region. That is, at the western boundary of the island a magnetic neutral sheet is situated.
- b) In Figs.2a and 2b a system of fieldlines is visible connecting the negative polarity of HR 16863 with the positive polarity of HR 16862. It corresponds to the arch filament system connecting the flare places in the umbra of the leader of HR 16863 with those in the trailing spot of HR 16862. Now look for these field lines in Fig.2c, where field lines for a larger value of α are displayed. The field topology has drastically changed. Now most of the considered field lines are high reading and run from the umbra of HR 16863 to far distant points in the eastern part of the region.

4. Discussion

The region west of the delta is relatively field-free. This seems to be one of the reasons why nearly all flux from the positive island is connected to the main spot in the E (but not the only reason; for the positive feature in the S-W of HR 16863 a corresponding field structure was not found!). The field structure encountered here for the delta is in good agreement with the observation that in delta configurations consisting of a parent spot and a satellite spot the satellite has practically no penumbra at its outer boundary {9}. It may be that the flare productivity of such delta configurations is generally due to the presence of neutral sheets at the penumbra-free

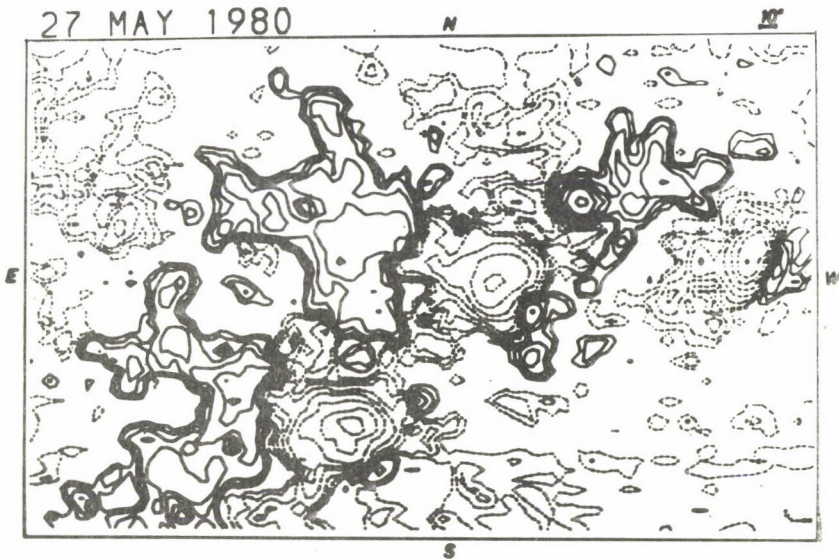


Fig.1. Photoelectric longitudinal magnetogram obtained at the solar observatory Einsteinurm in Potsdam on 27 May 1980, with a resolution of 6.1" in the N-S and 4.0" in the E-W direction. Contour levels are 20, 40, 80, 160, 320, 640, 1280, and 2560 G. Solid contours refer to positive fields, dashed to negative. HR 16862 is the bipolar region in the N-E part. 16863 that in the central part, and 16864 that in the S-E part. Large spots were situated in the negative polarity 16862, the positive polarity of 16862, the negative polarity of 16863, and the negative polarity of 16864. In these four spots the magnetic field measurements have been corrected for stray light (7% in the spot centres).



Fig. 2a.



Fig. 2b.

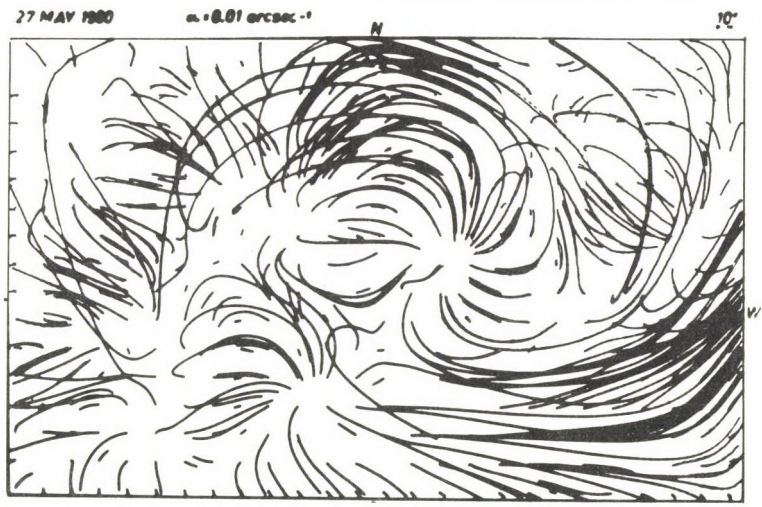


Fig. 2c.

Fig. 2a - 2c. Overview of the lines of force above the region of Fig. 1 for three values of the parameter α .

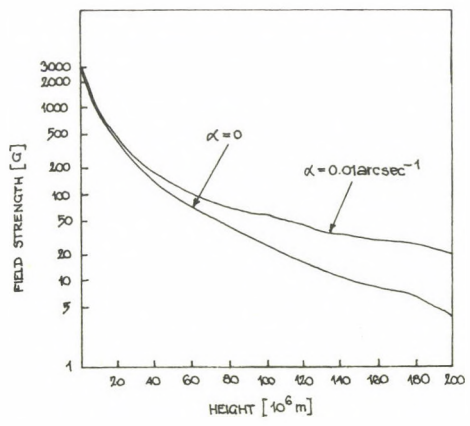


Fig. 3. Height dependence of the maximum field strength (of a given height level) for the potential field and a non-potential force-free field.

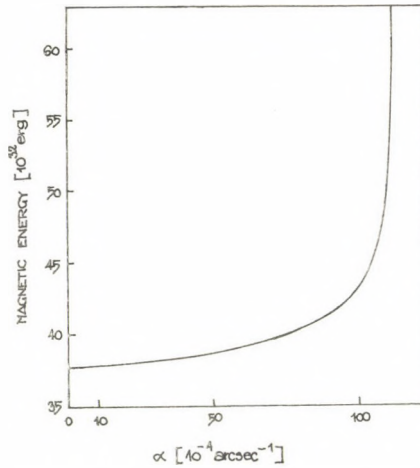


Fig. 4. Dependence of the magnetic energy content of the region on the parameter α . The unrealistically steep increase as $\alpha^2 \rightarrow \alpha_{\max}^2 = \pi^2 (L_x^{-2} + L_y^{-2})$, L_x and L_y denoting the extents of the magnetogram in both directions, is due to the boundary conditions of the used solution.

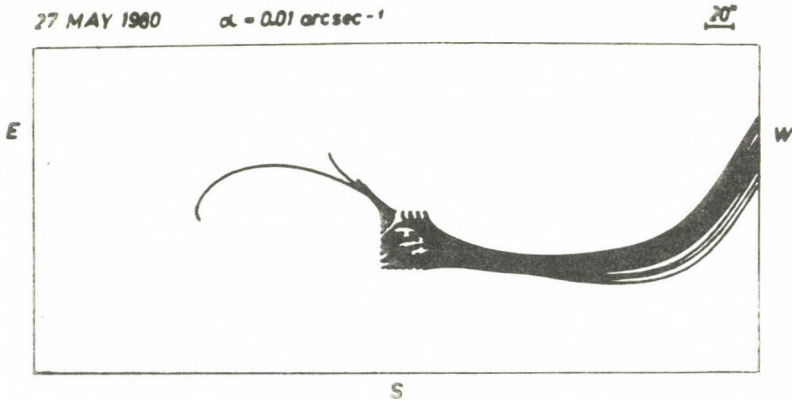


Fig. 5. Field lines starting from an rectangular area containing the positive isle in the N-W of the large leading spot of 16864 in its interior. At the western part of the boundary of this isle a neutral sheet is situated.

outer boundary of the satellites.

For an active region of July 1973, Seehafer and Staude [16] found a similar example (no delta configuration) with a magnetic neutral sheet producing chromospheric activity. In that case motions were observed pressing opposite fluxes together at the neutral sheet. Also in the present case motions were obviously present: New flux was emerging at the delta. Furthermore, the differential rotation of the Sun will lead to shearing motions at the sheet (complexes with strong fields undergo rigid rotational motions).

The parameter α of the force-free field is a measure of the extractable magnetic energy (Fig.4). When energy is fed into the field due to photospheric motions, α increase. In the case of the loop system connecting the leading spot of HR 16863 with the trailing spot of HR 16862 this increase is connected with changes in the magnetic field topology which are impossible under the frozen-in condition. It may be that (non-force-free) singular current sheets develop enabling the topological change in the overall magnetic structure. It seems more probably, however, that the considered development does not take place and that eruptive processes set in instead.

R e f e r e n c e s

- {1} Birn, J., Goldstein, H., Schindler, K., A theory of the onset of solar eruptive processes, *Solar Phys.* 57. 81, 1978
- {2} Gaizauskas, V., *The Crimean Solar Maximum Year Workshop*, Stanford University, SUIPR Report No.841. 17. 1980
- {3} Gaizauskas, V., *Progress report of FBS action Interval*, 2. 1981
- {4} Golovko, A.A., Kasinsky, V.V., Klochek, N.V., Magnetic fields and general space and time characteristics of the evolution and flare activity in the 21-29 May complex, (in Russ.) *ICM-SMY Crimean Workshop*, 2. 170, 1981
- {5} Heyvaerts, J., Priest, E.R., Rust, D.M., An emerging flux model for the solar flare phenomenon, *Ap.J.* 216. 123, 1977
- {6} Heyvaerts, J., Lasry, J.M., Schatzman, M., Witcnsky, P., Blowing up of two-dimensional magnetohydrostatic equilibria by an increase of electric current or pressure, *Astron. Astrophys.* 111. 104, 1982
- {7} Ioshpa, B.A., and 17 co-authors, The evolution of the complex of the active regions AR 16862-16864 in May 1980, (in Russ.) *ICM-SMY Crimean Workshop*, 2. 134, 1981

- {8} Jockers, K., Bifurcation of force-free solar magnetic fields: a numerical approach, *Solar Phys.* 56. 37, 1978
- {9} Künzel, H., Personal communication, 1983
- {10} Low, B.C., Evolving force-free magnetic fields. I. The development of the preflare stage, *Ap.J.* 212. 234, 1977
- {11} Makarova, E.A., and 9 co-authors, Some features of preflare situation in the complex HR 16862, 16863, 16864 on the 23-29 of May 1980, *ICM-SMY Crimean Workshop*, 2. 162, 1981 (in Russ.)
- {12} Mogilevsky, E.I., Homologous H α -flares in the umbra of AR complex MM-16862-3 in May 1980, (in Russ.) *ICM-SMY Crimean Workshop*, 2. 151, 1981
- {13} Petschek, H.E., Magnetic field annihilation, *AAS-NASA symposium on the physics of solar flares*, NASA SP-50, 425, 1964
- {14} Priest, E.R., Milne, A.M., Force-free magnetic arcades relevant to two-ribbon solar flares, *Solar Phys.* 65. 315, 1980
- {15} Seehafer, N., Determination of constant α force-free solar magnetic fields from magnetograph data, *Solar Phys.* 58. 215, 1978
- {16} Seehafer, N., Staude, J., Evidence for an X-type neutral sheet producing chromospheric activity, *Solar Phys.* 67. 121, 1980
- {17} Shilova, N.S., and 9 co-authors, H α umbral flares of the end of May 1980, (in Russ.) *ICM-SMY Crimean Workshop*, 2. 180, 1981
- {18} Spicer, D., An unstable arch model of a solar flare, *Solar Phys.* 53. 305, 1977

TIME VARIATION OF THE DIFFERENTIAL EMISSION MEASURE
OF HOT FLARE PLASMA

J. JAKIMIEC, R. MEWE, J. SCHRIJVER,
Astron. Observatory, Wrocław Space Res. Lab., Utrecht
J. SYLWESTER, B. SYLWESTER
Space Res. Center, Wrocław

Abstract:

We have investigated details of the time evolution of the flare differential emission measure (DEM) distribution in the temperature range 10-50 MK using high-resolution X-ray spectra recorded by the Bent Crystal Spectrometer aboard the Solar Maximum Mission satellite. We have found that for big flares the local maximum in the DEM distribution is systematically broader during the phase of flare increase than during the phase of decay. We have shown that this systematic effect is a result of development of a hot "wing" of the DEM local maximum during flare increase and its disappearance during flare decay. It turned out to be convenient to display the DEM evolution in a two-temperature diagram, \bar{T}_1 vs. \bar{T}_2 , where \bar{T}_1 and \bar{T}_2 are the values of the electron temperature calculated from the line ratio in the Fe XXV and Ca XIX spectrum, respectively.

ВРЕМЕННЫЕ ВАРИАЦИИ ДИФФЕРЕНЦИАЛЬНОЙ МЕРЫ ЭМИССИИ
ГОРЯЧЕЙ ВСПЫШЕЧНОЙ ПЛАЗМЫ

Я. ЯКИМЕЦ Р. МЕВЕ, Я. ШРИЙВЕР,
Астрон. Обс., Вроцлав Косм. Лаб., Утрехт
Я. СИЛЬВЕСТЕР, Б. СИЛЬВЕСТЕР
ЦНИ, Вроцлав

Абстракт:

Детально исследовано временное поведение распределения дифференциальной меры эмиссии ДМЭ во вспышках в температурном диапазоне 10-50·10⁶К на основании анализа рентгеновских спектров высокого разрешения, полученных на спутнике SMM при помощи спектрометра с изогнутым кристаллом. Найдено, что для больших вспышек ширина максимума распределения ДМЭ обычно больше для фазы нарастания, чем для фазы затухания вспышки. Показано, что этот эффект является следствием развития высокотемпературного "крыла" максимума распределения ДМЭ во время нарастания и его исчезновения во время фазы затухания. Показано, что наглядное представление об изменении распределения ДМЭ во время вспышки дает двумерная диаграмма, на которой определенные моменты развития вспышки характеризуются температурами \bar{T}_1 и \bar{T}_2 , где \bar{T}_1 и \bar{T}_2 - электронные температуры, вычисленные по отношению интенсивностей сателлитов к резонансной линии в спектрах FeXXV и CaXIX соответственно.

Investigations of X-ray and EUV flare spectra clearly show that the hot flare plasma ($1 < T_{(MK)} < 100$) is not isothermal, i.e. that there is some temperature distribution of the plasma. It is convenient to describe the distribution in terms of the differential emission measure (DEM) $\phi(T)$

$$\phi(T) = \frac{d \int N_e^2 dV}{dT} \quad (1)$$

Previous calculations of the hot flare plasma DEM (cf. {2}) showed that a local maximum in the temperature range $T > 10$ MK is a characteristic feature of flare DEM distributions. The spectra taken with the Bent Crystal Spectrometer (BCS) of the X-ray Polychromator on the Solar Maximum Mission (SMM) satellite (see {1}) provide a unique opportunity to investigate extensively the time evolution of this local maximum for various flares. Such a detailed investigation of the time development of the DEM is very important for a better understanding of the flare thermodynamics and specifying the mechanisms of flare heating.

We have calculated the DEM distributions by means of an iterative procedure worked out by Withbroe {6} and adapted to the hot flare plasma analysis by Sylwester {3} and Sylwester et al. {4}. Usually we have used 150 iteration steps, but some calculations have been performed with a larger number of steps to test the convergence of the procedure for the data set used here.

For the analysis we have used a set of spectral lines, which was chosen earlier as a group of lines suitable for flare diagnostics with the BCS (see {5}). Analysis of the emission functions of lines in Table 1 and calculated DEM distributions shows that this set allows the reliable determination of the DEM values in the temperature range between 10 - 50 MK. The integration time of the BCS spectra has been taken between 10 and 60 s depending on the flare intensity.

T A B L E 1

The specification of lines used in DEM calculations

No	λ [Å]	Ion trans.	Excitation	
1	1.8509	Fe XXV w	E	N.B. Here E means direct electron impact excitation, DR - excitation by the dielectronic recombination and IE - innershell excitation by electron impact. Note that the lines may contain some contribution from higher ($n \geq 3$) lithium-like DR satellite lines.
2	1.8610	Fe XXIV q	IE	
3	1.8662	Fe XXIV j	DR	
4	1.8729-47	Fe XXIII	DR	
5	1.8831-38	Fe XXII	DR	
6	3.1769	Ca XIX w	E	
7	3.2057	Ca XVIII k	DR	
8	3.2000	Ca XVIII q	IE	

We have found the following characteristic features of the DEM evolution:

- 1) The maximum of the DEM distribution for a given flare shifts towards higher temperatures during the flare growth and towards lower temperatures during decay of the flare. This is connected with the well-known fact of increase and subsequent decrease of the mean plasma temperature during the flare development.
- 2) The widths of the DEM distributions are systematically larger during the flare growth than during its decay. This means that the dispersion of the temperatures is larger during the flare growth than during flare decay (around the same mean temperature). This effect is the principal new result of the present investigation. It is illustrated in Fig.1.

It is most probable that the broadening of the DEM distributions during the flare growth result from strong plasma heating during this phase and we hope that this effect will help the understanding of the mechanism of flare heating.

To investigate the effects more comprehensively we have tried to find parameters which would be suitable to describe quantitatively such details of the DEM evolution. Standard "isothermal" temperatures \tilde{T}_i as determined from the intensity ratios of two pairs of iron and calcium lines, turned out to be appropriate for this purpose. The temperatures, \tilde{T}_i

($i=1$ for Fe and $i=2$ for Ca), were calculated from the ratios of the intensity of an appropriate dielectronic satellite line (line j in the Fe spectrum and line k in the Ca spectrum) to the intensity of the resonance line. The temperatures \tilde{T}_i are connected with the DEM distribution, $\varphi(T)$, in a rather complicated way, i.e.:

$$\frac{f_d(\tilde{T})}{f_r(\tilde{T})} = \frac{\int f_d(T) \varphi(T) dT}{\int f_r(T) \varphi(T) dT} \quad (2)$$

where $f_d(T)$ and $f_r(T)$ are the emission functions (see {4}) of the dielectronic satellite and the resonance line, respectively. Nevertheless, our empirical investigation showed that the parameters \tilde{T}_i are very convenient for our purposes. Moreover, \tilde{T}_i is a very sensitive indicator of the development of the high temperature wing in the DEM distribution.

The parameters \tilde{T}_1 and \tilde{T}_2 are very useful in presenting the DEM evolution for a given flare in a \tilde{T}_1, \tilde{T}_2 - diagram. For example, in Fig.2, such a diagram is shown for the large *X1/1B* flare of 14 July 1980. The part ABCD of the curve in this Figure corresponds to the flare growth. We see that the differences between the temperatures \tilde{T}_1 and \tilde{T}_2 are large during this phase of the flare development which means the broad DEM distribution. Phase DF corresponds to a slow cooling of the hot flare plasma. The whole DEM distribution slowly shifts to lower temperatures and the distribution becomes narrow (the differences between \tilde{T}_1 and \tilde{T}_2 are smaller now). We may call this phase "quasi-isothermal phase".

It is very interesting that all (~ 10) flares hitherto investigated by us evolve along the same sequence in our diagram during their decay phase. Moreover, smaller flares develop along this sequence during their increase (from left to right in our diagram), showing only short-term "spikes" towards higher values of \tilde{T}_1 during impulsive hard X-ray bursts. This strongly suggests that a flare evolves along the "quasi-isothermal" sequence, if only a basic mechanism of the flare heating having small efficiency and long duration is working (e.g. Joule heating).

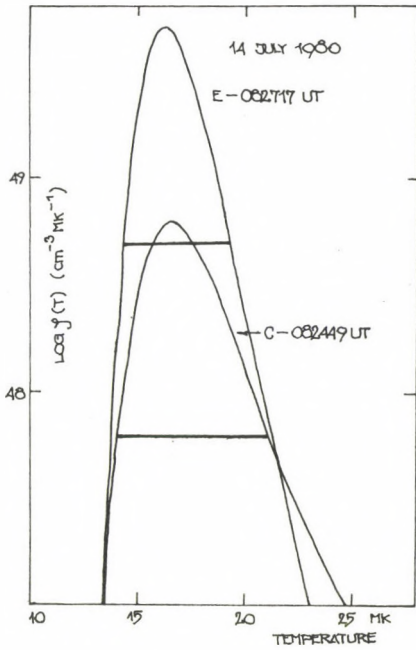


Fig.1.

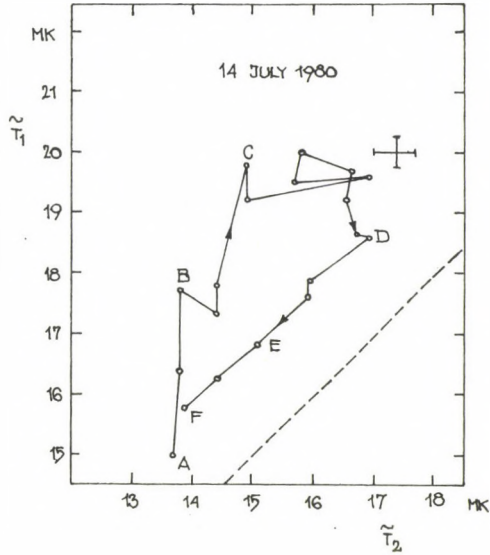


Fig.2.

Fig.1. The comparison of DEM distributions during the flare growth (C) and of the flare decay (E).

Fig.2. Time evolution of the flare of 14 July in \tilde{T}_1, \tilde{T}_2 diagram (the explanations are given in the text).

Our differential emission measure calculations allow the exhaustive investigation of the evolution of the energy content in the hot flare plasma. This will be done in another paper.

References

- {1} Acton, L.W., and 23 co-authors, The soft X-ray polychromator for the Solar Maximum Mission, *Solar Phys.* 65. 53, 1980
- {2} Sylwester, B., Jakimiec, J., Sylwester, J., Valnicek, B., Analysis of the physical conditions in a strong X-ray flare, *Adv. Space Res.* 1. No. 13. 239. 1981
- {3} Sylwester, J., *Thesis*, Wrocław University, 1977
- {4} Sylwester, J., Schrijver, J., Mewe, R., Multitemperature analysis of solar X-ray line emission, *Solar Phys.* 67. 285, 1980
- {5} Sylwester, J., Mewe, R., Schrijver, J., Analysis of X-ray line spectra from a transient plasma under solar flare conditions. III. diagnostics for measuring electron temperature and density, *Astron. Astrophys. Suppl. Ser.* 40. 335, 1980
- {6} Withbroe, G.L., The analysis of XUV emission lines, *Solar Phys.* 45. 301, 1975

THE DEVELOPMENT OF ACTIVITY IN HALE REGION 17098

(28 AUGUST - 8 SEPTEMBER 1980)

L. G E S Z T E L Y I, L. K O N D Á S

Heliophysical Observatory, Debrecen

Abstract:

Proper motions and some respects of chromospheric activities of a relatively simple large sunspot group were studied on the basis of full-disc white light photoheliograms and H_{α} filtergrams. The large sunspot group consisted of two, subsequently developing groups. In the course of their development, the umbrae of the two groups collided with each other, three times a δ -configuration developed by convergent motions of opposite polarity umbrae of the two groups of different age coming together into a common penumbra. In spite of this complexity, the observed chromospheric activity was relatively low.

РАЗВИТИЕ АКТИВНОСТИ В ОБЛАСТИ ХЕЙЛ № 17098

(28 АВГУСТА - 8 СЕНТЯБРЯ 1980 Г.)

Л. ГЕСТЕИ, Л. КОНДАШ

Гелиофиз.Обс., Дебрецен

Абстракт:

Собственные движения и некоторые проявления хромосферической активности относительно простой, большой группы пятен были исследованы на основе фотогелиограмм белого света и полного диска, а также H_{α} -фильтрограмм. Большая группа пятен состояла из двух, последовательно развивающихся групп. В течение их развития, тени обеих групп сталкивались друг с другом, три раза развивалась δ -конфигурация путем приближающихся движений теней противоположной полярности этих двух групп различной стадии, собираясь в общую полутень. Вопреки этой комплектности, наблюдаемая хромосферическая активность была относительно низка.

Observations and measurements

During the period of 28 August - 8 September, 1980, 280 full-disc photoheliograms were taken at the observing station of the Debrecen Heliophysical Observatory in Gyula. From this material 250 observations were used for the measurements (with the altitude of the Sun above the horizon 15°), the numbers of the daily observations and observing intervals are given in Table 1. The majority of the observations was obtained by L.Győri, the rest by Mrs.Zs.Lengyel and S.Rostás.

For the identification of the sunspots in the process of their development we used some full-disc observations and 35 mm frames of the group taken at Debrecen by B.Kálmán.

The $H\alpha$ filtergrams used were obtained in Debrecen. The observations were taken by Gy.Csepura, O.Gerlei, B.Kálmán and L.Kondás. The method of observations and reduction of measurements are the same as described by L.Dezső et al. {2}. The intervals of daily $H\alpha$ observations are given in Table 1.

The history of the sunspot group

In the Hale Region 17098 two bipolar groups developed subsequently with a difference of some days. When the region rotated onto the disc, the first spotgroup was at the end of the first stage of its development and the preceding polarity umbrae (1a, 1b) were moving westward (Figs.1,2). But for the next day (29 Aug.) a new bipolar spotgroup appeared very near to the other one. We mark this new group with numbers larger than ten, the odd numbers mark preceding, the even numbers following polarity umbrae, as in the case of the older group.

The preceding (N) polarity umbrae of the new group emerged so near to the main f (S) polarity umbra (2) of the older group that they were in common penumbra, thus forming the first δ -configuration in the sunspot group. But because of the different directions of their motions (Fig.1) umbra 2 separated from the common penumbra by 1 September.

The new group showed very fast development, its preceding polarity spots (11,13,15,17,19) were moving forward (W) with high velocity ($v = 0.2 \text{ km s}^{-1}$), and by 1 September they had

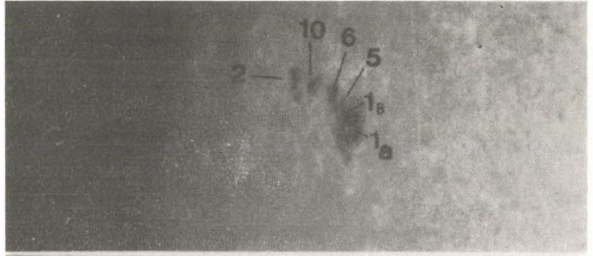
overtaken the older group; 1 and 11 were in common penumbra. The following (*S*) polarity umbrae of the older group (4,6,8) first collided with the new magnetic centre, when they were pushed by the fast moving new umbrae (11 and 19), so this collision resulted in a fast westward movement starting 30 August. (This case is like the case of the fast moving leading umbra on July 1974, marked by number 8 in the paper of Á.Kovács {5} which pushed several smaller spots in front of it {1}). Finally this smaller *S* polarity umbrae got jammed in between the large *N* polarity umbrae of the older and younger group (second δ -configuration) and died out. One subflare, accompanied by a surge rooted in these spots, was observed in Debrecen (Fig.3).

By 2 September umbrae 11 and 19 had overtaken umbra 1. As a result of their collision, umbra 1 had changed the direction of its motion from eastward to westward, and the velocity of umbrae 11 and 19 suddenly decelerated. Similar billiard-ball like collisions of umbrae of different age activities was described by B.Kálmán {4}, the behaviour of umbra 50 in Figs.1,2 of his paper.

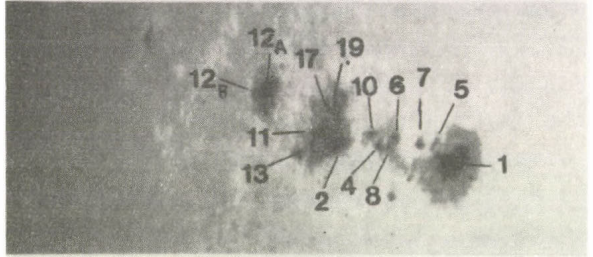
On 2 September, in the middle part of the group, (as is usual in regular sunspot group development) numerous new pores and spots formed. During 3 September two newly emerged umbrae (21a and 21b) were moving westward ($v=0.37 \text{ km s}^{-1}$) on 4 September we saw them in common penumbra with umbra 2: (the 3rd) δ -configuration developed in the center of the large group (Fig.1). On 5 September this opposite polarity spot pair showed a sea-horse like asymmetric penumbra. By 6 September this penumbra connection was broken between these spots. This case could be a new example for the tangential collision {1}. In spite of δ -configuration we did not observe considerable activity in this part of the group, which confirms H.Künzel's {6} result: δ -configuration formed after the end of the development of the spot group have no influence on the activity of the group.

By 6 September an interesting spiral-arm like structure

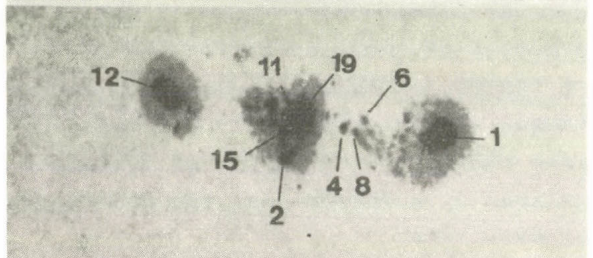
28 Aug.
11:50 UT



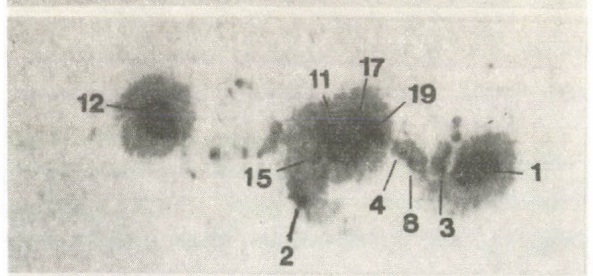
29 Aug.
11:31 UT



30 Aug.
10:20 UT



31 Aug.
12:57 UT



1 Sept.
6:03 UT

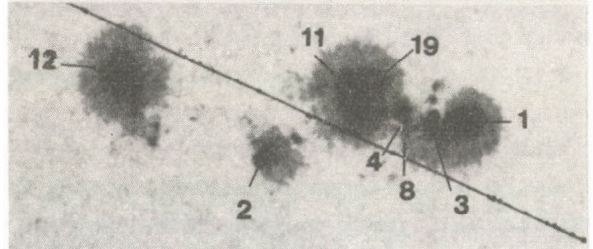
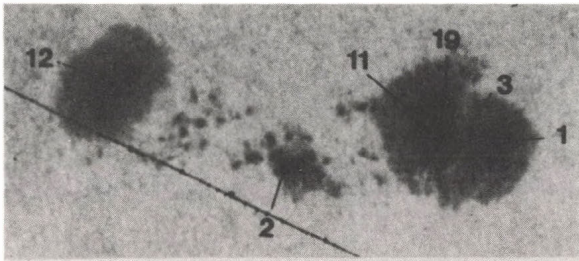
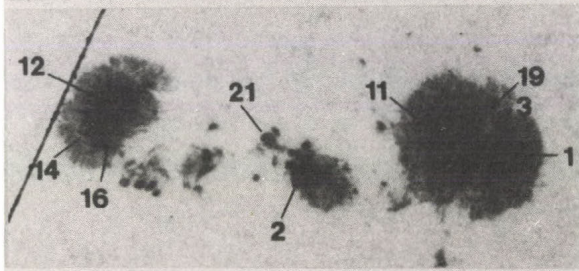


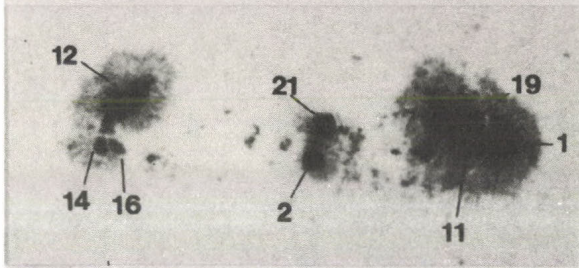
Fig. 1a. Development of the sunspot group in the period 28 Aug. - 1 Sept.



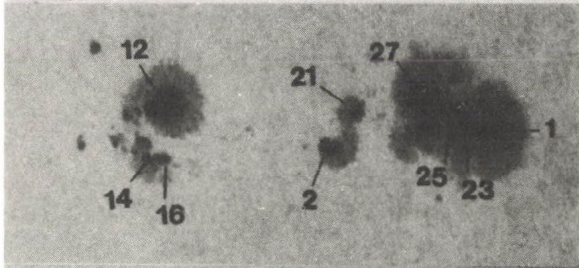
2 Sept.
13:44 UT



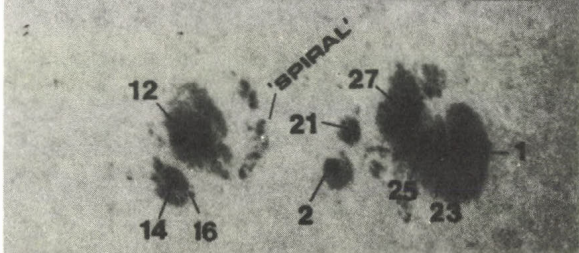
3 Sept.
9:59 UT



4 Sept.
7:30 UT



5 Sept.
12:25 UT



6 Sept.
8:59 UT

Fig.1b. Development of the sunspot group in the period 2 - 6 Sept.

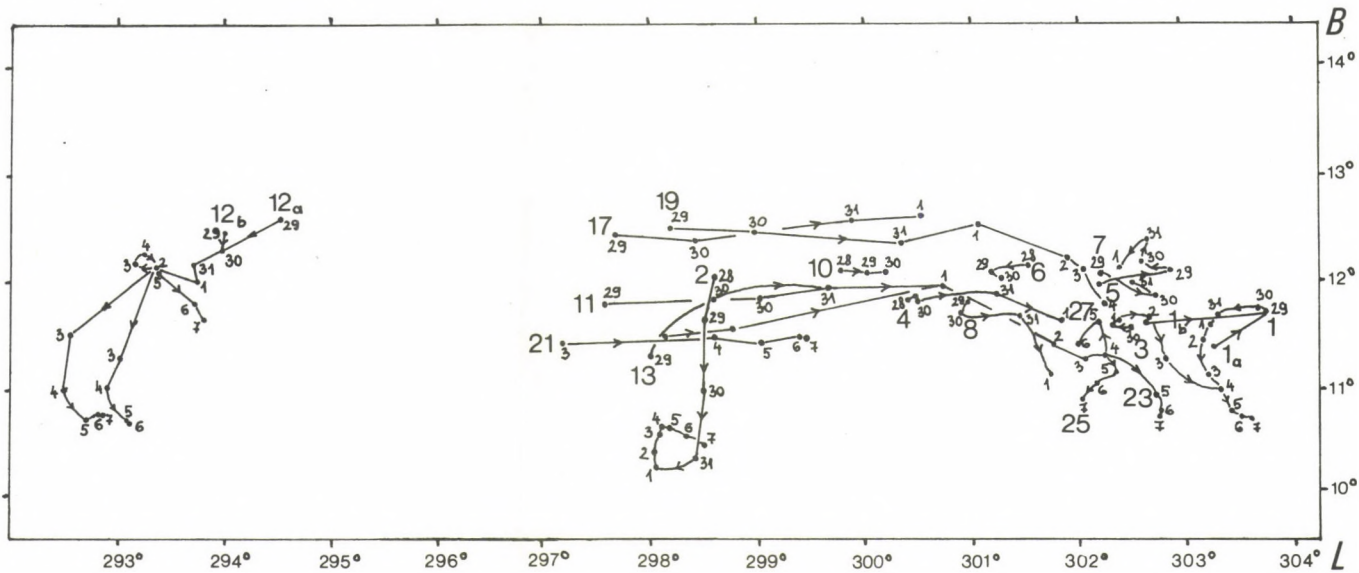
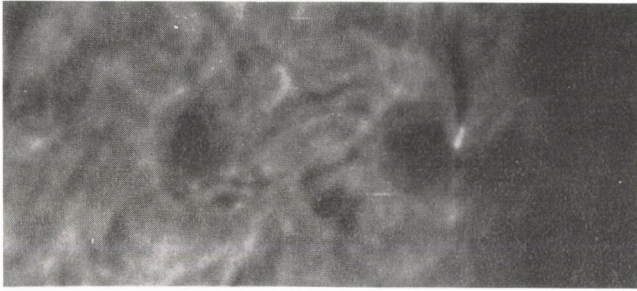
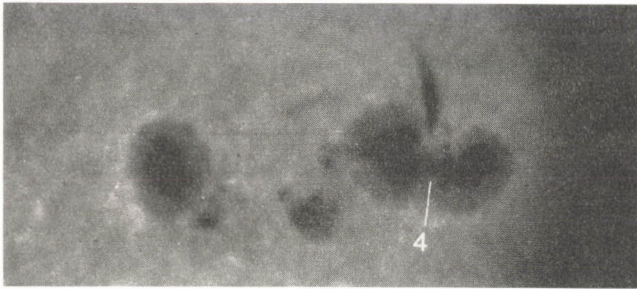


Fig.2. Trajectories of the main spots, 28 Aug. - 7 Sept.

The small numbers indicate the dates, larger ones the denotations of umbrae (cf. Figs.1a and 1b).



1 Sept.
13:12:31 UT
H α + 0.5 Å



1 Sept.
13:14:24 UT
H α + 1.0 Å

Fig.3. A subflare with surge between the two main leader spots. The small *f* polarity umbra 4 was decreasing during the day.

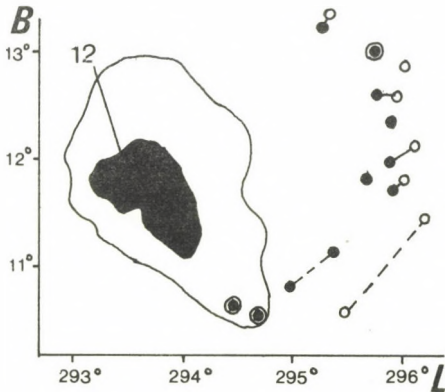
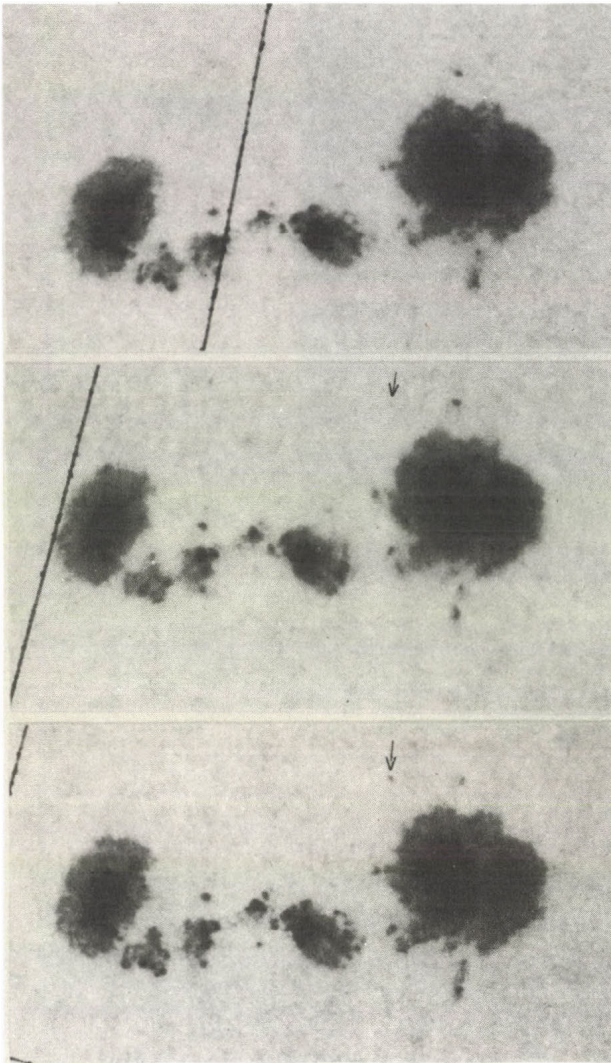


Fig.4. Displacement of the pores, i.e. deformation of the "spiral arm" like structure during 6 Sept. (morning (●), evening (○)).

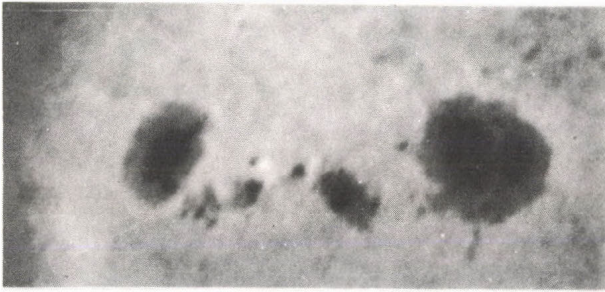


07:33:16 UT

07:43:08 UT

07:52:03 UT

Fig. 5a. Birth of a pore (photographs taken in white light).



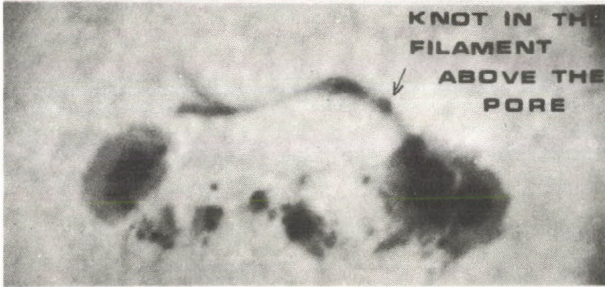
07:49:22 UT

H α - 1 Å



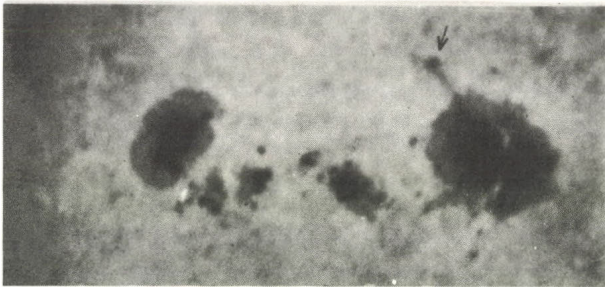
07:53:54 UT

H α + 1 Å



08:18:37 UT

H α + 1 Å



08:31:52 UT

H α - 1 Å

Fig.5b. The activation of a filament accompanied by the birth of the pore.

The material of observations

1980	white-light obs.	number of plates	H α obs.	number of quintets
	UT		UT	
Aug. 28	5:40 - 15:34	26		
29	6:00 - 15:04	31		
30	5:42 - 12:22	11		
31	12:56 - 13:58	4		
Sept. 1	5:57 - 13:35	8	13:12 - 13:46	7
2	11:19 - 14:37	11	12:04 - 16:25	5
3	6:17 - 15:55	44	5:19 - 16:20	61
4	6:09 - 15:51	47	5:06 - 16:08	98
5	6:00 - 15:35	44	5:28 - 12:24	49
6	6:36 - 15:05	14		
7	5:55 - 14:05	10		

appeared around the main S polarity spot. During the day the individual umbrae and pores of this spiral arm did not follow spiral-pattern movement, but moved off from umbra 12, almost radially (Fig.4), and by the next morning the spiral structure was broken.

The sunspot group in the Hale region 17098 rotated out from the disc on 8 September as a simple, old bipolar one.

Note on a filament activation

On 3 September in the north part of the region the birth of a pore was observed (Figs.5a and 5b), accompanied by filament activation. During this event we have quintets of H α filtergrams (H α +1 Å, H α +0.5 Å, H α centre) and full-disc white light heliograms every 5 and 10 minutes, respectively. On the basis of this observations we can say that the pores were faintly observable after 7 UT, but faded out at 7:39:56 UT. This time there was no pore in the photosphere. But in the next picture at 7:43:08 UT faint pore was once again seen, by 7:52:03 UT the pore became visible. The nearby filament activation was observed for the first time at 7:53:54 UT, when in the H α +1 Å frame the filament appeared conspicuously, invisible until this time. Very near to the new-born pore a knot appeared on the filament (pore's position $L = 300.79^\circ$, $B = +14.07^\circ$; knot's position $L = 300.70^\circ$, $B = +13.93^\circ$) showing that the pore really influenced the filament. The observed time-delay be-

tween the observation of the birth of the pore and start of filament activation is 645 sec. If we suppose that the height at the filament was of the order of 10 000 km above photosphere, the velocity of perturbation is fifteen to fifty times larger, than given by Bruzek and Bumba and Howard {8}. This case is like the case of 22 June 1980 when in the Hale region 16918 a 2B flare started after the birth of a pair of pores in the vicinity of a filament, and the first brightening of the flare was above one of these new-born pores {7},{3}.

Conclusion

The development of this large semi-complex sunspot group shows a counter-example to the rule, that high chromospheric activity, large flares usually happen when δ -configuration forms in a sunspot group. In this case a δ -configuration occurred three times, but in all of these cases the sunspot proper motions broke it, and these divergent motions could be the reason for the low flare-activity.

Acknowledgements

We wish to express our thanks to Dr P.Ambrož for making Ondrejov magnetograms available, we are also grateful to Karen L. Harvey who kindly put some Kitt Peak magnetograms at our disposal.

R e f e r e n c e s

- {1} Bumba,V.,Suda,J., Development of sunspots in the colliding magnetic fields of the June-July 1974 proton-flare group, *BAC*,34. 29, 1983
- {2} Dezső,L.,Gesztelyi,L.,Kondás,L.,Kovács,A',Rostás,S., Motions in the solar atmosphere associated with the white-light flare of 11 July, 1978, *Solar Phys.*67. 317, 1980
- {3} Gesztelyi,L., Sunspot group development in the Hale Region 16918 (16-23 June 1980) to be published in *Publ.Debrecen Obs.*Vol.4.
- {4} Kálmán,B., Magnetic fields and proper motions of sunspots. II. Group 420, October 1968, (in Russ.) *Izv.KrAO.*57. 122, 1977
- {5} Kovács,A', The development of the sunspot group associated with the white light flare of July 1974, *Publ.Debrecen Obs.*3. 197, 1977
- {6} Künzel,H., Variations of the maximum magnetic field strength in the main sunspots of the group N=11 , L=298 , rot Nr.1699 on September 2 to 4, 1980, *ICM-SMY Crimean Workshop*,2. 266, 1981
- {7} Martin,S.,Dezső,L.,Antalová,A.,Kučera,A.,Harvey,K.L., Emerging magnetic flux, flares and filaments - FBS interval 16-23 June 1980, *Adv.Space.Res.*2. Nr.11. 39, 1982
- {8} Tandberg-Hanssen,E., *Solar prominences*, D.Reidel Dordrecht, p.120, 1974

LOCATION OF SOURCES OF SOLAR NOISE STORMS
RELATIVE TO THE STRUCTURE OF EXTRAPOLATED CORONAL MAGNETIC FIELDS

P. A M B R O Ž

Astron.Inst., Ondřejov

Abstract:

A comparison is made of the positions of sources of solar radio noise storms, observed at 169 MHz, with the structure of the lines of force of the extrapolated coronal magnetic field in a current-free approximation. The typical position of the permanent radio source was found at the top of the coronal arch connecting the active region with the opposite polarity of the background magnetic field in its immediate vicinity. No direct relation was found between the flare activity in the active region and the presence of the radio source. A hypothesis is presented concerning the relation between the occurrence of noise storm sources and the process of evolutionary reconnection of the coronal magnetic field.

ПОЛОЖЕНИЕ ИСТОЧНИКОВ СОЛНЕЧНЫХ ШУМОВЫХ БУРЬ ОТНОСИТЕЛЬНО
СТРУКТУРЫ ЭКСТРАПОЛИРОВАННЫХ КОРОНАЛЬНЫХ МАГНИТНЫХ ПОЛЕЙ

П. АМБРОЖ

Астрон.Инст., Ондřejов

Абстракт:

Проведено сравнение положений источников солнечных шумовых бурь, наблюдавшихся на частоте 169 МГц, со структурой системы силовых линий коронального магнитного поля, рассчитанной в потенциальном приближении. Было найдено, что долгоживущий источник шумовых бурь находится на вершине корональной арки. Она соединяет область избытка магнитного потока одной полярности в активном центре с фоновым магнитным полем противоположной полярности в его окрестности. Не обнаружено прямой связи всплывочной активности в активных областях с присутствием исследованных радиоисточников. Предлагается гипотеза о существовании связи между появлением источников шумовых бурь и процессом перестройки корональных магнитных полей.

1. Introduction

The special observation interval included in the "Coordinated Observations of Type I Bursts Noise Storms" in the post-SMY phase, May 17-24, 1981, is exceptional in that the position of a permanent radio source could be determined daily in the course of eight observation days. The results of positional observations made by the radioheliograph in Nancay on a frequency of 169 MHz were made available by Mercier and presented summarily by Aurass et al. {1}. The objective of the project was to make use of these positional observations and to compare the positions of the individual radio sources with the structure of the magnetic lines of force, calculated for actual and corresponding times by numerical extrapolation of the results of observations of the photospheric magnetic field. The actual calculation is based on the solution presented by Sakurai and Uchida {3}, using a computer program written by the present author for the EC 1040 computer of the Astronomical Institute of the Czechoslovak Academy of Sciences in Ondřejov. A more detailed report on the program is being prepared for publication in the Bull.Astron.Inst.Czech.

2. Calculation of the magnetic field lines

To compute the model configurations of magnetic lines of force in the solar corona, we have used the daily observations of the longitudinal component of photospheric magnetic fields made at the Mt.Wilson Observatory. On the basis of the daily maps of May 12, 13, 14, 17, 21, 22 and 23, 1981, the synoptic map for Carrington rotation No.1708 was constructed in the usual way for heliographic longitudes ranging from 0° to 190° and heliographic latitudes ranging from -50° to $+50^\circ$. This map was used to determine the positions, dimensions and intensities of the magnetic field for 338 circular solenoids, giving the best description of the distribution of the observed intensities of the magnetic field and, simultaneously, optimally satisfying the requirements of the modelling and extrapolation technique.

As regards computations of this type, we know that the way in which the origins of the magnetic lines of force are

generated has a decisive effect on determining the character of the computed line-of-force configurations; It can be guaranteed that the origins of the lines of force will be generated in regions of the solar surface where measurable magnetic fields are present. Drawing on experience in comparing similar computations with available pictures of the solar corona, made in the soft UV radiation range, the author is of the opinion that the computed line-of-force configurations, particularly in places where their divergence is small, are very close to coronal formations which actually exist as densified plasmatic coronal archs. The density and temperature profiles across and along the arch greatly depend on the geometric shape of these formations, the intensity and degree of divergence of the magnetic field, as well as on the thermodynamic properties of their anchoring on the solar surface.

Assume that the coronal arches represent magnetic flux tubes and, once established, they are stable relative to the slow evolution of magnetic fields at the level of the photosphere. Changes in the magnetic flux distribution at the level of the photosphere may be a combined process of vertical field divergence from the lower subphotospheric layers, but also the result of horizontal convective motion of plasma which may be responsible for the redistribution of the magnetic flux. From this point of view, we consider the continuous evolution of the magnetic field in the corona as normal and natural development. For example, the generation of a new island of the opposite polarity, or the generation of a new active region will cause substantial changes in the structure of the coronal magnetic field which can be characterized by relatively slow, principal reconnections of the whole configuration. On the other hand, very rapid processes are also observed here, which are connected with the generation of magnetohydrodynamic instabilities associated with flares or with the activation of eruptive prominences.

The calculated configurations of magnetic lines of force are based on the assumption of an integral effect of all given

return-flux sources on the overall distribution of the magnetic potential in the space above the spherical surface of the photosphere on which the boundary conditions are defined. All the computed configurations are current-free and are based on the distribution of boundary conditions obtained by the synoptic method, i.e. gradually over a 12-day period. The computation has been conducted simultaneously for a substantial part of the solar surface with a single set of input data. Consequently, the computation does not take into account short-term evolutionary changes in the course of the interval involved. For these reasons, the computations do not include the contributions of the magnetic flux from the individual sunspots in the active centres.

The situation in the distribution of the magnetic lines of force shown in Figs. 1a - 1h, therefore, is based on a single definition and single computation of the configuration. The figures represent an orientation of the extrapolated configuration of the coronal magnetic field and solar disk which corresponds to the actual orientation of the solar disk relative to the observer at the time the positions of the radio sources were determined.

3. Comparison of the calculations and observations

In the first stage of the project, the positions of the separate detected radio sources on frequency 169 MHz were analyzed relative to the appropriately oriented configurations of the coronal magnetic field in the interval between May 17 and 24, 1981. The positions of the radio sources in the northern hemisphere are related primarily to the extensive active region Hale No. 17644. In the southern hemisphere, where all the radio sources observed after May 20, 1981 were located, their distribution was divided mainly between active regions Hale No. 17652 and 17653.

Among all the observed radio sources, we looked for sources which we could assume to belong, with the highest probability, to a single permanent radio source. It was found that only one radio source satisfied this condition sufficiently.

Special emphasis in the literature on noise storms is

being put on the question of typical location of the radio source relative to the structure of the corona and, particularly, relative to its magnetic field. Fig.2 shows all the radio sources observed by Mercier during the whole interval schematically as dotted clouds in a projection which positions the most probable location of the permanent source of the noise storm close to the solar disk centre. The compilation was made using the relations between the observed position of radio sources and lines of force for every day as indicated by Figs.1a-1h. The problem was to render the typical noise storm source an agglomeration of many individual positions derived from partial observations.

The found permanent noise storm source can be located in a single arch-like formation originating in active region Hale No.17653 towards the south-west. The position of this structure and the most probable mean position of the permanent radio source correspond very well with each other and, therefore, the probable distance of the source from the solar centre ρ can be estimated from the known height of the points computed on the lines of force. By analysing the geometry of the points of intersection of the lines of sight to the same source on several days, we were able to determine the following statistical mean values of all three heliographic coordinates of the source:

$$L = 125.6^\circ \pm 2.5^\circ$$

$$B = -25.6^\circ \pm 1.4^\circ$$

$$\rho = (1.332 \pm 0.075) R_\odot$$

In the course of this analysis, it was found that the measured positions of the permanent source did not correspond to a single stationary source. As evidenced by the probable errors of the results of the measurement given above and also by the scatter of the superimposed sources in Fig.2, the permanent source is confined to a single concrete magnetic configuration; however, within it its position varies within small intervals in all three coordinates. This, together with the analysis of the distribution of the photospheric magnetic field

MAY 17, 1981

L: 154.6

B: -2.4

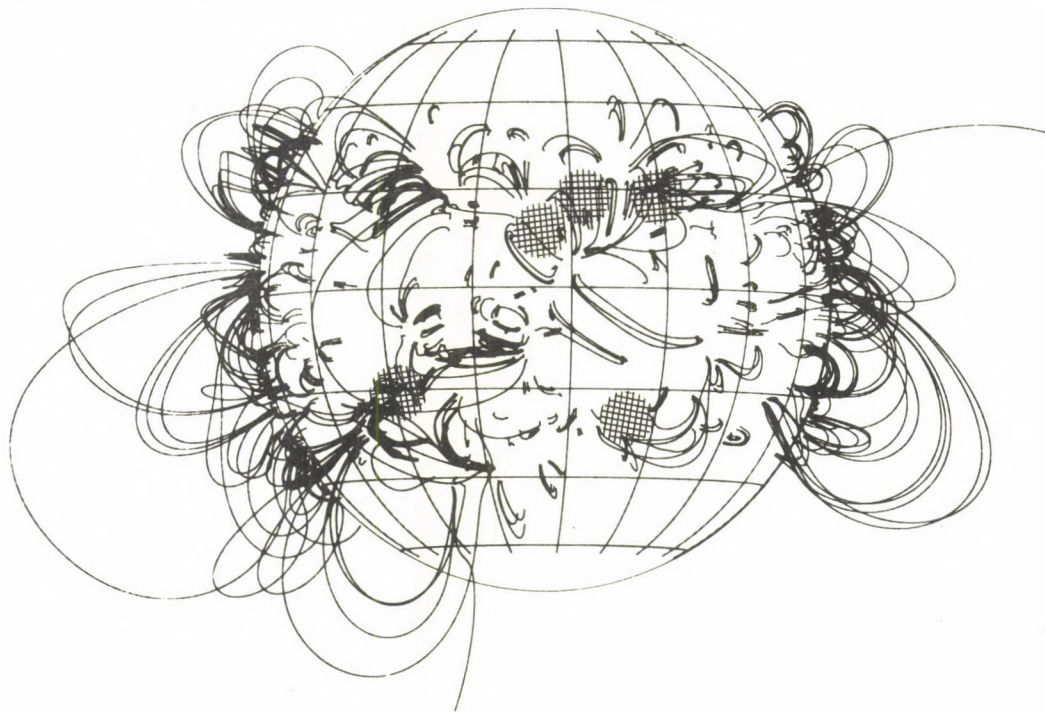
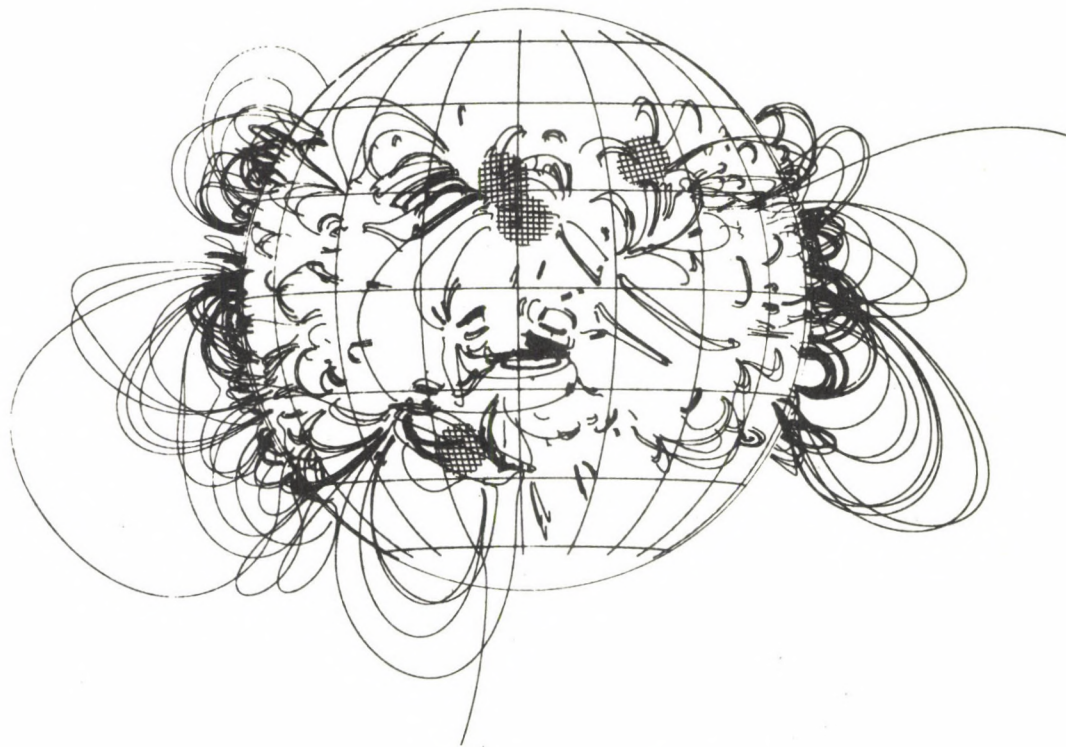
*Fig. 1a.*

Fig. 1a-1h. Comparison of positions of radio sources (hatched circles) on a frequency of 169 MHz with the structure of lines of force of the extrapolated coronal magnetic field in a current-free approximation for the individual days from May 17 to 24, 1981.

MAY 18, 1981

L₀: 141.4B₀: -2.3*Fig.1b.* The same as Fig.1a.

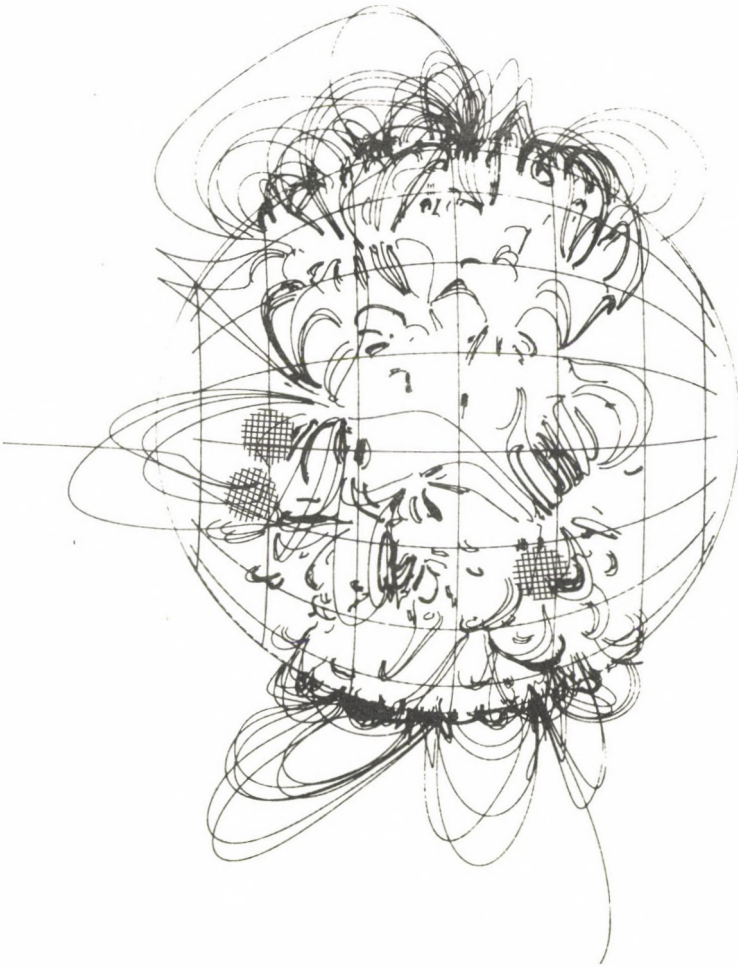
MAY 19, 1981



Fig. 1c. The same as Fig. 1a.

L.: 128.1
B.: -2.2

MAY 20, 1981



L.: 114.9
R.: -2.1

Fig. 1d. The same as Fig. 1a.

MAY 21, 1981

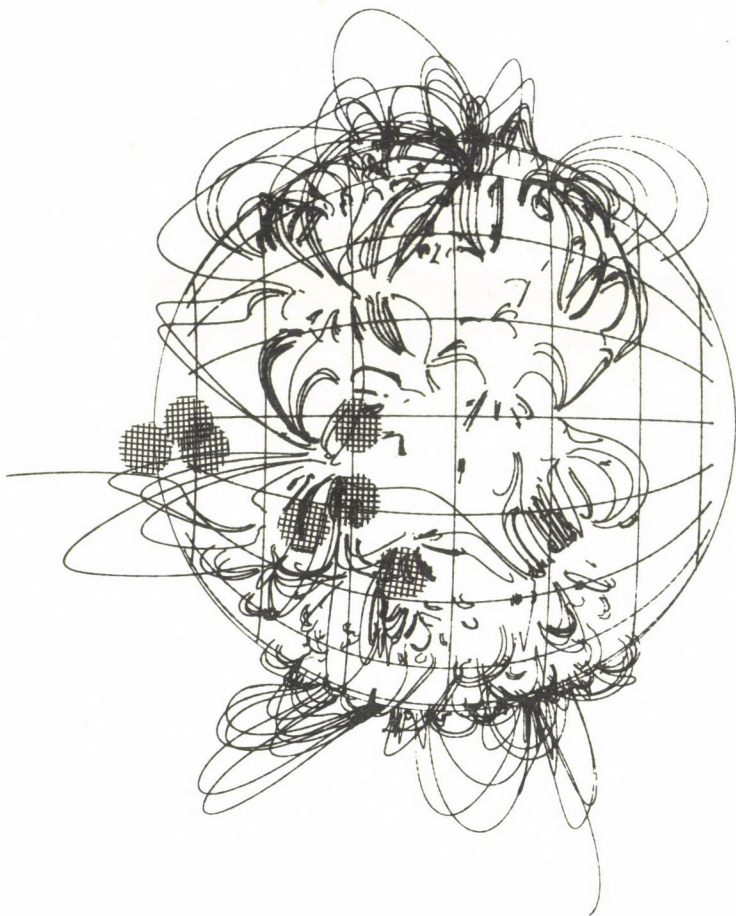


Fig. 1e. The same as Fig. 1a.

L: 101.7
B: - 2.0

MAY 22, 1981



L: 88.4
B: -1.8

Fig. 1f. The same as Fig. 1a.

MAY 23, 1981

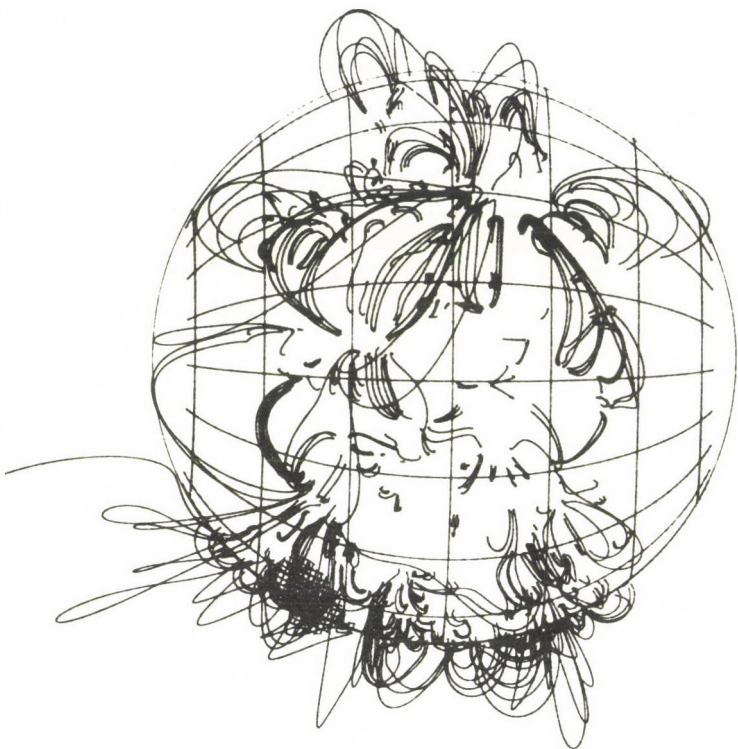


Fig. 1g. The same as Fig. 1a.

L: 75.2
B: -1.7

MAY 24, 1981

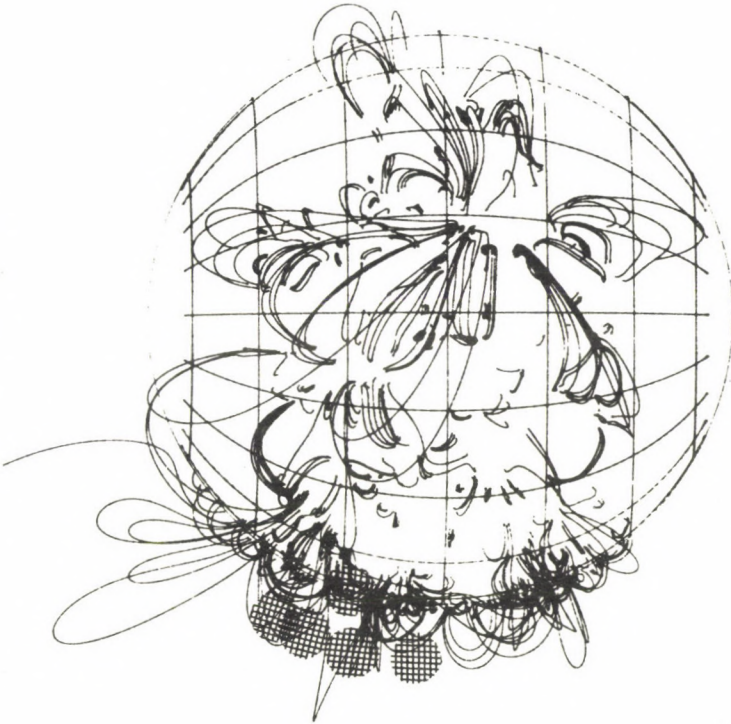


Fig. 1h. The same as Fig. 1a.

L_o: 61.0
B_o: -1.6

MAY 1981

169 MHz

L : 130.0

B : -35.0

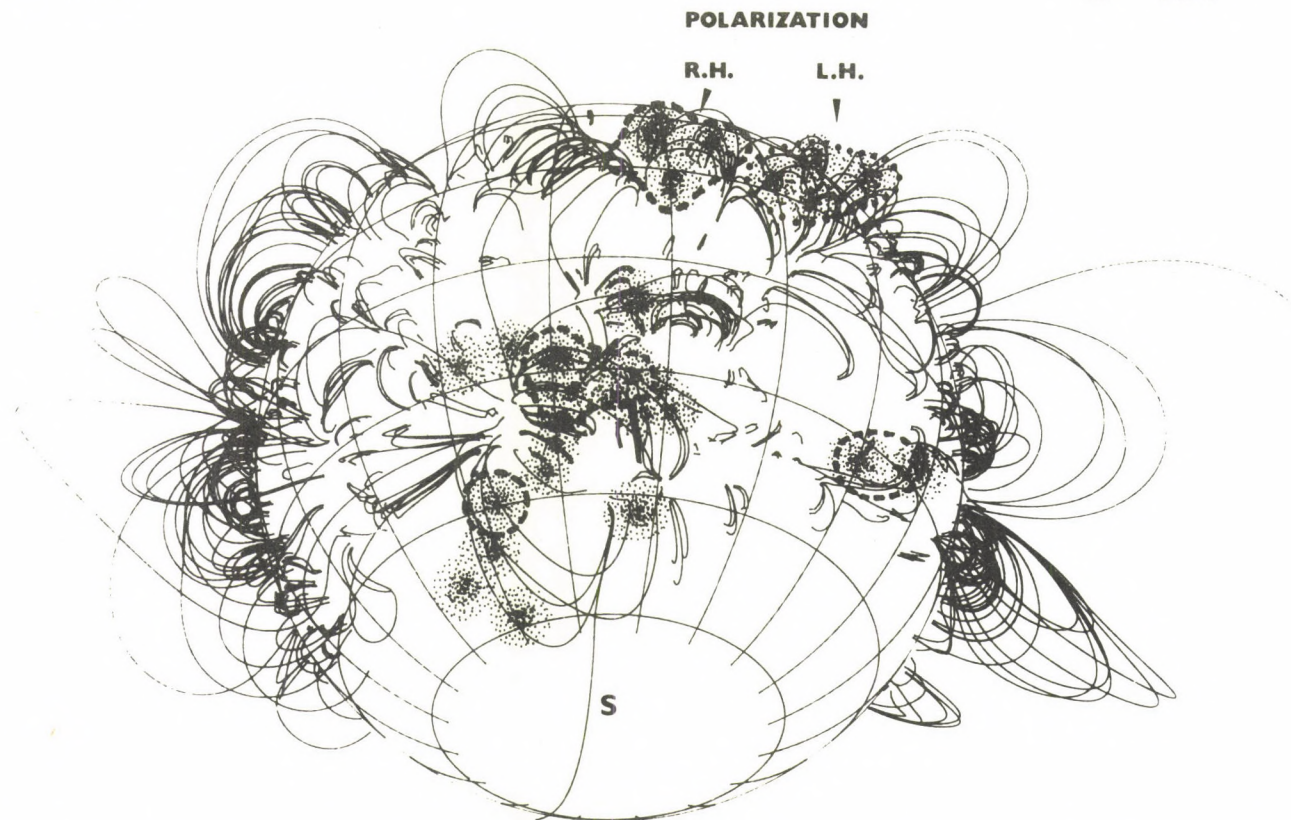


Fig. 2. Synthetic picture of the location of all observed radio sources (dotted "clouds") relative to the structure of lines of force of the coronal magnetic field.

in the region studied (Fig.3), where structural changes were observed, is considered to be an argument in favour of the opinion that substantial evolutionary restructuring of the coronal magnetic field takes place in the region where the permanent radio source is observed.

The positions of all 35 radio sources, observed during the pertinent interval and referred to the solar disk, constituted the initial data for the following statistical analysis.

The first question concerned the location of sources relative to any arch-like structure of the line-of-force configuration. By comparing the position of the source directly, relative to the distribution of the lines of force for the corresponding orientation of the solar disk, it was possible to determine quite unambiguously that 25, i.e. 71.1%, of all observed sources were located at the top of the line-of-force arch. Of the remaining 10 sources 4, i.e. 11.6%, were projected on to the arm of the arch and 6, i.e. 17.1%, on to the foot of the arch. However, it should be emphasized that the foot of the arch, for example, is, in a number of cases, the seat of the active centre where the configuration of lines of force is very compact and, consequently, is not reflected in our extrapolation model at all. One may, therefore, very well assume that the percentage representation of sources which coincide with the top of the loop arch is even larger and, therefore, that this location is statistically dominant.

Another question is the relation of the position of the noise storm source to the active region and the type of arch-like structures in the corona. An absolute majority of 28 observed sources, i.e. 80% of all observed cases, is located on the arch-like structures which start in the well developed centres and connect them with the ambient background magnetic field of opposite polarity. Not a single radio source is located on the lines of force which connect the separate active centres. Seven sources, i.e. 20%, are located outside these characteristic formations. Only in four cases, i.e. 11.6%, are the sources projected on to the position of the active centre.

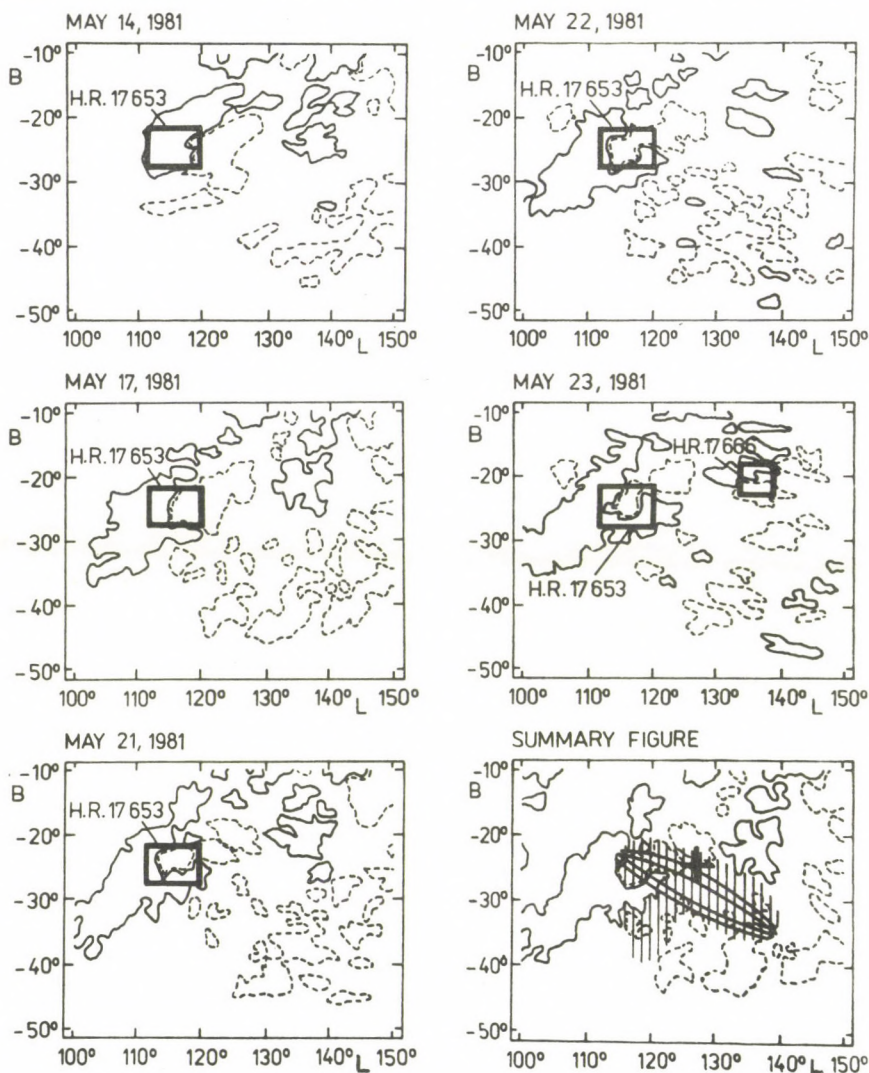


Fig. 3. Evolution of the structure of the photospheric magnetic field at an intensity level of 5 gauss for particular region transformed into the rectangular heliographic net. The full line indicates (+) polarity, the dashed line (-) polarity. The summary figure on the r.h.s. at the bottom shows the structure of magnetic regions from which the initial data for extrapolating lines of force were derived; the connection of the line-of-force arch is shown schematically. The positions of the permanent radio source, derived from Fig. 2 (hatched) and from the statistical determination of its position (full cross) are also given.

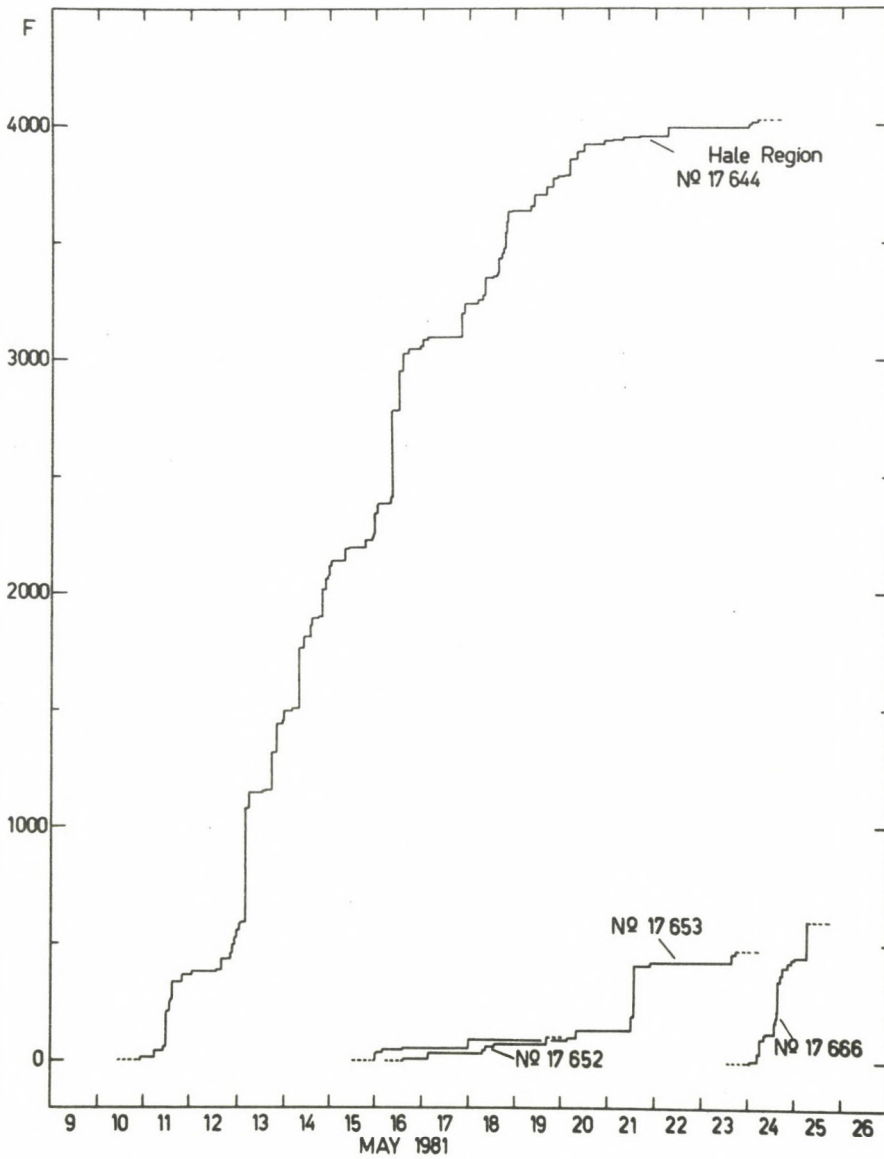


Fig. 4. Summation curves of the flare index F for the individual active regions observed on the solar disk in the interval of May 17 to 24, 1981.

The determined permanent radio source satisfies both of the statistical conclusions reached above and is located on the line-of-force arch which connects the positive polarity of the magnetic field of Hale region No.17653, positioned at $L = 113.7^\circ$, $B = -21.3^\circ$, with the region of negative polarity of the background magnetic field, positioned at $L = 140.3^\circ$, $B = -36.6^\circ$.

4. Discussion

A. Photospheric magnetic field evolution

Using the daily Mt. Wilson observations, charts of the distribution of the magnetic field intensity at the level of the photosphere has been constructed in Fig.3; it reflects the intensity level of 5 gauss so that the positive polarity is shown by the full line and the negative by the dashed line. The depicted region covers the whole magnetic system which has most probably taken part in forming the noise storm source. By comparing the situation in the polarity distribution between May 17 and 23, 1981, we can see that certain changes occurred in the distribution of the magnetic field in the very bipolar magnetic region coupled with active region Hale No.17653, as well as in the space where the opposite foot of the line-of-force arch is located. Whereas the magnetic fields in active region 17653 displayed a simple configuration with the S (-) polarity as leading and N (+) polarity as following at the beginning of the studied interval, the map of May 17 already shows that the following polarity in its southern part is moving very conspicuously to the west, surrounding the S polarity, and as of May 21 has moved in front of the region of leading polarity.

The data for extrapolating the lines of force in this region were compiled from magnetic observations made on May 17 and 21, 1981. The extrapolation calculation clearly indicates that the connection of the magnetic lines of force inside active region No.17653 is so close that, on the scale we are using, the lines of force could not be plotted at all. This means that the bipolar system itself does not reach up very high into the corona and apparently has no more substantial significance for our deliberations. On the other hand, the

connection of the positive polarity in the eastern part of the active region with the negative polarity located at $L = 140.3^\circ$, $B = -36.6^\circ$, does reach up into the corona quite distinctly and, with regard to the computed configuration, runs out to a distance $\rho = 1.25 - 1.30 R_\odot$ from the solar centre which correspond to 175-200 thousand km above the solar surface. This distance agrees very well with the level of the corresponding critical plasma frequency for 169 MHz. As in the interval from May 14 to 17, 1981, conspicuous qualitative changes occurred in the morphology of the field distribution in the neighbourhood of active region Hale No. 17653, so equally marked changes occurred in the sector of heliographic longitudes between 125° and 150° on May 21-23, 1981. The dominantly distributed negative polarity is interspersed by small islands of positive polarity which cause the region of negative polarity to disintegrate. As a result of horizontal displacements of the regions with opposite polarities, beginning with May 23, 1981, at position $L = 140^\circ$, $B = -22^\circ$ we can observe the interaction of the two opposite polarities and, at the same time, the emergence of the active region and sunspot group denoted Hale No.17666.

In connection with this very rapid change in distribution of the photospheric magnetic fields, one may also expect dramatic changes in the force conditions in the upper and middle corona, which will probably be reflected in changes of magnetic connections and, consequently, also in the structure of lines of force above the region in question. One may, therefore, assume that the space above the region being studied, in which the permanent noise storm source was observed, was a place of principal restructuring of the corona, its magnetic field, the distribution of the plasma density and, possibly, of the current density during the time of observation.

B. Flare activity

From the point of view of chromospheric activity, active region Hale No.17653 displayed very few morphological changes and very few flares. On the other hand, the newly created region 17666, in which the flare activity was very lively, ap-

peared and began to produce flares only on May 23, 1981 when the permanent source was already above the western limb of the Sun.

For the purpose of analysing the relation between the observed radio sources and flare activity of nearly all regions simultaneously present on the disk during the observation interval, summation curves of the flare index F were constructed using Křivský's method {2}. For completeness the very ample flare activity of active region Hale No.17644 in the northern hemisphere was also included. Since in principle the slope of the summation curve increases with the energy produced by the flare per unit time, we can claim that the onset of flare activity in the newly created region Hale No.17666 is quite compatible with the trend in the development of region No.17644. As regards the other two regions, 17652 and 17653, we can say that they displayed very little flare activity with the exception of the flare of May 21, 1981 of importance 1F. Nevertheless, the permanent radio source was indeed observed in the immediate vicinity of region No.17653 during the whole interval involved.

5. Conclusion

We may conclude, therefore, that radio noise storm sources, observed on 169 MHz, usually occur at the tops of coronal archs which connect the active centres with the surrounding magnetic regions of the background magnetic field. At 169 MHz the height of the source corresponds to the height of the critical frequency at a level of about 200 thousand km above the photosphere. The presence of the permanent source is most probably associated with the macroscopic restructuring of the corona, its magnetic field, distribution of plasma density and current density. This involves restructuring of an evolutionary nature which takes place continuously over a number of hours or even days. We assume that this is so because we have observed directly the evolutionary changes in the distribution of the measured magnetic fields at the photosphere level and, at the same time, also small changes in the position of the "permanent" radio sources in the region of the corona. The flare

activity did not affect the existence of noise storm sources conspicuously as can be seen from the behaviour of the summation curves of the flare index. As far as any connection has been outlined, this was only done in the sense that the changes in the corona and flare situation in the chromosphere are the consequence of a single evolutionary process at the level of the photosphere and below it. Moreover, the effects resulting in noise storms are apparently due to quasi-stationary development, whereas flare manifestations represent the catastrophic consequences of sudden destabilization.

R e f e r e n c e s

- {1} Aurass,H., Böhme,A., Fomichev,V.V., Gnezdilov,A.A., Krüger,A., Mercier,C., Tlamicha,A., Urpo,S., The radio emission and active region development during the May 15-25, 1981 period, *Inst.Theor.Astrophys.Report 57*, Oslo, 1983
- {2} Křivský,L., Trends of flare activity in the July 1974 proton region *BAC*, 26, 203, 1975
- {3} Sakurai,T., Uchida,Y., Magnetic field and current sheets in the corona above active regions, *Solar Phys.*52, 397, 1977

THE RADIO BURSTS OF 13 AND 16 MAY 1981 AND ASSOCIATED EVENTS
IN THE RADIO BRIGHTNESS DISTRIBUTION ABOVE AN ACTIVITY COMPLEX

V.F. MEL'NIKOV[†], V.P. NEFED'JEV[‡],
T.S. PODSTRIGAČH[†], V.S. PROKUDINA^{*},
N.N. POTAPOV[‡], G.Ya. SMOL'KOV[‡]

† NIRFI, Gorkij

‡ SibIZMIR, Irkutsk

* Shternberg Astron. Inst., Moscow

Abstract:

A comparison is made of the radio bursts of 13 and 16 May 1981, observed at centimetric and decimetric radio wavelengths, with chromospheric flares. It is shown that the features in the radio emission spectrum and in the bursts polarization are related to those in the spatial development of flare ribbons and arches.

ВСПЛЕСКИ РАДИОИЗЛУЧЕНИЯ 13 И 16 МАЯ 1981 Г. И СОПУТСТВУЮЩИЕ
ИМ ЯВЛЕНИЯ В РАСПРЕДЕЛЕНИИ РАДИОЯРКОСТИ НАД АКТИВНЫМ КОМПЛЕКСОМ

В.Ф. МЕЛЬНИКОВ[†], В.П. НЕФЕДЬЕВ[‡], Т.С. ПОДСТРИГАЧ[†],
В.С. ПРОКУДИНА^{*}, Н.Н. ПОТАПОВ[‡], Г.Я. СМОЛЬКОВ[‡]

† НИРФИ, Горный

‡ СИБИЗМИР, Иркутск

* ГАИШ, Москва

Абстракт:

Проведено сопоставление всплесков радиоизлучения 13 и 16 мая 1981 г., наблюдавшихся на волнах сантиметрового и дециметрового диапазонов радиоволн, с хромосферными вспышками. Показано, что особенности в спектре радиоизлучения и в поляризации всплесков связаны с особенностями в пространственном развитии вспышечных лент и арок.

On 13 and 16 May 1981 large flares developed in Active Complex 3106/3112 on the Sun. This report presents the results of an investigation of these flares, as observed at centimetric and decimetric wavelengths. We have used in this study the observations from NIRFI (9100, 2950, 950, and 650 MHz), from SibIZMIR (5770 MHz) and from IZMIRAN (204 MHz). In addition, we analyzed the optical observations of these flares from the High-Mountain Expedition of the Sternberg Astronomical Institute (Alma-Ata) and from Debrecen Observatory (Hungary).

The radio bursts of 13 and 16 May 1981 (see Fig.1 and 2) are marked by their association with powerful chromospheric 3B class flares. At the moment of maximum the radio emission fluxes at 3.3 cm wavelength were very high, namely 4000 s.f.u; for the 13 may burst and 2000 s.f.u; for the event of 16 May. While the time profiles at cm wavelength are in general similar, there are differences in the fine structure during the maximum phase of flares. The time profile of the radio burst of 16 May was very strongly modulated during that period. In contrast, the time profile of the 13 May event is very smooth. It is evident from Figs.1 and 2 that there are considerable differences in the decimetric emission of the flares.

The activity at metric wavelengths was also quite different. During the flare of 13 May, beginning at 3:50 UT only isolated series of III type bursts with low intensity were observed. At the time of the 16 May flare the events at metric wavelengths were considerably more powerful. From 8:12 to 11:05 UT a IV type emission was observed. In the period from 8:24 to 8:40 UT there was an intense II type burst. Thus the radio bursts related to the large flare arising in the same sunspot complex differ somewhat in the manner of development which is believed to be caused by 1) changes in the magnetic field topology in the active complex, which could have occurred from 13 to 16 May; 2) differences in the temporal evolution of the flare. Comparison of flare observations at radio and optical wavelengths can help to clarify to which chromospheric phenomena the aforementioned features of the bursts are related.

A detailed analysis of the changes in the active complex which occurred in the period 13 - 16 May, was made by Banin {1}, who pointed out that the general distribution of the active complex magnetic field had largely been preserved. According to an analysis of the flare evolution carried out by Banin et al. {2}, along with some typical features inherent in both flares (two-ribbon structure and the location of flares near the same spot) there were noticeable differences, which are related to the character of the development of chromospheric flares and to the loop structure. We have less detailed chromospheric observational data on the 13 May flare than on the 16 May flare. Nevertheless, these data are sufficient to make conclusion about the changes in the flares. The evolution of the flare is smooth without any rapid changes in the flare area. No rapid appearance and development of separate kernels in the flare was observed. The time profile of the centimetric burst was also very smooth. For the flare of 16 May we have rather detailed observations in the $H\alpha$ -line (in the center and in the wings of the line). We have used them to compare some features of the development of the flare and the burst. Fig.3 presents sketches of the stages of flare development at times when its spatial structure underwent dramatic changes. Before 8:20 UT the flare developed smoothly. The ribbons increased both in area and brightness. The cm burst changed smoothly as well. Between 8:21 and 8:27 UT a noticeable restructuring of the flare in the northern half of the N -polarity ribbon occurred (see Fig.3). At the same time an appreciable enhancement of the radio flux at 3.3, 5.2 and 10 cm wavelengths was observed. From that time till 8:33 UT the ribbon configuration remained virtually unchanged. The radio flux showed only minor fluctuations. A comparison of the $H\alpha$ -films taken at 8:33 UT and 8:36 UT revealed a violent spreading of the emission toward the leading spot of N -polarity. It is evident from the $H\alpha$ -filtergrams obtained at 8:36 UT that the emitting region reached the sunspot umbra. It was at that time that the most violent enhancement of the burst occurred and the shape of the spectrum

altered so that a rise towards 3 cm wavelength was observed. Besides, the time profile was greatly jagged at 3 cm wavelength. Moreover, the fluctuations decreased with increasing wavelength, becoming weak towards 10 cm wavelength. From this it follows that additional sources of the radio emission responsible for the temporal fluctuations at 3 cm wavelength have a rather steep spectrum, falling down towards 10 cm wavelength.

The burst of 16 May was also observed in the polarization at 5.2 cm wavelength. Prior to the start of an intensive development of the burst, individual peaks on time profiles I and V were well-correlated. The similarity between the time profiles breaks down during the most intensive development of the flare. An example of a burst recorded at its maximum is given in Fig.4. It is quite evident that the changes in the total intensity and polarization are anti-correlated. This indicates that the observed emission of the burst includes contributions from separate sources with the opposite sense of polarization, resulting in the bipolarity of the burst structure.

The foregoing analysis of the flares suggests some assumptions about the spatial structure of the generation region of cm bursts. For the flare of 16 May two sources are distinguishable in this region. The principal source is quasi-stationary and is physically and spatially connected with the evolution of a two-ribbon structure, with its emission intensity varying smoothly. The maximum of its emission corresponds to the maximum phase of development of a chromospheric flare. If we assume that the angular size of the source is comparable with the size of the region of $H\alpha$ -emission, then during the maximum phase the brightness temperature is of order $2 \cdot 10^8$ K. The emission spectrum at 3-10 cm wavelengths is nearly smooth.

Another source has a different nature. It is connected with a rapid change in the flare near the leading spot. Its emission is concentrated in the short wavelength part of the spectrum and it has a much smaller angular size.

As mentioned previously, the post-maximum phase of the 16 May event was marked by a strong increase in the decimetric

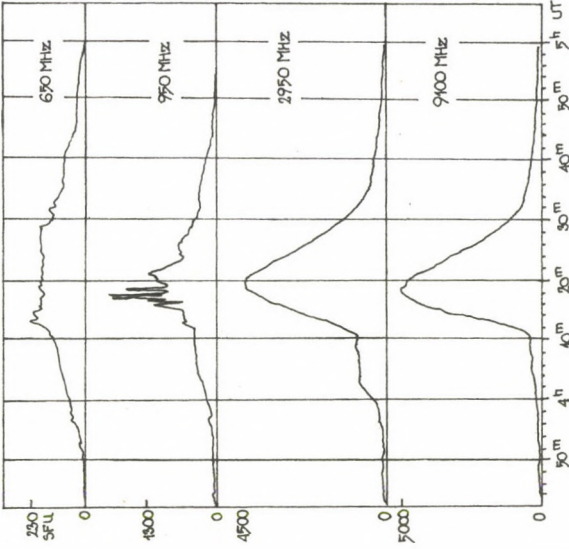


Fig. 2. The burst of 16 May 1981

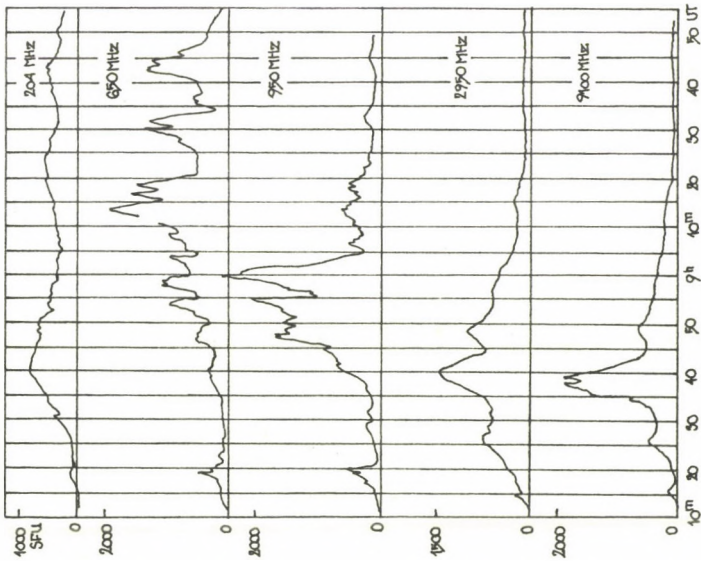


Fig. 1. The burst of 13 May 1981

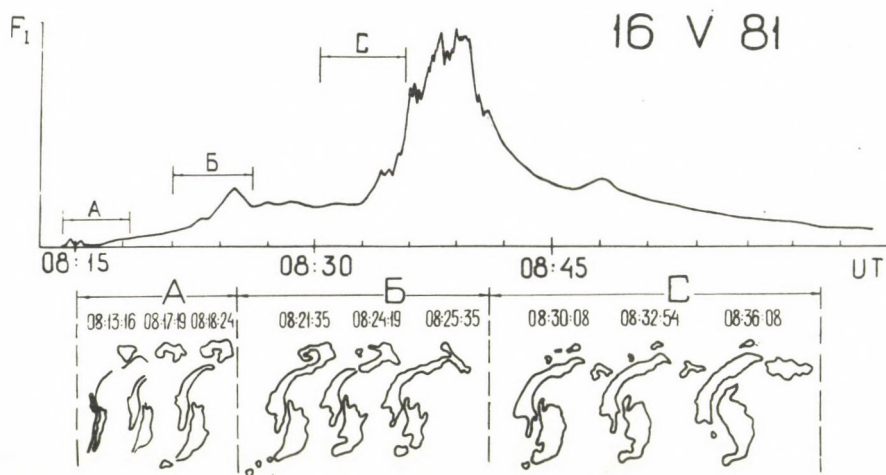


Fig. 3. Stages of development of the 16 May flare.

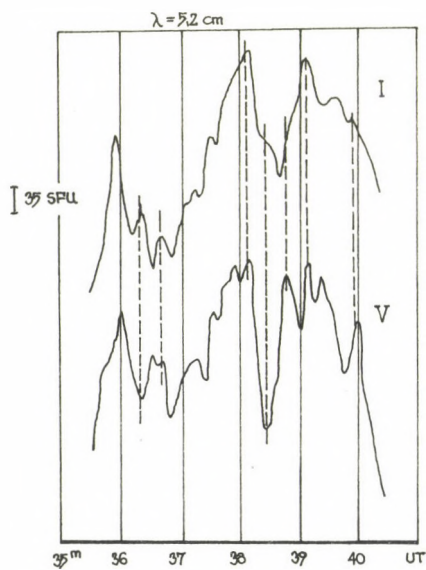


Fig. 4. Time profile of a burst at the time of maximum.

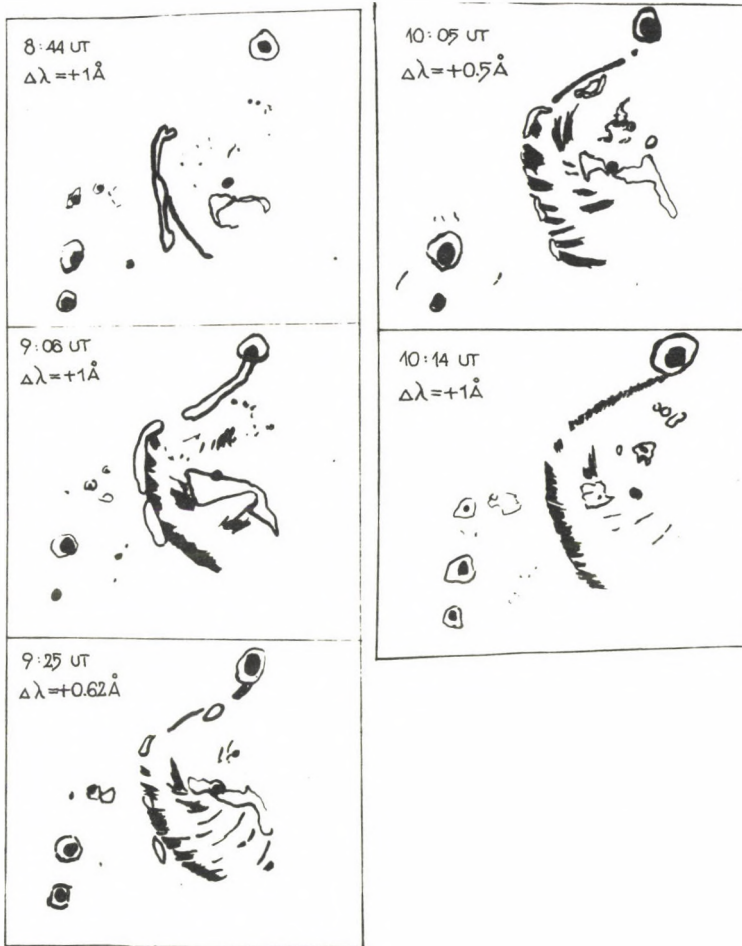


Fig.5. Stages of development of the arch system of 16 May.

and metric bursts but this was much less pronounced in the flare of 13 May.

A most striking feature of the optical emission in the post-maximum phase of the 16 May flare was the emergence and rapid formation of a loop system, accompanied by a gradual fading of the emission and by a diminution of the flare ribbon's area (see Fig.5). The $H\alpha$ -filtergrams obtained within 9:02 - 9:12 UT show a well-discernible loop system oriented along a neutral line of the longitudinal magnetic field, $H_{||}=0$. The footpoints of these arches are rooted in the emitting flare ribbons of N - and S -polarity, with a characteristic size of $30-50 \cdot 10^6$ m.

A loop structure was observed in the absorption in the red wing of the $H\alpha$ -line, showing a displacement from the line center, $\Delta\lambda = +0.75 \div +1 \text{ \AA}$. Such a displacement is indicative of a motion with the velocity $30 \div 45 \text{ km s}^{-1}$ along the arches downwards to the surface. The foots of the loop system in the form of narrow dark filaments near the neutral magnetic line, $H_{||} = 0$, were revealed in the $H\alpha$ -filtergrams shortly after the cm burst maximum. As the loop system evolved, it gradually stretched along the neutral line towards the leading spot of the active region, reaching it at 10:14 UT. At the center of the active complex the process of development of the loop system was completed by 9:30 UT. From that time on it did not alter its appearance, with the only exception of a slight change in the fine structure. As a steady-state structure the arcade was seen in the wing of the $H\alpha$ line till 10:40 UT. In the radio range the cm burst maximum was followed by a considerable change in spectral characteristics of the radio emission, coincident in time with the formation of a loop structure. This largely applies to a major enhancement of the decimetric component of the emission. A series of abrupt rises and falls of the intensity resembling individual radio bursts was observed at these wavelengths to occur at 10-15 min intervals. At 8:39 UT the radio emission spectrum became U-shaped, with maxima in the cm and dm range, a typical feature of pro-

ton events. By 8:45 the spectrum became W-shaped, with an additional maximum at the frequency 1 GHz. After 9:04 the spectral maximum was sharply displaced toward lower frequencies in the dm range (Fig.6). The post-maximum phase of the 13 May flare was accompanied by a development of loop systems. But these arches were of opposite polarities. Unlike the 16 May arches, these were also observed in the emission. The footpoints of the 13 May arches were rooted in *N* and *S* polarity sunspots whereas those of 16 May rested against the flare ribbons.

The dm radio emission in the 13 May flare differed from the dm radio emission on 16 May in a substantially lower intensity. It is known that dm radio emission sources are located at the tops of magnetic field loops. The differences in the development of dm bursts indicate that the physical conditions differed greatly in the magnetic field loops of 13 and 16 May. These differences may be relevant both to the height of the loop tops and to the density of material and temperature within them. The dissimilar character of the development of the 13 and 16 May bursts at dm wavelengths is explainable by assuming that the magnetic field loops in the 16 May flare were higher and hotter and the density was lower than in the 16 May flare loops.

In the framework of the above assumption, the less intense development of the burst at dm wavelengths in the 13 May flare might be associated with a stronger absorption of radio waves in a cool and dense plasma of the arches. In particular, absorption becomes essential if for the arches of 13 May we assume that the temperature $T_e \sim 10^5$ K and the density $N_e \sim 10^{12} \text{ cm}^{-3}$. Precisely such conditions at loop tops were reported by Banin {1} for the flare of 13 May.

The absorption becomes poorly observable at the temperature $T_e \sim 10^7$ K and density $N_e \sim 10^{10} \div 10^{11} \text{ cm}^{-3}$. It is likely that precisely such conditions existed at magnetic field loop tops in the 16 May flare.

Acknowledgements

We are grateful to B.Kálmán and V.G.Banin, who provided us with the chromospheric observations. Special thanks are due to

V.G.Mikhalkovsky for his assistance in preparing the English version of the manuscript and typing the text.

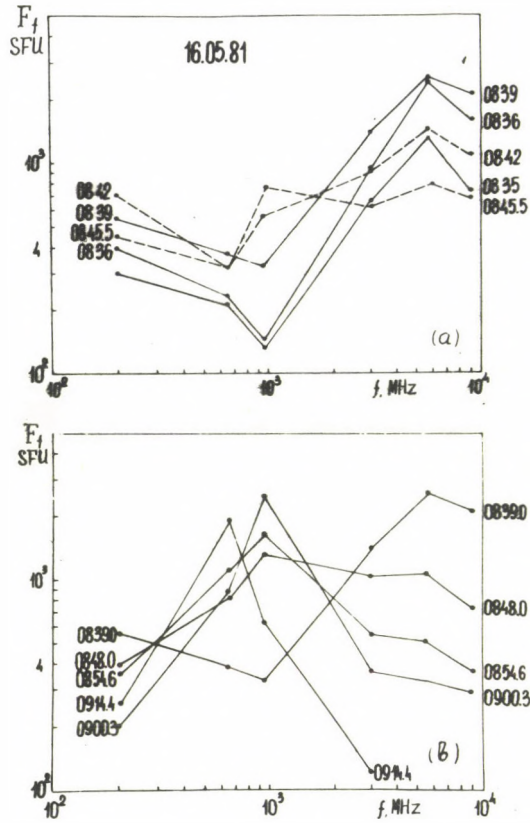


Fig. 6. Spectra of the 16 May burst for separate moments of time.

References

- {1} Banin, V.G., The activity complex and large flares of May 1981, (in Russ.) *Issl. SibIZMIR*, 65, 1983
- {2} Banin, V.G., Borovik, A.V., Yazev, S.A., The large solar flares of 13 and 16 May 1981, (in Russ.) *Issl. SibIZMIR*, 65, 1983

ФОТОСФЕРНЫЕ СЛОИ ВСПЫШЕК 14 И 15 МАЯ 1981 Г.

В КОМПЛЕКСЕ АР 3106+3112

К.В. А Л И К А Е В А

ГАО, Киев

Н.Н. К О Н Д Р А Ш О В А, П.Н. П О Л У П А Н, Т.И. Р Е Д Ю К

Астрон.Обс.НГУ, Киев

Абстракт:

Приведены результаты спектральных фотографических наблюдений активного комплекса АР 3106+3112 14 и 15 мая 1981 г. Изучены закономерности изменений профилей ряда фраунгоферовых линий в процессе вспышек разных баллов. Выявлены колебания всех параметров профилей этих линий, их ослабление и уширение вблизи максимумов вспышек. Сделаны оценки физических характеристик среды.

PHOTOSPHERIC LAYERS OF FLARES FOR MAY 14, 15, 1981

IN AR 3106+3112

K.V. ALIKAEVA

Acad.Astron.Obs.,Kiev

N.N. KONDRASHOVA, P.N. POLUPAN, T.I. REDYUK

Univ.Obs.,Kiev

Abstract:

The results are given of spectral photographic observations of active complex AR 3106+3112 for May 14, 15, 1981. The regularities are studied in profile variations of seven Fraunhofer lines forming at photospheric heights of 160-500 km during flares of various importance. Profile characteristics (depth, width, equivalent width) are found to oscillate at about 20 min periods. Near flare maxima, the lines are weakened and broadened. Before flares, the behaviour of sensitive to magnetic field lines and of insensitive ones is different. Evaluations of medium physical parameters indicate that the greatest temperature variations (up to 400 K) take place in the vicinity of flare maxima, gas pressure grows by 15%. During flares, the amplitude of general velocity field increases by 20-50%. According to radial velocity calculations, the matter motion may oscillate, velocity changes both in quantity and sign. The velocity values are largest at heights of 220-240 km, where upward motion prevails.

Спектральные фотографические наблюдения комплекса 3106+3112 проводились на Горизонтальном солнечном телескопе АЦУ-5 ГАО АН УССР. Одновременно с помощью кинокамеры делались снимки H α -фильтрограмм наблюдаемой области. На рис. 1 представлен вид этого комплекса 14 и 15 мая 1981 г. 14 мая наблюдения охватывали вспышку балла 3b (начальная стадия пропущена) и вспышку балла 1f. 15 мая более активным был другой флоккул активной области, в котором за время наблюдений произошли две субвспышки и вспышка балла 1n. Данные о вспышках, взятые из Solar Geophysical Data, приведены в табл. I.

Для изучения выбраны семь фраугноферовых линий железа, титана и хрома в области $\lambda\lambda 5210-5250 \text{ \AA}$ с разными центральными интенсивностями различной чувствительностью к изменениям физических условий среды. В рассмотрение включены как линии, нечувствительные или мало чувствительные к магнитному полю ($\lambda\lambda 5223, 5222 \text{ \AA}$), так и линии, имеющие большие факторы Ланде (табл. II). Геометрические высоты h образования центров линий вычислены в рамках модели Холвегера-Мюллер. Область образования этих линий охватывает протяженную по высоте часть фотосферы от 160 до 500 км выше уровня $\tau_{5000}=1$. В число рассматриваемых линий входят линии, используемые при измерениях магнитных полей с помощью магнитографа ($\lambda\lambda 5250$ и 5253 \AA). Точность магнитографических измерений существенно зависит от чувствительности линий к изменениям физических условий в активной области. Были проведены расчеты профилей этих линий для моделей атмосферы Солнца, отличающихся температурой (в пределах $\pm 800 \text{ K}$) или плотностью (в 0.6 - 1.6 раз) от модели спокойной фотосферы. Зависимости параметров профилей линий от температуры и плотности представлены на рис. 2. По оси ординат отложены изменения центральных глубин $\delta d_0 = \frac{d_{AO} - d_{H\Phi}}{d_{H\Phi}}$ и полуширин $\delta \Delta \lambda_{1/2} = \frac{\Delta \lambda_{AO} - \Delta \lambda_{H\Phi}}{\Delta \lambda_{H\Phi}}$, а по оси абсцисс - разность температур в активной и невозмущенной фотосфере и отношение соответствующих плотностей. Как видно из этого рисунка, обе линии в одинаковой мере чувствительны как к температуре, так и плотности, причем их центральные глубины практически не зависят от изменения плотности для "плотных" моделей. Полуширины этих линий не зависят от температуры, но

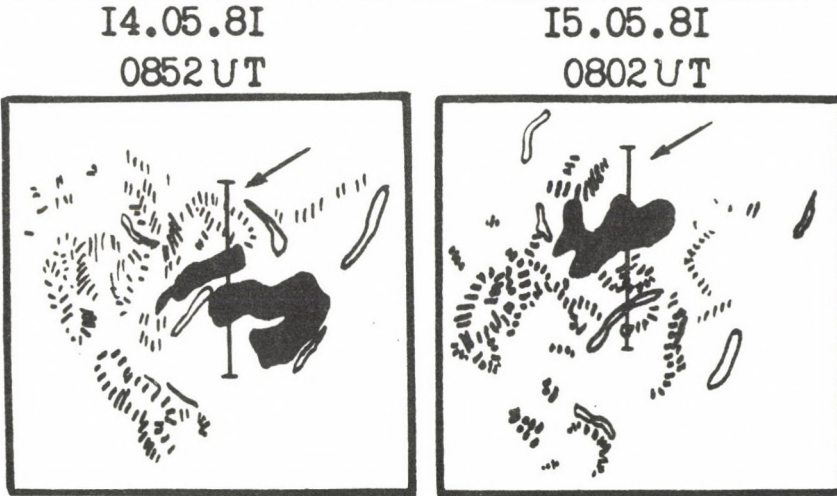


Рис.1. Зарисовка с Na-фильтраграммы активного комплекса AR 3106+3112 14 и 15 мая 1981 г.: ■ - вспышки, --- - граница флоккулов, / - волокна. Стрелка указывает положение щели спектрографа.

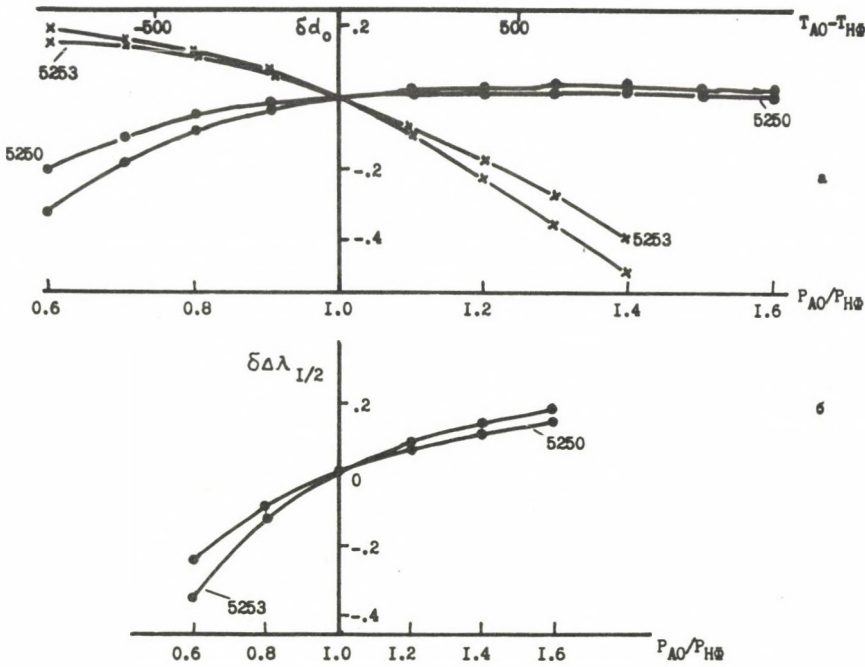


Рис.2. Изменения центральной глубины (а) и полуширины (б) линий $\lambda\lambda$ 5250 и 5253 Å в зависимости от температуры (x) и плотности (o).

зависят от плотности: для моделей с повышенной плотностью приблизительно одинаково, а для моделей с пониженной плотностью линия $\lambda 5253 \text{ \AA}$ более чувствительна. Таким образом, использование линии $\lambda 5253 \text{ \AA}$ вместо $\lambda 5250 \text{ \AA}$ в магнитографических наблюдениях магнитных полей в факелах и вспышках не дают выигрыша в точности.

Для анализа наблюдаемых изменений в линиях рассмотрены отклонения центральных глубин δd_0 , полуширин $\delta \Delta \lambda_{1/2}$ и эквивалентных ширин δW от соответствующих значений в невозмущенной фотосфере. Эти отклонения характеризуют изменения физических условий фотосферных слоев на данных геометрических высотах. Общие закономерности изменений профилей линий в процессе вспышки таковы:

1. Все параметры профилей во время вспышек подвержены колебаниям, превышающим ошибку измерений, период колебаний составляет 15-30 минут.
2. Все линии ослаблены и уширены, особенно вблизи максимумов вспышек. Ослабление тем больше, чем глубже линия образуется.
3. Различие поведения чувствительных и мало чувствительных к магнитному полю линий проявляется в ослаблении (приблизительно на 10 %) магниточувствительных линий перед вспышками и кратковременном усилении их в начальной стадии вспышек.

Такое поведение линий можно объяснить увеличением температуры и плотности в предмаксимальной фазе вспышек и их уменьшением в стадии спада, а также колебаниями поля крупномасштабных движений и магнитного поля. Возможно, эти колебания являются проявлением воздействия на фотосферу ударных волн, распространяющихся из вышележащих ярусов атмосферы {1}.

Малые изменения центральных глубин линий в зависимости от температуры и газового давления среды описываются формулами, приведенными в работе Бадалян и Обридко {2}. Применяя эти формулы к нескольким линиям, образующимся практически на одной высоте, можно оценить как температуру, так и давление. Во избежание ошибок за счет влияния магнитного поля использовались линии, мало чувствительные к нему. На рис. 3 представлены данные о физических условиях на высоте 170-180 км для вспышки

балла 3b 14.05.81 и для вспышки балла 1n 15.05.81. Можно отметить довольно значительные колебания физических параметров на протяжении вспышек. Наибольшее изменение температуры (до 200 К во вспышке 3b и до 400 К во вспышке 1n) наблюдается около максимумов соответствующих вспышек. Отклонения давлений от их значений в невозмущенной фотосфере достигают в отдельные моменты 15%. Значительные временные колебания давления хорошо коррелируют с ходом лучевых скоростей на рассматриваемых высотах.

Лучевые скорости были определены на высотах 130–260 км. Максимальные значения скоростей достигают ± 2.5 км/с (ошибка в определении скорости составляет ± 0.25 км/с). В одной и той же области на данной высоте с течением времени движение может носить колебательный характер, т.е. подъем сменяется опусканием вещества и наоборот. Периоды колебаний в среднем составляют около 20 минут. Однако есть ряд высот (220–240 км), где в это же время в течение 3–4 часов наблюдается однонаправленное движение, а именно, подъем вещества. Абсолютные значения скоростей здесь наибольшие. На рис. 4 представлен ход лучевых скоростей на трех различных высотах в тех же вспышках, что и на рис. 3. Как упоминалось выше (рис. 3), лучевая скорость коррелирует с давлением. Отмечена и корреляция с полуширинами линий.

По полуширинам слабых линий $\lambda\lambda 5222$ и 5223 \AA была вычислена амплитуда общего поля скоростей в активном комплексе на высоте около 150 км (рис. 5). Значения амплитуды поля скоростей и их изменения во времени, полученные по обеим линиям, в целом хорошо согласуются между собой, что свидетельствует о небольшом влиянии на линию $\lambda 5223 \text{ \AA}$ магнитного поля и, возможно, о малых изменениях напряженности магнитного поля в процессе развития области на данном уровне фотосферы. Скорость нетепловых движений на уровне фотосферы в активной области в среднем на 20 % превышает скорость в невозмущенной фотосфере. В мощной вспышке 14.05.81 и после нее наблюдаются резкие колебания амплитуды поля скоростей.

Таким образом, в процессе эволюции активного комплекса на всех уровнях фотосферы от области температурного минимума до наименьшей из рассмотренных нами высот (130 км) происходят различного

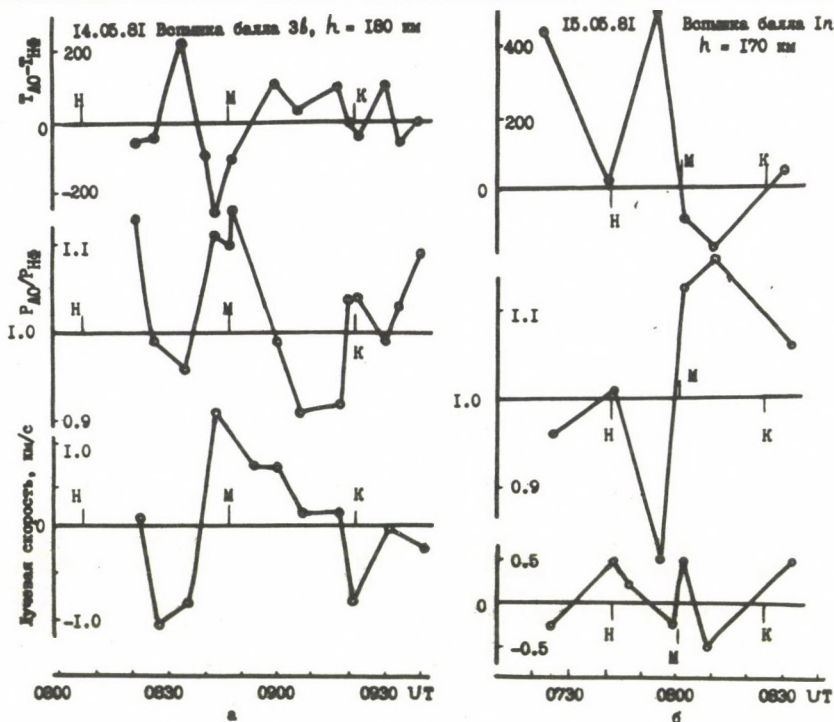


Рис. 3. Ход разностей температур и отношений давлений в активной области и невозмущенной фотосфере, а также ход лучевых скоростей во время двух вспышек: 14.05.81 (а) и 15.05.81 (б).

ТАБЛИЦА 1

Данные о вспышках 14 и 15 мая 1981 года

Дата	Начало UT	Максимум UT	Конец UT	Координаты		Балл
				ϕ	λ	
14.05.81	0808	0848	0923	+20	-32	3b
14.05.81	1000	-	1050	+21	-36	1f
15.05.81	0741	0801	0824	+12	-24	1n
15.05.81	1026	1042	1100	+11	-22	sf
15.05.81	1206	1211	1222	+11	-21	sn

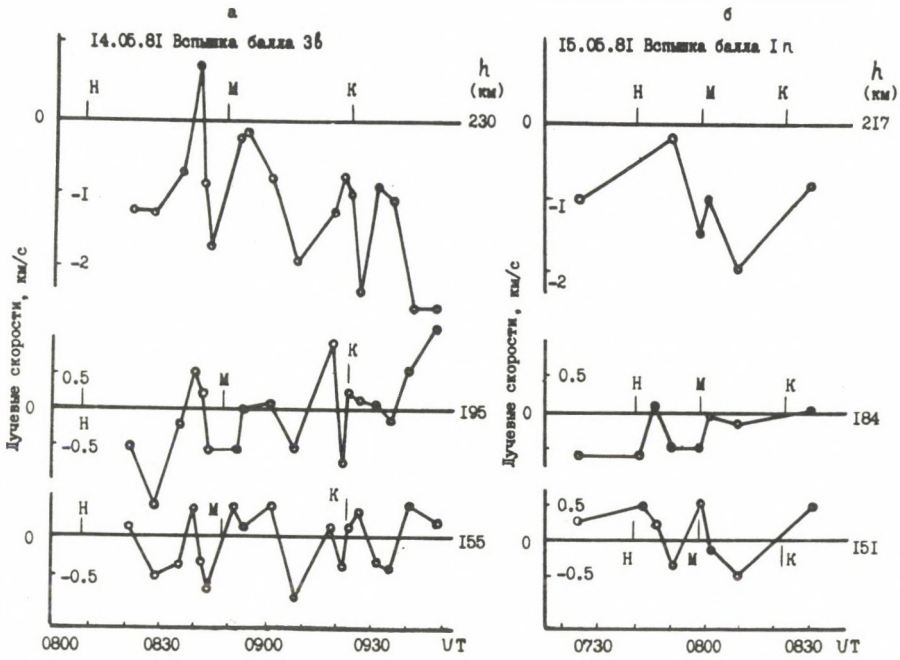


Рис. 4. Лучевые скорости на разных высотах во время вспышек разных баллов.

14.05.81

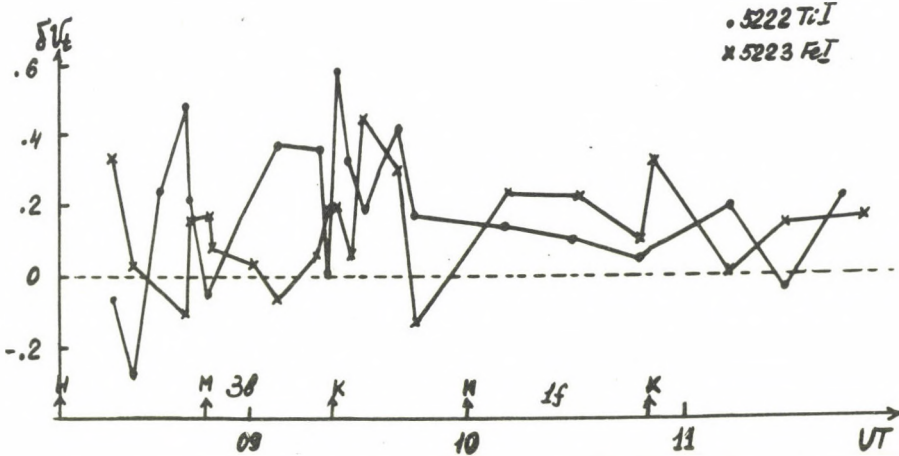


Рис. 5. Изменения во времени амплитуды поля скоростей в комплексе AR 3106+3112 на высоте $h = 150$ км.

ТАБЛИЦА 2

Список используемых линий, их характеристики
и высоты образования

λ	Элемент	Центральная глубина	h	EP	Фактор Ланде
Å			км	эв	
5210.392	Ti I	0.808	506	0.05	5/4 -5/5
5250.216	Fe I	0.772	435	0.12	3
5247.574	Cr I	0.760	409	0.96	5/2
5253.468	Fe I	0.700	314	3.28	3/2
5223.190	Fe I	0.350	180	3.63	1/2 -0/0
5222.685	Ti I	0.222	176	2.08	0-0
5211.535	Ti II	0.380	166	2.59	8/7 -8/7

рода изменения физических условий. Обнаружены колебания физических параметров среды на всех высотах фотосферы во время вспышек. Интересным и требующим подтверждения фактом является корреляция изменений во времени давления и лучевых скоростей. Вызывает интерес также и аномальное поведение лучевых скоростей на высотах 220-240 км. Изменения амплитуды общего поля скоростей на высоте 150 км в процессе развития активной области в целом невелики, они максимальны во время мощной вспышки балла 3b. Различие поведения сильно и мало чувствительных к магнитному полю линий перед вспышками свидетельствует, по-видимому, о довольно важной роли магнитного поля в верхних слоях фотосферы для создания предвспышечной ситуации.

Л и т е р а т у р а

- {1} Алтынцев, А.Т., Банин, В.Г., Куклин, Г.В., Томозов, В.М., *Солнечные вспышки*, с.133, Наука, Москва 1982
- {2} Бадалян, О.Г., Обридко, В.Н., О вариациях интенсивностей фотосферных линий и непрерывного спектра при малых изменениях физических параметров, *Астрон.Ж.* 52. 561, 1975

THE RADIO EMISSION AND ACTIVE REGION DEVELOPMENT
DURING THE PERIOD OF MAY 15 - 25, 1981

H. AURASS, A. BÖHME, A. KRÜGER
ZISTP (HHI), Berlin(GDR)

Abstract:

The activity of May 21, 1981 is described and special attention is given to the m-wave enhancement. This particular burst activity is dominated by a three step strong and broad band continuum rise (step I: 10:45 UT; step II: 11:51 UT; step III: 12:38 UT). Step I and III behave like noise storm onsets. The corresponding soft X-ray event, the missing short-cm activity, and the evidence of type IV-like dm structures long before the start of an observed flare (confirmed for step III, only) lead to the conclusion that the centre of the disturbance must be at greater heights in the corona.

РАДИО ЭМИССИЯ И РАЗВИТИЕ АКТИВНЫХ ОБЛАСТЕЙ
В ПЕРИОД 15 - 25 МАЯ 1981 Г.

Х. АУРАС, А. БЁМЕ, А. КРЮГЕР

ЦИСЭФ (HHI), Берлин (ГДР)

Абстракт:

Показано развитие солнечной активности в метровом диапазоне. Особенно обсуждаются увеличение континуума 21-ого Мая 1981 г. Наблюдалось шаговое развитие (первый шаг 10:45 УТ, второй шаг 11:51 УТ, третий шаг 12:38 УТ). Кажется, что шаг I и шаг III были увеличения типа шумовых бурь. Некоторые факты (связанное явление мягкого рентгеновского излучения, отсутствие активности в диапазоне кратких микроволн, наблюдение явления как в всплесках типа IV в дециметровом диапазоне уже до начала регистрируемой вспышки) поддерживают предположение, что источник явления может быть расположен в больших высотах короны.

The activity within the interval can be classified as follows (see Fig.1 and {1}):

1. The variable noise storm activity during whole the interval.
2. A type IV burst on May 16, starting 8:30 UT, followed by a type IV mB burst at 11:40 UT, lasting till May 17.
3. A dm burst on May 18, 08:00 - 09:20 UT.
4. A strong noise storm enhancement on May 21, mixed with some kind of type IV activity, which very slowly decays during May 22 and was perhaps masking the "background" noise storm.

Some further facts must be noted:

- a) The activity is essentially connected with the active regions of Hale number 17644 and 17653, having a high resp. very low S-component efficiency.
- b) There was a low flare activity.
- c) Mercier's 169 MHz radioheliograph data {1} reveal a very complicated source structure past May 18, 1981. There are several equally polarized noise storm sources, sometimes positioned far away from active regions.

The May 21, 1981 event is characterized by some special peculiarities:

1. According to *Solar-Geophysical Data*, the m-wave enhancement is associated in time with a rather strong soft X-ray outburst, starting near 11 UT and lasting until 16 UT. An analogy with the X-ray - noise storm correspondence as described in {2} is possible. The unusual absence of short-cm (and optical flare) emission leads to the conclusion that the centre of the disturbance must be at greater heights in the corona.
2. The m-wave continuum emission grows in three steps. No flare is reported which corresponds with step I or step II (visual flare patrol, only).
 - a) Step I (Fig.2): The continuum rise starts at 234 MHz at 10:45 UT, then a burst component activation follows 10:50 UT at 113 MHz, and 11:10 UT at 64 MHz. A small gradual rise and fall burst begins at 3 GHz at 11:10 UT, and later at 2 GHz and at 1.47 GHz.

The m-wave continuum enhancement proceeds, starting 11:20 UT

- at 113 MHz and near 11:35 UT at 64 MHz;
- b) Step II (Fig.2): This step starts over the 234 MHz - 30 MHz range within a 1 min interval at 11:51 UT. In particular, the steep intensity development at 64 MHz is a rare effect. Mercier's 169 MHz data reveal a slowly moving source, originating away from the former noise storm sources and dominating the activity at 12 UT and later. Fig.3 illustrates the situation. A slow source movement was already reported for noise storm enhancements and type IV mB bursts {3},{4}, and is not quite unusual.
- c) Step III: After a short relaxation, the m-wave enhancement continues in the following manner:
- | | |
|----------|------------|
| 12:38 UT | at 234 MHz |
| 12:42 UT | at 113 MHz |
| 12:43 UT | at 64 MHz |
| 13:00 UT | at 40 MHz |
| 13:05 UT | at 300 MHz |

Following *Solar-Geophysical Data* Prompt Reports, a subflare was observed in the region 17653 starting 12:45 UT and being well correlated with a small superposed peak of the 1.47 GHz emission. A peculiar behaviour was observed in the dm range between step II and step III, see Fig.4: Two peaks of right handed polarized emission were observed at 778 MHz without remarkable and correlated effects at the adjacent observing frequencies. Strong decimetric burst components of bandwidths smaller than about 500 MHz are not in principal unusual in this spectral range, as indicated by former observations {5} and theoretically discussed by Kuipers {6}. These emissions are evidently not directly related to the impulsive or explosive flare phases, as is typically the case, and may be considered as an indication for a highly inhomogeneous source structure. This is further supported by the observation of an irregular intermediate drift burst pattern in the 640 - 800 MHz range during the 12:23-12:28 UT interval (Karlický, private communication), which definitely occurred before step III, causing flare.

The described continuum evolution is of special interest in the frame of Böhme's {7} extensive statistical work, basing

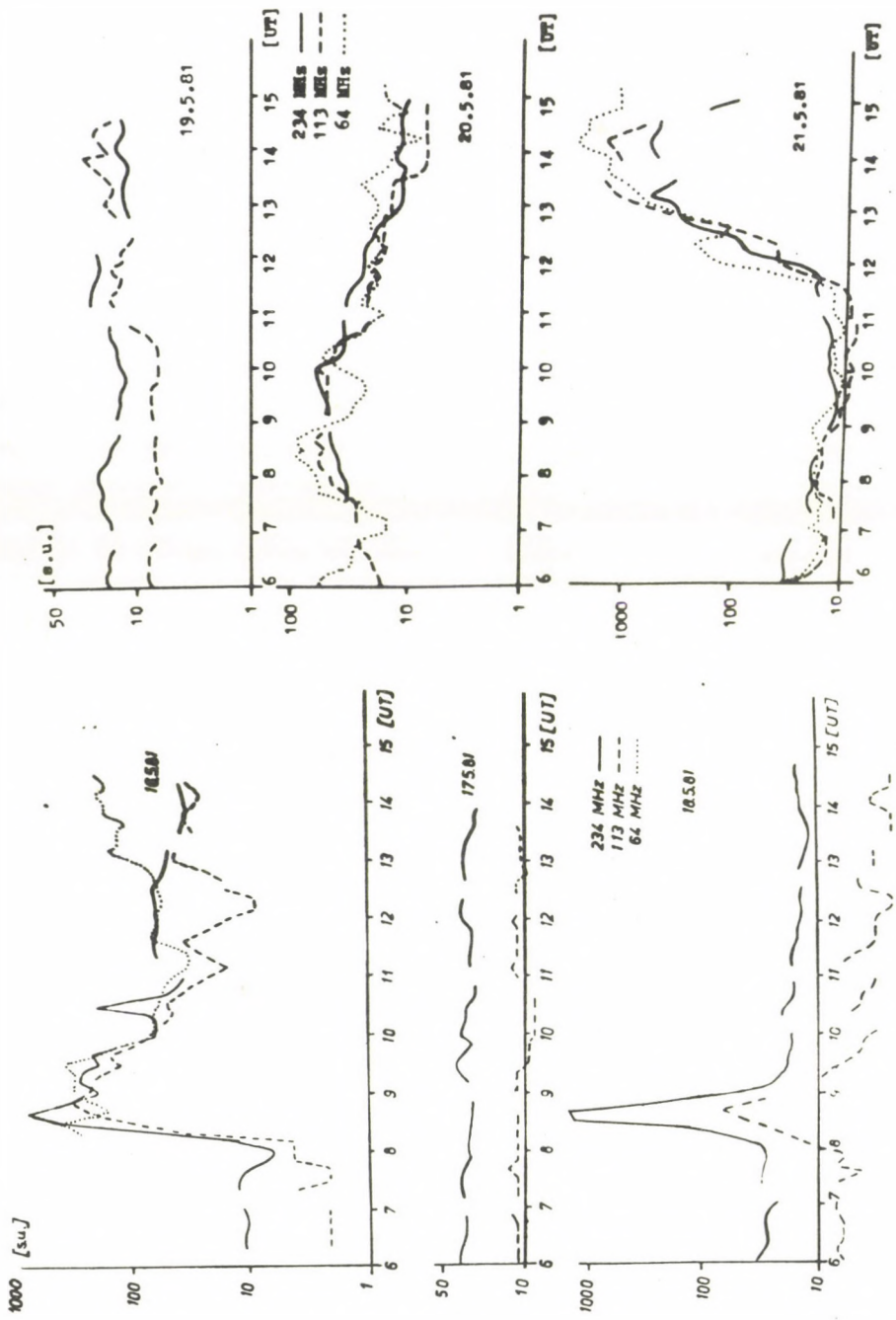


Fig. 1b.

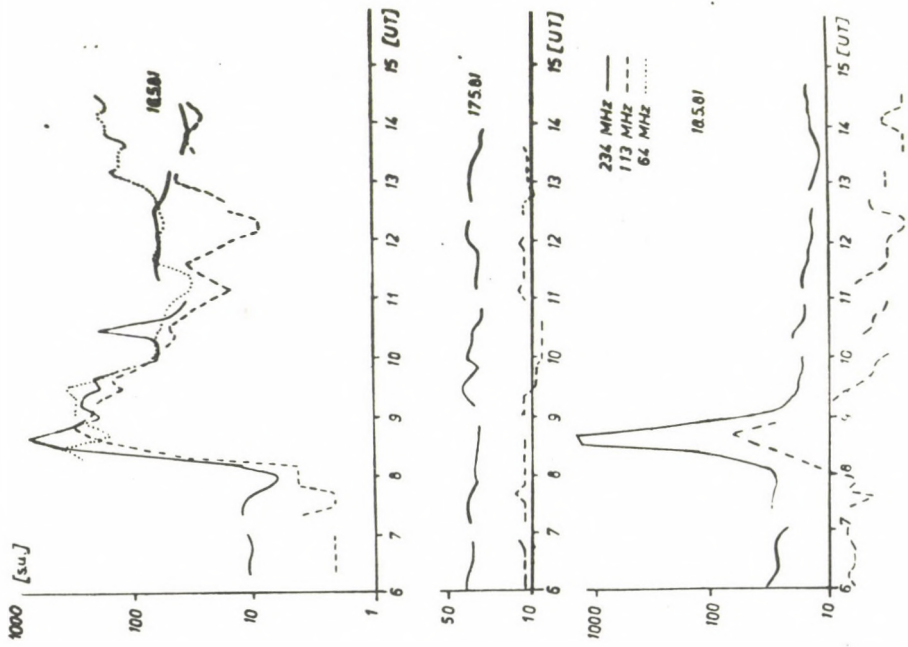


Fig. 1a.

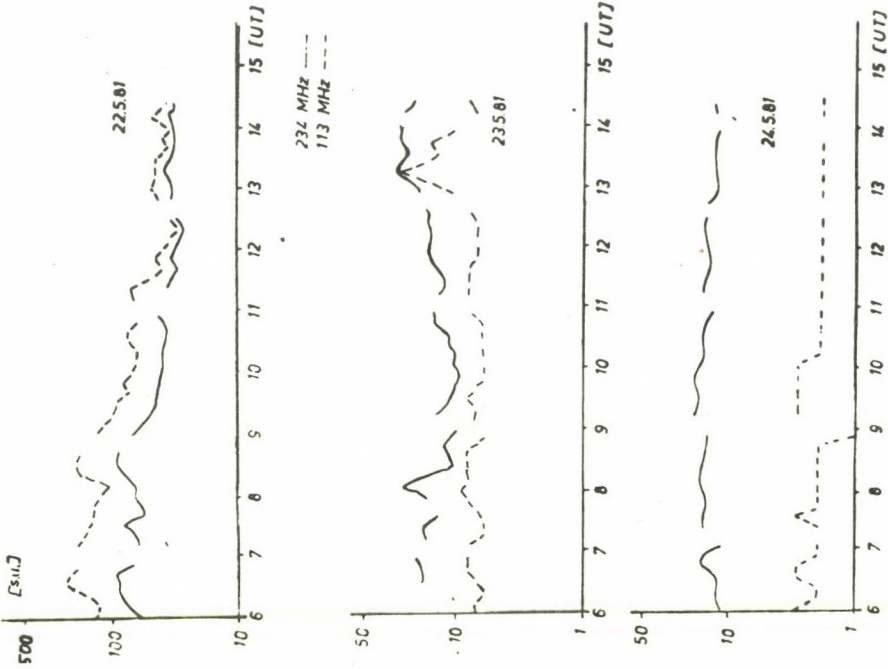


Fig. 1a - 1c. 10 min - continuum flux mean values
May 1981

Fig. 1c.

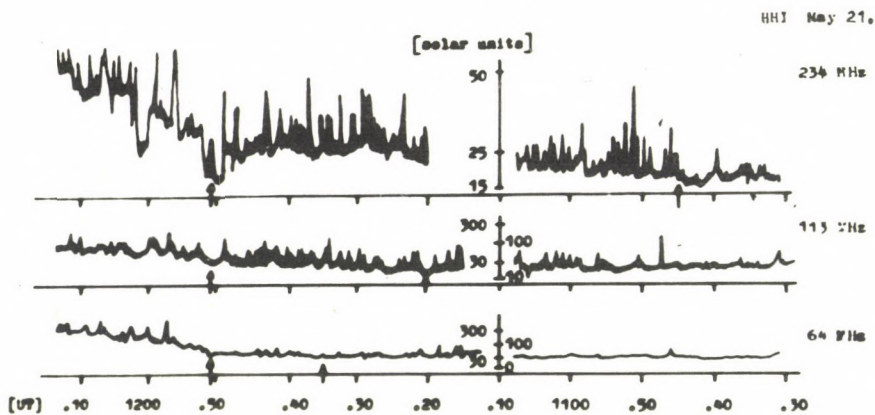


Fig. 2. The noise storm enhancement on May 21, 1981. The arrows mark the starting times given in the text.

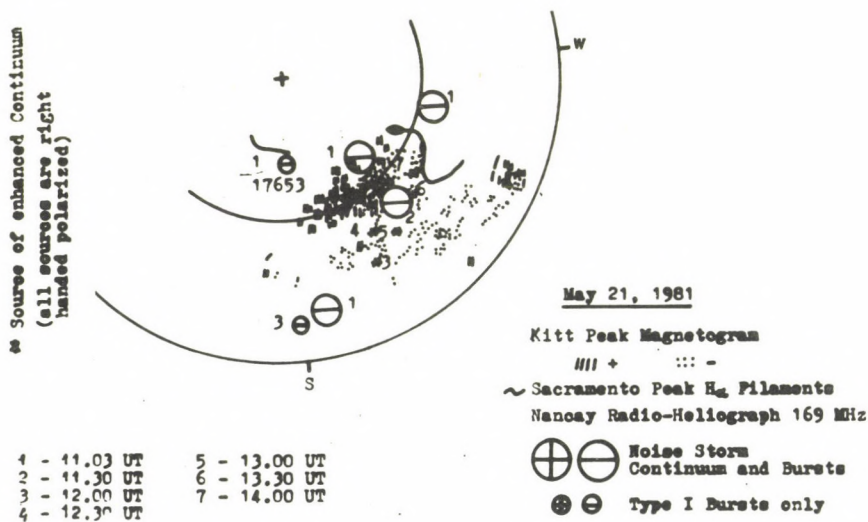


Fig. 3. The situation near active region 17653.

on 6 HHI single frequency records, including the onset behaviour of all the rise + I type noise storms (following the *HHI Solar Data* classification) during the 20th activity cycle from 1964-1976 (about 140 events). Böhme has divided the ensemble into the subgroups "flare related" and "non-flare related" noise storms, significantly differing in the onset behaviour and the covered spectral range. Step I of the May 21, 1981 event discussed fits the mean pattern of a non-flare related noise storm well, step III belongs to the subclass flare related noise storm onset.

Step II onset is a remarkable effect because of no flare correlation was observed and the fast, broadband continuum rise. Fig.5 gives some continuum intensity spectra drawn from the HHI single frequency records. The spectra 12:15 UT, 12:25 UT and 12:40 UT characterize the enhancement and the break following the step II onset. The spectral gap near 113 MHz, together with the highly polarized emission at 40 MHz are rare and unusual phenomena. In our experience {8} past step III the high polarization degree at 113 MHz and 40 MHz together with the observed spectral shape favours the assumption, that the event is a very broad band noise storm or type IV mB burst. In {9} enhanced emission is reported from 2 MHz - 540 MHz spectrograph observations on May 21 and May 22, 1981.

On the whole the May 21, 1981 event is surely not a typical type IV burst. It belongs to a small class of events showing very low cm-wave and very high m-wave emission. Another example of this kind was the August 28, 1966 12 UT burst.

R e f e r e n c e s

- {1} Aurass,H., Böhme,A., Fomichev,V.V., Krüger,A., Mercier,C., Tlamicha,A., Urpo,S., to be published in *4th CESRA Workshop*, 2. 1982
- {2} Lantos,P., Kerdraon,A., Rapley,G.G., Bentley,R.A., *Astron.Astrophys.*101. 33, 1981
- {3} Clavelier,B., Jarry,M.F., Pick,M., *Ann.d'Astrophys.*31. 5, 523, 1968
- {4} Kerdraon,A., Mercier,C., to be published in *4th CESRA Workshop*,1. 1982
- {5} Krüger,A., Fürstenberg,F., Fricke,K., *HHI Suppl.Ser.Solar Data*,2. Nr.5. 187, 1971

- {6} Kuijpers, J., *Solar Phys.* 36. 157, 1974
- {7} Böhme, A., submitted to *Solar Phys.* 1983
- {8} Böhme, A., submitted to *Solar Phys.* 1983
- {9} Pintér, S., Grigoreva, V.P., to be published in *4th CESRA Workshop*, 2.1982

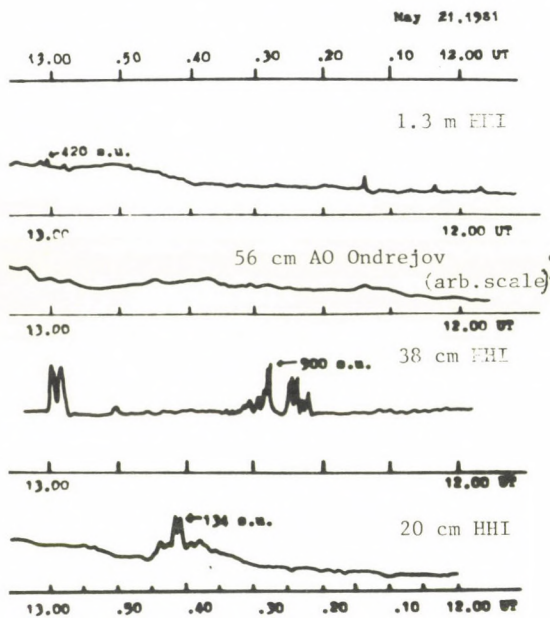


Fig. 4. Peculiar behaviour in the dm range between 12:00 and 13:00 UT.

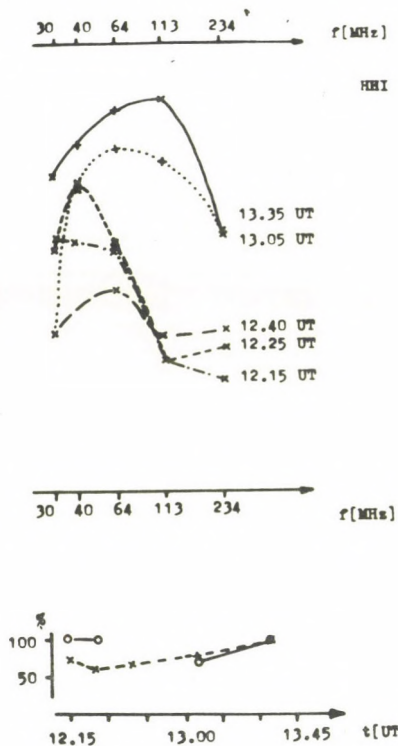


Fig. 5. Continuum intensity spectra during the m-wave enhancement on May 21, 1981.

bottom: Degree of circular polarization
 × 113 MHz
 o 40 MHz

PECULIARITIES OF THE DEVELOPMENT OF FLARE ON MAY 16, 1981
AS OBSERVED IN OPTICAL, X-RAYS AND RADIO WAVES

V.N. I S H K O V, A.K. M A R K E E V, V.V. F O M I C H E V,
G.P. C H E R N O V, I.M. C H E R T O K

IZMIRAN, Troitsk

O.B. L I K I N, N.F. P I S A R E N K O

Inst.Space Res., Moscow

B. V A L N Í Č E K, M. K A R L I C K Ý,

A. T L A M I C H A, F. F Á R N Í K

Astron.Inst., Ondřejov

B. K Á L M Á N

Heliophys.Obs., Debrecen

Abstract:

On the basis of X-ray, visual and radio observations of the large flare of 16 May 1981 the conclusion may be drawn that a large flare is a long duration energy release process, and can be interpreted as a sum of smaller flares throughout the active region.

ОСОБЕННОСТИ РАЗВИТИЯ ВСПЫШКИ 16 МАЯ 1981 Г.

ПО НАБЛЮДЕНИЯМ В РЕНТГЕНОВСКОМ, ОПТИЧЕСКОМ И РАДИОДИАПАЗОНАХ

В.Н. ИШКОВ, А.К.МАРКЕЕВ, В.В.ФОМИЧЕВ, Г.П.ЧЕРНОВ, И.М.ЧЕРТОК

ИЗМИРАН, Троицк

О.Б. ЛИКИН, Н.Ф.ПИСАРЕНКО

ИНИ, Москва

Б. ВАЛНИЧЕК, М. КАРЛИЦКИЙ, А. ТЛАМИХА, Ф. ФАРНИК

Астрон.Инст., Ондржейов

Б. КАЛМАН

Гелиофиз.Обс., Дебрецен

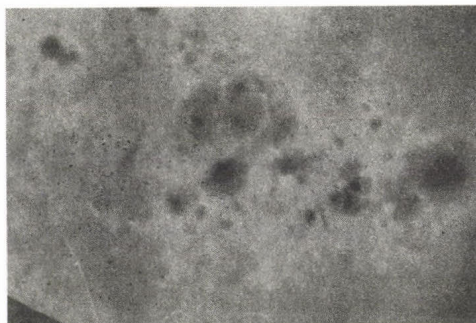
Абстракт:

На основе рентгеновских, оптических и радионаблюдений большой хромосферной вспышки 16 мая 1981 г. можно сделать вывод, что большая вспышка представляет собой процесс энерговыделения большой длительности, и может быть объяснена как сумма меньших вспышек в активной области.

The results of the analysis of the flare of May 16, 1981, the last one out of series of the large flares connected with passage of the complex active region HR 17644 are given in this report. This flare was observed during the International Post SMY program and XII STIP interval. The analysis is based on the observations in optical, X-rays and radio regions. The optical ($H\alpha$) observations were made with a coronagraph through 0.5 Å bandpass Halle $H\alpha$ filter at Debrecen Observatory and with a tower solar telescope at IZMIRAN. X-rays measurements in the range 2-360 keV have been obtained by the Czechoslovak photometer aboard the Prognor-8 satellite. The radio observations were carried out at two observatories: Ondrejov (the dynamic radio spectra in the frequency band 150-1000 MHz and the intensity-time profiles at the fixed frequencies 260, 536 and 890 MHz) and IZMIRAN (the dynamic spectra in the frequency range 45-236 MHz and the intensity-time profiles at the fixed frequencies 204 and 3000 MHz). The analysis of the whole observational data set allows the following peculiarities of the flare development to be picked out:

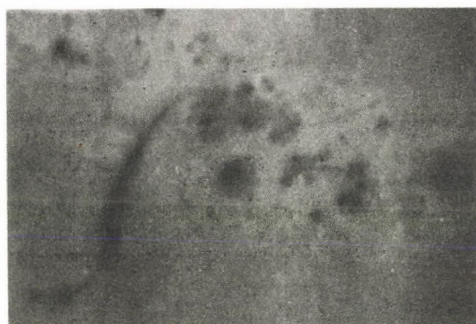
1. The flare of May 16, 1981 is an example of long duration energy release process which in the course of its development covered the extended area in HR 17644. The energy release processes took place in different sites of the flare region and had different manifestations at optical, X-rays and radio waves.
2. Development of the flare in $H\alpha$ occurred in two stages: the low energy stage when the flare developed at an area between the spot groups and was practically spotless (before 08:20 UT), and the main stage when the flare developed in the spot group and the flare knots arose or penetrated the spot penumbra (Figs.1,2).
3. Localization and evolution of the flare knots indicate that two connection systems between the different regions in this spot group (between the regions I and II, as well as I and III in Fig.2) existed. This connection was probably realized through loop like structures which became visible

- during the post maximum phase of the flare as an arch system.
4. During the pre-maximum stage of the flare the correlation was observed between the relatively sharp variations in the rate of increase in soft X-rays (2-8 keV) and the brightenings of the existing spaced H α knots and in the arising of the new ones (the parts 1,2 and 3 on the intensity-time profile of X-rays in Fig.3 correspond to the brightenings of regions II, I and II in Fig.2, respectively).
 5. A close time correspondance between the arising of the different peaks in hard X-rays (20-80 keV) and microwave emission and the brightenings of the different H α knots (Figs.1,2,3) exists.
 6. During the evolution of the flare the considerable variations in the frequency spectrum of microwave emission were observed. The maximum of spectrum moved to the short wave part of cm-region when H α emission had approached the sunspots (08:25 and 08:38 UT); meanwhile, during the initial spotless phase of the flare and the decay stage the maximum of spectrum was situated at dm-waves (Fig.4, the variation of f_{max} is shown in Fig.3b). However, any significant variations in power index of accelerated electrons were not observed in the limits of measurement accuracy (Fig.3b, lower part).
 7. Development of the flare was accompanied by the arising of two shock waves which issued at different times (08:14-08:15 UT and 08:20-08:21 UT, Fig.5) from the different flare sites. Propagation of these shocks in the corona resulted in generation of two type II radio bursts (08:19:12-08:31:00 UT and 08:30:35-08:43:30 UT, Fig.6).
 8. Dynamic spectrum of the second type II radio burst had an unusual, fine structure in the form of numerous short-lived elements with the bandwidth to 10 MHz, negative frequency drift 5-30 MHz s $^{-1}$ and life time at fixed frequency 0.1 s (08:36:10-08:38:00 UT and 08:41:20-08:43:30 UT, Fig.6). This fine structure is believed to belong to the second

Fig. 1a.

1981 May 16
H α + 1 Å
filtergrams

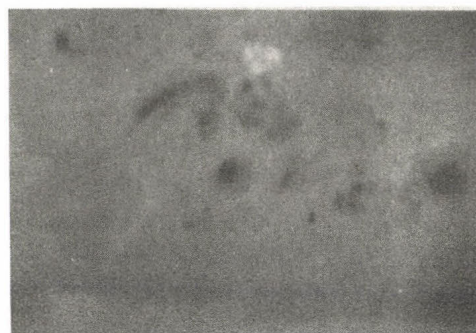
07:34:01 UT

Fig. 1b.

07:58:23 UT

Fig. 1c.

08:01:26 UT

Fig. 1d.

08:12:53 UT

Fig. 1e.



1981 May 16

H α + 1 Å

filtergrams

08:20:35 UT

Fig. 1f.



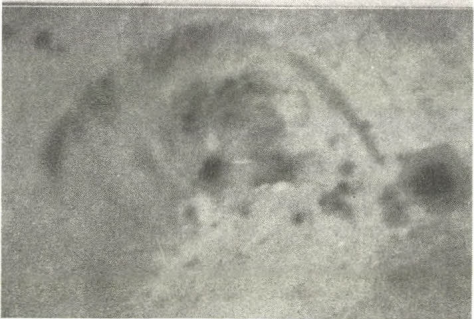
08:26:01 UT

Fig. 1g.



08:39:46 UT

Fig. 1h.



10:05:21 UT

harmonic band and to be connected with propagation of the shock waves through the inhomogeneities with the scale of 10^7-10^8 cm.

9. The beginning of the wide band pulsations with a time scale of seconds in type IV radio burst at dm-waves (08:24:30 UT) and at m-waves (08:41:30 UT) correlate with the development and the brightening of $H\alpha$ knots in penumbra of the sunspots (Figs.6,7). This fact indicates that pulsations appear when the flare processes affect the magnetic loops with footpoints situated in the umbra or penumbra of sunspots.
10. During the post maximum phase of the flare the different fine structure at dm-waves and m-waves (zebra pattern, pulsations, fiber bursts, absorptions) were observed in the dynamic spectrum of type IV burst (Fig.8). The appearance of zebra pattern (09:11 UT and 09:42 UT) followed the brightenings of tops of the arch flare system.

The results of the complex analysis of the flare on May 16, 1981 given above allow the conclusion to be drawn that a big solar flare with a complicated space-time structure is to be considered as a totality of a number of less intensive flares occurring at different moments in time and in different parts of active regions. In this case the sequence of an energy release process can be accompanied by X-rays and radio bursts with different characteristics (in particular, by radio bursts with different frequency spectra and fine structures), and by a generation of more than one shock wave with their own trajectories.



Fig. 2.

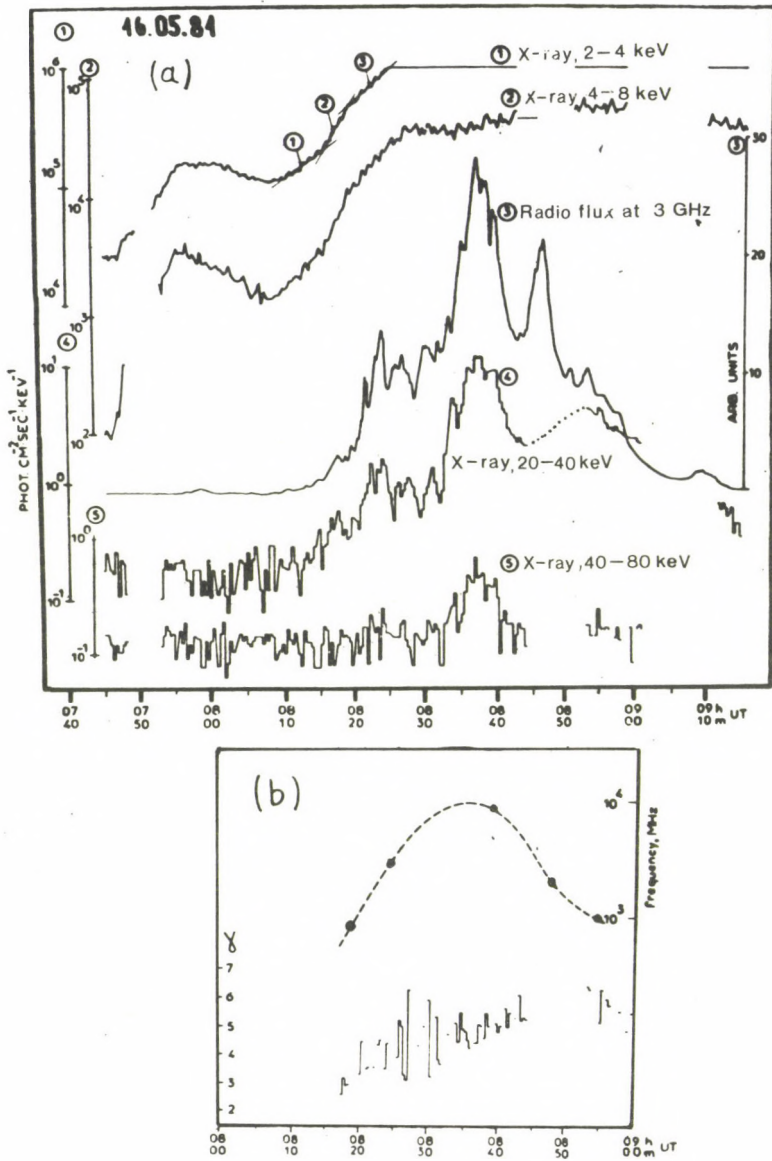


Fig. 3.

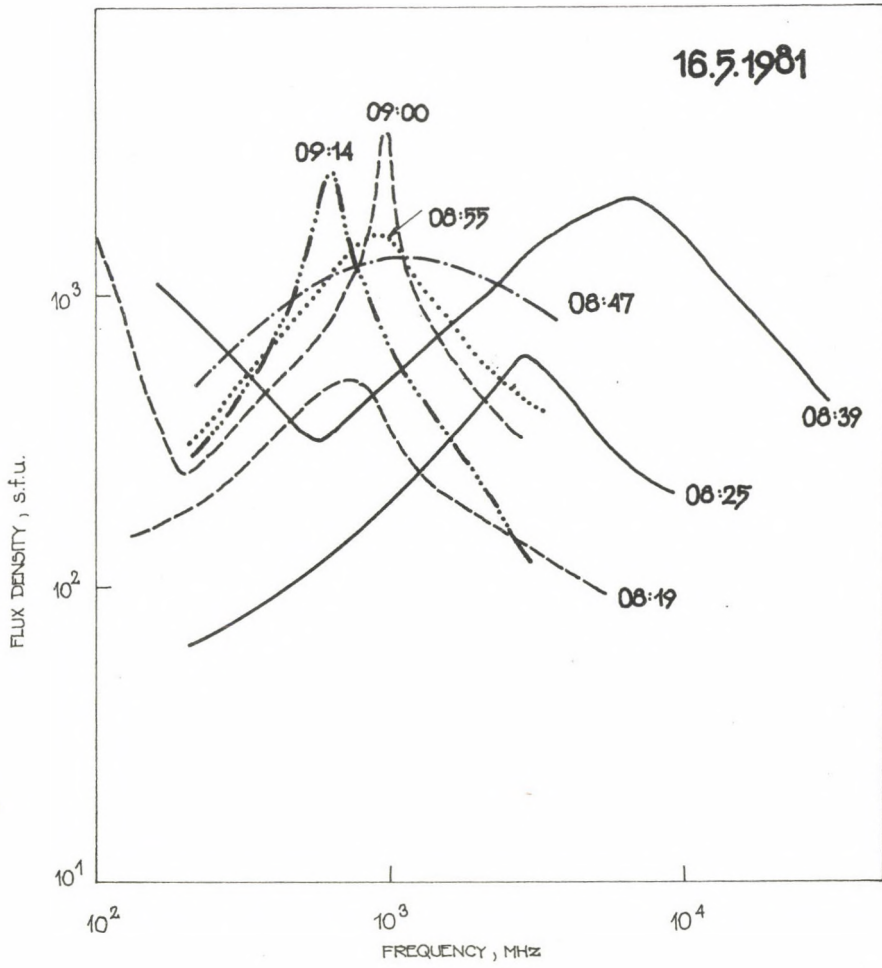


Fig. 4.

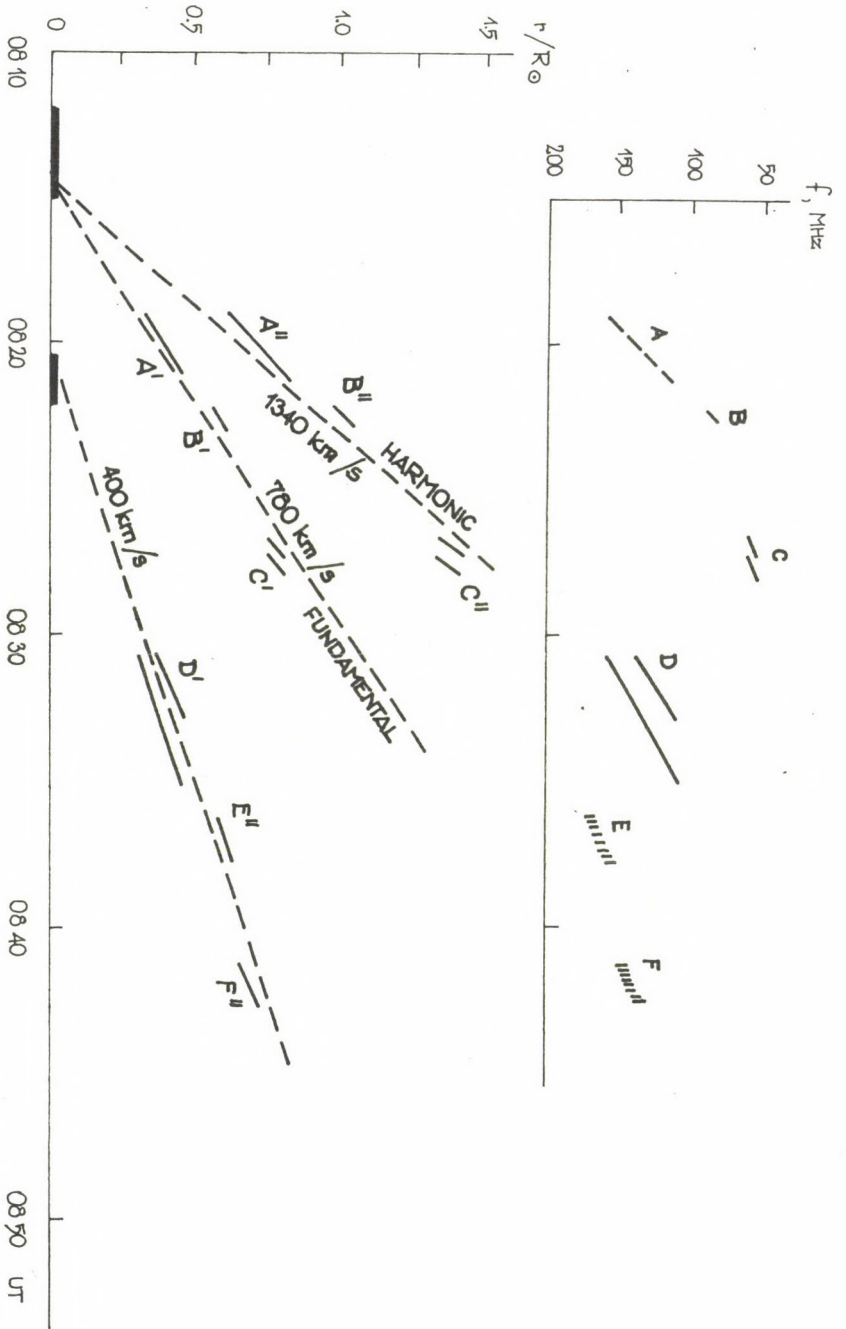


Fig. 5.

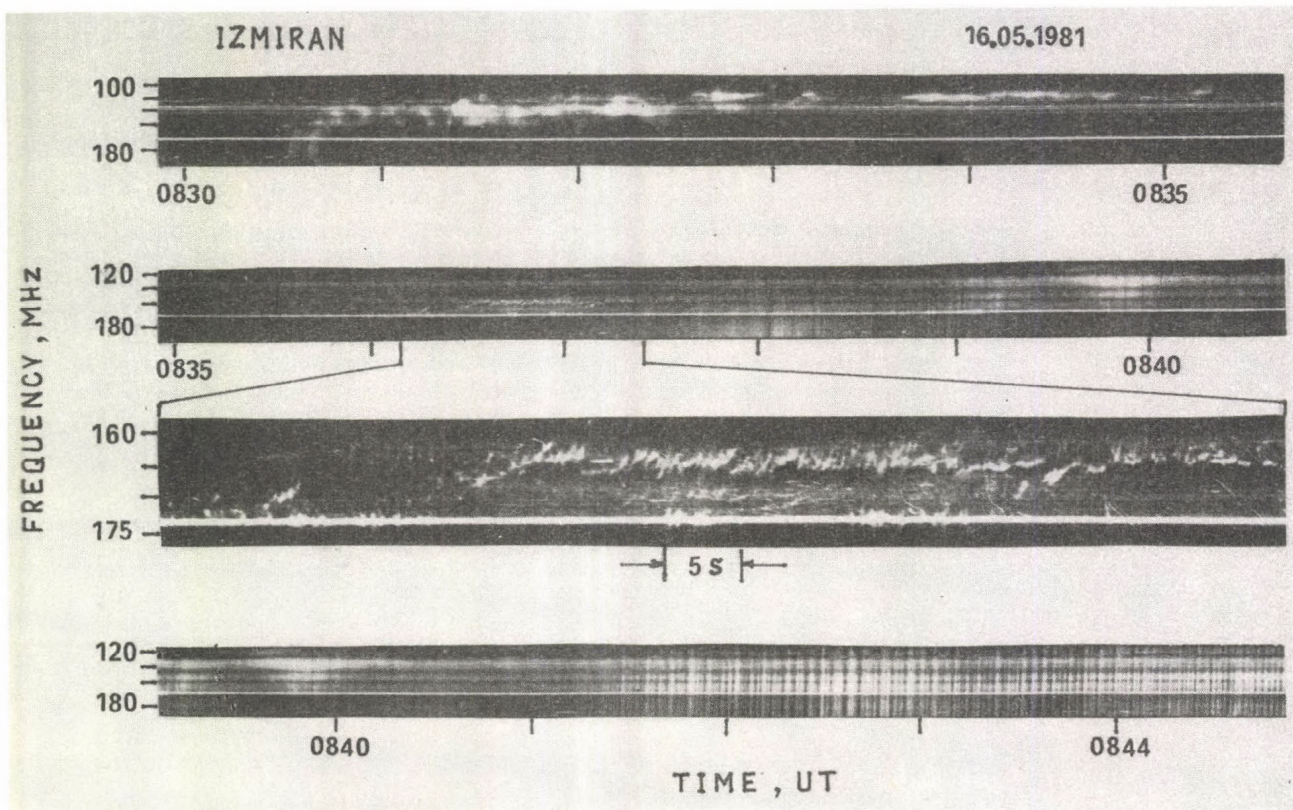


Fig. 6.

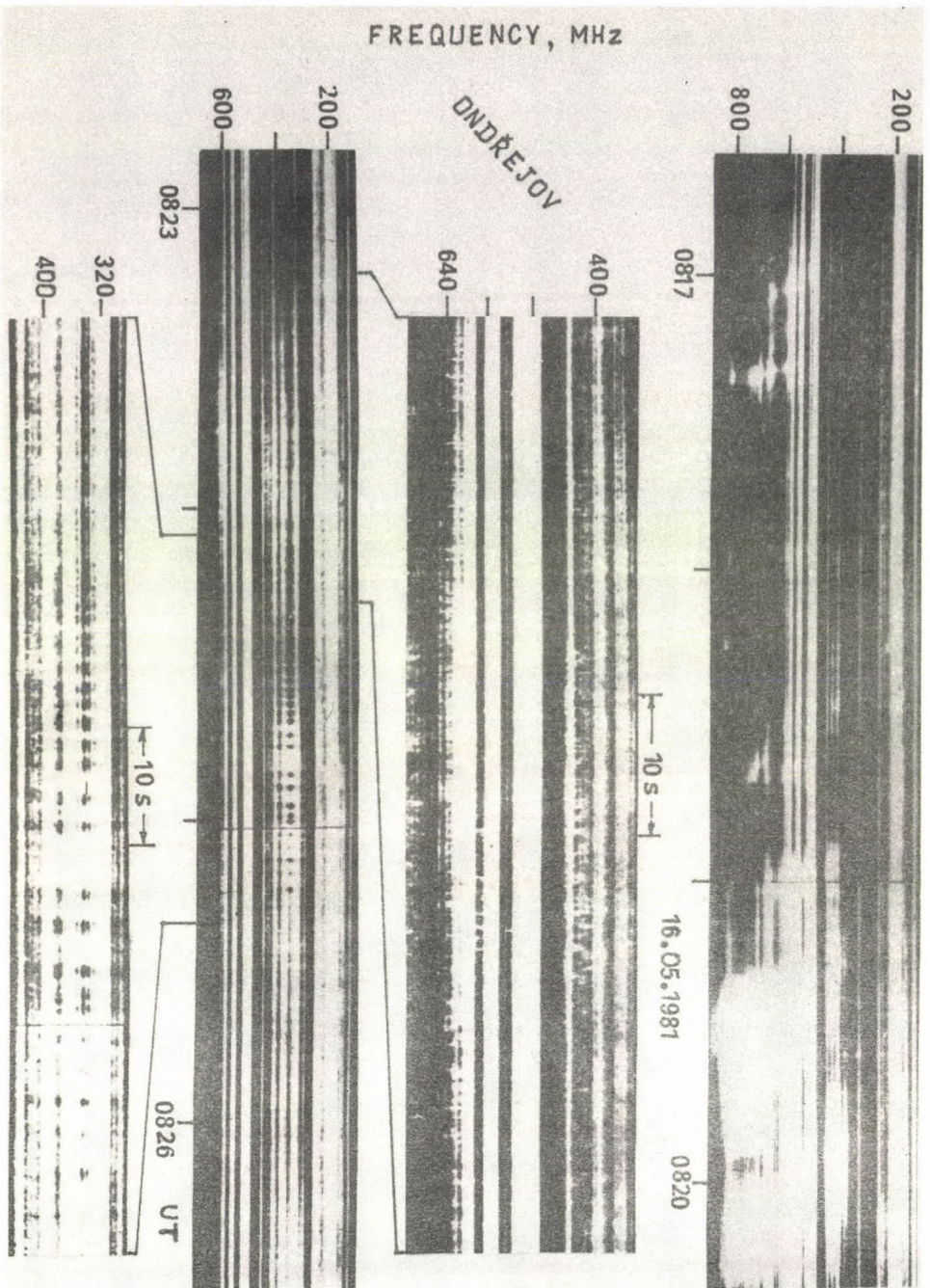


Fig. 7.

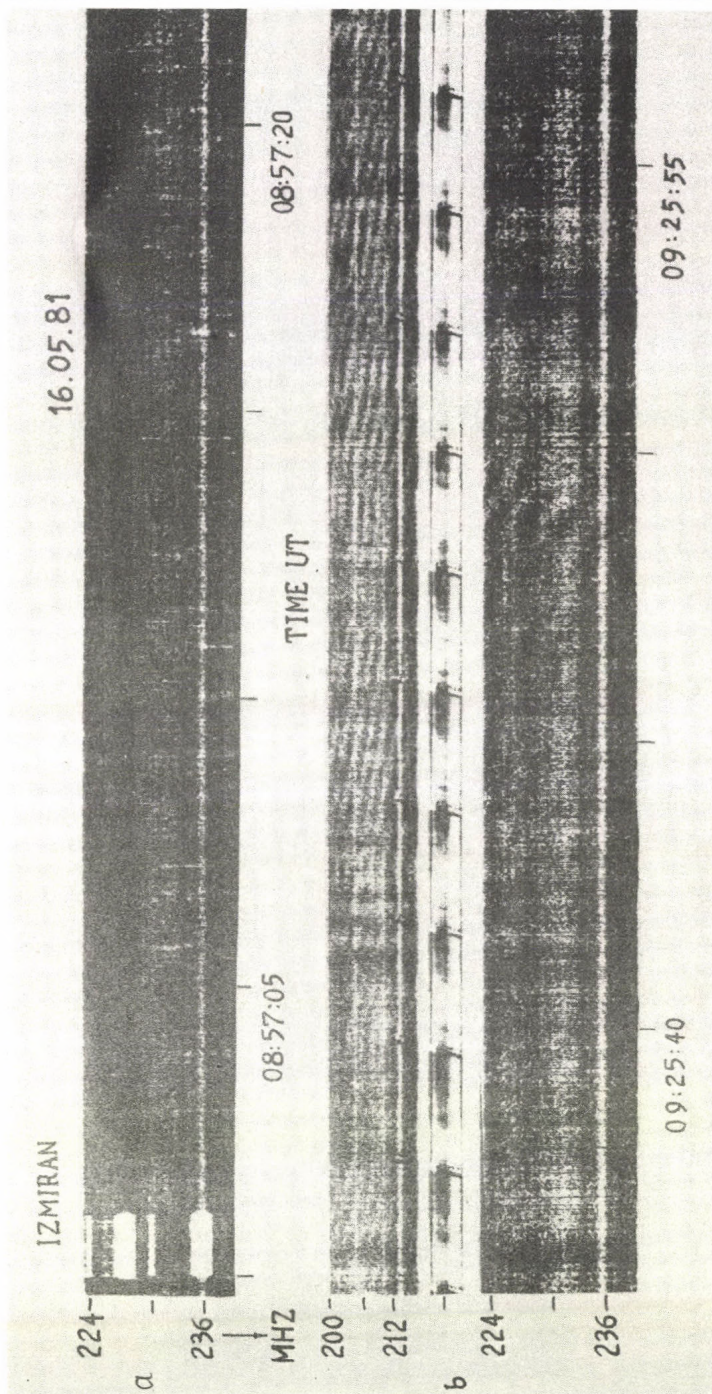


Fig. 8a,b.

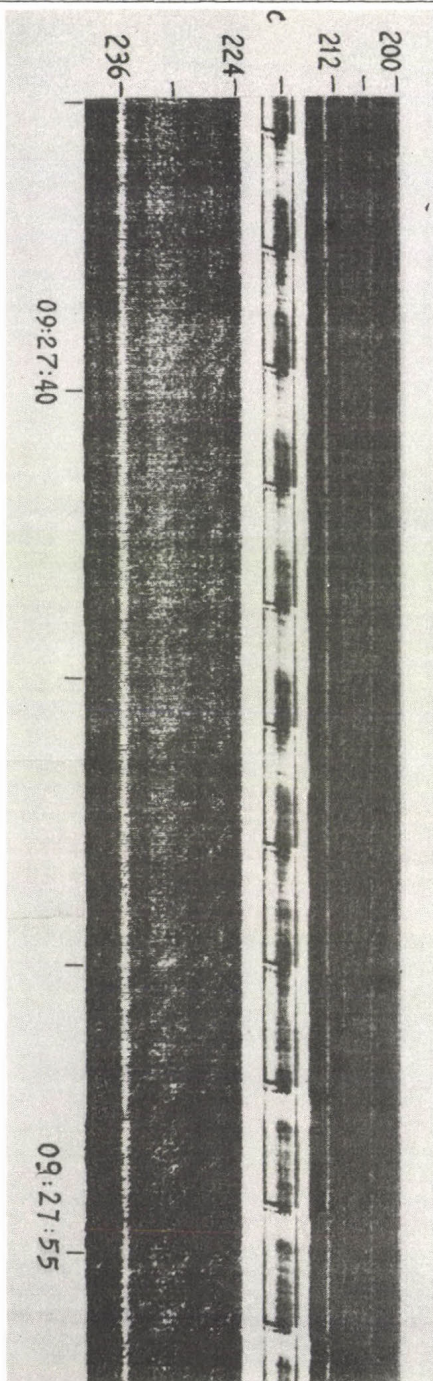


Fig. 8c.

PROPER MOTIONS IN HALE REGION 17644 (MAY 1981)
AND THE MAY 16 FLARE

B. K Á L M Á N, I. N A G Y

Heliophysical Observatory, Debrecen

Abstract:

Proper motions of sunspot umbrae in the Hale region 17644 are given for the period 13-19 May 1981, and some peculiarities of the 16 May flare are discussed.

СОБСТВЕННЫЕ ДВИЖЕНИЯ В ОБЛАСТИ ХЭЙЛ № 17644 (МАЙ 1981)
И ВСПЫШКА 16 МАЯ

Б. КАЛМАН, И. НАДЬ

Гелиофиз.Обс., Дебрецен

Абстракт:

Даются собственные движения солнечных пятен в активной области Хэйл № 17644 для периода 13-19 мая 1981 года, и обсуждаются некоторые особенности вспышки 16 мая.

Hale region 17644 was a very complex active region, consisting of at least two bipolar groups with an irregular cluster of spots between them. Due to its complexity it produced several large flares {1}, {2}, among them the 3B flare of 16 May 1981. The detailed description of this flare in X-rays, H α and radio bands has been published elsewhere, together with data on the flare-ribbon dynamics {3}.

On the basis of more than 140 full-disk photoheliograms, made in the Debrecen Observatory and its Gyula observing station, the heliographic coordinates and proper motions of the more significant spots in Hale region 17644 were determined in the period 13-19 May 1981, including the large 3B flare of May 16.

In the analysis the $H\alpha$ observations of the 16 May flare were also used, made by the large 53-cm coronagraph of the Debrecen Observatory through a 0.5 Å passband Halle filter. The white-light observations were made by L.Győri (Gyula) and L.Kondás (Debrecen), the ones in $H\alpha$ by O.Gerlei and one of us (I.N.).

The evolution of the region during the disk passage is shown in the accompanying photographs (Fig.1), a series of rectified drawings in Carrington coordinates is also given for the measured period (Fig.2). From the measured points average positions were determined for 0.2^d, 0.4^d, 0.6^d and 0.8^d UT each day, these averages are shown in the Figs.3,4. The date is shown on the trajectories of the spots, at the beginning and the end.

The most interesting results are the following:

Around the main zero line, where the large flare of May 16 occurred, the spots of different polarity move differently, and parallel to the zero line (spots 7,8,A,D,E). Meanwhile spot C moves perpendicularly to the zero line, pushing it northward.

Adjacent spots 3,4,5,6 move in a very similar way, although they do not exist at the same time.

Spot A after the large flare, which occurred nearby, drastically diminishes in size, and begins to move rapidly northwards.

A strange, similar and simultaneous change occurs in the character of the motion of spots 10,G,F at 16-17 May, they began to move in the direction of the (past) large flare.

In this complex the convergence and coalescence of spots of the same magnetic polarity {4} was observed again (spot 2 and an another small spot reaches the leader spot 1 and they coalesce). But another type of the interaction is also observed. In the middle of the group spot 14 emerges on 15 May, with a characteristic westward motion of the p polarity. It collides with the older spot 9, and rebounds, pushing the old spot southwards (see Fig.4). This type of interaction has already

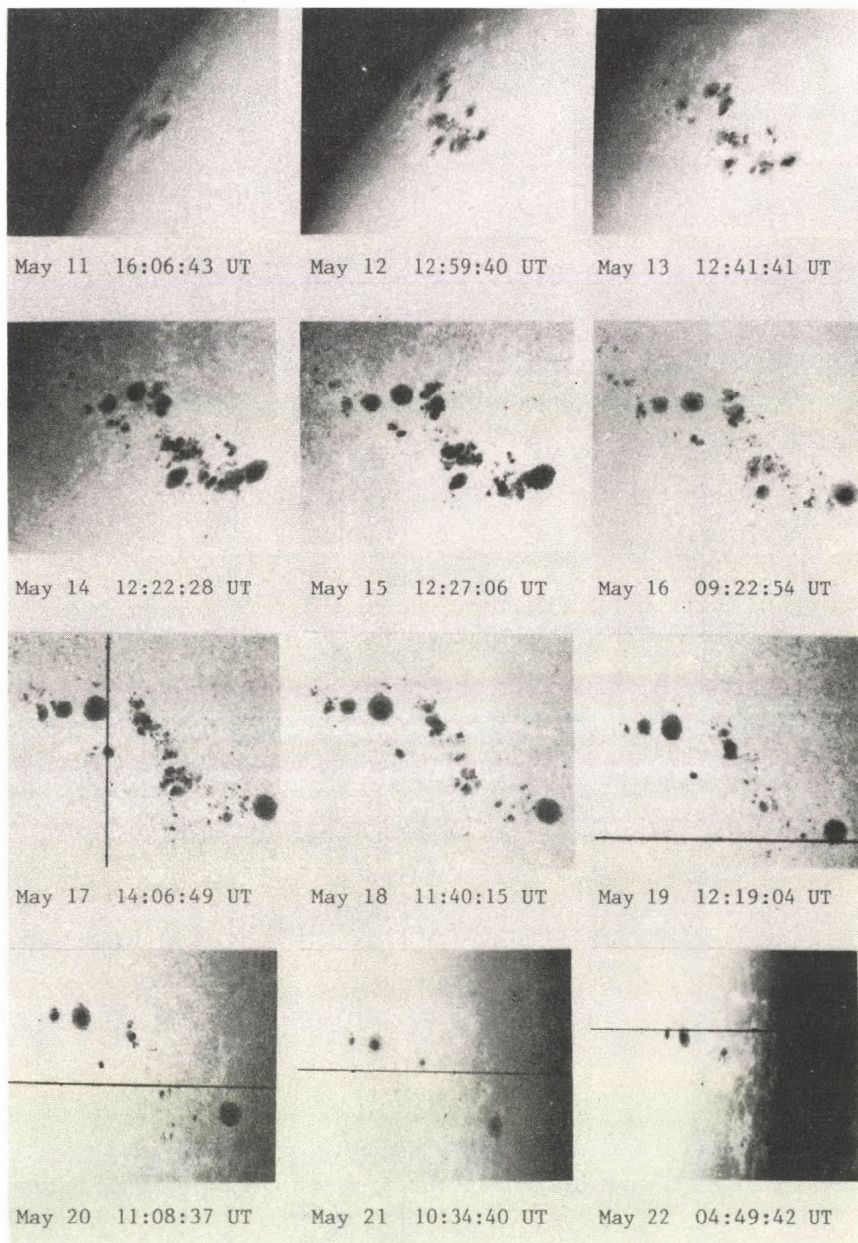


Fig.1. The evolution of Hale Rgn 17644, 11-22 May 1981.

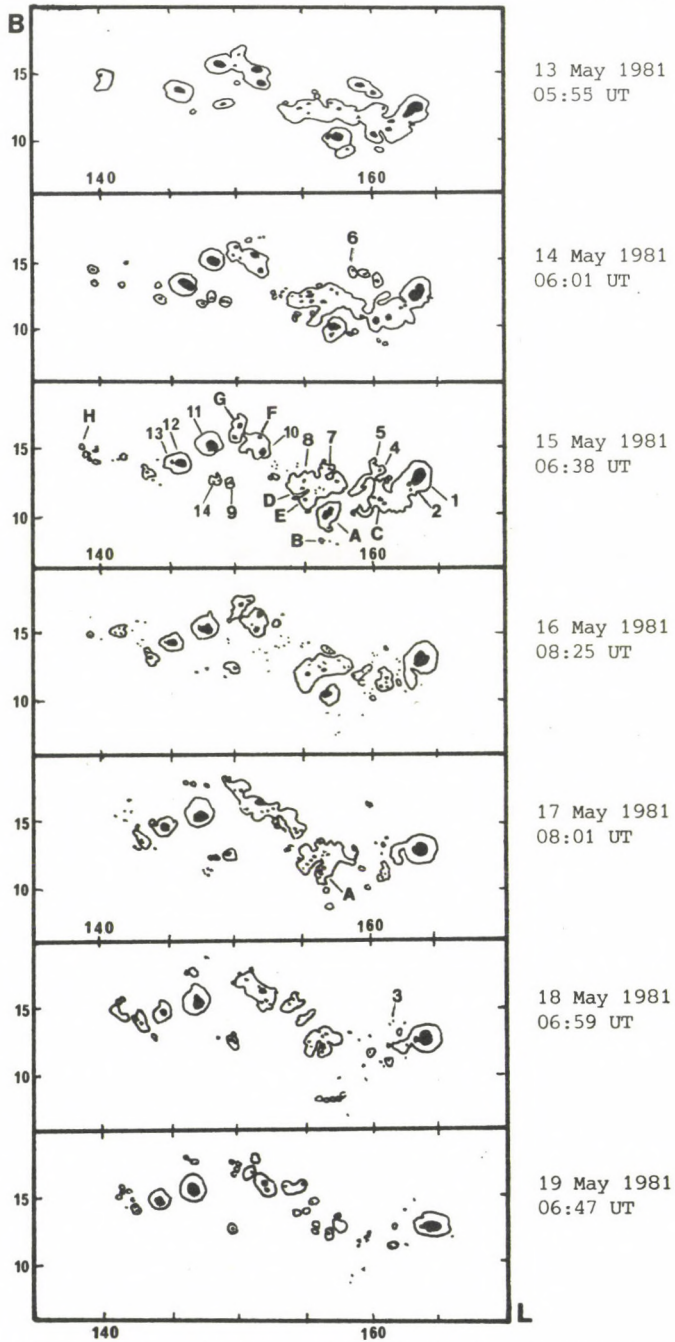


Fig.2. Rectified drawings in Carrington coordinates of Region 17644

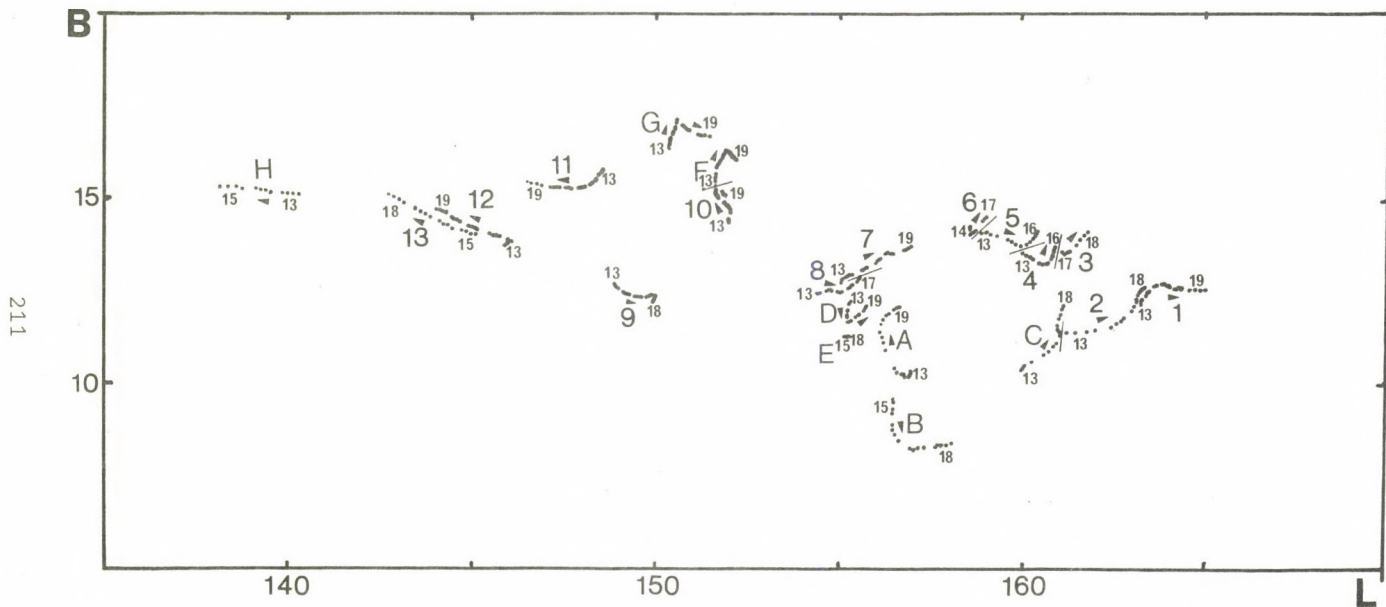


Fig.3. Trajectories of sunspot umbrae in Hale Rgn. 17644 between 13-19 May 1981. The positions for 0^d.2, 0^d.4, 0^d.6 and 0^d.8 UT for each day are given. Numbers denote preceding (N), letters - following (S) magnetic polarity. The dates of the first and last day of observation are shown by small numbers at the beginning and at the end of each trajectory.

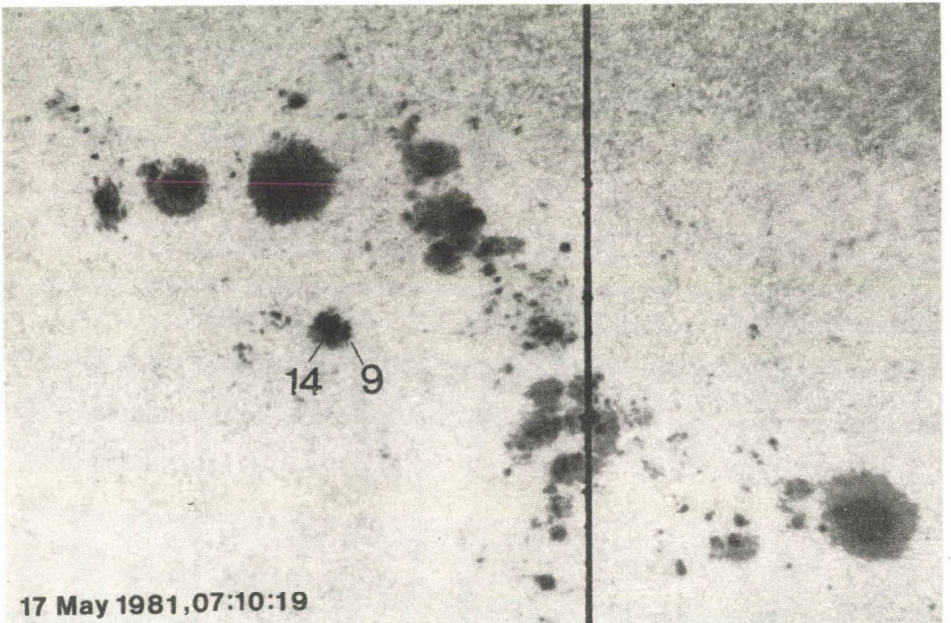
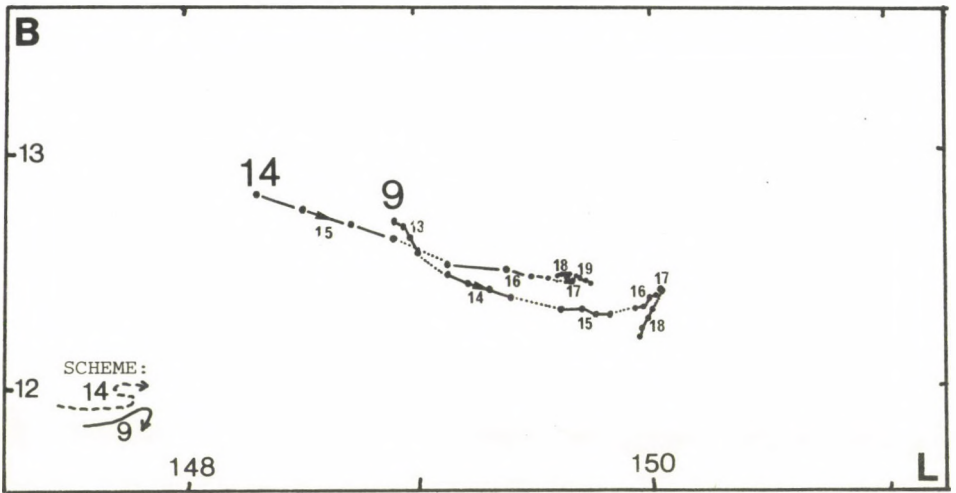


Fig.4. Trajectories of colliding spots 9 and 14 (top) and a photograph of the group on 17 May 1981 (bottom)

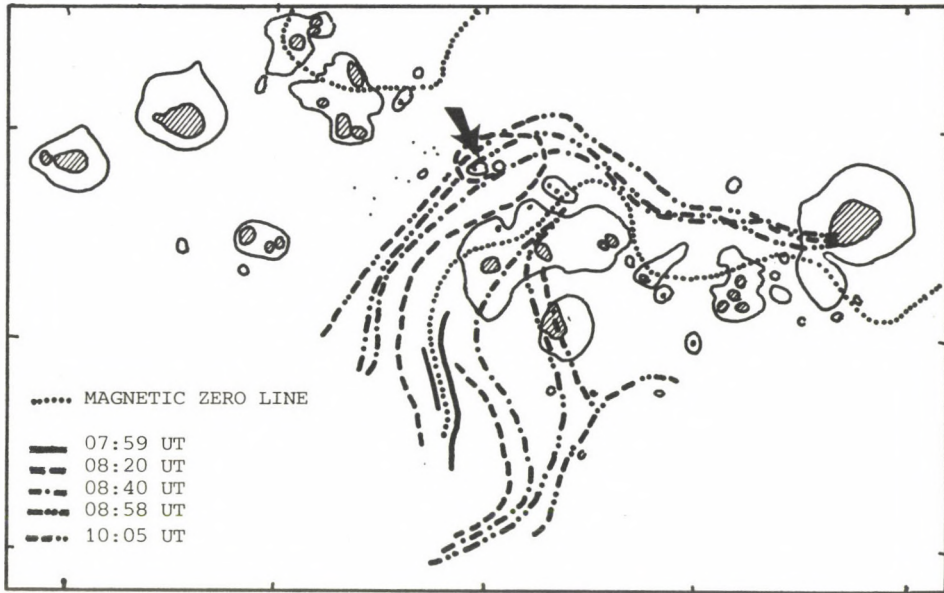


Fig.5. The movement of the flare ribbons in the flare of 16 May 1981. The arrow points to the small sunspot, surrounded by the "curl" (cf. Fig.6)

been observed in interactions of "old" and "new" activity {5}. From coordinate measurements of the flare ribbons (see Fig.) it became clear that the short-lived "curl" feature of the *NE* flare ribbon {3} formed around a small sunspot (arrow in Figs.5,6) in the first minutes of the flare.

Finally, the authors wish to thank Miss Ágnes Dobai, student of astronomy in Eötvös University, Budapest, for valuable help in measuring and computing the heliographic coordinates of the spots. The computations were performed partially on the PDP 11/40 computer of the ATOMKI (Nuclear Research Institute), Debrecen.

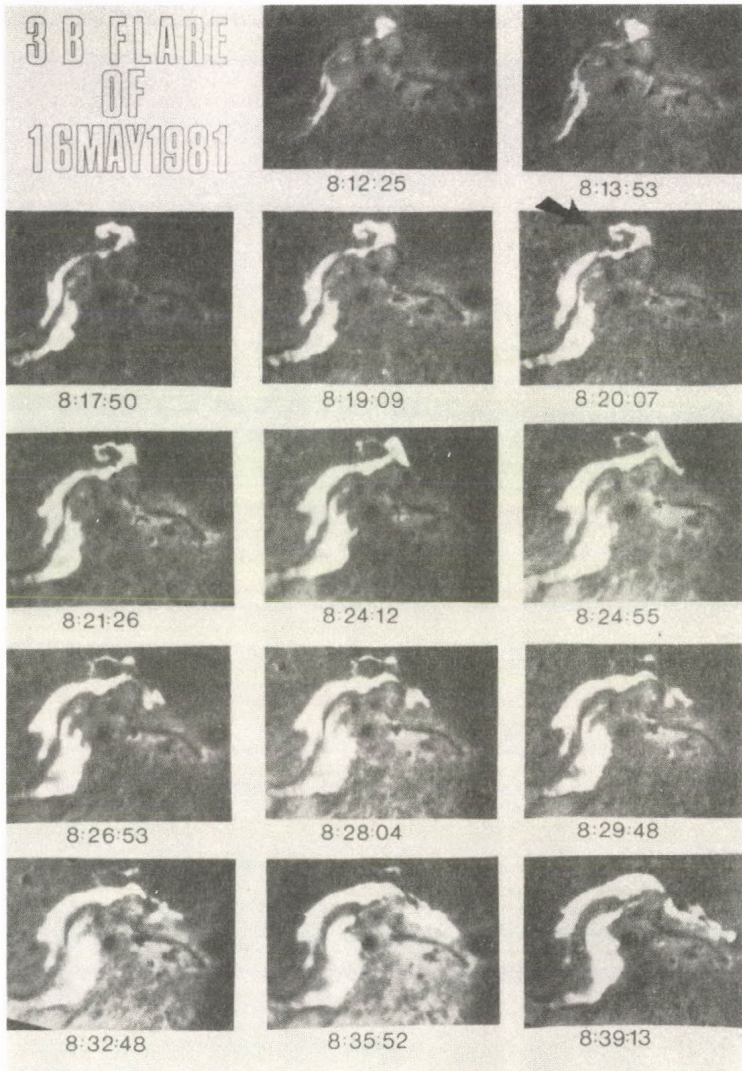


Fig.6. The evolution of the "curl" feature on the NE flare ribbon (arrow)

References

- {1} Hiei, E., Tanaka, K., Watanabe, T., Akita, K., Optical and X-ray flare event of 13 May 1981, *Proc. Hinotori Symp. on Solar Flares*, Tokyo, p.208, 1982
- {2} Banin, V.G., Borovik, A.V., Yazev, S.A., The large solar flares of 13 and 16 May, 1981, (in Russ.) *Issl. SibIZMIR*, 65. 151, 1983
- {3} Fárnik, F., Kaastra, J., Kálmán, B., Karlický, M., Slottje, C., Valníček, B., X-ray, H α , and radio observations of the two ribbon flare of May 16, 1981, *Solar Phys.* 1983 in press.
- {4} Dezső, L., Gyertyános, Gy., Gerlei, O., Kálmán, B., Kovács, A., Proper motions of sunspots observed simultaneously with the measurements on the satellite "IK-1", *Soln.-Zem.Fiz.3.* 151, 1972 (in Russ.)
- {5} Kálmán, B., Magnetic fields and proper motions of sunspots. II. Group 420, October 1968, (in Russ.) *Izv. KrAO.57.* 122, 1977

ИЗМЕНЕНИЕ ПРОФИЛЕЙ H_{α} И H_{β} В ПРОЦЕССЕ ВСПЫШКИ 16 МАЯ 1981 Г.

К.В. АЛИКАЕВА, И.Ф. НИКУЛИН,

ГАО, Киев

ГАИШ, Москва

П.Н. ПОЛУПАН

Астрон. Обс. НГУ, Киев

VARIATION OF H_{α} AND H_{β} PROFILES DURING MAY 16, 1981 FLARE

K.V. ALIKAEVA,

I.F. NIKULIN,

Acad. Astron. Obs., Kiev

Shternberg Astron. Inst., Moscow

P.N. POLUPAN

Univ. Obs., Kiev

Abstract:

Using H_{α} -filtergrams, the development of active complex 3106+3112 for May 16, 1981 including a strong two-ribbon flare is traced. Variations of H_{α} and H_{β} line profiles in the course of this flare development are followed. At beginning of the flare the profile shape in the two flare knots is conditioned by the matter rise, while in the vicinity of the brightness maximum and during the fading phase downward motions prevail. The comparisons of the observed H_{α} profiles with the theoretical ones, computed for various model flares at the assumption on Gaussian distributed macroscopic motions, indicate that as the flare brightness grows up to maximum, the electron density at the transition layer/chromosphere boundary increases several times, velocities diminish, and the boundary itself descends.

По $H\alpha$ -фильтрограммам прослежено развитие активного комплекса 3106 + 3112 16 мая 1981 г. с 06 до 10 час. всемирного времени (рис. 1). К 16 мая восточной части комплекса сформировался новый кольцеобразный флоккул В (рис. 1а). В 0750 UT в нем возникла вспышка. По-видимому, эта вспышка инициировала мощную вспышку балла 3В, которая началась в 0800 UT вблизи пятна на месте, где 14 мая также наблюдалась мощная вспышка. Одновременно произошло поярчание отдельных флоккульных узлов к юго-востоку от активной области. Это наталкивает на мысль об общем провоцирующем агенте, распространяющемся от первой вспышки.

Развитие вспышки 3В шло скачками. В 0825 UT началось разделение узлов по обе стороны от нейтральной линии. Один узел (Б) трансформировался к 0832 UT в мощную вспышечную ленту, огибающую хвостовое пятно. В 0835 узел А в свою очередь вытягивался в направлении пятна лидера, которого достиг в 0837 UT. Обе ленты вспышки пульсировали по яркости до 0846 UT, достигнув максимума площади в 0842 UT (рис. 1б). После этого ленты продолжали раздвигаться, теряя яркость и площадь.

Спектральные наблюдения этой большой вспышки проводились в ГАО АН УССР в Киеве и на станции ГАИШ в Алма-Ате. Спектры в области $H\alpha$ получены с интервалом времени 1-3 мин и охватывают все стадии развития обеих вспышек. Спектры в области $H\alpha$ и H и K Ca II получены вблизи максимума вспышки 3В. Центральная интенсивность $H\alpha$ достигает значения 1,3 от интенсивности непрерывного спектра. Профили обеих водородных линий, как правило, асимметричные, имеют провал интенсивности в центре линии. В начальной фазе наблюдается синяя асимметрия, большая протяженность крыльев, причем в отдельные моменты преобладает синее крыло. Вблизи максимума и после него крылья менее протяженные, а красное крыло систематически больше синего.

Для двух узлов мощной вспышки А и Б рассмотрены центральные интенсивности, положение и контраст синего и красного пиков $H\alpha$ в различные моменты времени. Контрастом мы называем отношение интенсивности пика к центральной интенсивности линии (рис. 2).

Нарастание интенсивности $H\alpha$ происходит до 0840–0846 UT скачками, что подтверждается фильтрограммами. Ход центральной интенсивности явно противоположен ходу контрастов пиков. С увеличением центральной интенсивности контраст уменьшается.

В начальной фазе вспышки в обоих узлах синий пик интенсивнее красного. В узле А красный пик начал преобладать, начиная с 0818 UT, а в узле Б – начиная с 0842 UT. Совершенно так же меняется и положение пиков относительно несмещенного центра линии, и поэтому на графике не приводится. В начале вспышки синий пик смещен больше, чем красный, а затем картина меняется на противоположную. Такие особенности профилей $H\alpha$ можно объяснить следующим образом: 1. В начальной фазе вспышки происходит подъем вещества одновременно в обоих узлах. В узле А начиная с 0818, а в узле Б с 0824 UT преобладают нисходящие движения. По $H\alpha$ -фильтрограммам, снятым в Алма-Ате, хорошо видно, что эти ленты, расположенные по разные стороны от нейтрального волокна, соединяются системой тонких дуг. По-видимому, вблизи максимума и в фазе затухания вспышки вещество стекает от вершин петель в хромосферу. 2. Уменьшение контраста пиков при возрастании центральной интенсивности может быть связано с замывающим действием турбулентности. Характер профилей указывает на весьма сложный характер макроскопических движений в области свечения $H\alpha$ и непостоянство функции источника вдоль луча зрения. Все это должно учитываться при построении моделей вспышек.

Мы сравнили наблюдаемые профили $H\alpha$ с взятыми из литературы теоретическими, основанными на разных моделях вспышек. Четыре эмпирические модели Динха {1} различаются высотой и электронной плотностью на границе переходный слой/хромосфера. Модель, использованная в работе Кэнфилда и Атея {2}, учитывает распределение плотности и температуры с высотой, обусловленное распространяющейся ударной волной с числом Маха от 5 до 15. Соответствующие этим моделям теоретические профили дают провал интенсивности в центре $H\alpha$, однако он слишком велик. Если учесть макроскопические движения, то удастся теоретические профили приблизить к наблюдаемым. Мы рассчитали для всех моделей профили с учетом макроскопических скоростей от 10 до 100 км/с с

16.05.1981

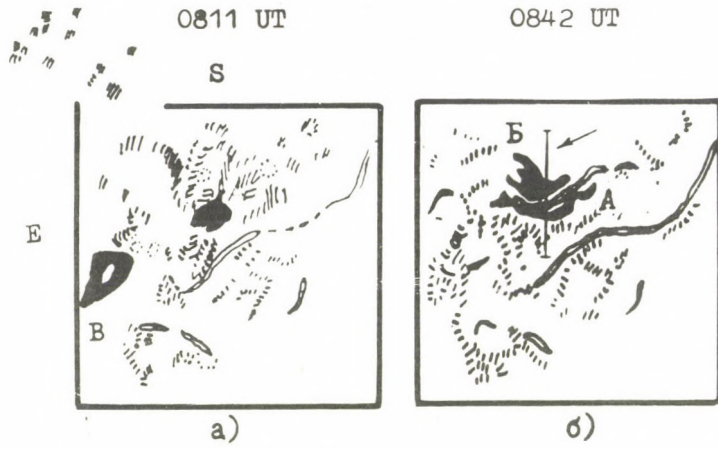


Рис. 1.

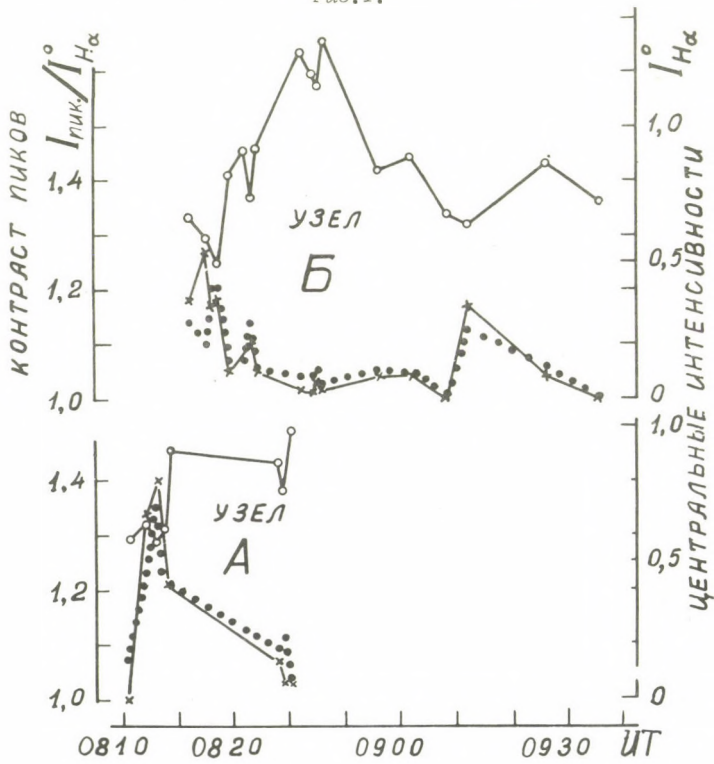


Рис. 2.

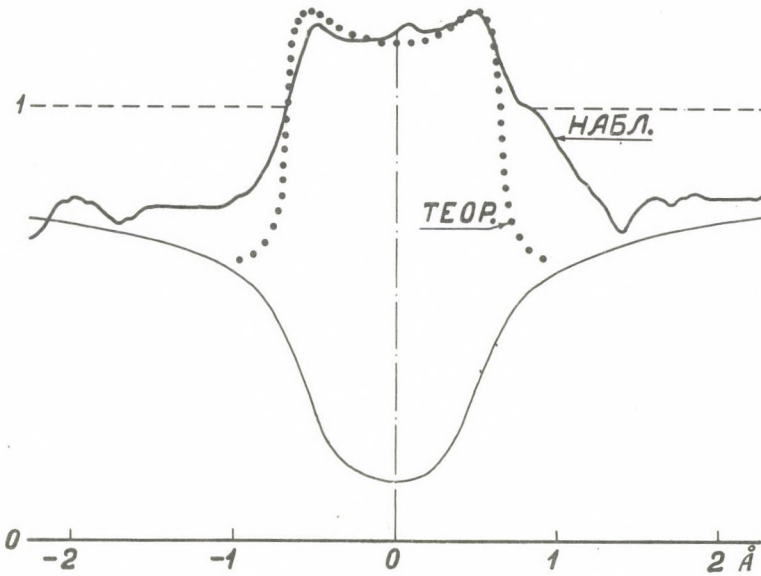


Рис.3. Сравнение наблюдаемого профиля $H\alpha$ с теоретическим (модель Динха No 3, $V_{\mu a} = 40 \text{ км с}^{-1}$)

Рис.1. Зарисовки активного комплекса 3106+3112 16.05.1981:
 а) начальная стадия вспышки ЗВ
 б) вблизи максимума этой вспышки

Рис.2. Изменение центральной интенсивности и контраста пиков линии $H\alpha$ в процессе развития двух узлов вспышки ЗВ:
 интенсивность центра $H\alpha$ (—○—), синего пика (—x—),
 красного пика (•••)

гауссовым распределением (рис.3). Из сравнения с наблюдениями следует: 1. Модель Кэнфилда-Атея не дает согласия с наблюдениями, т.к. приводит к очень большим значениям интенсивности пиков и большому расстоянию между пиками. Однако качественно она объясняет асимметрию линии и различную интенсивность синего и красного пиков. 2. Модели Динха приводят к неплохому согласию с наблюдениями в центральной части профиля $H\alpha$, но не объясняют протяженных крыльев и асимметрию линии (рис. 3). 3. На разных этапах развития вспышки 3В следует привлекать разные модели Динха. В таблице приведены данные о физических условиях на границе переходного слоя по моделям Динха и $V_{\mu a}$. Как видно из нее, вблизи максимума интенсивности $H\alpha$ граница переходного слоя опускается, плотность становится выше, а $V_{\mu a}$ даже уменьшаются.

Физические условия на границе переходного слоя во вспышке 3В

Время UT	Модель Динха	Переходный слой			$V_{\mu a}$ км с ⁻¹
		высота км	T К	$n_e \times 10^{-12}$ см ⁻³	
0829	1	1312	8300	4.6	73
0833	2	1189	8300	9.8	85
0834	2	1189	8300	9.8	63
0842	3	1073	8300	18.0	40
0844	2	1189	8300	9.8	40
0845	2	1189	8300	9.8	45

Л и т е р а т у р а

- {1} Dinh, Q.V., Spectral analysis of solar flares II, *Publ. Astron. Soc. Japan*, 32, 515, 1980
- {2} Canfield, R.C., Athay, R.G., Theoretical chromospheric flare spectra *Solar Phys.*, 34, 193, 1974

Publ. Debrecen Obs. Vol. 5

No. 3.

PAPERS ON MASS MOTION AND MAGNETIC FIELDS
IN SOLAR ACTIVE REGIONS

ФОНОВЫЕ МАГНИТНЫЕ ПОЛЯ И СОЛНЕЧНАЯ АКТИВНОСТЬ

Н.Н. СТЕПАНИН

КрАО, Научный

Абстракт:

На основе количественного изучения $H\alpha$ -карт крупномасштабных фоновых магнитных полей на Солнце и широтного распределения солнечной активности за полтора цикла показано, что рассеянные поля хвостовых частей активных областей не определяют фоновые поля. Их вклад не отражается на величине площади, занимаемой полем соответствующего знака.

Определенные ранее в [5] количественные характеристики структур фоновых полей подтверждают предположение о том, что крупномасштабные фоновые магнитные поля на Солнце являются отражением конвекции третьего яруса с конвективными элементами порядка радиуса Солнца ($\lesssim 0.5 R_{\odot}$).

BACKGROUND MAGNETIC FIELDS AND ACTIVITY OF THE SUN

N.N. STEPANYAN

Crimean Astrophys.Obs., Nauchnyj

Abstract:

Having quantitatively investigated the $H\alpha$ -charts of the large-scale background magnetic fields and latitude distribution of the activity on the Sun for one and a half solar cycles, we showed that the scattered magnetic fields of the following polarity do not define the background magnetic field. Their contribution is negligible on the area occupied by the magnetic field of a corresponding sign.

Quantitative characteristics of the background field structures, obtained earlier, confirm the hypothesis that the large-scale background magnetic fields on the Sun are actually the reflection of convection with elements of an order of solar radius ($\lesssim 0.5 R_{\odot}$).

Хорошо известен такой наблюдательный факт как миграция рассеянных магнитных полей хвостовых частей активных областей к полюсам. По теории Беккока {1} эти рассеянные поля активных областей и создают фоновое поле Солнца. Смена знака полярного поля происходит из-за выхода этих полей в полярные области. В {2} авторы аналогичным образом интерпретировали наблюдения с магнитографом обсерватории Маунт Вилсон.

Сомнение в справедливости этого положения впервые было высказано А. Б. Северным в {3, 4}, где он указал на существенные трудности такого объяснения.

Нами предпринята попытка показать что фоновые магнитные поля - самостоятельное явление, и рассеянные поля активных областей не изменяют заметным образом площадь, занятую фоновым полем того или иного знака.

При изучении фоновых полей по $H\alpha$ - картам в {5} нами была введена величина A^+ - доля площади 10 градусной широтной зоны Солнца, занятая (+) полем в одном обороте.

Изменение A^+ с широтой и временем для периода ноябрь 1964 - декабрь 1980 мы представили в виде графика, по оси абсцисс которого откладывалось время, а по оси ординат - широта. В клетке, соответствующей широтному интервалу φ_i и k -му обороту, помещалось соответствующее их значение A^+_{ik} .

В аналогичном виде были представлены данные о солнечной активности за тот же период. Характеристикой солнечной активности служила суммарная мощность всех флоккулов, наблюдавшихся в широтной зоне φ_i в течение k -го оборота (M_{ik}). Под мощностью одного флоккула мы понимаем произведение его площади (выраженной в м.д.п.) на яркость (в относительных единицах). Обе эти величины были взяты из {6}.

Графики A^+_{ik} и M_{ik} , содержащие данные за каждый оборот, были осреднены во всех широтных зонах по пяти оборотам. Полученный таким образом усредненный график для мощности флоккулов представлен на рис. 1. Области с разной штриховкой соответствуют различным значениям M (обозначения в нижней части рис. 1). На графике хорошо виден тривиальный эффект уменьшения широты зоны пятнообразования с развитием цикла.

Данные о фоновых полях (A_{1k}^+) представлены в несколько ином виде. Для каждого оборота находилась широта, на которой A^+ имела максимальное значение. Полученные таким образом точки для соседних оборотов соединялись плавной сплошной линией. Эти линии также представлены на рис. 1. Сплошные линии относятся к максимумам A^+ , т.е. преобладанию (+) полярности, пунктирные к максимуму (-) полярности. Толщина линии грубо соответствует высоте максимума.

В {5} мы рассматривали эту картину распределения "волн" поля преимущественной полярности, приводящего к смене знака полярных полей. Сейчас обратим внимание на связь распространения "волн" с активностью.

В рассматриваемом нами XX цикле в N - полушарии полярность хвостовых частей активных областей была положительной. В S - полушарии - отрицательной. Если бы фоновые поля являлись рассеянными полями хвостовых частей активных областей, от зон с максимальным значением мощности флоккулов M распространялись бы к полюсам "волны" (+) поля в N - полушарии и (-) поля в S - полушарии. На самом деле такой закономерности не видно.

Так в N - полушарии в 1969 г. при росте активности от соответствующих широт распространялись к N - полюсу "волна" (-) поля, а самая мощная волна (+) поля, приведшая к окончательной смене знака полярного поля, началась в S - полушарии и гораздо раньше максимума M.

В S - полушарии "волна" (-) поля, приведшая к смене знака полярного поля, начала распространяться во время максимальной активности Солнца, к тому же с низких широт.

Данные о фоновых полях и мощности флоккулов были сравнены также количественно.

Значения A^+ и M для последовательных оборотов в каждой 10-градусной зоне можно рассматривать как отдельные временные ряды $A_{\varphi i}^+$ и $M_{\varphi i}$. Нами были построены кросскорреляционные функции различных комбинаций пар этих рядов как типа $A_{\varphi i}^+ - A_{\varphi j}^+$ и $M_{\varphi i} - M_{\varphi j}$, так и $A_{\varphi i}^+ - M_{\varphi j}$.

Для фоновых полей A^+ в соседних широтных зонах коэффициент

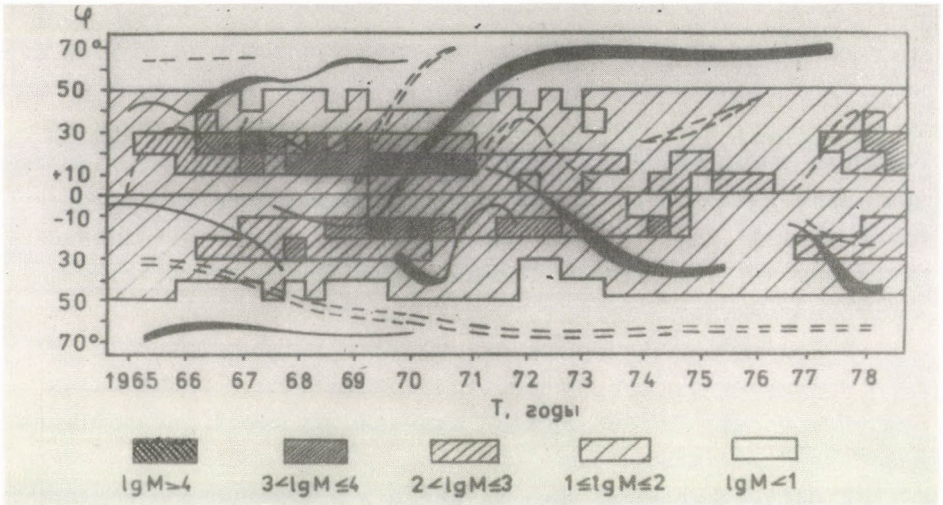


Fig. 1.

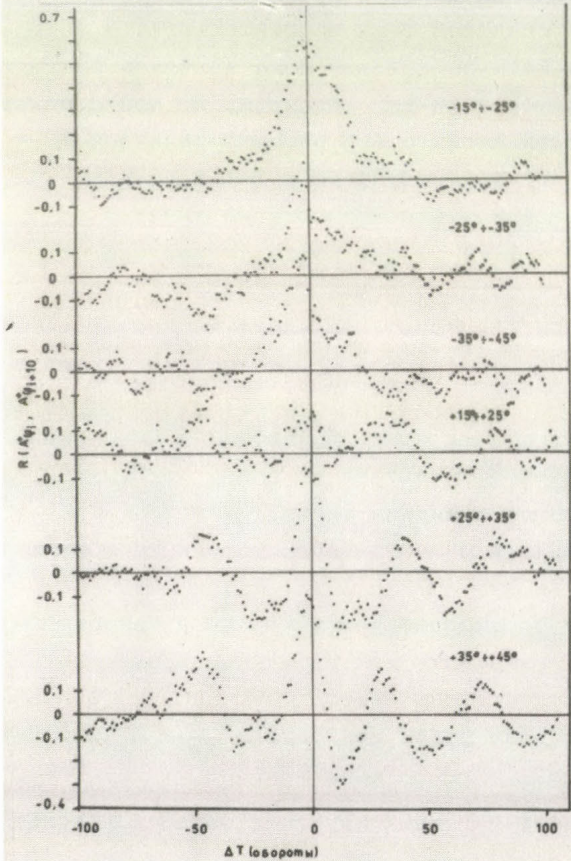


Fig. 2.

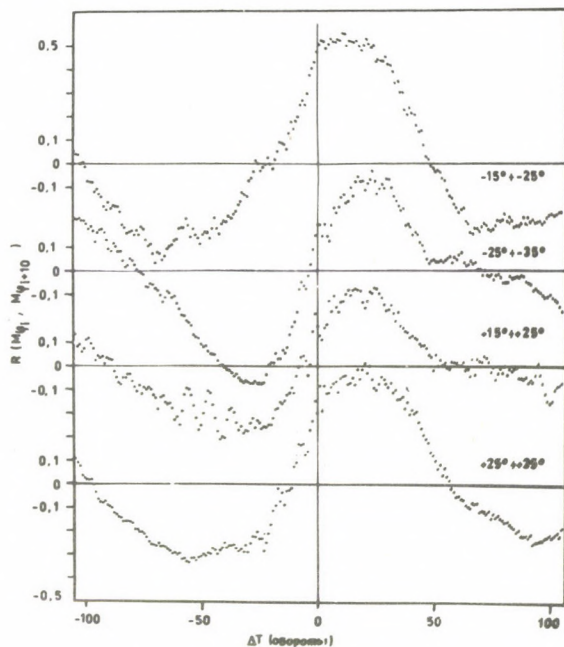


Рис.3. Кросскорреляционные функции мощности флоккулов в соседних широтных зонах (При 95 процентном уровне значимости корреляционная связь имеется при $R > 0.2$ [19]).

Рис.1. Изменение со временем широтного распределения активности (штриховка разной плотности) и преобладания поля (+) полярности (сплошные линии) и (-) полярности (пунктир).

Рис.2. Кросскорреляционные функции A^+ (доля площади 10 градусной зоны, занятая (+) полем) в соседних широтных зонах. (при 95 процентном уровне значимости корреляционная связь имеется при $R > 0.2$ [19]).

кросскорреляции $R(A^+_{\phi_i}, A^+_{\phi_i+10})$ является значимым ($R > 0,2$) для широт выше 20° в обеих полусферах (рис. 2). Причем максимум кросскорреляционной кривой сдвинут относительно $\Delta T = 0$ на ~ 3 оборота. Знак смещения свидетельствует о распространении "волн" фоновых полей к полосам со скоростью $\sim 3^\circ$ за оборот или ~ 15 м/сек.

Кросскорреляционные кривые для $M_{\phi_i} - M_{\phi_i+10}$ представлены на рис. 3. На них мы видим сдвиги максимумов на $\Delta T \sim 20$ оборотов. Знак сдвига свидетельствует о перемещении активности к экватору. Скорость смещения ~ 3 м/сек. Это значение согласуется с тем, что можно определить по данным за несколько циклов из {7}.

Что касается кросскорреляции типа $A^+_{\phi_i} - M_{\phi_j}$, то ни в одном варианте ϕ_i, ϕ_j коэффициент корреляции не достигал значения $0,2$ ни при каком сдвиге ΔT . Это свидетельствует о том, что значимой корреляции между фоновыми полями и мощностью флоккулов в соседних, более отдаленных или тех же самых широтных зонах нет.

Отсюда можно сделать вывод, что рассеянные поля хвостовой полярности не определяют полностью фоновые поля. Их вклад не отражается на величине площади, занимаемой полем данного знака.

В литературе не раз встречалось предположение, что на Солнце может присутствовать конвекция трех ярусов (см., например, {8}). Отражением первых двух ярусов в фотосфере являются грануляция и супергрануляция. Конвекции третьего яруса могут соответствовать крупномасштабные структуры фоновых магнитных полей.

По вопросу о наличии третьего яруса конвекции с размером ячеек, сравним с радиусом Солнца, еще нет единого мнения и убедительных свидетельств "за" и "против" такого предположения.

Ранее нами были определены по $H\alpha$ -картам количественные характеристики структур фоновых полей {5}. А именно, было найдено, что средние размеры структур $L = 300000$ км $= 3 \cdot 10^{10}$ см скорости их движения U от 5 до 50 м/сек ($[0,5 \div 5] \cdot 10^3$ см·сек $^{-1}$), распределение по времени жизни τ имеет 3 максимума на $3, 7$ и 10 оборотах ($[0,6 \div 1.4 \div 2] \cdot 10^7$ сек).

Если предположить что фоновые поля - отражение 3-го яруса конвекции, то полученные нами значения L, U и τ для структур фоновых полей должны удовлетворять некоторым соотношениям

{8, стр. 20}, вытекающим из представления о турбулентной конвекции {9, 10}.

Во-первых, чтобы быть наблюдаемой, конвекция должна быть квазистационарной, т.е. турбулентное число Рейнольдса R_{1t} должно находиться в пределах $10 \div 100$.

$$R_{1t} = ULv_t^{-1} \quad (1)$$

где U - скорость основного масштаба, L - его размер, v_t - турбулентная вязкость, определяемая мелкомасштабными вихрями, создающими эффективное трение для крупномасштабных конвективных движений.

Величина v_t для верхнего грануляционного яруса $\sim 10^{11} - 10^{12}$ и несколько больше, 10^{13} , во втором ярусе. Предполагается, что в пределах конвективной зоны v_t меняется не слишком сильно.

Из наших данных мы можем по формуле (1) оценить v_t , подставив $R_{1t} = 10 \div 100$; $L = 3 \cdot 10^{10}$ см и $U = (0,5 \div 5) 10^3$ см·сек⁻¹.

Для v_t получим величину $0,5 \cdot 10^{12} \div 1,5 \cdot 10^{13}$, что не противоречит приведенным выше значениям, т.е. супергрануляция может определять v_t для конвекции третьего яруса.

Кроме того, для конвективных ячеек характерное время жизни τ должно быть порядка L/U . В нашем случае $\tau = L/U = (0,6 \div 2) 10^7$ сек = $3 \div 10$ оборотам Солнца.

Эти же числа получены нами непосредственно из наблюдений. Эти соотношения могут служить количественным подтверждением представления о том, что крупномасштабные фоновые магнитные поля являются проявлением конвекции третьего яруса с конвективными элементами, сравнимыми по размеру с радиусом Солнца ($\approx 0,5R_\odot$).

Выше мы показали, что магнитные поля активных областей существенно не отражаются на распределении фоновых полей по поверхности Солнца.

Остановимся кратко на обратной проблеме - влиянии крупномасштабных полей на распределении активных областей.

Хорошо известен факт возникновения новых активных областей на стыках супергранул. Именно в этих местах происходит концентрация поля, т.к. силовые линии и трубки магнитного поля

"сгребаются" к границам радиальными движениями вещества в супергрануле. Нечто подобное можно ожидать и в структурах крупномасштабных полей.

Многие авторы исследовали неравномерность распределения активности по диску Солнца. Было найдено, что существует некоторая концентрация групп пятен к активным долготам {11, 12}, границам секторов межпланетного поля {12, 13} к стыкам гигантских гранул {14}.

Но во всех подобных исследованиях получено, что такая концентрация проявляется только для мощных активных центров со сложной магнитной структурой, сильными или протонными вспышками. Чем слабее активные области, тем меньше концентрация их в "особых точках" поверхности Солнца. В {15}, например, было показано, что при рассмотрении всех групп пятен (включая униполярные) не наблюдается их концентрации к активным долготам и границам секторов.

На этом основании можно сделать вывод, что место возникновения активных областей не зависит от крупномасштабных структур. Но тот уровень развития, которого данная область достигнет, зависит от места ее возникновения.

Упомянутые выше гигантские гранулы - описанные в {16} крупномасштабные структуры солнечной активности в зонах пятнообразования. По-видимому, на этих широтах структуры фоновых крупномасштабных полей совпадают с гигантскими гранулами.

Проекция границ секторов межпланетного поля на поверхности Солнца также совпадает с границами крупных структур фоновых полей.

В {17} было показано, что существует тесная корреляционная связь между фоновым полем и общим магнитным полем Солнца как звезды. Общее магнитное поле Солнца, в свою очередь определяет структуру межпланетного поля {18}.

Таким образом, вывод о связи уровня максимального развития активной области с границами секторов и гигантских гранул можно отнести к границам секторов и гигантских гранул можно отнести к границам структур крупномасштабных фоновых полей.

В заключение перечислим выводы, полученные нами в результате количественного изучения $H\alpha$ -карт крупномасштабных фоновых магнитных полей и широтного распределения активности за полтора цикла.

1. Структуры крупномасштабных фоновых магнитных полей являются проявлением конвекции третьего яруса с размером ячеек, сравнимым с радиусом Солнца ($\approx 0,5R_{\odot}$).

2. Смена знака полярных полей происходит путем распространения к полюсам "волн" поля. Такие "волны" распространяются от приэкваториальных зон со скоростью ~ 15 м/сек. Начало этих "волн" не связано по широте и времени с солнечной активностью. Рассеянные магнитные поля хвостовых частей активных областей не дают заметного вклада в эти "волны".

3. Активные области возникают независимо от расположения крупномасштабных структур, равномерно на всех долготах. Но максимально достижимый ими уровень развития оказывается выше вблизи границ крупномасштабных структур.

Л и т е р а т у р а

- {1} Babcock, H.W., The topology of the Sun's magnetic field and the 22-year cycle, *Ap.J.* 133. 572, 1961
- {2} Howard, R.H., LaBonte, B.J., Surface magnetic fields during the solar activity cycle, *Solar Phys.* 74. 131, 1981
- {3} Severny, A.B., Is the Sun a magnetic rotator? *Nature*, 224. 53, 1969
- {4} Severny, A.B., The fluctuations of the general magnetic field of the Sun, *Quart. Journ. R.A.S.* 12. N.4. 363, 1971
- {5} Степанян, Н.Н., Фоновые магнитные поля на Солнце в 1964-1978 гг. *Изв. КрАО.* 65. 43, 1982
- {6} *Solar-Geophysical Data*
- {7} Брей, Р., Лоухед, Р., *Солнечные пятна*, с.384, МИР, Москва, 1967
- {8} Каплан, С.А., Пикельнер, С.Б., Цытович, В.Н., *Физика плазмы солнечной атмосферы*, с.255, библиогр. с.228., Наука, Москва, 1977
- {9} Каплан, С.А., Спектр магнито-гидродинамической турбулентной конвекции, *Астрон. Ж.* 40. 1047, 1963
- {10} Unno, W., On the applicability of the linear theory to the problem of convection in stellar atmosphere, *Publ. Astron. Soc. Japan*, 13. 276, 1961
- {11} Vitinskij, Ju. I., On the problem of active longitudes of sunspots and flares. *Solar Phys.* 7. 210, 1969

- {12} Bumba, V., Obridko, V. N., "Bartels" active longitudes, sector boundaries and flare activity, *Solar Phys.* 6. 104, 1969
- {13} Левицкий, Л. С., О связи солнечных космических лучей с энергией 10 Мэв с хромосферными вспышками. *Изв. КрАО*, 49. 36, 1974
- {14} Bumba, V., Howard, R., Martres, M. J., Soru-Iscovici, J., Patterns of active region magnetic field development, *IAU Symp.* 35. 13, 1968
- {15} Браиловская, И. Ю., Коваль, А. Н., Огирь, М. Б., Степанян, Н. Н., Некоторые параметры флоккулов, определяющие вспыхивающую активность, *Солн. Данн.* 6. 88, 1972
- {16} Bumba, V., Howard, R., Large-scale distribution of solar magnetic fields, *Ap. J.* 141. 1502, 1965
- {17} Котов, В. А., Степанян, Н. Н., Щербакова, З. А., Роль фонового магнитного поля и полей активных областей и пятен в общем магнитном поле Солнца, *Изв. КрАО*, 56. 75, 1977
- {18} Severny, A. B., Wilcox, J. M., Scherrer, P. H., Colburn, D. S., Comparison of the mean photospheric magnetic field and the interplanetary magnetic field, *Solar Phys.* 15. 3, 1970
- {19} Налимов, В. В., *Применение математической статистики при анализе вещества*, с. 379. Физматгиз, Москва, 1960

ИЗМЕНЕНИЕ МАГНИТНЫХ ПОЛЕЙ СОЛНЕЧНЫХ ПЯТЕН В СВЯЗИ СО ВСПЫШКАМИ

А.Н. КОВАЛЬ, Н.Н. СТЕПАНИН

КрАО, Научный

VARIATIONS IN THE MAGNETIC FIELDS OF SUNSPOTS RELATED TO FLARES

A.N. KOVAL', N.N. STEPANYAN

Crimean Astrophys.Obs., Nauchnyj

Abstract:

The spectrograms of sunspots obtained at the tower telescope - BST-2 of the Crimean observatory with polarization analyzer have been examined. We have measured the magnetic fields of sunspots by Zeeman-splitting of eight spectral lines originating at different depths in the solar atmosphere (from 60 km to 1200 km).

The consideration of the observational data obtained with 1 h time resolution showed, that:

1) In sunspots there are several kinds of magnetic field distribution according to height, but mostly the maximum magnetic field strength occurs at a height of 400-600 km.

2) The appearance of the flare coincides with an increase of magnetic field in the adjacent sunspots. After the end of the flare the field decreases. The maximum change in the field occurs at heights $h=400-600$ km.

3) The averaged rates of sunspot magnetic field variations for $h=400-600$ km level before (or during) the flare, after the flare and in the absence of the flare are 356 ± 75 , -324 ± 64 and -48 ± 23 G h^{-1} respectively.

The detailed study of the magnetic field of two sunspot groups during the flares, of importance 1B and 2N and with time resolution 1-7 min, permits us to conclude, that:

1) The most pronounced field variations take place in the umbrae which are located on both sides of the line of polarities reversal and their magnetic fields evolve in opposite directions: one polarity increases while the other decreases.

2) The displacement of the neutral line occurred during the flare. Its value varied with the height of solar atmosphere. It may be interpreted as a change in the force tubes inclination during the flare.

3) The relationships between the strengths of field change, which were determined by lines, originated at the same depth but with different temperature sensitivities.

4) By Zeeman-splitting of the metal emission lines, the magnetic field is the same or even stronger than that derived by the absorption lines in the sunspot below the emission.

Ранее нами было изучено изменение магнитных полей пятен на двух уровнях в атмосфере Солнца в связи с развитием активных областей: появлением и ростом пятен, возникновением усов и выбросов и вспышечной активностью {1}. Статистически было получено, что перед вспышкой в пятнах, близких к месту возникновения вспышки, разность $\Delta H = H_{\text{верх}} - H_{\text{ниж}}$ растёт, а после вспышки уменьшается и становится отрицательной, а затем принимает прежнее значение. Изменения магнитных полей более значительны на верхнем уровне. Пятна, далекие от вспышки, не показывают таких изменений.

Так как в {1} измерения магнитных полей пятен проводились 2-4 раза в день и только в двух линиях, мы решили продолжить начатые исследования с большим разрешением по высоте и по времени.

1. Наблюдательный материал

Для измерения магнитных полей были выбраны 8 линий, образующихся на разной глубине в атмосфере Солнца (от 60 до 1200 км), а также с разной чувствительностью к температуре. Список линий и их характеристики приведены в табл. 1 (λ - длина волны, элемент, $g\lambda^2$ - величина магнитного расщепления, I_{ϕ} - интенсивность линии в невозмущенной фотосфере, $I_{\text{п}}$ - интенсивность линии в пятне, h - высота образования линии). Высоты образования линий в пятне определены по {2}.

Наблюдения проводились на башенном телескопе БСТ-2 Крымской астрофизической обсерватории. Спектрограммы пятен с применением поляризационной оптики получены в четвертом порядке дифракционного спектрографа с дисперсией $0,37 \text{ \AA}/\text{мм}$. Одновременно на пластинке (пленке) получался участок длин волн $\lambda 6102 \text{ \AA} - \lambda 6153 \text{ \AA}$.

Мы анализируем наблюдательный материал полученный, начиная с 1972 г. Особенно подробные наблюдения магнитных полей выполнены для большого комплекса пятен, наблюдавшегося в мае-июне 1980 г. по программе ГСМ. Поляризационные спектрограммы всех пятен комплекса получались с интервалом около 1 часа в течение 8-10 часов ежедневно. Летом 1981 г. проведены наблюдения магнитных полей пятен во время вспышек. Спектрограммы

получались с интервалом 1-7 минут на протяжении всей вспышки.

2. Измерения и результаты

Средняя квадратичная ошибка одного измерения магнитного поля имеет значение от 50 до 100 гс в зависимости от резкости линии соотношения ее глубины и полуширины и величины магнитного расщепления.

Для всех изученных пятен по данным для всех восьми линий были построены графики, показывающие ход напряженности магнитного поля с высотой. Этот ход поля с высотой оказался разным для разных пятен. На рис. 1 представлены типичные примеры распределения напряженности магнитного поля с высотой. В исследованных нами пятнах наиболее часто встречающимся является распределение поля с максимальной напряженностью на высотах 400-600 км.

Рассмотрим соотношение магнитных полей, измеренных по линиям, разбитым попарно на следующие группы: 1) Линии образуются на примерно одной высоте и имеют одинаковую температурную чувствительность (линии 6,8); 2) Линии образуются на разных высотах, но их температурная чувствительность одинакова (линии 2,6); 3) Линии образуются на одной высоте, но имеют разную температурную чувствительность (линии 2,4).

На рис. 2 представлены попарные соотношения магнитных полей пятен, полученные из измерений этих линий. Из графиков видно, что: 1) Измеренные по линиям 6 и 8 магнитные поля практически одинаковы; 2) Определенные по линии 2 магнитные поля в основном выше на ~ 500 гс. чем по линии 6 для пятен с любыми напряженностями. Это свидетельствует о наиболее частой встречаемости распределения поля в пятнах с максимумом на высоте 400-600 км; 3) измеренные по линиям 2 и 4 магнитные поля в пятнах с напряженностью $\lesssim 3000$ гс различаются, в основном, не сильно. При $H \gtrsim 3000$ гс появляется значительное число пятен, в которых поле, измеренное по линии 4, более чувствительной к температуре, существенно больше, чем по линии 2. К этому графику мы вернемся позднее.

Чтобы уменьшить влияние ошибок в определении высот образования линий при изучении изменений магнитных полей пятен со

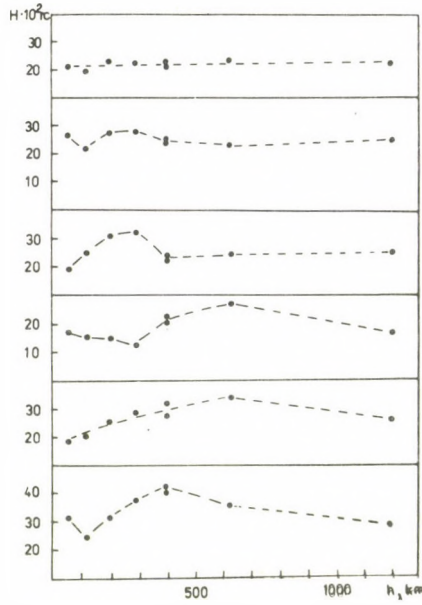


Рис. 1. Примеры наиболее часто встречающегося распределения магнитного поля с высотой в изученных пятнах.

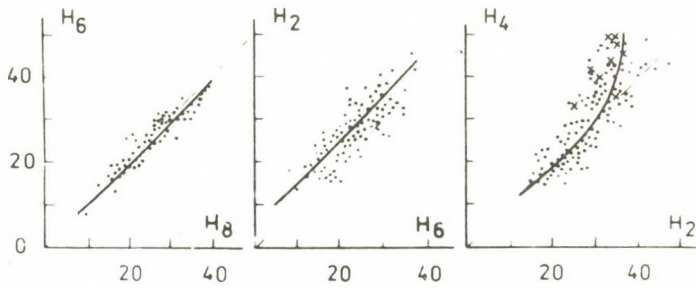


Рис. 2. Парные соотношения магнитных полей пятен, измеренных по разным линиям.

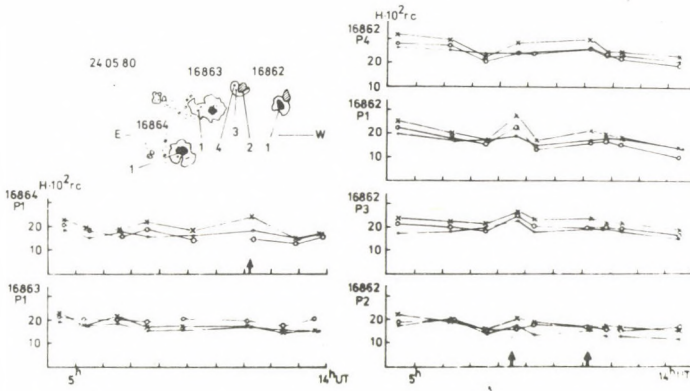


Рис.3. Изменение со временем магнитного поля пятен на трех уровнях в комплексе групп пятен 24.05.80 г. и его сопоставление со вспышками. Точки - нижний уровень, кресты - средний, кружки - верхний. Моменты вспышек отмечены стрелками на оси абсцисс. Положения узлов вспышек нанесены штриховкой на зарисовках групп пятен. Цифрами обозначены исследуемые ядра пятен. Значок P с цифрой обозначает номер ядра, к которому относятся измерения.

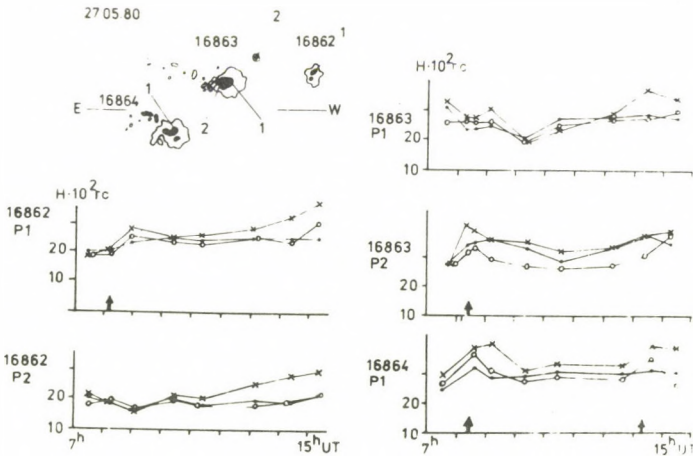


Рис.4. То же, что на рис.3, но для комплекса 27.05.80 г.

временем, мы разделим наши линии на три группы в зависимости от высоты их образования: нижний уровень ($h=60-300$ км), средний уровень ($h=400-630$ км) и верхний уровень ($h=1200$ км). Поля измерялись по всем линиям, затем бралась средняя напряженность магнитного поля по линиям данной группы. Напряженность поля на нижнем уровне определялась по четырем линиям (3,5,6,8), на среднем - по трем линиям (2,4,7) и на верхнем - по одной.

Измерения магнитного поля со временем на этих трех уровнях были сопоставлены со вспышками. На рис. 3-6 представлены результаты измерений для нескольких групп пятен. Моменты вспышек нанесены стрелками на оси абсцисс. В верхней части рисунка даны зарисовки пятен и цифрами отмечены исследуемые разрезы, а также нанесены положения вспышек по наблюдениям на КГ-1 и КГ-2.

Из анализа изученного материала можно сделать вывод: вспышки совпадают по времени с ростом поля близлежащих пятен. Чаще всего максимальный рост поля происходит на среднем уровне. После вспышки поле уменьшается. Пятна в той же группе, удаленные от вспышки, или пятна соседних групп в это время не показывают изменений поля, или изменения имеют другой характер.

Оценим реальность изменений магнитных полей в связи со вспышками и их отличие от эволюционных изменений магнитных полей пятен. Для всех наших наблюдений мы определили скорость изменения магнитного поля ΔH гс/час перед вспышками (во время вспышек), после них и для периодов без вспышек. На рис. 7 результаты таких определений представлены в виде гистограмм, на которого отложено число случаев (в процентах) для каждого значения ΔH для этих трех интервалов на нижнем, среднем и верхнем уровнях в атмосфере Солнца. В табл. 2 приведены средние значения ΔH гс/час. Как видно из рис.7 и табл. 2, в период вспышек наблюдается рост поля со средней скоростью несколько сот гаусс в час, а после вспышки уменьшение поля происходит со скоростью того же порядка. Наибольшие изменения происходят на среднем уровне. Наибольшая дисперсия значений H наблюдается для периодов перед вспышкой. В период без вспышек скорость изменения поля около - 50 гс/час, что соответствует найденной в [14] средней скорости изменения поля в пятнах. Отрицательное значение,

возможно, объясняется ухудшением качества изображений, приводящим к фиктивным уменьшениям поля от утра к полудню (большинство наблюдений проводилось в первую половину дня).

Таким образом, из табл. 2 видно, что изменения магнитных полей в период вспышки и после нее существенно превосходит изменения в спокойный период развития группы пятен.

Анализ наших наблюдений также показал, что значительные изменения магнитных полей пятен происходят в течение небольших интервалов времени, порядка часа и меньше. Поэтому следует еще более улучшить временное разрешение, чтобы получить более подробную картину изменений магнитного поля в связи со вспышками.

3. Результаты измерений магнитных полей пятен с высоким временным разрешением во время вспышек.

Летом 1981 г. мы провели ряд наблюдений магнитных полей пятен во время вспышек с временным разрешением 1-7 минут. Для двух вспышек получены наблюдения с самого начала и они были изучены нами в первую очередь.

А. Вспышка балла 1 В 23. VII. 1981 г. Вспышка началась в $7^{\text{h}} 10^{\text{m}}$ UT, достигла максимума в $7^{\text{h}} 20^{\text{m}}$, закончилась в $8^{\text{h}} 15^{\text{m}}$. Наблюдения магнитных полей пятен начаты через 10 минут после начала вспышки.

Результаты измерений магнитных полей пятен во время вспышки представлены на рис. 8. В верхней части рисунка приведена зарисовка группы пятен, отмечены исследуемые ядра, штриховкой нанесено положение узлов вспышки. Наиболее яркие узлы вспышки были расположены вблизи разреза 2. Без детального сравнения с развитием вспышки мы пока не будем рассматривать колебания магнитного поля, которые хорошо видны в некоторых ядрах, а рассмотрим картину изменения магнитного поля в целом.

Ядра 1 и 2 имели N полярность, ядра 3 и 4 S-полярность.

В ядре 1 только для линий, образующихся на среднем уровне, наблюдается небольшой рост поля в течение вспышки. Наибольшие изменения магнитного поля происходили в ядре 2, вблизи которого находился самый яркий узел вспышки: поле растет на всех уровнях,

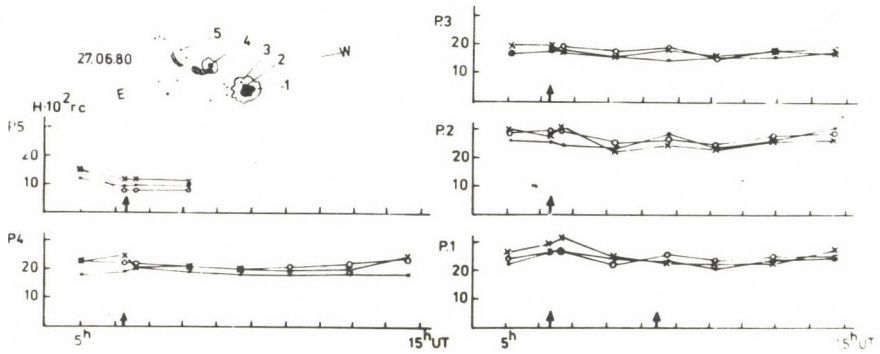


Рис. 5. То же, что на рис. 3, но для 27.06.80 г.

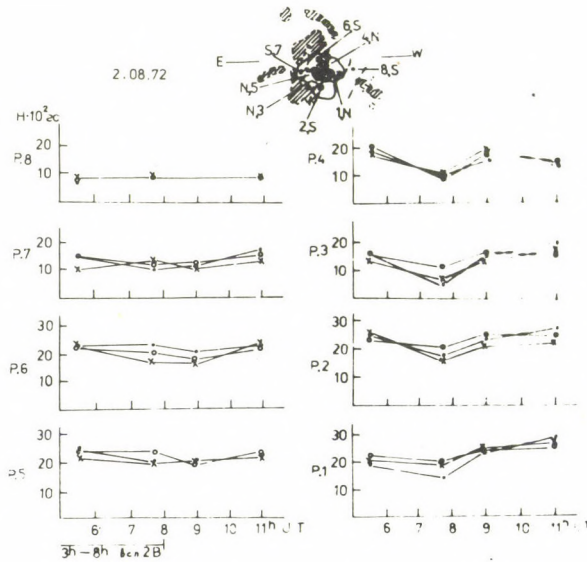


Рис. 6. То же, что на рис. 3, но для 2.08.72 г.

ТАБЛИЦА 1

NoNo п/п	λ	Элемент	$g\lambda^2$	I_{ϕ}	I_{Π}	h км
1	6102.72	Ca I	$74.1 \cdot 10^{-10}$	9	25	1200
2	6108.15	Ni I	40.4	6	8	400
3	6111.05	Ni I	46.6	2	0	60
4	6119.54	V I	41.6	1	8	400
5	6128.99	Ni I	56.5	1	2	120
6	6136.99	Fe I	75.3	3	4	200
7	6141.72	Ba II	41.4	7	12	630
8	6151.63	Fe I	69.2	4	6	290

ТАБЛИЦА 2

Уровень	М о м е н т		
	перед вспышкой г час ⁻¹	после вспышки г час ⁻¹	без вспышки г час ⁻¹
Нижний	165 ± 49	-198 ± 39	-38 ± 15
Средний	356 ± 75	-324 ± 64	-48 ± 23
Верхний	291 ± 56	-340 ± 61	-40 ± 19

ТАБЛИЦА 3

Время UT	H ₆₁₃₇ г	H ₆₁₃₈ г	H ₆₁₄₂ г
	6:28	2100	2200
6:29	3000	3100	-

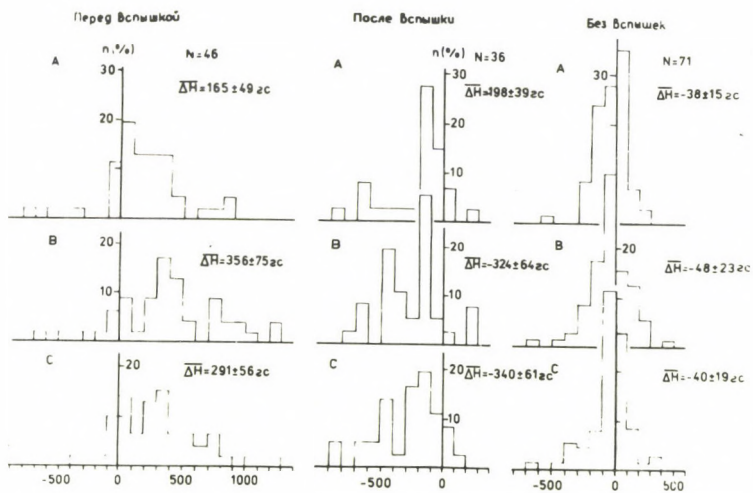


Рис. 7. Распределение скорости изменения магнитного поля пятен перед вспышками, после вспышек и без них для трех уровней в атмосфере Солнца. А - нижний, В - средний, С - верхний уровни.

но наибольший рост поля выявляется по линиям 2, 4 и 7. В ядре 3 происходит уменьшение поля, которое также более выражено в линиях 4 и 7. В ядре 3 напряженность магнитного поля во время вспышки практически не изменяется: слабое уменьшение поля в линиях 5, 6, 8.

Таким образом, наибольшие изменения поля происходили в ядрах, расположенных вблизи линии раздела полярностей (ядра 2 и 3), при этом поле N полярности усиливалось, а поле S полярности уменьшалось. Эти изменения поля соответствуют результатам, полученным в [3].

Одной из особенностей ядра 4 является огромная разность напряженностей магнитного поля, определенного по линиям 4 и 2, достигающая 1700 гс. В других ядрах этой группы разность $\Delta H = H_4 - H_2$ была около 300-1000 гс. Эффект увеличения разности ΔH в пятнах, на которых располагалась эмиссия вспышек, наблюдался нами для ряда вспышек. Так, 27. VI. 80 г. в спокойный период развития группы пятен при наблюдениях с 5^h до 15^h UT (шесть измерений магнитных полей) $\Delta H = H_4 - H_2$ изменялась от 300 до 500 гс., а во время вспышки 1 В достигла значений 1000-1200 гс.

Выше мы уже говорили, что в пятнах с напряженностью поля больше 3000 гс линия 4, более чувствительная к температуре, чаще показывает более высокое значение напряженности поля рис. 2. На этом же рис. 2 крестиками нанесены измерения магнитных полей пятен, относящихся к моментам вспышек. Практически все они находятся в области $H_4 > H_2$.

Так как линия 4 усиливается в пятне, т.е. образуется в более холодных элементах, то рост поля в ней по сравнению с линией 2 свидетельствует о росте магнитного потока от холодных элементов. Такой рост может происходить за счет увеличения относительного числа холодных элементов или за счет повышения в них магнитного поля.

В. Вспышка балла 2 12. VIII. 1981 г. В 5^h30^m начал ярчать флоккул, в 6^h20^m - 6^h30^m вспышка достигла максимальной яркости и в 7^h практически закончилась. Измерения магнитных полей пятен начаты в 5^h45^m. Наиболее яркий узел вспышки был расположен между ядрами 4 и 5 (см. рис. 9), а в момент максимума яркости

эмиссия частично заливала ядро 4. Ядро 4 было N полярности, ядро 5 - S полярности. В промежутке между ядрами 4 и 5 поле еще два раза меняло знак: к ядру 4 примыкало поле S полярности (р 4.а), затем шло поле N полярности. То есть самый яркий узел вспышки располагался в области с очень сложной структурой магнитного поля.

Исследовались изменения магнитного поля во время вспышки в ядрах 1, 4, 5 и в области S полярности, примыкавшей к ядру 4 (р 4.а). В ядре 1 происходили небольшие изменения поля, наиболее заметные в линиях 1 и 7: небольшое падение напряженности поля к моменту максимума вспышки и восстановление к прежнему значению. В ядре 5 заметных изменений поля не происходило. Наибольшие изменения поля были в ядре 4 и в области примыкавшей к нему S полярности. В ядре 4 во время вспышки поле уменьшается во всех линиях, а к концу вспышки начинает восстанавливаться. В примыкавшей области S полярности (р 4.а) поле растет на всех уровнях (см.рис.9).

Кроме роста поля S -полярности во время вспышки происходило смещение нулевой линии между ядром 4 и р 4а. Причем это смещение в спектральных линиях 2 и 6 (их можно отнести в среднем к высоте 300 км) отличалось от смещения в линиях 1 и 7 (образующихся в среднем на высоте 1000 км).

Изменение расстояния нулевой линии от центра ядра 4 на этих уровнях показано на рис.10. Такой вид кривых можно интерпретировать как изменение наклона трубок силовых линий поля во время вспышки. Схематически это показано на рис. 11.

Использование спектральных линий, образующихся на разных высотах, позволяет нам проследить картину сдвига нулевой линии магнитного поля в плоскости, проходящей через щель спектрографа (линия ОВ на рис.11) и луч зрения (ОА на рис.11). В плоскости фотосферы, перпендикулярной ОАВ, условно изображено пятно с ядром 4 и нулевой линией (пунктир), пересекающей щель спектрографа в точке С. Линии СД₁, СД₂ и СД₃ - сечения поверхности нулевого магнитного поля с плоскостью ОАВ в последовательные моменты времени (5^h50^m, 6^h20^m, 6^h30^m). К концу вспышки (7^h10^m) эта линия приблизилась к СД₁.

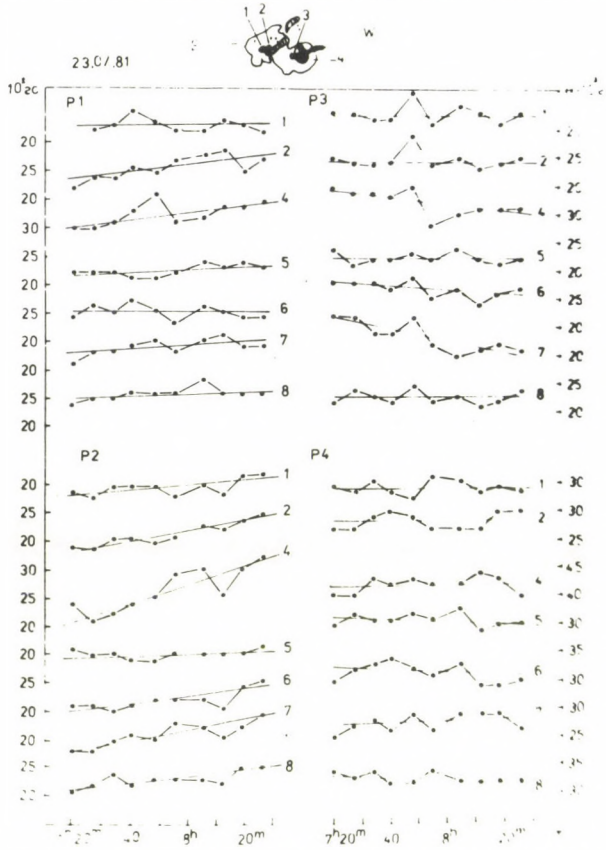


Рис.8. Изменения магнитных полей в группе пятен во время вспышки балла 1В 23.07.81 г. В скобках - номера линий, по которым определялось поле (согласно таблице 1).

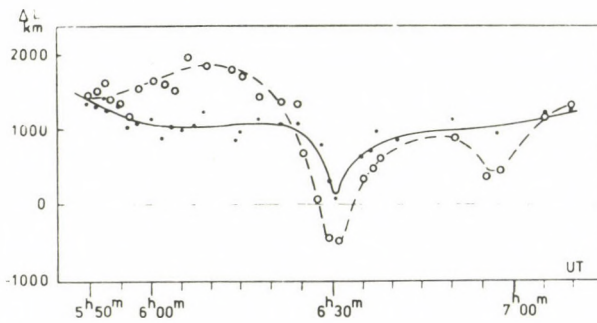


Рис.10. Изменение со временем положения границы раздела полярностей относительно центра ядра 4 12.08.81 г. Точки - положение границы в линиях 6.8, кружки - линиях 1.7.

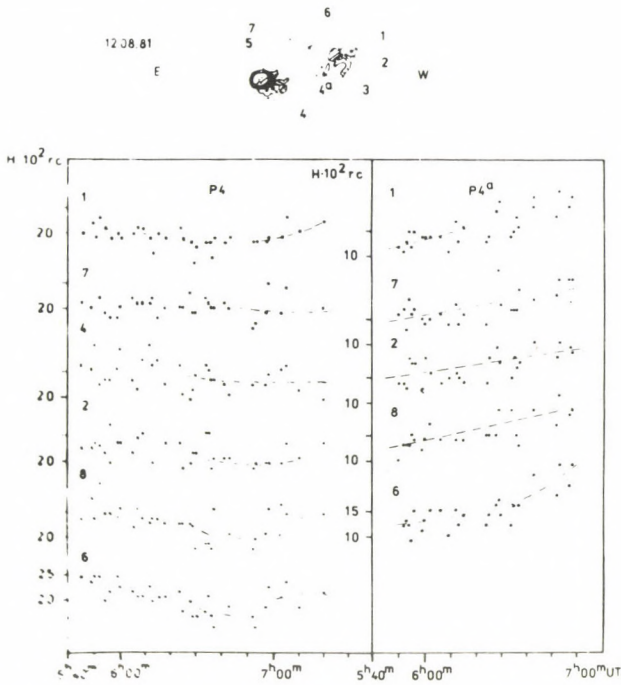


Рис.9. Изменение магнитного поля в ядре 4 и области S полярности (р 4а) во время вспышки балла 2N 12.08.81 г.

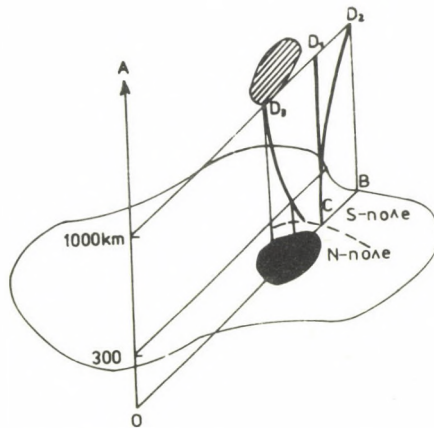


Рис.11. Схематическое изображение сдвига нулевой линии магнитного поля в плоскости, проходящей через щель спектрографа и луч зрения. Залитый овал - ядро 4, заштрихованный овал - эмиссия вспышки.

Оценки скорости движения линии раздела полярностей для высот около 1000 км дают величину ~ 10 км/сек.

В $6^{\text{h}}28^{\text{m}} - 6^{\text{h}}30^{\text{m}}$ вблизи ядра 4 ряд линий металлов виден в эмиссии. В линиях FeI $\lambda 6136,6 \text{ \AA}$ и $\lambda 6137,7 \text{ \AA}$, а также в линии Ba II $\lambda 6141,7 \text{ \AA}$ эмиссия довольно сильная и видна на двух соседних полосках поляризационной спектрограммы. Это дает возможность определить напряженность и знак магнитного поля в месте свечения металлов во вспышке. Результаты измерений представлены в таблице 3, из которой видно, что напряженность магнитного поля в месте свечения металлов такая же, или даже несколько выше, чем определенная по линиям поглощения в пятне. Основная часть эмиссии располагалась на нулевой линии и в области S полярности. Поле в области эмиссии также имеет S полярность.

Таким образом, наблюдения магнитных полей пятен во время вспышек с высоким временным и пространственным разрешением на нескольких уровнях атмосферы Солнца подтверждают и частично дополняют картину изменений, происходящих в активной области в связи со вспышками {4,5}.

Существенные изменения происходят в магнитных полях пятен. Меняется величина поля, распределение его с высотой, наклон трубок поля, соотношение горячей и холодной компоненты в пятне.

Л и т е р а т у р а

- {1} Коваль, А.Н., Степанян, Н.Н., Изменение магнитных полей пятен на двух уровнях в связи с развитием активных областей, *Солн.Данн.* 1. 83, 1972
- {2} Mattig, W., The geometrical height-scale and the pressure equilibrium in the sunspot umbra, *Solar Phys.* 8. 291, 1969
- {3} Ribes, E., Study of the correlation between flares and the evolution of magnetic field, *Astron. Astroph.* 2. 316, 1969
- {4} Зверева, А.Н., Северный, А.Б., Магнитные поля и протонные вспышки 7 июля и 2 сентября 1966 года, *Изв. КРАО.* 41-42. 97, 1970
- {5} Гопасюк, С.И., Огирь, М.Б., Северный, А.Б., Шапошникова, Е.Ф., Структура магнитных полей и ее изменения в районе солнечных вспышек, *Изв. КРАО.* 29. 15, 1963

CHANGES IN THE LARGE-SCALE CURRENT SYSTEMS
IN THE COURSE OF THE EVOLUTION OF AN ACTIVE REGION

S. I. G O P A S Y U K,

B. K Á L M Á N,

V. A. R O M A N O V

Crimean Astrophys. Obs.,
NauchnyjHeliophys. Obs.,
DebrecenState University
KrasnoyarskAbstract:

The evolution of the magnetic field structure in sunspot group SD 207/1969 (MtW. 17310) was studied between 8-14 June 1969 using a novel method: the azimuths of the observed transversal magnetic field component were compared with the azimuths of the H_t of a potential field computed from the distribution of the observed longitudinal component. Furthermore the vertical electric current density was computed from Maxwell's equations. On the resulting charts the differences in azimuths and the strong currents with densities up to 20 000 A/km² have a strong correlation with the activity in the group (spot transformations and evolution, proper motions) and with flare activity. This method may be useful for operative flare forecasting from magnetic field measurements.

ЭВОЛЮЦИЯ КРУПНОМАСШТАБНЫХ ТОКОВЫХ СТРУКТУР

ЗА ВРЕМЯ РАЗВИТИЯ АКТИВНОЙ ОБЛАСТИ

С. И. ГОПАСЮК

Б. КАЛМАН

В. А. РОМАНОВ

КрАО
НаучныйГелиофиз. Обс.
ДебреценГос. Университет
КрасноярскАбстракт:

В работе изучена эволюция магнитного поля групп пятен С.Д. 207/1969 (MtW. 17310) с 8 по 14 июня 1969 г по новому методу: азимуты наблюдаемого поперечного компонента магнитного поля сравнивались с азимутами H_t , вычисленными из потенциального распределения по наблюдаемому продольному компоненту. Далее была вычислена плотность вертикальных токов из уравнений Максвелла. На полученных картах большие отклонения азимутов и сильные токи до 20000 А/км² хорошо коррелируют с активностью в группе (преобразования и эволюция пятен, собственные движения), и со вспышечной активностью. Данный метод может быть использован для прогнозирования вспышек из магнитных измерений.

1. Introduction

The search for the laws of evolution of solar active regions is important for understanding the basic physics of solar activity. The main direction in these investigations was and is the study of the evolution of magnetic fields in the solar atmosphere, and analysis of the physical processes caused by these changes {1},{4},{7}.

This paper is the continuation of a series of analysis of the structure of the magnetic field in active region No 207 (*Solnechnye Dannye*) or McMath No 10135, Mt. Wilson No 17310. The measurements of the magnetic field were made by the vector-magnetograph of the Crimean Astrophysical Observatory with simultaneous registration of all three components of the H vector in the λ 5250 Å *Fe I* spectral line, in all phases of evolution of the sunspot group between 8-14 June 1969. The detailed description of the observations and the reduction of the material is described in {4},{6}.

On the basis of these magnetic measurements, using both photoheliograms from the Debrecen Heliophysical Observatory, and magnetic spectroheliograms from Meudon Observatory, a detailed study of the connection between penumbral structure and magnetic field vector was made {6}, the proper motions of the umbrae and the penumbral structure were compared with the structure of the magnetic field {4}, and the connection between the evolution of the group and its magnetic field changes and vertical electric currents was investigated {5}. However, some problems remained open after these papers:

1) In {5} the vertical current density j_z was computed using the following expression:

$$\frac{4\pi}{c} j_z = \frac{\partial H_y}{\partial x} - \frac{\partial H_x}{\partial y} \quad (1.1)$$

i.e. by numerical differentiation of tangential components H_x , H_y . But in numerical differentiation, the errors in measurements of H_x , H_y , may significantly influence the accuracy of the result (the relative error of j_z may be significantly greater than that of H_x , H_z).

2) Even the process of numerical differentiation has some inherent inaccuracy (in the course of the measurement one reading was taken every 3.4", and the distance between scans was 6.7").

3) The tangential component may have two directions, differing by 180°. In {4} this ambiguity was resolved by intuition using superposition of charts of longitudinal and tangential components. This method may be erroneous in the case of complicated field geometry.

4) The computed distribution of j_z allows us to distinguish between positive and negative current areas, and makes it possible to derive the average rotational component along the boundaries. It is difficult to say on the basis of only these data, how strongly the currents influence the magnetic field, i.e. how far the magnetic field is from a potential one. From the physical point of view this non-potentiality can characterize the activity of the group.

5) Numerical differentiation gives j_z in the depth of formation of the λ 5250 Å *Fe I* line. No information can be gained about currents above this level (e.g. in the chromosphere, corona).

If, in addition to the aforementioned points, we consider the real complexity of currents flowing in the solar atmosphere, it becomes clear why {5} reaches a conclusion about insignificant changes in the principal large-scale current structure during the observations. In reality, as will be shown later, the redistribution of current structure occurs very intensively. But to show this we need a special reduction of the observations, which will be described now.

In this paper we investigate, how close the magnetic field of the given active region (AR hereinafter) is to a potential field, which was computed for each observation from the distribution of the vertical field component H_z . Such computations allow us to decide at which time of observations the magnetic field was near potential, and at which time strongly non-potential. A more detailed analysis is also poss-

ible: From the charts of the magnetic field, places of near potential field can be determined and also other places, where the real measured field disagrees strongly with the computed potential field. If these places of disagreement are sure (the magnitude of the disagreement is greater than the measurement errors of the magnetic field, and there are many points of measurement in these areas), then we can say that in these disturbed areas, or in the vicinity of them, strong currents are flowing. In such a way we can follow the evolution of current systems in the AR during the time of observations.

As in our case we can derive the existence of currents above the level of the measurement of magnetic fields (e.g. in the chromosphere and corona), we can follow the correlation between redistribution of current structure and flare activity in the group.

All computations of potential magnetic fields were performed by one of us (V.A.R.) on the ES-1033 computer of the Computing Center of the Krasnoyarsk Filial of the Siberian Branch of the USSR Academy of Sciences, for the plots a "Digigraf" plotter was used.

2. Mathematical formulation of the problem. Analysis of the potentiality of observed solar magnetic fields

The magnetic field of the AR is computed in a Cartesian coordinate system, in a semi-infinite volume, the lower boundary of this is the plane, where the distribution of H_z is given. As the currents, causing this field, are below this level, we can write the Maxwell equations:

$$\operatorname{rot} H = 0 \quad (2.1)$$

$$\operatorname{div} H = 0 \quad (2.2)$$

On the lower boundary we give a boundary condition for the normal component:

$$H_n \uparrow_G = H_z \quad (2.3)$$

Naturally the solution must vanish in the infinity:

$$H \rightarrow 0 \quad \text{if } R \rightarrow \infty \quad (2.4)$$

From equations (1.2) and (1.4) we can derive

$$\oint H_z dG = 0 \quad (2.5)$$

This system of (2.1-2.3) with conditions (2.4,2.5) is a Neumann boundary problem for the Laplace equation in a semi-infinite volume. A unique solution for this system exists {2}.

For real magnetograms condition (2.5) is not true because of measurement errors and lack of information from the whole AR of the distribution of H_z . In this case we can get an approximate solution for a finite volume. Problems connected with the mathematical foundations for solving this system by Fourier series, with the accuracy of the solution, and with the implementation of a simple algorithm for small computers were studied and published separately {3}.

The distribution of H_z in the model is identical on the lower boundary plane with the measurements, but as regards the tangential components, these are generally different. Comparing these distributions, we can determine how far the observed distribution of the magnetic fields is from a potential one. Such a comparison is possible because the registration of longitudinal and transversal components of the magnetic field proceeds separately {7}, and in the computations the tangential components are not involved.

Disagreements between observed and computed tangential components are caused by currents, flowing above the level of formation of the spectral line, in which the magnetic fields were measured, i.e. in our case the λ 5250 Fe I line. In {8} the necessity for taking currents flowing below and above the formation level of the spectral line used for magnetic measurements separately into account was discussed for the first time. In this paper we do not want to reconstruct the spatial structure of these currents, only delineate those areas where such currents flow above the level of line formation (i.e. this is a partial solution for a more general problem, outlined in {8}).

For comparison of observed and computed magnetic fields we must know the accuracy of potential field calculations and magnetic field measurements. For this purpose we analyse these problems on the example of the measurements and calculations of one day, this allows us to show the data for other days more concisely.

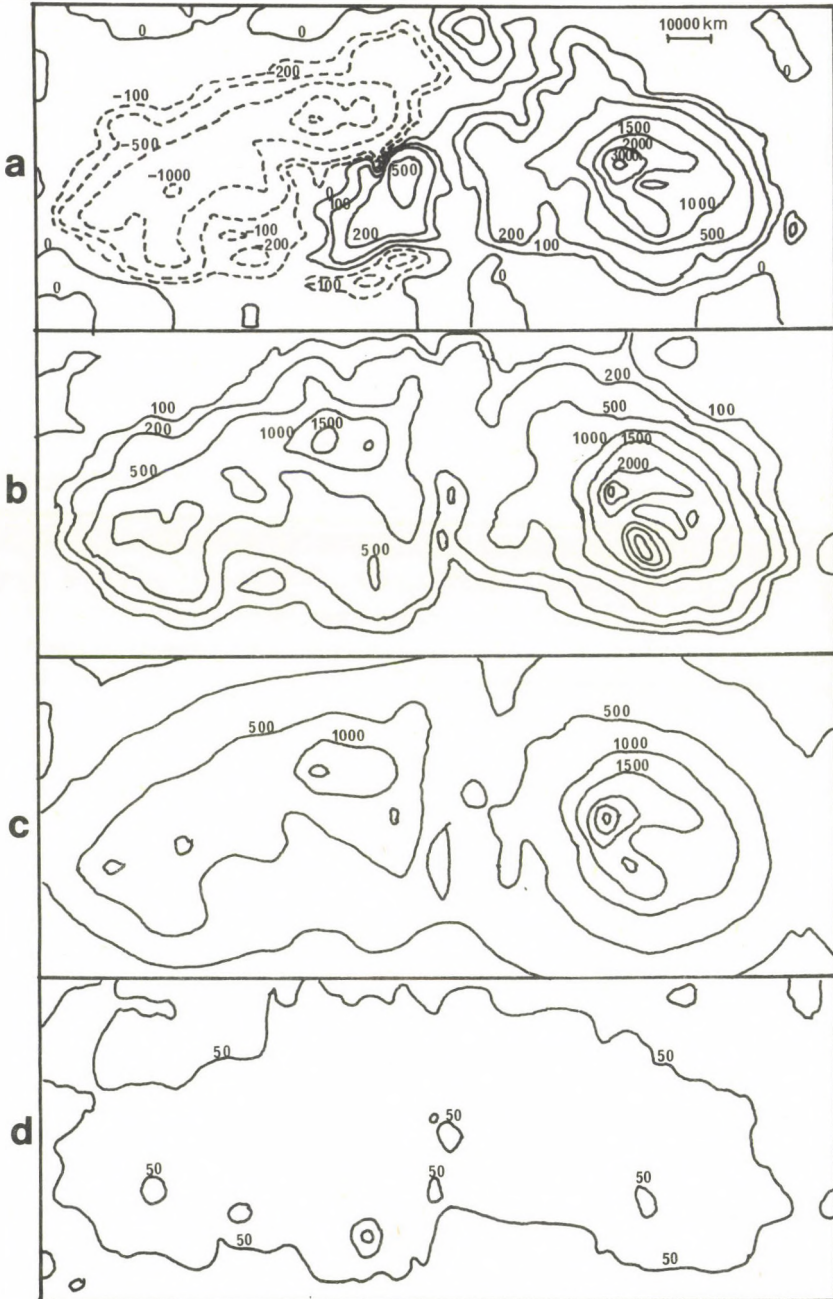


Fig.1. a) isogausses of H_2 (measured) for 8 June 1969, b) isogausses of measured H , c) isogausses of computed H , d) discrepancy between b & c, (%).

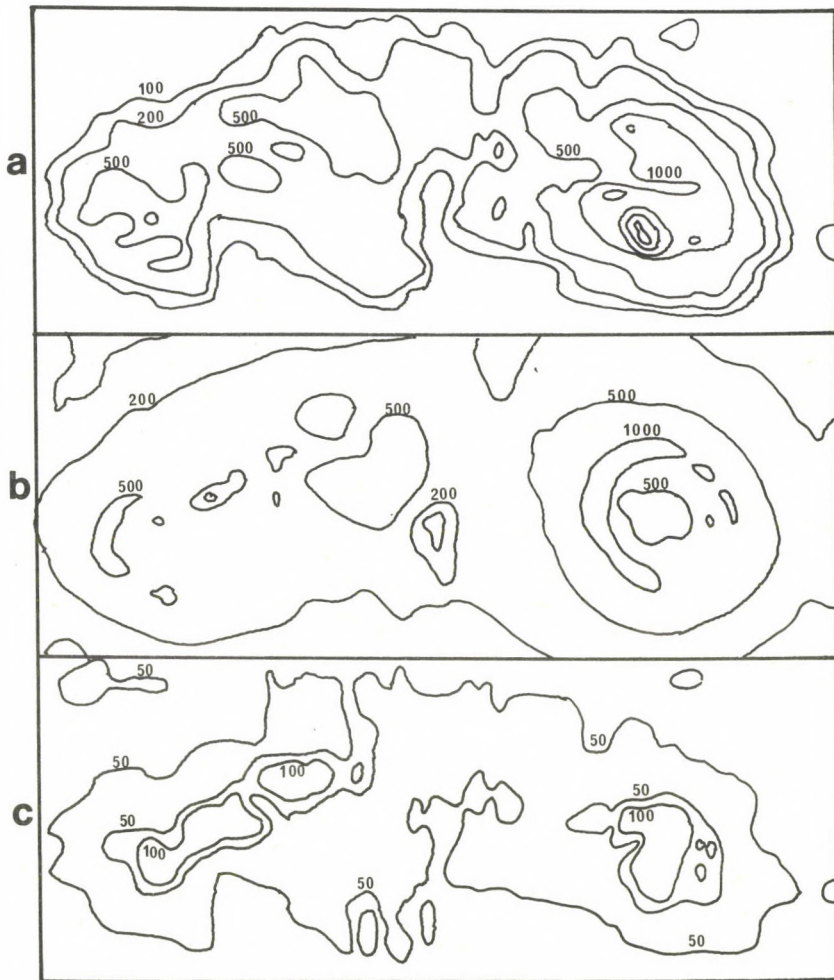


Fig.2. a) isogausses of the absolute value of the tangential component of the measured magnetic field for 8 June 1969,
b) isogausses of the absolute value of the tangential component of the magnetic field, computed from the potential model,
c) the discrepancy between a & b in %

In Fig.1a the chart of distribution of H_z is shown for 8 June 1969. The potential fields are computed on the bases of such charts. The magnetic flux of northern polarity in this chart is 31% higher than that of southern polarity. This imbalance of magnetic fluxes remains similar for the other days, and leads to the non-fulfillment of condition (2.5). Notwithstanding this, the measurements of the longitudinal component of the magnetic fields are very accurate, having a sensitivity of about 10 G {7}. This is very important because this accuracy determines the accuracy of the potential model (the errors of computation do not exceed 3-4%, except in very rare cases {3}).

In Figs.1b,c,d: a) the distribution of the absolute value of the magnetic field $|H|$ from observations, b) the same from the computed potential model on the same level and c) the disagreement between the two above charts in percents are shown:

$$\Delta = \frac{|H_{pot} - H_{meas}|}{|H_{pot}|} \times 100\% \quad (2.6)$$

The contour lines are drawn at 50% and 100% disagreement level, in this chart disagreements of more than 100% were not found. In practice we have good agreement between measured and computed field in the whole AR, except at the borders of the chart (this will be discussed later).. This good agreement is due to the fact that the component H_z , which is used in computing $|H|$, is identical in the measurements and in the computed field. Therefore $|H|$ is not a good parameter for the analysis, and will not be used further.

In the upper right corner of Fig.1 a scale is drawn, showing the linear extent of the charts, as this is the same for all the charts, it is shown only once.

In Fig.2 in the same manner as in Fig.1b,c,d, the absolute values of the tangential component of the magnetic field $|H_t|$ are shown. The discrepancies in these charts are significantly more, and greater. Let us see the differences at the borders of the charts. These are caused by two factors:

- 1) by the 31% imbalance of magnetic fluxes and the cor-

responding inaccuracy of the potential model. This factor is not serious because an imbalance of 30% causes large differences only on the 2-3 rows of the computing grid points at the very edge of the chart, and its influence is negligible in the inner parts {3}.

2) by the low sensitivity of the magnetograph to the transversal field (100 G {7}). This is the principal factor. On the border areas, the computed magnetic field component has a value of the order of 200 G, and the accuracy of the measurements is 100 G. This leads to the fact that the contour line of 50% discrepancy practically coincides with the 100 G iso-gauss line in the observations. This is also the cause of the differences at the border of the $|H|$ chart in Fig.1d. Differences in the central parts of the charts are classified as real, and treated separately.

In Fig.3 a) a drawing of the AR for 8 June 1969, solid line delineates umbrae, dashed line - penumbrae, b) chart of the differences of the azimuths in the potential model and in the measurements are shown. The contour lines are drawn at the 45° and 80° level, i.e. significantly higher than the accuracy of the measurement of this parameter. The ambiguity of the azimuths in the observations is resolved so that the angle between the computed and observed azimuths is always taken it less, or equal to 90° . This method is not in contradiction with methods of {4}, and, what is important, it generates the least differences between the potential model and the reality, thus maximally assuring the reality of the differences for this parameter.

In Fig.3c, the chart of vertical current density j_z is given, computed by formula (1.1) by numerical differentiation, the same way as in {5}. This result is purely from observations, only azimuths are taken from the potential model. For deriving the accuracy of the numerical differentiation by formula (1.1) we computed the distribution of j_z for the potential model for all the days of observation. In all of the cases the value of current density did not exceed 3000 A km^{-2} , at the same time

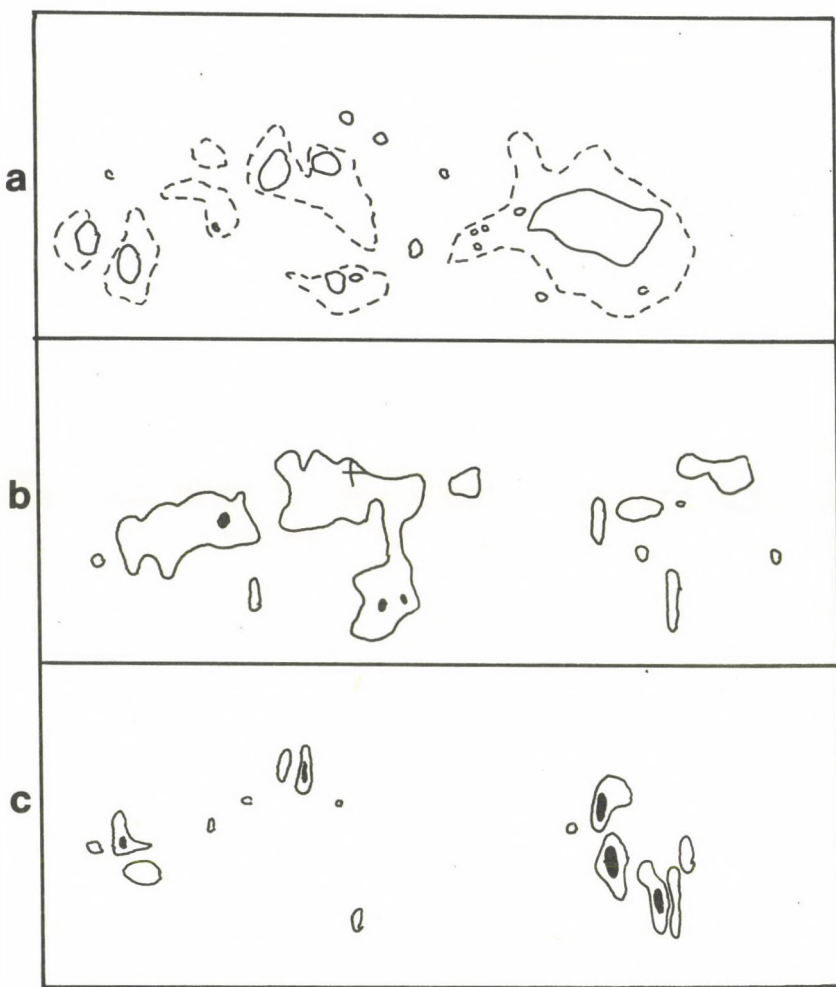


Fig.3. a) the drawing of the sunspot group for 8 June 1969, full line - umbra , dashed line - penumbra,

b) the differences of azimuths of the observed and computed tangential component of the magnetic field. Full line - 45° difference, black area - more than 80° difference.. Cross - flare site.

c) vertical electric current densities, computed from Maxwell equations. Full line - $j_z = 10\,000\text{ A/km}^2$, black areas - j_z greater than $20\,000\text{ A/km}^2$.

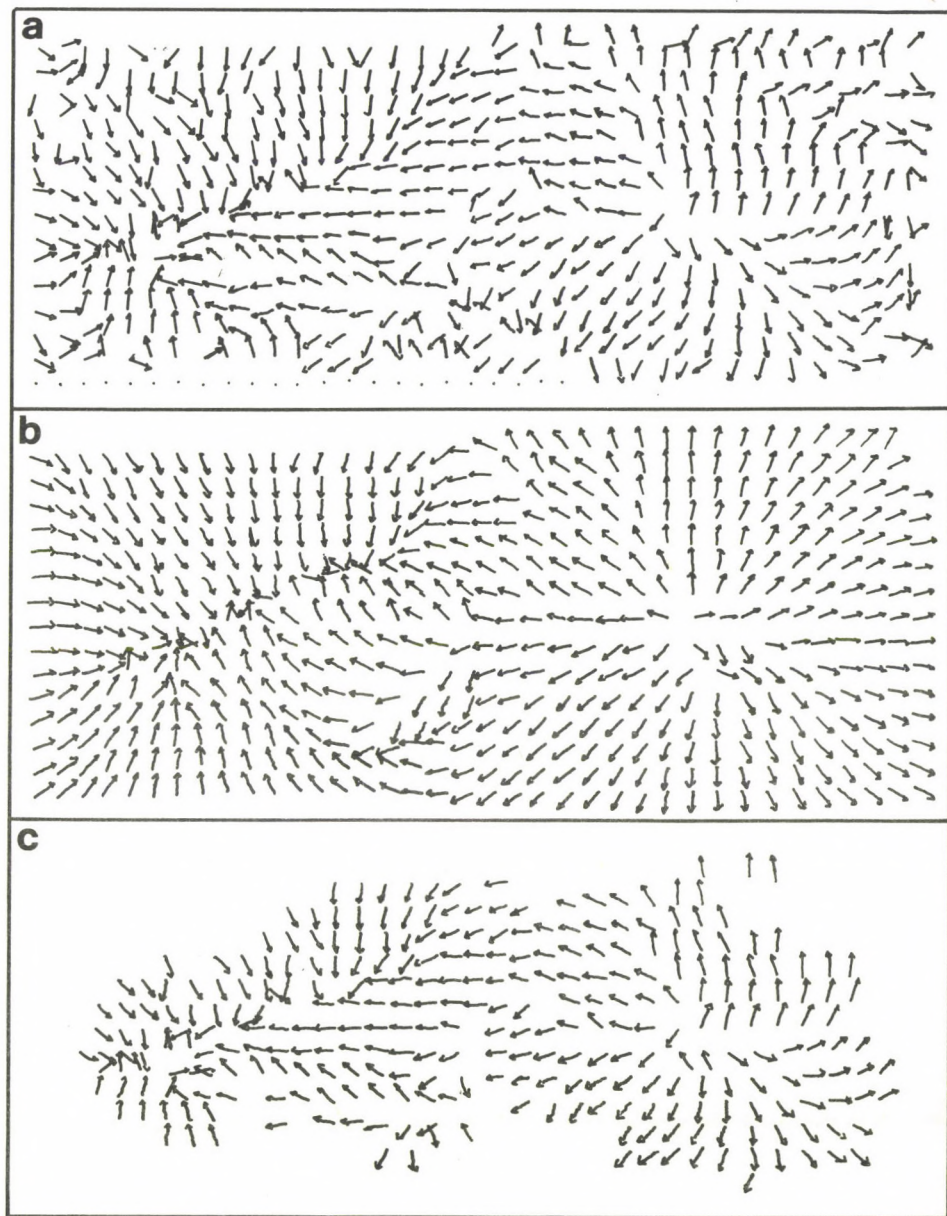


Fig.4. a) azimuths of the measured tangential magnetic field for 8 June 1969,
b) azimuths of the tangential field from the potential model,
c) azimuths of the measured tangential field, omitting points with
 H_t less, than 100 gauss.

in some places current densities of $10\,000\text{ A km}^{-2}$ and $20\,000\text{ A km}^{-2}$ were computed (Fig.3) from observations. The differences of azimuths in the potential model and in the observations are due to currents flowing above the level of magnetic measurements. The charts of the distribution of j_z show the in- and outflow of these currents in the studied volume. It is natural to suppose that the currents are strongest around the source regions, so the charts of 3b and 3c should be similar. But strong currents with densities $10\,000 - 20\,000\text{ A km}^{-2}$ do not disturb significantly the magnetic fields, (e.g. in the case of strong magnetic field, as in the leader spot) in all cases. On the contrary, in the areas of weak magnetic fields, weak currents can already cause large disturbances, but we cannot study these because of the inaccuracy of computations by formula (1.1).

So the charts of vertical current density j_z and charts of differences between observed and computed from the potential field azimuths are complementary. Furthermore, the latter are more reliable, as the measurements of the azimuths is more accurate. Therefore, in the subsequent analysis these charts of azimuth differences will be used to study the potentiality of the magnetic field of the AR.

In all the charts in this paper the scale is the same, and the same area of the solar surface is shown for charts of one and the same day. This facilitates the comparison of different disturbances in different charts, and the comparison of current inflow and outflow areas with sunspots. In Fig.4b the chart of azimuths of H_t is shown; it is computed from the potential model. In Fig.4a we have the chart of observed azimuths of H_t , from this chart the one in Fig.4c was derived, where azimuths for points with $|H| > 100\text{ G}$ are not shown, as they are chaotic because of measurement errors. The azimuth difference chart of Fig.3b was derived from comparison of Figs.4b&c.

3. Evolution of the large-scale current system of the sunspot group, its connection with the proper motion of spots and flare activity centres

In the following we will use the symbols and results of papers {4}, {5}, and especially the results of {5}.

On 8 June 1969 (Fig.3) the sunspot group is a typical bipolar one, with separate preceding and following parts, the following part is not very large. In the preceding part we can follow the motion of umbrae 2,3 to the large leader umbra 1, and there were large changes in the shape of umbra and penumbra of the leader spot (Fig.5 for 9 June 1969). In these places the largest currents of the day flowed, but they did not disturb the tangential component: the difference between the azimuths of the potential and observed field is not very large.

The most interesting evolution took place in the central and eastern parts of the group, where the following part began to form. In these areas the currents were weaker, but they strongly deformed the magnetic field. In this place we observed the converging motion of umbrae b_1 & b_2 (on the next day there was a single umbra $b_{1,2}$) and the motion of umbra b_3 to these. In that area we might observe strong currents, large differences in azimuths and a subflare was observed.

Solar flares were observed on the coronagraph KG-1 of the Crimean Astrophysical Observatory, from these observations we derived the place and time of flares. As usual, the time of observation of magnetic fields and observations on the coronagraph coincided, which makes this series of observations especially interesting.

Proper motions of umbrae $a_1, a_2, a_3, e_1, e_2, e_3$ were registered on this day, also the decay of umbra c , which ended on 9 June 1969. On all these places there are distinct differences in the azimuths of H_t .

On 9 June 1969 two measurements of the magnetic field were made, with a time difference of $1^h 20^m$. In Figs.5,6 the results of analysis of these data are shown.

From H_α observations on this day an activation of the

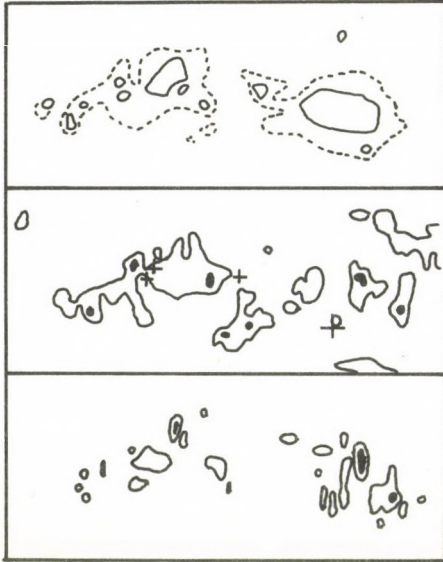


Fig.5. The same, as Fig.3, for the first measurement of 9 June 1969

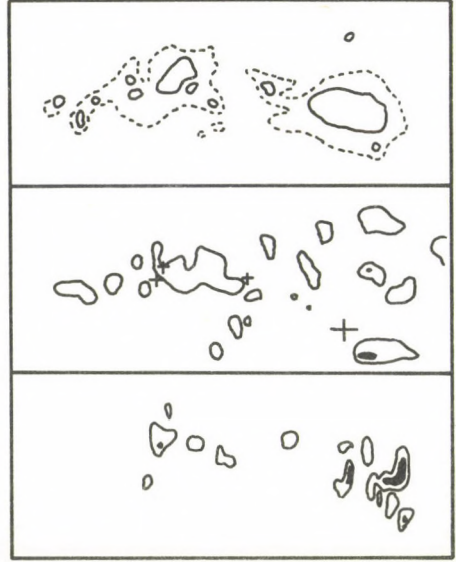


Fig.6. The same, as Fig.3, for the second measurement of 9 June 1969.

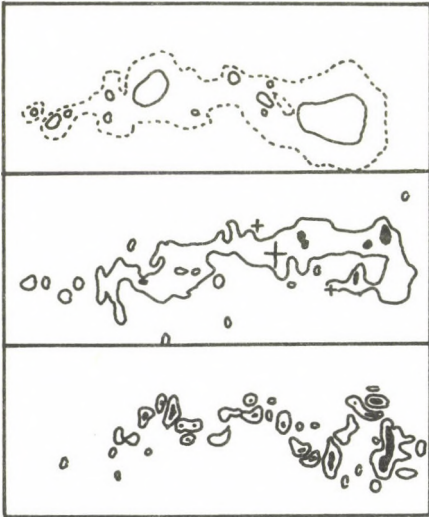


Fig.7. The same, as Fig.3, for the measurement of 10 June 1969

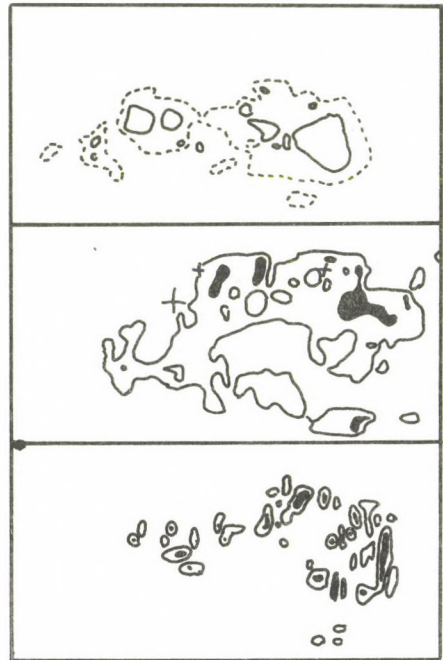


Fig.8. The same, as Fig.3, for the measurement of 11 June 1969

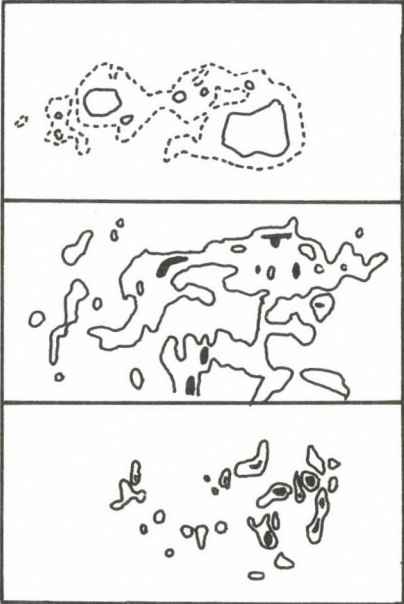


Fig.9. The same, as Fig.3, for the measurement of 12 June 1969

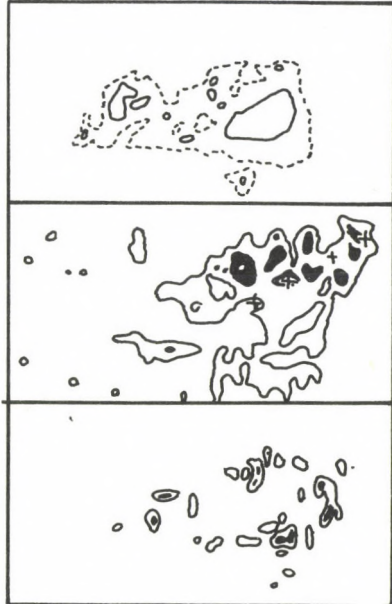


Fig.10. The same, as Fig.3, for the first measurement of 13 June 1969

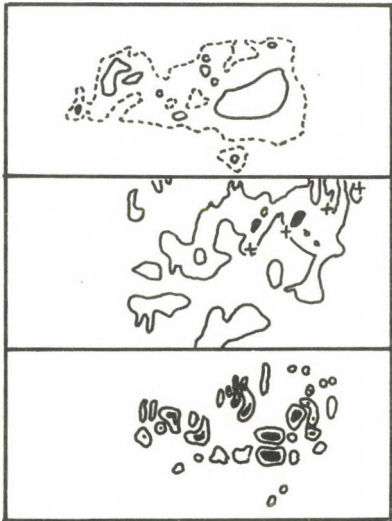


Fig.11. The same, as Fig.3, for the second measurement of 13 June 1969

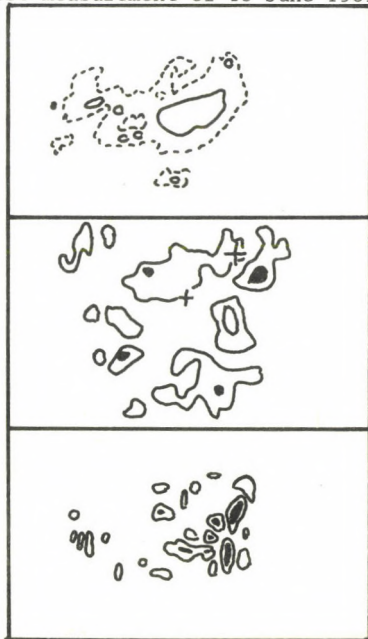


Fig.12. The same, as Fig.3, for the measurement of 14 June 1969

central part of the group began. On the magnetic charts we could see the increase of the magnetic field, umbrae 1 & 2 merged completely (two subflares observed in this place) umbra c decays finally (on 10 June it is completely invisible) - on this place a subflare also occurred. Active proper motion of spots a_1 , a_2 , a_3 , e_1 , e_2 , e_3 were connected with differences in azimuths of H_t and enlargement of current areas. Fig.5 shows the coincidence of two subflares and a current filament with current density $20\ 000\ \text{A km}^{-2}$. Connection of flares with strong currents was already found in {9}.

There was an activation in the preceding part of the group. The areas of currents near the leader spot, to the north and south of it greatly enlarged. To the south an importance 1 flare was observed (large cross in Figs.5,6), to the north a small island of following magnetic polarity began to form, the disturbances from this field are markedly visible in the chart of azimuths.

On 10 June 1969 there was the maximum of activity in this group. Its appearance was strongly changed: practically all the umbrae were within a common penumbra. The areas with strong currents enlarged further, and occupied practically the whole central part of the AR, excluding only spots a_1 , a_2 ; these had disappeared by the following day.

The preceding part of the group was the most active. To the north of the leader spot a new umbra (δ) was formed, to the east umbra 2 actively develops, in the vicinity of which an importance 1 flare was observed. It is worth mentioning the very compact form of the area with large differences between the observed and computed azimuths of H_t . In practice it coincides with the area of the common penumbra. This peculiarity of Fig.7 will be discussed later.

11 June 1969 was the first day of the decay of the group (Fig.8). Very large activity in proper motions of the umbrae in the group was observed. The structure of the group simplified quickly. Umbra 2 coalesced with the leader one, and the umbrae of group α almost disappeared.

The areas of large difference in azimuths of H_t greatly enlarged. They expanded far from the area of the penumbra, and their distribution was qualitatively different from the one in the phase of growth of the group (Figs.7,8). During the phase of growth of the AR the magnetic field increased mainly in its central part: the strongest currents flowed there and the greatest disturbances in magnetic field and sunspot proper motions were there. Therefore, the greatest azimuth differences were also observed in the central part of the group.

During the phase of decay, there is a basically different situation. The magnetic field already occupied a large volume of the solar atmosphere. The decay of such a configuration is impossible without decay on the edges, moreover, in the beginning of the decay it occurs most intensively in the periphery, gradually spreading to the centre the areas with large, up to 80° and more differences in azimuths of H_t , measured and computed from the potential model, and the places of flares in Fig.8 deserve attention). This process remained qualitatively the same on the following days too (Figs.9-12).

From 12 to 14 June 1969 (on 13 June there were two observations of the magnetic field) the process of decay was complicated by an increase of the magnetic field on the southern part of the group and on the northern side of the leader spot. The latter caused great differences in the magnetic field of the AR from the potential one, and some subflares on that place.

14 June 1969 was the last day of observations of this AR. The process of decay was going on. Generally, the activity of the group diminished noticeably (cf.Figs.8 and 12). The areas with great differences in azimuths of H_t , and accordingly with large currents, shrank markedly. There remained a faint flare activity on the northern border of the leader spot.

4. Conclusions

The results of our computations has shown the whole complexity of the physical processes going on in the active region during the process of its evolution. The changes in the struc-

ture of the spots and in the magnetic field were accompanied by the formation of large-scale current systems, flowing in the areas of the most intensive transformations. The flare-active centres coincided well with places of large difference of the magnetic field of the AR from the potential one. The electric currents, causing the difference of the magnetic field from a potential field, flowed higher than the level of formation of the spectral line used for magnetic field measurements (in our case the λ 5250 Å Fe I), i.e. in the upper photosphere and chromosphere. During the observations the structure of large-scale currents changes significantly, in accordance with changes in the structure of sunspots and the dynamics of the group. Even small disturbances can be detected by this method, which are accompanied by subflares. This method can be used for operative forecasting of solar flares, for its use it is sufficient to have data of distribution of Hz and structure of azimuths of Ht. It does not require much computing time.

Finally the authors wish to thank Prof.V.S.Sokolov and members of the Krasnoyarsk Computing Centre of the USSR Acad.Sci., V.V.Denisenko for constant attention and help, and M.B.Ogir' (Crimean Astrophys.Obs.) for making the observational material on the coronagraph KG-1 accessible.

R e f e r e n c e s

- {1} Gopasyuk, S.I., The character of the spot magnetic field in the corona, *Izv.KrAO.34.* 288, 1965 (in Russ.)
- {2} Godunov, S.K., *Uravneniya matematicheskoy fiziki*, (in Russ.) Nauka, Moskva 1971, p416
- {3} Denisenko, V.V., Romanov, V.A., Method of computation of force-free $\alpha = \text{const}$ fields induced by a single source in a flat layer (in Russ.) *Dep.VINITI, No.1796.* 1982
- {4} Kálmán, B., Magnetic fields and proper motions of sunspots, (in Russ.) *Izv.KrAO.55.* 60, 1976
- {5} Kálmán, B., Evolution of sunspot groups and their magnetic fields, I. (in Russ.) *Soln.Dann.12.* 69, 1978
- {6} Kálmán, B., Connection between the structure of penumbra of sunspots and the magnetic field vector, *Izv.KrAO.60.* 114, 1979 (in Russ.)
- {7} Severny, A.B., Observations of transversal and longitudinal magnetic fields connected with solar flares (in Russ.) *Izv.KrAO.31.* 159, 1964
- {8} Hagyard, M., Low, B.C., Tandberg-Hanssen, E., On the presence of electric currents in the solar atmosphere, *Solar Phys.* 73. 257, 1981
- {9} Moreton, G.E., Severny, A.B., Magnetic fields and flares in the Region CMP 20 September 1963, *Solar Phys.* 3. 282, 1968

THE STUDY OF THE DYNAMIC PROCESS OF UMBRAL FLASHES

R.B. T E P L I T S K A Y A, I.P. T U R O V A, G.V. K U K L I N

SibIZMIR, Irkutsk

Abstract:

A detailed analysis has been made of Umbral Flashes in two sunspots. The results are: 1) The dynamic process of UF operates throughout the entire layer of formation of the H and K CaII line central reversals. 2) The shape of the H and K line profile depends upon the position of a sunspot on the solar disk. 3) The parameters of the oscillatory process, viz. the amplitude and the phase relations, are also dependent on the sunspot's position. 4) An attempt to interpret the results under items 1) through 3) leads us to conclude an intrinsic relationship among the UF phenomenon, fine structure elements of the umbra at the photospheric level, and the rope-like configuration of the sunspot magnetic field.

ИССЛЕДОВАНИЕ ДИНАМИЧЕСКОГО ПРОЦЕССА "ВСПЫШКИ В ТЕНИ"

Р.Б. ТЕПЛИЦКАЯ, И.П. ТУРОВА, Г.В. КУКЛИН

СИБИЗМИР, Иркутск

Абстракт:

Выполнен подробный анализ "вспышек в тени" в двух пятнах. Получены следующие результаты. 1) Динамический процесс "вспышки в тени" ("UF") охватывает всю толщину слоя образования центральных обращений линий H и K CaII. 2) Форма контуров линий H и K зависит от положения пятна на диске Солнца. 3) Параметры колебательного процесса - амплитуды, фазовые соотношения - также зависят от положения пятна. 4) Попытка интерпретировать результаты 1)-3) приводит к заключению о родстве хромосферного явления UF с элементами тонкой структуры тени на фотосферном уровне и со жгутовой конфигурацией магнитного поля пятен.

The emergence of interest in the dynamic process of Umbral Flashes (hereinafter referred to as UF) in sunspots has been stimulated for several reasons. Among these we may note the following.

I) It is the most powerful and easiest-to-study quasi-periodical process occurring in the chromosphere of a sunspot umbra, i.e. in conditions where the plasma dynamics is governed by the magnetic field. Hence, analysis of UF properties must show what the peculiarities of wave propagation and resonance are in the solar atmosphere in the presence of a strong magnetic field.

II) As with other modes of solar oscillations, the triggering mechanism for UF lies underneath the visible solar surface. Therefore, a study of UF may shed light on the state of deeper layers of the sunspot; it is a typical problem in solar "seismology".

III) UF are associated with the transport of a certain amount of mechanical energy, i.e. they should be taken into account when examining the energy deficit in sunspots.

Although there exists an extensive literature dealing with UF (see, e.g., a review by Moore {6}), observations of UF in their classical form are scarce. The "true" UF represent a phenomenon of a strong brightening of emission reversals of the H and K Ca II lines (as well as a brightening in the infra-red triplet lines) {1}, {13}; evidence for an increase in the $H\alpha$ line intensity is very rare {6}. Meanwhile, velocity fluctuations seen in $H\alpha$ were often referred to UF. In addition to the references just cited, UF were studied by Kneer et al. {3}, Zhugzhda and Makarov {14} and Lites et al. {5}. In the present paper we will consider the following questions relevant to the above general problems.

a) What are the differences between the oscillation parameters of the chromosphere of different type of sunspot? We are principally concerned with phase relations between Doppler shift and brightness in the H and K Ca II lines.

b) How does the sunspot's position on the solar disk influence the observable characteristics of the UF process?

c) How do the H and K line profiles in different phases of the UF process and the line profiles in the maximum phase with different positions of a sunspot on the disk, behave?

1. Spatial and temporal characteristics

In connection with the aforementioned problems, a detailed spectrophotometric study was made of the H and K lines in the umbrae of two sunspots. The first one was observed at the centre and at the limb of the disk ($\mu = 0.96$ and 0.60), and the second one was observed only at the limb ($\mu = 0.60$). Hereinafter they are referred to as sunspots No 2 and No 1 respectively. The groups, including these sunspots, differed in the rate of their evolution in magnetic structure and in the degree of flare activity. A more complicated configuration of magnetic field and a higher activity are inherent in sunspot No 1 (a bipolar group of D class). Sunspot No 2 is a unipolar one, of J class. Visual inspection of spectrograms reveals discernible changes of the type of weak UF in sunspot No 1. During the four days available for observations sunspot No 2 was characterized by strong UF. The observation conditions and data reduction are identical for both sunspots. The sequences of spectrograms covered time intervals of 20-23 minutes, with pictures taken every 40 seconds. As wavelength standards we used photospheric lines in two "quiescent" areas surrounding the sunspot while the intensities were referenced to those in H and K line centers, also measured there.

Photometric recording of the two sunspots was carried out by a number of scans, spaced by 1" or 2" apart along the direction of the spectrograph slit. The results presented below are relevant only to the scans within the umbra.

Fig.1 shows a typical case of time variation of the K line profile at one of the points of the sunspot No 2 umbra (disk centre). Following the goal of qualitative definition of the profiles, we determined the parameters indicated in Fig.2. These are: I_{max} (or $r_{max} = (I_{max} - \bar{I}_{max})/\bar{I}_{max}$, where \bar{I}_{max} is the time-averaged I_{max}), $\Delta\lambda_{max}$ and $\Delta\lambda_{1/2}$.

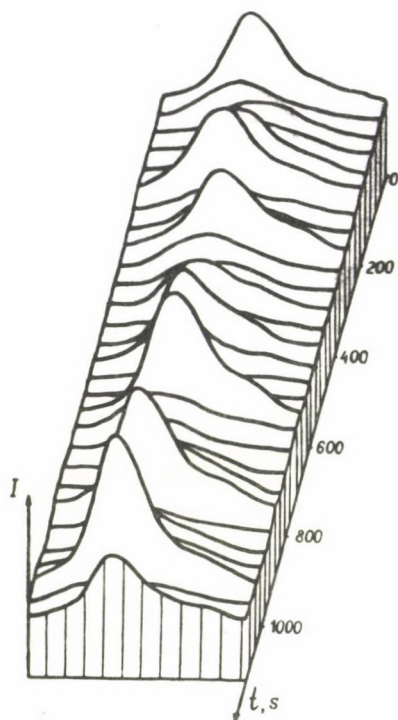


Fig. 1.

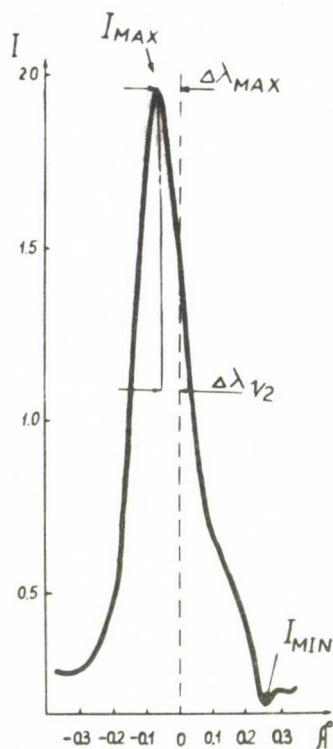


Fig. 2.

Fig. 1. The time sequence of K line profiles in the middle of the sunspot No 2 umbra (disk centre).
The intensity scale is arbitrary.

Fig. 2. The K line profile at the time of maximum brightness.
The parameters I_{max} , $\Delta\lambda_{max}$ and $\Delta\lambda_{1/2}$ are shown for which a spectral analysis was completed.

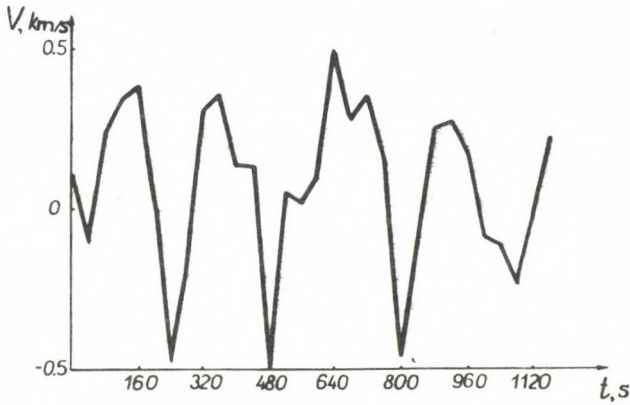


Fig.3. The five-minute oscillations in a quiet region, as deduced from differential Doppler shifts of the reference lines. The figure demonstrates the reliability of determination of line-of-sight velocities.

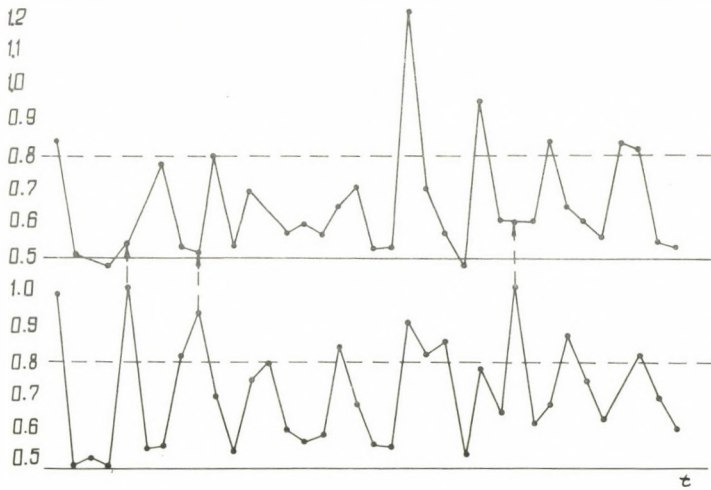


Fig.4. The time variation of the intensity I_{\max} at the top of the K line emission peak in two adjacent umbral parts. The arrows indicate the moments when the values of I_{\max} are opposite in phase.

The reliability of measurement of the parameters listed above is illustrated in Fig.3 and 4. Fig.3 shows km s^{-1} -scaled plots of differential Doppler shifts of the reference lines in two areas of the quiet region; their variation reflects the presence of five-minute oscillations (with a period of 275 s and a r.m.s. amplitude of 266 m s^{-1}). Fig.4 presents I_{max} , as measured in two adjacent scans, spaced by $2''$ apart. The arrows indicate the times when brightness fluctuations were almost opposite in phase. The figure gives convincing evidence that the close proximity of very bright regions (UF maxima) does not make too a large contribution of scattered light which could distort the picture of the process involved in neighbouring areas.

In searching for a periodicity we applied the method of correlational periodogram analysis {4}, which offers some numerical advantages over the classical spectral analysis of time series. Correloperiodograms (CPG) virtually yield the same results as do the power spectra (Fig.5). Figs.6 and 7 show the CPGs for three parameters in the middle of sunspot No 2 umbra (disk centre) and the CPGs for the parameter r_{max} in the same sunspot, when it was far from the centre.

Periods T. Figs.6 and 7 present a striking feature of "monochromaticity" of the UF process. It consists not only in the fact that most power is concentrated in one peak only but also in the fact that in some areas of the umbra all the parameters fluctuate with the same period. It should be noted, however, that the parameter $\Delta\lambda_{\frac{1}{2}}$ in sunspots with $\mu = 0.6$ is small and its behaviour is not sensitive to CPG-analysis.

Despite the overall closeness of period for different parameters at the same point of the umbra, there are spatial changes in the periods as we pass from one point to the other.

The values of periods obtained all distinguish themselves by fairly good reliability, namely the peak identified on CPG correspond to a confidence level higher than 0.99.

Amplitudes. R.m.s. amplitudes (symbol \wedge) of the parameter $\Delta\lambda_{max}$ in sunspots at the disk limb are smaller than ones

within the sunspot at the disk centre. If the value of $\hat{\Delta\lambda}_{max}$ are interpreted as a result of an upward motion of the gas, then they must diminish as $\cos\theta$ towards the limb. Such is not the case, however: $\hat{\Delta\lambda}_{max}$ reduced to the disk centre, are greater as might be expected with a purely vertical upward motion.

R.m.s. amplitudes illustrate the intensity of the UF process insufficiently clearly. Maximum amplitudes are more representative. Thus, the greatest blue shifts at the disk centre and at the limb in sunspot No 2 correspond to velocities of 7.0 and 6.4 km s⁻¹ while the strongest enhancements of intensity as compared to the intensity in the minimum phase, correspond to 4.75 and 2.56.

Phases. The phase difference between fluctuations of velocity and brightness is important for the identification of the wave mode. We are faced here with an unexpected phenomenon. Sunspot No 2 at the disk centre yields a phase difference between blue shift and intensity of 0.19 T. This result agrees well with Fig.7 from a paper by Beckers and Tallant [1]. Such a phase difference, close to a quarter of a period, is characteristic of standing waves. However, both observations at the limb give a nearly zero phase difference, inherent in propagating waves.

At the centre of the disk the displacements $\Delta\lambda_{max}$ and $\Delta\lambda_{1/2}$ fluctuate nearly coherently and their amplitudes differ little from each other. One gets the impression that the greater part of the chromosphere oscillates as a whole. As for the limb, the situation is quite different. As mentioned previously, $\Delta\lambda_{1/2} \ll \Delta\lambda_{max}$, so it is not possible to determine the phase difference.

Visual inspection of spectrograms reveals quite well that not a single but several UF are projected onto the slit. This is also demonstrated by Fig.4. In order to determine the number of UF systems located along the slit length used, it is convenient to utilize the phase curves (Fig.8). The figure shows four areas of sunspot No 2 at the limb. In scans 4 and 5 the phases show a nearly parallel change. It is natural to believe

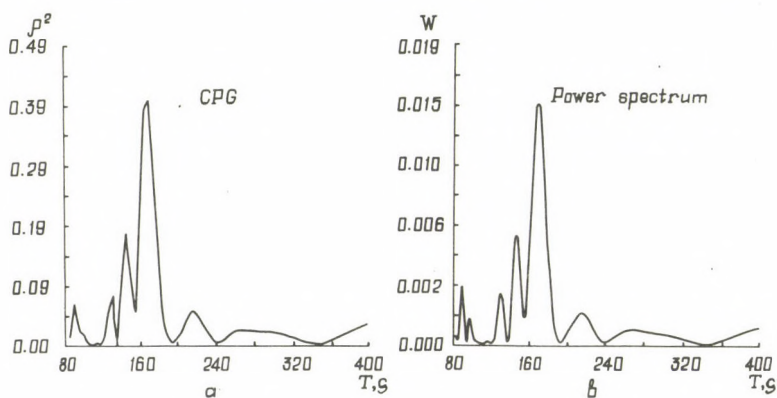


Fig. 5. The comparison of the two methods of spectral analysis. The correloperiodograms (CPG) and the power spectrum, calculated for the same data series, (Γ_{\max}) are shown.

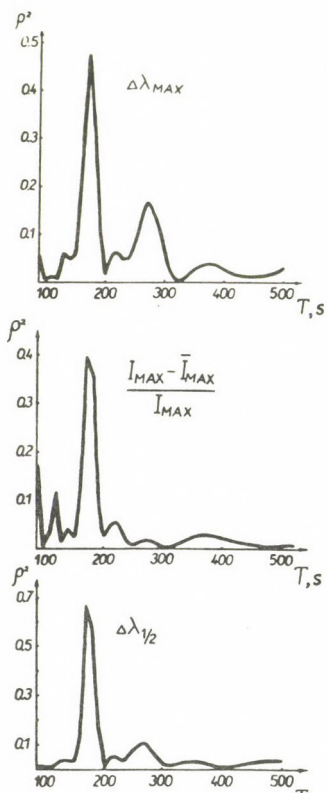


Fig. 6. The correloperiodograms for three parameters in the middle of sunspot No 2 umbra (disk centre).

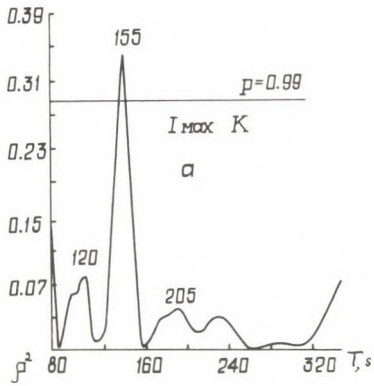


Fig.7. The correloperiodogram for the parameter r_{max} in the umbra of the same sunspot No 2 (at limb). The 0.99 significance level is labelled.

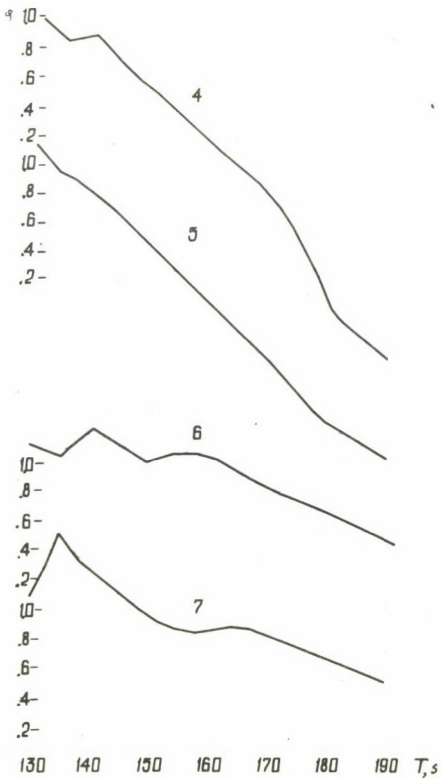


Fig.8. Examples of phase curves $\phi(T)$ (sunspot No 2, at the limb). Area numbers are shown near the curves.

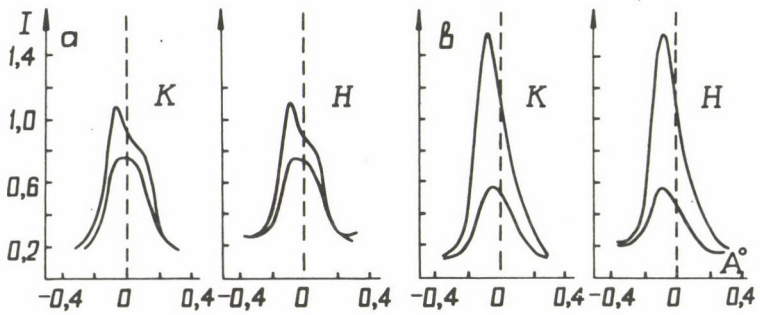


Fig. 9. Typical H and K Ca II line profiles at minimum and maximum brightness variation. Sunspot No 1 - at the limb; sunspot No 2 - at the disk centre.

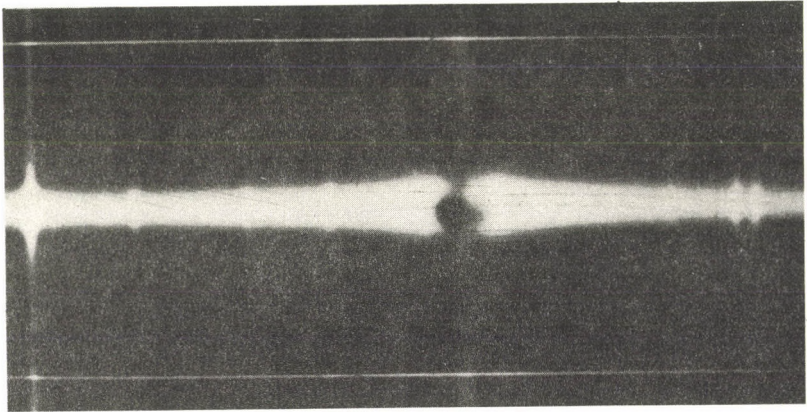


Fig. 10. The umbral spectrum at the moment of UF maximum (K line). A red "tail" is discernible.

T A B L E 1

Results of statistical analysis of oscillations
in the No 1 and No 2 sunspot chromosphere

Sunspot	No 1		No 2	
		$\mu = 0.60$	$\mu = 0.60$	$\mu = 0.96$
Periods(T)	s	150 - 200	150 - 180	170 - 190
$\Delta\lambda_{\max} (\mu = 1)$	km s ⁻¹	3.2	2.4	1.9
$\Delta\lambda_{1/2} (\mu = 1)$	km s ⁻¹	0	0	1.65
\hat{r}_{\max}		0.14	0.20	0.30
$\Delta\phi(r_{\max}, -\Delta\lambda_{\max})$		0.01	0.02	0.19
$\Delta\phi(\Delta\lambda_{\max}, \Delta\lambda_{1/2})$		-	-	0

The phase differences are $\Delta\phi$ are given in fractions of T.

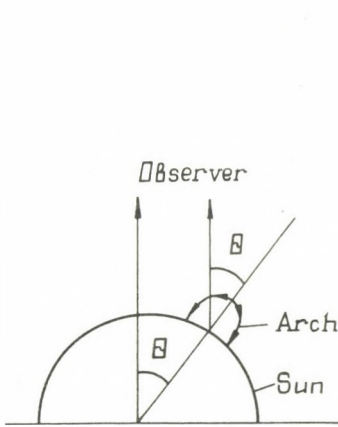


Fig.11a.

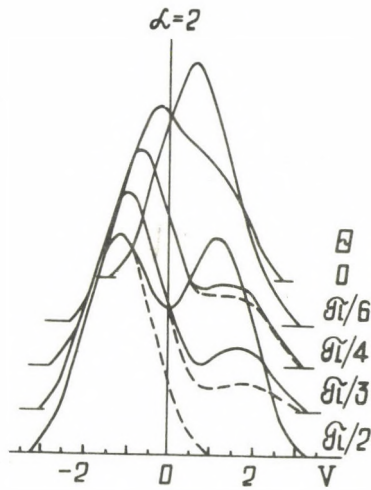


Fig.11b.

Fig.11a. The scheme of a luminous chromospheric arch, on which Ostapenko {8} based his calculations.

Fig.11b. The calculated normalized profiles of the emission line {8}.

that these scans are covered by a common system of UF. The phase curves of scans 6 and 7 are similar but there is no complete confidence in their commonality. In places where the identification of a UF system is reliably done, a "phase velocity" projected onto the slit direction can be measured. It is rather large, of 100-150 km s⁻¹, which exceeds the velocity of horizontal migration of UF towards the penumbra, as obtained by Beckers and Tallant {1} and Wittman {13}.

Table 1 summarizes the results of a statistical analysis of oscillations in the chromosphere of sunspots No 1 and No 2.

This table demonstrates that the differences between the parameters of the oscillations are mostly due to the location of a sunspot on the solar disk and, to a lesser extent, they are associated with individual properties of sunspots. The sunspot's moving away from the disk centre leads to a decrease in the amplitude of brightness fluctuations, to a change in the phase relation between Doppler shifts and intensity and to a reduction of $\Delta\lambda_{1/2}$ -shift. Moreover, there arise signatures of a presence of horizontal components of the gas velocity.

2. Peculiarities of H and K line profiles in Umbral Flashes

To discuss the physical conditions in the umbra in different phases of UF it is useful to examine the corresponding features of the H and K line profiles. First, one may use such an important diagnostic tool as the intensity ratio I_{K_3}/I_{H_3} . The first attempt was made by Firstova {2}, who compared the line profiles at maximum activity in the area of UF and in an adjacent area of the umbra. We have repeated the measurements, using a considerably more extensive data set and examining the profiles not in different areas but in one and the same, at moments corresponding to different phases however.

In determining I_{K_3}/I_{H_3} any possible alteration in the photometric system over as long as 30 Å between the centres of the two lines, should be taken into account, which is achieved by some precautions being taken when calibrating the measurements. Our choice of the calibration method failed to

yield absolute values for the sought-for ratios. However, it permits their reliable comparison at different phases. It has become clear that the ratios I_{K_3}/I_{H_3} at moments of minimum and maximum intensity are the same. Since it is known that on average the ratio of central intensities for the umbra gets rather close to unity (≈ 1.2), one may conclude that irrespective of the oscillation phase the umbral chromosphere is an optically thick medium.

When the phases of the UF process are known for the moments the spectrograms were taken, it is then easy to combine the line profiles according to close values of the phase and to determine typical average profiles. Fig.9 shows such profiles for sunspot No 1 ($\mu = 0.6$) and sunspot No 2 ($\mu = 0.96$). It is evident that for the phases $\varphi = 0$ and $\varphi = 0.5$ the profiles are dissimilar all along the central reversals. Consequently, the UF process presumably involves the whole thickness of the atmosphere, where emission peaks are formed.

A most striking feature of the H and K Ca II line profiles at moments close to maximum brightness moments, is their blue asymmetry. However, even a visual inspection of spectrograms reveals time-coincident weak brightenings, also seen in the red wing. At the centre of the disk they appear as a diffuse red "tail", extending from the bright point in the blue wing. On an average profile it looks like a small deformation of the smooth variation of intensity. The deformation is more pronounced on original spectra against the background of the surrounding unperturbed umbra (Fig.10). At the limb the red brightening manifests itself in an intensification of the double-peaked shape of the line profile.

The presence of red brightening at moments of UF maximum occurs as a rule, rather than an exception. We have looked through a further 27 temporal sequences of spectrograms, with a reliably traceable behaviour of UF. In 20 cases red brightenings are well-defined but in seven cases we have no unambiguous identification. In this case there is no relationship of doubtful cases with some location or other of the sunspot on

the disk. Thus, the presence of blue asymmetry at various distances from the disk centre gives evidence for the not purely vertical motion of the gas while red brightenings, also independent of sunspot location, suggest that conversely directed flows of material take part in the formation of the line.

3. Umbral flashes and the fine structure of the umbra

It is necessary to find a type of motion, at which the line profiles and the parameters of oscillations behave as described above. A similar asymmetry of the emission lines was detected by Ostapenko {8}, who calculated the line profiles emitted by an arch of a dense material located in the chromosphere. Emission elements travel from the top of the arch on both sides down towards its photospheric foot-points (Fig.11a). The size of the arch is such that it covers the entire spectrograph slit. Fig.11b reproduces Ostapenko's figure, showing normalized profiles emitted by *the whole* of the arch for the case when the emission intensity has a maximum at its top (solid curves indicate the case when the emission from the rear part of the arch does not experience absorption, and dashed curves show the case when the emission from the front branch only is observable; time profiles correspond to an intermediate variant). The agreement between the shape of the profiles and our observations is violated because at the disk centre the line is totally shifted towards the red. However, in order to get a fuller qualitative analogy, it is sufficient to assume that there is an additional purely vertical upward motion of the arch.

In the frame of a traditional model of the umbra with a homogeneous magnetic field, motions of such a type are not possible. However, the idea of a rope structure of the sunspot field, proposed by Severny {11}, has led to the concept of a two-stage structure of the umbra, i.e. a field enclosed within narrow, isolated tubes below the visible surface and a homogeneous field above it {7},{9},{10}. Such a model was applied to explain the fine structure of the umbral photosphere. Thus, Fig.12 reproduces Fig.1 from a review by Spruit {12}, showing

the configuration of the magnetic field. The arrows schematically outline the ways in which convection is realized. One is of circulation type, very deep within the columns without field, and the other is oscillatory convection in subphotospheric layers of flux tubes. Parker {10} showed that in columns without field residing beneath the visible surface, an oscillatory convection takes place too. The concomitant upward injections of a hot gas may be responsible for phenomena of granules and umbral dots at the photospheric level of the sunspot.

Spruit {12} made the assumption that Umbral Flashes also arise due to a "punching of a hole" in the magnetic field, similar to bright points in the umbra. We feel that the present observations support this hypothesis. The right part of Fig.12 is a schematic representation of the magnetic field and of the velocity field in the places of ejection. Such an interpretation of the origin of UF is capable of explaining qualitatively the following facts.

1. Complex form of emission lines - pseudo-arch in the umbral chromosphere with a rise of material at its top and with a quasi-horizontal spreading along magnetic "walls".

2. Bright emission - nonlinear effects connected with a large velocity amplitude in places of gas out-break.

3. "Monochromaticity" of oscillations and the phase relation between velocity and brightness, observable at the disk centre - capture of waves by the chromospheric cavity; a source of waves is provided by oscillatory convection immediately beneath the photosphere. The phase relation, as seen at the limb, - the concomitant transverse motion of material along curved field lines.

4. The behaviour of the parameter $\Delta\lambda_{1/2}$ at different points of the disk - a result of the variation of the line profile shapes with different μ .

5. The increased intensity of the total emission reversal at UF maximum - a result of the heated gas' coming from below.

This simple interpretation of UF phenomenae encounters, however, some difficulties, of which the UF size is the main

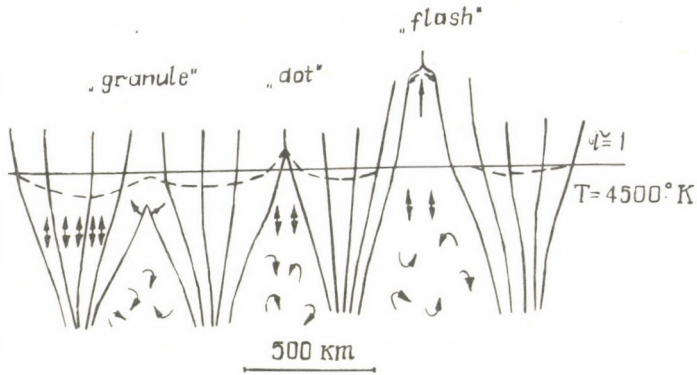


Fig. 12. A schematic configuration of the magnetic field and velocity field in the rope model of the sunspot's magnetic field. The left part of the figure is taken from a review by Spruit {12}. Usual convection (\curvearrowright) occurs between tubes of force, and oscillatory convection (\updownarrow) occurs within tubes of force. Oscillatory convection also develops at the subphotospheric layers of the columns without field {10}. The isotherm $T = 4500$ K is shown, illustrating the formation of line structure, i.e. spot granulation and umbral dots. The right hand part of the figure shows the supposed structure of the magnetic field and velocity field in areas where the gas penetrates into the chromosphere. A pseudo-arch is produced. At its top the gas is welling up, while on the sides it spreads quasi-horizontally along the field lines.

one. According to Beckers and Tallant {1}, an Umbral Flash is, on average, 2200 km in diameter, greatly exceeding a mean diameter of an umbral dot. Such dimensions of the field-free column cast some doubts on the possibility of oscillatory convection. In addition, an image of so large a feature cannot entirely be covered by the spectrograph slit (the working width of the slit utilized by us corresponds to 460 km on the Sun). Finally, the scheme in Fig.12 suggests a largely transverse magnetic field for UF, whereas Beckers and Tallant {1} detected and measured a longitudinal field, typical of the umbra. A way out of the above difficulties lies in the fact that UF is composed of several knots; a fragmentation of UF with the time and a consolidation of the knots were directly observed by Beckers and Tallant. Admitting this possibility, we proceed from the analogy with umbral light bridges, resolvable into a conglomeration of umbral dots and which, as opined by Obridko {7} and Parker {10}, may share a common origin with them.

References

- {1} Beckers, J.M., Tallant, P.E., Chromospheric inhomogeneities in sunspot umbrae, *Solar Phys.* 7. 351, 1969
- {2} Firstova, N.M., The ratio of maximum intensities of H and K CaII lines in umbral flashes, *Astron. Zh.* 57. 666, 1980 (in Russ.)
- {3} Kneer, F., Mattig, W., Uexküll, M., The chromosphere above sunspot umbrae. III. Spatial and temporal variations of chromospheric lines, *Astron. Astrophys.* 102. 147, 1981
- {4} Kopecký, M., Kuklín, G.V., Concerning the 11-year variation of average lifetime of a sunspot group. *Issl. SibIZMIR*, 2. 167, 1971 (in Russ.)
- {5} Lites, B.W., White, O.R., Packman, D., Photoelectric observations of propagating sunspot oscillations, *Ap.J.* 253. 386, 1982
- {6} Moore, R.L., Dynamic phenomena in the visible layers of sunspots, *Space Sci. Rev.* 28. 387, 1981
- {7} Obridko, V.N., On the origin of the umbral dots, *Astron. Zh.* 51. 1272, 1974 (in Russ.)
- {8} Ostapenko, V.A., Note on the emission line profile asymmetry of solar flares, I. *Soln. Dann.* 1978, No.6. 80, (in Russ.)
- {9} Parker, E.N., Sunspots and the physics of magnetic flux tubes. I. The general nature of the sunspot, *Ap.J.* 230. 905, 1979

-
- {10} Parker, E.N., Sunspots and the physics of flux tubes. IX. Umbral dots and longitudinal overstability, *Ap.J.* 234. 333, 1979
- {11} Severny, A.B., On the nature of solar magnetic fields, *Astron.Zh.* 42. 217, 1965 (in Russ.)
- {12} Spruit, H.C., Small scale phenomena in umbras and penumbras. The role of convective processes, *The physics of sunspots*, (Cram, L.E., Thomas, J.H. eds.) *Sac. Peak Obs. Conf.*, 359, 1981
- {13} Wittman, A., Some properties of umbral flashes, *Solar Phys.* 7. 366 1969
- {14} Zhugzhda, Yu.D., Makarov, V.I., On the dynamics of the chromosphere above sunspots, *Solar Phys.* 81. 245, 1982

STUDIES OF KINEMATIC ELEMENTS
IN TWO MULTICENTER SUNSPOT GROUPS

Z. B. K O R O B O V A

Astron. Inst., Tashkent

Abstract:

Some features of kinematic elements (KE) in two multicenter sunspot groups were studied using Tashkent full-disc white light heliograms. KE and morphological elements do not reveal any relationship. A KE coincides with a unipolar or multipolar spot or with part of a spot. It may also contain an extended stream including several spots. Relation of KE to large-scale photospheric magnetic fields is less clear. The line of polarity reversal is in most cases, the dividing line between two adjacent KE. At the same time, a KE can contain spots of both polarities. Sunspot trajectories in the leading polarity regions show the best similarity. Interactions of KE are greatly influenced by the meridional drift.

ИССЛЕДОВАНИЕ КИНЕМАТИЧЕСКИХ ЭЛЕМЕНТОВ
В ДВУХ МНОГОЦЕНТРОВЫХ ГРУППАХ СОЛНЕЧНЫХ ПЯТЕН

З. Б. КОРОБОВА

Астрон. Инст., Ташкент

Абстракт:

Изучена связь кинематических элементов (КЭ) с морфологией и крупномасштабным магнитным полем двух протяженных групп солнечных пятен. Показано, что КЭ не связаны с морфологическими элементами группы пятен. Нет однозначного соответствия между КЭ и крупномасштабным магнитным полем активной области. КЭ могут совпадать с отдельными пятнами, составлять часть пятна или охватывать несколько пятен, расположенных в областях разной полярности. Наибольшая однородность достигается в КЭ, находящихся в области ведущей полярности. При взаимодействии КЭ существенную роль играет меридиональная циркуляция.

Active regions MCM 16239 (August 1979) and HR 17644 (May 1981) are known to have complex magnetic structure and large extension on longitude. Both regions obviously evolved from the merging of several close bipolar systems. In this note the properties of kinematic elements (KE) in the sunspot groups of these AR are studied by analysing the trajectories of the sunspot proper motions. Some earlier papers {1},{2},{3},{4} have also dealt with the same problem.

The full-disc white light heliograms were obtained in Tashkent using the photoheliograph AFR-3 with the diameter of the Sun's image of 74 mm. The positions of the umbrae were determined by means of an UIM-23 coordinate measuring instrument. The Carrington coordinates were calculated with Iskra-124.

Sunspot motions in the groups are shown in Figs.1 and 2. The denotations of umbrae at the trajectories as well as at the relevant umbrae contours inserted were made with large numbers. The small numbers indicate the dates of the first and the last observation. The KE are marked with Latin letters.

MCM 16239 (1979). The group was studied in the period of August 23-29. It was born in the invisible hemisphere and developed rapidly. It appeared on the east limb as a large group consisting of three main spots each of δ -configuration. The leading and following spots remained during the whole passage across the disc, while the central spot disappeared on the disc.

Turning to the KE in Fig.1 one can see that kinematic elements do not coincide with morphological ones. Most of the umbrae in all the spots moved westward forming a common stream along a parallel (KE-A). The trajectories were the most similar and motion was the most rapid in the leading part of the stream, mean speed being 150 m s^{-1} . It is important to add that KE-A contained regions of both polarities. Umbrae 13, 14, 18, 19, 20 of the following polarity moved in the same way and did not disturb the homogeneity of the stream.

Every large spot contained an island of the following polarity with rotational motion (KE-B, KE-C, KE-D). During August 24-26 umbrae 1, 2 of KE-B and umbrae 3, 4, 5 of KE-A

embedded in a common penumbra moved in opposite directions.

KE-C and KE-D disappeared by August 28. It is interesting that umbra 6 in KE-C showed a slow movement like the other umbrae of this KE, but after the latter had disappeared, umbra 6 rapidly increased its velocity and exhibited a trajectory similar to the umbrae of the adjacent KE-A.

Analysing the umbral trajectories in the group the relationship between umbral motion and the line of polarity reversal position studied in {5} can be seen. Umbrae of KE-A located near the stable part of the line move along it. Umbra 5 turned towards the equator after approaching the zero line which runs in the meridional direction west of the group. KE-C and KE-D, occupying the gulfs of the following polarity, showed rotational motion.

HR 17644 (1981). The group was studied in the period of May 13-21. The group was located where the three groups of the former rotation were but no spot of these two rotations could be identified. The group HR 17644 seems to be the coalescence of remnants of the April groups and the spots born on the invisible hemisphere. During the period studied the central multipolar part of the group underwent a slow disintegration and decay.

Contrary to the previous case, this group shows some correspondence between kinematic and morphological elements (see Fig.2). KE-C containing the leading spot with satellites moved westward along the line of polarity reversal, the trajectories showing good similarity. After the disappearance of the satellites the speed of the leading umbra 1 increased to 200 m s^{-1} .

KE-L containing a large multicenter spot of following polarity revealed irregular trajectories. Umbra 7 drifted slightly equatorward. Umbrae 6, 8 showed an anticlockwise rotation. Umbrae 9, 10, 23 moved westward along the line of polarity reversal. All the umbrae except 23 were rotated onto the visible disc, so the date of their emergence is unknown. Taking into account the conclusions made in {5} it can be supposed that umbrae with different trends of motion differ in their age.

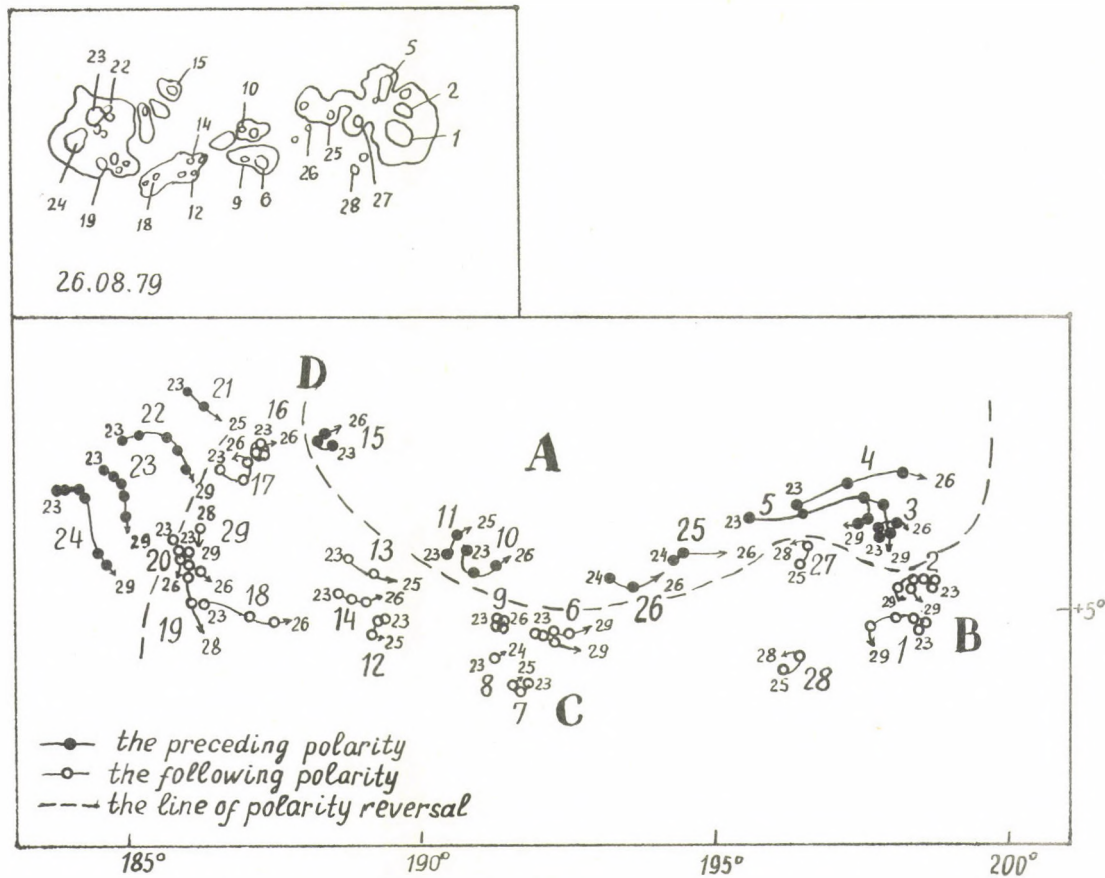


Fig. 1. Sunspot proper motions in McM 16239 on August 23-29, 1979
(no observations on August 27).

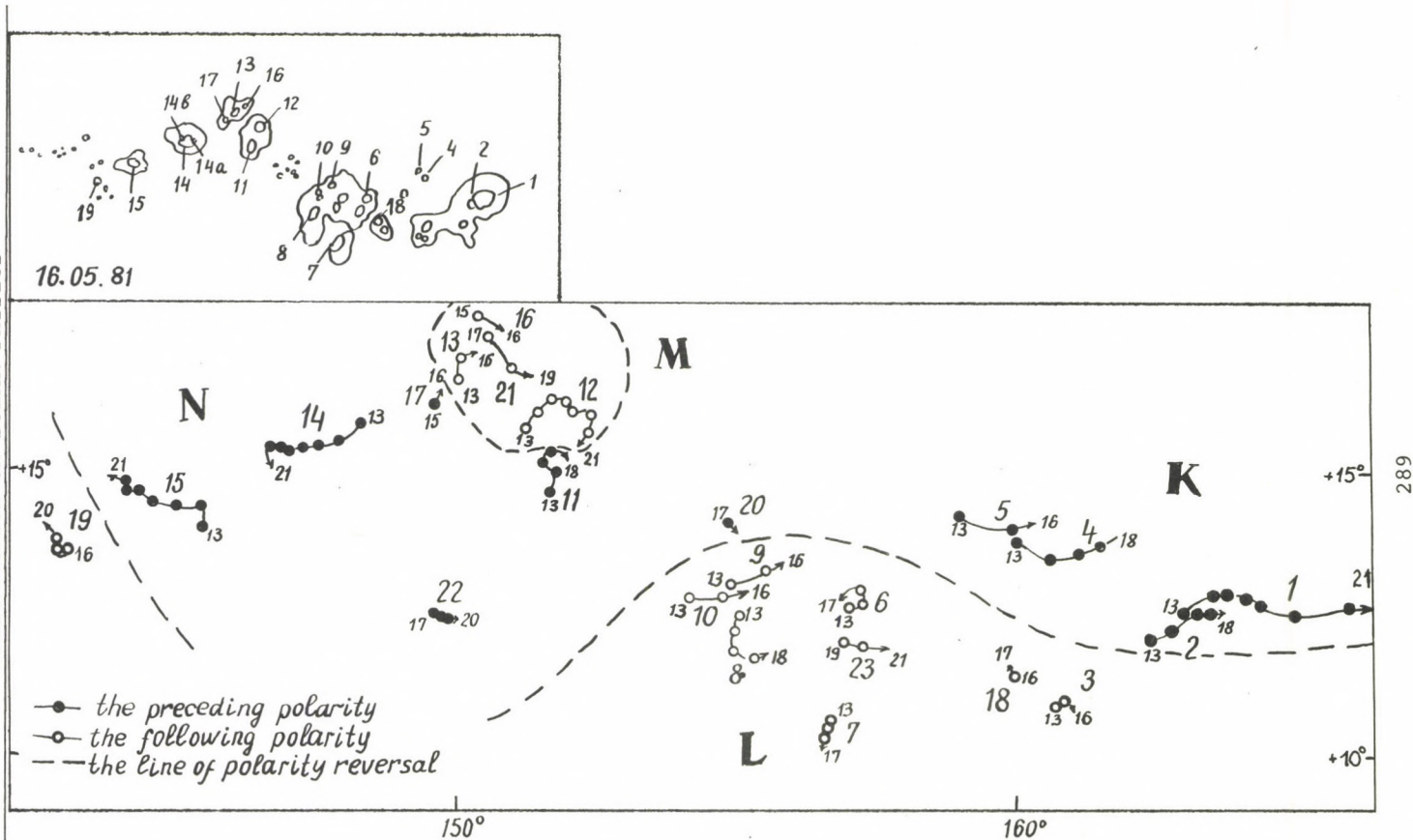


Fig. 2. Sunspot proper motions in HR 17644 on May 13-21, 1981
(no observations on May 17).

In fact, only in the May rotation did the polarity reversal line reach the position shown in Fig.2. In April here there was a deep gulf of the following polarity to the region of the preceding one. So the rotational motion of the old umbrae seems due to their emergence near the curved zero line, while new umbrae show more straight trajectories.

KE-M contained a multipolar spot with clockwise rotation.

In KE-N umbrae 14, 15 and 19 of both polarities moved eastward. This motion, non-typical in a bipolar configuration, seems due to repulsion of KE-N from KE-M. The positions of two stable satellites 14a and 14b of the umbra 14 made the revelation of the anticlockwise rotation of the whole spot possible.

Conclusion

1. Kinematic and morphological elements do not reveal any relationship. A KE coincides with an unipolar or multipolar spot or with a part of a spot. It may also be an extended stream including several spots.

2. Relations of KE to large-scale photospheric magnetic fields is less clear. The line of polarity reversal is mostly the dividing line between two adjacent KE. At the same time a KE can contain spots of both polarities.

3. Sunspot trajectories of KE in leading polarity regions show good similarity, especially at the western part of the group near the leader spots. KE exhibit rotational motion in the following polarity regions, irregular trajectories dominating over regular vortices.

4. Interactions of KE are greatly influenced by the meridional drift. In the vicinity of latitude 16° where the drift has the least speed {6}, KE repulsing from KE-M moved nearly along a parallel. On the latitudes of $5-8^\circ$ the closing part of KE-A, carried by the latitudinal drift did not interact with KE-D embedded in the same penumbra. Adjacent KE move independently if they are separated with a stable line of polarity reversal oriented along a parallel.

References

- {1} Kuklin, G.V., Syklen, A.E., Proper motions in a multi-center sunspot group, (in Russ.) *Результаты наблюдений и исследований в период МСС, 1. 64*, Наука, Москва 1966
- {2} Palamarchuk, L.E., On formation of a kinematic element and the hierarchy of dynamics in an active region, (in Russ.) *Soln.Dann.* 1973, No.10. 71.
- {3} Ikhsanov, R.N., Configuration of the magnetic field and motions in sunspots and sunspot groups, (in Russ.) *Soln.Dann.* 1974, No.12., 81.
- {4} Korobova, Z.B., Tishchenko, V.M., Tshai, A.A., Baturin, V.V., Proper motions in multicentral groups, *Солнечные процессы и их наблюдения* 57, Издат.ФАН, Ташкент, 1973 (in Russ.)
- {5} Korobova, Z.B., Sunspot proper motions and configuration of stable H α filaments in the active region of August 1979, *Soln.Dann.* 1982, No.11. 98. (in Russ.)
- {6} Tuominen, J., Kyröläinen, J., On the latitude drift of sunspot groups and solar rotation, *Solar Phys.* 79. 161, 1982

PHASE-COHERENCE OF CHROMOSPHERIC OSCILLATIONS
WITHIN AN ACTIVITY COMPLEX AND DYNAMIC PROCESSES IN A FILAMENT
DURING THE FLARES ON 6 OCTOBER 1979

V.E. MERKULENKO, L.E. PALAMARCHUK,
V.I. POLYAKOV
SibIZMIR, Irkutsk

СИНФАЗНОСТЬ КОЛЕБАНИЙ ХРОМОСФЕРЫ
В ПРЕДЕЛАХ КОМПЛЕКСА АКТИВНОСТИ И ДИНАМИЧЕСКИЕ ПРОЦЕССЫ В ВОЛОКНЕ
ВО ВРЕМЯ ВСПЫШЕК 6 ОКТЯБРЯ 1979 Г.

В.Е. МЕРКУЛЕНКО, Л.Э. ПАЛАМАРЧУК, В.И. ПОЛЯКОВ
СибИЗМИР, Иркутск

Abstract:

On 6 October 1979 at the Sayan Observatory a birefringent filter in the H β line was used to observe an activity complex, consisting of two groups, SD 461 and SD 462. During the observational period from 5:16 to 8:26 UT the activity complex produced 6 flares. Filtergrams in the wings of the H β \pm 0.2 \AA line were used to construct 40 maps of line-of-sight velocity and brightness field. The analysis of the maps showed that coherent variations of the velocity are related not only to the filament with a near-by chromosphere but also to a considerable part of the neighbouring active region. The observed oscillatory process seems to be a reflection of the impulsive emergence of a magnetic field from subphotospheric layers. Maximum darkening of the filament under investigation occurs simultaneously with the maximum downward velocity of the gas. Along the filament there was a rotation oriented in the opposite direction, and in the phase of the erupted part of the filament there was a reversal of the rotation. The start of flares that occurred sequentially in the activity complex, is particularly associated with abrupt changes of line-of-sight velocities and was accompanied by short-time outbursts of magnetic field rise.

1. Introduction

As is known, a flaring filament gives rise to a variety of phenomena that are presumably associated with a restructuring of the active region magnetic field. These are the rapid darkening, expansion or upward motion, disintegration into several parts, transition to emission, ejection of a part of the filament, and total disappearance {21}. Particular emphasis is being placed on the eruption stage of the filament. Filament oscillations should be recognized as an important feature of their dynamics. Prior to a limb flare in a loop prominence, Malvill and Schindler {10} observed radial and torsional oscillations of a period of 75 min and an amplitude of $1-2 \text{ km s}^{-1}$. Flare-productive regions provide evidence for oscillations of suddenly activated filaments over periods between 5 and 40 min {17},{18}. A description of a flare-produced "winking" filament, as observed in the wing of the $H\alpha$ line, is given by Hyder {5}. The oscillations observable in a filament, are most probably related to those covering the entire active region. Tanaka {25} found that flares occur 10-40 min after five-minute oscillations become coherent in areas of a linear size of about $1.2 \cdot 10^5 \text{ km}$.

Apart from oscillations, rotation is observable in a filament. According to Rust {20}, a simplification of the filament structure after a flare is suggestive of its "untwisting". A great deal of evidence for rotation in eruptive prominences is reported by Rompolt {19}.

Questions concerning the oscillations in the active region as well as filament rotation deserve particular attention in connection with the problem of flare energy accumulation. According to the calculations of Mullan {13}, during 20 minutes of coherent oscillations, which are dealt with by Tanaka {25}, the chromosphere is capable of accumulating energy in the order of 10^{34} erg. The wave nature of the production of flares was discussed by Osterbrock {15}, Piddington {16} and Mogilevskij {12}. The flare is regarded as a product of the energy release in discrete portions from subphotospheric layers in some places near the neutral line or as a consequence of a sudden enhance-

ment of the Alfvén wave flux emanating from subphotospheric layers where magnetic flux tubes undergo a pre-twisting. The presence of a gradient of angular rotation velocity along the filament must give rise to a longitudinal current and, therefore, to the development of a helical instability. According to a model suggested by Hirayama {4} such instability gives rise to an uplifting of the filament, below which a neutral layer, that determines the appearance of a flare, is formed.

Thus, the question of coherent oscillations over a large area in the active region before a flare and the spectrum of these oscillations as well as the dynamic behaviour of the flaring filament require further study. It should be noted that when considering so complex and contradictory a phenomenon as the flare, it is important to derive information about large-scale motion of a plasma at least at a chromospheric layer over a long time interval spanning consecutive stages of preparation and formation of a flare. To some extent, this problem will be solved in the present paper.

2. The sequence of dynamical processes related to the flares of 6 October 1979

With the aid of a birefringent filter in the line $H\alpha \pm 0.2 \text{ \AA}$ an out-eclipse coronagraph observed an activity complex, composed of two groups, *SD* 461 ($\varphi = 24^\circ$, $\lambda = -40^\circ$) and *SD* 462 ($\varphi = 16^\circ$, $\lambda = -50^\circ$). The observing time was from 5:16 to 8:26 UT.

Fig.1 is a sketch of the activity complex groups and of the location of the main flare knots (dotted lines), dark filaments and well-discernible fibrilles. It is seen that there are fibrilles that interconnect the complex groups. One aggregation of fibrilles, Φ_1 , connects the leader of *SD* 461 to plage areas near the filament in front of the leader of *SD* 462, while the other one, Φ_2 , links the follower of *SD* 461 to the leader of *SD* 462. A faster motion of *SD* 462 on the disk, reported by Dezső et al. {2}, might have led to a characteristic curvature of the second aggregation of fibrilles as well as to a "raking-up" of the field in front of the leader of *SD* 462. The then produced enhancement of the magnetic field gradient near the

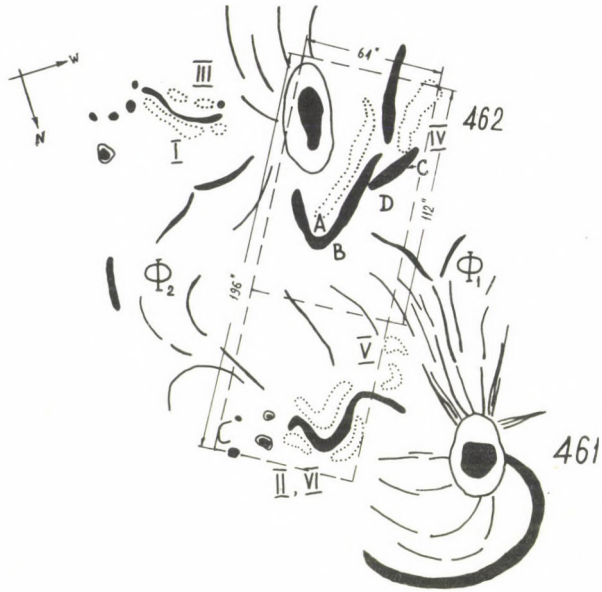


Fig.1. A sketch of a sunspot group of SD 461 and SD 462 and the main flare knots on 6 October 1979.

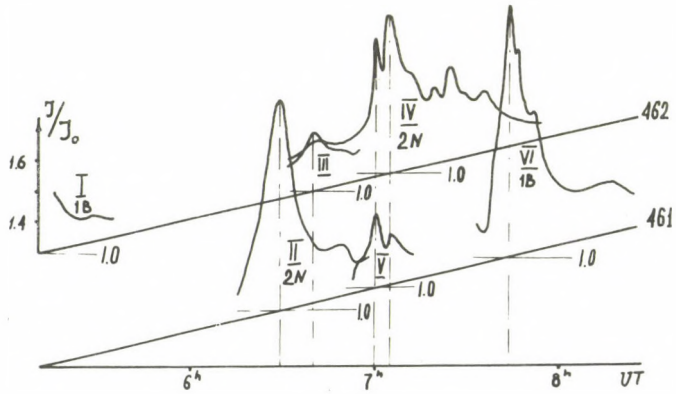


Fig.2. Light curves of the series of the 6 October 1979 flares.



Fig.3. Chart of longitudinal magnetic field near filament.

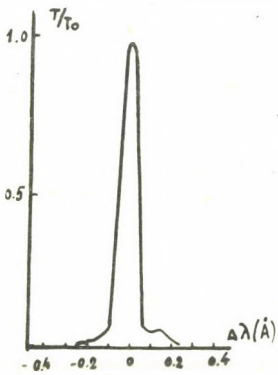


Fig.4. Birefringent filter transmission band in the H β line.

neutral line might be important for the flare to appear. A description of flares from this complex, as observed in the $H\alpha$ -line, is given by Ishkov and Obashev {6} and Bhatnagar et al. {1} and results of VLA radio observations can be found in {3}.

A sequence of flare production in the complex is indicated by light curves in Fig.2 for the time interval under investigation. Inclined lines are drawn for purposes of easing a distinction of flares, belonging to *SD* 461 and *SD* 462. The start of the observations coincided with the decay phase of flare I in *SD* 462. At 6:15 UT flare II originated in *SD* 461 and had a maximum at 6:30 UT. During its decay phase subflare III occurs in the follower of *SD* 462 and flare IV of *2N* class in front of the leader of the same group. At 6:55 UT subflare V occurs in *SD* 461 and the double-peaked brightness of this flare is coincident in time with that of flare IV. During the decay phase of flare IV at 7:35 UT, flare VI of *1B* class occurs in *SD* 461. This latter was considered in detail by Stepanov et al. {23}.

An area $64'' \times 112''$ was photometered. Since 7:02 UT the photometered area was enlarged to $64'' \times 196''$. A dash line in Fig.1 outlines the boundaries of the area photometered.

Fig.3 presents a magnetic field chart for the area $64'' \times 112''$ (Fig.1), obtained using a processed magnetogram taken with the SibIZMIR panoramic magnetograph. Solid lines denote *N*-polarity while dotted lines indicate *S*-polarity. A contour of a filament appears shaded for the time of its maximum brightness at 5:54 UT. Heavy dashed are drawn along the polarity separation line. The magnetogram was obtained at 2:07 UT, i.e. about 3 hr before the beginning of the observations.

A calculation of the velocity and brightness fields was performed using filtergrams in the wings of $H\beta \pm 0.2 \text{ \AA}$. The birefringent filter centered on $H\alpha$ has a bandpass of 0.09 \AA . A bandpass profile is shown in Fig.4. A displacement of the band within $\pm 1.5 \text{ \AA}$ does not give rise to any noticeable "ghosts" the fact that secures line-of-sight velocity measurements, devoid of instrumental errors. The spatial resolution was initially $1.5''\text{-}2''$ but it degraded to $3''\text{-}4''$ toward the end

of the observations. The microphotometer slit covered an area of $2'' \times 2''$. The charts of brightness and line-of-sight velocity were obtained for 40 nonequidistant instances for the entire period of observations. The calculation technique is detailed by Stepanov et al. {23}.

Now, we shall examine the sequence of the main moments of development of the events using a series of line-of-sight velocity maps (Figs.5a-i). The regions of upward motion of the gas are shaded on the maps. Solid lines correspond to the following velocities of upward motion $V = 0; -1; -2; -4; -6; -8;$ and -10 km s^{-1} . Dotted lines indicate downward velocities $V = 2; 4; 6;$ and 8 km s^{-1} . Heavy dashes delineate areas of downward motion with $V > 10 \text{ km s}^{-1}$. Dots outline the filament and the other darkest areas taken from the brightness map for the given moment of observation. It should be borne in mind that spatial scales along the axes do not coincide and they are indicated on the map for time 5:16 UT.

Time 5:16 UT (start of observations). The entire area exhibits a downward motion of the gas with the velocity of $2-4 \text{ km s}^{-1}$. The comparison with the magnetic field chart shows that areas of upward motion of the gas generally lie on the neutral line of the magnetic field or nearby.

Time 5:54 UT. The gas downward motion intensified abruptly throughout the area. The filament reaches a maximum of darkening.

Time 6:35 UT. There is an increase of the area of the portions occupied by the rising gas as well as of the values of upward velocities. The areas of an upwardly moving gas are located preferentially on the outer boundary of the filament with respect to the sunspot. A region of gas upward motion is discernible in the part of the filament, henceforth referred to as the segment (region C in Fig.1).

Time 6:53 UT. Again, there is a preferential downward motion of the gas. Against the downward motion a segment is observable with the upward velocity in excess of 10 km s^{-1} . Apparently, this moment should be regarded as a start of erup-

tion in the segment.

Time 6:59 UT. Over the greater part of the area under study there is a sharp increase of the gas rise velocity. Crosses indicate ribbon flares. The ribbon intensity attains a continuous spectrum level and, therefore, the velocities there were not determined.

Time 7:02 UT. Almost throughout the area the gas upward motion changed abruptly to downward. It is interesting that the edges of flare ribbons are bordered by areas of both upward and downward gas, with the downward velocities, on occasions, exceeding 10 km s^{-1} .

Time 7:15 UT. There is an intensification of upward motion in the middle part of the filament as well as in several places at the edges of flare ribbons. In the remaining area the gas moves preferentially downward with the velocity of $1-2 \text{ km s}^{-1}$.

Time 7:33 UT. Along the filament, a weak upwardly moving gas persists. Outside the filament, a slow downward motion continues.

Time 7:35 UT. There is an abrupt increase in the upward velocity of the gas along the filament which is possibly associated with a flare onset in the neighbouring group *SD 461*.

Later on, the area under consideration presents itself as a stable picture of a preferential downward motion of the gas. Upward motion continues along the filament only.

3. Coherence of velocity oscillations

within an activity complex and relation to flares

The above description of dynamic processes provides evidence for line-of-sight velocity oscillations, covering a significant area. We now demonstrate the presence of coherence of the oscillations in the filament, on a chromospheric area in front of the leader of *SD 462* and in the follower part of the group of *SD 461*. With this end in mind, we shall perform preliminarily a sliding smoothing of the velocity values inside the filament. After that, we shall determine average velocities within and outside the filament for positive (downward motion) and negative (upward motion) values separately. Fig.6 is useful

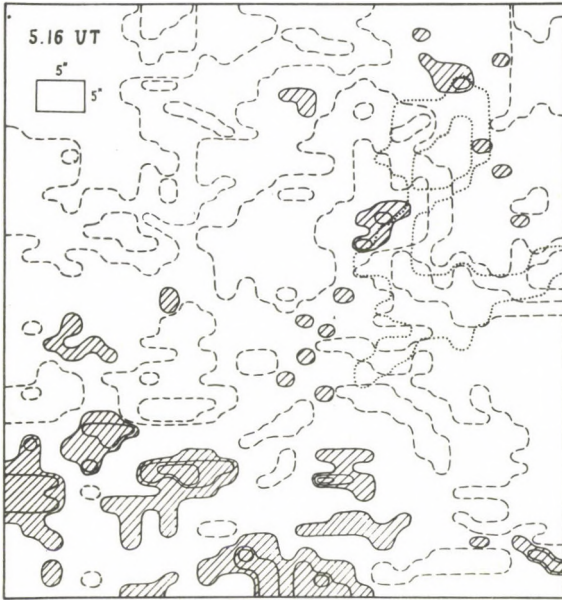


Fig. 5a.

Fig. 5a - 5i. Maps of line-of-sight velocities in the filament and its vicinities for the moments 5:16, 5:54, 6:35, 6:53, 6:59, 7:02, 7:15, 7:33 and 7:35 UT.

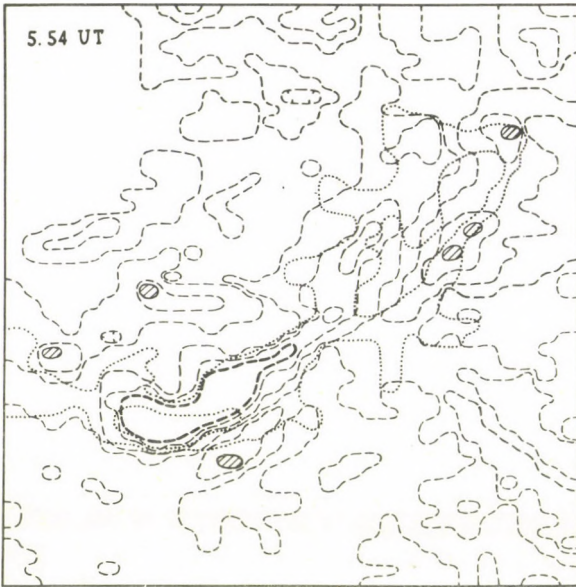


Fig. 5b.

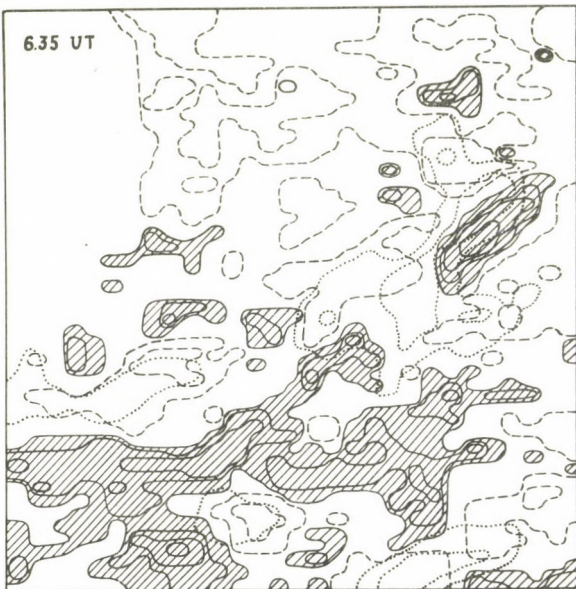


Fig. 5c.

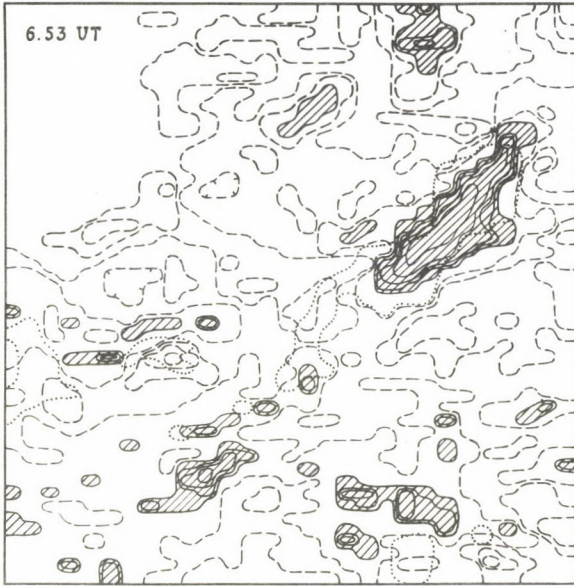


Fig. 5d.

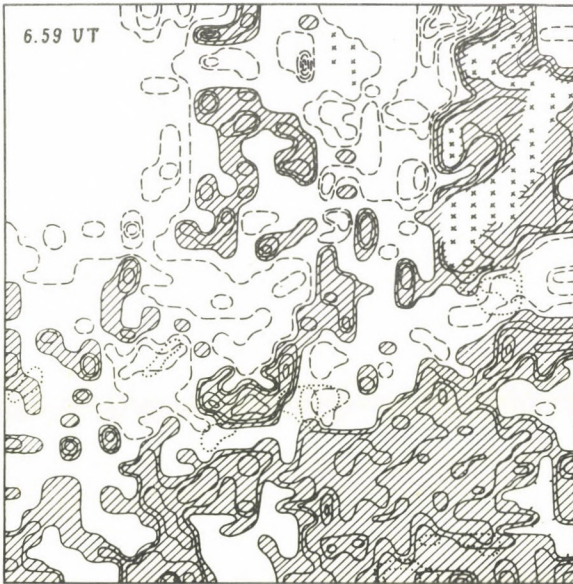


Fig. 5e.

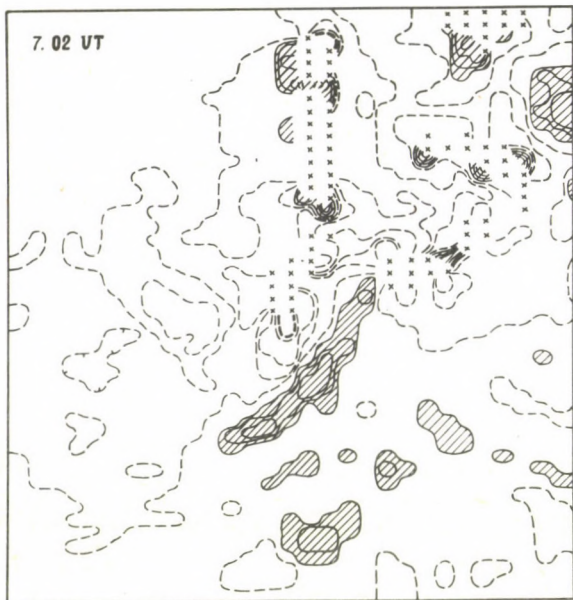


Fig. 5f.

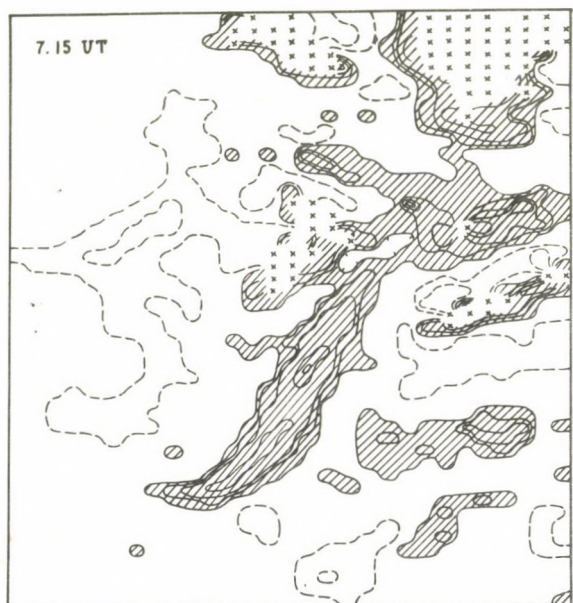


Fig. 5g.

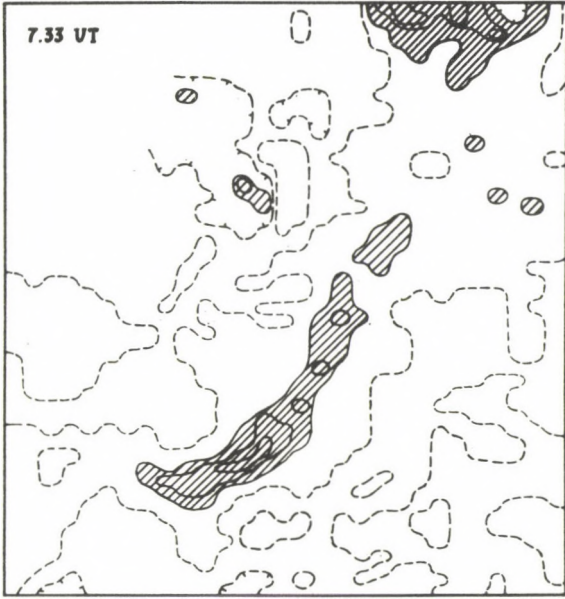


Fig. 5h.

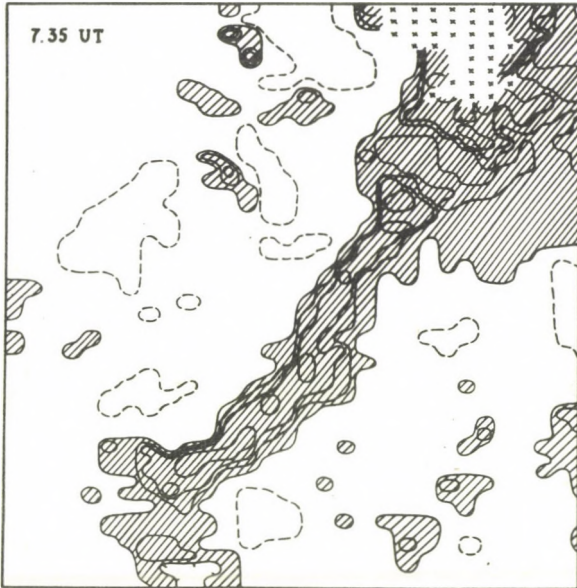


Fig. 5i.

for getting an idea of the time variation of these quantities. Vertical bars on the time axis indicate the moments for which line-of-sight velocity maps were drawn. Curves *b* correspond to upward velocities and curves *c* correspond to downward velocities. Solid lines indicate average upward and downward velocities in the filament; dashed curves indicate those outside the filament. Starting from the moment 7:02 UT when the area photometered was enlarged, it was possible to obtain similar curves for the lower part of *SD* 461. The average upward velocity for this area is represented by curve *a* and, accordingly, the downward velocity is indicated by curve *d*.

An examination of the curves in Fig.6 permits us to make the following conclusion. Throughout the observing interval coherent changes of both the up- and downward velocities of the gas take place over a significant area of the activity complex. Particularly high downward velocities are observed between 5:40 UT and 6:20 UT when flares were lacking in the complex. The arrows on the time axis in Fig.6 indicate the moments of flare brightness maxima. It should be noticed that the series of flares followed a decrease in the downward velocity and an increase in the upward velocity. Moreover, the flare onset was accompanied by particularly abrupt velocity "splashes".

Thus, the behaviour of line-of-sight velocities as well as the flare activity prove to be associated with some oscillatory process, coherently operating over the greater part of the activity complex.

These oscillations may be interpreted from the point of view that the observed changes of the line-of-sight velocity imply disturbances propagating from subphotospheric layers along magnetic flux tubes. Let us give some arguments in favour of this supposition.

1) For a magnetic field strength of 2 gauss and a density $\rho \sim 10^{-14} \text{ g cm}^{-2}$ in fibrilles that interconnect the groups of *SD* 461 and *SD* 462 7, the Alfvén velocity must be $V_A \approx 5 \cdot 10^6 \text{ cm s}^{-1}$. The groups are about 200" apart and therefore, the time required for disturbances to propagate through the chromosphere would

be ≈ 50 min. However, according to Figs.5 and 6, for example at 7:03 UT, disturbances in the form of an abrupt downward motion occur simultaneously in both groups.

2) The zero-different line-of-sight velocity on the neutral line of the magnetic field may be regarded as an indication of the gas' moving together with the magnetic field {9}. Line-of-sight velocities recorded along neutral lines that pass through the area under investigation, and averaged over the length of these lines, are represented by a dotted line in Fig.6. We will consider these average values as the radial component of the magnetic field velocity. Since the magnetogram that was used to determine the position of the neutral line $H_{||} = 0$, was taken approximately 3 hr before our observations some uncertainty remains as to whether the thus determined magnetic field velocity is accurate. Comparison of the changes of line-of-sight velocities in the filament and in its vicinities and of the magnetic field velocity with light curves for flares shown in Fig.2, clearly reveals that, firstly, the line-of-sight velocities and magnetic field velocities vary coherently in phase and, secondly, short-duration "splashes" of upward motion of the magnetic field precede the flares.

3) Fig.7 presents a result of spectral analysis of the variations of smoothed velocity values within the filament. A dashed line indicates the 90% confidence level. On the resulting correlogram significant periods of 65, 40, 28, 18, and 13 min are distinctly seen. Oscillations with such periods cannot result from a resonance excitation of MHD-waves in the active region corona because their periods are an order of magnitude lower {17}.

Thus, it may be concluded that the observed oscillatory process, phase-coherent for different portions of a significant part of the activity complex, seems to be a response to the disturbances which propagate from subphotospheric layers, and possibly, determines the impulsive character of uplifting of the active region magnetic field. A similar conclusion is arrived at by Ogir {14}, who investigated the brightness of

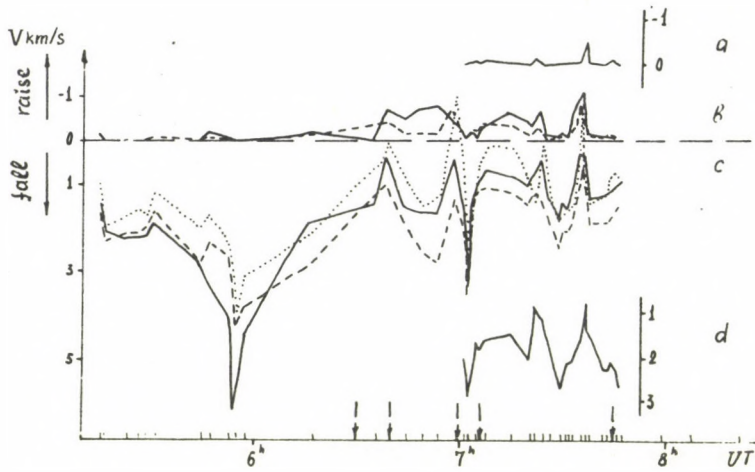


Fig. 6. The time variation of line-of-sight velocities in and outside the filament and magnetic field velocity (for details see text).

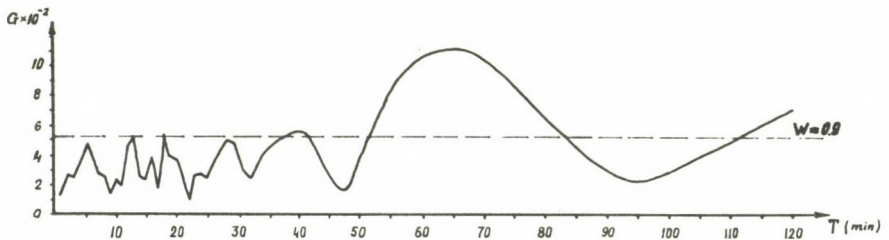


Fig. 7. Correloperiodogram of line-of-sight velocity oscillations in the filament.

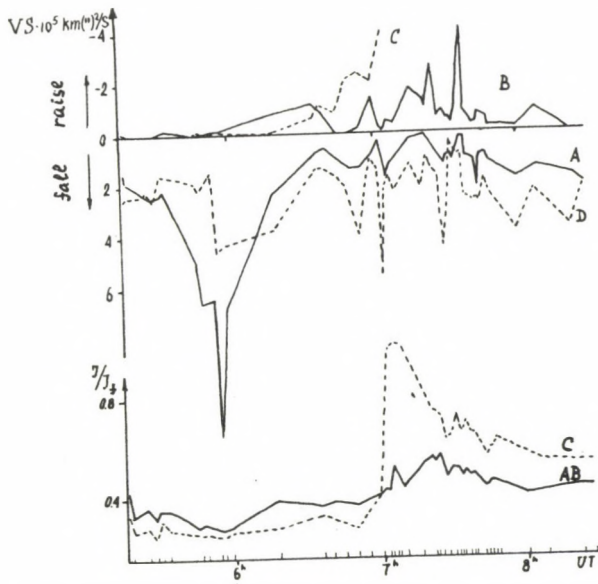


Fig.8. The flow velocity variation in zones A, B, C, and D and brightness variation in adjacent portions of the filament.

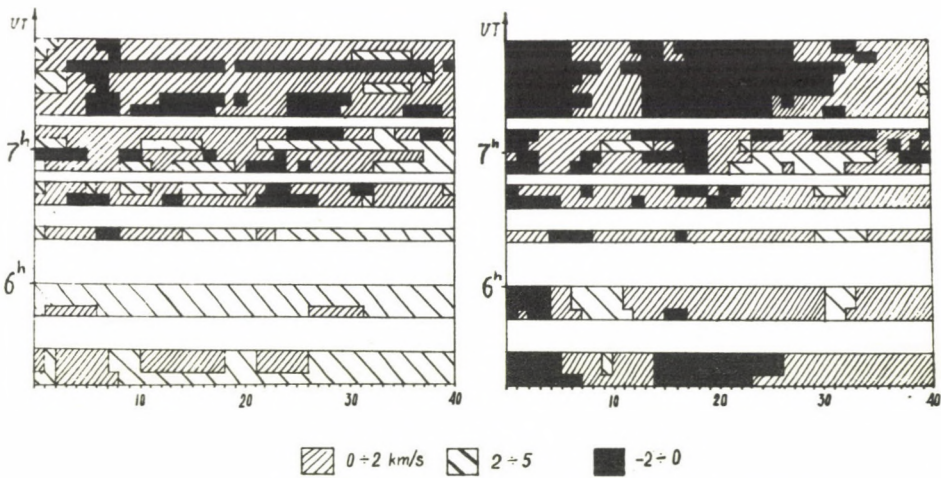


Fig.9. Diagrams of velocity V_s and rotation velocity V_ϕ changes along the filament.

floculi in relation to flare activity over the entire solar disk. As far as the flares are concerned, these are likely associated with a restructuring of the magnetic field during an impulsive emergence of the magnetic field, covering a significant area.

4. Some features of the filament dynamics

The series of maps of line-of-sight velocities in the filament and in its vicinity reveal identifiable zones, in which the velocity did not change sign throughout the observing interval. Letters *A, B, C* and *D* in Fig. 1 label such four zones. Zones *A* (fall) and *B* (rise) are located on either side of the curved part of the filament. Zone *C* (rise) belongs to the segment, where in the place of its eruption a flare knot appeared. Zone *D* (fall) adjoins zone *C* and is located within the bounds of the *S*-polarity magnetic field hill. Thus, these zones occupy a quite definite place as the elements of the filament's dynamic structure.

Examine now the variation in brightness of the velocity flow in these zones (Fig. 8). The ordinate axis indicates the value of an average velocity flow $\overline{v_i S_i}$ through the area of zone S_i , determined for each *i*-th moment. Curves for flow variation in the zones are labelled by corresponding letters. The behaviour of these curves, on the whole, patterns after that of average velocities in Fig. 6. Consequently, coherent oscillations also manifest themselves in areas on the solar surface that are far smaller compared with the activity complex.

The bottom part of Fig. 8 presents brightness curves of the filament between zones *A* and *B* (solid line) and for zone *C* (dashed line). It is worth noting that the stage of maximum darkening of the filament, observable prior to flare IV, refers to the period of maximum fall of the gas. Of greatest interest is the behaviour of zone *C*. The originally gradual increase of velocity at 6:59 UT changes to an abrupt uplifting and, apparently, to eruption when the velocities exceed 10 km s^{-1} . It is at that moment that zone *C* changes from absorption to emission. Thus, a violent climb of a part of the

filament which is, beyond doubt, associated with a rearrangement of the magnetic field, gives rise to a flare.

The relatively good phase coherence of the velocity flow curves for zones A and B suggests that this part of the filament is able to have rotation. Following the goal of investigating the possible rotation at 40 points along bands 4" wide, symmetric with respect to the N axis, smoothed velocity values were determined. The half-sum of a symmetric pair of velocity values may be interpreted as a velocity V_S as a whole along the line of view. Then, the half-difference would yield a rotation velocity V_ϕ of the filament. The variation of V_S and V_ϕ along the filament with time is plotted in Fig.9, in which case V_S and V_ϕ were averaged within five-minute intervals. The correspondence between the shading intensity and the velocity value appears below the plots. The V_S plot shows that before 6:35 UT there is a preferential descent of the gas. Thereafter, there appear separate rising portions that gradually expand and after the flare IV commencement, include nearly all the filament. An exception are butt-end of the filament where descent is mostly observed.

The V_ϕ plot proves to be more informative. Individual portions of the filament (along the N axis) do not reverse, as is evident from the plot, the direction of their rotation throughout the observations. These are portions 1-7 and 13-21 with an anticlockwise rotation, as viewed from the northward end of the filament ($V_\phi < 0$) and portions 7-13 and 34-40 with a clockwise rotation ($V_\phi > 0$). For portions 21-34 the sense of rotation reversed during flare IV. This last portion belongs to a segment, erupted before the flare. This means that on the place of the disappeared part of the filament there remains some reversive system of rotational motion.

The value of azimuthal component of magnetic field B_ϕ , which may result from twisting, will be $B_\phi \approx B_Z \Delta t \frac{V_\phi}{\Delta Z}$, where B_Z is a poloidal component of magnetic field, Δt is the time of twisting, and ΔZ is the length of the twisted portion. It is known that if B_ϕ exceeds B_Z , then a helical instability

is able to start developing. In our case, according to the plot, $\Delta t = 75$ min, and $\Delta Z = 14''$. Taking into account that the velocities are underestimated on the plot because the difficulties inherent in the methods made it impossible for us to measure large values of V we adopt $V_{\phi} \geq 4$ km s⁻¹. Then $\frac{B_{\phi}}{B_z} \geq 1.8$ and, therefore, the conditions become appropriate for the helical instability to develop and to lead to a gradual rise of the filament, as observed before the flare. In the absence of other disturbances, such a metastable state is able to persist for any length of time.

The question remains unclear regarding the reason for subsequent eruption. One may conjecture that a part of the field lines from the surroundings of the leader of *SD 462* close on *S*-polarity hills of a weak adjacent bipolar region and, passing below the filament, sustains the latter. The spinning filament must entrain these field lines. If the filament executes at least one rotation about its axis, then on its boundary there must arise a layer, in which a "shear" of field lines changes by 180°. As has been shown by Spicer {22}, under the action of a wave-like disturbance coming from below, such a layer must give rise to a tearing instability, with a concomitant gas heating and particle acceleration. For the rotation rate $V_{\phi} = 4$ km s⁻¹ and filament radius of 4'' the time of one rotation will be 1.3 h. This coincides with the rotation time of the segment before the flare. Consequently, necessary, but not sufficient conditions for the tearing instability can arise in the segment we observed. Finally, we must suppose that a trigger for this instability is represented by short-duration violent jump in the upward motion of magnetic field, which are only one stage in the entire phase-coherent process, covering a significant area within the activity complex, or even a greater one. As shown previously, there are good grounds for such an assumption because violent intensifications of the magnetic field rise are correlated with the flare onset.

The mechanism for the filament eruption due to the

tearing instability is universal with respect to the type of flare model, i.e. it is able to "operate" both in models with a closed magnetic configuration and in models with an open configuration. The flares under investigation are explainable in terms of models of these two types. For example, in flares II and IV, occurring in the follower part of the active region, the process of filament eruption extends magnetic loops and renders the magnetic configuration open {8}. Flare IV occurs at the junction of two active regions in the already open magnetic configuration {24}. In either case the mechanism suggested by Spicer, may account for the filament eruption and a subsequent flare.

5. Conclusions

The main results of the present work may be summarized as follows.

1. Throughout the observing interval, phase-coherent changes of both up- and downward velocities of the gas were taking place over a significant portion of the activity complex.
2. A maximum darkening of the filament was observed at maximum downward velocity of the gas.
3. The flare onset is associated with particularly abrupt changes of line-of-sight velocities and it took place during short-duration impulsive upliftings of the magnetic field.
4. Along the filament under study the rotation had different direction. In the part of the filament where eruption occurred, the rotation reversed direction.
5. The oscillatory process observed over a significant area, seems to be a response to a disturbance which propagates from subphotospheric layers and determines the impulsive character of magnetic field upward motion.

Acknowledgements

We wish to thank Dr L.V.Ermakova, who provided us with the magnetograms. Thanks are also due to V.G.Mikhalkovsky for his assistance in the preparation of the manuscript.

References

- {1} Bhatnagar, A., Jain, R.M., Shelke, R.N., H α solar observations during SERF and FBS intervals of April 6-12 and May 22-28, *ICM-SMY Crimean Workshop*, 2. 202, 1981
- {2} Dezső, L., Kálmán, B., Kondás, L., Two-ribbon flares, observed in the period 5-9 October 1979, *ICM-SMY Crimean Workshop*, 2. 97, 1981
- {3} Felli, M., Lang, K., Willson, R., VLA observation of solar active regions. I. The slowly varying component, *Ap.J.* 247. 325, 1981
- {4} Hirayama, T., Theoretical model of flares and prominences. I. Evaporating flare model, *Solar Phys.* 34. 323, 1974
- {5} Hyder, C.L., Winking filaments and prominence and coronal magnetic fields, *Z.Astrophys.* 63. 78, 1966
- {6} Ishkov, B.N., Obashev, S.O., Chromospheric observations of the flare event on October 6, 1979, (in Russ.) *ICM-SMY Crimean Workshop*, 2.85, 1981
- {7} Kaplan, S.A., Pikel'ner, S.B., Tsyтович, V.N., *Plasma physics of the solar atmosphere* (in Russ.) p.73, Nauka, Moscow 1977
- {8} Kopp, R.A., Pneuman, G.W., Magnetic reconnection in the corona and the loop prominence phenomenon, *Solar Phys.* 50. 85, 1976
- {9} Kuklin, G.V., Stepanov, V.E., Motion of gas and magnetic field in a sunspot, I. (in Russ.) *Soln.Dann.* 1. 55, 1963
- {10} Malvill, J.M., Schindler, M., Oscillations of a loop prominence preceding a limb flare, *Solar Phys.* 70. 115, 1981
- {11} Merkulenko, V.E., Towards the dynamics of sunspot magnetic field uplifting in the corona and some resonance features of a coronal active region, (in Russ.) *Astron.Zh.* 43. 1179, 1966
- {12} Mogilevskij, E.I., Energetics and phenomenology of large solar flares, *Fiz.soln.akt.* 3, 1980 (in Russ.)
- {13} Mullan, D.J., Flare triggering by coherent oscillations, *Ap.J.* 185 353, 1973
- {14} Ogir', M.B., Intercorrelation between active solar regions according to H α observations on May 25, 28 and 29 1980, *ICM-SMY Crimean Workshop* 2. 197, 1981 (in Russ.)
- {15} Osterbrock, D.E., The heating of the solar chromosphere, plages and corona by magnetohydrodynamic waves, *Ap.J.* 134. 347, 1961
- {16} Piddington, J.H., A model of solar flares and faculae, *Solar Phys.* 31. 229, 1973
- {17} Ramsey, H.E., Smith, S.F., Flare-initiated filament oscillations, *Astron.J.* 70. 688, 1965
- {18} Ramsey, H.E., Smith, S.F., Flare-initiated filament oscillations, *Astron.J.* 71. 197, 1966
- {19} Rompolt, B., Rotational motion in fine solar structures
Warszawa-Wroclaw, 1975
- {20} Rust, D., An active role for magnetic fields in solar flares, *Solar Phys.* 47. 21, 1976

- {21} Smith, S.F., Ramsey, H.E., The flare-associated filament disappearance, *Z. Astrophys.* 60. 1, 1964
- {22} Spicer, D.S., The thermal and non-thermal flare. A result of non-linear threshold phenomena during magnetic field line reconnection, *Solar Phys.* 53. 249, 1977
- {23} Stepanov, V.E., Ermakova, L.V., Merkulenko, V.E., Palamarchuk, L.E., Polyakov, V.I., Klochek, N.V., Motion in flare knots and magnetic fields in the 6 October 1979 flare, *Issl. SibIZMIR*, 56. 98, 1981 (in Russ.)
- {24} Sweet, P., The neutral point theory of solar flares, *IAU Symp.* 6. 123, 1958
- {25} Tanaka, K., Chromospheric oscillation in the H α plage, *Bull. Amer. Astron. Soc.* 4, 393, 1972

A NOTE ON FLARE LOOPS

L. D E Z S Ő, Á. K O V Á C S

Heliophysical Observatory, Debrecen

Abstract:

It is shown that even the flash phase of a typical flare consisted mainly of loops, when the bulk of energy release took place, consequently the flare phenomenon may be regarded as a loop system temporarily in a highly excited state.

ЗАМЕТКА О ВСПЫШЕЧНЫХ ПЕТЛЯХ

Л. ДЕЖЁ, А. КОВАЧ

Гелиофиз.Обс., Дебрецен

Абстракт:

Показано, что даже всплеск-фаза типичной вспышки состояла большей частью из петель, когда большинство энерговыведения состоялось. Следовательно вспышечное явление может быть рассмотрено как система петель временно во высоковозбужденном состоянии.

G.W.Pneuman put forward as an "interesting speculation ... that perhaps the post-flare loops are not <post-flare> at all - rather, they are the flare" {1}. Indeed, the major flare event of 11 July 1978, which was by no means exceptional, was predominantly a bright loop prominence system {2}. This became visible even in "white" light as proved by the original photos listed in Table 1, and demonstrated here in Figs.1-4.

For the sake of brevity, let us simply refer to the paper {2} quoted and also use the designations to be found there.

In Fig.1 the heavy contours marking the positions of white light emission relative to that of the filament and nearby umbrae, are self-explanatory proof for the existence of white

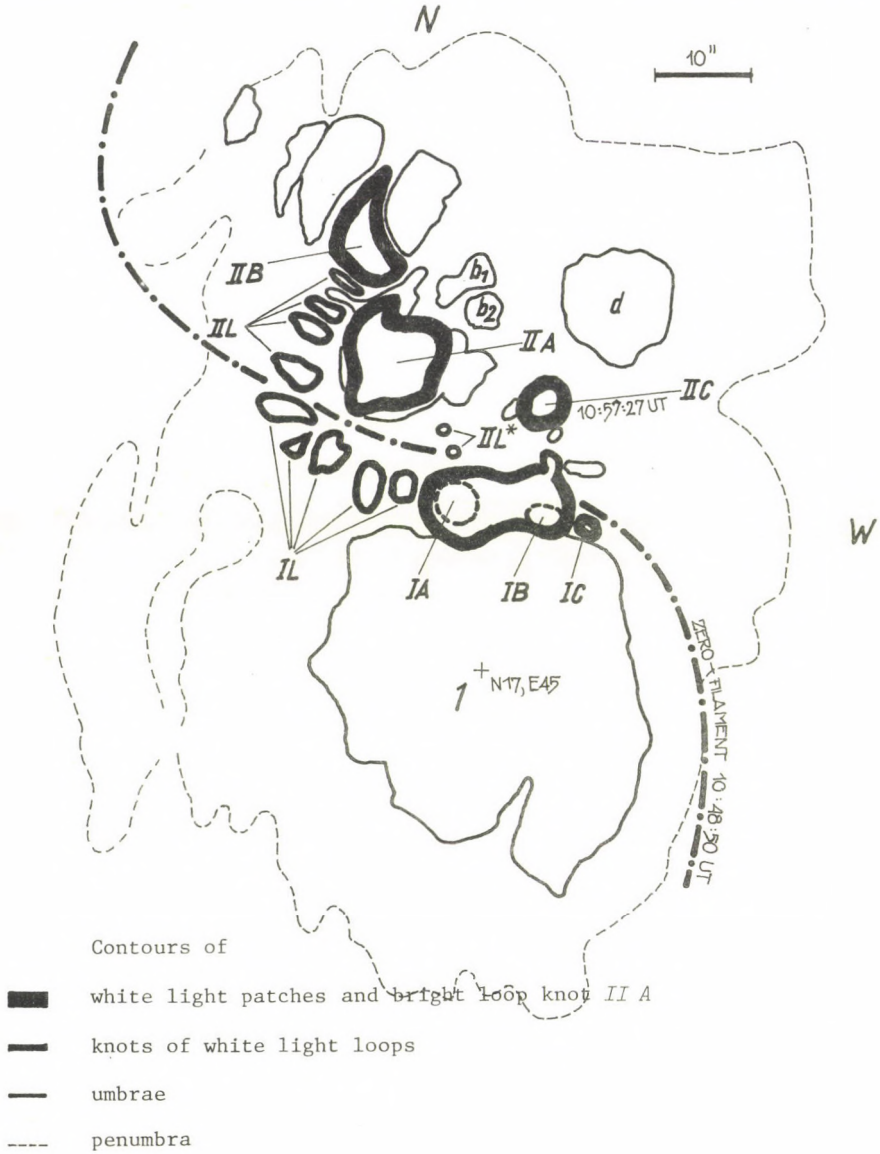


Fig.1. White light flare loops over the naked eye spot on 11 July 1978 (cf. *Fig.2*). All contours at 10:53:55 UT, with the exceptions of *II C* and of the filament.

T A B L E 1

The photographs available to study the white light patches
seen in the great sunspot of 11 July 1978

Numbering in chronological order	Time of exposure <i>UT</i>	Obtained at
1.	<u>10:44:09</u>	Gyula (Gy)
2/Gy	10: <u>53:55</u>	Gy
2/H-P	10:53:55	Haute-Provence (H-P)
3.	10: <u>54:02</u>	H-P
4.	10:54:21	Gy
5.	10:54:52	H-P
6.	10: <u>55:10</u>	H-P
7.	10:55:43	H-P
8.	10:55:45	H-P
9.	10: <u>56:35</u>	H-P
10.	10:56:35	H-P
11.	10:56:37	H-P
12.	10:56:44	Gy
13.	10: <u>57</u> circ.	Miskolc (M)
14.	10:57:27	H-P
15.	10: <u>58</u> circ.	M
16.	10:59:19	Gy
17.	<u>11:00:56</u>	Gy
18.	11: <u>02:31</u>	Gy
19.	11:02:43	H-P
20.	11: <u>04:34</u>	Gy

The name of observers are as follows:

S.Rostás, Gyula (the Observing Station of Debrecen Observatory){2}

F.Rouvière, Haute-Provence (France){3}

J.Kelemen, Miskolc (Hungary){4}

Data of the telescopes, filters, photomaterial, etc. used are given in the papers {2} and {3} for Gyula and Haute-Provence respectively, while in Miskolc the photographs were taken in the prime focus of a small Zeiss refractor (\emptyset 8 cm, $f=120$ cm) on colour film Orwochrom ut 18, without any filter.

10:53:55 UT

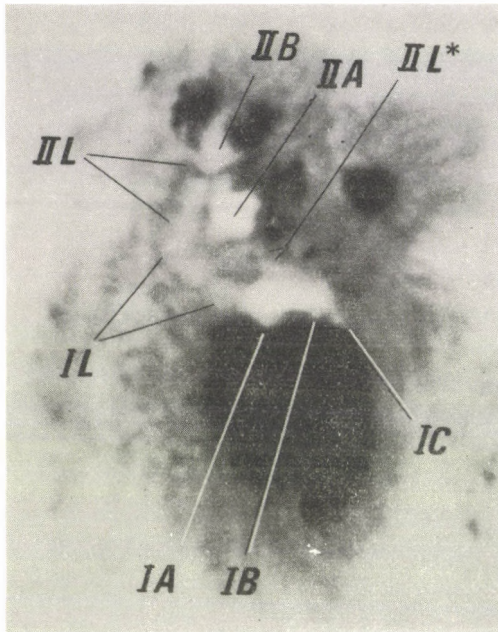


Fig.2. Print of photograph 2/Gy of Table 1.

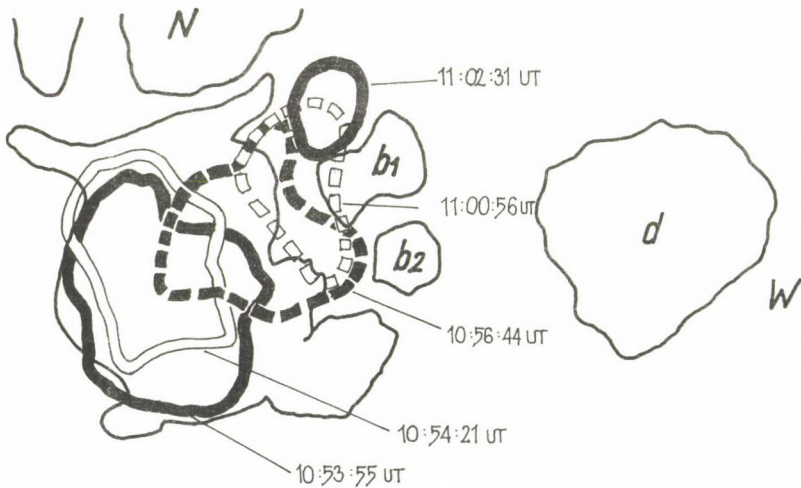


Fig.3. Apparent motion of loop knot II A of the white light flare on 11 July 1978.
(Umbra contours at 10:44 UT.)

10:54:02 UT

10:57:27 UT

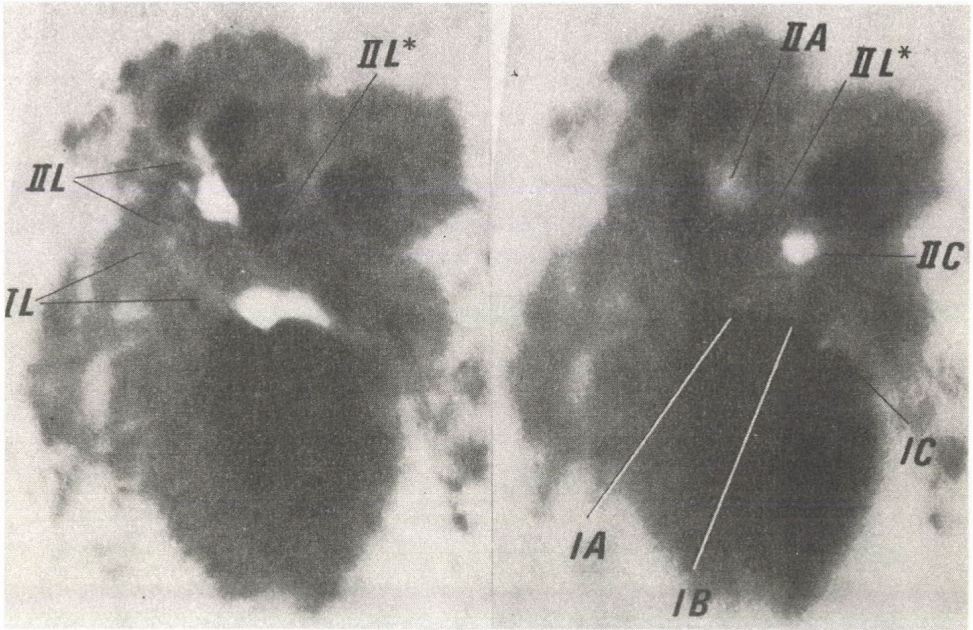


Fig.4a. Prints of photographs 3 and 14 of Table 1.

circ. 10:57 UT

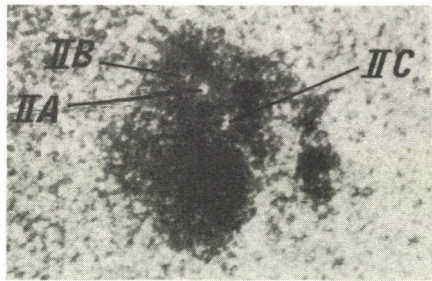


Fig.4b. Print of photograph 13 of Table 1.

light flare loops. We have only taken those white light patches into consideration which were distinctly recognizable as identical at least on one pair of simultaneous (or quasi-simultaneous) photographs, one of them obtained in Hungary, the other in France.

The indisputable examples are conspicuous in Figs.2 and 4. The nice loop *II L* could be followed for more than 2 minutes, and the faint and short *L** probably for twice as long. The bright white patches *II B* and *II C* reveal the likely impact places of loops while *II A* is a large knot of a loop. This is still moving with high speed at a great distance above the photosphere, as disclosed by Fig.3. But *I A* and *I B* have also reached considerable elevation, since some parts of umbra *I* and the so-called zero-line was covered by them for a while.

We think that (during the impulsive phase of the flare) all the bright white light patches were produced by streams of particles accelerated in a restricted part of the active region. This view is supported by the simultaneous occurrence of white light and strong γ -ray emission. The acceleration of particles, no doubt, took place just under the zero-filament (i.e. on the zero line of the longitudinal magnetic field), where a high gradient existed between the *p* polarity giant umbra (*I*) and the ensemble of umbrae (*b*, *b*₁, *b*₂, ...) of *f* polarity, especially because of their converging motion.

Acknowledgements are due to Drs F.Rouvière and J.Kelemen who kindly put their photographs at our disposal.

R e f e r e n c e s

- {1} Pneuman G.W., Coronal manifestations of eruptive prominences (Theory) in *Physics of Solar Prominences* (eds.E.Jensen et al.) Proceedings, IAU Coll.No.44, 281,(Oslo) 1978
- {2} Dezső L., Gesztelyi L., Kondás L., Kovács A., Rostás S., Motions in the solar atmosphere associated with the white light flare of 11 July 1978, *Solar Phys.* 67, 317, 1980
- {3} Rouvière F. a) Photographie solaire avec un télescope de 20 centimètres, *L'Astronomie*, 93, 185, Avril 1979
b) Éruption du 11 juillet 1978, commentaires sur l'évolution de la tache concernée, *L'Astronomie*, 94, 179, Avril 1980
c) (Institute de Mathematiques et Sciences Physiques, Université de Nice) Photographs. *Private Letter* of December 22,1980
- {4} Kelemen J.(Urania Observatory,Budapest) Photographs. *Private Letter* of July 18,1978.

CORONAL MAGNETIC STRUCTURES RELATED TO SOLAR FLARES

B. I. RYABOV, A. R. SPEKTOR

Radioastrophys. Obs., Riga

Abstract:

The common properties of active region coronal magnetic field, derived from radio data, such as the potential character and the relative stability with respect to faint solar flares are discussed. Active region coronal magnetic field has a tendency to form potential structure on the scales $\geq 10^9$ cm and to conserve this structure during 10^1 - 10^2 minutes interval, as before and after a subflare or a flare of importance 1 in the AR. One of the available radio methods for diagnostics of the peculiarities in coronal magnetic structure is described. The method based on expected polarization effect would permit us to localize the neutral point of the coronal magnetic field and to evaluate electron density in its vicinity.

МАГНИТНЫЕ СТРУКТУРЫ В СОЛНЕЧНОЙ КОРОНЕ СВЯЗАННЫЕ СО ВСПЫШКАМИ

Б. И. РЯБОВ, А. Р. СПЕКТОР

Радиоастрофиз. Обс., Рига

Абстракт:

Рассмотрены такие общие свойства коронального магнитного поля активных областей на Солнце как потенциальный характер и относительная устойчивость структуры при слабых вспышках. Установлено что корональное магнитное поле АО на масштабах $\geq 10^9$ см имеет потенциальную структуру и сохраняет её по крайней мере в интервале 10^1 - 10^2 минут как до так и после субвспышки или вспышки балла 1 в АО. Описан один из возможных методов диагностики особенностей структуры коронального поля, который основан на ожидаемом из модельных расчётов эффекте двойной смены знака круговой поляризации радиоизлучения ядра ЛИ. Метод позволяет обнаружить нулевую точку коронального магнитного поля и оценить электронную концентрацию в ее окрестности.

Introduction

It is generally accepted that the flare process is determined by the storage of "free" magnetic energy (the energy of currents above the photosphere, i.e. a non-potential excess of the field) in the upper chromosphere and lower corona {1}. From such a point of view, no fixed connection is seen between the flare occurrence and the magnetic field changes on the photosphere level {2}. However, the magnetic field changes directly connected with a flare must be looked for in the solar corona because the flare energy is released there {1}. It was confirmed by the fact that 90% of the flare radiative energy is concentrated in X-rays and UV wavelengths.

For the examination of coronal magnetic field structure in a solar active region (AR) radio observations would be preferred. This is because of their directivity and unambiguous interpretation {3},{4}. In this paper we draw attention to a few common properties of AR coronal field derived from radio data, such as the potential character and the relative stability with respect to faint flares. One of the available radio methods for diagnostics of the peculiarities in coronal magnetic structures is described.

As brief review of the existing flare theories {5} shows that the search of coronal magnetic structures would permit us to clarify not only the flare process, but also the processes of energy accumulation and release.

Potential magnetic field

There are two necessary conditions allowing potential magnetic field to occur in the solar corona {6}:

$$(1) \quad \beta < 1 \quad \text{where} \quad \beta = \frac{2nkT}{H^2/8\pi}$$

$$(2) \quad \alpha L < 1 \quad \text{where} \quad \alpha \vec{H} = \text{rot } \vec{H},$$

here L is a minimum length at which a potential field still exists in the corona. Table 1 lists values of α and β derived from the observations of ARs at various wavelengths. Since these values are relatively small and the conditions (1), (2) are satisfied at heights of 20 to 100 thousand kilometers

T A B L E 1

AR coronal magnetic field characteristics β (1) and α (2)

α^{-1} 10^9 cm	β	Height above photosphere; parameters assumed values	Wave- length range	Comments
>5	--	$0.18 \cdot 10^9$ cm	<i>Hα</i>	Model force-free magnetic field compared with H chromospheric patterns {7}.
0.9-5.2	--	Inner corona H = 640 G	<i>Hα</i>	Model force-free magnetic field compared with H α chromospheric patterns (while flares) {8}.
2.3-3.3	--	Inner corona		Model simulations {9}.
$2 \cdot 10^2$ - 10^3	--	Inner corona	<i>X, UV</i>	Model force-free magnetic field compared with X and UV patterns coronal {10}.
--	< 1.3 < 1.2	10^{10} cm, H = 5 G $2 \cdot 10^9$ cm, H = 17 G	<i>X</i>	Hot, dense coronal loops are assumed {11}.
--	< $7 \cdot 10^{-3}$	$\leq 3 \cdot 10^9$ cm H = 100 gs	<i>X</i>	Results of model simulations compared with AR X-ray observations {12}.
--	$8 \cdot 10^{-5}$	$4 \cdot 10^8$ cm $n = 5 \cdot 10^9$ cm $^{-3}$	<i>cm</i>	Model simulation of gyro emission compared with AR radio observations {13}.
--	$4.4 \cdot 10^{-5}$ $2 \cdot 10^{-4}$	10^9 cm $2 \cdot 10^9$ cm	<i>cm</i> <i>cm</i>	Model simulation of gyro emission compared with AR radio observations {14}.
--	$7 \cdot 10^{-1}$ 1	$7 \cdot 10^9$ cm $\geq 1.8 \cdot 10^{10}$ cm	<i>X</i> <i>m</i>	Data of radio observations compared with coronal loops X-ray observations {15}.
1.4	--	$< 2 \cdot 10^8$ cm	<i>6 cm</i>	Radio observations of AR made with the help of the radio telescope WSRT {16}.
--	$7 \cdot 10^{-6}$	$2 \cdot 10^8$ cm H = 700 G	<i>6 cm</i>	

above the photosphere, the potential magnetic field could exist there on the scales $\alpha^{-1} = L \gtrsim 10^9 \text{cm}$.

The validity of the potential approximation is additionally confirmed by a comparison of results of potential field simulation with real coronal structures, observed at various wavelengths {7},{8}. The data of radiotelescope RATAN-600 observations with angular resolution 20-50" and radio brightness simulated with the help of potential approximation of the AR coronal magnetic field are compared in Figs.1, 2. The coincidence of the sign of model circular polarization with the observed one checks the potential approximation (see {9} for details).

The conclusion on the potential character of the coronal magnetic field in AR seems to contradict both the evidence of inhomogeneity of solar corona and the assumption of flare energy source, that is, the presence of coronal currents. Indeed, the estimation of an energy excess for force-free magnetic field (fff) over potential one in corona {10}:

$$(3) \quad \Delta E = \frac{1}{8\pi} \int (H_{\text{fff}}^2 - H_{\text{pot}}^2) dV$$

allows some authors {10},{11},{12},{13} to suggest that the magnetic energy abundance released during a flare is roughly equal to flare energy.

Note, it is proposed here that the estimation mentioned above (3) should not lead to unambiguous conclusions with respect to the structure of the coronal magnetic field of AR. Besides, the accuracy of (3), while α is taken from $H\alpha$ chromosphere patterns without any coronal data may be expected to be poor. Indeed, different methods of the model simulation by themselves lead to inaccuracy of one magnitude {14}. However, the knowledge of characteristic length of potential field ($L \approx 10^9 - 10^{10} \text{cm}$) eliminates above mentioned contradictions, that is coronal currents may exist at smaller lengths.

Stability of magnetic field structure

Former {15} polarizational radio observations made once per day with a moderate angular resolution ($\approx 1.5'$) led to the

conclusion that the sign of circular polarization of a local source of radio emission (LS) remains unchanged during a flare activity in AR. The sensitivity of the radio measurements (by the degree of circular polarization) to the coronal structure was high enough. Relevant radio observations were made before or after a subflare and/or a flare importance 1 in AR. For this reason the structure of AR coronal magnetic field at the heights $4 \cdot 10^9 - 10^{10}$ cm is stable at the time interval $10^1 - 10^2$ minutes and on the scales $\geq 10^9$ cm.

Some H α {16} and radio {17} observations confirm such a conclusion. The relative stability of the coronal structure is pronounced by circular polarization of microwave bursts too. The sign of the burst circular polarization remains the same as the slowly varying component {18}. Possibly, it is not the case with a short time interval {19}.

To illustrate relative stability of AR coronal magnetic field in Figs.1, 2 radio scans of the LS connected with the spot group No 193, 1979 (by *Solnechnye dannye*) are shown. It is worth drawing attention to none disturbance in the distribution along LS of circular polarization while subflare occurs at the time of radio observation at 4V 1979 (Fig.1b, {20}). The corresponding distribution of total intensity (Fig.1a) has a clear distortion. Meanwhile, the LS west core circular polarization would be highly sensitive to variations in the structure of the coronal magnetic field because it is affected by quasi-transverse propagation of radio waves in the corona (Fig.1d, 2d). However, neither deviation from model potential magnetic field, nor any fluctuations of a large scale coronal field ($\geq 10^9$ cm are needed to explain the radio observations).

Diagnostic of magnetic structure peculiarities

As was pointed out in Section 2, non-potential insertions to AR coronal magnetic field could be expected at length scale of the order of magnitude $\approx 10^8$ cm at the heights $2 \cdot 10^9 - 10^{10}$ cm. Therefore, searching for such a peculiarity of coronal magnetic structure like a neutral point (NP) or neutral sheet {5} demands angular resolution better than a few arc seconds.

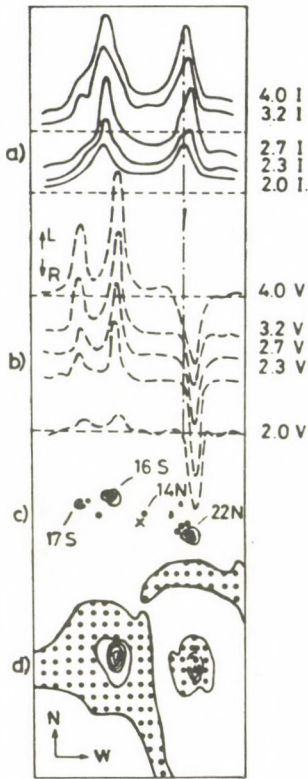


Fig. 1.

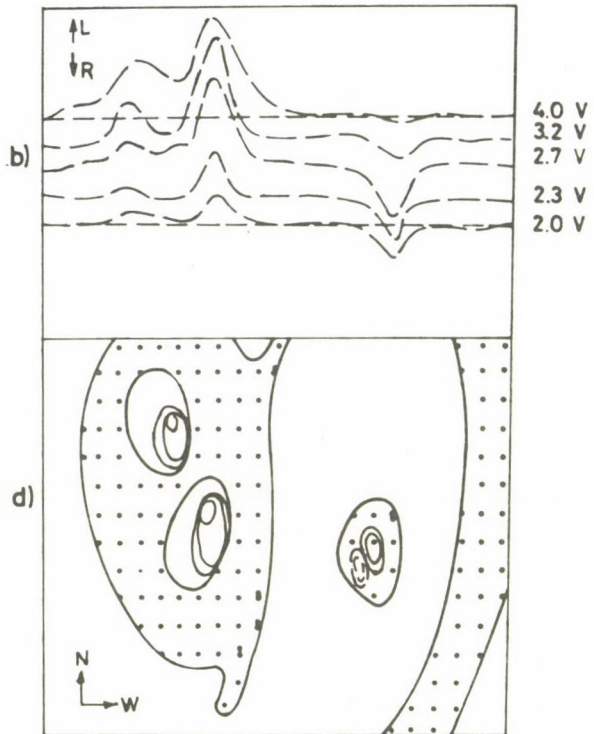


Fig. 2.

Fig. 1. Radio scan of spot group No 193, 1979 at five wavelengths was taken at 4V with the help of the radiotelescope RATAN-600 in total intensity (a) and circular polarization (b). Spot group No 193 by *Sol-nechnye dannye* (c). Result of model simulation of the QTR (represented by dots in the plain of view) and of the source of microwave emission (d).

Fig. 2. Radio scan of spot group No 193, 1979 at five cm wavelengths taken at 5V with the help of the radio telescope RATAN-600 in circular polarization (b). Result of model simulation of the QTR and source of microwave emission (d).

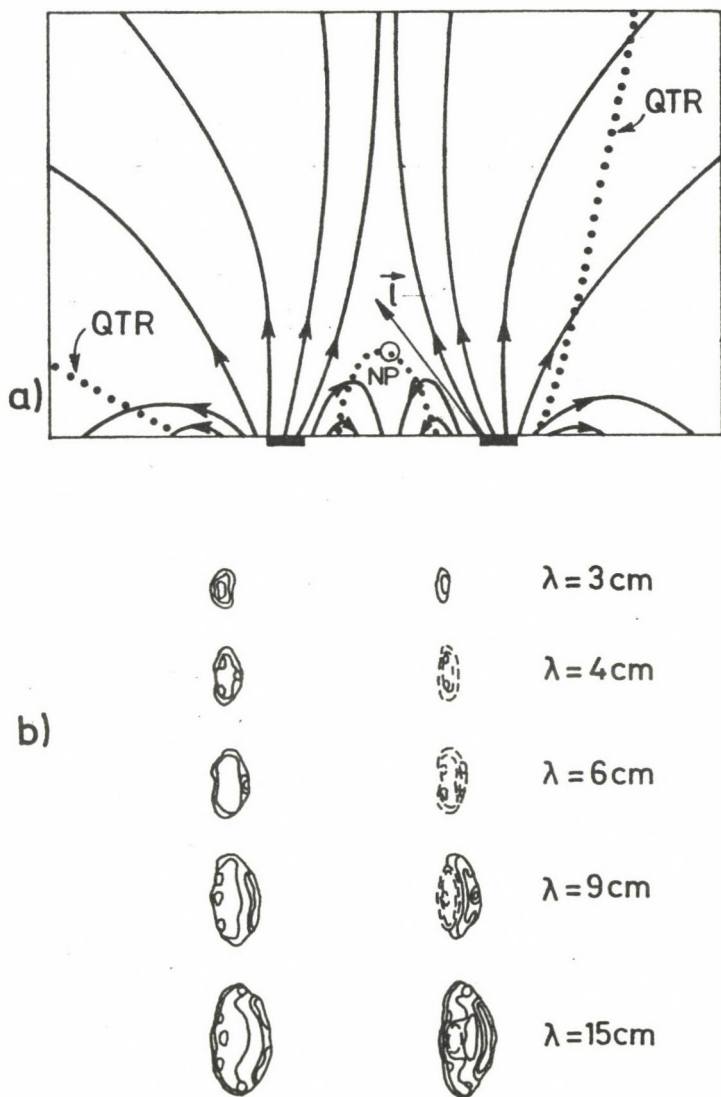


Fig. 3. Coronal magnetic field of two sunspots with the neutral point in vertical plane (a). Result of model simulation of microwave circular polarized sources above sunspots at five wavelengths in the plain of view (b). Note the double sign inversion through wavelength range in the case of radio emission passed through NP vicinity.

The neutral sheet and NP diagnostic methods worked out up to now {21},{22} assume radio observations as most direct and unambiguous {3},{4}. Fig.3 illustrates a new one based on the effect of double sign inversion of LS circular polarization pronounced by model calculations in the case of radio wave passage through quasi-transverse region (QTR) in the nearest vicinity of NP ($r \approx 10^8 - 10^9$ cm, where QTR must be presented). In QTR the sense of circular polarization depends on the parameter {23}:

$$(4) \quad Q \approx 1.8 \cdot 10^{-25} n H^3 L_\alpha \lambda^4, \quad \text{where} \quad L_\alpha = \alpha \left| \frac{d\alpha}{dz} \right|^{-1}$$

is a characteristic scale at which an angle α between \vec{H} and the direction z of wave propagation vary, λ is wavelength. The method permits us to estimate not only the position of NP in the solar atmosphere, but also the electron density n in the vicinity of the NP.

Concluding remarks

Thus, we have considered briefly restrictions on some properties of the AR coronal magnetic structure, which may be useful with respect to solar flares. On the basis of polarizational radio observations one could suggest a coronal magnetic field tendency to form potential structure on the scales $\geq 10^9$ cm and to conserve this structure before and after $10^1 - 10^2$ minutes interval of a subflare or/and importance 1 flare in the AR. There are some radio observations with a high angular resolution {24},{25} which suggest changes related to a flare in coronal structure on the small scale $\leq 5 \cdot 10^8$ cm.

The method presented (Fig.3) should be assistant both in the discovery of such a peculiarity as neutral point in coronal field and in diagnostics of the coronal plasma in its vicinity. In turn, NPs are the characteristics of a total structure of AR coronal magnetic field {6}, being possibly, the locus of solar flare origin.

References

- {1} Somov, B.V., Energy accumulation and release in solar flares (in Russ.), *XIII Leningrad seminar on cosmophysics*, 6, Leningrad 1982
- {2} Michard, R., Solar magnetic fields in association with flares *IAU Symp. 43*. 359, 1971
- {3} Beckers, J.M., The measurement of solar magnetic fields, *IAU Symp. 43*. 3, 1971
- {4} Gelfreikh, G.B., Microwave diagnostics of the magnetic fields of the Sun, (in Russ.), in: *Dynamics of current sheets and physics of solar activity*, p.116, Riga 1982
- {5} Švestka, Z., What should be observed on the Sun, *Solar Phys.* 47.375, 1976
- {6} Molodensky, M.M., Syrovatsky, S.I., Magnetic field of active regions and its neutral points, (in Russ.) *Astron. Zh.* 54. 1293, 1977
- {7} Newkirk, G.Jr., Large scale solar magnetic fields and their consequences *IAU Symp. 43*. 547, 1971
- {8} Dulk, G.A., McLean, D.J., Coronal magnetic fields, *Solar Phys.* 57.279, 1978
- {9} Peterova, N.G., Ryabov, B.I., Restoring polarized emission of local sources and the structure of coronal magnetic field, (in Russ.) *Astron. Zh.* 58. 1070, 1981, (English transl. in *Soviet Astron.* 25.No.5)
- {10} Seehafer, N., Staude, J., Force-free magnetic field extrapolation for the complex sunspot group of August 1972, *A.N.* 300. 151, 1979
- {11} Rust, D.M., Nakagawa, Y., Neupert, W.M., EUV emission, filament activation and magnetic fields in a slow-rise flare, *Solar Phys.* 41 397, 1975
- {12} Tanaka, K., Nakagawa, Y., Force-free magnetic fields and flares of August 1972, *Solar Phys.* 33. 187, 1973
- {13} Sakurai, T., Calculation of force-free magnetic field with non-constant α , *Solar Phys.* 69. 343, 1981
- {14} Seehafer, N., A comparison of different solar magnetic field extrapolation procedures, *Solar Phys.* 81. 69, 1982
- {15} Gelfreikh, G.B., Peterova, N.G., Ryabov, B.I., Local source polarization as criterion of coronal magnetic fields changes during solar flares, *Theses of the session Radio Emission of the Sun*, (in Russ.) Kislovodsk, USSR, 1978
- {16} Ishkov, V.M., Korobova, Z.B., Mogilevsky, E.I., Arch systems of large solar flares, (in Russ.) *Fiz. soln. akt.* 93, 1979
- {17} Marsh, K.A., Zirin, H., Hurford, G.J., VLA observations of solar flares, interpreted with optical, X-ray, and other microwave data, *Ap.J.* 228. 610, 1979
- {18} Peterova, N.G., Rodrigues, R., Some results of microwave bursts and sources of S-component polarizational investigation (in Russ.) *Soln. Dann.* No.2. 47, 1977
- {19} Bachurin, A.B., Dvoryashin, A.S., Erushev, I.H., Cvetkov, L.I., Polarized radio emission of the powerful active region on the Sun at July 1974 at the wavelengths 1.9, 2.5, 3.5 cm, *Izv. KrAO.* 61. 37, 1980

-
- {20} Akhmedov, Sh. B., Bogod, V. M., Gelfreikh, G. B., The results of the study of the local source of solar active region McMath 159740 on SMY program using RATAN-600, *ICM-SMY Crimean Workshop*, 2, 45, 1981
- {21} Kuznetsov, V. D., The analysis of possibility of the solar flare study and forecast by the characteristics of preflare emission, *ICM-SMY Crimean Workshop*, 1, 233, 1981
- {22} Zheleznyakov, V. V., Zlotnik, E. Ya., Thermal cyclotron radio emission of neutral current sheets in the solar corona, *Solar Phys.* 68. 317. 1980
- {23} Cohen, M. H., Magnetoionic mode coupling at high frequencies, *Ap. J.* 131. 664, 1960
- {24} Kundu, M. R., Schmahl, E. J., Velusamy, T., Vlahos, L., Radio imaging of solar flares using the Very Large Array: new insight into flare process, *Astron. Astrophys.* 108. 188. 1982
- {25} Lang, K. R., High resolution interferometry of the Sun at 3.7 cm wavelength, *Solar Phys.* 36. 351, 1974

RADIOEMISSION OF WEAK SOURCES AND MAGNETIC FIELD STRUCTURE

S.I. AVDYUSHIN⁺, M.M. ALIBEGOV⁺,
A.F. BOGOMOLOV^o, V.A. BUROV⁺, E.I. ZAJTSEV^o,
S.P. LEONENKO^o, B.A. POPERECHEENKO^o

⁺Inst. Appl. Geophys., Moscow

^oMoscow Power Inst., Moscow

РАДИОИЗЛУЧЕНИЕ СЛАБЫХ ИСТОЧНИКОВ И СТРУКТУРА МАГНИТНОГО ПОЛЯ

С.И. АВДЮШИН⁺, М.М. АЛИБЕГОВ⁺, А.Ф. БОГОМОЛОВ^o, В.А. БУРОВ⁺,
Е.И. ЗАЙЦЕВ^o, С.П. ЛЕОНЕНКО^o, Б.А. ПОПЕРЕЧЕНКО^o

⁺ Инст. Прикл. Геофиз., Москва

^o Моск. Энерг. Инст., Москва

Абстракт:

В работе рассматриваются результаты измерений степени поляризации радиоизлучения Солнца 24 - 28 июля 1982 г. Наблюдения проводились на 64-метровом радиотелескопе ТНА-1500 в Медвежьих Озерах на частотах 8.3 и 3.7 ГГц. Анализ радиокарт позволяет выделить два типа структур: 1) области слабополяризованного ($P < 0.3 - 0.5 \%$) излучения и 2) области с относительно высокой ($P \geq 1 \%$) степенью поляризации, совпадающие с группами пятен и флоккулами. Наблюдаемая степень поляризации в структурах первого типа дает (для выбранной модели солнечной атмосферы) величину поля в переходном слое около 5 Гс. Сравнение структуры крупномасштабного поля, представленной на Стенфордских картах, с картами поляризованного излучения на 3.7 ГГц показывает их хорошее соответствие. Динамика поляризации радиоизлучения локальных источников над флоккулами и малыми группами пятен указывает на возможную двухкомпонентную структуру магнитных полей в них: протяженные области слабых полей ($B \approx 10-15$ Гс) с компактными участками сильных полей ($B \approx 500-1000$ Гс).

July 24-28, 1982 was characterized by a very low level of solar activity. Only 3-5 weak sunspot groups covering the area less than 100 mh were observed within this period.

The solar disk mapping was carried out at 8.3 and 3.7 GHz using the single disk radiotelescope TNA-1500 with a 64 m parabolic antennae. In the course of observations Stokes parameters I and V were measured. Instrumental characteristics are presented in Table 1.

Mapping by passage method was carried out 2-3 times a day. The scan distance was 2 angular min. Calibration was based on an assumed temperature of 220°K for the Moon {1}. 2-3 radio images of the Sun were obtained daily. The measured brightness temperature of the quiet Sun was equal to $1.1 \cdot 10^4$ K and $2.3 \cdot 10^4$ K for the frequencies 8.3 GHz and 3.7 GHz, respectively. The emission polarization degree was calculated according to the expression:

$$P = T_V/T_I - P_p \quad (1)$$

where T_V , T_I - measured Stokes parameters;

P_p - parasitic polarization degree (PPD).

Parasitic polarization values were obtained according to minimum solar brightness temperature regions which were usually located near the filaments. It was assumed that in mentioned regions true radioemission polarization was equal to zero.

Throughout the whole observation period at 3.7 GHz PPD appeared practically constant and was equal $P_p \approx (2.4 \pm 0.2)\%$, whereas at 8.3 GHz it varied within the range of 2-3%. In general, we have solved the problem by means of extracting spatially and temporally stable structures.

The aim of the observations during the mentioned period was to reveal the relation between radioemission parameters and magnetic field features in the quiet and weakly disturbed regions of the Sun. The analysis of solar radiocharts permitted the extraction of two types of structures: (i) regions with weakly polarized ($P \leq 0.3-0.5\%$) emission which cover the major part of the surface, and (ii) regions with relatively strong ($P \geq 1\%$) polarization which coincide with sunspot groups and

plages. Absolute coordinate calibration of radio images was accomplished by measuring sunspot positions on the full-disk, image and by using these spots as a reference to determine absolute position on the heliograms. Polarization observations of undisturbed solar regions showed that the mean polarization degree is equal to 0.3-0.4% (for 3.7 GHz). Calculations were made to choose solar atmosphere parameters to get a better agreement between the calculated and the observed data. On the basis of models used in {2}, {3} the solar atmosphere model was adopted (see Table 2). It is seen that effective emission layers are located at a very narrow height interval of 2199 - 2247 km above the photosphere and in fact have a common source of generation at the observation frequencies. In the presence of magnetic field brightness temperature remains practically unchanged but polarization degree increases. For example, when the field strength is equal to 20 gauss the polarization degree, according to the chosen model, is $P(3.7 \text{ GHz}) \approx 1\%$, $P(8.3 \text{ GHz}) \approx 0.5\%$. The calculations were made for quasi-longitude propagation of thermal bremsstrahlung. The propagation equation (2) was solved numerically:

$$T_{Bj} = \int_0^{\infty} T_e(\tau_j) \exp(-\tau_j) d\tau_j \quad (2)$$

Here $\tau_j = \int_0^S \kappa_j(z) dz$ - optical depth along the line of sight;

$$\kappa_j = \frac{0.12 n_e^2}{\tau_e^3 (f \pm f_B)^2} \quad \text{- absorption coefficient of emission with frequency } f \text{ in the magnetic field \{4\};}$$

f_B - gyrofrequency;
 $j = o, e$ - o-wave, e-wave; minus sign corresponds to e-wave, plus sign to o-wave.

Calculations show that the observed polarization degree correspond to the transition zone field strength 4-6 gauss.

The relation between emission polarization degree at 3.7 GHz and the large-scale solar magnetic fields becomes

T A B L E 1

Frequency GHz	HPBW	Scale K/mm		Fluctuation threshold K
		I	V	
8.3	2.1'	100	3	3
3.7	4.4'	500	15	8

T A B L E 2

h 10^3 km	T_e $^{\circ}K$	n_e cm^{-3}
2.250	$8.8 \cdot 10^4$	$4.0 \cdot 10^9$
2.249	7.9	4.4
2.2482	7.0	5.0
2.2477	6.1	5.7
2.2473	5.3	6.7
2.2469 *	4.4	8.0
2.242 * *	3.2	$1.5 \cdot 10^{10}$
2.235 * *	2.0	1.8
2.199 *	$8.4 \cdot 10^3$	3.0

* - denote the layers giving the bulk emission at both frequencies

T A B L E 3

Group No (date of central meridian passage)			July	July	July	July	July
			24	25	26	27	28
No 248 (July 26.3)	A	mh	0	90	62	0	0
	P(8.3)	%	2.1	2.3	0	0	0
	P(3.7)	%	3.3	3.3	1	1	1
No 253 (July 28.7)	A	mh	-	-	95	20	0
	P(8.3)	%	-	-	0	0	0
	P(3.7)	%	-	-	0.5	0.7	0.5

Here A - area, in millionth of the solar helisphere (mh),
P(f, GHz) - maximum measured polarization degree

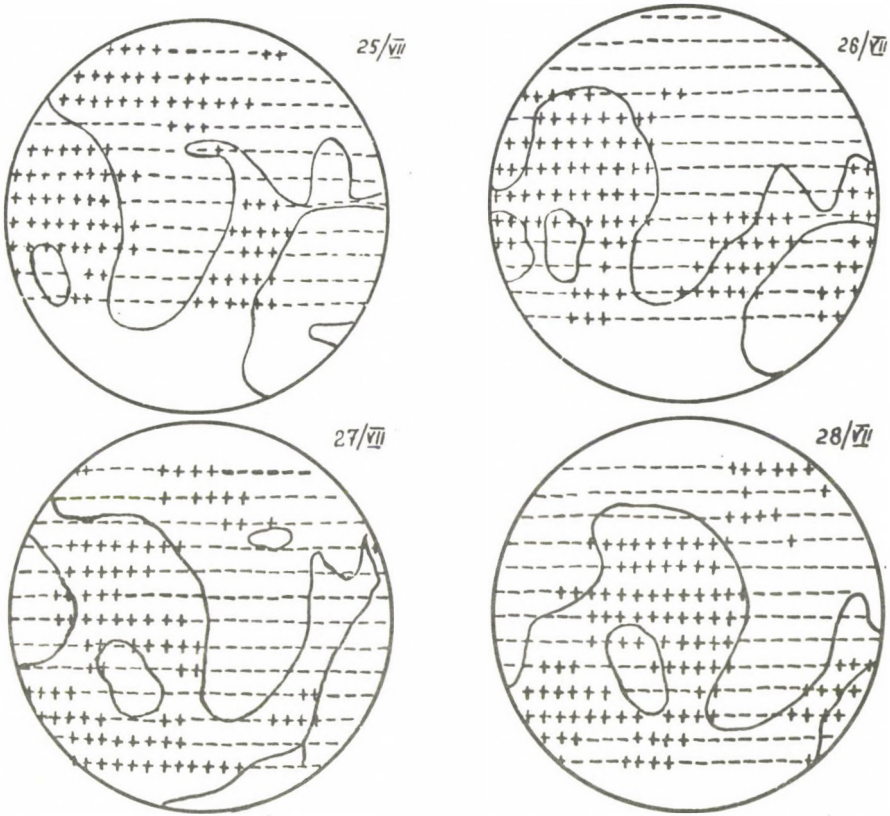


Fig. 1. Radioemission of weak sources and magnetic field structure.

evident when comparing polarization charts with Stanford photospheric magnetic field maps obtained from optical measurements in FeI line on July 25-28, 1982 (see Fig.1). Along with polarization map ("+" - right-hand polarization, "-" - left-hand polarization), the figure presents zero magnetic field line from photospheric observations. The agreement seems to be rather good taking into account possible distortions at distances exceeding 60° from the central point. It becomes still more evident if individual regions with fixed polarization sign moving due to the Sun rotation are considered. However, it should be noted that while calculating magnetic field strength on the basis of polarization degree, we use, in fact, the gradients of concentration (n_e) and temperature (T_e) of electrons in the transition zone. Slight variations of these parameters can essentially change the value of the calculated field, the true magnetic field being constant.

A few small sunspot groups were observed on the Sun during the considered period of July 24-28, 1982. Sunspot groups Nos 248 and 253 (according to *Solnechnye Dannye*) were found to be the most convenient for the analysis due to their isolation and location in the vicinity of the central meridian. Data on groups Nos 248 and 253 are presented in Table 3. The table shows that in group No 248 abrupt polarization changes took place on the night of 25-26 July: at 3.7 GHz polarization degree decreased three times, and at 8.3 GHz it almost disappeared. The assumption of gyroresonant nature of radioemission can account for the observed phenomenon. The existence of increased polarization at both frequencies on July 24-25 indicates the field strength of about 1000 gauss in the coronal region above the group No 248 (radioemission was determined by the 3rd and 4th harmonics of the gyrofrequency). Polarization degree fall starting from July 26 accounted for the coronal field strength decrease to 500 gauss. The emission at 8.3 GHz became undetectable since the 4th gyrolevel is optically thin, and the emission at 8.3 GHz is determined by the 3rd harmonic of gyroresonance. Assuming that the source was a point one, we can consider the

influence of HPBW. Calculations provide polarization degree which is more than one order of magnitude higher than that presented in Table 3. Since variations of the integral region radio flux were weak it can be inferred that radioemission exposes two components: weakly polarized extended halo and compact highly resonant gyroresonance source. Note that polarization changes in sunspot group No 248 preceded spot disappearance by a day.

Within the period of observations polarization in group No 253 did not undergo any substantial changes. The observed polarization degree can be interpreted in terms of both bremsstrahlung mechanism in the presence of magnetic field with $H \approx 10-15$ gauss, and, as in the above case, gyroresonance emission mechanism in the magnetic field of 500 gauss.

The results of radioemission polarization observations at 3.7 and 8.3 GHz point to the two-component source structure of the plages and small sunspot groups: the extended area with a weak magnetic field and compact kernels of strong field embedded in the corona. The model combines measurements carried out in {5} where the fields up to 400 gauss were registered, and in {6} where the fields of several tenths of a gauss were reported.

R e f e r e n c e s

- {1} *Планеты и спутники*, МИР, Москва, 1974
- {2} Fürst, E., Hachenberg, O., Hirth, W., The center-to-limb variation of the Sun at centimetric wavelengths, *Astron. Astrophys.* 36. 123, 1974
- {3} Vernazza, J.E., Avrett, E.H., Loeser, R., Structure of the solar chromosphere. III. Models of the EUV brightness components of the quiet Sun, *Ap.J. Suppl.* 45. 635, 1981
- {4} Kundu, M.R., *Solar radio astronomy*, University of Michigan Radio Astronomy Observatory, 1964
- {5} Gelfreikh, G.B., Snegirev, S.D., Fridman, V.M., Shejner, O.A., Investigation of magnetic fields of solar flocculi by radio astronomical observations, (in Russ.) *Изв. высш. учеб. заведений. Радиофизика*, 18. №12. 1764, 1975

- {6} Bogod, V.M., Gelfreikh, G.B., Measurements of the magnetic field and the gradient of temperature in the solar atmosphere above a flocculus using radio observations, *Solar Phys.* 67, 29, 1980

ЭВОЛЮЦИЯ И ВСПЫШЕЧНАЯ АКТИВНОСТЬ
БОЛЬШОЙ ГРУППЫ СОЛНЕЧНЫХ ПЯТЕН ИЮЛЯ 1982 Г.

И. САТТАРОВ, З.Б. КОРОБОВА

Астрон.Инст., Ташкент

Абстракт:

Исследована большая группа солнечных пятен BBR 18474 июля 1982 г. Показано, что группа состояла из отдельных фрагментов, первоначально находившихся в общей полутени, но развивавшихся независимо. Область появления новых биполярных систем смещалась с востока на запад. Развитие биполярных систем вблизи линии раздела полярностей сопровождалось появлением двуленточных вспышек, вдали от нее—"точечных". Наиболее яркие узлы двуленточных вспышек располагались на границах между кинематическими элементами группы.

DEVELOPMENT AND FLARE ACTIVITY
IN THE LARGE SUNSPOT GROUP IN JULY 1982

I. SATTAROV, Z.B. KOROBOVA

Astron.Inst., Tashkent

Abstract:

A large sunspot group in BBR 18474 (July 1982) was studied at the East limb. It consisted of some independently developing fragments in the common penumbra. Regions of emergence of new bipolar systems drifted westward. f-spots of these systems appeared when p-spots began to decay. Flares occurred in the regions of new bipolar systems. The zone of flare appearance expanded from the center regions of the group to its borders in accordance with the drift of the region of sunspots emergence. The development of the new bipolar systems near the line of polarity reversal was usually associated with two-ribbon flares. The flares far from the line are small in size. The most intensive dots of the flares are situated at the boundaries of the kinematical elements of the group.

Введение

Известно, что вспышечная активность области зависит от ее эволюционной фазы {1-2} и магнитной конфигурации {3}. Частота появления вспышек достигает максимального значения вблизи максимума площади группы {1-2}. Однако мощные вспышки могут наблюдаться как на стадии роста, так и на стадии спада площади группы {4} и их возникновение зависит от степени усложненности ее магнитной конфигурации. Группы могут рождаться со сложной магнитной конфигурацией, (например, группа июля 1961 г.) и могут становиться таковыми в результате образования новых ядер внутри или вблизи существующих пятен (например, группа июля 1978 г.) [5]. Новые пятна неустойчивы и вблизи них часто наблюдаются вспышки {5-7} и выбросы {8}. Изучение процесса формирования сложной группы пятен, выявление закономерностей, приводящих к вспышкам, представляет большой интерес. Здесь мы приводим результаты изучения развития большой группы солнечных пятен и обсуждаем их в связи со вспышечной активностью области.

Общие характеристики активной области

Большая группа солнечных пятен июля 1982 года развилась в активной области, проходившей по диску Солнца по крайней мере пять раз. Эта активная область примыкала к более ранней АО, существовавшей в течение четырех солнечных оборотов с января по апрель 1982 г.

Изучаемая активная область развилась в западном направлении. Площадь флоккульного поля в линии кальция имела максимальную площадь в августе. Группа пятен достигла наибольшего развития в июле. В мае на ее месте было униполярное пятно, окруженное сателлитами. В июле группа представляла собой большое многоцентровое пятно преимущественно ведущей полярности и цепочки мелких ядер хвостовой полярности, вытянутой на восток. 8 июля группа пятен появилась на восточном краю Солнца в виде большого скопления ядер в общей полутени. 13 июля площадь группы превысила 3000 м.д.п. (рис.1). К 19 июля площадь ее уменьшилась до 1200 м.д.п., а протяженность по долготе достигла 27°.

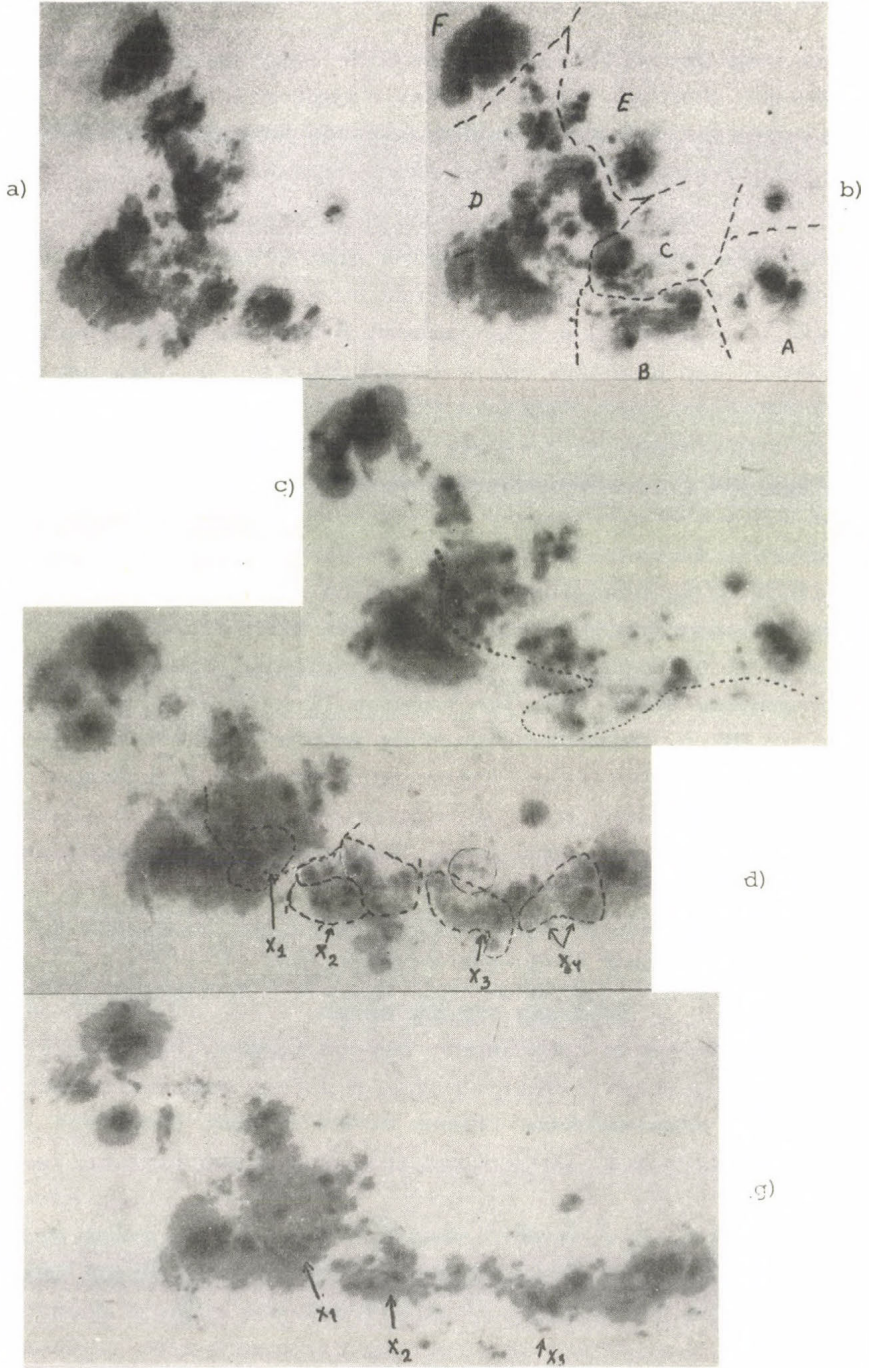
По мере развития активной области существенно изменилось направление основной линии раздела полярностей (ЛРП): в июньском прохождении она имела меридиональное направление, тогда как в июле оказалась вытянутой вдоль параллели {9}.

Материалы наблюдений и их обработка

Большая группа солнечных пятен июля 1982 г. 10 июля была объявлена как объект для наблюдений по программе "Солнечные вспышки", предложенной В.А. Кратом. В Ташкенте наблюдения проводились как в белом, так и монохроматическом (H_{α}) свете на двух телескопах: хромосферно-фотосферном АФР-2,3 (полный диск, диаметр изображения 74 и 16 мм) и горизонтальном солнечном телескопе АЦУ-5 (избранный участок при диаметре изображения Солнца 600 и 160 мм). Данные об интервалах времени наблюдений приводятся в таблице. Координаты и площади пятен и их ядер измерялись на координатно-измерительной машине УИМ-23. По измеренным прямоугольным координатам на ЭКВМ "Искра-124" вычислены их фотогелиографические координаты. Тем же способом был произведен обмер контуров вспышек 12 и 15 июля, снятых на телескопе АЦУ-5. Площадь пятен и их ядер измерялась по изображению на фотогелиограммах, спроектированному с 30-кратным увеличением на специально подготовленный экран УИМ-23. Были обработаны все снимки отличного, хорошего и удовлетворительного качества. Отождествление ядер на снимках за соседние дни производилось после вычисления их гелиографических координат и собственных движений в течение каждого дня.

Эволюция группы пятен

Развитие группы происходило внутри конфигурации, состоявшей из трех основных пятен, которые к началу июльского прохождения А0 уже существовали. Группу можно условно разделить на несколько фрагментов. Они обозначены латинскими буквами на рис. 1 б. Развитие группы связано с образованием новых пятен во фрагментах С, Е и пятен-сателлитов в D, B, A. По темпу развития фрагменты группы отличались друг от друга, и каждый фрагмент развивался независимо. Северо-восточное пятно F достигло максимальной площади 14 июля (см.рис.2), после чего начало



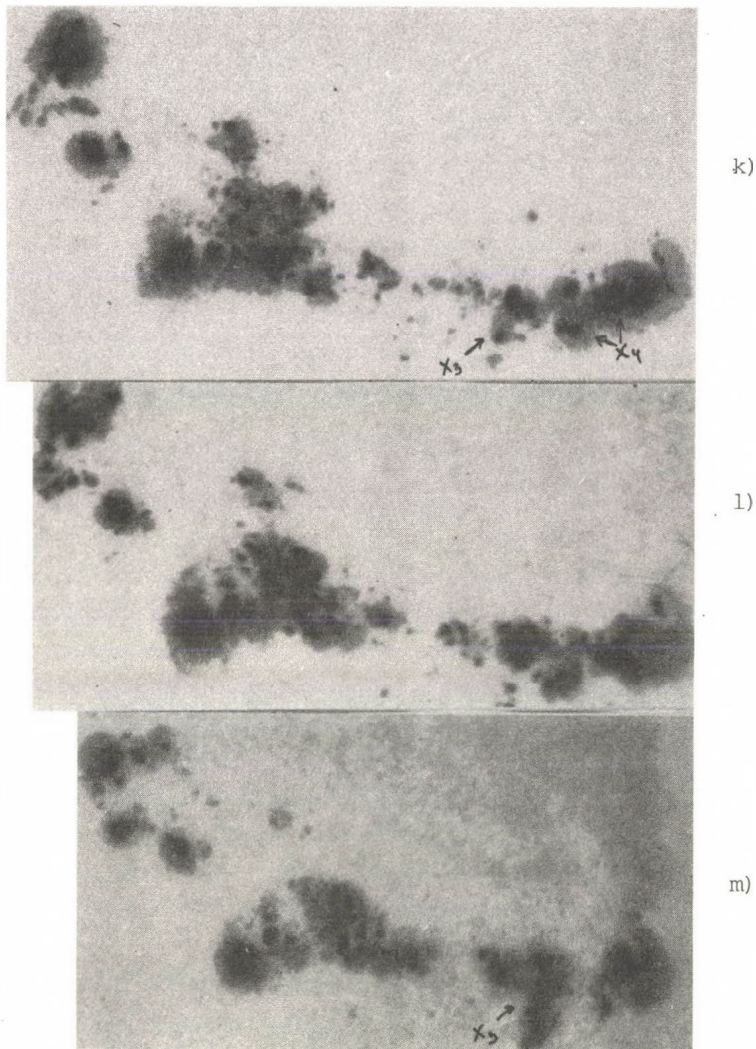


Рис.1. Снимки группы пятен июля 1982 г. с 11 по 18 июля.
А, В, С, D, Е, F - фрагменты группы,
X₁, X₂, X₃, X₄ - новые всплывающие биполярные системы.
Точечный пунктир - основная ЛРП.

уменьшаться. Пятна фрагмента Е, составлявшие биполярную систему, достигли максимальной площади 12 июля. Однако увеличение общей площади группы (см. рис. 2а) с 11 по 13 июля связано с развитием центральной части, которая достигла максимума площади 13 июля (см. рис. 2b). Последнее произошло в результате образования новых ядер X_1 , заполнивших беспятенную область между большим ядром D и пятнами Е (см. рис. 1). Новые ядра X_1 достигли максимальной площади (100 м.д.п.) 15 июля, после чего стали быстро разрушаться. Фрагмент С начал быстро развиваться 12 июля, 13 июля отделился от D и достиг максимальной площади 14 июля (см. рис. 1 и 2). Как видно из рис. 1, он соединен с головным пятном В цепочкой пор. От головного пятна В в сторону большого ядра D тянется вторая цепочка пор. Между этими цепочками проходила основная ЛРП и над ними находились ленты вспышек 12 июля. Сравнение фотогелиограмм, полученных до и после вспышек свидетельствует о том, что в этих районах после вспышек появились новые ядра X_2 (см. рис. 1с). Эти новые ядра составляют тесную биполярную систему, N-ядра которой достигли максимальной площади 14 июля, а S-ядра - 14 июля. За головным пятном В, которое, как будет показано, быстро двигалось на запад, 14 июля начинает образовываться новая тесная биполярная система X_3 , (см. рис. 1d), которая в отличие от менее устойчивых X_1 и X_2 превратилась 18 июля в крупное пятно δ -конфигурации. 14 июля между А и В начинается процесс образования новой биполярной области X_4 который привел к объединению в одну полутень фрагментов А и В. Эта быстро развивающаяся система достигла максимального развития 15-16 июля и после 17 июля начала быстро разрушаться (см. рис. 1 и 2).

Последовательность образования и близость новых ядер разноименной полярности, а также, как будет показано ниже, тонкая структура хромосферы дают основание полагать, что между пятнами А и D в течение 10-18 июля всплыли четыре новых магнитных потока: X_1 вблизи большого пятна 10 июля, X_2 - северо-восточнее пятна В 12 июля, X_3 -вблизи головного пятна В 14 июля и X_4 между А и В также 14 июля. Зона всплывания потоков перемещалась с востока на запад. Пятна (ядра) противоположной поляр-

ТАБЛИЦА

Дата 1982	АФР-3,2				АЦУ-5			
	Фотогелиограммы		H α -фильтрограммы		Широкополосные снимки		H α -фильтрограммы	
	h m	h m	h m	h m	h m	h m	h m	h m
10.07	03 08	- 11 13	03 20	- 06 00	06 40	- 07 35	06 40	- 07 35
11.07	03 02	- 08 07	03 12	- 06 04	09 02	- 10 51	09 02	- 10 51
12.07	07 04	- 12 31	07 17	- 08 35	04 30	- 07 30	04 30	- 07 30
13.07	07 15	- 10 20	07 34	- 10 30	08 12	- 09 00	08 12	- 09 30
14.07	03 28	- 10 02	07 30	- 10 35	09 31	- 10 54	09 31	- 10 54
15.07	03 08	- 09 00	06 45	- 07 53	07 30	- 10 35	07 30	- 10 35
16.07	03 00	- 05 55	06 58	- 09 04	08 58	- 09 04	05 45	- 07 53
17.07	03 00	- 10 25	02 48	- 06 00	02 48	- 05 30	08 58	- 09 04
18.07	03 02	- 08 00	06 50	- 07 00	04 15	- 04 48	02 48	- 05 30
			04 15	- 04 48	06 50	- 07 00	06 50	- 07 00
			03 09	- 06 02	04 15	- 04 48	04 15	- 04 48

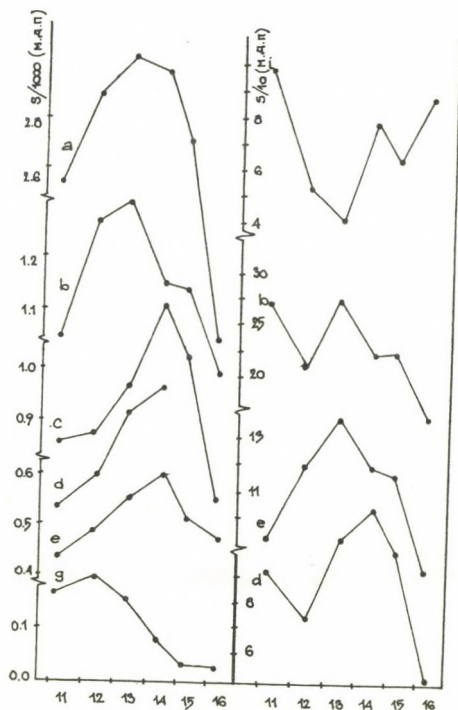


Рис. 2. Изменение площади группы (левая половина) и ядер (правая половина) в течение 11-16 июля: а - суммарная площадь всей группы, б - фрагмента D, с - фрагментов А+В+С, d - фрагментов В+С, е - фрагмента F, г - фрагмента E, и - фрагмента А.

ности, входящие в каждую систему X, или находятся в общей полутени (X_3, X_4), или так близки друг к другу (X_1, X_2), что между ними видна лишь тонкая (шириной 10^4 км) светлая полоска. Следует отметить, что в группе преобладают ядра N-полярности над S-полярностью. Отношение их суммарных площадей 13 июля превосходило 3,5. В новых биполярных системах также преобладают ядра N-полярности которые появляются первыми и начинают разрушаться (X_1, X_2) тогда, когда соответствующие им ядра S-полярности находятся в стадии роста. Все новые биполярные системы развились внутри треугольника, образованного тремя большими пятнами фрагментов A, D, F.

Движение пятен

На рис. 3а и 3б приведены траектории пятен в период с 11 по 18 июля 1982 г. Видно, что отдельные части группы входили в разные кинематические элементарные (КЭ). Каждый КЭ, кроме собственного направления движения, в большей или меньшей степени участвовал в общем сдвиге к экватору.

Лидирующая часть группы двигалась на запад (КЭ-I). В отдельные дни скорость этого КЭ превышала 200 м/с. Центральная часть группы (КЭ-II) двигалась к экватору. Это движение охватило разные части большого неправильного пятна. Пределы этого КЭ не ограничились размерами центрального пятна т.к. сходные траектории имели и пятна, удаленные от него. В юго-восточной части центрального пятна, в одной полутени с КЭ-II находился КЭ-III, двигавшийся на восток. В том же направлении двигался КЭ-IV, содержащий большое пятно лидирующей полярности. Новые пятна появлялись между удалявшимися друг от друга пятнами, следом за ними или в разрывах между ними.

Вспышечная активность области

По предварительным данным {9}, в АО, содержащей данную группу, наблюдалось более 240 вспышек, в том числе 2 балла 3, 13 - балла 2, 47 - балла 1. Наиболее вспышечно-активным был период 11-12 июля, когда в течение 34 часов наблюдалась одна вспышка балла 3 и 6 вспышек балла 2 (см. рис. 4). Следующий, более слабый всплеск вспышечной активности охватил вторую поло-

вину 14 июля и первую половину 15 июля. В каждый из последующих дней происходила одна вспышка балла 2 и по три-четыре балла 1. В течение 10-16 июля нами было зарегистрировано 5 двуленточных вспышек: одна балла 3 (12 июля), две балла 2 (12 и 15 июля), две балла 1 (11 и 13 июля) и более 15 компактных вспышек.

Для изучения распределения вспышек по АО мы нанесли вспышки по их координатам {9} на гелиографические карты. Изучение таких карт показало, что 10 июля вспышки концентрировались в северных районах D и в районах E, 11 и 12 июля в районах между пятнами D и B, 13 июля в южных районах B. 15 июля зона вспышек охватывает районы F и A, которые до сих пор показывали малую вспышечную активность. 17 июля в центральных частях (D и B) вспышечная активность уменьшилась и вспышки преобладали в районах A и F. Как уже отмечалось во фрагменте A в этот период образовалась система X_4 , а в F-цепочка неустойчивых пятен и пор.

Вспышечная активность области, по-видимому, связана с образованием биполярных систем, т.к. вблизи них часто находятся наиболее быстрые эмиссионные детали вспышек. Эти биполярные системы образовались на основной ЛРП. Максимум вспышечной активности в районах новых биполярных систем совпадает с начальной стадией развития каждой из них. Так было 10-11 июля в районе E (максимум площади пятен - 12 июля), 12 июля в районе X_1 (максимум 15 июля) и X_2 (максимум 14 июля) и 15 июля в районах X_3 и X_4 (максимум 16 июля).

В случае образования биполярных систем у основной ЛРП наблюдаются двуленточные вспышки. Когда такие системы или ядра паразитной полярности образуются вдали от ЛРП районы E, наблюдаются компактные "точечные" вспышки. Районы образования последних на магнитограммах видны как вкрапления паразитной полярности. На магнитограммах Китт Пик {9} такие вкрапления имеются на северо-западе D, в районах E и окружают полукольцом с севера район F.

Уровень вспышечной активности понижается при упрощении структуры магнитного поля и повышается при усложнении ее. Так,

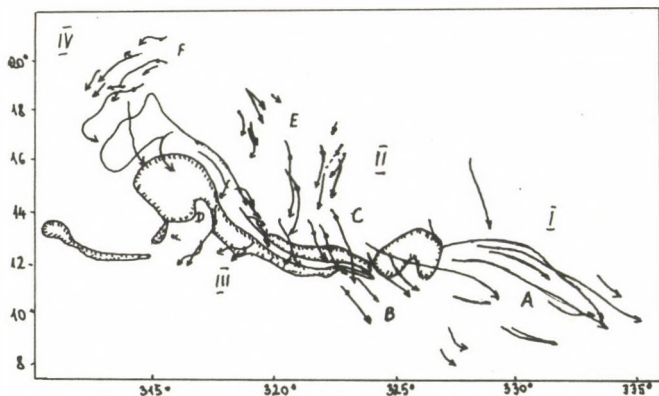


Рис. 3а.

Траектории пятен
11-18 июля 1982 г. и
контуры вспышки
12 июля, 9:33 UT.

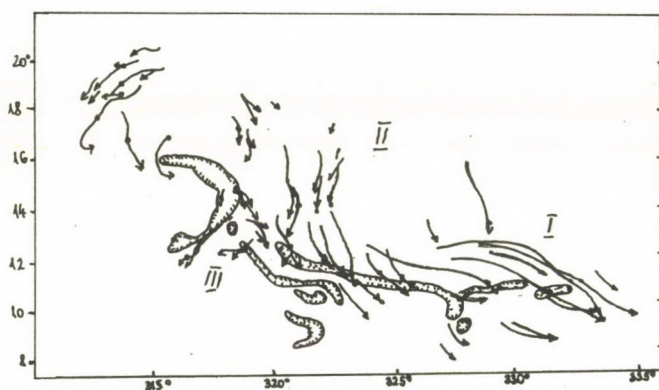


Рис. 3б.

Траектории пятен
11-18 июля 1982 г. и
контуры вспышки
15 июля, 3:12 UT.

(точкой на траектории показано положение пятна в день вспышки)

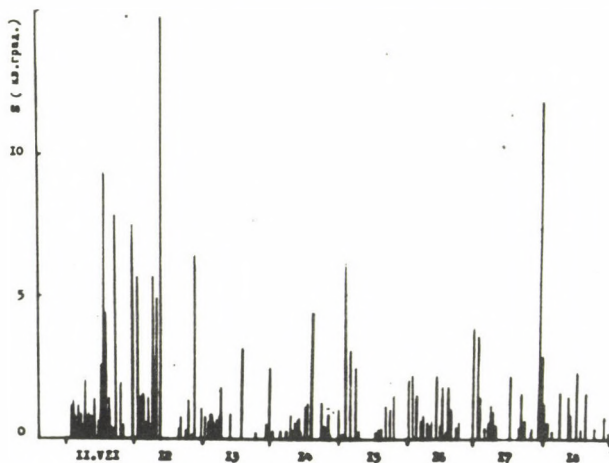
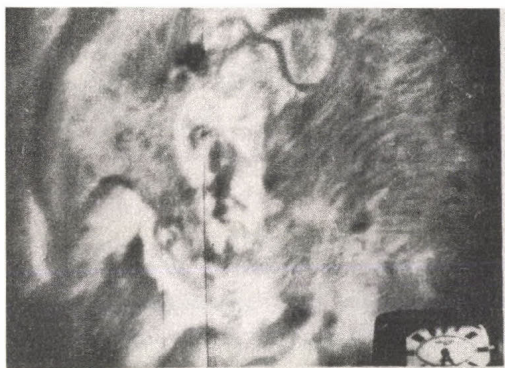


Рис. 4.

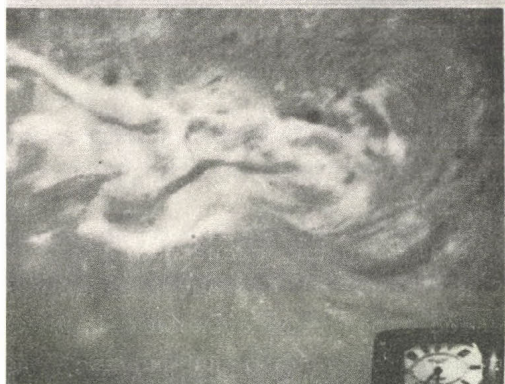
Вспышечная активность
группы в течение
11-18 июля.



a)



b)



c)

Рис. 5. $\text{H}\alpha$ -фильтрограммы A0, полученные в Ташкенте 11 (а), 12 (б) и 15 (с) июля 1982 г.

после 11 июля N-ядра в D разрушились на их месте 15 июля появились S-ядра. С новой S областью слились ранее существовавшие в этом фрагменте S-поля. Одновременно в D произошло затухание вспышечной активности. Напротив, появление 18 июля S-ядер в F сопровождалось усилением вспышечной активности в этом фрагменте.

На снимках в H_{α} (см. рис. 5) 13-15 июля в этих районах наблюдается много арочных волокон. Они видны также в районах образования новых ядер в E и вблизи X_4 . По-видимому, в этих районах также происходит всплывание нового магнитного потока.

Контуров двух мощных вспышек 12 и 15 июля нанесены на карту собственных движений пятен (рис. 3а и 3б). Обращает на себя внимание тот факт, что вспышки располагались над районами фотосферных сдвигов, происходящих как вдоль так и поперек жгутов вспышки. Наиболее яркие жгуты вспышек находились на границе между кинематическими элементами, т.е. в районах резкой смены направлений движения фотосферных потоков, где в дальнейшем происходили разрывы пятна.

В то же время скорость движения пятен в районе вспышек не превысила скорости движения пятен вдали от них. Не было общего увеличения скорости движения пятен и в дни с повышенной вспышечной активностью. Аналогичное явление отмечается и в {10}.

Как показывают отпечатки фильтрограмм (см. рис. 5), общий вид этих и других дуэнточных вспышек в изучаемой области позволяет отнести их к разряду гомологичных. Такие вспышки нередко наблюдаются в группах с большими собственными движениями пятен {11,12}. Однако совмещение рис. 3а и 3б не показывает совпадения контуров вспышек. Отклонение от более полной гомологичности объясняется изменениями, происшедшими в структуре группы с 12 по 15 июля из-за движения пятен. Общий меридиональный дрейф привел к сдвигу к экватору линии раздела полярностей, что привело к сдвигу по широте лент вспышек. Кроме того, область вспышки 15 июля продвинулась на запад, что связано с быстрым движением в этом направлении КЭ-I и заполнением разрыва между КЭ-I и КЭ-II новыми пятнами.

Выводы

1. Группа пятен состояла из отдельных фрагментов, первоначально находившихся в одной полутени, но развивавшихся независимо.

2. Область появления новых биполярных систем в полутени группы смещалась с востока на запад.

3. Хвостовые компоненты новых биполярных систем появлялись тогда, когда их лидеры уже начинали разрушаться.

4. Связь вспышечной активности с развитием группы пятен проявлялась в следующем:

а) вспышки возникали в районах новых биполярных систем. В соответствии с перемещением области образования новых пятен зона вспышечной активности расширялась от центральных районов группы к периферийным.

б) развитие новых биполярных систем вблизи ЛРП сопровождалось появлением двуленточных вспышек, а вдали от ЛРП - компактных "точечных" вспышек.

в) наиболее яркие узлы вспышек располагались на границах между кинематическими элементами.

Л и т е р а т у р а

- {1} Giovanelli, R., *Ap. J.* 89. 555, 1939
- {2} Слоним, Ю.М., *Труды Ташкент. Астрон. Обс. в. сер. 2.* 1957
- {3} Гопасюк, С.И., Огирь, М.В., Северный, А.Б., Шапошникова, Е.Ф., *Изв. КрАО.* 22 15, 1963
- {4} Sivaraman, K.R., *Solar Phys.* 6. 152, 1969
- {5} Саттаров, И., *Астрон. Ж.* 60. 350, 1983
- {6} Martres, M.T., Michard, R., Soru-Iscovici, I., Tsap, T., *IAU Symp.* 35., 318, 1968
- {7} Огирь, М.В., Шапошникова, Е.Ф., *Изв. КрАО.* 34. 272, 1975
- {8} Огирь, М.В., *Изв. КрАО.* 43. 165, 1971
- {9} *S.G.D. Prompt rep. No. 456, 457, Part I.* 1982
- {10} Ишков, В.И., Коробова, З.Б., Могилевский, Э.И., Старкова, Л.И., *Физ. солн. акт.* 48, 1980
- {11} Коробова, З.Б., Ишков, В.И., Могилевский, Э.И., *Физ. солн. акт.* 3, 1976
- {12} Могилевский, Э.И., *FCM-SMY Crimean Workshop.* 2. 151, 1981

ЭВОЛЮЦИЯ СТРУКТУРЫ, СОБСТВЕННЫХ ДВИЖЕНИЙ И НЕКОТОРЫХ
ОСОБЕННОСТИ БОЛЬШИХ ВСПЫШЕК В МОЩНОЙ ВСПЫШЕЧНО-АКТИВНОЙ
ОБЛАСТИ ИЮНЯ-ИЮЛЯ 1982 г.

В.Н. И Ш К О В[†], З.Б. К О Р О Б О В А^{*}

Э.И. М О Г И Л Е В С К И Й[†]

[†] ИЗМИРАН, Троицк

^{*} Астрон. Инст., Ташкент

Абстракт:

Проведен предварительный анализ эволюции мощной вспышечно-активной области (№203 по С.Д.) в июне-июле 1982г. Детально определены собственные движения в этой группе в течение трех оборотах Солнца, во время которых выделяются кинематические элементы в центральной, головной и хвостовой частях группы. Рассмотрено эволюционное распределение местоположений вспышек от оборота к обороту. Рассмотрена возможная полуколичественная схема эволюции рассматриваемой активной области.

EVOLUTION OF STRUCTURE, PROPER MOTIONS AND
SOME PECULIARITIES OF LARGE FLARES IN THE ACTIVE REGION
OF JUNE-JULY 1982

V.N. ISHKOV[†], Z.B. KOROBVA^{*}, E.I. MOGILEVSKIJ[†]

[†] IZMIRAN, Moscow

^{*} Astron. Inst., Tashkent

Abstract:

A preliminary analysis of a large active region of June-July 1982 with high flare activity (SD No 203) is given. The sunspots proper motions during three solar rotations were determined. Some kinematical elements in the preceding, central and following parts of the groups were found. The evolution of the flares distribution in three rotations is shown. A probable semiquantitative scheme of the active region evolution is discussed.

(1). В июне-июле 1982 г. в северной полусфере ($\varphi \approx 8^\circ \div 18^\circ \text{N}$, $L \approx 305^\circ \div 325^\circ$) достигла наибольшего развития вспышечно-активная область с очень динамичной группой пятен (группы пятен №№ 203- в июне; 228-229 - в июле; 261 - в августе по "СД"). Площадь этой группы в июле достигла рекордной величины за последние два солнечных цикла: $S_{\text{M}}^{\text{P}} \approx 3300$ ед. В период май-август в этой АО зарегистрировано только умеренных и больших рентгеновских вспышек 128 балла М и 11 балла Х, причем самые мощные произошли в июле (9,12-го и др.). Мы располагали достаточно полными наблюдениями (особенно за июль месяц): получали почти ежедневно ряд серии H_{α} фильтрограмм, ежедневные карты магнитных полей на башенном телескопе с магнитографами в линиях Ва II и Fe (одновременно), фотогелиограммами.

Настоящее сообщение носит предварительный характер, т.к. обработка и особенно анализ материалов столь сложной АО нами, по сути, еще только начаты.

(2). В отличие от вида группы в мае (группа № 171 по "СД", правильное пятно ведущей полярности и мелкие пятна и поры и соседняя группа пятен) в июне группа появилась из-за Е края в виде очень большого сложного многоядерного пятна " δ " магнитной конфигурации и ряда пятен и пор, которые располагались по большой дуге вдоль линии смены магнитной полярности (NL). Характерно, что большинство ядер в группе были вытянуты вдоль дуги (однозаходной спирали), в продолжении которой располагалось (как в июне так и в июле) уходящее к большим широтам большое волокно, которое чутко отражало вспышечные явления в группе {1}.

Из построенной карты собственных движений пятен в этой группе в июне 1982 г. (рис.1.) видно, что выделяются три кинематических элемента: КЭ-Е - головной, КЭ-Ф - вредный и КЭ-Г - хвостовой частей группы, в КЭ-Е пятна ядра двигались к экватору и на запад (средняя скорость в отдельные дни достигла 60 м/сек). В КЭ-Ф - также преобладал западный дрейф и смещение к экватору. Особый интерес представлял район с координатами $\varphi \approx 11^\circ \text{N}$, $L \approx 312^\circ$. В этом месте, где отмечались глубокие изгибы линии раздела магнитной полярности (NL), попадавшие туда в различные

дни пятна разрушались. В хвостовом и более высокоширотном КЭ-G пятна двигались вдоль дуги к полюсу, хотя часть пятен, близких к КЭ-F имели также тенденцию смещения к экватору и на запад.

Как в июне так и в июле-августе отмечалось общее смещение ($\Delta L \approx 10^\circ$ за оборот) на запад всей группы; это указывало на существование общего устойчивого подфотосферного потока, превышавшего размеры группы.

В июле, как это следует из карты (рис.2.), выделяются также головная, срединная и хвостовая части с четырьмя кинематическими элементами. Лидирующая часть группы (КЭ-A) двигалась преимущественно на запад (средняя скорость движения пятен доходила до 200 м/сек). В головной части находились также новые пятна, которые появились в июне-июле на невидимой части Солнца. Весьма сложной по структуре и кинематике была срединная часть группы. В очень сложных, тесно расположенных многоядерных пятнах (некоторые - " δ " конфигурации) можно было выделить два кинематических элемента: КЭ-B - с преобладанием движений вдоль NL в направлении на SW и КЭ-C - с движением ядер S-полярности к востоку. В хвостовой части (этих больших пятен в июне не было) наблюдались преобладающие смещения к SE.

Пятна (также как и NL) располагались также по большой спрямленной дуге, но наклон ее к экватору существенно изменился: произошел ее поворот против часовой стрелки. Эта тенденция (поворот к экватору) сохранилась и в августе (рис.3.). Деформация общей структуры группы в июле достигла такого положения, что пятна и NL образовали уже двухзаходную спираль ("S" - образного вида).

Следует еще отметить, что характерной особенностью эволюции группы (особенно в июле) - это быстрое заполнение разрывов в полутени пятна, возникавших из-за движений ядер, новыми ядрами и "клочками" полутени.

(3). Местоположения вспышек, характеризуя наиболее активные места в группе, в процессе эволюции заметно изменялись. На рис. 4 а, д очерчены места концентрации вспышек в июньском и июльском оборотах Солнца. В июне очаги вспышек последовательно смещались от центральной части (в период 12÷16 июня) к северо-

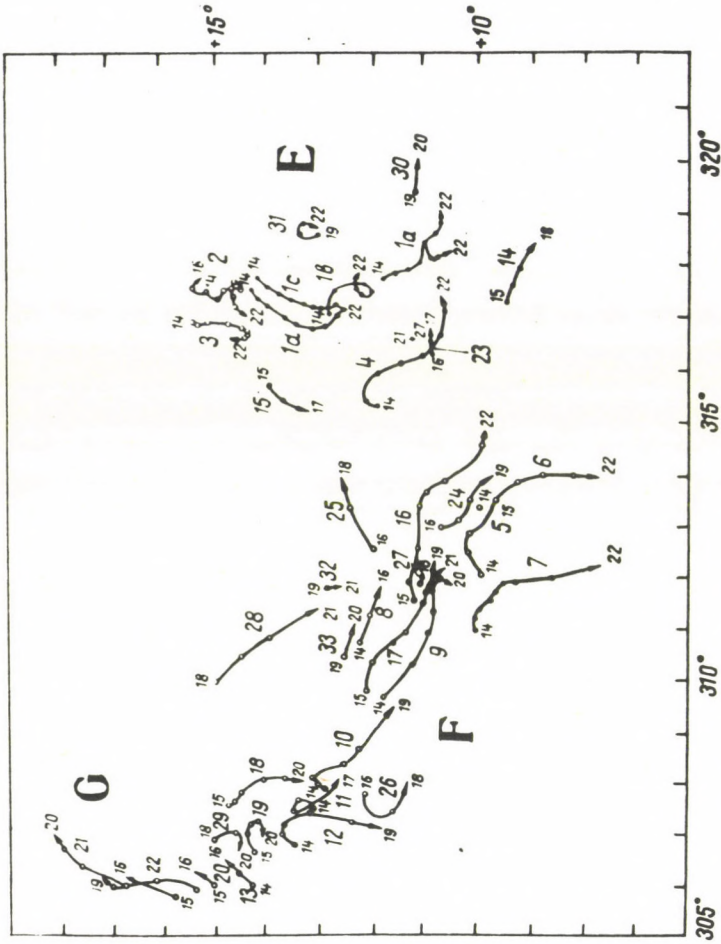


Рис. 1. Собственные движения пятен в группе НР 18422 14-22 июня 1982 г.

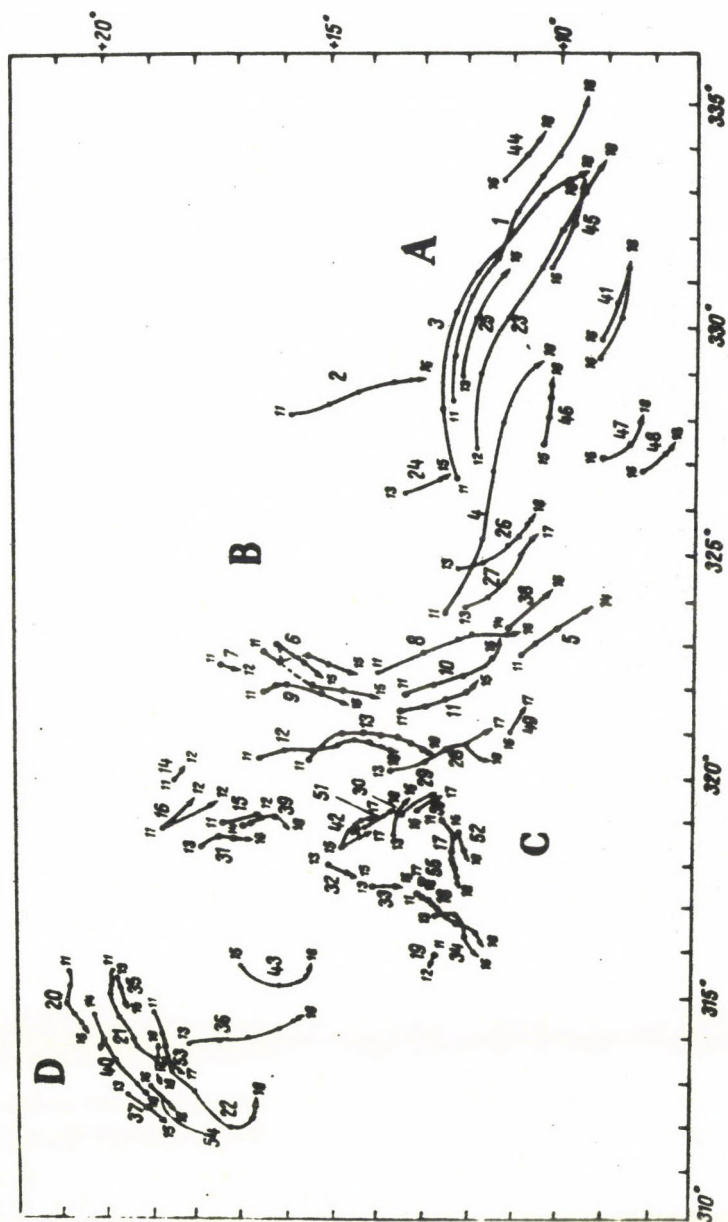


Рис. 2. Собственные движения пятен в группе VBR 18474 11-18 июля 1982 г.

-востоку (и к волокну) и на запад, где основное магнитное поле N-полярность взаимодействовало с полем S полярности. Следует подчеркнуть, что отмеченное выше место "гибели" попавших туда пятен, выделяется также тем, что в период 20-22 июня, когда начался переход от однозаходного к двухзаходному расположению пятен, резко увеличилось число вспышек.

В июле при выходе из-за E края основные и самые большие вспышки (9, 12-го и т.д.) концентрировались в центральной части АО. Но примерно с 17 июля вспышки появились преимущественно в E части группы вблизи волокна и в головной части группы, где у NL были перегибы. Смещение очагов вспышки также видно на примере протекания очень больших вспышек. Так (см. рис. 5d) мощная двухленточная вспышка 12 июля на первом этапе наблюдалась в центральной и хвостовой частях группы и затем появились вспышечные ленты и резкая активизация волокна уже за пределами самой группы. Более полное рассмотрение особенностей бывших вспышек в этой АО - предмет нашего дальнейшего исследования.

(4). Рассматриваемая нами АО может позволить выявить некоторые особенности эволюции, которые необходимы для построения будущей количественной модели вспышечно-активных областей. Образование и развитие АО можно рассматривать как своеобразный процесс самоорганизации магнитоплазменных элементов в структуре, характерные для АО (петли, волокна, арки и т.д.). Попытка обосновать такой синергитический подход в гелиофизике сделан в работе одного из авторов [2]. Образование и эволюция магнито-плазменных структур можно представить следующей системой уравнений:

$$\frac{\partial m_i}{\partial t} = F_i(m_1, \dots, m_n, \vec{r}, t) + \operatorname{div} \sum_j D_{ij}^L \nabla m_j - \operatorname{div} m_i \sum_j D_{ij}^{NL} \nabla m_j .$$

Здесь: m_i - исходные элементы магнитоплазменных структур с координатами \vec{r} , t - время; D^L и D^{NL} - соответственно линейный и нелинейный коэффициент диффузии. Нелинейная функция F определяет мультипарные взаимодействия между элементами m_i . Эта система уравнений, выражая закон сохранения, определяет структуризацию магнитоплазменных элементов. В результате нелинейных

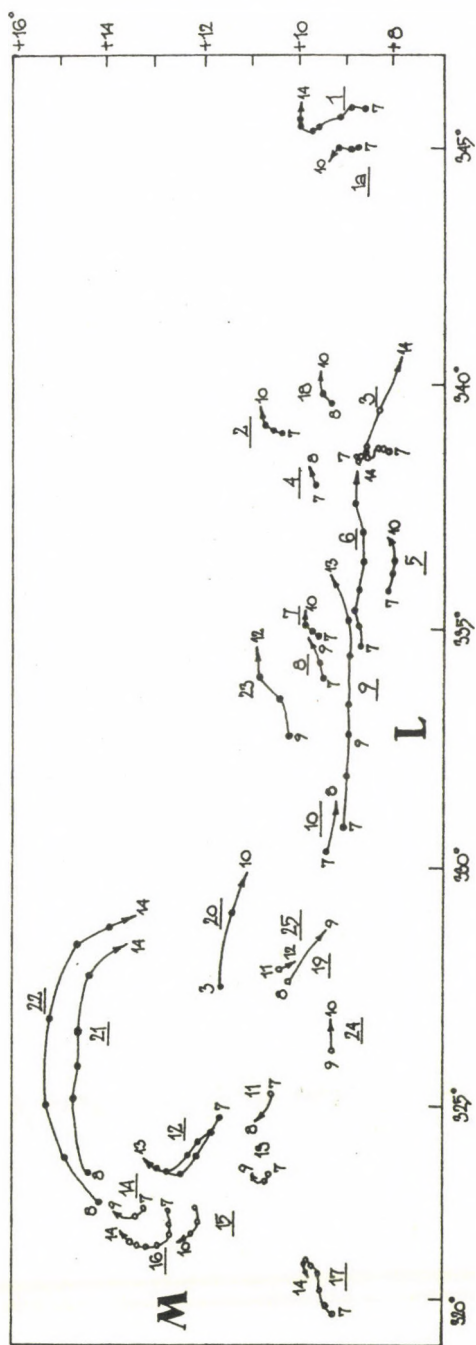


Рис. 3. Собственные движения пятен в группе BVR 18511 7-14 августа 1982 г.

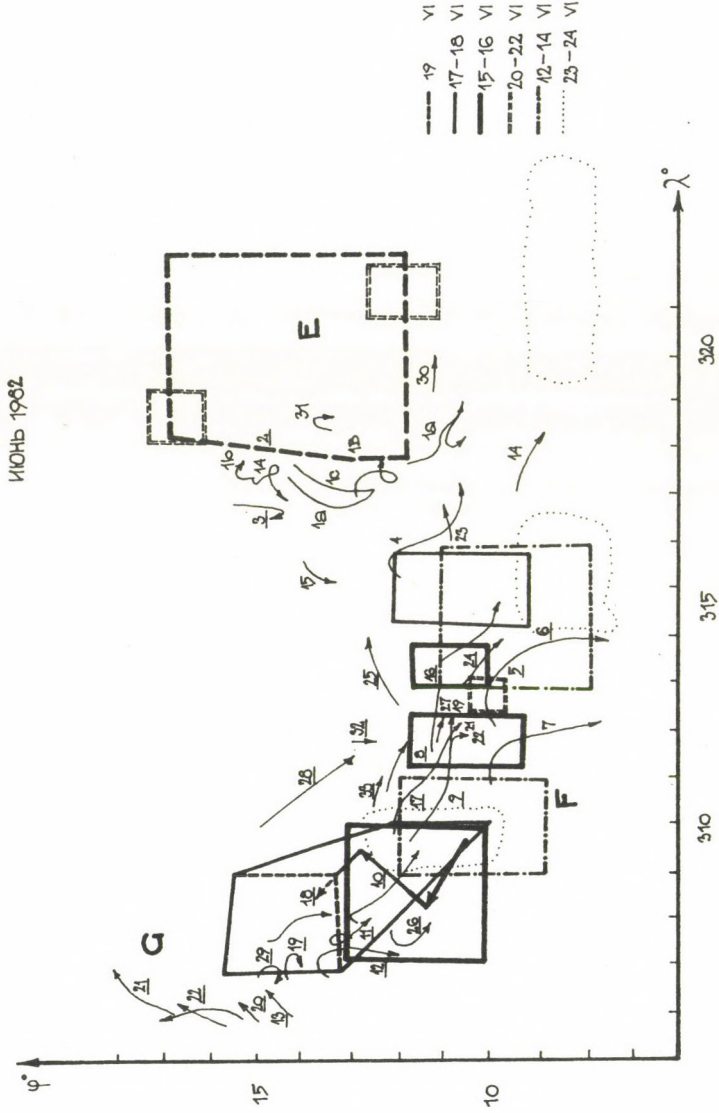


Рис. 4а.

ИЮЛЬ 1962

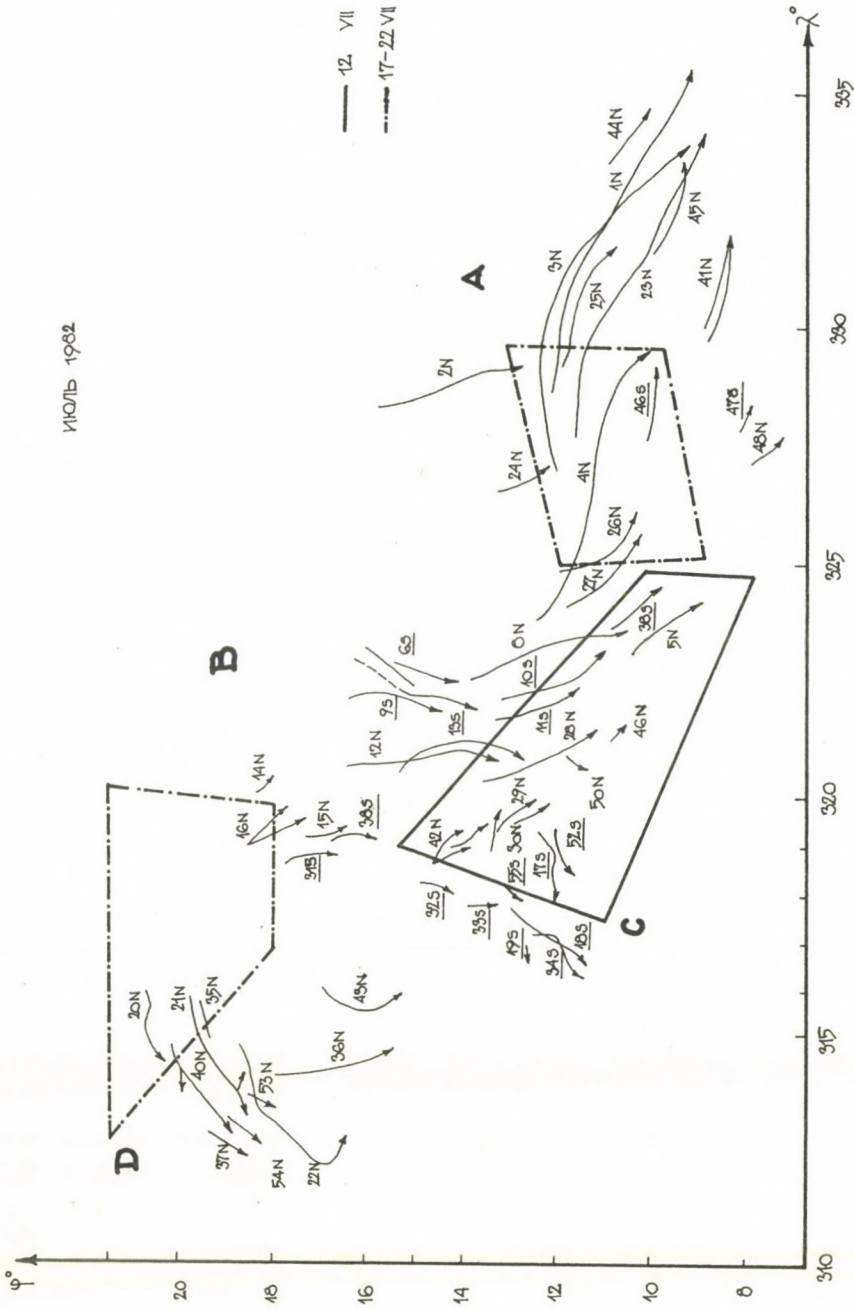
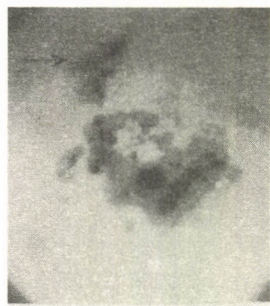


Fig. 46.



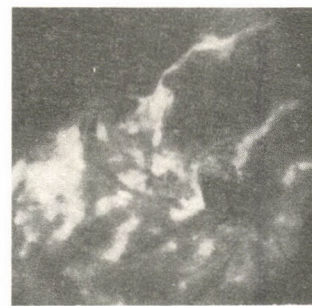
15.06.82 12:54 UT
H α + 0.5Å



18.06.82 13:00 UT
H α - 0.5Å



19.06.82 H α 4:47 UT
малая вспышка



21.06.82 H α 4:23 UT

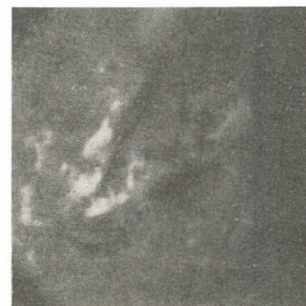
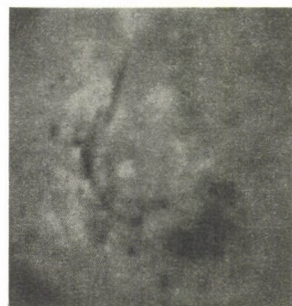
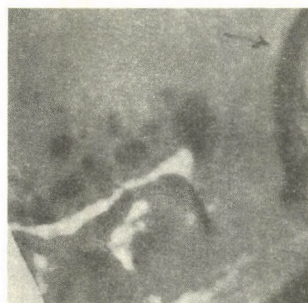
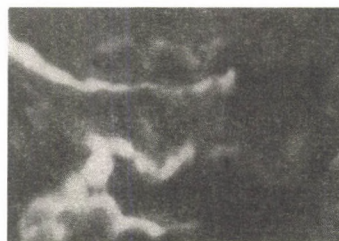
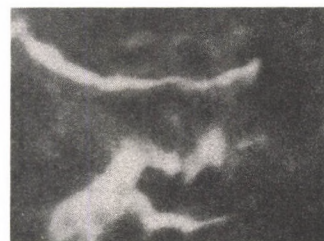


Рис. 5а. Эволюция вспышечно - активной области в июне 1982 г.
Развитие общей структуры А0 с переходом от однозаходной к двухзаходной спирали.

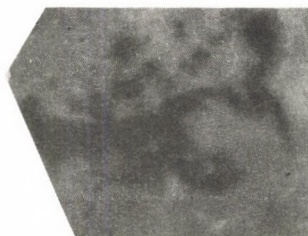
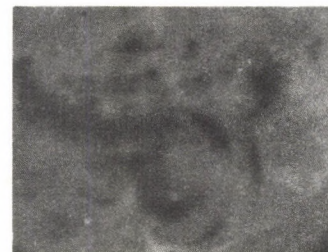
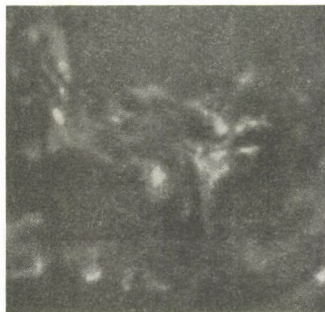
10:05 UT $H\alpha+1.0\text{\AA}$

арки над "разрушенным"
волоком при развитии
вдоль канала волокна
второй части двухлен-
точной вспышки

365

10:19 UT $H\alpha$ 11:37 UT $H\alpha$ 11:46 UT $H\alpha$

Системы арок AFS-a

11:37 UT $H\alpha+1.5\text{\AA}$ 11:46 $H\alpha+1.0\text{\AA}$ 

14:40 UT $H\alpha$
Системы послемаксимальных
арок типа AFS-b

Рис. 56. Фрагменты развития большой ($I=2$) двухленточной вспышки 12 июля 1982г.

взаимодействий и потока элементов (два последних члена справа) образуются устойчивые подсистемы, с уменьшением числа "свободных" элементов и параметров порядка (переход от хаоса к порядку).

Однако в этой схеме фигурируют близкодействующие электромагнитные взаимодействия, при которых могут возникать и эволюционировать отдельные структуры в АО. Если рассматривать следующую дискретную иерархическую структуру (активная область, комплекс АО, группы пятен), то следует учесть дальнедействующие (полевые) силы, природа которых нам пока неизвестна. В этом случае можно попытаться воспользоваться моделью образования структур в неоднородных нелинейных колебательных *активных средах* [3]. В нашем случае такой активной средой является конвективная зона, где в результате турбулентного динамо, диссипативных процессов и локального подтока энергии формируется АО (группы пятен и т.д.), отражение которого наблюдается прежде всего в фотосфере. В качестве такой *автоволновой* модели может служить спиральная волна с ревербератором (волновозбудителем) [3], которая описывается нелинейным параболическим уравнением Колмогорова-Петровского-Пискунова.

Из приведенного выше феноменологического описания развития АО следует, что ее общую структуру можно рассматривать как отражение неподвижной (точнее с медленным поворотом против часовой стрелки) спиральной волны. В июне вдоль одноходового спирального волнового фронта группировались пятна. В конце июньского периода наблюдений, а затем это особенно четко оформилось в июле, в центральной части группы проявился выход дополнительной энергии (это отразилось в концентрации и в характере собственных движений пятен в группе в этом месте вспышек), что привело к переходу к двухзаходной спиральной автоволне. Известно, что для многих вспышечно-активных областей также характерна особенность в развитии вспышек в центральной ее части: для вытянутых по долготе (например, АО в августе 1979 г., комплекс мая 1981 г. и т.д.) и для компактных групп (например, август 1972 г. и др.). Существование спиральных структур в АО как целое и в отдельных ее частях при наличии волновозбудителя

в центре спирали (например, поворот большого пятна и т.д.) можно обнаружить во многих случаях, например, по расположению NL и волокна. Установление степени соответствия наблюдаемых спиральных структур в АО автоволновым процессам – предмет последующего изучения. Смысл предлагаемого подхода в понимании эволюции АО как отражение автоволнового процесса в конвективной зоне состоит в том, чтобы при этом найти количественное описание эволюции и выявить природу сил, формирующих структуру АО.

Л и т е р а т у р а

- {1} Шилова, Н.С., Старкова, Л.И., *Физ.солн.акт.* 99, 1983
- {2} Могилевский, Э.И., *Физ.солн.акт.* 56, 1983
- {3} Сб. *Автоволновые процессы в системах с диффузией*, ИФФ АН СССР, Горький, 1981

RESULTS OF VECTOR MAGNETOGRAPHIC MEASUREMENTS
IN THE ACTIVE REGION SD 228/229 ON 15 JULY 1982

G. B A C H M A N N, A. H O F M A N N, J. S T A U D E
"Einsteinurm" Solar Obs., Potsdam

Abstract:

We first present measurements of vector magnetic fields in an active region of 15 July 1982 obtained with the new code-impulse magnetograph working in the wing of FeI 5250 line. Linear polarization down to 0.004 corresponding to transverse magnetic fields of about 150 G has been taken into account. The direction of the transverse magnetic fields is compared with dark chromospheric structure elements in H α filtergrams and with the contours of sunspots obtained by means of a heliogram. For long-lived stable structures, such as the central part of the zero-line filament or systems of fibrils and threads, the correspondance is good, in contrast to short-lived. Also in regions with weak magnetic fields no correspondance is found. This probably highlights the errors in our results, which are of the order of 0.004.

РЕЗУЛЬТАТЫ НАБЛЮДЕНИЙ ВЕКТОРА МАГНИТНОГО ПОЛЯ
В АКТИВНОЙ ОБЛАСТИ С.Д.228/229 15 ИЮЛЯ 1982 Г.

Г. БАХМАНН, А. ХОФМАНН, Й. ШТАУДЕ
Солн.Обс. "Эйнштейнтурм", Потсдам

Абстракт:

15 июля 1982 были получены с новым кодовоимпульсным магнитографом, работающим в крыле линии Fe 5250, первые результаты об измерениях векторных магнитных полей в активной области. Была рассмотрена линейная поляризация до предела 0.004, которая соответствует 150 Г. Направление поперечного поля сравнивается с темными хромосферными структурными элементами, видимыми на H α фильтрограммах, и с контурами пятен, полученными с помощью гелиограммы. Для долгоживущих, стабильных структур таких как центральная часть волокна вдоль нулевой линии продольного поля или систем фибрилл и нит существует хорошее соответствие, в противоположность короткоживущим. Также в районах слабых магнитных полей соответствия не существует. Возможно что это указывает на ошибки в наших результатах, которые порядка 0.004.

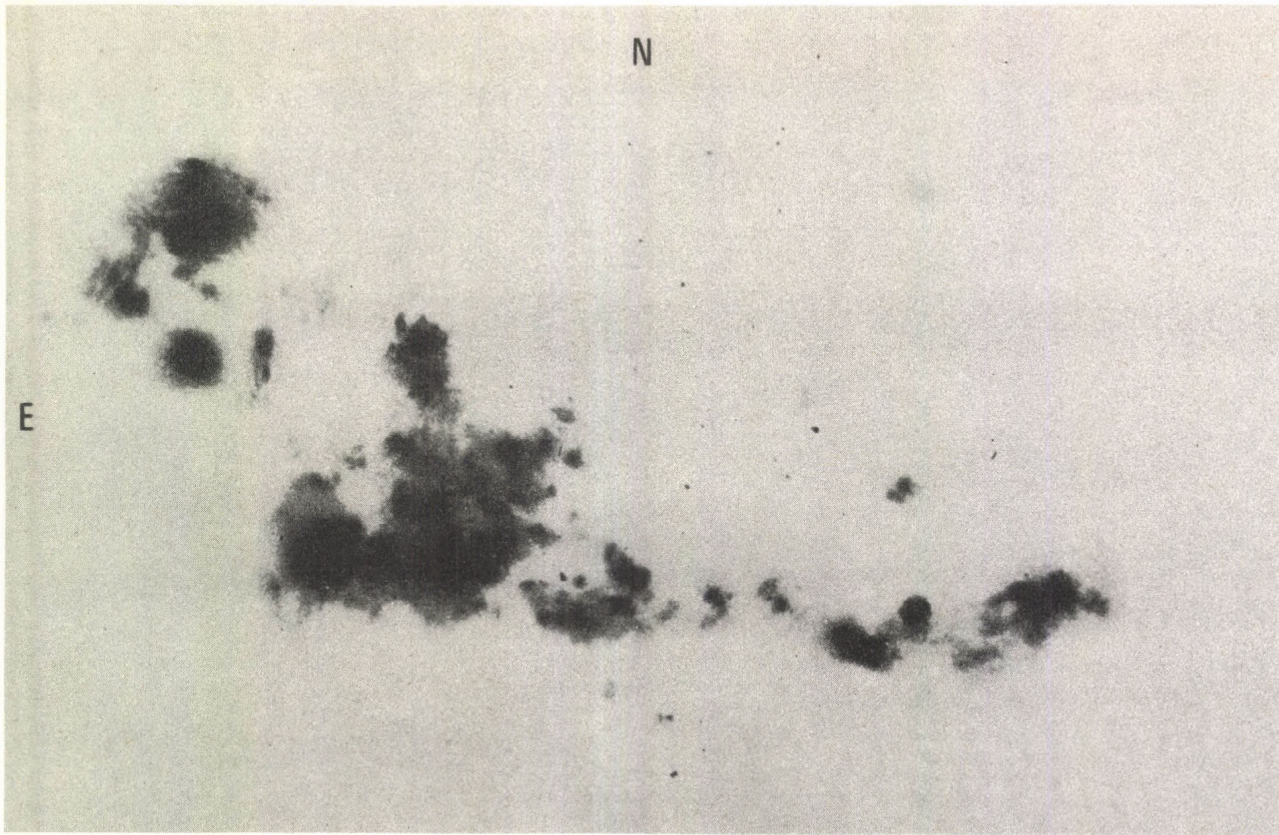
1. Observations

A new code-impulse vector magnetograph was used for measurements of solar magnetic fields in selected active regions in July 1982. The optical scheme of the analyzer is the same as that given by Stepanov et al.{3}.

Measurements of the Stokes parameters, of the brightness in continuum and line core, and of the Doppler shift are recorded on magnetic tape, while the active region is scanned with an aperture of about 3.6 arcseconds and an integration time of 0.03 seconds. The Stokes parameters are measured in the red wing of the spectrum line FeI 5250.2 Å. An exit slit of 120 mÅ selects the light and a photomultiplier EMI 9502 B converts it into electric signals.

The calibration of the whole instrumental system is carried out by means of polarizer and quarterwave plate in front of the first coelostat mirror before and after each scanning of an active region. Eight equidistant different position angles are used to calibrate for linear polarization and also eight for circular polarization. This allows the elimination of differences in the illumination of the magnetograph. After this the intensity crosstalk into the magnetic signals is recorded without polarizing optics. For the complete calibration procedure about 10 minutes are necessary.

By means of the calibration measurements information is obtained on the sensitivity of the magnetograph and on the instrumental polarization of the tower telescope, which depends on time. During the scanning of an active region the linear polarization caused by the telescope is compensated for by means of a tilted glass plate in front of the spectrograph. Without compensation the sensitivity of the magnetograph of about 0.001 would not be realizable. The results presented are obtained in the active region *SD* 228/229, which on 15 July had the mean position of N12 W02. We use a magnetogram recorded at 13:22 to 14:13 UT, a heliogram of 05:34 UT and a H α filtergram of 07:33 UT.



371

Fig.1. Sunspot groups SD 228/229 on 15 July 1982, 05:34 UT.
Photographic positive from heliogram obtained with the Einstein tower telescope.



Fig. 2. Photographic positive from $H\alpha$ filtergram of the same active region at 07:33 UT obtained with the chromospheric telescope of the Potsdam Solar Observatory.

373

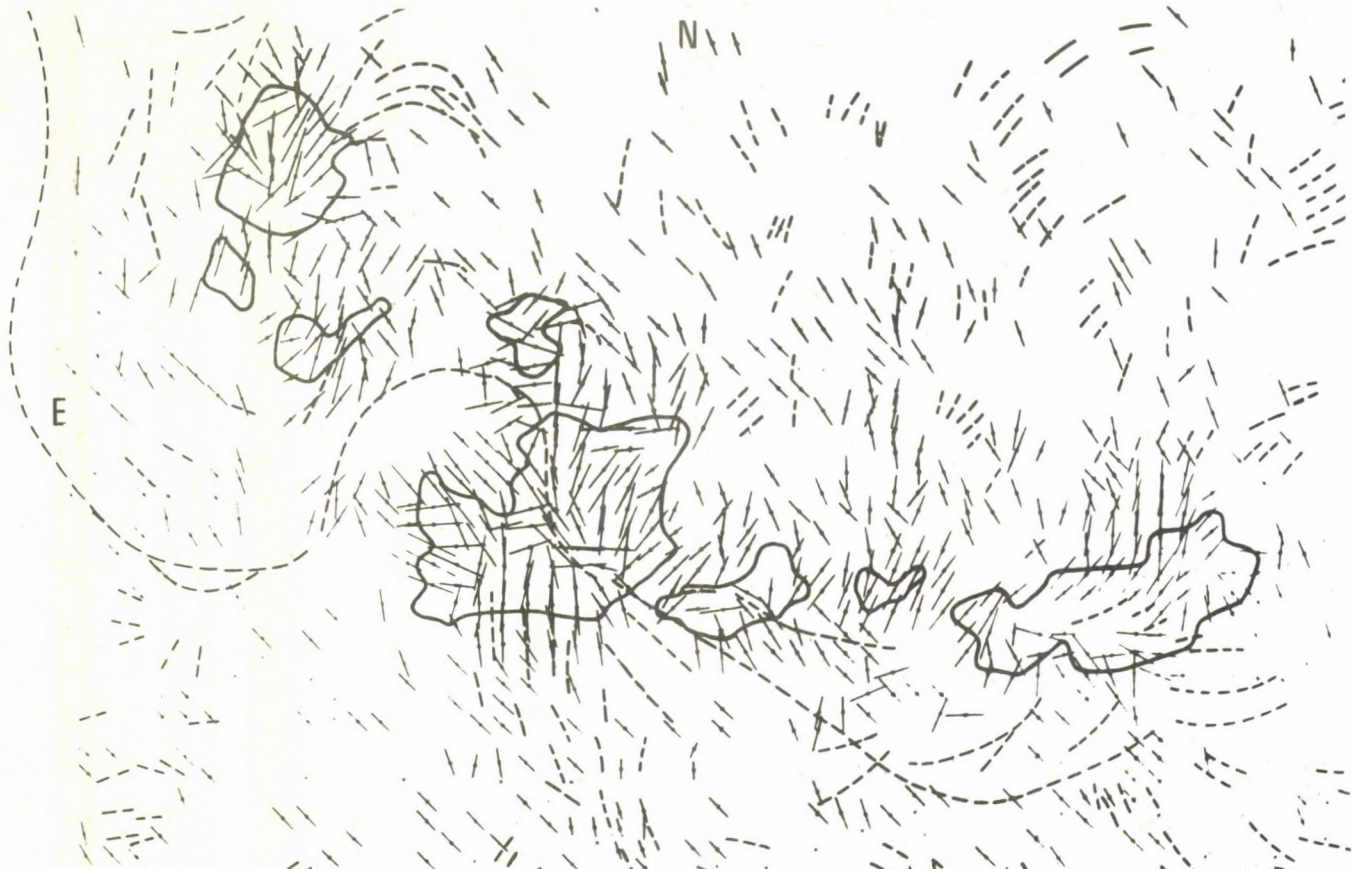


Fig. 3. Contour map of sunspots in the active region, azimuth and strength of the transverse magnetic field in logarithmic scale (line segments; points mark the position of the measurement), and directions of dark chromospheric structure elements (dashed lines).

15 July 1982

 H_{\parallel}

1322-1413 UT

N

N12 W02

270 x 390"

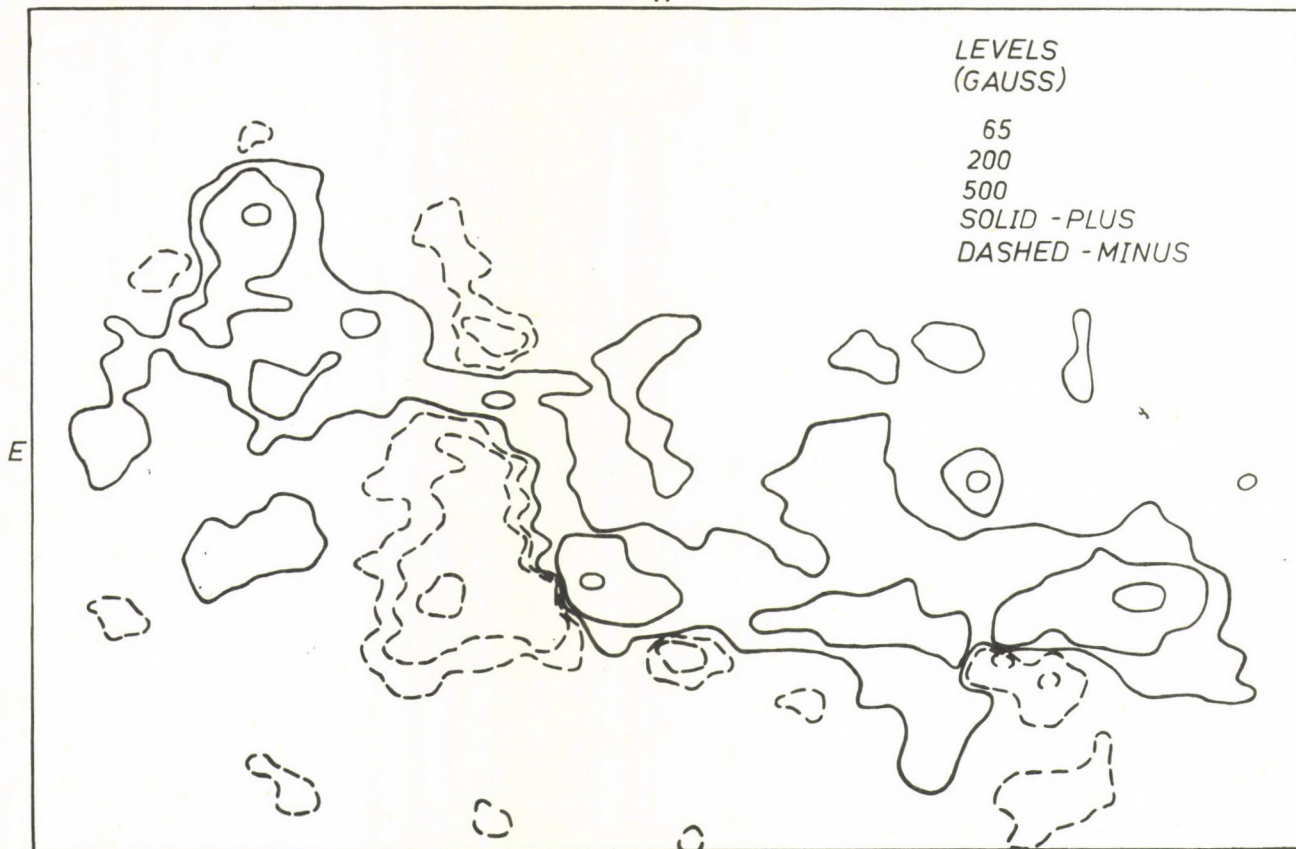


Fig. 4. Map of the longitudinal magnetic field in the active region SD 228/229 obtained in the FeI line 5250.2 Å.

2. Results

By means of the calibrations we calculated the Mueller matrix B of our system. B transforms the true Stokes vector S into the observed one S' corresponding to $S' = B \cdot S$. To the calculated matrices B a linear least square fit is applied to attain more correct results. After this the elements of the matrix should be correct within ± 0.005 .

In each scan across the active region we selected only some positions with larger amounts of linear polarization. The correction of the measurements is carried out with the inverse matrix to B , but taking the compensation by the tilted glass plate into account. Linear polarizations are found between 0.001 and 0.072, where the lower limit is determined by the noise. In future, smoothing of data by computer should diminish the detection limit of polarization to about 0.0001.

The limiting polarizations 0.001 and 0.072 correspond to transverse magnetic fields of about 100 and 700 G, respectively, where the influence of scattered light is not yet taken into account. Because this has its maximum influence in sunspots, corrections for scattered light should therefore shift the upper limit upward. The lower limit is also influenced by errors in the matrix B .

Fig.1 shows the photoheliogram from which the contours of the sunspots have been determined. Relative to these contours we present the transverse magnetic field in a logarithmic scale in Fig.3 and the azimuth in comparison with the directions of dark chromospheric structure elements as shown in Fig.2. From the magnetographic measurements the isogauss map of the longitudinal magnetic field shown in Fig.4 was also obtained.

At the boundaries of umbrae respective penumbrae the field direction is, in most cases, radially outward. Within the sunspot groups the zero-line filament shows the same direction as the transverse magnetic field. The same behaviour is to be seen in dark structure elements westward of the large sunspot in the NE part of the AR and southward of the large

sunspot in the SE part.

In contrast, the correlation with short-lived loops in the SW part and also with spicule bushes is worse.

Already many years ago it was suggested by Foukal {1} and Zirin {4} that dark chromospheric structures follow the field lines deeper in the atmosphere when the transverse field is strong, but higher in the atmosphere when the field is weak. Our result gives clear evidence of these earlier suggestions. Similar results have recently been found with the vector magnetograph of the Marshall Space Flight Center {2}, too. The influence of proper motions of sunspots in connection with transverse fields is very interesting and should be investigated in more detail.

R e f e r e n c e s

- {1} Foukal, P., Morphological relationships in the chromospheric H α fine structure, *Solar Phys.*19. 59, 1971
- {2} Hagyard, M. J., Cumings, N. P., West, E. A., Smith, J. E., The MSFC vector magnetograph, *Solar Phys.*80. 33, 1982
- {3} Stepanov, V. E., Grigor'ev, V. M., Kobanov, N. I., Osak, B. F., Electro-optic analyzer of polarization with code-pulse control, (in Russ.) *Issl. SibIZMIR*, 37. 147, 1975
- {4} Zirin, H., Fine structure of solar magnetic fields, *Solar Phys.*22. 34, 1972

DETERMINATION OF THE ACTIVE REGION MAGNETIC FIELD STRUCTURE
USING VECTOR-MAGNETOGRAPHIC MEASUREMENTS

V.M. G R I G O R' E V, B.F. O S A K, V.L. S E L I V A N O V
SibIZMIR, Irkutsk

Abstract:

Some methodical questions concerning magnetic field vector observations in solar active regions are discussed. The observation results on the magnetic field configuration of the single sunspot of 19 May 1983 (E24, S27) and of the leading sunspot in the active region of 24 June 1983 (W08, N17) are given.

ОПРЕДЕЛЕНИЕ СТРУКТУРЫ МАГНИТНОГО ПОЛЯ АКТИВНЫХ ОБЛАСТЕЙ
ПО ИЗМЕРЕНИЯМ НА ВЕКТОР-МАГНИТОГРАФЕ

В.М. ГРИГОРЬЕВ, Б.Ф. ОСАК, В.Л. СЕЛИВАНОВ
СИБИЗМИР, Иркутск

Абстракт:

Обсуждаются методические вопросы наблюдения вектора магнитного поля в активных областях на Солнце. Приводятся результаты наблюдений конфигурации магнитного поля одиночного пятна за 19.05.83 (E24, S27) и ведущего пятна в активной области за 24.06.83 (W08, N17).

It is known that in the past decade the development efforts received by vector-magnetographs and observations with them have been substantially reduced. This was occasioned by a variety of almost insurmountable difficulties, namely the need to take into account instrumental polarization and scattered light as well as the complexity of the interpretation of magnetographic observations due to the desired accuracy of allowing for the inverse Zeeman effect in the spectral line profile.

For the SibIZMIR vector-magnetograph described by Stepanov et al. [1], investigations were carried through and a technique developed for solving these two questions.

An analysis of the errors within the electro-optical modulator of the magnetograph completed by Grigoryev and Selivanov [3] showed that for magnetographs with a square modulation the influence of instrumental polarization is substantially smaller than that for magnetographs with sinusoidal modulation while the instrumental miscentering effect of the line (see, e.g. [4]) is negligible and it is possible to eliminate it completely.

Taking into account the instrumental polarization and calibration of the magnetograph by determining an instrumental matrix of the instrument by imposing a known polarization at the telescope entrance [2] and by a subsequent correction for magnetographic data matrix. As a result, the magnetic field parameters are calculated from the equation:

$$S' = A \cdot S = A \cdot I \cdot \begin{pmatrix} 1 \\ \varphi(H, \gamma) \cos 2\chi \\ \varphi(H, \gamma) \sin 2\chi \\ f(H, \gamma) \end{pmatrix}$$

where $S=(I, Q, U, V)$ is the Stokes vector of emission (dashes denote the observed Stokes-vector to distinguish it from the true one), H is the magnetic field strength, γ is an angle between the magnetic field strength vector and the line of sight, χ is the magnetic field vector azimuth in the plane of projection, and $f(H, \gamma)$, $\varphi(H, \gamma)$ are the calibration curves for a lon-

gitudinal and a transverse component of magnetic field, calculated for a magnetosensitive spectral line using a given model of the solar atmosphere.

Scattered light is taken into account following a method proposed by Bachman et al. [1]. However, we do not record an exact scattering function but make only a crude estimate of the fraction of scattered light from the surrounding photosphere in a sunspot by comparing the "umbra-photosphere" contrast with a true one (see, e.g. [6]).

A portion of solar image is scanned with a scanning device controlled by a CM-2 computer. Information is recorded on magnetic disk and after off-time processing, magnetic field parameter charts are put into a digital printer.

The time taken for an active region magnetic field to be recorded is normally between 30 min and 1.5 h, with a scanning rate of $4'' \text{ sec}^{-1}$, the spectrograph entrance slit of $4'' \times 2''$ and a step between scans of $4''$. The time constant of the magnetograph is 1s. The magnetograph sensitivity in the channels of longitudinal and transverse components of the magnetic field is $5 \cdot 10^{-4}$ in polarization degree units.

Fig.1 presents a chart of magnetic field vector distribution in a single sunspot for 19 May 1983 (E24,S27). Dotted lines show the location of sunspot's umbra and penumbra, while arrows indicate the direction of the magnetic field vector in the plane of projection H_{\perp} , their length being proportional to the magnitude of H_{\perp} . For the purpose of easing the representation, the direction of the arrows is drawn the same as for a magnetic field of *N* polarity, while the true polarity was *S* and the maximum strength H_m in the sunspot umbra was 2830 G. Solid lines show isolines of longitudinal component of the magnetic field H_{\parallel} for the following values: 100, 300, 500, 1000, and 2000 G.

Fig.2 presents a chart of the magnetic field vector distribution in a leading sunspot of the active region on 24 June 1983 (W08,N17), the designations remaining the same. Isolines of longitudinal component are drawn for the values: 100, 200,

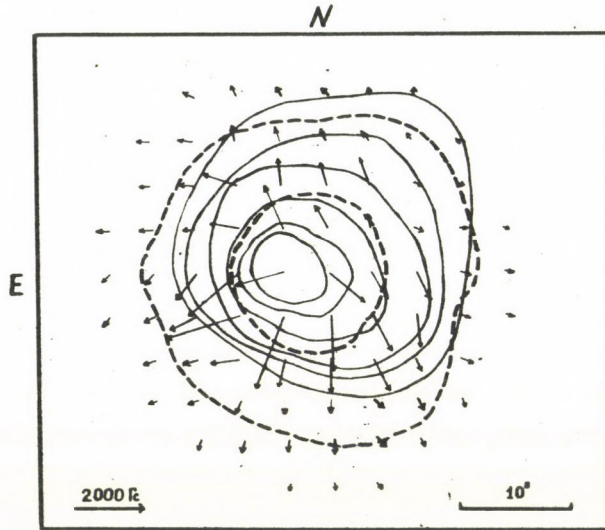


Fig.1. Chart of magnetic field vector distribution for the sunspot E24S27 (19 May 1983)

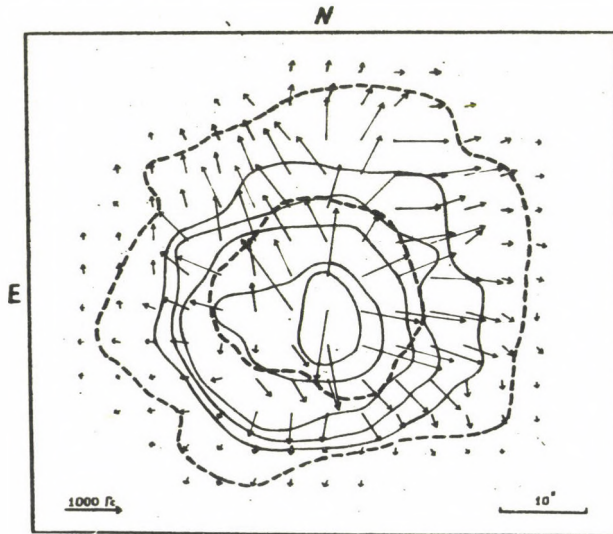



Fig.2. Chart of magnetic field vector distribution for the sunspot W08N17 (24 June 1983)


 a) E24S27 (19.05.83)


 б) W08N17 (24.06.83)


 в) W19N17 (25.06.83)

Fig. 3. Sketch of sunspots in white light.

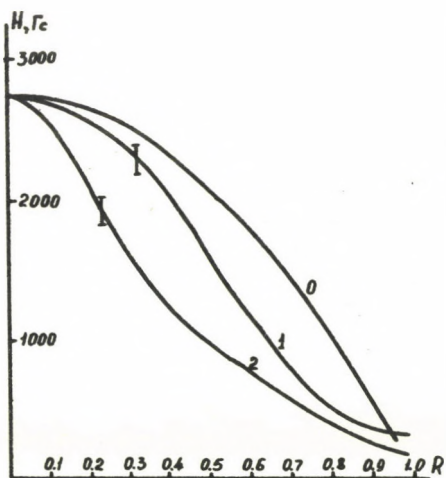


Fig. 4. Radial distribution of magnetic field strength in sunspots.

500, 1000, 1500, and 2000 G. The magnetic field polarity is *N* and the maximum strength in the sunspot umbra was 2910 G.

One may note a comparatively more complex field configuration in the sunspot, involved in the active region. Here the deviations of the transverse field H_{\perp} from radial distribution are very large and there is a well-defined tendency for the magnetic field line to concentrate into several flux tubes, closing, apparently, on different elements of the active region.

Fig.3 shows sketches in integrated light of a single sunspot for 19 May 1983 (a), a sunspot in the active region for 24 June 1983 (b) and of the same sunspot for 25 June 1983 (c). It is evident from Fig.3 (c) that the sunspot umbra divided into several cores.

Fig.4 presents cores of the magnetic field strength H in sunspot radius, normalized to $H = 2700$ G. Index 0 denotes the relationship $H = H_m / (1 + r^2 + r^4 + r^8 + r^{16})$, proposed by Wittman {8} as most realistically reflecting the strength behaviour in sunspots. Indices 1 and 2 denote curves for a single sunspot and a sunspot in the active region, respectively. An example of these two sunspots illustrates that for a sunspot with a more complex configuration of magnetic field its deviation of radial distribution from curve 0 is significant. On the boundary penumbra-photosphere for both sunspots the magnetic field strength is ≈ 200 G. Many authors (see, e.g.{5}) pointed out that the boundary penumbra-photosphere follows the isogausses $\approx 500 \div 1000$ G. In such a case the underestimated values of strength seem to be due to the fact that the data were not corrected for light blurring while image motion was $\approx 5''$ in these observations.

Acknowledgements

The authors express their gratitude to Dr Kobanov N.I. and Melentyeva G.K. for help with the work.

References

- {1} Bachmann, G., Jäger, F.W., Künzel, H., Pflug, K., Staude, J., Methodical experiences regarding the measurements of solar magnetic fields at the Sonnenobservatorium Einsteinturm, *HHI-STP Report*, No.4. Berlin, 1975
- {2} Grigoryev, V.M., B.F.Osak, Pflug, K., Selivanov, V.L., Determination of instrumental polarization of a solar telescope and calibration of a solar magnetograph, *Phys.Solariterr.* 14. 81, 1980
- {3} Grigoryev, V.M., Selivanov, V.L., The influence of instrumental polarization upon the formation of magnetograph signals with a pulse-code modulation, (in Russ.) *Soln.Dann.* 1978, No.2. 80,
- {4} Jäger, F.W., Instrumental polarization concerning magnetographic measurements, *Solar Phys.* 27. 481, 1972
- {5} Kálmán, B., The connection of the sunspot penumbra structure with the magnetic field vector, (in Russ.) *Izv.KrAO.* 60. 114, 1979
- {6} Selivanov, V.L., Estimation of scattered light in magnetographic data, (in Russ.) *Issl.SibIZMIR*, 60. 87, 1982
- {7} Stepanov, V.E., Grigoryev, V.M., Kobanov, N.I., Osak, B.F., An electro-optical polarization analyzer with pulse-code control, *Issl.SibIZMIR*, 37. 147, 1975
- {8} Wittmann, A., *Thesis*, Georg-August Universität, Göttingen, 1973

Felelős kiadó: Szeidl Béla

Hozott anyagról sokszorosítva

8414467 MTA KESZ Sokszorosító, Budapest. Felelős vezető: dr. Héczey Lászlóné



Publications of Debrecen Heliophysical Observatory

Vol.	No.		Year	Page
1	1-4	Statistical Investigations of Sunspots	1964	1-108
		<i>5 et seq. follows</i>		
2	1-11	Proceedings of the 6th Regional Consultation on Solar Physics	1971	1-217
3	1-5	Proceedings of the Intercosmos Symposium on Solar Physics	1977	1-310
4	1-2	Sunspot Group Development	1980-1981	1-60
		<i>3 et seq. follows</i>		
5	1-3	Proceedings of the 11th Regional Consultation on Solar Physics	1983	1-384
		P a r t 1		
	4-5	Proceedings of the 11th Regional Consultation on Solar Physics	1983	385-666
		P a r t 2		

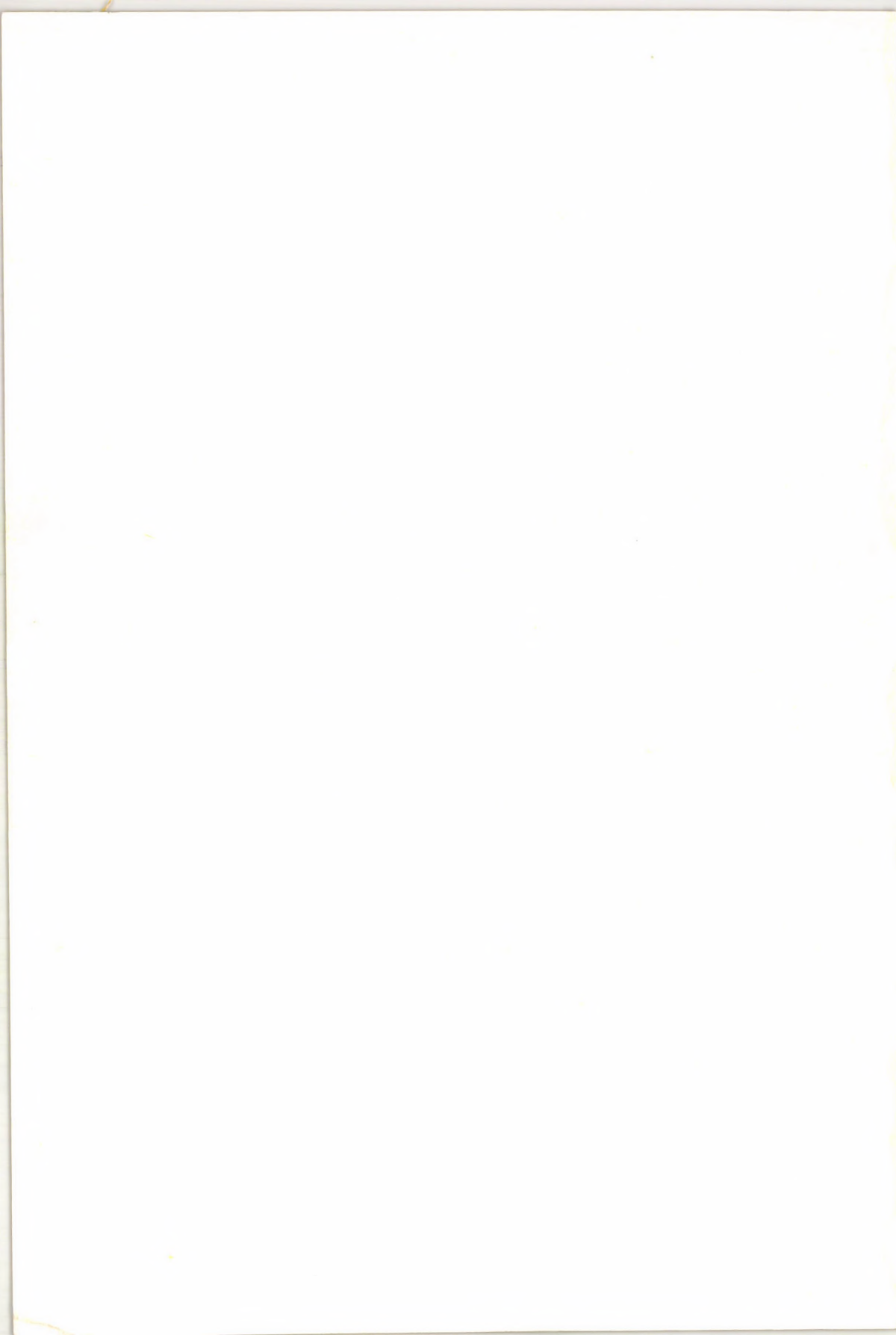
PUBLICATIONS
OF
DEBRECEN
HELIOPHYSICAL OBSERVATORY
OF THE
HUNGARIAN ACADEMY OF SCIENCES

ПУБЛИКАЦИИ
ДЕБРЕЦЕНСКОЙ
ГЕЛИОФИЗИЧЕСКОЙ ОБСЕРВАТОРИИ
ВЕНГЕРСКОЙ АКАДЕМИИ НАУК

A MAGYAR TUDOMÁNYOS AKADÉMIA
DEBRECENI
NAPFIZIKAI OBSZERVÁTORIUMÁNAK
KÖZLEMÉNYEI

VOLUME 5, PART 2

11th Regional Consultation on Solar Physics
Debrecen, Hungary
1983



PUBLICATIONS
OF
DEBRECEN
HELIOPHYSICAL OBSERVATORY
OF THE
HUNGARIAN ACADEMY OF SCIENCES

ПУБЛИКАЦИИ
ДЕБРЕЦЕНСКОЙ
ГЕЛИОФИЗИЧЕСКОЙ ОБСЕРВАТОРИИ
ВЕНГЕРСКОЙ АКАДЕМИИ НАУК

A MAGYAR TUDOMÁNYOS AKADÉMIA
DEBRECENI
NAPFIZIKAI OBSZERVATÓRIUMÁNAK
KÖZLEMÉNYEI

VOLUME 5

Nos. 4-5

Proceedings of the
11th Regional Consultation on Solar Physics
PART 2

DEBRECEN
1983

EDITORS:

L.DEZSŐ and B.KÁLMÁN

Heliophysical Observatory
Hungarian Academy of Sciences

H-4010 D E B R E C E N

HUNGARY

ISSN 0209-7567

(Publ.Debrecen Obs.,Vol.5, Part 2, Nos.4-5, pages 385-666)

Publ. Debrecen Obs. Vol. 5

No. 4.

MISCELLANEOUS PAPERS ON THEORETICAL ASPECTS
OF SOLAR ACTIVITY

ЗОНАЛЬНЫЕ ТЕЧЕНИЯ В СОЛНЕЧНОЙ КОРОНЕ

Г.В. КУКЛИН, В.Е. СТЕПАНОВ

СибИЗМИР, Иркутск

THE ZONAL STREAMS IN THE SOLAR CORONA

G.V. KUKLIN, V.E. STEPANOV

SibIZMIR, Irkutsk

Abstract:

The zonal streams in the solar corona were investigated using the corona rotation observations during the years 1969-71. The coronal zonal streams are compared with corresponding streams in the photosphere during the same time period. It is shown that both in the photosphere and in the corona the streams of the same direction are located in the same heliolatitude intervals. However, the average coronal stream velocities are equal to 230 m s^{-1} , that means they are larger by two orders than the photographic ones.

Four variants of possible explanations of streams origin are considered. It is shown that these streams are most likely to appear due to the presence of the pressure gradients caused by extremely small relative pressure variations (10^{-4} - 10^{-5}) and apparently are an effect of cyclonic streams or of heliostrophic wind. Therefore observations of the zonal streams in the solar corona confirm indirectly the reality of the photospheric zonal streams discovered by Howard and La Bonte [1].

1. Введение

Говард и Лабонт {1} по наблюдениям лучевых скоростей в линии 5250 А при помощи магнитографа на обсерватории Маунт Уилсон обнаружили зональные движения в фотосфере Солнца. Наблюдения охватывают период с января 1968 года по декабрь 1979 г. Зональные восточнoзападнoе течения большого масштаба определялись вычитанием из скорости вращения на данной широте, усредненной за 4 кэррингтоновских оборота, скорости, соответствующей сглаженной картине дифференциального вращения.

Были установлены следующие закономерности:

1. Зоны быстрого и медленного вращений возникают вблизи полюсов и смещаются к экватору за 22 года. Эти зоны начинают свой дрейф на каждом полюсе примерно в одно и то же время. Авторы связывают зону быстрого вращения около полюсов в 1975 году с началом цикла солнечной активности 22 по цюрихской нумерации (см. карту зональных течений на фиг. 1 {1}).
2. В обоих полушариях картина течений симметрична относительно экватора. Средняя величина скорости зональных течений равна 3 м/с, хотя отдельные значения достигают 10 м/с.
3. Центр тяжести зоны пятнообразования, отождествляемый с положением максимума магнитного потока, приблизительно совпадает с полярной границей зоны быстрого вращения, т.е. с линией максимума сдвига с поле скоростей.

В работе {2} и {3} эти зональные движения истолковываются как крутильные колебания большого масштаба, имеющие прямое отношение к эволюции магнитной активности на Солнце. При обсуждении обнаруженного явления в связи с моделью $\alpha - \omega$ динамо авторы приходят к выводу, что наблюдаемые зональные течения не могут быть объяснены в рамках этой модели.

Целью настоящей работы является установление связи фотосферных крупномасштабных зональных течений с такими же движениями в солнечной короне. Для этого мы сравниваем избытки скорости вращения короны и фотосферы за один и тот же промежуток времени (1969-72 гг.).

2. Зональные течения в короне

Исследования вращения короны по доплеровским сдвигам линии FeX λ 6374 Å относительно линий поглощения в ореоле с введением необходимых поправок за смещение линий ореола выполнены по наблюдениям произведенным в 1969-72 гг. {4}. Они показали, что в этот период в интервалах гелиографических широт 5-40° и 65-70° имело место уменьшение скорости вращения короны. На рис. 1 приведена кривая зависимости вращения короны от широты по наблюдениям, сведенным в один квадрант. Жирная линия представляет аппроксимацию данных о вращении по известной формуле

$$\frac{1}{r} \tilde{v}_\lambda = (A + B \sin^2 \varphi + C \sin^4 \varphi) \cos \varphi. \quad (1)$$

Коэффициенты А, В и С определены по методу наименьших квадратов (см. Прил.). Тонкая линия представляет наблюдаемую зависимость скорости вращения короны от широты. Нетрудно видеть что в различных интервалах широт существует как замедленное, так и ускоренное вращение короны.

Для сравнения фотосферных и корональных течений мы по карте избытков скоростей вращения в фотосфере (фиг. 1 {1}) построили изменение этих величин с широтой за тот же промежуток времени, когда были выполнены наблюдения вращения короны. Эти результаты приведены на рис. 2а. Аналогичная картина избытков скоростей вращения короны, усредненная за весь промежуток наблюдений 1969-72 гг., приведена на рис. 2в.

На рис. (2 а, в) сплошные вертикальные линии соответствуют средним картинам дифференциального вращения в фотосфере и короне согласно формуле (1). Сразу видно, что в фотосфере (рис. 2 а) эта линия не обеспечивает равенства нулю среднего значения избытка скорости от экватора до полюса и преобладают восточные течения (замедленное вращение фотосферы). Поэтому необходимо сместить нульпункт в сторону отрицательных скоростей на 1 м/с (штриховая вертикальная линия). В {5} (см. рис. 4 а), где объединены зональные скорости северного и южного полушарий, эта ошибка в средней скорости вращения за исследуемый период авторами устранена. Штриховые кривые показывают

Т А Б Л И Ц А 1

Фотосфера		Корона		Фотосфера		Корона	
Положение границ зональных течений (V=0)	Экссесс давления на границах	Положение границ зональных течений (V=0)	Экссесс давления на границах	Положение максимальных скоростей течения	Величина скорости течения	Положение максимальных скоростей течения	Величина скорости течения
°	Дин см ⁻²	°	10 ⁻⁶ Дин см ⁻²	°	м с ⁻¹	°	м с ⁻¹
4 ± 1.5	-	-	-	0 ± 2.5	-2.9	-	-
18.5 ± 2.5	-0.8	22.5 ± 3.5	-0.2	9 ± 4.0	+3.0	-	-
35.5 ± 4.5	+0.9	43.0 ± 1.5	+1.2	24.5 ± 5	-2.1	35.0 ± 3.5	-320
60.0 ± 2.0	-3.9	61.0 ± 1.0	-1.6	51 ± 5	+2.3	53.5 ± 3.5	+300
-	-	-	-	-	-	67.0 ± 3.5	-250

Т А Б Л И Ц А 2

Широта	Скорость вращения короны	Срkv. ошибка измерения	Избыток скорости вращения короны	Срkv. ошибка оценки
φ °	v_λ км с ⁻¹	σ км с ⁻¹	Δv_λ км с ⁻¹	σ км с ⁻¹
5	2.073	± 0.086	+ 0.069	± 0.060
15	1.969	± 0.071	+ 0.059	± 0.055
25	1.676	± 0.072	- 0.047	± 0.062
35	1.165	± 0.069	- 0.287	± 0.054
45	1.240	± 0.070	+ 0.114	± 0.058
55	1.086	± 0.057	+ 0.297	± 0.045
65	0.167	± 0.071	- 0.321	± 0.058
75	0.130	± 0.070	- 0.122	± 0.058
85	0.126	± 0.052	+ 0.050	± 0.049

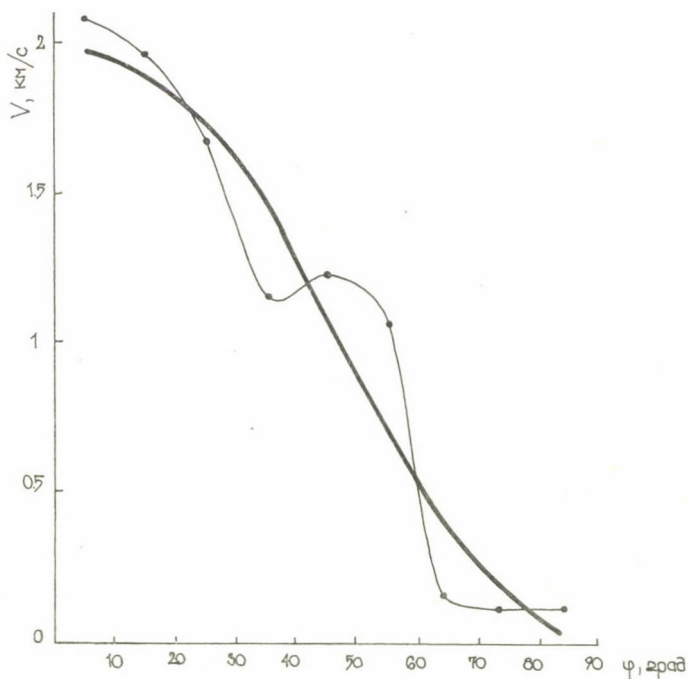


Рис.1. Зависимость наблюдаемых $(V_\lambda)_o$ и сглаженных $(V_\lambda)_c$ скоростей вращения короны в 1969-72 гг. (приведенные к одному квадранту) от широты φ .

интервал возможных погрешностей, соответствующий среднеквадратической ошибке измерений, равной ± 70 м/с для короны.

Прежде всего мы видим неплохое подобие течений в фотосфере и в короне, как по положениям изменений знака избытков скоростей ($\Delta V=0$), так и по направлению течений. Однако эксцессы скоростей в короне достигают по модулю 350 м/с, т.е. превышают таковые в фотосфере на два порядка.

В табл. 1 даны средние гелиографические широты положений точек пересечения кривых на рис. 2 а, в и скорректированных нульпунктов, т.е. положений максимумов сдвига скоростей (столбцы 1,3), положений экстремумов скоростей течений (столбцы 5,7) и их величины для фотосферы и короны (столбцы 6,8). Нам не удалось оценить точность определения избытков скоростей в фотосфере, приведенных в {1}, но, повидимому, ошибки не превышают 1 м/с. В таком случае погрешности оценок широт в табл. 1 примерно одинаковы и для фотосферы и для короны. Тогда положения максимумов сдвига скоростей в фотосфере и в короне, практически, совпадают. Положения же экстремумов скоростей в фотосфере и в короне различаются более существенно, особенно в интервале $25-35^\circ$, где в короне максимум имеет большую широту, чем в фотосфере. Скорее всего это связано с меньшей надежностью определения величин экстремумов и их положений по карте, как в фотосфере, так и в короне.

Таким образом, общий характер изменения с гелиографической широтой зональных течений и в короне и в фотосфере свидетельствует о динамической связи фотосферных и корональных движений.

Идея существования в короне зональных течений была высказана в работе {4} и использована в {7} при необходимости объяснить сравнительно быстрые явления ускорения и замедления вращения секторной структуры межпланетного магнитного поля. Предполагалось что в широтной зоне существования активных областей чаще температура и давление в короне должны отличаться от таковых в спокойной зоне (на одной и той же высоте над фотосферой). Тогда должны возникнуть меридиональные градиенты давления, обуславливающие ветры, которые под действием кориолисовой

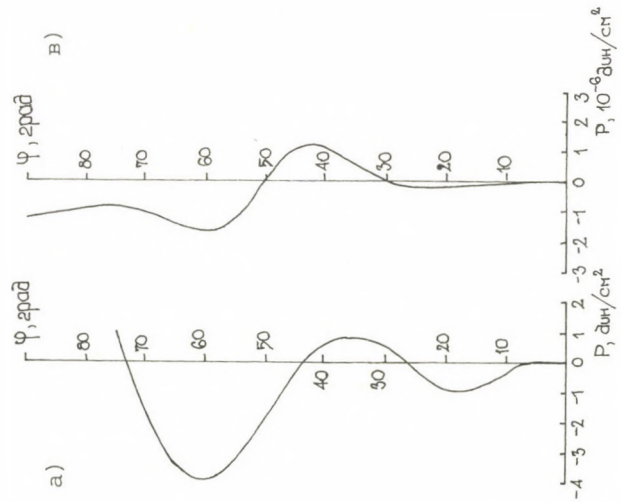


Рис. 3. Зависимость вариации давления P в фотосфере (а) и в короне (в) от широты ϕ .

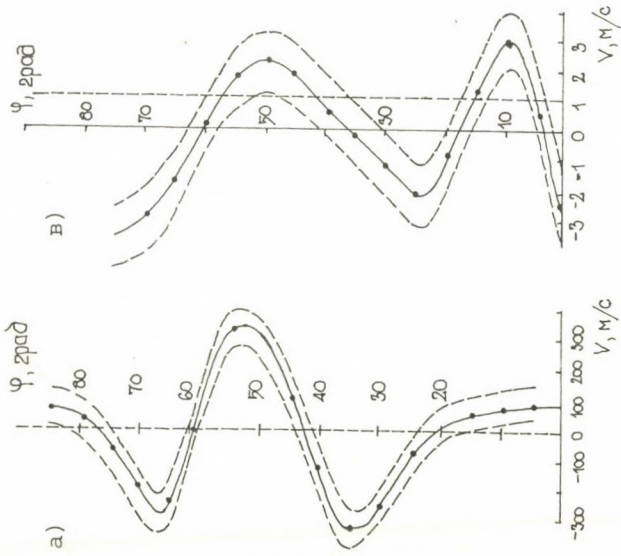


Рис. 2. Зависимость избытков скоростей вращения $\Delta V_\lambda = (V_\lambda)_0 - (V_\lambda)_c$ в фотосфере (а) и в короне (в) от широты ϕ .

силы приобретают зональную составляющую. Действительно, данные наблюдений {4} показывают, что в 1969-72 гг. в короне существовала структура зональных течений (избытков скоростей вращения), которая качественно согласовывалась с картиной временных изменений вращения секторной структуры межпланетного магнитного поля {7}.

Вполне очевидно, что выявление зональных течений, т.е. избытков скорости вращения короны, необходимо производить относительно некоторой глобальной картины дифференциального вращения, принятой за референц-основу. Как уже упомянуто выше, мы сочли возможным аппроксимировать глобальную картину дифференциального вращения короны выражением типа (1) (см. Прил.)

$$V_{\lambda} = (C_0 + C_1 \sin^2 \vartheta + C_2 \sin^4 \vartheta) \sin \vartheta, \quad \vartheta = \frac{\pi}{2} - \varphi. \quad (1')$$

Надо иметь в виду, что использование указанной аппроксимации подразумевает существование двухуровневой иерархии меридиональной циркуляции, поддерживающей глобальную картину дифференциального вращения: циркуляция с витком от полюса до экватора, на которую накладывается вторичная, бizonaльная циркуляция с двумя витками разных направлений в высоких и низких широтах. Эта картина в зависимости от роста или убывания с высотой над фотосферой абсолютной величины скорости приводит к истечению солнечного ветра и транспорту солнечных магнитных полей в межпланетную среду: либо из средних широт, либо из приполярных и приэкваториальных областей.

3. Возможные объяснения зональных течений в атмосфере Солнца

Возможны 4 варианта подхода к решению проблемы о корональных зональных течениях. Мы попытаемся дать им грубую оценку.

Первоначально мы пренебрежем влиянием вязкости фотосферного и коронального вещества и магнитных полей. Нас интересует характер изменения давления в области зональных течений. В цилиндрических координатах (ω - расстояние от оси вращения, z - расстояние от экваториальной плоскости) уравнения установившегося вращения имеют следующий вид {12,13}

$$\frac{1}{\rho} \frac{\partial P}{\partial \tilde{\omega}} = - \frac{\partial \pi}{\partial \tilde{\omega}} + \Omega^2 \tilde{\omega} ,$$

$$\frac{1}{\rho} \frac{\partial P}{\partial z} = - \frac{\partial \pi}{\partial z} .$$
(2)

Здесь ρ - плотность вещества, P - давление, π - потенциал гравитационных сил, Ω - угловая скорость вращения. При переходе к сферическим координатам (r - радиус-вектор, ϑ - коширота), учитывая, что

$$\tilde{\omega} = r \sin \vartheta, \quad z = r \cos \vartheta,$$

получаем

$$\frac{1}{\rho} \frac{\partial P}{\partial r} + \frac{\partial \pi}{\partial r} = \frac{v_\lambda^2}{r}$$

$$\frac{1}{\rho} \frac{1}{r} \frac{\partial P}{\partial \vartheta} + \frac{1}{r} \frac{\partial \pi}{\partial \vartheta} = \frac{v_\lambda^2}{r} \operatorname{ctg} \vartheta .$$
(3)

где $v_\lambda = \tilde{\omega} \Omega = r \Omega \sin \vartheta$ - линейная скорость вращения. Если считать, что уровенная поверхность ($\pi = \text{const}$) несущественно отличается от сферы, то

$$\frac{\partial P}{\partial \vartheta} \approx \rho v_\lambda^2 \operatorname{ctg} \vartheta$$
(4)

Тогда вариация давления ΔP , связанная с зональными течениями, может быть найдена численным интегрированием следующего уравнения

$$\frac{\partial}{\partial \vartheta} (\Delta P) = \rho [(v_\lambda^2)'_o - (v_\lambda^2)'_c] \operatorname{ctg} \vartheta .$$
(5)

Здесь индексом "o" помечены наблюдаемые значения скорости вращения, а индексом "c" - сглаженные по формуле (1).

Вычисления для фотосферы выполнены при $\rho = 2.89 \cdot 10^{-7} \text{ г/см}^3$

и

$$A = 2.867 \times 10^6 \text{ с}^{-1}, \quad r = 6.96 \times 10^9 \text{ см} ,$$

$$B = -0.3415 \times 10^6 \text{ с}^{-1}, \quad C = -0.4895 \times 10^6 \text{ с}^{-1} .$$

Значения A, B, C взяты по Говарду и др. [3]. Сглаженные значения скорости вычислялись по формуле (1), а наблюдаемые были получены прибавлением к этим величинам избытков согласно рис. 2.а.

Результаты вычислений показывают, что максимальные величины $|\Delta P|$ в фотосфере достигают нескольких дин/см², т.е. $|\Delta P/P|$ является малой величиной порядка 10^{-5} (рис. 3а).

В случае движений в короне мы непосредственно взяли данные наблюдений Степанова и Тягун {4}, усредненными за 1969–72 гг. и приведенными к одному квадранту. Далее мы воспользовались данными Краинберга и Теплицкой {9} для короны в максимуме активности (1969–70 гг.). Тогда для высоты 20" над лимбом (14.5 тыс. км) получаем следующие значения: электронная плотность $n_e \approx 5.5 \times 10^8$, газовое давление $P \approx 0.17$, электронная температура $T_e \approx 1.15 \times 10^6$ °К, массовая плотность $\rho \approx 1.2 \times 10^{-15}$. По формулам для полностью ионизированной водородной плазмы {10} можно оценить электропроводность $\sigma_0 \approx 8.4 \times 10^{15}$ CGSE, динамическую вязкость $\mu \approx 0.15$ и кинематическую вязкость $\nu \approx 1.3 \times 10^{14}$. Принимая $r \approx 7.105 \times 10^{10}$ см, можно вычислить производную газового давления вдоль меридиана и после численного интегрирования оценить вариации давления на различных гелиоширотах. Соответствующие оценки показывают, что наблюдаемая картина избытков скоростей вращения может быть обусловлена относительными вариациями давления порядка 10^{-5} (рис. 3).

Таким образом, мы видим, что области максимального и минимального давлений соответствуют $\Delta v_\lambda = 0$. При этом минимумы давлений совпадают с границами перехода от западного зонального течения к восточному при переходе к более высоким широтам. Поскольку одна из границ перехода, согласно {1}, расположена в "центре тяжести" пятнообразования, следует заключить, что в этой области в среднем в фотосфере имеет место пониженное давление. Следовательно, в этой области, как и в аналогичной области в высоких широтах, следует ожидать гелиострофического ветра, возможность которого предсказана Б.М. Рубашевым {6}.

В этом случае {8}

$$\begin{aligned} -2\Omega v_x \sin\varphi &= \frac{1}{\rho} \frac{\partial P}{\partial y}, \\ 2\Omega v_y \sin\varphi &= \frac{1}{\rho} \frac{\partial P}{\partial x}, \\ -g + 2\Omega v_y \cos\varphi &= \frac{1}{\rho} \frac{\partial P}{\partial z}. \end{aligned} \quad (6)$$

Здесь κ - направление по касательной на юг (в северной полусфере), γ - к востоку и ось z - по вертикали вверх, g - ускорение силы тяжести.

Произведем оценку, каковым должно быть изменение давления, чтобы в фотосфере появилась зональная скорость v_γ равная 3м/с. Из (6) следует, что

$$\frac{\partial P}{\partial \kappa} = 2\rho\Omega v_\gamma \sin\varphi.$$

Полагая $\rho = 2.89 \times 10^{-7}$ г/см³, $\Omega = 2.865 \times 10^{-6}$ рад/сек и $g = 2.731 \times 10^4$ см/сек² получим при $\varphi = 18^\circ 5'$ $\partial P / \partial \kappa = 1.5 \times 10^{10}$. Следовательно, на протяжении крупномасштабных течений ($\sim 10^{10}$ см) при давлении в фотосфере $\sim 10^5$ дин см⁻², падение давления в месте $\Delta v_\lambda = 0$ составляет всего 1 дин см⁻², что подтверждает величины эксцессов давления, вычисленных выше.

Рассмотрим теперь, как изменяются зональные течения в короне в зависимости от изменения температуры с высотой. Выражая ρ во втором и третьем уравнениях (6) через T и P и дифференцируя v_λ / T по z , а третье уравнение по κ и исключая $\frac{\partial^2 \ln P}{\partial \kappa \partial z}$, получим согласно {8}

$$\frac{\partial v_\gamma}{\partial z} = \frac{v_\gamma}{T} \frac{\partial T}{\partial z} + \frac{g}{2\Omega \sin\varphi} \frac{1}{T} \frac{\partial T}{\partial \kappa}.$$

Интегрируя это уравнение от z_0 до z получим:

$$v_\gamma = \frac{T}{T_0} v_\gamma^0 + \frac{gT}{2\Omega \sin\varphi} \int_{z_0}^z \frac{1}{T^2} \frac{\partial T}{\partial \kappa} dz. \quad (7)$$

Представляя $\ln T$ в короне ломаными линиями, можно получить следующую аппроксимацию:

$$\text{при } z_0 < z < z_1 \quad T = T_0 (z/z_0)^{0.65},$$

$$\text{при } z_1 < z < z_2 \quad T = T_1 (z/z_1)^{0.88},$$

где $z_0 = 2630$ км, $z_1 = 3510$ км, $z_2 = 39800$ км, $T_0 = 10^4$, $T_1 = 1.2 \times 10^5$ и $T_2 = 10^6$ град.

При средних скоростях зональных движений в максимумах в фотосфере (см. табл. 1) $\Delta v_\phi = 2$ м/с получим следующее уравнение

$$\Delta v_{\text{кор}} = 345 + 2.33 \times 10^{-4} \left\langle \frac{\partial T}{\partial \kappa} \right\rangle \quad (\text{в м/с})$$

Беря разность температур в корональной конденсации и в спокойной короне, легко оценить, что $\langle \frac{\partial T}{\partial k} \rangle \ll 1$. Поэтому, скорость в короне зональных течений, как показывают вычисления равна 345 м/с, что хорошо согласуется с наблюдаемой скоростью зональных течений в короне, равной 300 м/с. Таким образом, описание наблюдаемых зональных течений в короне хорошо согласуется с простой теорией гелиострофического ветра.

Во втором варианте вычислений мы воспользовались вариантом постановки задачи об установившемся течении вязкой несжимаемой жидкости в сферической системе координат (r, ϑ, λ) согласно Седову [11]. В этом случае, опираясь на соображения теории размерностей, предполагается, что наблюдаемые компоненты скорости могут быть представлены в виде

$$\begin{aligned} \frac{1}{\rho} P - p &= \frac{v^2}{r^2} F(\vartheta), \quad v_r = \frac{v}{r} f(\vartheta), \\ v_\vartheta &= \frac{v}{r} \varphi(\vartheta), \quad v_\lambda = \frac{v}{r} \psi(\vartheta) = r\Omega(\vartheta) \sin\vartheta. \end{aligned} \quad (8)$$

где $F(\vartheta)$, $f(\vartheta)$, $\varphi(\vartheta)$ и $\psi(\vartheta)$ - безразмерные функции безразмерного аргумента. Ожидаемое решение предполагает, что скорости убывают с удалением от начала координат обратно пропорционально этому расстоянию при постоянстве v . В действительности с высотой и скорость, и кинематическая вязкость в короне возрастают. Естественно, что подстановка наблюдаемых значений позволит получить решение с точностью до "наоборот", т.е. с противоположным знаком, но с примерно реальным значением порядка величины искомого неизвестного. Тогда в случае осевой симметрии нетрудно получить соотношения [11]

$$\begin{aligned} \varphi &= (\psi' + \psi \operatorname{ctg} \vartheta)' / (\psi' + \psi \operatorname{ctg} \vartheta), \\ f &= -(\varphi' + \varphi \operatorname{ctg} \vartheta), \\ F &= \varphi\varphi' - f' - \psi^2 \operatorname{ctg} \vartheta, \\ F &= \frac{1}{2} [f^2 + \varphi^2 + \psi^2 + f'' + f' (\operatorname{ctg} \vartheta - \varphi)]. \end{aligned} \quad (9)$$

Из наблюдений для короны мы располагаем зависимостью $v_\lambda(\vartheta)$. Непосредственные вычисления показали, что учет газоки-

нетической вязкости, вычисленной по модели {9}, приводит к "возникновению" меридиональной циркуляции в короне со скоростями порядка $v_{\vartheta} \approx 10^2$ м/с. Дальнейшие вычисления показали, что оценки величины горизонтального градиента давления вдоль поверхности Солнца приводят к ожидаемым относительным вариациям порядка 10^{-4} , т.е. лишь на порядок выше, чем в случае полного пренебрежения вязкостью. Этот результат звучит весьма ошеломляюще: для возникновения зональных течений достаточно крайне мизерных вариаций давления.

В третьем варианте вычислений мы воспользуемся полной системой уравнений вращения вязкой жидкости при произвольной зависимости скоростей вращения и характеристик среды от сферических координат. Тогда компоненты тензора вязких напряжений определяются следующими выражениями, заимствованными у Тассуля {12},

$$\begin{aligned} \tau_{rr} &= 2\mu \frac{\partial v_r}{\partial r}, & \tau_{r\vartheta} &= \tau_{\vartheta r} = \mu \left[\frac{1}{r} \frac{\partial v_r}{\partial \vartheta} + r \frac{\partial}{\partial r} \left(\frac{v_{\vartheta}}{r} \right) \right], \\ \tau_{\vartheta\vartheta} &= 2\mu \left(\frac{1}{r} \frac{\partial v_{\vartheta}}{\partial \vartheta} + \frac{v_r}{r} \right), & \tau_{\vartheta\lambda} &= \tau_{\lambda\vartheta} = \mu \frac{\sin \vartheta}{r} \frac{\partial}{\partial \vartheta} \left(\frac{v_{\lambda}}{\sin \vartheta} \right), \\ \tau_{\lambda\lambda} &= 2\mu \left(\frac{v_r}{r} + \frac{v_r}{r} \operatorname{ctg} \vartheta \right), & \tau_{\lambda r} &= \tau_{r\lambda} = \mu r \frac{\partial}{\partial r} \left(\frac{v_{\lambda}}{r} \right), \end{aligned} \quad (10)$$

а сами уравнения стационарного движения согласно {12} имеют вид

$$\begin{aligned} \rho \left(-\frac{v_{\vartheta}^2}{r} - \frac{v_{\lambda}^2}{r} + v_r \frac{\partial v_r}{\partial r} + \frac{v_{\vartheta}}{r} \frac{\partial v_r}{\partial \vartheta} \right) &= \\ &= -\frac{\partial}{\partial r} (\rho \pi) - \frac{\partial P}{\partial r} + \frac{1}{r \sin \vartheta} \left[\frac{\sin \vartheta}{r} \frac{\partial}{\partial r} (r^2 \tau_{rr}) + \frac{\partial}{\partial \vartheta} (\tau_{r\vartheta} \sin \vartheta) \right] - \\ &- \frac{1}{r} (\tau_{\vartheta\vartheta} + \tau_{\lambda\lambda}), \\ \rho \left(-\frac{v_{\lambda}^2}{r} \operatorname{ctg} \vartheta + v_r \frac{\partial v_{\vartheta}}{\partial r} + \frac{v_{\vartheta}}{r} \frac{\partial v_{\vartheta}}{\partial \vartheta} + \frac{v_r v_{\vartheta}}{r} \right) &= \\ &= -\frac{1}{r} \frac{\partial}{\partial \vartheta} (\rho \pi) - \frac{1}{r} \frac{\partial P}{\partial \vartheta} + \frac{1}{r \sin \vartheta} \left[\frac{\sin \vartheta}{r} \frac{\partial}{\partial r} (r^2 \tau_{\vartheta r}) + \frac{\partial}{\partial \vartheta} (\tau_{\vartheta\vartheta} \sin \vartheta) \right] + \\ &+ \frac{1}{r} (\tau_{r\vartheta} - \tau_{\lambda\lambda} \operatorname{ctg} \vartheta), \\ \rho \left(\frac{v_r v_{\lambda}}{r} + \frac{v_{\vartheta} v_{\lambda}}{r} \operatorname{ctg} \vartheta + v_r \frac{\partial v_{\lambda}}{\partial r} + \frac{v_{\vartheta}}{r} \frac{\partial v_{\lambda}}{\partial \vartheta} \right) &= \\ &= \frac{1}{r \sin \vartheta} \left[-\frac{\sin \vartheta}{r} \frac{\partial}{\partial r} (r^2 \tau_{\lambda r}) + \frac{\partial}{\partial \vartheta} (\tau_{\lambda\vartheta} \sin \vartheta) \right] + \frac{1}{r} (\tau_{r\lambda} + \tau_{\vartheta\lambda} \operatorname{ctg} \vartheta). \end{aligned} \quad (11)$$

Оценим фигурирующие здесь величины, полагая, что по вертикали (по радиусу) характерным масштабом является высота

уровня наблюдений над фотосферой, а для кошироты $\vartheta \approx 45^\circ$ надо использовать значение радиуса $R_0 \approx 7.105 \times 10^{10}$ см. Одновременно будем считать, что в грубом приближении явление меридиональной циркуляции может быть описано как соленоидальное движение несжимаемой жидкости. Обозначая

$$v_{\vartheta} = u,$$

имеем

$$v_r \approx 0.08 u.$$

Инерционный член $\rho \frac{D}{Dt} w \approx 5.5 \times 10^{-26}$ μw .

Компоненты тензора вязких напряжений

$$\begin{aligned} \tau_{rr} &\approx 1.1 \times 10^{-10} \mu u, & \tau_{\vartheta\vartheta} &\approx 1.1 \times 10^{-10} \mu u, & \tau_{\lambda\lambda} &\approx -2.9 \times 10^{-11} \mu u, \\ \tau_{r\vartheta} = \tau_{\vartheta r} &\approx 6.7 \times 10^{-10} \mu u, & \tau_{\vartheta\lambda} = \tau_{\lambda\vartheta} &\approx 1.9 \times 10^{-6} \mu, & \tau_{\lambda r} = \tau_{r\lambda} &\approx 2.3 \times 10^{-5} \mu. \end{aligned}$$

Здесь амплитуда зональных течений принята равной $\Delta v_{\lambda} \approx 3.5 \times 10^4$ см/с. Тогда из третьего уравнения (11) следует $u \approx 0.8 \times 10^7 \mu$ (12). Второе уравнение (11) позволяет оценить горизонтальный градиент газового давления (максимум), обеспечивающий наблюдаемые избытки скорости вращения и соответствующие вязкие напряжения. Во втором уравнении мы полагали, что потенциал p не зависит от координаты ϑ .

Используя первое уравнение (11), мы получим, что члены, содержащие скорости (динамические по физической природе) на несколько порядков меньше основных членов, которые отражают наличие в короне гидростатического равновесия. Следовательно, в целом корона слабо реагирует на динамические эффекты, т.е. её стратификация достаточно стабильна.

Оценим порядок величины скорости меридиональной циркуляции из соотношения (12). Подставляя ранее найденное значение μ , получаем скорости порядка 10 км/с. Столь высокие скорости меридиональной циркуляции вызывают некоторое сомнение в своей реальности, т.е. вязкость должна быть существенно меньше. Однако в этом случае число Рейнольдса будет менее 10^3 , т.е. нет условий для развития турбулентности, которая могла бы заметно, на 2-3 порядка снизить эффективную вязкость.

Таким образом, можно сделать вывод, что если вязкость в короне имеет газокинетическую природу, то должны наблюдаться

большие скорости меридиональной циркуляции и давление не играет никакой существенной роли в формировании зональных течений. По-видимому, этот вывод имеет силу только в случае пренебрежения влиянием магнитных полей.

Иошимура {2} разработал механизм крутильных колебаний большого масштаба в рамках динамо теории. Для определения эффективной глубины действия этого механизма он использовал соотношение (5.3) в{2}, которое может быть записано в следующем виде

$$\langle \Delta v_{\lambda} \rangle \approx \frac{1}{\delta \pi r} N_{\rho}^0 N_{\theta}^0 \frac{1-K}{\gamma R_0}, \quad (13)$$

где $\langle \Delta v_{\lambda} \rangle$ - средняя абсолютная величина избытка скорости вращения, R_0 - радиус слоя, N_{ρ}^0 и N_{θ}^0 - средние значения полоидальной и тороидальной компонент общего магнитного поля, γ - декремент затухания для характерного масштаба ℓ ($\gamma \approx \nu/\ell^2$) и $1-K$ - множитель порядка единицы, зависящий от характера граничных условий (открытые или закрытые). Полагая $\ell = R_0 \Delta \theta$, где $\Delta \theta \approx 0.3 (17^\circ)$, мы получим для короны

$$\langle \Delta v_{\lambda} \rangle \approx 1.6 \times 10^9 N_{\rho}^0 N_{\theta}^0 \quad (13')$$

откуда следует, что $N_{\rho}^0 N_{\theta}^0 \approx 10^{-5}$ в короне, если наблюдаемые зональные течения в короне ($\langle \Delta v_{\lambda} \rangle \approx 10^4$) обусловлены механизмом Иошимуры. Поскольку N_{ρ} и N_{θ} в короне порядка 1-10 гс, то наблюдаемые зональные течения в короне не вызываются механизмом Иошимуры, точнее, его действие не распространяется из подфотосферных слоев вверх в корону.

Следовательно, необходимо располагать сведениями о локальных магнитных полях в короне (волокна, эфемерные АО и пр.) в отношении к зональным течениям в короне, так как они могут проявить себя в картине зональных течений в качестве механизма эффективной вязкости. Эта задача требует специального отбора данных и способа их обработки и в этой статье не рассматривается.

4. Обсуждение

Анализ избытков скорости дифференциального вращения короны,

определенных по доплеровским смещениям красной корональной линии показывает:

1) существование средних зональных течений в полярных областях и на низких широтах в зоне солнечной активности в короне;

2) в фотосфере и в короне положение максимумов сдвигов скоростей и направленных течений совпадают в пределах ошибок измерений лучевых скоростей;

3) оценки величин скоростей зональных течений в короне на два порядка превышают таковые в фотосфере и близки к 300 м/с (см. табл.1.).

Если пренебречь эффектами вязкости и магнитных полей, то в рамках представлений газовой динамики и гидродинамики звезд для возникновения указанных зональных течений и в фотосфере и в короне достаточно иметь относительное понижение газового давления на 10^{-5} в областях, совпадающих с переменной знака зональной скорости. Тогда, как мы видим, зональные течения направлены примерно вдоль изобар, причем области низкого давления остаются слева в северном и справа в южном полушариях. Центробежной силой, возникающей при искривлении траекторий, можно практически пренебречь на расстояниях более 20 тыс. км от центра кривизны траектории. Следовательно, в этом приближении зональные течения, наблюдаемые и в фотосфере и в короне, могут быть истолкованы как проявление гелиострофического ветра, либо как циклонические и антициклонические течения.

Важным вопросом является - почему в зоне центра тяжести активных областей в среднем наблюдается пониженное давление. Скорее всего, вполне правдоподобно считать, что антициклоническая ситуация наблюдается в период роста развития активных областей, сопровождающегося увеличением напряженности магнитного поля и повышением в связи с этим общего давления, а циклоническая - в период уменьшения напряженности и соответственно уменьшения общего давления. Поскольку продолжительность угасания активных областей значительно превышает продолжительность их роста, возможно, это в среднем и приводит к уменьшению давления. Также вероятно это объясняет, почему согласно

Ричардсону {18} вихревая структура хромосферы в окрестностях пятен в обоих полушариях Солнца в 75% случаев соответствует циклонической картине и в 25% случаев - антициклонической. Также следует ожидать в среднем понижения давления и на высоких гелиографических широтах, где согласно {1} зарождается новый цикл.

Является ли наблюдаемая картина избытков скоростей вращения в фотосфере и в короне следствием чисто зональных течений, которые должны поддерживаться меридиональной циркуляцией со сложной структурой или вихрей циклонической и антициклонической природы, все равно следует ожидать что наблюдения позволят обнаружить вариации общей картины меридионального дрейфа, величины которых должны быть порядка выявленных избытков скоростей вращения, если будет реализована соответствующая программа наблюдений. Конечно, это достаточно сложная задача, т.к. обнаруженные в последнее время меридиональные течения имеют скорости от 10 до 40 м/с {14-16}.

Скорее всего, явление избытков скоростей вращения фотосферы, обнаруженное на обсерватории Маунт-Уилсон, и их дрейф к экватору имеют определенное отношение к механизму солнечной активности, к солнечным магнитным полям. Трудно сомневаться в том, что очередное возникновение зоны быстрого вращения в приполюсной области фотосферы не связано со следующим циклом. Если действительно зональные течения в короне динамически обусловлены фотосферными зональными течениями, то и в короне следует ожидать экваториального дрейфа. К сожалению, сравнительно короткий ряд наблюдений вращения короны не дает возможности определенно сказать о направлении смещения зональных течений: к экватору подобно картине, полученной Говардом и Лабонтом {1} для фотосферы или к полюсам подобно волокнам и ЛРП крупномасштабных магнитных полей.

В заключение авторы благодарят сотрудников СиБИЗМИР и ИЗМИРАН, способствовавших своими замечаниями улучшению этой работы.

Приложение

Оценка величин зональных течений и её погрешность
 Обычно для оценки коэффициентов A, B и C в выражении (1) или коэффициентов C_0, C_1 , и C_2 в равносильном выражении (1') применяется метод наименьших квадратов в его классическом варианте: из совокупности условных уравнений вида (1) или (1') составляется система нормальных уравнений для неизвестных, которая и решается. Однако нетрудно заметить что с приближением к полюсу (рост φ или убывание ϑ) и с ростом номера неизвестного (C_0, C_1, C_2) в условных уравнениях коэффициенты быстро убывают. В матрице нормальных уравнений элементы по этой же причине быстро убывают с ростом номера и строки и столбца. В результате точность определения C_1 и C_2 быстро ухудшается. Помимо этого наиболее существенный вклад в коэффициенты нормальных уравнений дают условные уравнения для низких широт. В силу сказанного полученное этим путем выражение вида (1) будет неплохо представлять картину распределения скоростей вращения с широтой в приэкваториальной зоне и с существенно меньшей точностью в приполярной зоне

Избежать этого дефекта можно путем перехода от условных уравнений вида (1) или (1') к эквивалентным условным уравнениям вида.

$$v_\lambda = B_0 \sin \vartheta + B_1 \sin 3\vartheta + B_2 \sin 5\vartheta. \quad (A 1)$$

Теперь уже коэффициенты при неизвестных B_0, B_1 и B_2 во всех условных уравнениях будут иметь один порядок и то же самое будет верно для нормальных уравнений. Более того, оказывается выгодным использовать свойство ортогональности функций $\sin k\vartheta$ на интервале $(-\frac{\pi}{2}, +\frac{\pi}{2})$.

Рассмотрим теперь вопрос об оценке величин избытков скоростей вращения. По существу избытки скоростей суть невязки отдельных условных уравнений вида (1) или (A1). В общем случае каждому условному уравнению можно приписать свой вес p_i , обратнопропорциональный квадрату погрешности δ_i свободного члена (наблюдаемое значение v_λ). Введем обозначения согласно {17}:

A - вектор-столбец неизвестных (коэффициенты в (1) или (A1)),

X - матрица условных уравнений,

P - диагональная матрица весов условных уравнений,

L - вектор-столбец свободных членов (наблюдения v_λ),

$D = L - XA$ - вектор-столбец невязок (избытки Δv_λ).

Тогда система нормальных уравнений имеет вид

$$(X^T P X) A = X^T P L, \quad (A2)$$

откуда

$$A = (X^T P X)^{-1} X^T P L. \quad (A3)$$

Следовательно,

$$D = (E - X(X^T P X)^{-1} X^T P) L = FL \quad (A4)$$

Таким образом, интересующие нас невязки (избытки) линейно выражены через свободные члены (наблюдения). Если полагать что отдельные условные уравнения соответствуют независимым измерениям, то диагональная матрица P^{-1} является корреляционной матрицей вектора L . Тогда корреляционная матрица G вектора D определяется соотношением

$$G = F P^{-1} F^T \quad (A5)$$

и содержит на главной диагонали квадраты погрешностей оценок невязок (избытков).

Для наблюдений короны Степанова и Тягун {4} вычисления по формулам этого приложения (см. табл. 2) убедительно показывают, что выделенные по регулярному ходу избытков скорости зональных потоков Δv_λ вполне значимы.

Л и т е р а т у р а

- {1} Howard, R., La Bonte, B.J., The Sun is observed to be a torsional oscillator with a period of 11 years, *Ap.J.* 239. L33, 1980
- {2} Yoshimura, H., Solar cycle Lorentz force waves and the torsional oscillations of the Sun, *Ap.J.* 247. 1102, 1981
- {3} La Bonte, B.J., Howard, R., Torsional waves on the Sun and the activity cycle, *Solar Phys.* 75. 161, 1982
- {4} Stepanov, V.E., Tyagun, N.F., Investigation of coronal rotation by the spectroscopic method, *IAU Symp.* 71. 101, 1976

- {5} La Bonte, B.J., Howard, R., Solar rotation measurements at Mount Wilson III. Meridional flow and limbshift, *Solar Phys.* 80. 361, 1982
- {6} Рубашев, Б.М., *Проблемы солнечной активности*, Наука, Москва, 1964
- {7} Kuklin, G.V., Obridko, V.N., *Preprint SibIZMIR*, 10, 1982
- {8} Хргиан, *Физика атмосферы*, Гидрометеиздат, Ленинград, 1969
- {9} Krinberg, I.A., Teplitskaya, R.B., On the adjustment of outer solar layer models, *Solar Phys.* 25. 305, 1972
- {10} Спитцер, Л., *Физика полностью ионизованного газа*, ИЛ, 1957
- {11} Седов, Л.И., *Методы подобия и размерности в механике*, 4-е изд., ГИТТЛ, Москва, 1957
- {12} Тассуль, Ж.-Л. *Теория вращающихся звезд*, МИР, Москва, 1982
- {13} Крат, В.А., *Фигуры равновесия небесных тел*, ГИТТЛ, Москва, 1950
- {14} Beckers, J.M., Observations of solar rotation and meridional flows at the Sacramento Peak Observatory, *Osserv. Astrofis. Catania Publ.* No. 162. 166, 1978
- {15} Duvall, T.L. Jr. Large-scale solar velocity fields, *Solar Phys.* 63.3, 1979
- {16} Howard, R., Evidence for large-scale velocity features on the Sun, *Ap. J.* 228. L45, 1979
- {17} Линник, Ю.В., *Метод наименьших квадратов и основы теории обработки наблюдений*, Физматгиз, Москва, 1962
- {18} Richardson, R.S., The nature of solar hydrogen vortices, *Ap. J.* 93.24, 1941

ПРОБЛЕМА ПЕРВИЧНОГО ИСТОЧНИКА ЭНЕРГИИ И
ВЕЩЕСТВА СОЛНЕЧНЫХ ВСПЫШЕК

Э.И. МОГИЛЕВСКИЙ

ИЗМИРАН, Москва

Абстракт:

Обсуждаются некоторые новые результаты наблюдений солнечных вспышек последних лет. Сделано заключение о том, что выдвинутая ранее автором гипотеза о волновом выходе из подфотосферы энергии и вещества вспышки (МГД солитонами, пакетами МГД волн) согласуется с наблюдениями.

THE PROBLEM OF THE PRINCIPAL SOURCE OF ENERGY AND
THE MASS OF SOLAR FLARES

E. I. MOGILEVSKIJ

IZMIRAN, Moscow

Abstract:

Some results of the observations of solar flares in the past years are discussed. The author concludes that the observations are in accordance with his former hypothesis about the wave-type output of energy and the matter of flares from below the photosphere (as MHD solitons, MHD wave packets).

1. Одной из основных проблем природы солнечных вспышек является задача установления первичного источника энергии и вещества импульсных и больших двухленточных вспышек. Наиболее разработанной и принятой большинством исследователей является модель предвспышечного накопления энергии в магнитном поле на высотах короны активной области (АО) в виде токовых слоев с последующей реализацией этой "свободной" (токовой компоненты) магнитной энергии во время вспышек. Эту модель условно назовем "стандартной" или моделью "А". Поскольку, однако, эта модель встречает ряд принципиально непреодолимых трудностей, в частности, в объяснении ряда наблюдательных данных {1}, то была предложена другая гипотеза (назовем ее "моделью Б"), состоящая в том, что первичные источники вспышки (энергии и вещества) расположены под фотосферой. В этой модели предполагается, что незадолго до и во время вспышки энергия и вещество транспортируются волновыми модами (МГД-солитоны, цуги быстрых магнитозвуковых волн) в верхнюю хромосферу и корону АО, где и происходят основные процессы вспышки. Международная программа "Год солнечного максимума" (раздел "FBS") среди первых основных задач предусматривала исследования первичных источников вспышки. "Сценарий" развития всего комплекса явлений вспышек, вероятно, может несущественно изменяться с переходом к модели "Б" первичных источников. Однако, как будет показано ниже, при этом снимаются многие отмеченные {1} трудности, а совокупность новых (полученных в последние годы) данных получает естественное объяснение. Вынос энергии и вещества из подфотосферных глубин волновыми МГД модами важен как для исследования предвспышечного состояния АО, так и вообще, в определении энергобаланса в эволюции вспышечно-активных областей.

2. Чтобы яснее представить себе качественное различие моделей "А" и "Б", рассмотрим кратко современную модель геомагнитной суббури. Аналогия между последними и солнечными вспышками неоднократно обсуждалась в литературе {2,3} и, несмотря на существенное различие в масштабах этих явлений, полезность такой аналогии продолжает привлекать внимание исследователей. Известно {3}, что токовый слой (или "двойной"

слой по Альвену) по оси хвоста магнитосферы Земли (согласно прямым измерениям на КА) является источником надтепловых частиц, которые, попадая в высокие геомагнитные широты, вызывают геомагнитные возмущения (суббури), полярные сияния и т.д. Деформация магнитосферы во время взаимодействия магнитосферы с замагниченной плазмой солнечного ветра определяет неустойчивость токового слоя хвоста магнитосферы и сброс в приполярные зоны надтепловых частиц. Однако (и это принципиально важно!) энергия суббури (и всей геомагнитной бури) равна той *внешней* по отношению к магнитосфере энергии, которая привносится солнечным корпускулярным полем. Эмпирически Акасофу {2} ввел индекс:

$$E = VB^2 F(\theta) \ell_0^2 \quad \{\text{эрг/с}\}, \quad (1)$$

где $F(\theta)$ - функция полярного угла θ вектора межпланетного магнитного поля; V - скорость солнечной плазмы (ветра) в окрестности Земли, и $\sim \ell_0^2$ - эффективная площадь магнитосферы, через которую происходит поступление энергии из солнечного потока. Экспериментальные оценки дают для ℓ_0 значение $\sim 7R_\oplus$, хотя, очевидно, что ℓ_0 является функцией плотности (ρ), скорости (v), величины поля (B) и угла θ в солнечном потоке. Очевидно, что E есть поток привнесенной в магнитосферу энергии солнечного геоэффективного потока. Последующие исследования показали, что суммарная энергия межпланетного магнитного поля (солнечного корпускулярного потока), которая при благоприятном угле θ (для пересоединения ММП с полем магнитосферы Земли) направления вектора поля поступила в магнитосферу, равна энергии геомагнитного возмущения суббури и всей геомагнитной бури. Величина E для геомагнитных возмущений различной интенсивности варьирует от $\sim 10^{18}$ до 10^{20} эрг.с⁻¹. Токовый слой хвоста магнитосферы способствует преобразованию этой поступившей энергии в ускоренные и сбрасываемые в полярные зоны частицы, однако геомагнитное поле при этом не аннигилировало. Структура деформированной магнитосферы (также, как и токовые слои хвоста) относительно быстро восстанавливается после прекращения поступления энергии от проходящего в окрестности Земли солнечного корпускулярного потока.

В случае солнечных вспышек токи (токовые слои), которые существуют в хромосфере и короне АО это подтверждается, например, наличием петельных и других структур короны и тем, что в сложных АО поле близко к токовой бессиловой конфигурации играют примерно ту же роль, что и токи в хвосте магнитосферы Земли. Но основная энергия вспышки (и инжектированная в межпланетную среду замагниченная плазма) с необходимостью должна быть привнесена извне. По модели "Б" - это энергия серии уединенных МГД возмущений, которая идет из подфотосферных глубин АО. В этом и состоит основное отличие моделей "А" и "Б", в результате которого меняется понимание комплекса наблюдаемых явлений в АО, связанных со вспышками.

В модели "А" во время вспышки должна реализоваться энергия токовой компоненты поля короны в АО. Проверенные расчеты показывают {4}, что во время больших вспышек реализация всей "свободной" энергии поля АО (токовой компоненты) должна была бы заметным образом отразиться на всей структуре магнитного поля АО. Новые расчеты {5} показали, что изменения корональных токов (полей) непосредственно связаны с перестройкой фотосферного поля за время вспышки ($t \sim 10^3$ с). Отсюда следует, что из-за больших характерных размеров токов (т.е. большой самоиндукции) за время вспышки может быть реализовано не больше 10% свободной энергии АО {6}, что почти на два порядка меньше энергии больших вспышек. Неоднократные попытки измерить во время вспышек вариации магнитных полей в фотосфере АО {7,8,9} не позволили обнаружить такие изменения, которые были присущи только вспышкам. Обычно наблюдаемые изменения (качественно и по амплитуде) не отличались от вариаций магнитных полей, которые характеризуют неспышечную эволюцию активной области.

Однако в последние годы с помощью видеомагнитографа удалось обнаружить кратковременное существование маломасштабных ($\approx 3 \div 5''$) сильных ($B \approx 10^2 \div 10^3$ Г) магнитных полей вблизи линии смены полярности. Эти "магнитные транзиенты" {10,11} появлялись вблизи тех мест и в то время, где отмечалась вспышечная эмиссия. Характерно, что магнитные транзиенты наблюдались при вспышках вне центральной зоны диска, т.е. у них преобладала H_{\perp} компо-

нента поля. Последующие спектроскопические определения магнитных полей в местах эмиссии вспышек {12} также фиксировали кратковременные большие ($\leq 10^2 \div 10^3$ G) магнитные поля. Эти пока еще небесспорные (с экспериментальной точки зрения) наблюдения собственно вспышечных нестационарных магнитных полей малого масштаба в какой-то мере напоминают ранее рассчитанные {1} сильные локальные волновые возмущения (МГД-солитоны), т.е. указывают на возможную справедливость модели "Б" о первичных источниках вспышек. Проведенные оценки энергии этих нестационарных возмущений подя {10} показали, что магнитные транзиенты содержат энергию, сравнимую с энергией больших вспышек.

3. Эксперименты на КА "SMM" совместно с наблюдениями с наземными телескопами в период осуществления программы "ГСМ" (1979-80 гг) позволили получить для нескольких солнечных вспышек достаточно полную картину последовательности появления вспышечной эмиссии в оптике, мягком и жестком рентгене, далекой УФ области и в радиодиапазоне. Перечислим кратко те результаты программы "ГСМ", которые содержат информацию о первичных источниках энергии и вещества вспышек.

а). Комплекс наблюдений прилибровой вспышки 29.06.80 (рентгеновский балл - M4), согласно {13}, подтвердил данные предыдущих наблюдений на SMM о том, что жесткая ($25 \div 300$ кев) эмиссия исходит из оснований корональных петель (т.е. с высот фотосферы или хромосферы) и начинается одновременно с H α -эмиссией вспышек раньше на 2-3 минуты, чем мягкая рентгеновская эмиссия с вершины и в самих петлях. Развитие импульсной фазы вспышки удалось проследить на снимках с высоким разрешением в линиях переходной зоны (O V; $\tau \sim 2.5 \cdot 10^5$) и горячей вспышечной плазмы (Fe XXI; $\tau \sim 1.1 \cdot 10^7$). Вначале появилась эмиссия в O V (яркая точка, а затем петля с движением вещества вверх) и лишь затем по более высокой петле ($h \approx 30000$ км) появилась эмиссия в Fe XXI.

б). В ряде случаев, когда удавалось получить спектрограммы в импульсной фазе в УФ и видимом диапазонах отмечался доплеровский сдвиг или "голубая асимметрия", указывающие на начальный подъем вещества.

в). В последние годы опубликованы работы {14,15}, в которых по

ряду детальных спектроскопических данных показано, что непрерывная эмиссия "белых вспышек" связана с фотосферным излучением ионов H^- . Эта эмиссия появлялась на несколько минут (до 8^m) раньше мягкой рентгеновской эмиссии корональных петель.

г). В период программы ГСМ детально исследовались некоторые $H\alpha$ вспышки в ядрах больших солнечных пятен {16,17}. Это отнюдь не редкое (во многих больших вспышках также отмечалась изолированная яркая $H\alpha$ эмиссия в больших пятнах), но еще мало изученное явление указывает на возможность появления вспышечной $H\alpha$ эмиссии на малых высотах в поле пятна одной магнитной полярности (т.е. где нет эффекта пересоединения магнитных полей). При этом микроволновые радиовсплески практически не наблюдались.

д). Принципиально новые результаты получены в последние годы на КА по изучению релятивистских электронов (они генерируют континуум γ -излучения) и протонов. Последние вызывают монохроматическое ядерное излучение в γ -диапазоне. Наиболее сильные ядерные линии 2,2 Мэв (реакция захвата нейтрона протоном), 4,4 Мэв (^{12}C); 6,1 Мэв (^{16}O). Не вдаваясь в подробное рассмотрение этого имеющего самостоятельный интерес вопроса {18,19}, отметим только следующее:

(I). Наблюдения на КА "SMM" и "Hinotori" существенно увеличили число случаев вспышек с γ -линиями. С повышением чувствительности приемников оказалось что многие (если не все) вспышки сопровождаются импульсной ($\Delta t \sim$ десятки секунд) или продолжительной (от сотен до полутора тысяч секунд) ядерной эмиссией.

(II). Спектр релятивистских протонов и электронов ($E > 1$ Мэв) в источнике оказался степенной и удивительно постоянный (со степенью 2). Общее число ускоренных протонов $\sim 10^3$ раз (т.е. в отношении m_p/m_e) превышало число электронов с той же энергией. Это в сочетании с работами советских исследователей {20} показало, что ускорение электронов и протонов происходит одновременно в относительно плотных ($> 10^{12} \text{ см}^{-3}$) слоях АО. Долгое время существовало представление о двухступенчатом ускорении частиц во вспышке: импульсное первичное ускорение электронов (например, при разрыве токового слоя) и вторичное ускорение на фронте вспышечной ударной волны. Новые данные по γ -спек-

троскопии указывают на одноступенчатый механизм ускорения, действующий на очень малых высотах (в фотосфере или хромосфере) в АО. Установленное для ряда вспышек соотношение $T_{\frac{1}{2}}^i > T^e$, где $T_{\frac{1}{2}}^i$ - температура многозарядных ($z > 2$) ионов (i), а T^e - температура электронов, свидетельствует об отсутствии (или малой эффективности) в процессе ускорения турбулентности.

(III). Хотя имеется некоторое различие между кратковременной и продолжительной ядерными эмиссиями вспышек [19], общим для них является то, что они начинаются одновременно с жестким рентгеновским излучением, которое, как отмечалось выше, генерируется в основании вспышечных петель, т.е. на уровне фотосферы или хромосферы. Учитывая малые величины сечений ядерных взаимодействий (т.е. ядерные реакции требуют относительно большие плотности вещества), следует заключить, что и ядерная эмиссия (особенно длительная) происходит с фотосферного уровня АО и с самого начала импульсной фазы.

е). В программе наблюдений на КА "SMM" большое внимание уделялось исследованию с внезатменным коронографом и другими приборами явлениям корональных транзиентов, т.е. выброса на большие высоты и ряда случаев - в межпланетную среду огромных замагниченных плазменных облаков. Корональные транзиенты (в картинной плоскости) напоминают преимущественно по форме вытянутую арку. Часть корональных транзиентов непосредственно связана со вспышками. Существенно то, что оценка общей массы корональных транзиентов ($\approx 10^{16}$ г) превышала (на 1-2 порядка) массу коронального вещества всей АО. Суммарная энергия для транзиента вспышки 5.09.79 г магнитного поля $E_{\text{mag}} \approx 10^{31}$ эрг, тогда как $E_{\text{мех}} \approx 10^{30}$ эрг, а суммарная энергия эмиссии вспышки $E_{\text{рад}} \approx 10^{29}$ эрг. Такие характеристики инжектируемых в межпланетную среду вспышечных корональных транзиентов указывают на то, что их масса и энергия транспортировались из основания АО (фотосферы и хромосферы). Кроме того важно подчеркнуть, что на генерацию корональных транзиентов расходуется энергия на $\approx 1,5$ порядка больше, чем на все виды вспышечной эмиссии. Такие массы и соотношение энергий в корональных транзиентах возможны,

если их выход обусловлен источниками на уровне фотосферы или под фотосферой {21}.

Из всего вышеизложенного следует, что совокупность различных наблюдений последних лет указывает на то, что первичное энерговыделение вспышек происходит преимущественно в основании АО (на фотосферно-хромосферном уровне). Это может служить аргументом в пользу гипотезы модели "Б". Принципиальная важность выбора модели первичного источника требует постановки серии прямых экспериментов, в которых с достаточной определенностью выявились бы основные положения модели "Б". На башенном телескопе ИЗМИРАН подготовлена и действует кроме двухканального магнитографа также двухканальный высокочувствительный измеритель лучевых скоростей (интегральный интерференционный фотоэлектрический тахометр) {22}. С помощью этой аппаратуры предполагается провести соответствующие серии программных наблюдений, которые позволили бы выяснить степень справедливости обсуждаемой модели "Б".

Л и т е р а т у р а

- {1} Могилевский, Э.И., Энергетика и феноменология больших солнечных вспышек, *Физ.солн.акт.*, 3, 1980
- {2} Akasofu, S.I., Energy coupling between the solar wind and the magnetosphere, *Space Sci.Rev.*, 28, 121, 1981
- {3} Akasofu, S.I., *Physics of magnetospheric substorms*, *Astrophysics and Space Science Library*, Vol.47, D.Reidel Dordrecht, 1977
- {4} Могилевский, Э.И., Утробин, В.Г., Использование карт магнитного поля для расчета токовой компоненты поля в атмосфере вспышечно-активных областей, *Phys.Solariterr.*, 13, 102, 1980
- {5} Low, B.C., Hu, I.Q., The energy of electric current sheets, *Solar Phys.*, 81, 107, 1982, 84, 83, 1983
- {6} Yeh, T., Diffusive hydromagnetic flow in the vicinity of a neutral point, *Ap.J.*, 207, 837, 1976
- {7} Зверева, А.М., Северный, А.Б., Магнитные поля и протонные вспышки 6 июля и 2 сентября 1960 г., *Изв.КрАО*, 41-42, 97, 1970
- {8} Tanaka, K., Measurements and analysis of magnetic field variation during a class 2b flare, *Solar Phys.*, 58, 149, 1978
- {9} Harvey, K.L., Harvey, I.W., A study of magnetic and velocity fields in an active region, *Solar Phys.*, 47, 233, 1976
- {10} Zirin, H., Tanaka, K., Magnetic transients in flares, *Ap.J.* 250, 791, 1981

- {11} Zirin, H., Heidig, D.E., Continuum emission in the 1980 July 1 solar flare, *Ap.J.*, 248, L45, 1981
- {12} Лоцицкая, Н.И., Лоцицкий, В.Г., Существуют ли "магнитные транзиенты" в солнечных вспышках? *Письма в АЖ*, 8, 500, 1982
- {13} Poland, A.T., Machado, M.E., Wolfson, C.I., Frost, K.J., Woodgate, B.E., Shine, R.A., Kenny, P.J., Cheng, C.C., Tandberg-Hanssen, E.A., Bruner, E.C., Henze, W., The impulsive and gradual phases of a solar limb flare as observed from the Solar Maximum Mission satellite, *Solar Phys.*, 78, 201, 1982
- {14} Hiei, E., A continuous spectrum of a white light flare, *Solar Phys.* 80, 113, 1982
- {15} Барановский, Э.А., Коваль, А.Н., К вопросу о непрерывной эмиссии вспышек *Изв. КРАО*, 45, 35, 1982
- {16} Могилевский, Э.И., Гомологичные H α -вспышки в ядрах комплекса активных областей MM-16862-3 в мае 1980 года, *ГСМ-SMY Crimean Workshop*, 2, 151, 1981
- {17} Шилова, Н.С., Бабин, А.Н., Делоне, А.Б., Кирюхина, А.И., Макарова, Е.А., Якунина, Г.В., Мамедов, С.Г., Мусаев, М.М., Оруджев, Э.Ш., Сеидов, А.Г. H α -вспышки в тени пятен в конце мая 1980 года, *ГСМ-SMY Crimean Workshop*, 2, 180, 1981
- {18} Кужевский, Б.М., Гамма-астрономия Солнца и исследование солнечных космических лучей, *Успехи физических наук*, 137, 237, 1982
- {19} Ковальцов, Г.А., Кочаров, Г.Е., Вспышечные гамма-кванты, протоны и электроны, *Препринт ФТИ*, 799, 1982
- {20} Курт, В.Г., Логачев, Ю.И., Писаренко, Н.Ф., и др., Ускорение частиц в малых вспышках, *Труды 9. Ленинградского семинара по космофизике*, 128, 1978
- {21} Wagner, W.I., Hildner, E., House, L.L., Sawyer, C., Sheridan, K.V., Dulk, G.A., Radio and visible light observations of matter ejected from the Sun, *Ap.J.*, 244, L123, 1981
- {22} Горский, С.М., Кожеватов, И.Е., Куликова, Е.К., Использование двухлучевой интерференции в аппаратуре для исследования динамики солнечной атмосферы, *Иссл. СибИЗМИР*, 52, 116, 1980

ДИНАМИКА ЭНЕРГИЧНЫХ ПРОТОНОВ В СОЛНЕЧНЫХ МАГНИТНЫХ ПЕТЛЯХ
ЭФФЕКТЫ ДИСПЕРСИИ АЛЬВЕНОВСКИХ ВОЛН

В.А. МАЗУР, А.В. СТЕПАНОВ

СибИЗМИР, Иркутск

Абстракт:

Показано, что дисперсия альвеновских волн, связанная с учетом гиротропии $\omega/\omega_i \ll 1$, приводит к канализации альвеновских волн в неоднородностях плотности плазмы (дуктах) корональных петель. Установлено, что если радиус дукта R и скорость Альвена A удовлетворяют соотношению $\xi = \omega^2 R / \omega_i A > 1$, то рефракция не нарушает квазипродольный характер распространения альвеновских волн и усиление волн в петлях может быть значительным.

Во вспышечных петлях $\xi \sim 10^2$, поэтому изотропизация ускоренных в петлях протонов на альвеновских волнах приводит к быстрому уходу протонов в конус потерь и гибели их в солнечной хромосфере. Это объясняет наблюдаемый в некоторых вспышках дефицит энергичных протонов в межпланетной среде по сравнению с их числом, ожидаемым по гамма-излучению. В источниках пульсирующих всплесков IV типа где $\xi \sim 1$ pitch-угловая диффузия протонов на альвеновских волнах определяет длительность цуга пульсаций. "Хорошими" для удержания энергичных протонов являются высокие ($\sim 1R_\odot$) корональные магнитные петли без дуктов.

DYNAMICS OF ENERGETIC PROTONS ON SOLAR MAGNETIC LOOPS

ALFVEN WAVE DISPERSION EFFECTS

V.A. MAZUR, A.V. STEPANOV

SibIZMIR, Irkutsk

Abstract:

It is shown that the Alfvén wave dispersion associated with the gyrotropy $\omega/\omega_i \ll 1$, leads to waveguiding of Alfvén waves in plasma density inhomogeneities (ducts) of coronal loops. It was found that if the radius R of the duct and the Alfvén velocity A satisfy the condition $\xi = \omega^2 R / \omega_i A > 1$, then refraction does not violate the quasi-longitudinal propagation of Alfvén waves, and wave amplification on loops may become substantial.

$\xi \sim 10^2$ in flaring loops; thus isotropisation of loop-accelerated protons by Alfvén waves forces the protons to escape rapidly into the loss-cone and to precipitate in solar chromosphere. This explains the deficit of ≥ 10 MeV protons expected from the γ -ray emission, in interplanetary space observable in some flares as compared to their number. In sources of pulsations of type IV radio emission where $\xi \sim 1$, the pitch-angle diffusion of protons due to Alfvén waves determines the pulse train duration. Large ($\sim 1R_\odot$) coronal magnetic loops without ducts are good candidates for the storage of energetic protons.

1. Введение

Ускоренные при солнечной вспышке энергичные протоны могут, как известно, длительное время (часы-дни) удерживаться в корональных петлях - адиабатических магнитных ловушках {8}. С другой стороны, в некоторых вспышках наблюдалось интенсивное гаммаизлучение, вызываемое протонами с энергией 10 Мэв, а потоки протонов в межпланетной среде были значительно меньше ожидаемых {9}. Такие явления свидетельствуют о быстрой гибели ускоренных протонов в плотных слоях атмосферы Солнца.

Разнообразие в поведении энергичных протонов в солнечной атмосфере может быть связано с различными условиями удержания протонов в корональных петлях. Если энергия плазмы и быстрых частиц сравнима с энергией магнитного поля, $\beta = 8\pi\rho/V^2 \sim 1$, то магнитная петля разрушается из-за отсутствия равновесия или МГД-неустойчивости. Энергичные протоны выходят из ловушки за время $\tau \sim \ell/A \sim 1-10^2$ с, где $\ell \sim 10^8-10^{10}$ см - характерный масштаб петли, $A \sim 10^8$ см/с - скорость Альвена. При $\beta \ll 1$ максимальное время удержания определяется кулоновскими соударениями и в зависимости от энергии протонов составляет величину от нескольких часов до нескольких дней {7}. Wentzel {10} обратил внимание на то, что энергичные протоны в корональных петлях формируют распределение с "конусом потерь". В результате развивается циклотронная неустойчивость альвеновских волн с частотой $\omega \approx \omega_i A/v \approx 10^{-2} \omega_i$ и с длиной волны $\lambda \approx 2\pi v/\omega_i \lesssim 10^7$ см. Здесь v - скорость протонов, $\omega_i \lesssim 10^4$ с⁻¹ - гирочастота протонов. Инкремент неустойчивости максимален для волн, распространяющихся вдоль магнитного поля {4}

$$\gamma \approx 0,4\omega\eta\beta_h, \quad \eta > \omega/\omega_i \quad (1)$$

и резко уменьшается при $k_{\perp} > (\omega/\omega_i)^{1/2} k_{\parallel}$. Здесь η - степень анизотропии энергичных протонов, связанная с величиной пробочного отношения $\sigma = V_{\max}/V_{\min}$ соотношением $\eta = 3/2(\sigma - 1)$, $\beta_h = 8\pi P_h/V^2$, P_h - давление энергичных протонов, k_{\perp} и k_{\parallel} - поперечное и продольное по отношению к магнитному полю волновые числа. Изотропизация протонов на альвеновских волнах должна приводить к уходу протонов в конус потерь и гибели их в хромосфере Солнца через несколько секунд после ускорения, что противоречит данным о длительном удержании протонов.

Решающим фактором в динамике энергичных протонов в солнечной короне по мнению Wentzel [10] является кривизна магнитного поля петли. Рефрагирующие альвеновские волны быстро выходят из режима квазипродольного $k_{\perp} < (\omega/\omega_i)^{1/2} k_{\parallel}$ распространения, при котором усиление альвеновских волн эффективно, их амплитуда остается на низком уровне и они не влияют на динамику энергичных протонов. В рамках той же идеи более строго эволюцию рефрагирующих альвеновских волн в корональных петлях исследовали на основе приближения геометрической оптики Меерсон и др. [6]. Они пришли к заключению, что наиболее важным с точки зрения удержания протонов параметром является параметр β_h . Если β_h меньше некоторого критического, то удержание определяется не изотропизацией протонов на альвеновских волнах, а кулоновскими соударениями и магнитным дрейфом.

В настоящей работе учтены два новых обстоятельства. Во-первых, наличие в корональных петлях дактов - неоднородностей плотности плазмы, вытянутых вдоль магнитного поля. Во-вторых, дисперсия альвеновских волн, связанная с конечностью величины $U \equiv \omega/\omega_i \ll 1$, которая при определенных условиях приводит к канализации альвеновских волн в дактах [5]. В результате волны сохраняют квазипродольный характер распространения и усиление волн может быть значительным. Поэтому динамика энергичных протонов в солнечной короне определяется не только параметрами протонов, но, в большей степени, свойствами корональных петель.

2. Корональная петля - альвеновский волновод

Исследования рентгеновского излучения Солнца выявили существование в корональных петлях дактов - магнитных трубок, в которых плотность плазмы превышает плотность окружающей среды [3]. Дополнительным свидетельством существования дактов в солнечной короне являются пульсации радиоизлучения IV типа, которые, вероятнее всего, обусловлены МГД-колебаниями дактов. При распространении волн в поперечно-неоднородной (по отношению к магнитному полю) плазме большое значение имеет их поперечная дисперсия. Обычно дисперсией альвеновских волн пренебрегают, полагая $\omega = k_{\parallel} A$. В этом случае в неоднородной плазме не

существует собственных альвеновских колебаний. Эволюция среднего волнового вектора пакета альвеновских волн описывается уравнением

$$\frac{d\vec{k}}{dt} = - \frac{\delta\omega}{\delta\vec{r}} . \quad (2)$$

Отклонение волнового вектора от направления магнитного поля при движении пакета от вершины петли, согласно (2), можно характеризовать поперечным волновым числом $k_{\perp} \sim \omega t/R$, где $t \sim \ell/A$ - время прохождения пакетом пути ℓ/R - радиус дакта. Поскольку волны выходят из режима усиления при $k_{\perp} \sim \sqrt{u} k_{\parallel}$, то пакет пересечет усиливаться пройдя путь $\ell \sim \sqrt{u}R$. Без дактов этот путь значительно больше: $\ell \sim \sqrt{u}L$, где L - продольный размер петли ($L \gg R$). Дакты, на первый взгляд, увеличивают рефракцию альвеновских волн в \vec{k} - пространстве и, следовательно, ухудшают усиление волн в корональных петлях.

Ситуация радикально меняется при учете дисперсии альвеновских волн. Простейшая схема позволяющая исследовать эффекты дисперсии - это двухжидкостная гидродинамика, в которой пренебрегается инерцией электронов и столкновениями частиц. Кроме рассматриваемой здесь "холодной" дисперсии, порядок величины которой u , учет конечного ларморовского радиуса ионов приводит к "горячей" дисперсии, порядок величины которой $k_{\perp}^2 \rho_i^2$. При $\beta \ll 1$ "горячая" дисперсия больше "холодной", если $k_{\perp} > \beta^{-1/4} k_{\parallel}$. Нас интересует квазипродольное $k_{\perp} \lesssim \sqrt{u} k_{\parallel}$ распространение, т.е. "холодная" дисперсия, связанная с инерцией ионов. В этом приближении известное электродинамическое уравнение для компоненты электрического поля волны \vec{E}_{\perp} , перпендикулярной магнитному полю $\vec{B} = (0, 0, B)$ имеет вид

$$\text{rot rot } \vec{E}_{\perp} = \frac{\omega^2}{A^2} \frac{1}{1-u^2} (\vec{E}_{\perp} + iu [\vec{E}_{\perp}, \frac{\vec{B}}{B}]) . \quad (3)$$

Эффекты дисперсии наиболее просто пояснить на примере однородной плазмы. Полагая $\vec{E} \sim \exp(-i\omega t + i\vec{k}\vec{r})$ из (3) получаем

$$\omega = k_{\parallel} A \left[1 - \frac{u^2}{2} - \frac{u}{2} \left(\frac{k_{\perp}^2}{k_0^2} + \sqrt{1 + \frac{k_{\perp}^4}{k^4}} \right)^{-1} \right], \quad (4)$$

где $k_0^2 = 2uk_{\perp}^2$. Видно, что дисперсия существенна при квазипродольном распространении, $k_{\perp} \lesssim k_0$, и полностью обусловлена малой поправкой $u \equiv \omega/\omega_i \ll 1$.

Важным свойством поперечной дисперсии альвеновских волн является ее положительность, $\delta\omega/\delta k_{\perp} > 0$, т.е. направления групповой скорости и поперечной компоненты волнового вектора совпадают. Тогда нетрудно понять что дакт может играть роль волновода для альвеновских волн. В самом деле, пусть в начальный момент времени пакет альвеновских волн находится в стороне от оси дакта, на которой значение скорости Альвена $A = B/\sqrt{4\pi n_i n_o}$ минимально. Согласно уравнению (2) поперечный волновой вектор пакета начинает увеличиваться в направлении оси дакта и появляется групповая скорость в ту же сторону. После прохождения пакетом оси дакта поперечный волновой вектор меняется в обратном направлении и пакет повернет назад. Эти сравнительно медленные колебания накладываются на быстрое движение пакета с альвеновской скоростью вдоль магнитного поля. При этом, что особенно важно, поперечное волновое число меняется в ограниченных пределах, что создает возможность значительного усиления альвеновских волн.

3. Модель цилиндрического волновода

Геометрическая оптика даёт только качественную картину явления. Для более полного описания нужно обратиться к уравнению (3) для поля. Ограничиваясь для простоты аксиально-симметричными возмущениями $\vec{E}_{\perp} = \vec{E}_{\perp}(r) \exp(-i\omega t + ik_{\parallel} z)$ из уравнения (3) находим связь между компонентами E_r и E_z :

$$E_r = iu \frac{\omega^2}{A^2} [k_{\parallel}^2 (1-u^2) - \omega^2/A^2]^{-1} E_z. \quad (5)$$

Из соотношения (5) видно, что волна будет альвеновского типа (левополяризованная) при $k_{\parallel}^2 (1-u^2) > \omega^2/A^2$.

Вводя новую переменную $\psi = r^{1/2} E_z$, из (3) получаем уравнение Шредингера

$$\frac{d^2 \psi}{dr^2} - U(r) \psi = 0 \quad (6)$$

Для профиля плотности вблизи оси дакта

$$n_o(r) = n_o(0) (1-r^2/R^2) \quad (7)$$

потенциал можно представить в виде

$$U(r) = q^2 \left(\frac{r^2}{R^2} + \delta + 2u^2 - \frac{u^2}{\delta + r^2/R^2} \right) + \frac{3}{4r^2}, \quad (8)$$

где $q = \omega/A_0$, $A_0 = B/\sqrt{4\pi\epsilon_0 n_0(0)}$. Граничными условиями для уравнения (6) являются требования ограниченности функции $\psi(r)$ при $r=0$ и $r \rightarrow \infty$. Уравнение (6), (8) с такими граничными условиями рассматриваем как задачу на собственные значения. При $\omega = \text{const}$ роль собственного значения играет параметр δ , который связан с продольным волновым числом k соотношением

$$k_{||}^2 = q^2 \frac{1+\delta}{1+u^2}, \quad 0 < \delta \ll 1.$$

Рассмотрим частный случай, когда область локализации решений столь мала, что $r^2/R^2 \ll \delta$. Тогда решение уравнения Шредингера (6) с потенциалом (8), удовлетворяющее граничному условию при $r=0$ имеет вид

$$\psi = r^{3/2} \exp\left[-\left(1 + \frac{u^2}{\delta^2}\right) \frac{qr^2}{R}\right] \Phi\left(-(\epsilon-1), 2; \left(1 + \frac{u^2}{\delta^2}\right) \frac{qr^2}{R}\right), \quad (9)$$

где $\Phi\{x, y; z\}$ - вырожденная гипергеометрическая функция, а

$$\epsilon = \frac{1}{4} \left(1 + \frac{u^2}{\delta^2}\right)^{-1/2} \left(\frac{u^2}{\delta} - \delta - 2u^2\right) qR.$$

Решение удовлетворяет второму граничному условию (при $r \rightarrow \infty$), если $\epsilon - 1 = n$, $n = 0, 1, 2, \dots$. Тогда функция Φ есть полином Эрмита степени n . Из последнего равенства находим

$$\delta = \delta_n = u - u^2 - \frac{2\sqrt{2}(n+1/2)}{qR}. \quad (10)$$

Характерный масштаб локализации решений с малыми номерами n , как следует из (9), порядка $\Delta r \sim \sqrt{R/q}$. Требование $(\Delta r)^2/R^2 \ll \delta$ приводит к неравенству

$$\xi = uqR \gg 1. \quad (11)$$

Масштаб Δr определяет характерное поперечное волновое число $k_{\perp} \sim (\Delta r)^{-1} \sim \sqrt{q/R}$. Из (11) следует, что $k_{\perp} \ll \sqrt{u} k_{||}$ т.е. найденные решения удовлетворяют условию квазипродольности распространения. Отсюда, в частности, вытекает что эти решения обладают круговой поляризацией: $E_r = iE_{\phi}$. В этом можно убедиться, используя

соотношения (5) и (10). Моды с небольшими номерами n имеют масштаб локализации решения $\Delta r \ll R$. При увеличении номера n , как следует из анализа уравнения (6), масштаб локализации решения возрастает: $\Delta r \sim R$. Итак, при $\xi \gg 1$ в плазменном дакте существует целый набор квазипродольных собственных альвеновских мод, эффективно усиливающихся при циклотронной неустойчивости.

Леонович и др. [5] показали, что в плоской геометрии собственные альвеновские моды существуют при любом значении параметра ξ . В цилиндрической геометрии необходимым условием существования собственного решения уравнения (6) является требование $U_{\min} < 0$. Здесь U_{\min} - минимальное значение потенциала (8), вид которого представлен на рис. 1. Из (8) следует, что при $\xi^2 = u^2 q^2 R^2 < 3/4$ потенциал везде положителен и собственных решений нет. Поскольку при $\xi \gg 1$ существует целый набор решений, то ясно, что имеется некоторое критическое ξ_c такое, что при $\xi > \xi_c$ волноводные решения есть, а при $\xi < \xi_c$ их нет. По порядку величины $\xi_c \sim 1$. Итак, при $\xi < \xi_c$ эффект дисперсии недостаточно силен для существования волноводных решений и альвеновские волны испытывают сильную рефракцию при распространении в дактах корональных петель. В этом случае условия для значительного усиления волн отсутствуют.

Изложенный вывод чувствителен к профилю плотности плазмы. Исследование уравнения (6) для скачкообразного профиля показывает, что собственные решения существуют для любого значения параметра ξ . Вид потенциала $U(r)$ для такого профиля показан на рис. 1 штриховой линией. На наш взгляд, профиль (7) лучше описывает реальное распределение плазмы, чем скачкообразный профиль. Поэтому мы сохраним свой вывод об отсутствии волноводных решений при $\xi < 1$.

4. Обсуждение

4.1. Вспышечные петли

Наблюдения рентгеновского и гамма-излучения солнечных вспышек показывают, что в некоторых случаях протоны с энергиями порядка десятков Мэв ускоряются, как и электроны, на импульсной фазе вспышки [9]. Первоначальное энерговыделение происходит, по-видимому, в магнитных петлях с размерами $R \sim 10^8$ см

и $L \sim 10^9$ см и с плотностью плазмы $n_0 \sim 10^{10} - 10^{11} \text{ см}^{-3}$, на порядок превышающей плотность плазмы вне петель {3}. Вспышечная петля, следовательно, является дактом. Во вспышечной петле с $\nu \geq 200$ Гс параметр $\xi = \omega^2 R / \omega_i A \gtrsim 10^2$. Это означает, что альвеновские волны не выходят из режима квазипродольного растраскивания по всей длине петли и эффективно усиливаются энергичными протонами, что, в свою очередь, приводит к интенсивной диффузии протонов в конус потерь. Представим коэффициент пичч-угловой диффузии в виде {4}

$$D \approx \frac{B_A^2}{B^2} \omega_i, \quad (12)$$

где B_A - амплитуда магнитного поля альвеновских волн. При достаточно низком уровне альвеновской турбулентности значение B_A^2 можно определить из линейной теории

$$B_A^2 = B_{Af}^2 \exp \Gamma, \quad (13)$$

где B_{Af}^2 - уровень тепловых альвеновских шумов, который в области $k_{\perp} \lesssim \sqrt{v} k_{\parallel}$ по порядку величины равен

$$B_{Af}^2 \sim u T (\omega_i / v)^3, \quad (14)$$

T - "температура" энергичной компоненты. Коэффициент усиления волн $\Gamma = 2\gamma L/A$ с учетом (1) имеет вид $\Gamma \approx 0,8 \omega_i \beta_H \eta L/v$. Полагая $\nu = 200$ Гс, $n_0 = 10^{10} \text{ см}^{-3}$, $L \sim 10^9$ см, $T = 15$ Мэв находим, что при $\eta = 0.1$ и сравнительно небольшом давлении энергичной компоненты $\beta_H = 10^{-3}$ величина усиления $\Gamma \approx 30$. Тогда с учетом (14) получаем $B_A^2 / B_{Af}^2 \approx 5 \times 10^{-8}$. Подставляя последнее значение в коэффициент диффузии (13), находим характерное время удержания протонов во вспышечной петле: $\tau \sim D^{-1} \sim 10$ с. Очевидно, что с ростом β_H время пичч-угловой диффузии τ уменьшается, однако в этом случае в коэффициент усиления вместо L нужно подставлять значение $A\tau$, поскольку τ становится меньше времени прохождения пакетом длины петли $\sim L/A \sim 10$ с. Таким образом, если протоны ускоряются во вспышечных петлях, то они быстро, за время менее секунды диффундируют на альвеновских волнах в конус потерь и гибнут в плотных слоях солнечной атмосферы, вызывая при этом гамма-излучение. Отсюда понятно, почему в некоторых вспышках наблюдается значительный дефицит протонов в межпланетном пространстве по сравнению с числом протонов, дающих гамма-излучение {9}.

4.2. Источники пульсации радиоизлучения IV типа

Недавно Зайцев и др {2} на основе анализа связи пульсаций радиоизлучения IV типа с энергичными протонами в межпланетном пространстве пришли к выводу, что секундные пульсации связаны с МГД-колебаниями источника радиоизлучения. При этом предполагается, что часть ускоренных во вспышку протонов захватывается в высокие ($\sim 1R_{\odot}$) корональные петли с повышенной плотностью плазмы (дакты), которые являются резонаторами для быстрых магнитозвуковых (БМЗ) волн. При определенном давлении энергичных протонов β_H возбуждаются БМЗ-колебания петли, которые модулируют радиоизлучение. При уменьшении β_H БМЗ-колебания петли быстро затухают, поэтому длительность цуга пульсаций (несколько минут) определяется фактически временем удержания протонов в корональной петле. Кулоновские соударения приводят к времени удержания от нескольких часов до нескольких дней. Рассмотрим поэтому диффузию протонов в конус потерь петли на альвеновских волнах.

Пусть магнитное поле в вершине петли $B_L = 1$ Гс, в средней части $B_{L/2} = 10$ Гс, а у пробки $B_m = 100$ Гс. Полагая радиус дакта $R \approx 10^9$ см $v \approx 10^{10}$ см/с, $A(z) = 10^8$ см/с = const, находим параметр $\xi = \omega^2 R / \omega_i A$ в различных частях петли: $\xi_L \approx 10$, $\xi_{L/2} \approx 1$, $\xi_m \approx 0.1$. Альвеновские волны, следовательно, находятся в квази-продольном режиме распространения в верхней половине источника пульсаций радиоизлучения IV типа, т.е. длина усиления порядка размера петли L . Из соотношений (12)-(14) определим величину давления протонов, необходимую для объяснения наблюдаемой длительности цуга пульсаций

$$\beta_H \approx \frac{A}{\eta \omega L} \ln \left(\frac{B^2 v^3}{\tau_0 u T \omega_i^4} \right). \quad (15)$$

Для $\eta = 10^{-2}$, $B = 1$ Гс, $v = 10^{10}$ см/с, $L = 5 \times 10^{10}$ см, $\tau_0 \approx 2 \times 10^2$ с из (15) находим $\beta_H \approx 0.1$. Такая величина β_H как показывают оценки, легко достигается при вспышке.

4.3. Высокие корональные ловушки

Из радиогелогографических наблюдений следует, что пульсации радиоизлучения IV типа исходят из компактного источника,

вложенного в более протяженный источник континуального излучения {1}. Это означает, что поперечные размеры высоких ($\sim 1R_{\odot}$) корональных магнитных ловушек, удерживающих энергичные электроны и протоны, значительно превышают соответствующие размеры дактов. Если дакты с $R \sim 10^8 - 10^9$ см плотно "упакованы" в такой ловушке, то, как следует из раздела 4.2, длительное удержание протонов маловероятно из-за изотропизации протонов на альвеновских волнах. Если в ловушке нет дактов, либо дакты занимают небольшую часть объема ловушки, то усилению альвеновских волн препятствует, как указывал Wentzel {10}, кривизна магнитного поля. Длина усиления снижается: $l \sim \sqrt{u}L$. Из соотношения (15) следует, что в таком случае диффузия энергичных (> 10 Мэв) протонов на альвеновских волнах при $\eta \approx 10^{-2}$; $V = 1$ Гс, $A = 10^8$ см/с приводит к времени удержания порядка кулоновского $\tau_0 \sim 10^5$ с, даже когда давление энергичных протонов достаточно высокое: $\beta_H \approx 0.3$. Итак, в высоких ($\sim 1R_{\odot}$) корональных ловушках без дактов наиболее вероятно длительное удержание энергичных протонов.

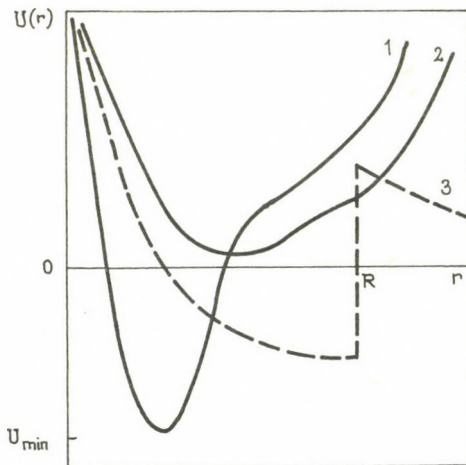


Рис.1. Форма потенциала $U(r)$ для профиля плотности (7) при следующих значениях параметра ξ : (1) $\xi \gg 1$, (2) $\xi = \sqrt{3}/2$. Штриховой линией (3) обозначена зависимость $U(r)$ для скачкообразного профиля плотности.

Л и т е р а т у р а

- {1} Caroubalos, C., Pick, M., Rosenberg, H., Slottje, C., A high resolution study in time, position, intensity, and frequency of the radio event of January 14, 1971, *Solar Phys.* 30, 473, 1973
- {2} Zajtsev, V.V., Stepanov, A.V., Chernov, G.P., Pulsations of type IV radio bursts as an indicator of protonability of solar flares, *Preprint SibIZMIR*, 12, 1983
- {3} De Jager, C., On the seats of elementary flare bursts, *Solar Phys.* 64, 135, 1979
- {4} Kennel, C.F., Petschek, H.E., Limit on stably trapped particle fluxes, *J.G.R.*, 71, 1, 1966
- {5} Леонович, А.С., Мазур, В.А., Сенаторов, В.Н., Альвеновский волновод, *Ж.Э.Т.Ф.*, 85, 141, 1983
- {6} Меерсон, Б.И., Рогачевский, И.В., Сасоров, П.В., Об удержании высокоэнергичных протонов в солнечной короне, сб. *Динамика токовых слоев и физика солнечной активности*, с.172, Зинатне, Рига, 1982
- {7} Newkirk, G., Coronal magnetic fields and energetic particles, *IAU Symp.* 57, 473, 1974
- {8} Svestka, Z., *Solar flares* D.Reidel Dordrecht, 1976
- {9} von Rosevinge, T.T., Ramaty, R., Reames, D.V., Interplanetary particle observations associated with solar flare gamma-ray line emission, *Proc. 17. Intern. Cosmic Ray Conf.* 3, 28, Paris, 1981
- {10} Wentzel, D.G., Condition for "storage" of energetic particles in the solar corona, *Ap.J.* 208, 595, 1976

A COMPARISON BETWEEN HIGHLY RESOLVED S-COMPONENT OBSERVATIONS
AND MODEL CALCULATIONS USING FORCE-FREE MAGNETIC FIELD
EXTRAPOLATIONS

N. S E E H A F E R, J. H I L D E B R A N D T, A. K R Ü G E R
ZISTP (HHI), Berlin (GDR)
SH. A K H M E D O V, G. B. G E L ' F R E J K H
Pulkovo Obs., Leningrad

СРАВНЕНИЕ НАБЛЮДЕНИЙ С-КОМПОНЕНТА С ВЫСОКИМ РАЗРЕШЕНИЕМ
С МОДЕЛЬНЫМИ РАСЧЕТАМИ, ИСПОЛЬЗУЮЩИМИ БЕССИЛОВЫЕ
ЭКСТРАПОЛЯЦИИ МАГНИТНОГО ПОЛЯ

Н. ЗЕЕХАФЕР, Й. ХИЛЬДЭБРАНДТ, А. КРЮГЕР
ЦИСЭФ, Берлин (ГДР)
Ш. АХМЕДОВ, Г. Б. ГЕЛЬФРЕЙХ
Пулково Обс., Ленинград

Abstract:

Extensive model calculations of solar radio emission features were presented for the complex of solar active regions Hale No 16862, 16863, and 17864 on May 27, 1980 using force-free extrapolated magnetic fields with constant α and a treatment of radiative transfer of S-component emission. The photospheric magnetic field data were taken from magnetographic measurements whereas the required height distribution of temperature and electron density have been adopted from semi-empirical sunspot models by Staude {13} and Bromboszcz et al. {3} which are based on recent X-, EUV-, optical, and radio observations.

In contrast to the simpler magnetic field structure used in other studies the complex source structure of the S-component emission is clearly represented exhibiting a dip of brightness temperature above the sunspot centres, a weakly polarized region with maximum intensity surrounding the centres, and broken ring or horse-shoe structures of high circular polarization at the outer edges of the gyromagnetic source regions. The results of the calculation are compared with the observations of the WRST (6 cm) and RATAN-600 (3.2 cm). While a number of typical features are well represented in both calculation and observation, the comparison of structural details underlines the sensitive dependency of the radio emission on the angle θ between the ray path and magnetic vector. Moreover, the existence of hot regions near the tops of magnetic loops connecting one polarity with the other is indicated.

1. Introduction

Observations of solar active regions with high spatial resolution (a few arcsec) in the microwave range have stimulated some progress in the field of emission models of the S-component (cf. e.g. {4}, {2}, {9}, {7}). Assuming the same main radiation processes (gyromagnetic emission and Coulomb bremsstrahlung) the differences between various S-component models are related to the use of different parameter distributions (electron density, temperature, and magnetic field vector). Because of the strong influence of the magnetic vector on the emission quantities (it determines the positions of the gyroresonance layers), recently some attempts were made to use magnetic field models based on real photospheric observations and theoretical extrapolations of these fields to greater heights.

This paper briefly presents the results of model calculations combining advanced model distributions of thermodynamic plasma parameters and extrapolated magnetic field distribution.

2. Model

The model used for our calculations was described by Krüger et al. {7}. The electron density and temperature distributions are based on the sunspot model of Staude {13} which is very similar to the more recent model of Lites and Skumanich {8} using the latest measurements in the EUV-region. The extrapolation to the corona was done by assuming a constant heat flow (which can be used to influence the thickness of the transition layer) according to the work of Alissandrakis et al. {2}. The temperature distribution was restricted to a maximum value of $1.8 \cdot 10^6$ K, whereas the coronal density monotonically decreases with height.

The distribution of the magnetic field can be chosen either as an analytical one (e.g. dipole model, cf. {6}) or as the non-symmetric distribution of the magnetic field vector extrapolated from magnetographic measurements with the method of Seehafer {10}, {11} assuming a constant α .

The equation of radiative transfer is solved numerically for an inhomogeneous, horizontally stratified medium assuming straight ray paths and vertical incidence.

We assume gyroemission and Coulomb bremsstrahlung as the only important emission processes in the microwave range; the corresponding absorption coefficients are taken into account in a very general manner.

3. Observations

Our model calculations are based on the magnetogram of May 27, 1980 obtained with the magnetograph of the Einstein tower in Potsdam. The whole magnetogram has an extension of 374 000 km × 237 000 km with a resolution of about 6" (4000 km); cf. [12]. The radio observations used for comparison were obtained in the first case with the WRST [1] at 6 cm in the form of two-dimensional maps of the Stokes parameters I and V with an E-W resolution of about 4" and a N-S resolution of about 11". Unfortunately the published data are for May 25, 1980, while in our calculations the magnetogram of May 27, 1980 have been used. But it seems that most of the structures were stable over a period of some days.

In the second case we compared our results with observations made with the RATAN-600. These observations are given in the form of a profile in E-W direction because of the antenna beam width of 27"×21' at 3.2 cm. After data reduction one can obtain integral properties (flux density, averaged degree of polarization) of the sources, which are also comparable with the computations at different frequencies (9.4, 11, 13, and 15 GHz).

4. Discussion of results

The results of our calculations are presented in Figs. 2 and 3 (4.9 GHz) and Figs. 6 and 7 (9.4 GHz) in the form of maps of the total intensity (in temperature units corresponding to $\bar{T}_b = 0.5(T_b^o + T_b^e)$) and the degree of (circular) polarization ($p = |T_b^o - T_b^e| / (2\bar{T}_b) \times 100\%$), respectively.

Typical features are the dips of the brightness temperature above the sunspot centres (the ordinary mode is suppressed

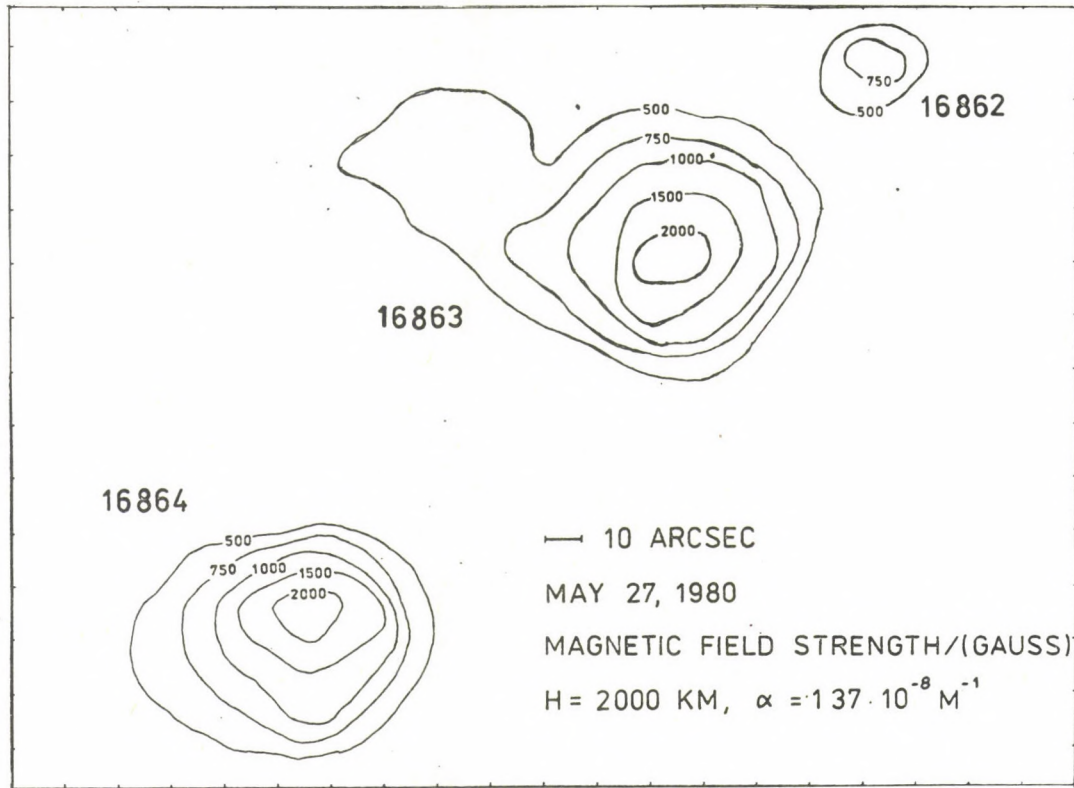
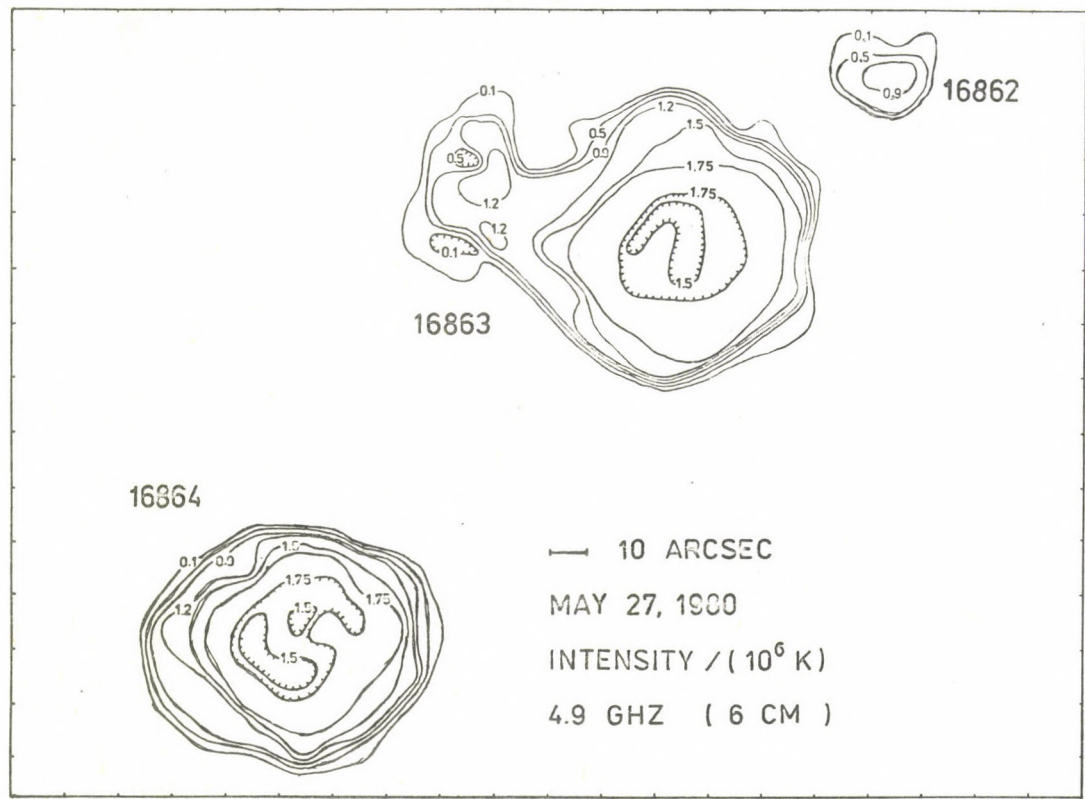


Fig.1. Magnetic field strength at a height level of 2000 km above the photosphere (position of the transition region to the corona) extrapolated from magnetographic data.



435

Fig. 2. Calculated total intensity (in temperature units) at 4.9 GHz. The dip at the spot centre and the ring of maximum intensity around the centre are typical; also the correspondence between the source size and the magnetic structure (cf. Fig. 1).

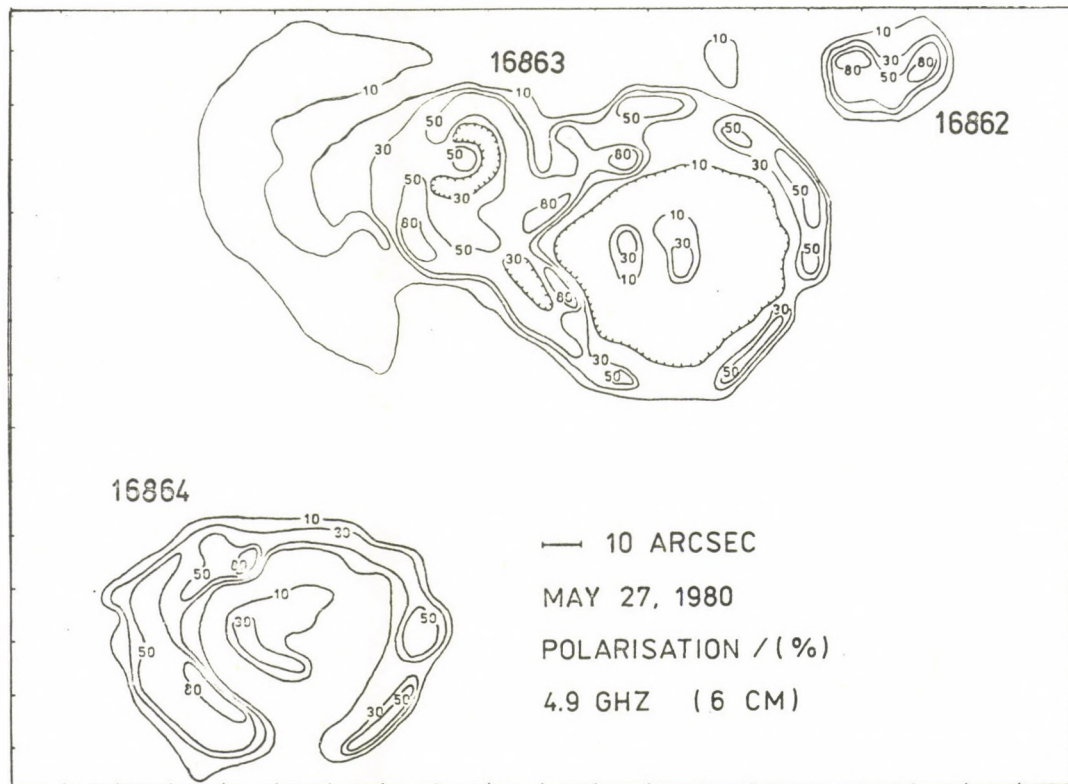


Fig. 3. Calculated map of the degree of (circular) polarization at 4.9 GHz. The regions with highest intensities correspond to those of weakest polarization (optically thick second-harmonic emission in both modes) and at the outer edge of the source a more or less broken ring of strong polarization appears (third-harmonic emission in the extraordinary mode).

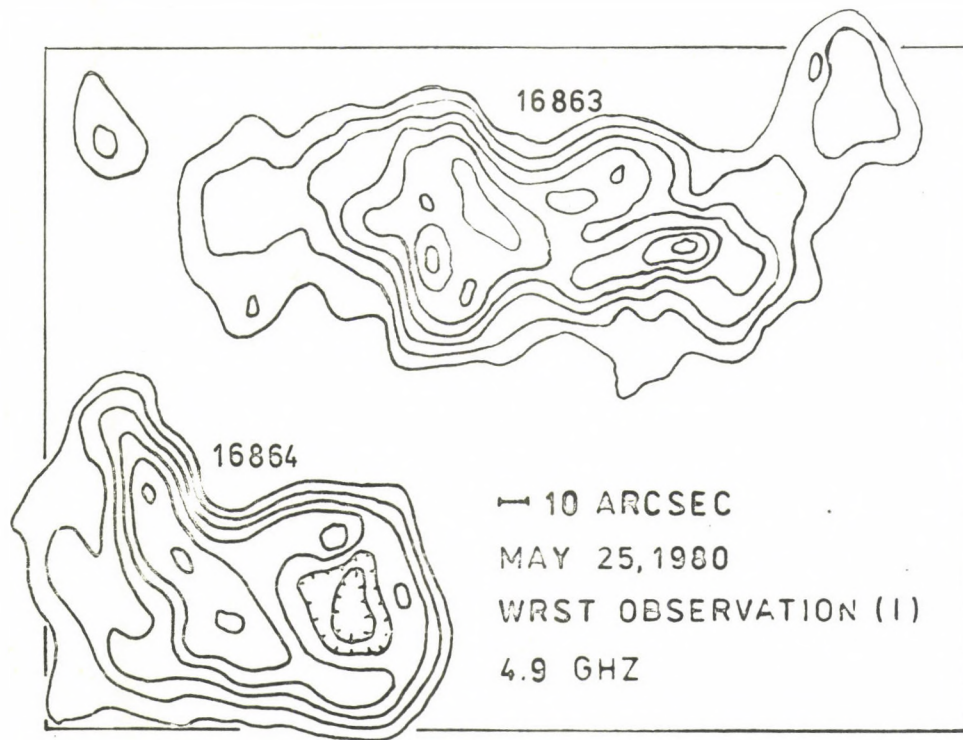


Fig. 4. WRST observations of the intensity at 4.9 GHz on May 25, 1980.

For the spot group No 16864 a dip at the centre is also observed; the principal shape of the source is in sufficient accordance with the calculations. This cannot be said for group No 16863, especially in the eastern part. The much higher observed temperatures (up to $3.8 \cdot 10^6 \text{K}$) cannot be obtained from the calculations (the temperature model is restricted to $T_{\text{max}} = 1.8 \cdot 10^6 \text{K}$) and indicate the existence of hot regions near the tops of magnetic loops connecting one polarity with the other.

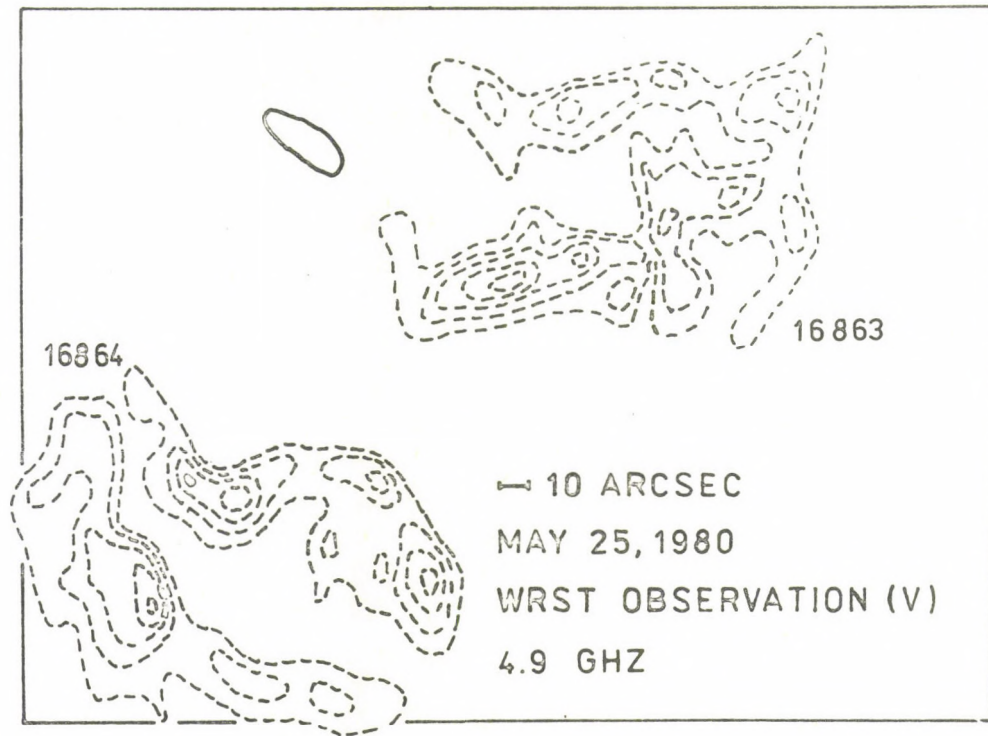


Fig. 5. WRST observations of the polarization (Stokes parameter V) at 4.9 GHz on May 25, 1980. Accordance with the calculation is better for spot group No 16864 as in Fig. 4 for the intensity. Nevertheless, both groups show the expected ring or sickle-shaped structure with maximum polarization at the boundary of the sources.

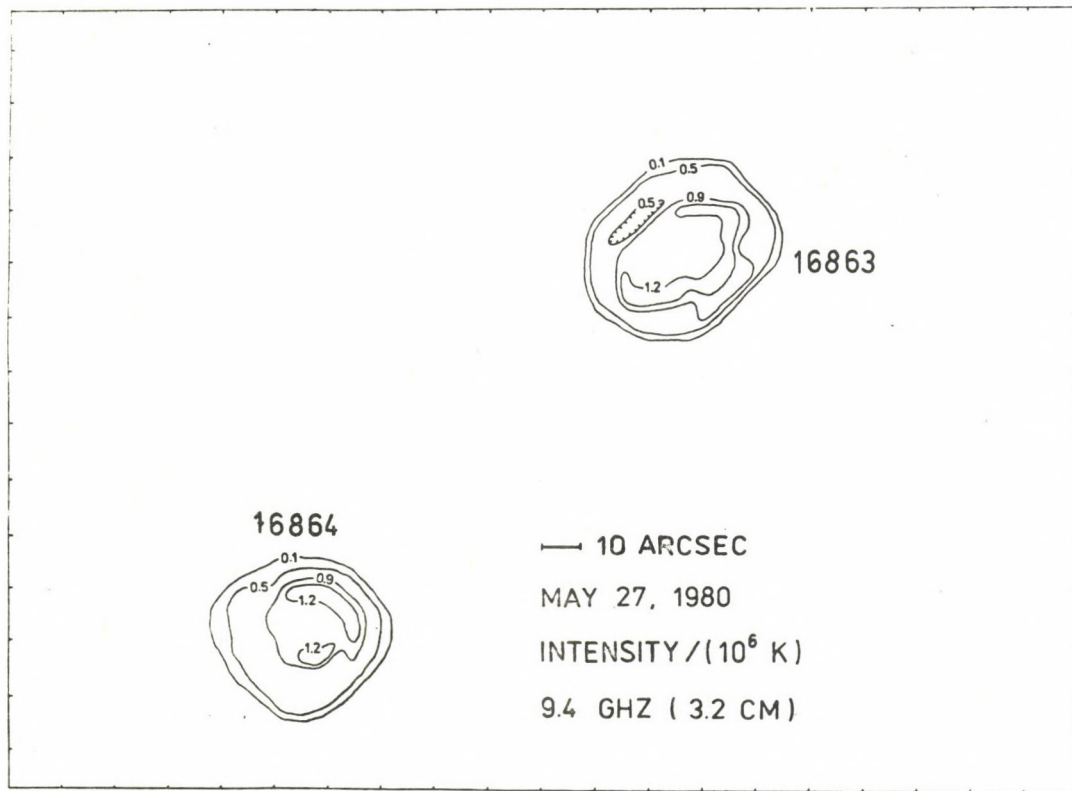


Fig. 6. The same as in Fig. 2 but for 9.4 GHz (3.2 cm).

It can clearly be seen that it is only in a small sickle-shaped part that second-harmonic emission occurs; the radiation of the other parts of the sources is mainly caused by third-harmonic emission in the extraordinary mode.

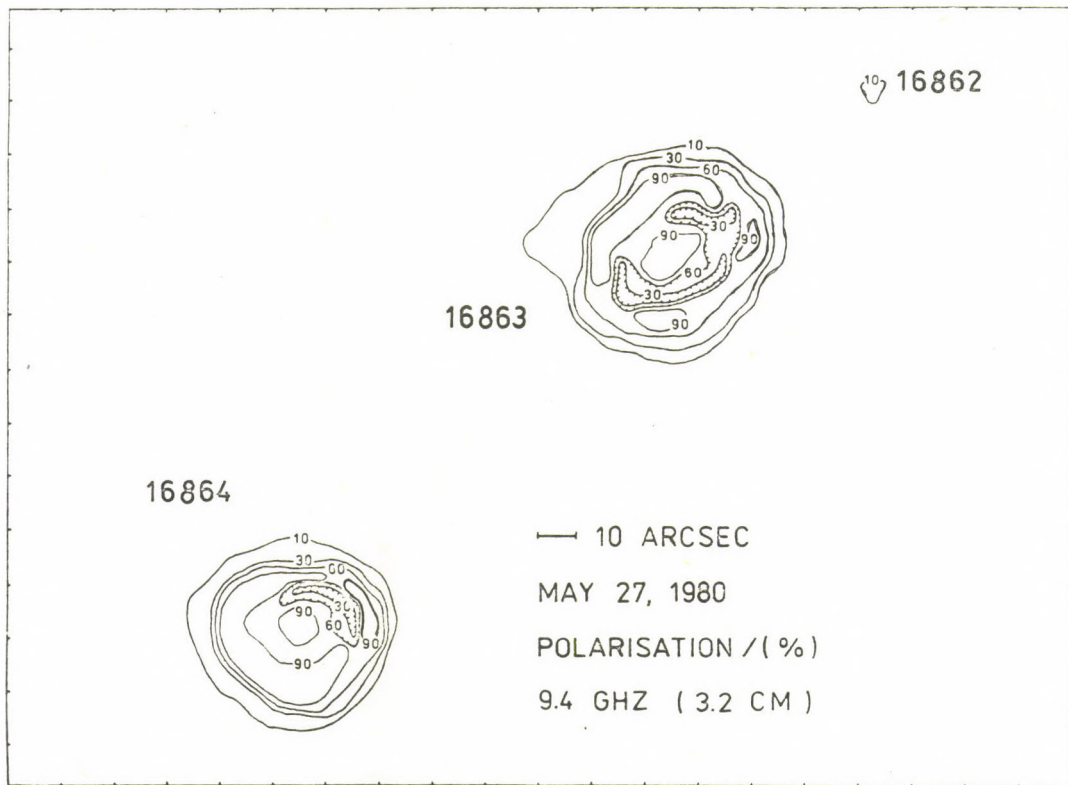


Fig. 7. Calculated map of the degree of circular polarization at 9.4 GHz (3.2 cm).
The explanation for the weakly or highly polarized parts of the sources is given in Fig. 6
(the dips in the degree of polarization are associated with maximum intensity).

at small angles θ) surrounded by rings of maximum intensity (second-harmonic emission in both modes). At the outer boundary of the gyromagnetic sources the polarization is strong (third-harmonic emission in the extraordinary mode). The fine structures are mainly caused by the distribution of the angle θ , which is a sensitive parameter for gyroemission.

The comparison with the WRST maps (Figs.4 and 5) shows a sufficient agreement (in spite of the different observation days!) for the spot group No 16864 (also a dip in brightness and a broken ring polarization). This is not the case for the group No 16863, especially for the eastern part, which is associated with a plage region. The much higher observed temperatures (more than $3 \cdot 10^6$ K) cannot be obtained from the calculations (because the temperature model is restricted to $T_{max} = 1.8 \cdot 10^6$ K) and indicate the existence of hot regions near the tops of magnetic loops connecting one polarity with the other. Nevertheless, for the polarization both groups show the expected ring or sickle-shaped structures with maximum values at the boundary of the sources.

At 9.4 GHz (Figs.6 and 7) the source sizes are much smaller (only in a narrow sickle-shaped part second-harmonic emission with $T_b > 10^6$ K occurs); the larger part of the source area is associated with third-harmonic emission in the extraordinary mode, therefore, the averaged degree of polarization is higher than for 4.9 GHz. The comparison with RATAN-600 measurements was possible after integration of our discrete temperature values along small strips of 500 000 km extent in N-S direction. Of course, the result is largely in accordance with the observation, but is only of a qualitative nature, since the antenna temperature is not directly comparable with our calculated brightness temperature.

The whole fluxes and averaged degrees of polarization have also been compared at different frequencies; surprisingly, the differences between the calculations and measurements were smaller than 20%.

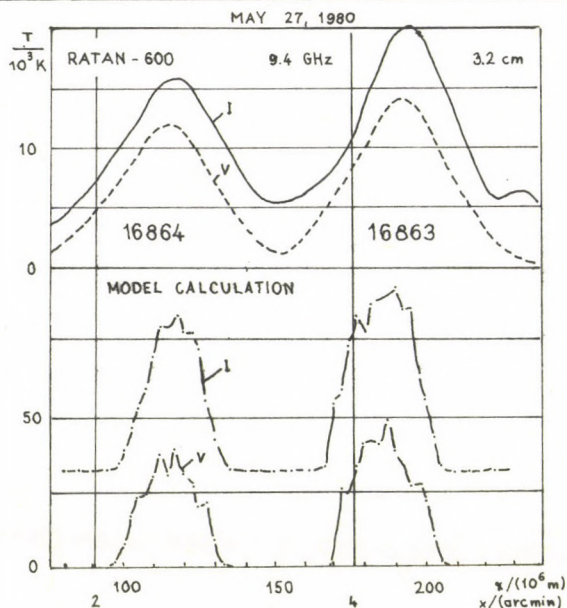


Fig. 8. A comparison between RATAN-600 measurements and our calculations at 9.4 GHz (3.2 cm). Because of the one-dimensional emission patterns of the RATAN-600 we have integrated our values along small strips of 500 000 km extent in N-S direction. The result is only of qualitative nature, since the antenna temperature is not directly comparable to our calculated brightness temperature.

References

- [1] Alissandrakis, C.E., Kundu, M.R., *Ap.J.* 253, L49, 1982
- [2] Alissandrakis, C.E., Kundu, M.R., Lantos, P., *Astron. Astrophys.* 82, 30, 1980
- [3] Bromboszcz, G., Jakimiec, J., Siarkowsky, M., Sylwester, B., Sylwester, J., Obridko, V.N., Fürstenberg, F., Hildebrandt, J., Krüger, A., Staude, J. *Prepr. IZMIRAN*, 11a, 1982
- [4] Gelfreikh, G.B., Lubyshev, B.I., *Astron. Zh.* 56, 562, 1979
- [5] Hildebrandt, J., *Thesis*, Berlin, 1983
- [6] Krüger, A., Fürstenberg, F., Hildebrandt, J., Akhmedov, Sh.B., Bogod, V.N., Korzhavin, A.N., *this issue* 1983
- [7] Krüger, A., Hildebrandt, J., Fürstenberg, F., Staude, J., *HHI-STP Report* 14, 1, 1982
- [8] Lites, B.W., Skumanich, A., *Ap.J. Suppl.* 49, 293, 1982
- [9] Pallavicini, R., Sakurai, T., Vaiana, G.S., *Astron. Astrophys.* 98, 316, 1981
- [10] Seehafer, N., *Solar Phys.* 58, 215, 1978
- [11] Seehafer, N., *Thesis*, Berlin, 1979
- [12] Seehafer, N., *this issue* 1983
- [13] Staude, J. *Astron. Astrophys.* 100, 284, 1981

VARIATION OF CIRCULAR AND LINEAR POLARIZATION IN BURST EMISSION
AS A CONSEQUENCE OF DYNAMIC PROCESSES IN THE SOLAR ATMOSPHERE

V. P. N E F E D ' E V

SibIZMIR, Irkutsk

Abstract:

We explore the possibility of assessing the physical conditions in the solar atmosphere at the time of flare development, using polarization characteristics of bursts. In particular, it is shown that during the impulsive phase the magnetic field strength in the corona changes by a factor of < 2 . An example of a linearly polarized burst is given. We discuss some likely processes in the solar atmosphere (a change in the magnetic field line orientation; expansion of the generation region, etc.) which might be responsible for the linear polarization sign change.

ИЗМЕНЕНИЕ КРУГОВОЙ И ЛИНЕЙНОЙ ПОЛЯРИЗАЦИИ В ИЗЛУЧЕНИИ
ВСПЛЕСКОВ КАК СЛЕДСТВИЕ ДИНАМИЧЕСКИХ ПРОЦЕССОВ В АТМОСФЕРЕ СОЛНЦА

В. П. НЕФЕДЬЕВ

СИБИЗМИР, Иркутск

Абстракт:

Обсуждается возможность оценки физических условий в атмосфере Солнца во время развития вспышек по изменению поляризационных характеристик всплесков. В частности, показано, что во время импульсной фазы напряженность магнитного поля в короне изменяется в < 2 раза. Приведен пример всплеска с линейной поляризацией. Обсуждаются возможные процессы в атмосфере Солнца (изменение ориентации силовых линий магнитного поля; расширение области генерации и т.д.), которые могут вызвать изменение знака линейной поляризации.

Disturbances arising at the time of flare development cause alterations in physical conditions at various levels of the solar atmosphere. The present paper explores the possibility of assessing the character of these changes by analysing the polarization characteristics of the radio burst emission.

Several bursts with a polarization sign change were recorded at 5.2 cm wavelength at SibIZMIR in August 1981. An example of such bursts is shown in Fig.1. Some of the bursts recorded by us were observed at other cm wavelengths in Japan and in Switzerland. In response to our request, co-workers from these observatories provided us with copies of recordings of these bursts. We have been able to investigate the polarized component at other wavelengths during a reversal of the circular polarization at 5.2 cm wavelength.

It turned out that in all cases, as the burst progressed, the polarization sign change at 5.2 cm wavelength was accompanied by a sign change of the circular polarization over the frequency range. An example of the bursts is given in Fig.2.

It is known {4} that the polarization sign change can occur over the wavelength range as a result of radio wave propagation through a quasi-transverse magnetic field. Fig.3 is a schematic of the burst generation region and of the structure of a quasi-transverse magnetic field along the path of propagation of the radio emission. The circular polarization changes sign at the frequency of the observations $f = f_t$

$$f_t \sim \frac{N_e^{\frac{3}{4}} H_0^{\frac{3}{4}}}{\left| \frac{d\alpha}{dz} \right|^{\frac{1}{4}}} \quad (1)$$

In this case, at the frequency $f \gg f_t$, the polarization sign remains unchanged, whereas at frequencies $f \ll f_t$ it is reversed. The sign change of circular polarization over the frequency range will be accompanied by that at a fixed frequency when the conditions in the region of quasi-transverse propagation will be changed so that $f_{5.2} \leq f_t$. From (1) it is evident that f_t is the most critical with respect to the change of H . When the degree of polarization goes to zero at 5.2 cm wavelength,

$f_{5.2} = f_t$. Specifying the value of $N_e \sim 10^8 \text{ cm}^{-3}$; $\frac{d\alpha}{dz} \sim 10^{-10}$ will yield for the magnetic field strength a value ~ 10 Gs. A fluctuation of the magnetic field strength around this value will lead to a sign change of the polarization at a fixed frequency. Using burst recordings taken at other frequencies we are able to determine the upper bound of the oscillation amplitude of the magnetic field strength. A sign change of the circular polarization is observed only at one wavelength, namely at 5.2 cm. At longer and shorter wavelengths, different from the 5.2 cm wavelength by less than a factor of 2, there is no circular polarization reversal. From this it follows that fluctuations of the magnetic field strength in the region of quasi-transverse propagation certainly do not exceed a factor of 2 in the impulsive phase.

Apart from the circular polarization the radio burst emission exhibits on occasions, a linearly polarized component (Stokes parameters Q, U). It is known that the linearly polarized emission is very critical to physical conditions both in the generation region and along the propagation path. A departure of these conditions from optimum ones causes the degree of linear polarization either to change (decrease) substantially or to disappear totally. The strong dependence of the degree of linear polarization on physical conditions leads to the fact that the linear polarization in the radio burst emission is rarely observed [1]. However, in cases where it is nevertheless recorded, there is an additional possibility of making an analysis of short-time processes, occurring in the solar atmosphere at the time of a flare.

With the purpose of recording the four Stokes parameters ($I, V, Q, \text{ and } U$) [2], observations at 3.2 cm wavelength were carried out at SibIZMIR during 1968-1970. A linearly polarized component was recorded in the emission of a number of bursts. Fig.4 shows an example of such bursts. The observations obtained at SibIZMIR did not only confirm the fact that the radio burst emission involves linearly polarized components but also they revealed some interesting features in the manner of variation

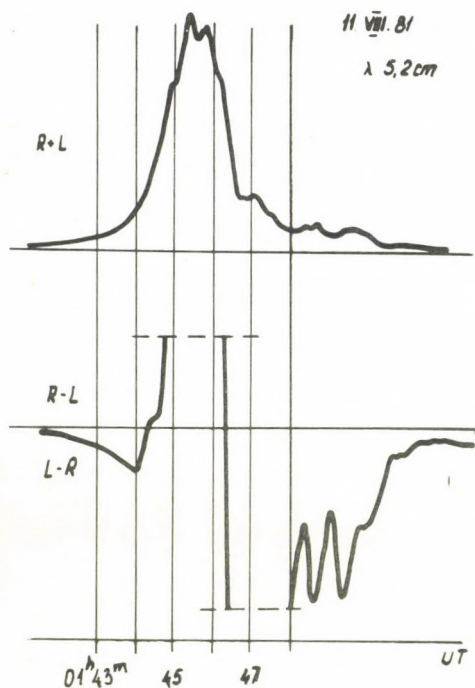


Fig. 1. 5.2 cm burst with a sign change of the circular polarization.

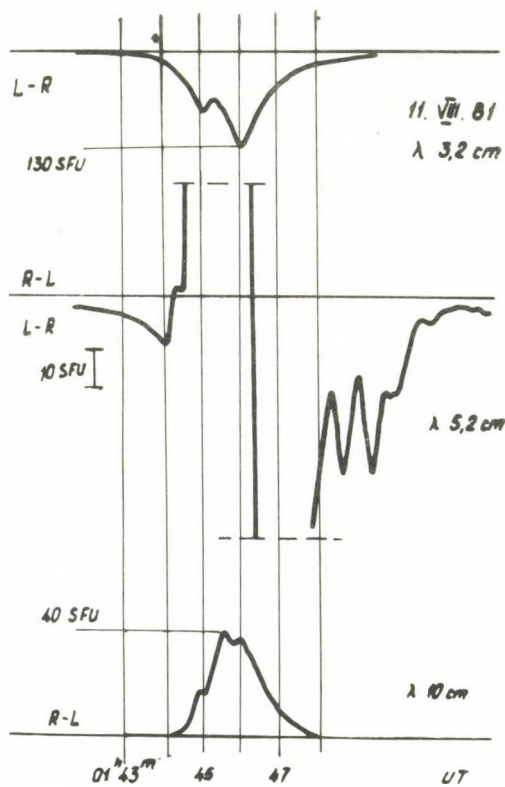


Fig. 2. Example of a burst in which a sign change of the circular polarization at 5.2 cm wavelength was accompanied by that over the frequency range.

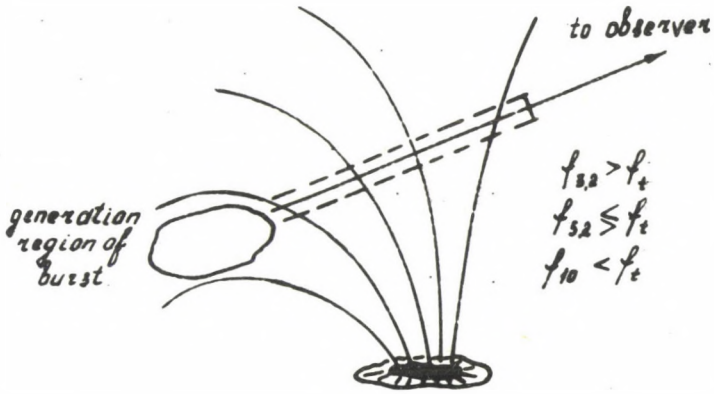


Fig.3. Radio wave propagation in a quasi-transverse magnetic field.

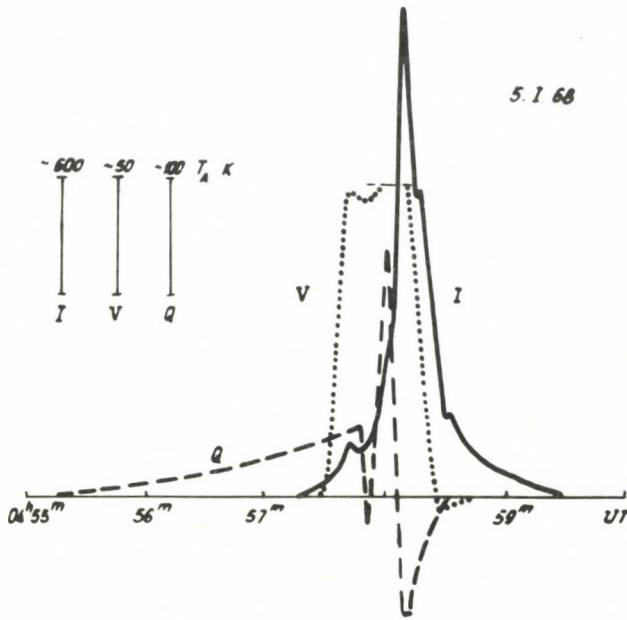


Fig.4. Example of a burst, whose emission exhibited a linearly polarized component.

of the linearly polarized emission flux. It is evident from the example shown in Fig.4 that the flux of linearly polarized emission arose and gradually increased before the impulsive phase of the burst. During the impulsive phase the character of variation of the linearly polarized emission flux changed dramatically, namely, a threefold sign change is observed.

An enhancement of the radio emission flux with a linear polarization before the impulsive phase of burst development was attributed to processes occurring in the current sheet at the flare onset {3}. Estimates were also made of the electron density in the current sheet ($N_e \sim 10^{12} \text{ cm}^{-3}$), of its thickness ($< 10^3 \text{ cm}$) and of the characteristic scale of electron density variation ($\sim 10 \text{ cm}$). The impulsive phase of development of the burst was preceded by a gradual change in these parameters.

The fact that the linear polarization changes sign during the impulsive phase of burst development offers evidence that the burst impulsive phase is not merely an increase in brightness of pre-existing generation regions. The brightness enhancement is accompanied by a development of large-scale processes and a substantial change in physical conditions in the atmosphere above the flare on a time scale of about 10 s. These processes may include: I. A change in the orientation of magnetic field lines by 90° . The orientation change of field lines may result from magnetic field line reconnection in a current sheet. II. The displacement of the region of burst generation from the top of the arch down to its base, giving rise to a generation region within the region with a different orientation of magnetic field lines. III. A change in the thickness of the emitting region as the result of its expansion or contraction. This will result in a change of the phase difference between normal waves (ordinary and extraordinary) which will cause the polarization plane to rotate under the action of the Cotton-Mouton effect {5}.

In this paper it was not our intention to conduct a thorough study and make quantitative estimates of the conditions in the solar atmosphere, using data on radio burst

polarization. This would require information about the spectrum of a polarized radio emission. The examples given here and their qualitative consideration show, however, that the polarized radio emission is a sensitive indicator of the development of dynamical processes in the solar atmosphere.

Acknowledgements

I would like to thank Drs H.Aurass, A.Magun and S.Enome for providing me with copies of radio burst recordings. Thanks are also due to V.G.Mikhalkovsky for his assistance in preparing the English version of the manuscript and typing the text.

References

- {1} Matzler,Ch., *Proc.4th Meeting of the CESRA*, Berne, 1974
- {2} Nefedjev,V.P., On elliptic polarization in the 3.2 cm line solar radioburst emission, (in Russ.) *Issl.SibIZMIR*,31, 38, 1974
- {3} Nefed'ev,V.P., On the possibility to estimate physical conditions in the current sheet region during the development of a chromospheric flare, (in Russ.) *Pis'ma v AZh*,5, 96, 1979
- {4} Zheleznyakov,V.V., *Radio emission of the Sun and planets* (in Russ.) Nauka, Moscow 1964
- {5} Zheleznyakov,V.V., *Electromagnetic waves in cosmical plasma* (in Russ.) Nauka, Moscow 1977

A MODEL OF THE OSCILLATIONS IN THE CHROMOSPHERE
AND TRANSITION REGION ABOVE SUNSPOT UMBRAE

Yu. D. ZHUGZHDA, J. STAUDE,
IZMIRAN, Troitsk "Einsteinurm" Solar Obs., Potsdam
V. LOCÁNS
Radioastrophys. Obs., Riga

Abstract:

In an earlier paper the present authors proposed a model for the interpretation of velocity and intensity oscillations with periods between 2 and 3 minutes observed above umbrae. The oscillations are explained by the resonant transmission of slow mode magneto-acoustic waves which are semi-trapped in a chromospheric cavity. The model has now been improved by more detailed calculations and corroborated by recently published observations: Our calculations are in good agreement with a) the height dependence of the observed phase difference between velocity and intensity oscillations, and with b) the frequency spectrum of oscillations in the transition region above sunspots observed on the SMM spacecraft during the SMY.

МОДЕЛЬ КОЛЕБАНИЙ В ХРОМОСФЕРЕ И ПЕРЕХОДНОМ СЛОЕ
НАД ТЕНЬЮ СОЛНЕЧНЫХ ПЯТЕН

Ю. Д. ЖУГЖДА, И. ШТАУДЕ
ИЗМИРАН, Троицк Солн. Обс. "Эйнштейнтурм", Потсдам
В. ЛОЦАНС
Радиоастрофиз. Обс., Рига

Абстракт:

В предыдущей работе авторами была предложена модель для интерпретации колебаний скорости и интенсивности с периодами от двух до трех минут, наблюдаемых над тенями. Эти колебания мы можем объяснить резонансным пропусканием замедленных магнито-звуковых волн, частично захваченных в хромосферном резонаторе. В данной работе модель была усовершенствована более подробными вычислениями и подтверждена последними результатами наблюдений. Хорошо согласуются между собой вычисления и наблюдения следующие величины: а) зависимость разности фаз колебаний скорости и интенсивности от высоты, б) спектр частот колебаний в переходном слое над солнечными пятнами, наблюдаемых на спутнике "SMM" во время ГСМ.

1. Introduction

Velocity and, often, intensity oscillations have been observed in spectral lines formed at different levels in the atmosphere of sunspot umbrae. In the chromosphere and the transition region to the corona the periods of these oscillations range from $P_i \approx 120$ to 200 sec (s). There is no correlation with the oscillations observed at lower, photospheric levels in a much broader range of $P_i \approx 2$ to 8 min. Moreover, a clear correlation among the parameters P_i , the oscillation amplitude, the umbral area, and the magnetic field B does not exist for the oscillations in the chromosphere and transition region, which will be considered in particular.

In a recent paper of the present authors {6} observations and different suggestions for the interpretation of the umbral oscillations have been discussed; this will not be repeated here. We proposed an interpretation by the resonant transmission of slow mode magneto-acoustic waves in the strong magnetic field of an umbra ($c_s^2 \ll v_A^2$, where c_s is the sound speed and v_A the Alfvén speed). These waves are semi-trapped in a chromospheric cavity. The model provides an independent method of checking semi-empirical models of the umbral chromosphere because the resonant periods depend on the extent of the chromosphere.

The model proposed in {6} has now been improved by new calculations and checked by recently published observations. We shall see that our model is well corroborated by recent observations. Finally we outline possible improvements which should be considered in future model calculations.

2. Numerical calculations

2.1. Model atmospheres

Our method to derive the sunspot model atmospheres has been described by Staude {3} and summarized briefly in {6}; a more detailed description of the used computer programs and examples of umbral atmospheres in tabular form can be found in a report by Staude {4}. The semi-empirical model atmospheres are based on spectroscopic observations including recent EUV

data. The procedures consider non-LTE radiative transfer effects, the formation of molecules as well as positive and negative ions of hydrogen, moreover, He and 9 other elements are taken into account with two steps of ionization. The equations of state, of radiative transfer, and of hydrostatic equilibrium are solved in a self-consistent way by iterations. A turbulent velocity v_{tu} is included in the hydrostatic equilibrium computation as a turbulent contribution to the total pressure.

Starting from the original umbral model atmosphere of Staude {3}, three different grids of model atmospheres have been derived. The first grid SO is an extension of that from our earlier paper {6} from 3 to 6 models; these models are derived by changing linearly the extent of the chromosphere between the temperatures $T = 3000$ K (the minimum T_{min}) and $T = 22\ 000$ K, while the models are unchanged at photospheric levels. Two other grids S1 and S2 have been derived assuming different models of $v_{tu}(T)$ ($v_{tu} = 0$ in S2; a monotonous increase of $v_{tu}(z)$ with increasing geometrical height z in S1) and different masses at the base of the corona for the different models. Fig.1 shows $T(z)$ for S1 and S2.

The height dependence of all physical quantities such as c_s , v_A , mass density ρ , gas pressure P , and γ the ratio of specific heats, have been calculated separately for each model using the procedures mentioned above.

2.2. Wave propagation

The basic physical assumptions and the method for the computation of the propagation of slow mode magneto-acoustic waves though the sunspot umbral atmosphere have been described by Zugzda and Locāns {5} and in {6}. The calculations are based on an analytic solution of the equations of ideal magneto-hydrodynamics assuming a compressible stratified medium with constant values of B , gravity g (both assumed in parallel direction), γ , and $\beta = dT/dz$, moreover, $c_s^2 \ll c_A^2$. The solution does not depend on the horizontal wave number k_{\perp} . Wave energy can propagate only in a direction along B while the

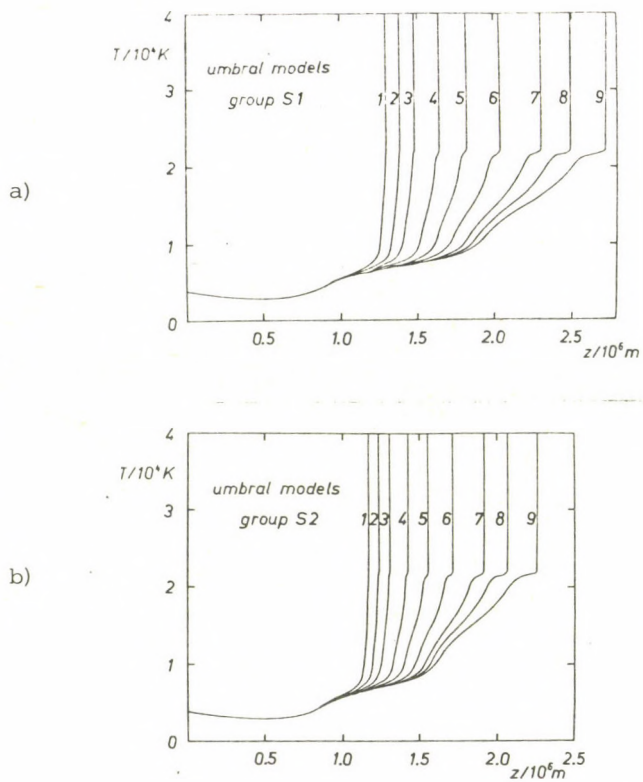


Fig. 1. Height dependence of temperature for different sunspot model atmospheres:
 (a) grid of models S1 with a turbulent velocity monotonously increasing with height;
 (b) grid S2 with zero turbulent velocity.

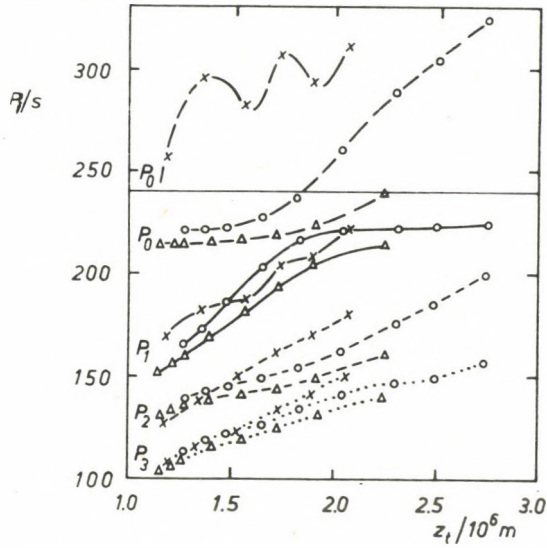


Fig.2. Resonance periods P_i versus height z_t of the transition region for the grids of models S0 (x), S1 (o), and S2 (Δ). The horizontal straight line indicates the cutoff frequency $\omega_0 = c_s / (2H_0)$ for acoustic waves; our calculations for larger P_i are less reliable.

phase velocity could show an arbitrary angle to B depending on k_{\perp} ; in the special case $k_{\perp} = 0$ the slow mode is similar to a pure acoustic wave. We consider only vertically propagating waves. The model atmosphere is subdivided into a sufficiently large number of layers which are connected to each other by appropriate boundary conditions; in each layer the assumptions for the analytic solution (e.g., $\beta = \text{const.}$) are supposed to be strictly valid.

Compared to our earlier computations {6} the following modifications have been introduced: The equations have been formulated in Lagrangian coordinates instead of Eulerian coordinates.

This choice facilitates an exact treatment of boundary conditions in the thin transition region which in practice oscillates as a whole. v_{tu} has been considered in the computation of wave propagation by using an effective gravity. Finally, we also publish values of the height dependence of amplitudes and phases of the oscillations.

3. Discussion of the results

3.1. Dependence on the model atmosphere

The main results of our earlier investigation {6} are confirmed by the present more detailed calculations. For each model we get a spectrum of resonances, that is, the transmission of the atmosphere for wave propagation has sharp maxima at a number of discrete periods P_i . A special period, e.g. the fundamental resonance P_1 , generally increases with increasing extent of the sunspot chromosphere for a given grid of model atmospheres (see Fig.2). This provides a method of checking empirical model atmospheres by comparing calculated and observed spectra of oscillations, that is, a "sunspot seismology". However, the dependence of the P_i on the chromospheric extent is somewhat different for the different grids of model atmospheres, therefore more detailed and simultaneous observations of both oscillations and spectro-photometric data are required in order to reduce the remaining ambiguities in the construction of sunspot model atmospheres. In the following

subsection we will show that SMM observations of oscillations in the sunspot transition region could help to progress in this direction.

Fig.2 shows some examples for $P_i(z_t)$, for $i = 0, 1, 2, 3$ and for the grids S0, S1 and S2 (z_t is the height at the base of the transition region with $T = 42\ 000\ K$, for T_{\min} we have $z \approx 500\ km$ for all models) which are used for this approach. The resonance P_0 is mainly of photospheric origin (see the discussion in {6}), it is not considered in the further discussion. Fig.3 gives the height dependence of amplitudes and phases for the oscillations of T , P , z , and velocity u for the period P_1 of model S15 as an example. The oscillations are defined as follows:

$$z = z_0 + h \quad \text{with } h = |h| \cos(\varphi_h - \omega_i t),$$

$$T = T_0 + T' \quad \text{with } T' = |T'| \cos(\varphi_T - \omega t), \text{ etc.}$$

with $\omega_i = 2\pi/P_i$. The subscript 0 indicates a quantity in the equilibrium state, and a dash marks a Lagrangian variation. The height dependence is similar for other model atmospheres and periods. In Subsection 3.3. these results will be compared with recent observations.

3.2. Comparison with observations in the transition region

Velocity and, sometimes, simultaneous intensity oscillations in transition region lines have been observed with high accuracy on the SMM spacecraft {1}. Periods of 129-173 s, velocity amplitudes of 0.8-3.5 km s⁻¹, and intensity variations of 6% - 9% have been reported. Maximum intensity is in phase with maximum blue shift. In some cases also oscillations of the line widths with the some periods and with amplitudes of about 1 km s⁻¹ have been observed.

The observations of u show significant power at one of two periods P_i , if the 0.999 confidence level (approximately 3σ in a normal distribution) of {1} is applied. This seems to contradict the results from our model calculations which produce a spectrum of resonances. The use of a less strong confidence level, however, results in a larger number of resonant

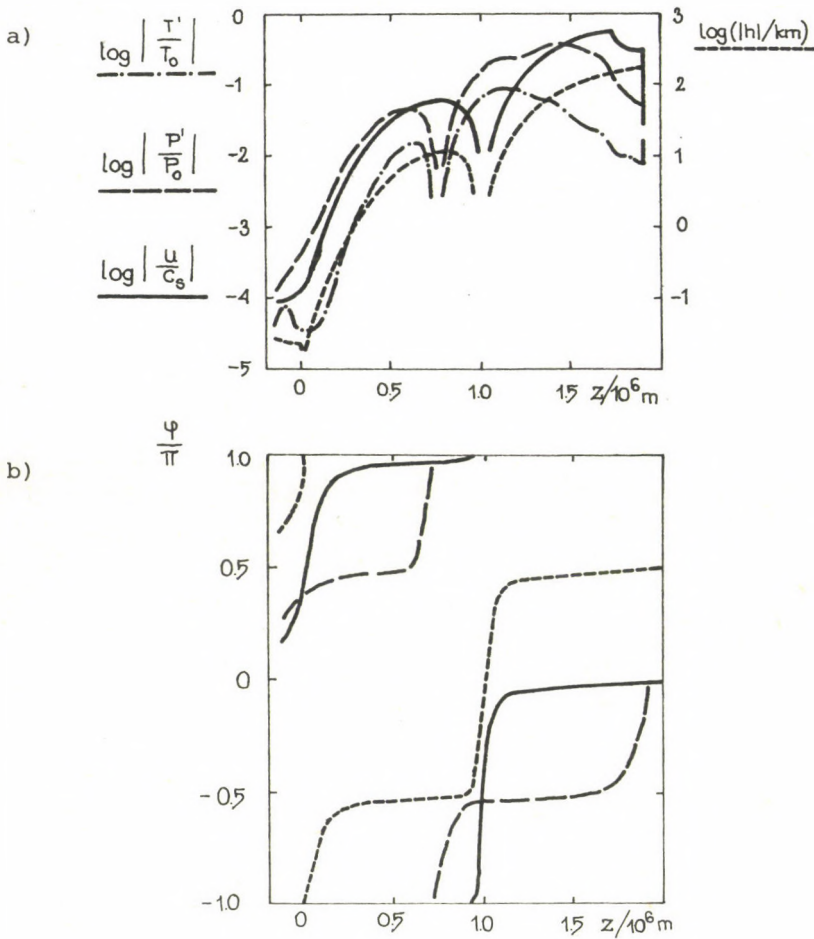


Fig.3. (a) relative amplitudes of the oscillations with period P_1 of velocity $|u/c_s|$, pressure $|P'/P_0|$, temperature $|T'/T_0|$, and the plasma displacement $|h|$ versus height z ;

(b) phases $\varphi(z)$ for these oscillations (the phases for T' , P' , and ρ' coincide). All calculations refer to sunspot model S05, an energy flux of $F_0 = 10^4 \text{ erg cm}^{-2} \text{ s}^{-1}$ from the convective zone and an amplitude of $u = 5.0 \text{ km s}^{-1}$ for P_1 in the transition region, but the results are similar for other models, periods, and amplitudes.

peaks; e.g., a 0.977 level (2σ) shows 5 significant peaks in Fig.6a of {1}. The observed periods P_i could be determined with a relative error of 6% - 8%. Within this accuracy the resonant peaks in each time series in {1} could be identified with the calculated spectrum of oscillations for at least one of our models. For instance, in Fig.4 of {1} the periods $P_1 = 173$ s and $P_2 = 139$ s (136 s in the intensity power) show significant power in u ; this could be identified with our models S12 ($P_1 = 173$ s, $P_2 = 143$ s), S24 ($P_1 = 170$ s, $P_2 = 140$ s), or S17 ($P_1 = 222$ s, $P_2 = 176$ s, $P_3 = 147$ s); the latter case could be realized if P_1 is weakly excited and P_2 is the first visible resonant peak. Similarly, Fig.6a of {1} shows peaks at 154 s, 137 s, 113 s, 100 s, etc.; this could be identified with spectrum of our models S22 ($P_1 = 155$ s, $P_2 = 133$ s, $P_3 = 109$ s, etc.) or S15 (starting with $P_2 = 154$ s, $P_3 = 135$ s, etc.). In this way our "sunspot seismology" provides at least a restriction in the number of possible umbral models. Considering in addition the results from spectroscopic observations {4},{6}, the models with larger chromospheric extent and weakly excited period P_i seem more reliable. The small number of observations of the umbral chromosphere and transition region available at present, however, does not yet allow us to exclude the other models under discussion.

We also estimated the influence of the waves (fluctuations of thermodynamic parameters, of the thickness of the transition region, shift of the line - emitting region, etc.) on the oscillations of EUV line intensities. The calculated amplitudes and phases are in good agreement with the observed ones if we assume isothermal ($\gamma \approx 1$) rather than adiabatic ($\gamma \approx 5/3$) oscillations; this could be a hint of the importance of radiative relaxation.

3.3. Height dependence of phases

Crucial observations for a test of our model assumptions are the height dependence of the phases $\varphi(z)$ and in particular the phase differences $\Delta\varphi(z)$ between oscillations in velocity u and intensity I' , the latter being produced by variations

of P' and T' . Such data have been reported by Kneer et al. {2}, who observed a number of chromospheric lines in an umbra (Ca II H , K , and IR lines, Na I $D1$ and $D2$, $H\alpha$); these data could be completed by the SMM observations of {1} (transition region). The relevant results could be summarized as follow: The measured phase velocity is $\ll v_A$ thus indicating slow mode waves. In the lower chromosphere $\Delta\phi \approx \pi$, the phases quickly change with increasing height. $\Delta\phi \approx \pi/2$ at the level of $D1$ formation, thereupon it decreases slowly to 0.42π at the level of $D2$, to 0.38π at the level of $H\alpha$ formation, and finally to $\Delta\phi = 0$ in the transition region.

For comparison with our model calculations we computed height levels of line formation for different chromospheric lines, at first in our original sunspot model. Ascribing these heights to the observations mentioned above and comparing them with the $\phi(z)$ curves from our model calculations (Fig.3) we get an excellent agreement.

This gives strong evidence for having considered the most important physical features in our model, while the simplifying assumptions obviously do not disturb the picture.

4. Conclusions

In the present paper we considered an isolated chromospheric resonator for slow mode magneto-acoustic waves being excited by a broad band, incident flux. In a real sunspot umbra we have three resonance layers (they will be described in more detail in another paper) which are coupled to each other by a level of wave transformation. Two resonators exist in the layer, photospheric and subphotospheric layers of the sunspot. For one of these resonators the properties of the waves in the convective zone are similar to those of pure acoustic waves, for the other they are more similar to slow mode waves which in a weak magnetic field hardly differ from pure Alfvén waves. A comparison between observations and calculations of the differences in amplitudes and phases of different harmonics becomes greatly complicated by the interaction of the different resonators. The height dependence of ampli-

tudes and the phase relations for the slow mode waves in our calculations, however, do not depend on the type of excitation of oscillations in the chromospheric resonator, that is, no matter whether it results from coupling with the complicated system of resonance layers or not.

Therefore, the good agreement of our computations with observations points to our model for the structure and dynamics of the umbra at chromospheric layers reflecting essential features of the nature of sunspots, notwithstanding our various simplifying assumptions. Possible improvements for our analysis suggest themselves. The computations should be carried out for more realistic models of the umbral transition region, also taking its assumed inhomogeneous structure into consideration which seems necessary to understand multiple wavelength observations. The influence of a 'plateau-type' chromosphere in comparison with our 'gradient' model atmosphere should be studied. The calculations should include the contribution of the fast mode waves, effects of radiative relaxation, and the coupling with the other resonators. Finally, the variations of B and of all thermodynamic quantities by the waves should be considered in line profile computations in order to enable an improved comparison with observations. Some such improvements are being prepared.

Acknowledgements

We would like to thank Drs J.B.Gurman and J.W.Leibacher for the helpful discussion by correspondence.

R e f e r e n c e s

- {1} Gurman, J.B., Leibacher, J.W., Shine, R.A., Woodgate, B.E., Henze, W.,
Transition region oscillations in sunspots, *Ap.J.* 253. 939, 1982
- {2} Kneer, F., Mattig, W., Uexküll, M., The chromosphere above sunspot umbrae.
III. Spatial and temporal variations of chromospheric lines,
Astron.Astrophys. 102. 147, 1981
- {3} Staude, J., A unified working model for the atmospheric structure of
large sunspot umbrae, *Astron.Astrophys.* 100. 284, 1981

-
- {4} Staude, J., Diagnostics of solar active regions in photosphere and chromosphere by means of the spectral polarimetry of Fraunhofer lines. A compilation of computer programs. *HFI-STP Report No. 14*. 24, 1982
- {5} Zhugzhda, Yu., D., Locans, V., Resonance oscillations in sunspots (in Russ.) *Pis'ma v A. Zh.* 7. 44, 1981
- {6} Zhugzhda, Yu., D., Locans, V., Staude, J., Seismology of sunspot atmospheres, *Solar Phys.* 82. 369, 1983

A POSSIBLE MODEL FOR GLOBAL OSCILLATIONS OF THE SUN
ACCORDING TO HILL'S OBSERVATIONAL DATA

V. E. MERKULENKO, V. I. POLYAKOV

SibIZMIR, Irkutsk

Abstract:

A sequence of periods in a spectrum, obtained by Hill and co-workers from solar diameter measurements, agrees to a high degree of probability with eigen-frequencies of a spherically symmetric layer, located at the base of the convection zone. The parameters of the layer are: thickness 10^4 km, depth of occurrence $0.56 R_{\odot}$, density $2.5 \cdot 10^{-1} \text{g cm}^{-3}$, temperature $2.5 \cdot 10^5 \text{K}$, and field strength $4.3 \cdot 10^7 \text{G}$. The field is composed of individual ropes with a preferred orientation in coordinate φ . The condition for resonance excitation on eigen-frequencies of the system is satisfied for oscillations in the layer in coordinate θ , owing to small damping. A response to these oscillations is suggested by strength fluctuations of the poloidal component of the general magnetic field of the Sun as well as by some small plasma density variation at the photospheric level.

ВОЗМОЖНАЯ МОДЕЛЬ ГЛОБАЛЬНЫХ КОЛЕБАНИЙ СОЛНЦА
ПО ДАННЫМ НАБЛЮДЕНИЙ ХИЛЛА

В. Е. МЕРКУЛЕНКО, В. И. ПОЛЯКОВ

СИБИЗМИР, Иркутск

Абстракт:

Последовательность периодов в спектре, полученном группой Хилла при измерении диаметра Солнца, с высокой степенью вероятности согласуется с собственными частотами сферически-симметричного слоя с магнитным полем, локализованного под конвективной зоной. Параметры слоя: толщина 10^4 км, глубина залегания $0.56 R_{\odot}$, плотность $2.5 \cdot 10^{-1} \text{г см}^{-3}$, температура $2.5 \cdot 10^5 \text{К}$, напряженность поля $4.3 \cdot 10^7 \text{гс}$. Поле состоит из отдельных жгутов с преимущественной ориентацией по координате φ . Для колебаний по координате θ ввиду малого затухания осуществляется условие резонанской раскачки на собственных частотах системы. Откликом на эти колебания, возможно, являются пульсации напряженности полоидальной компоненты общего магнитного поля Солнца, а также незначительная вариация плазмы на уровне фотосферы.

1. Introduction

In 1975 Hill and co-workers detected small oscillations of the solar diameter {10},{11},{12}. The spectrum of these oscillations is displayed in Fig.1. The periods vary from 6.5 to 110 minutes (m){3}. At the same time Severny's group made measurements of the difference between the velocities of the central part of the solar disk and the outer annular zone. Their study resulted in a reliable determination of a 160.01 m period {25},{26},{27}. That same period of oscillations was recorded independently by Brookes et al. {2} and further confirmed by Snider et al. {28} as well as by Scherrer et al. {21},{22}.

Until now no unambiguous interpretation of the 160.01 m period and of the Hill spectrum have been reported. The period 160.01 m may be associated with the g -mode at $n = 11$ and $l = 2$ for a standard model of the Sun, in which case, however, the periods 147 m and 171 m should be observed with the same probability but such is not the case {25}. The value 160.01 m is close to the fundamental harmonic of the pulsations of nearly uniform sphere having mass M_{\odot} and being of radius R_{\odot} , but the luminosity of such a sphere must be a factor of 10^5 lower than that of the Sun {25}. The theoretically predicted p -modes of radial oscillations of the Sun, for which $l = 0$, may be associated with a distribution of the periods in the Hill spectrum. Such calculations were performed by Scuflaire et al. {23}, Christensen-Dalsgaard and Gough {5}, Hill and Stebbins {11}, Iben and Mahaffy {14}, and Rouse {19}. The first column of Table 1 lists the observed periods of solar diameter oscillations according to data reported by Brown et al. {3} over the period range 6.5 - 110 minutes. An asterisk denotes periods that do not reach the 0.95 significance level in the spectrum. Columns 2 through 6 present values of periods of radial acoustic modes, inferred in terms of various models of the Sun. As is evident from the table, the observed periods of oscillations for each model cannot be fully identified with radial p -modes. In relation to this Rouse {19}, Boury et al. {1} and Johnson et al. {15} associate the Hill spectrum with nonradial oscil-

lations ($l \neq 0$), by confronting it with individual harmonics selected from a large set of theoretically predicted values of periods. However, the question remains open as to why preference should be given to one or another mode of oscillations.

The aforementioned difficulties in interpreting the Hill spectrum can be avoided, assuming that the separation of individual modes is brought about by a resonance excitation of these oscillations through some spherically-symmetric layer in the Sun's interior with physical parameters, dissimilar to the environment. Vainshtein et al. (29) pointed out that at the base of the convection zone the strength of the azimuthal (B_ϕ) component of the magnetic field is able to reach 10^6 G. As claimed by the authors of the last reference, it is necessary to account for the mechanism of field enhancement in terms of the effect of diamagnetic expulsion of the field out of the region of turbulent convection. In relation to this it is of interest to determine the parameters of a layer with a magnetic field, residing at the base of the convection zone, for which the eigen-frequencies of oscillations are close to those in the Hill spectrum.

2. Spectrum of eigen-frequencies of oscillations of a spherically symmetric layer with an azimuthal field component

The equation for plasma oscillations within a spherically symmetric layer with a magnetic field may be written as (16)

$$\rho_0 \frac{\partial^2 \vec{\xi}}{\partial t^2} = -\nabla(\vec{\xi} \rho_0 \nabla \psi + \gamma P_0 \nabla \vec{\xi}) + \frac{1}{4\pi} \left[\text{rot} B_0 \text{rot} [\vec{\xi} B_0] \right] + \frac{1}{4\pi} \left[\text{rot rot} [\vec{\xi} B] B_0 \right] \quad (1)$$

where $\vec{\xi}$ is plasma shift from the equilibrium position, ψ is the gravitational potential, B_0 is the magnetic field strength, and $\gamma = c_p/c_v$. The "zero" index stands for values of unperturbed parameters. Assume that $\vec{B}_0 = \vec{e}_\phi B_0/x$; $\vec{\xi} = \vec{e}_r \xi_r(r, \theta) + \vec{e}_\theta \xi_\theta(r, \theta)$, where $x = r/\tilde{a}$ and \tilde{a} is a radius of the layer base.

First we shall examine the condition where the parameter $\beta = 8\pi P/B_0^2 \ll 1$, i.e. the plasma is magnetized. Equation (1) then

becomes:

$$\frac{\partial^2 \xi_r}{\partial t^2} = \frac{V_a^2}{\tilde{a}^2} \cdot \frac{1}{x^2} \frac{\partial}{\partial x} \left[\frac{\partial \xi_r}{\partial x} + \frac{1}{x} \frac{\partial \xi_\theta}{\partial \theta} \right] \quad (2)$$

$$\frac{\partial^2 \xi_\theta}{\partial t^2} = \frac{V_a^2}{\tilde{a}^2} \frac{1}{x^3} \frac{1}{\sin \theta} \frac{\partial}{\partial \theta} \left[\sin \theta \left(\frac{\partial \xi_r}{\partial x} + \frac{1}{x} \frac{\partial \xi_\theta}{\partial \theta} \right) \right] \quad (3)$$

where $V_a = B_0 / \sqrt{4\pi\rho_0}$ is the Alfvén velocity. Upon substitution of the variable $U = \frac{\partial \xi_r}{\partial x} + \frac{1}{x} \frac{\partial \xi_\theta}{\partial \theta}$ equations (2) and (3) then yield:

$$\frac{\partial^2 U}{\partial t^2} \frac{\tilde{a}^2}{V_a^2} = \frac{\partial}{\partial x} \left(\frac{1}{x^2} \frac{\partial U}{\partial x} \right) + \frac{1}{x^4} \frac{\partial}{\partial \theta} \left[\frac{1}{\sin \theta} \frac{\partial}{\partial \theta} (U \sin \theta) \right] \quad (4)$$

We seek a solution in the form: $U = A e^{i\omega t} R(x) S(\theta)$. For a function that depends on θ , the solution will have the form:

$$S_n(\theta) = \sin \theta P_n(\cos \theta) \quad (5)$$

where $P_n(\cos \theta)$ is the first kind Legendre polynomial. The equation for the $R(x)$ function assumes the form:

$$x^2 \frac{d^2 R}{dx^2} - 2x \frac{dR}{dx} + \left(\frac{\omega^2 \tilde{a}^2 x^4}{V_a^2} - n(n+1) \right) R = 0 \quad (6)$$

where $n = 0, 1, 2, \dots$

The solution to this equation has the form:

$$R(x) = x^{3/2} I_\nu \left(\frac{1}{2} \omega \frac{\tilde{a}}{V_a} x^2 \right) \quad (7)$$

where I_ν is the Bessel's function, $\nu = \frac{1}{4} \sqrt{9 + n(n+1)}$. Generally the spectrum ω must be derivable from relationships that define the absence of a pressure jump on the boundaries of the layer and of a continuity of a normal component of the perturbed field. However, when the layer's thickness l is substantially smaller than the wavelength λ , i.e. $l \ll \lambda = V_a \tau_n$, where τ_n is the period of oscillations, during radial pulsations the layer will displace as an entity without any substantial deformation. This permits us to neglect derivatives with respect to x in equation (6). Moreover, because $l \ll \tilde{a}$, the variable x can be represented thus: $x = l + y$, where $y \ll l$. As a result, equations (6) and (7) yield to a first approximation:

$$\omega_n \approx \frac{V_a}{\tilde{a}} \sqrt{n(n+1)} = \omega_0 \sqrt{n(n+1)} \quad (8)$$

$$R_n \approx I_v \left(\frac{1}{2} \sqrt{n(n+1)} \right) = \text{const.} \quad (9)$$

Accordingly, taking (5) into account, the solution for U becomes:

$$U_n \approx c_n \exp \left(i \frac{V_a}{\tilde{a}} \sqrt{n(n+1)} t \right) \sin \Theta P_n \cos \Theta \quad (10)$$

whence

$$\xi_{\Theta, n} \approx c_n \exp \left(i \frac{V_a}{\tilde{a}} \sqrt{n(n+1)} t \right) \int_0^{\Theta} \sin \mu P_n \cos \mu \, d\mu \quad (11)$$

Thus, a layer with an azimuthal magnetic field, for which $l \ll \lambda$, must be dominated by pulsations with a shift in the coordinate Θ and with a peak amplitude in the equatorial region. The spectrum of eigen-frequencies of oscillations of the layer must, to a first approximation, be defined by the relationship (8). Assuming that $\omega_0 = V_a / \tilde{a} = 6.54 \cdot 10^{-4} \text{ s}^{-1}$ which corresponds to a period $T^{(0)} = 160.01$, as inferred by Severny from solar radial pulsation measurements, we will define the spectrum thus:

$$T_n = T^{(0)} [n(n+1)]^{-1/2}$$

The computational result is presented in the seventh column of Table 1, where the last column gives the relevant values of n . One can see that these periods confidently agree both in the number of maxima and in the values of Hill spectrum periods. An exception is the period 35.78 m with $n=4$. It appears to correspond to an average taken of two maxima on the spectrum with the periods 39.0 m and 32.1 m. Then this maximum would refer to the period 35.5 m which compares well with the predicted value. Fig.2 is a plot of $\lg T_n$ against n , also showing corresponding values of periods from the Hill spectrum.

The confidence of the agreement between the theoretical and observed spectra was evaluated using the following scheme: the value of $T_j^{(0)} = T_j \sqrt{j(j+1)}$ was determined for each value of the period in the Hill spectrum. Hence the r.m.s. deviation

$$\sigma = \left[\frac{1}{N} \sum T^{(0)} - \overline{T^{(0)}} \right]^{1/2} \text{ is } 3.56 \text{ m, in which case } T^{(0)} = \frac{1}{N} \sum_{j=1}^N T^{(0)} =$$

= 160.086 m and $N=24$. As a result, the parameter of Student

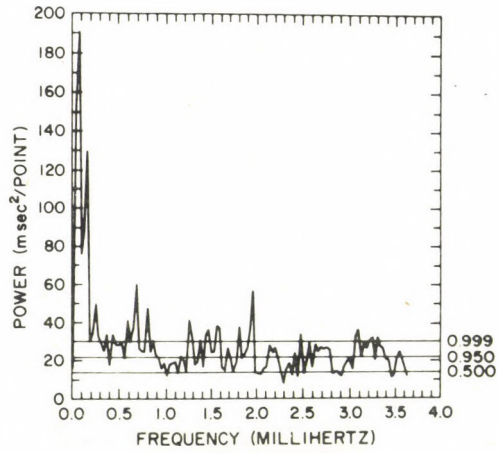


Fig. 1. Power spectrum of oscillations of the solar diameter according to observations of Brown et al. {3}

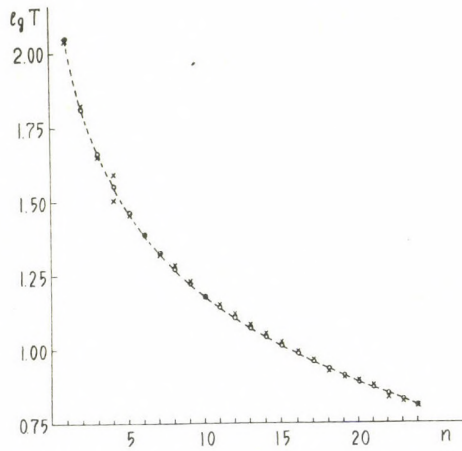


Fig. 2. Comparison of the computed values of periods with periods of Hill spectrum (••• - theory, x x x - experiment).

is 0.19. Thus, it can be asserted that theoretical and experimental values of the periods agree to within 0.85 probability.

Oscillation periods of solar diameter were calculated in {3} only up to 6.5 m ($n=24$). If we examine a theoretical spectrum for large values of n , then for the 5 minute oscillation region the frequency difference between the adjacent harmonics of the spectrum becomes constant $\Delta\nu = 0.1041 \cdot 10^{-3}$ Hz. The discreteness of the spectrum with equally-spaced peaks was found by Claverie et al. {6}. However, the frequency spacing of the peaks in the power spectrum of the observed 5 min oscillations is smaller, namely $0.0678 \cdot 10^{-3}$ Hz. Such a frequency difference is observable if $T^{(0)} = 245.82$ min is assumed as the principal period of oscillations in formula (12). Dittmer {8} found a period of 256 m, in close proximity to this period.

3. Physical parameters of a spherically symmetric layer with magnetic field

Now, we shall determine the parameters of a layer with a magnetic field, acting as a resonator at Hill frequencies. At its lower boundary the equilibrium condition may be written as:

$$\frac{B_0^2}{8\pi} + (\tilde{\rho}_i - \rho_e)gz + P_i = P_e \quad (13)$$

where $\tilde{\rho}_i$ is an averaged value of the density through the radial cross-section of the layer. The indices i and e denote the parameter values within and outside of the layer.

The last equation yields:

$$\frac{\tilde{\rho}_i}{\rho_e} = \frac{V_{se}^2 + \gamma g l}{V_a^2(0.5\gamma + \alpha) + \gamma g l} \quad (14)$$

where $V_{se}^2 = \frac{\gamma P_e}{\rho_e}$ is the square of sound velocity outside the layer and $\alpha = V_{si}^2/V_a^2$ is the ratio of the squared sound velocity within the layer to the Alfvénic velocity. In order to eliminate the action of the hydrostatic force on the layer it should be assumed that $\tilde{\rho}_i = \rho_e$. This results in

$V_{se}^2 = V_a^2(0.5\gamma + \alpha)$. Assume that $\alpha = 0.1$ and $\gamma = 5/3$. In doing so, in accordance with the expression (8) we find:

$$V_{se}^2 = \frac{\gamma P_e}{\rho_e} = 2.3 \cdot 10^8 T_e = 0.9 V_a^2 = 0.9 \tilde{a}^2 \omega_0^2 \quad (15)$$

Allowing for the value of ω_0 , this last expression will take the form:

$$T_e = 8.1 \cdot 10^6 \kappa^2 \quad (16)$$

where κ is the distance from the center of the Sun in fractions of solar radius. We will avail ourselves of a model {24} of the distribution of physical parameters of the Sun with depth. The T_e versus κ curve intersects the temperature variation curve at $\kappa_0 = 0.56$ from solar radius. For this depth $\rho_e = \rho_i = 2.5 \cdot 10^{-1} \text{g cm}^{-3}$. Taking into account that $\tilde{\alpha} = \kappa_0 R_\odot$ from equation (15) we find: $V_a = 2.4 \cdot 10^7 \text{g cm}^{-3}$. According to the adopted condition for oscillations of the layer, $\lambda \gg l$, hence the layer's thickness l may be assumed to be of the order 10^9cm . The field strength within the layer must be $B_0 = V_a \sqrt{4\pi \tilde{\rho}_i} = 4.3 \cdot 10^7 \text{G}$. When $\alpha = 0.1$, i.e. $V_{si}^2 = 0.1 V_a^2$, the condition of plasma magnetization is satisfied. Correspondingly, the temperature within the layer will be $2.5 \cdot 10^5 \text{K}$. Outside the layer, according to the model of Sears {24}, it is $2.5 \cdot 10^6 \text{K}$.

Thus, equilibrium in the layer must be realized through a substantial temperature drop. A deficit of radiant energy flux in the layer can be compensated for only by convective transfer. In a horizontal magnetic field convection has the form of extended rolls {4}. A variation of the angular rotation rate, as a result of convection along the length of the rolls, must cause the layer to split into a system of twisted quasi-parallel ropes. Presumably, this process must have no effect on oscillations in the layer in coordinate θ because in between the ropes the sound velocity is comparable to Alfvén velocity.

A temperature decrease in magnetic ropes as compared to the ambient medium may be associated with the thermal instability {17} which develops whenever $\frac{\partial}{\partial T} \left[\frac{L(T)}{T} \right] < 0$, where $L(T)$ is a function that depends on temperature only. From the form of the $L(T)$ function {7}, with proper account of the temperature distribution according to the model of Sears {24} it follows that the condition for the instability to develop will be satisfied. Possibly, this process is analogous to the production of prominences in the corona.

4. Discussion

The sequence of periods in the Hill spectrum can, to a high degree of probability, be brought into agreement with eigen-frequencies of oscillations of a spherically symmetric layer with a magnetic field, located below the convection zone at a depth of $0.56 R_{\odot}$. The thickness of the layer is order of 10^4 km. The density in the layer coincides with that of the surrounding plasma but the temperature is an order of magnitude lower. The field seems to consist of individual ropes, oriented in coordinate φ , with a strength of order $4.3 \cdot 10^7$ G. Global oscillations in the layer must proceed preferentially in coordinate Θ , i.e. across the magnetic field. Since for these oscillations the Alfvén velocity substantially exceeds the sound velocity, the damping will, therefore, be minimal which will determine their excitation on resonance frequencies. For radial oscillations the wavelength is an order of magnitude longer than the layer's thickness. On its boundary $V_a \geq V_{se}$, and therefore a shock wave must arise which will substantially decrease the amplitude of radial oscillations as compared to those in coordinate Θ . The following variant of a reconciliation between the oscillations on the solar surface and those within the layer seems to be plausible. Plasma shift ξ_{Θ} near the poles in the layer must lead to simultaneous oscillations of the poloidal component strength of the general magnetic field of the Sun, the component being undoubtedly associated with the layer. Indeed, the period 160.01 m has been discovered by Severny's group in the oscillations of the general magnetic field of the Sun [18]. It should be noted that near the poles in the photosphere there must be oscillation of plasma density resulting from plasma entrainment by a poloidal field during axially symmetric tangential shifts in coordinate Θ . Possibly, this effect was making the crucial contribution at the time of oscillation measurements in Hill's experiment. On the whole, it must be suggested that the global oscillations of the Sun with the period 160.01 m, as detected by Severny's group, cause a resonance excitation of meridional oscillations in a spheri-

T A B L E 1

Observed period (min)	Predicted period (min)						n
	Scufaire et al. (1975)	Christensen-Delsgaard and Gough (1976)	Hill et al. (1976a)	Iben and Mahafy (1976)	Rouse (1977)	Merkulenko and Polyakov (1983)	
110			167			160.01 113.14	1
66.16	62.71	62.22		66.14	75.82	65.32	2
44.66		41.98	46.9		45.50	46.19	3
39.0	41.10			40.81			
32.1	31.26	32.32	30.0	30.67	33.06	35.78	4
28.7						29.21	5
24.8	24.75	26.00		24.18	25.66	24.69	6
21.0	20.42	21.51	22.3		20.97	21.38	7
19.5		18.33	17.84	19.95		18.86	8
17.0*	17.36			16.90	17.81	16.87	9
15.1*	15.12	15.95			15.55	15.26	10
14.3*		14.13		14.75		13.93	11
13.3	13.38		14.88	13.05	13.84	12.81	12
12.1	12.02	12.64	12.77		12.49	11.86	13
11.4		11.54	11.19	11.72	11.38	11.04	14
10.7	10.94	10.60	9.96	10.65	10.44	10.33	15
9.9	10.05	9.81		9.77	9.67	9.70	16
9.3	9.30	9.12	8.98	9.03	9.00	9.14	17
8.5	8.65	8.52	8.17	8.39	8.41	8.65	18
8.0*	8.08					8.21	19
7.8		7.94		7.83	7.89	7.81	20
7.6	7.59	7.53	7.50	7.34	7.45	7.44	21
6.9		7.12		6.92	7.06	7.11	22
6.7		6.75	6.93		6.69	6.81	23
6.5		6.41	6.44	6.54	6.37	6.53	24

cally symmetric layer with a strong magnetic field below the convection zone with a spectrum of the form $\omega_n = \omega_0 \sqrt{n(n+1)}$. In the last years, apart from these basic frequencies in the oscillations of the solar diameter Hill obtained a number of additional peaks of the harmonics {30}.

Possibly, in the future, they can be associated with a more exact solution to the problem of oscillations of this layer.

Acknowledgements

We are grateful to Dr G.V.Kuklin for assisting in the evaluation of the reliability of the computed spectrum. Special thanks are due to V.G.Mikhalkovsky for his help in preparing the English version of the manuscript and typing the text.

R e f e r e n c e s

- {1} Boury,A.,Scuflaire,R.,Noels,A.,Gabriel,M., Nonradial oscillations of solar models with an initial discontinuity in hydrogen abundance, *Nonradial and nonlinear stellar pulsation* (Hill,H.A.,Dziembowski, W.,eds.) *Lecture Notes in Physics*,Vol.125. 342. Springer-Verlag, Heidelberg, 1980
- {2} Brookes,J.R.,Isaak,G.R.,van der Raay,H.B., Observation of free oscillations of the Sun, *Nature*,259. 92, 1976
- {3} Brown,T.M.,Stebbins,R.T.,Hill,H.A., Long-period oscillations of the apparent solar diameter: observations, *Ap.J.*223. 324, 1978
- {4} Chandrasekhar,S., *Hydrodynamic and hydromagnetic stability*, p.189. Oxford Univ.Press. 1961
- {5} Christensen-Dalsgaard,J.,Gough,D.O., Towards a heliological inverse problem, *Nature*, 259. 89, 1976
- {6} Claverie,A.,Isaak,G.R.,McLeod,C.P.,van der Raay,H.B.,Cortes,T.R., Solar structure from global studies of the 5-minute oscillation, *Nature*, 282. 591, 1979
- {7} Cox,D.P.,Tucker,W.H., Ionization equilibrium and radiative cooling of a low density plasma, *Ap.J.*157. 1157, 1969
- {8} Dittmer,P.H., An observational search for solar pulsations at periods from 7 to 70 minutes, *Ap.J.*224. 265, 1978
- {9} Field,G.B., Thermal instability, *Ap.J.*142. 531, 1965
- {10} Hill,H.A.,Stebbins,R.T., Recent solar oblateness observations: date, interpretation, and significance for earlier works, *Ann.N.Y.Acad.Sci.* 262. 472, 1975
- {11} Hill,H.A.,Stebbins,R.T., The intrinsic visual oblateness of the Sun, *Ap.J.*200. 471, 1975
- {12} Hill,H.A.,Stebbins,R.T.,Brown,T.M., Recent solar oblateness observations: date, interpretation and significance for experimental relativity, *Atomic Masses and Fundamental Constants* (Sanders,J.H. Wapstra,A.H.eds.) Vol.5. 622. Plenum Press, N.Y.-London, 1976
- {13} Hill,H.A.,Stebbins,R.T.,Brown,T.M., Oscillations of the Sun. *A summary of contribution to the March 12, 1976 meeting of the Royal Astronomical Society*, 1976
- {14} Iben,I.Jr.,Mahaffy,J., On the Sun's acoustical spectrum, *Ap.J.*209. L39. 1976

- {15} Johnson, W.W., Windet, D.E., Douglas, D.H., Van Horn, H.M., Time varying gravitational multipole moments corresponding to nonradial solar oscillations, *Nonradial and nonlinear stellar pulsation* (Hill, H.A. Dziembowski, W. eds.) *Lecture Notes in Physics*, Vol. 125. 357, Springer-Verlag, Heidelberg, 1980
- {16} Kadomtsev, B.B., Hydromagnetic stability of plasma. (in Russ.) *Voprosy teorii plazmy*, 2. (Leontovich, M.A. ed.) 132, Atomizdat, Moscow 1963
- {17} Kaplan, S.A., Pikel'ner, S.B., Tsytovich, V.N., *Physics of plasma of the solar atmosphere*, (in Russ.) 100. Nauka, Moscow, 1977
- {18} Kotov, V.A., Severny, A.B., Tsap, T.T., Observations of oscillations of the Sun, *M.N.* 183. 61, 1978
- {19} Rouse, C.A., On the first twenty modes of radial oscillation of the 1968 non-standard solar model, *Astron. Astrophys.* 55. L477, 1977
- {20} Rouse, C.A., On the nonradial oscillations of the 1968 nonstandard solar model, *Astron. Astrophys.* 71. 95, 1979
- {21} Scherrer, P.H., Wilcox, J.H., Severny, A.B., Kotov, V.A., Tsap, T.T., Observations of solar oscillations with periods of 160 minutes, *Nature*, 277. 635, 1979
- {22} Scherrer, P.H., Wilcox, J.H., Severny, A.B., Kotov, V.A., Tsap, T.T. Further evidence of solar oscillations with a period of 160 minutes, *Ap.J.* 237. L97, 1980
- {23} Scuflaire, R., Gabriel, M., Noels, A., Boury, A., Oscillatory periods in the Sun and theoretical models with or without mixing, *Astron. Astrophys.* 45. 15, 1975
- {24} Sears, R.L., Helium content and neutrino fluxes in solar models, *Ap.J.* 140. 477, 1964
- {25} Severny, A.B., Kotov, V.A., Tsap, T.T., Observation of solar pulsations, *Nature*, 259. 87, 1976
- {26} Severny, A.B., Kotov, V.A., Tsap, T.T., The study of solar pulsations and the problem of its interior, (in Russ.) *Uspekhi Fizicheskikh Nauk*, 128. 728, 1979
- {27} Severny, A.B., Kotov, V.A., Tsap, T.T., Solar oscillation and the problem of internal constitution of the Sun, (in Russ.) *Astron.Zh.* 56. 1113, 1979
- {28} Snider, J.L., Kearns, M.D., Tinker, P.A., Evidence for long-period global oscillations of the Sun, *Nature*, 275. 730, 1978
- {29} Vainshtein, S.I., Zeldovich, Ya.B., Ruzmaikin, A.A., *Turbulent dynamo in astrophysics*, (in Russ.) 262. Nauka, Moscow, 1980
- {30} Bos, R.J., Hill, H.A., Detection of individual normal modes of oscillation of the Sun in the period range from 2h to 10 min in solar diameter studies, *Solar Phys.* 82. 89, 1983

ON THE EFFECTS OF MAGNETIC ENERGY INCREASE
IN THE SUNSPOT CHROMOSPHERE

V. N. D E R M E N D J I E V

Acad. Astron. Dept., Sofia

Abstract:

A two-dimensional, hydromagnetic, time-dependent model is developed, which simulates the response of the sunspot umbral chromosphere plasma initiated by the emerging magnetic flux at the "foot" of an existing magnetic loop structure. The effects of the thermal conduction, gravity and Joule heating are taken into account and separate ion and electron temperatures are calculated. The increased magnetic flux leads to a somewhat modest collapse in the lower chromosphere and causes the plasma to flow upwards. It is hypothesized that such effects may provide a reasonable simulation of small-scale transient phenomena in the lower chromosphere, often in close relation to chromosphere plasma ejection events.

ОБ ЭФФЕКТАХ РОСТА МАГНИТНОЙ ЭНЕРГИИ
В СОЛНЕЧНОЙ ХРОМОСФЕРЕ НАД ПЯТНАМИ

В. Н. ДЕРМЕНДЖИЕВ

Астрон. Отд. Акад., София

Абстракт:

Разработана двумерная, гидромагнитная модель, которая симулирует отклик хромосферной плазмы над солнечным пятном на всплывание магнитного потока в "ножке" уже существующей магнитно-петлевой структуры. Эффекты теплопроводности, силы тяжести и джоулевой диссипации приняты во внимание и отдельно вычисляются ионная и электронная температуры. Возрастающий магнитный поток приводит к возникновению небольшого коллапса в нижней хромосфере и вызывает движение плазмы вверх. Высказывается предположение, что такие эффекты дают приемлимые симуляции мелко-масштабных нестационарных явлений в нижней хромосфере, которые часто тесно связаны с явлениями выбрасывания хромосферной плазмы.

1. Introduction

The increase of magnetic energy in the solar atmosphere is an object of considerable observational and theoretical interest and is usually explained with magnetic flux emergence. When such emergence occurs at the base of a pre-existing magnetic loop structure, it is treated as a possible mechanism of solar flares formation {6},{5}. However, a number of observations show that surges, sprays and bright points (Ellerman bombs) can also be formed.

As a rule, surges are observed in the regions of the solar atmosphere with relatively fast variations of the magnetic flux. The analysis of high resolution on- and off-band $H\alpha$ filtergrams of disk solar surges and their comparison with magnetic data {9} shows that surges are clusters of a large number of fine jets, thickness of 1" in diameter, apparently connected with the bright knots, or bombs in the lower chromosphere. According to Rust {11} the Ellerman bombs mainly appear in the regions with "satellite" polarity in close proximity to already existing strong magnetic field at photospheric level.

Bruzek {1} supposes that the cause of formation for both the bombs and the accompanying arch filaments is closely connected with the propagation through the chromosphere of expanding and increasing active region magnetic fields.

The aim of this paper is to model the magnetic energy increase in regions of strong local magnetic field with suitable equations and to investigate numerically the behaviour, i.e. the dynamical response of the plasma in the chromosphere above this region.

2. Magneto-hydrodynamic model

The model in cartesian coordinates describes an initial potential magnetic field configuration of bipolar sunspot groups at the "foot" of which a new magnetic flux emerges. This situation is expressed by equations (1) and (2)

$$B_x^I = B_0 \cos \left(\frac{\pi}{2} \frac{x_m - x}{x_m} \right) \exp \left(- \frac{\pi}{2} \frac{y}{x_m} \right)$$

$$B_y^I = B_0 \sin \left(\frac{\pi}{2} \frac{x_m - x}{x_m} \right) \exp \left(- \frac{\pi}{2} \frac{y}{x_m} \right)$$

$$x = i\Delta x, \quad i=0,1,2,\dots,k, \quad k\Delta x = D, \quad (1)$$

$$B_x = B^* \cos \left(\frac{\pi}{2} \frac{x}{d} \right) \left(1 + \frac{1}{B^*} \frac{dB}{dt} t \right)$$

$$B_y = -B^* \sin \left(\frac{\pi}{2} \frac{x}{d} \right) \left(1 + \frac{1}{B^*} \frac{dB}{dt} t \right)$$

$$t = 0,1,2,\dots,\tau, \quad d = \frac{D}{2} \quad (2)$$

where D is the diameter of the foot, B_0 - the magnetic induction at the base of the magnetic arch system of a semiwidth of x_m , B^* - the initial value of magnetic induction of the new field at the photosphere, $\frac{dB}{dt}$ - the growth of the magnetic field and τ - the duration of the magnetic pulse. In accordance with the observational data {2} we assume $B_0 = 1500$ G and $x_m = 15 \cdot 10^3$ km. The B_x component is tangent to the solar limb, while the B_y - component is radially directed upwards to the corona. The perturbations {2} increase linearly with the time and are continuously maintained throughout the time-dependent calculations.

To describe the behaviour of the chromosphere plasma above the place of magnetic flux emergence, we proceed from the equations in cartesian coordinates of two-dimensional magneto-hydrodynamics of a compressible media, making the following assumptions: 1) the investigated media is a completely ionized hydrogen plasma, 2) the velocity and magnetic field have only two components, 3) Joule heating is limited to the electrons, 4) separate thermal conductivities are computed for electrons and ions, 5) viscosity and radiation are neglected, 6) the transport coefficients are isotropic and 7) the thermodynamic properties of the media are described by the equation of the ideal gas.

Since we are studying plasma of a very low value of the parameter beta, $\beta \ll 1$ (β is the ratio of gas pressure to mag-

netic pressure), when computing the magnetic field small errors might increase, leading to fictitious effects of anomalous heating or cooling. Therefore, instead of the equation of total energy in conservative form, we use the equation of thermal energy in which all terms describing heating are obviously included.

Taking into account all these assumptions, time dependent equations can be written as follows:

$$\frac{\partial \rho}{\partial t} = -\frac{\partial}{\partial x}(\rho U) - \frac{\partial}{\partial y}(\rho V), \quad (3)$$

$$\frac{\partial}{\partial t}(\rho U) = -\frac{\partial}{\partial x}(\rho U^2) - \frac{\partial P}{\partial x} - \frac{\partial}{\partial y}(\rho UV) - \frac{B_y}{4\pi} \left(\frac{\partial B_y}{\partial x} - \frac{\partial B_x}{\partial y} \right), \quad (4)$$

$$\frac{\partial}{\partial t}(\rho V) = -\frac{\partial}{\partial y}(\rho V^2) - \frac{\partial P}{\partial y} - \frac{\partial}{\partial x}(\rho UV) - \frac{B_x}{4\pi} \left(\frac{\partial B_x}{\partial y} - \frac{\partial B_y}{\partial x} \right) - \rho g_0 \quad (5)$$

$$\frac{\partial B_x}{\partial t} = \frac{c^2}{4\pi} \frac{\partial}{\partial y} \left[\eta \left(\frac{\partial B_x}{\partial y} - \frac{\partial B_y}{\partial x} \right) \right] - \frac{\partial}{\partial y} (B_x V - B_y U), \quad (6)$$

$$\frac{\partial B_y}{\partial t} = \frac{c^2}{4\pi} \frac{\partial}{\partial x} \left[\eta \left(\frac{\partial B_y}{\partial x} - \frac{\partial B_x}{\partial y} \right) \right] - \frac{\partial}{\partial x} (B_y U - B_x V), \quad (7)$$

$$\begin{aligned} \frac{\partial}{\partial t}(\rho T_e) = & -(\kappa - 1)\rho T_e \left(\frac{\partial U}{\partial x} + \frac{\partial V}{\partial y} \right) - \frac{\partial}{\partial x}(\rho T_e U) - \frac{\partial}{\partial y}(\rho T_e V) - \frac{\gamma - 1}{R} \left[\frac{\partial}{\partial x} \left(\kappa_e \frac{\partial T_e}{\partial x} \right) + \right. \\ & \left. + \frac{\partial}{\partial y} \left(\kappa_e \frac{\partial T_e}{\partial y} \right) - \frac{\eta c^2}{(4\pi)^2} \left(\frac{\partial B_x}{\partial y} - \frac{\partial B_y}{\partial x} \right)^2 \right] + \frac{\rho(T_i - T_e)}{\tau_{eq}}, \quad (8) \end{aligned}$$

$$\begin{aligned} \frac{\partial}{\partial t}(\rho T_i) = & -(\kappa - 1)\rho T_i \left(\frac{\partial U}{\partial x} + \frac{\partial V}{\partial y} \right) - \frac{\partial}{\partial x}(\rho T_i U) - \frac{\partial}{\partial y}(\rho T_i V) - \frac{\kappa - 1}{R} \frac{\partial}{\partial x} \left(\kappa_i \frac{\partial T_i}{\partial x} \right) + \\ & + \frac{\partial}{\partial y} \left(\kappa_i \frac{\partial T_i}{\partial y} \right) + \frac{\rho(T_e - T_i)}{\tau_{eq}}, \quad (9) \end{aligned}$$

$$P = \rho R(T_i + T_e), \quad (10)$$

where the independent variables are x and y coordinates directed tangent to the solar limb and radially upwards to the corona respectively. κ is the ratio of specific heats, R is the gas constant, η is the electrical resistivity, κ_e and κ_i are electron and ion thermal conductivity, τ_{eq} is the electron-ion temperature equilibration time, c is the velocity of light and g_0 is the gravity on the surface of the Sun. The dependent variables are the density ρ , gas pressure P , horizontal, U , and vertical, V , velocity, horizontal, B_x , and vertical, B_y , components of the magnetic field induction, and electron, T_e , and ion, T_i , temperatures. Spitzer {12} formulas are used for pro-

perties η , κ_e , κ_i , and τ_{eq} and a value of $\kappa = 5/3$ is used for all calculations.

For the numerical solution of the model (1)-(10) we used a variation of Richtmyer's two-step method {10}. The principal advantage of the method is the fact that it is of a second order accuracy and that it is capable of a sharper shock resolution compared to other second order approaches. To overcome instability due to the time centering of the second space differences, we use the Dufort-Frankel scheme {4} which is unconditionally stable.

3. Results and discussion

We place a two-dimensional 60×100 network with a step $\Delta x = \Delta y = 10$ km at the lower chromosphere immediately over the photosphere at the foot of the magnetic loop structure, simulated with equation (1). This network forms the basic staggered spatial array for the computations. The network step is chosen so that high resolution in the regions of fast changing to be achieved, while the time step - to satisfy the Courant-Friedrich-Lewy condition for stability of the solution in every node of the network. The initial atmosphere is assumed to be motionless, with temperature and density satisfying the empirical sunspot chromosphere model of Lites and Skumanich {7}.

The model allows the current component in z direction. From the physical point of view, it is supposed that initially, the plasma has a zero velocity, whereupon it gains acceleration due to an impulsive increase of the magnetic pressure in a thin layer at the lower boundary (photosphere). This magnetic pressure jump, equivalent to a weak current at the boundary, is given by the perturbation {2} which simulates the emergence of a new magnetic flux.

The boundary conditions, except for the magnetic pulse on the lower boundary, are engaged in the calculations in such a way that the first-order extrapolation is satisfied {3}.

To demonstrate the possibilities of the model we give $B^* = 1000$ G and $\frac{dB}{dt} = 10$ G sec⁻¹. Of particular interest are the thermodynamic response of the solar chromosphere and the

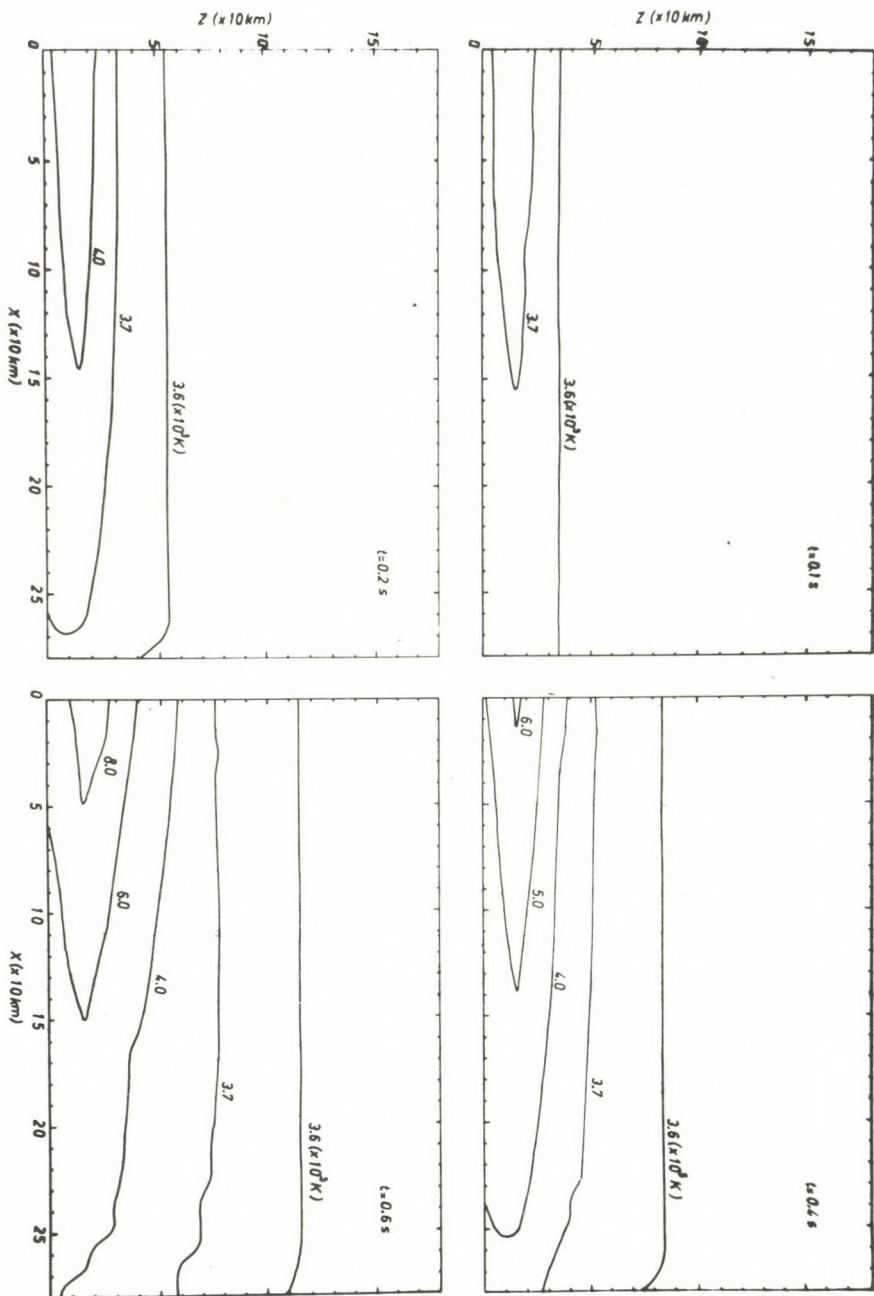


Fig. 1.

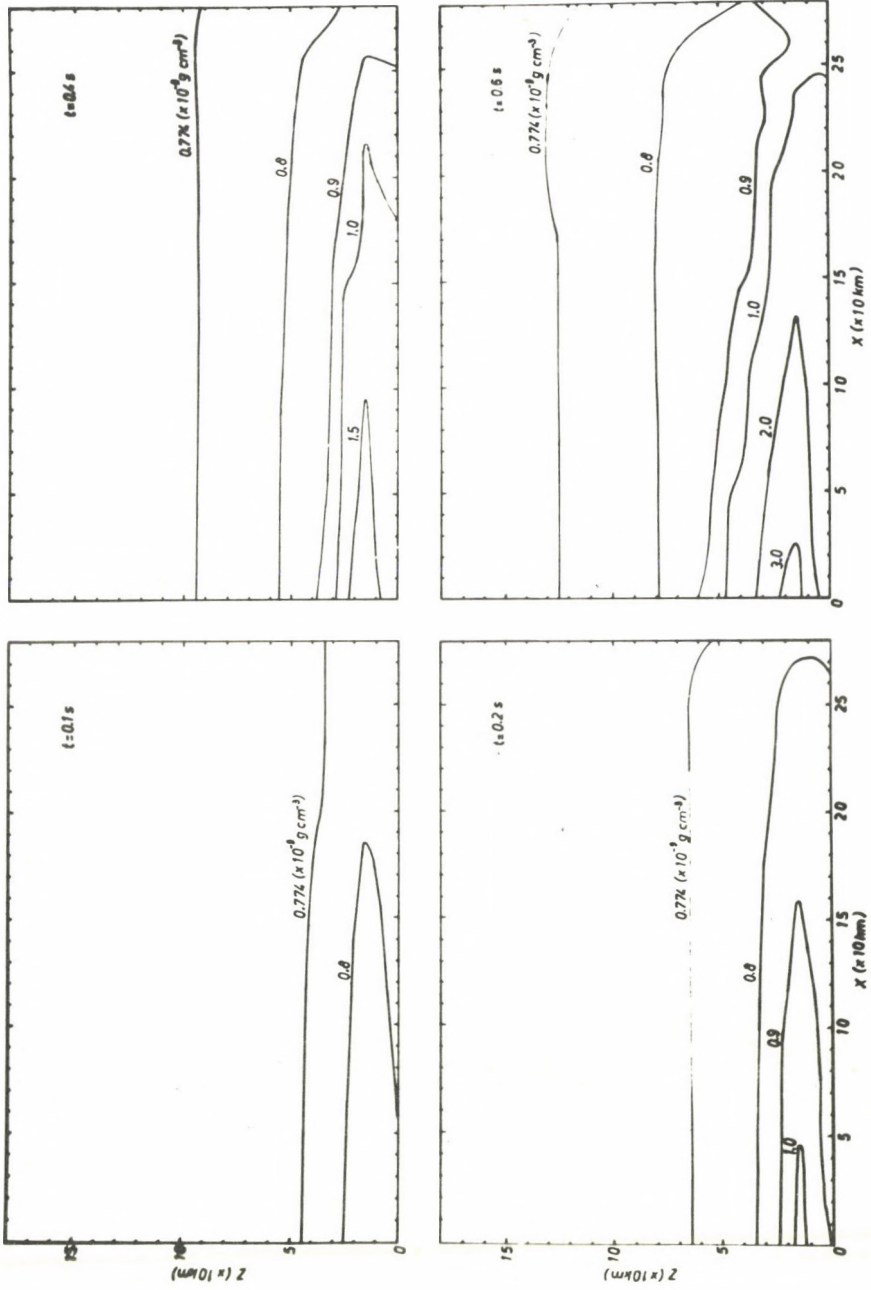


Fig. 2.

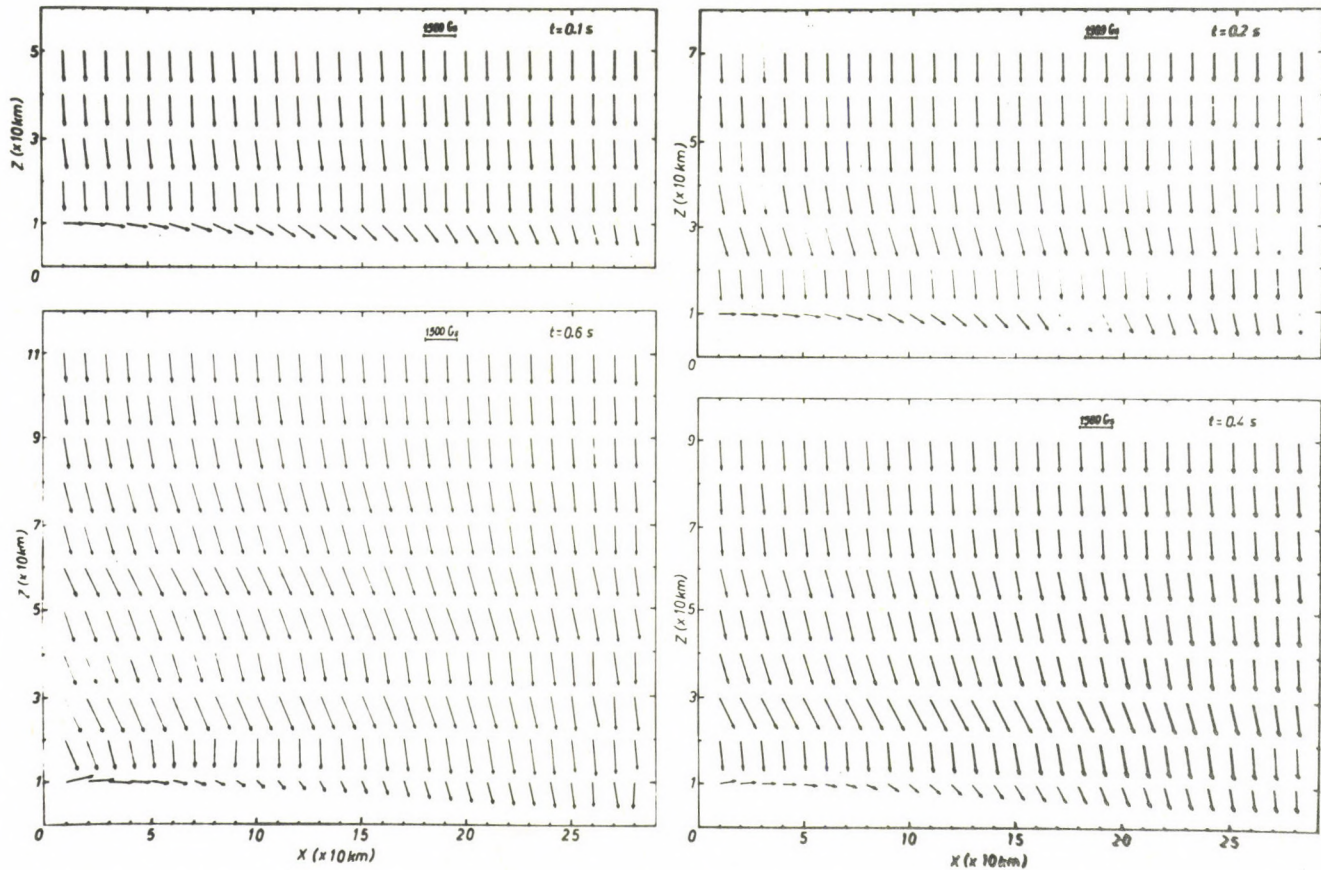


Fig. 3.

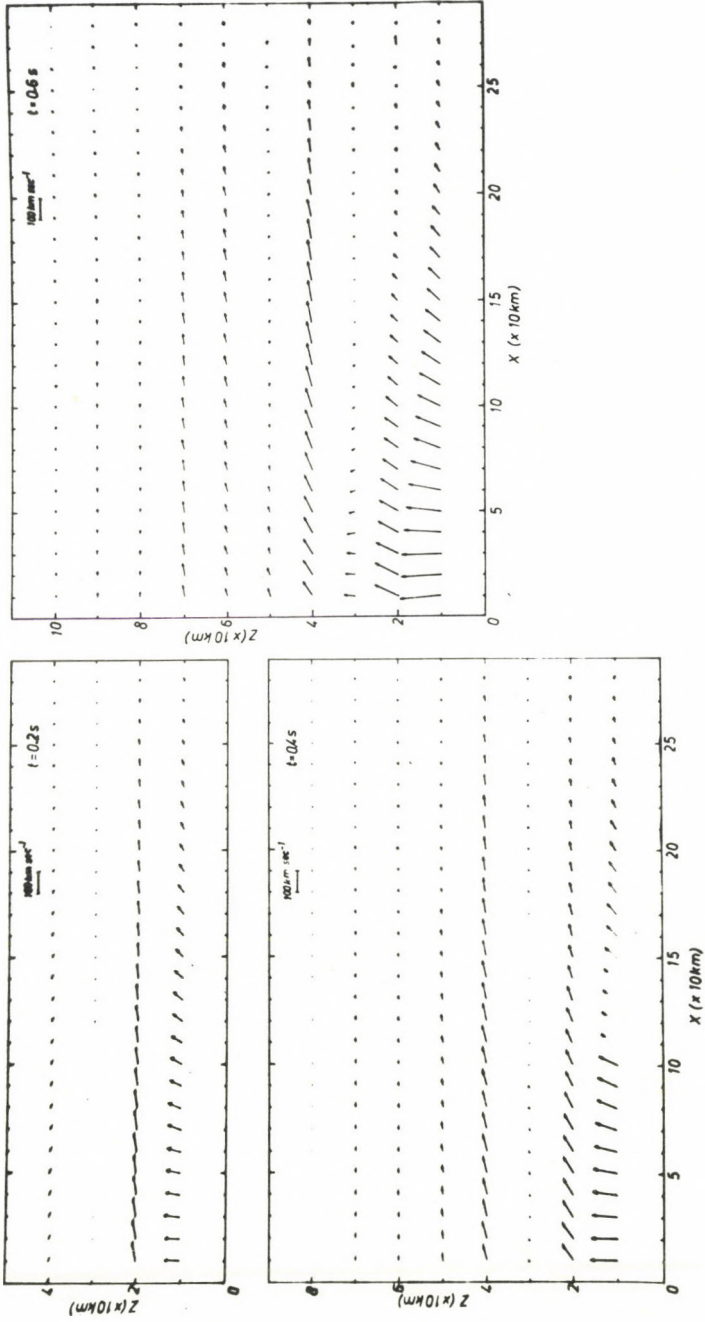


Fig. 4.

magnetic and velocity fields, established by the emerging flux.

The problem of displaying the output values has always been very difficult. The complete set of profiles for all representative times is an excessively large body of data. Therefore, we have selected four consecutive sets for the electron temperature, density and magnetic field profiles and three sets of velocity profiles to indicate the type of data available from this solution.

In Figs.1 and 2, a modest collapse can be traced, appearing immediately to the lower boundary around the axis of symmetry. We have to point out that due to the symmetry, the respective figures show only the right-hand part of the investigated region. The imperturbed regions are not shown either.

The magnetic field (Fig.3) remains imperturbed at larger heights, but it shows zigzags and is strongly deformed close to the place of the new magnetic flux emergence. The picture of the velocity field is also interesting (Fig.4). The plasma moves upwards in pulses, showing a vortex-like movement.

4. Conclusion

As Parker {8} suggests, the magnetic buoyancy in an electrically conductive atmosphere is large enough to bring a strand of flux from the general toroidal magnetic field up into the photosphere. This mechanism probably acts in the sub-photosphere layers, while above the photosphere, the electromagnetic processes are becoming substantial.

With the help of a two-dimensional magneto-hydrodynamic numerical experiment we investigate in our work the behaviour of the chromosphere plasma above the sunspot during the emergence of a new magnetic flux, taking the dissipation processes (neglecting the viscosity) into account. The essential result obtained is that an area of increased density and temperature is being created which may be interpreted as a bright point or bomb. The created temperature gradient can serve as an initial pulse which may produce a plasma flux in the direction of the lines of force of the quasistatic magnetic loop structures in the form of a surge or spray events.

Acknowledgements

I wish to thank Dr B.Rompolt for the very helpful discussions and Professor E.I.Mogilevsky for his valuable advice.

References

- {1} Bruzek,A., Bright points (moustaches) and arch filaments in young active regions, *IAU Symp.*35. 293, 1968
- {2} (Bruzek,A.,Durrant,C.J.eds.) *Illustrated glossary for solar and solar-terrestrial physics*, *Astrophysics and Space Science Library*, Vol.69. D.Reidel Dordrecht, 1977
- {3} Chu,C.K.,Sereny,A., Boundary conditions in finite difference fluid dynamic codes, *Journal of Comp.Phys.* 15. 476, 1974
- {4} Dufort,E.C.,Frankel,S.P., Stability conditions in the numerical treatment of parabolic differential equations, *Math.Tables and other aids to comp.* 7. 135. 1953
- {5} Heyvaerts,J.,Priest,E.R.,Rust,D.M., An emerging flux model for the solar flare phenomenon, *Ap.J.* 216. 213, 1977
- {6} Krivský,L., Interaction of magnetic fields and the origin of proton flares, *IAU Symp.*35. 465, 1968
- {7} Lites,B.W.,Skumanich,A., A model of a sunspot chromosphere based on OSO 8 observations, *Ap.J.Suppl.Ser.* 49. 293, 1982
- {8} Parker,E.N., The formation of sunspot from the solar toroidal field, *Ap.J.* 121. 491, 1955
- {9} Roy,J.-R., The magnetic properties of solar surges, *Solar Phys.* 28. 95, 1973
- {10} Rubin,E.L.,Burstein,S.Z., Difference methods for the inviscid and viscous equations of a compressible gas, *Journal of Comp.Phys.* 2. 178, 1967
- {11} Rust,D.M., Chromospheric explosions and satellite sunspot, *IAU Symp.*35. 77, 1968
- {12} Spitzer,L.Jr. *Physics of fully ionised gases*, 2nd ed. Interscience Publishers, New-York - London, 1962

СИНЕРГИТИЧЕСКОЕ ПОНИМАНИЕ ЭВОЛЮЦИИ СТРУКТУР
МАГНИТНЫХ ПОЛЕЙ НА СОЛНЦЕ

Э. И. М О Г И Л Е В С К И Й

ИЗМИРАН, Троицк

SYNERGIC EXPLANATION OF THE EVOLUTION
OF SOLAR MAGNETIC FIELD STRUCTURES

E. I. MOGILEVSKIY

IZMIRAN, Troitsk

1. Принципиальное отличие космической плазмы (в том числе замагниченной плазмы на Солнце) от лабораторной состоит прежде всего в том, что отсутствие в космосе ограждающих стенок, которые для лабораторной плазмы обуславливают выполнение всей законов сохранения, приводит к такой самоорганизации (образованию таких структур) плазмы в космосу, которая обеспечивает ее самоорганизации. Это означает, в частности, что в наблюдаемой атмосфере Солнца должны существовать такие точки, магнитные поля, скорости вещества (возможные при определенных структурах в плазме), которые обеспечивают квазистационарность солнечной атмосферы. Супергранулы по всей поверхности Солнца, соответствующие конвективным ячейкам Бенара, петельные и аркадные и другие структуры в короне и хромосфере, тонкоструктурные филаментарные магнитоплазменные элементы, из которых состоят наблюдаемые явления солнечной активности (пятна, факелы и т.д.) - все это иллюстрирует существование на Солнце процессов самоорганизации.

Указанную характерную особенность солнечной магнитоплазмы, которая определяет фундаментальные ее свойства, можно вывести из предложенного А.А. Власовым {1} соотношения структурности:

$$\int f(r, p) d\tau \propto \Phi(\bar{B}, \bar{J}, \bar{U}, \rho, \dots, t), \quad (1)$$

где $f^{(v)}$ - статистическая функция распределения микроэлементов

магнитоплазмы в фазовом пространстве (v) ; Φ - функция, устанавливающая взаимосвязь векторов поля (\vec{B}) , токов (\vec{J}) , макроскорости (\vec{U}) , плотности (ρ) и т.д. и времени (t) , которая обеспечивает самосохраняемость космической (солнечной) плазмы. Соотношение (1) определяет нерасходимость функции распределения и ее моментов, т.е. все законы сохранения при условии образования ряда дискретных структур. Характерной особенностью уравнения (1) является то, что при заданном потенциале взаимодействия для совокупности элементов любого масштаба образуется ряд дискретных структур (по Власову - "плазмOIDы"), при существовании которых возможна сама сохраняемость всей системы (в нашем случае замагниченная атмосфера Солнца).

Замечательным открытием в гелиофизике последнего десятилетия явилось обнаружение с помощью вакуумных солнечных телескопов элементарных тонкострунных филаментов-субгранул (sgf), которые в литературе называют "магнитными трубками потока", "филигри" и т.д. На уровне фотосферы они наблюдаются в виде резко очерченных дискретных точек сильного поля в сечении $\approx 0,2$ (т.е. всего несколько сот километров, что находится на пределе разрешающей возможности наземных телескопов). Напряженность поля в них $\approx 600 \div 1000$ G (в спокойных областях) и до $1,5 \div 3$ KG (в активных областях). Все известные нам явления солнечной активности (пятна, факелы, флоккулы, коронально-хромосферные петли и т.д.) состоят из совокупности ряда этих взаимодействующих элементарных магнитоплазменных волоконцев sgf. Активные области выделяются существенно большей локальной (в течение определенного периода) концентрацией (а следовательно - соответствующими структурными образованиями) элементарных субгранул (sgf). В спокойных областях субгранульные элементы сосредоточены в граничных узелках конвективных супергранул (аналог ячеек Бенара). А почти всю поверхность Солнца занимают крупномасштабные униполярные фоновые поля, слабое ($\approx 5 \div 10$ G) магнитное поле которых распределено равномерно бесструктурно. Активные области, как правило, возникают и развиваются на границе фоновых магнитных полей противоположной полярности. Фоновые магнитные поля также

как магнитные поля активных областей (АО) изменяются в течение 22-летнего цикла по закону Хэйла. Из изложенного следует, что вполне оправдана попытка синергитического рассмотрения эволюции наблюдаемых на Солнце дискретных структур магнитных полей, состоящих из ряда взаимодействующих самоорганизующихся элементов и, которые определяют практически все характерные свойства явлений солнечной активности {2}.

2. Как показывают наблюдения, элементарные субгранулы имеют ограниченное время существования на уровне фотосферы: от нескольких часов (для изолированных вне АО элементов) до десятка часов и нескольких дней - при вхождении *sgf* (т.е. при наличии их тесного взаимодействия) в состав пятен, факелов и т.д. (явления в АО). В то же время известно, что магнитные поля в АО существуют, по крайней мере, на порядок дольше. Это означает, что в АО происходит динамический процесс: диссипация или погружение "старых *sgf*" и всплытие "новых *sgf*", которые должны генерироваться в подфотосферных слоях (в конвективной зоне). Теория турбулентного динамо позволяет получить для крупномасштабных магнитных полей $B \approx 10^3 \text{G}$, тогда как в *sgf* наблюдаются поля $B \approx 10^3 \text{G}$. В настоящее время нет пока удовлетворительной гипотезы столь сильного усиления магнитного поля в субгранульных элементах {4}. Однако среди них наиболее перспективной является гипотеза усиления поля при автомоделных колебаниях в активной окружающей среде (плазме), пронизанной крупномасштабным (фоновым) полем.

3. Из уравнения структурности (1) вместе с уравнениями Максвелла для осесимметричного случая получается следующее выражение для функции распределения субгранульных элементов (*sgf*) в фоновом поле \vec{B} и конвективной скорости \vec{U} :

$$f(r, p) = A\rho(r, z - ut) \exp\left(-\frac{\epsilon}{k\theta_m} + aI\right), \quad (2)$$

где

$$I = r \sin\theta \left(U\phi + \frac{e}{mc} A\phi \right). \quad (3)$$

Здесь ρ - пространственная плотность субгранульных элементов (*sgf*) с координатами r, θ, z , общей энергией ϵ , макрочарядом e и с массой M ; $A\phi$ - компонента вектор-потенциала магнитного

поля, $k\theta_m$ - энергия случайных движений sgf ; A и a - постоянные нормировки. Особенностью функции (2) (в отличие от того, что имеет место в замагниченной лабораторной плазме) является то, что она *анизотропная*, т.е. стационарное фоновое магнитное поле (\bar{B}) и скорость конвекции (\bar{U}) определяют в выделенном направлении распределение и диффузию субгранульных элементов sgf . Если $\langle f \rangle$ - средняя напряженность магнитного поля sgf , то, проинтегрировав функцию распределения (2) по энергиям, можем перейти к совокупности дискретных магнитных элементов

$$\langle h \rangle = \int f d\epsilon \rightarrow \sum_{j=1}^n m_j \quad (4)$$

Поток этих элементов (с учетом вида функций) (2) и (3)):

$$\bar{F} = \sum_{j=1}^n D_j^L \nabla m_j - \sum_{j=1}^n \nabla m_j. \quad (5)$$

Здесь D^L - линейный коэффициент диффузии, который определен при дифференцировании в функции (2) члена плотности ρ . Нелинейный коэффициент диффузии D^{NL} можно получить дифференцируя функции (2) с учетом (3) по координатам (y у нас по z). Очевидно, что при этом появятся два слагаемых (из-за градиентов скорости $[\nabla \bar{U}]$), пропорциональных m , т.е.

$$D_j^{NL} \approx -C m_j (\alpha \nabla \bar{U} + \beta \nabla \bar{B}) \approx m_j S_j \quad (6)$$

где C , α , β , - соответствующие коэффициенты пропорциональности. Функция S_j определяет нелинейные потоки m_j - элементов при наличии градиентов скорости, поля и взаимодействия между n - элементами на малых расстояниях (r_d) по сравнению с характерными размерами (L) рассматриваемой структуры. Существенно подчеркнуть что анизотропность функции распределения элементов (2) определила *стимулированную* диффузию по градиентам скорости и поля и взаимодействием между субгранульными элементами.

Эволюцию системы sgf можно, следуя работе [5], представить нелинейным уравнением типа:

$$\frac{\partial m_i}{\partial t} + \text{div } \bar{F} = F_i(m_1, m_2, \dots, m_n, r, t), \quad (7)$$

где m_i - динамические переменные нашей системы магнитных

элементов; r - их координаты, t - время, а функция F_i - определяет мультипликативную нелинейность взаимодействия n - элементов. Подставив в (7) выражение (5), (6), получим нелинейное уравнение эволюции:

$$\frac{\partial m_i}{\partial t} = F_i(m_1, m_2, \dots, m_n, r, t) + \operatorname{div} \sum_{j=1}^n D_{ij}^L \nabla m_j - \operatorname{div} m_i \sum_{j=1}^n S_{ij} \nabla m_j. \quad (8)$$

4. Чтобы выяснить физический смысл нелинейной функции взаимодействия (F_i) в нашем конкретном случае (т.е. при образовании структур активных областей на Солнце), следует сделать следующие замечания.

а) Активная область (АО) на Солнце, занимающая относительно малую часть поверхности, можно рассматривать как ответвление "малого сечения" от общей конвективной зоны (сферический слой между ядром и фотосферой толщиной $> 0,2R_{\odot}$). В конвективной зоне (кроме, в принципе, многоярусной конвекции) генерируются и распространяются крупномасштабные колебания различных мод: волны Россби, стоячие волны колебаний Солнца как звезды, магнитозвуковые волны, которые генерируются турбулентностью. Тогда, согласно {6}, в узком канале связи АО с конвективной зоной будут распространяться простые волны, т.е. волны с произвольной амплитудой. Эти волновые процессы могут способствовать усилению магнитного поля и приводить к изгибным колебаниям субгранульных филаментов, определяя также их взаимодействие. Ниже будет также отмечено, что эти волновые процессы играют существенную роль в энергобалансе АО, особенно, когда речь идет об относительно быстрых явлениях таких как солнечные вспышки.

б) Рассмотрим характер парных взаимодействий m_1 и m_2 элементов. Их условно можно разбить на статическую и волновую части, т.е. магнитная энергия пары m_1 и m_2 будет состоять их двух частей:

$$W_{12} = E_{12}^{CT} + E_{12}^b = (E_1 + E_2 + E_{12})^{CT} + E_{12}^b. \quad (9)$$

Здесь E_{12}^{CT} :

$$E_1 \approx m_1^2; \quad E_2 \approx m_2^2; \quad E_{12} = \iint m_1(r) m_2(r) G_{12}(r, d) dt \quad (10)$$

где $G_{12}(rd) = G_{12}(|r_1 - r_2|)$ - функция Грина типа потенциала Дебая. Если элементы m_1 и m_2 колеблются с частотами ω_1 и ω_2 и фазами φ_1 и φ_2 так, что $\Omega = \omega_1 - \omega_2$; $\varphi = \varphi_1 - \varphi_2$, а электромагнитное трение с окружающей плазмой $\approx e^{-\gamma t}$, то тогда {2}:

$$E_{12}^b = \iint m_1(r) m_2(r) \frac{\cos\varphi - \left(\frac{\Omega}{\gamma}\right) \sin\varphi}{1 + \left(\frac{\Omega}{\gamma}\right)^2} dt. \quad (11)$$

Особенностью этого интерференционного члена является то, что в зависимости от значений параметров $\varphi \frac{\Omega}{\gamma}$, энергия волнового взаимодействия может быть $>$ или $<$ 0, что определит (в совокупности с другими членами [9]) притягивание или отталкивание взаимодействующих элементов. Это означает, что структуры могут и не образоваться при некоторых условиях колебаний взаимодействующих элементов. В этой схеме с волновым нелинейным взаимодействием образование структур требует, чтобы система была энергетически открытой, что обусловлено связью с энергоисточниками (в т.ч. колебаниями) в конвективной зоне. Это означает, что производство энтропии $(E) \frac{dE}{dt} < 0$, т.е. имеет место самоорганизация структур. Этот процесс, как, например, показано в {5}, носит пороговый характер и может быть описан по схеме фазовых переходов {5,7}.

В условиях Солнца, где из-за огромной непрозрачности вещества перенос энергии излучением является крайне медленным процессом. В образовании АО (и особенно магнитоплазменных структур, предопределяющих такие явления как солнечные вспышки), существенную роль (наряду с более медленным процессом - конвекцией) играют низкочастотные волновые МГД явления. Если в результате действия соответствующих сил, например, влияния сил Кориолиса, дифференциального вращения и т.д., образуется в процессе эволюции в подфотосферной зоне АО бессилловая магнитная структура (т.е. $[\bar{V} \text{rot} \bar{V}] = 0$ или $\text{rot} \bar{V} = k\bar{V}$). Отметим, что генерирующий эффект - спиральность [α -эффект] при турбулентном динамо, образует ток параллельно магнитному полю \bar{V} {3}, то при условии равномерного распределения энергий ($E_{\text{kin}} \approx E_{\text{mag}}$) должна иметь место соответствующая структура движений типа Громеко-Бельтрами, т.е. $\text{rot} \bar{U} = k\bar{U}$. В этом случае, как показано в нашей

работе {8}, возмущения (\bar{U}) описываются уравнением Картевега де-Вриза типа:

$$\frac{\partial U}{\partial t} + U \frac{\partial U}{\partial z} + \frac{1}{k^2} \frac{\partial^3 U}{\partial z^3} = - \left(\frac{\partial U}{\partial z} + \frac{U}{k^2} \frac{\partial^3 U}{\partial z^3} \right) \approx - \frac{\partial U}{\partial z} . \quad (12)$$

Правая часть характеризует слабое поглощение МГД возмущений. Уравнение (12), как известно, имеет солитонное решение

$$U = U_0 \operatorname{sech}^2 z \quad (13)$$

Это означает, что начальное подфотосферное волновое возмущение при распространении к фотосфере переходит в уединенное возмущение, при котором нелинейность уравновешивается слабой дисперсией в среде. Существует и более общее рассмотрение проблемы быстрого выноса поля и вещества в атмосферу Солнца МГД волнами (в т.ч. до и во время солнечных вспышек), которое выполнено Е.А. Руденчиком {9,10}. В одномерном (а затем в двумерном) приближении рассматривалась задача о распространении быстрой магнитозвуковой волны в стратифицированной атмосфере в горизонтальным (и арочным) магнитным полем. Полученное в общем случае решение этой нелинейной задачи показало, что в случае цугового характера начальных колебаний происходит эффективный вынос вещества и энергии достаточный, чтобы происходили солнечные вспышки.

Эти новые результаты находят свое подтверждение в некоторых наблюдениях ("магнитные транзиенты", цуговых характер колебаний в АО и т.д.). Принципиальная их важность состоит также и в том, что эффективный вынос энергии и вещества волновыми процессами позволяет обеспечить появление характерных дискретных магнитоплазменных структур в АО в том числе и тех (арочные хромосферно-корональные структуры и т.д.), которые наблюдаются во время вспышек. Таким образом, автоволновые процессы в активной среде играют важную роль в образовании и эволюции магнитоплазменных полей и движений в активных областях на Солнце.

Отметим также, что распад структур и самих активных областей указывает на прекращение поступления энергии в виде МГД волн. Это подтверждается измерениями Фурье спектров мощности

квазипериодических колебаний поля и скоростей на фазе распада АО.

Из приведенного весьма неполного анализа проблемы синергетического понимания эволюции магнитных полей на Солнце следует, что даже настоящее начальное рассмотрение может способствовать становлению обоснованной количественной модели эволюции активных областей на Солнце. Это весьма важно не только в плане фундаментальных, но также и для прикладных задач прогнозирования солнечных и солнечно-обусловленных геофизических явлений. Важно также, что такой подход позволяет установить характер тех солнечных наблюдений (исследование колебательного режима в АО, в оптике, радио и т.д.), которые должны с большей определенностью обосновать развиваемую точку зрения на природу эволюции АО на Солнце.

Л и т е р а т у р а

- {1} Власов, А.А., *Статистические функции распределения*, Наука, Москва, 1966
- {2} Могилевский, Э.И., Обоснование стохастичности краткосрочного прогноза солнечной активности, *Phys. Solariterr.* 16, 5, 1981
- {3} Вайнштейн, С.И., Зельдович, Я.Б., Рузмайкин, А.А., *Турбулентное динамо в астрофизике*, Наука, Москва, 1980
- {4} Паркер, Е., *Космические магнитные поля*, 1, МИР, Москва, 1982
- {5} Таланов, В.И., Стимулированная диффузия и кооперативные эффекты в распределенных кинетических системах, *Нелинейные волны. Самоорганизация*, с.47, Наука, Москва, 1983
- {6} Лайтхилл, Д., *Волны в жидкостях*, МИР, Москва, 1981
- {7} Хакен, Г., *Синергетика*, МИР, Москва, 1980
- {8} Могилевский, Э.И., Энергетика и феноменология больших солнечных вспышек, *Физ.солн.акт.*, 3, 1980
- {9} Руденчик, Е.А., Перенос вещества МГД волнами в звездных атмосферах, *Письма в АЖ*, 9, 504, 1983
- {10} Руденчик, Е.А., Распространение быстрых магнитозвуковых волн через арки магнитного поля на Солнце, *Физ.солн.акт.*, 19, 1983

NEW COMPUTATION RESULTS FOR THE SOLAR DYNAMO

I. K. C S A D A

Konkoly Observatory, Budapest

Abstract:

The analytical solution to the solar dynamo equation leads to a relatively simple algorithm for the computation in terms of kinematic models. The internal and external velocities taken to be in the form of axisymmetric meridional circulation and differential rotation, respectively. Pure radial expanding motions in the corona are also taken into consideration. Numerical results are presented in terms of the velocity parameters for the period of the field reversal, decay time, magnitudes and phases of the first four multipoles.

НЕКОТОРЫЕ ЧИСЛЕННЫЕ РЕЗУЛЬТАТЫ ДЛЯ СОЛНЕЧНОГО ДИНАМО

И. К. ЧАДА

Обсерватория Конколи, Будапешт

Абстракт:

Выражения, полученные при аналитическом решении уравнений, описывающих модель кинематического солнечного динамо, приводят к относительно простым алгоритмам для вычисления на ЭВМ. Внутренняя и внешняя скорости описываются в виде аксиально-симметричного меридианного потока и дифференциального вращения. Учитываются также и чисто радиально-экспансивные движения солнечной короны. Период и время затухания переворота, момент первых четырех мультиполей и фаза изменения магнитного поля выражаются численными данными в зависимости от параметров скорости.

The basic ideas of this report have already been presented in symposia and colloquia as well as being published in *Solar Physics* {1},{2},{3}. Now, some new results obtained in this field will be summarized with respect to solar research.

The physical conditions of the continuous existence of the magnetic field are formulated in terms of a solar dynamo. The present paper contains some new results in a simplified version, introduced as "kinematic dynamo" {4}. In this dynamo the velocity is supposed to be given and in the analysis it is considered to be able to generate a sizeable field from a small initial field.

A further, more generally known simplification of the dynamo is the "axisymmetric" model in the framework of the kinematic concept. Critical statements concerning the application of this model to the theory of the solar and stellar magnetism can be summarized by two objections.

The first objection points to the "negative feedback" which arises in this kind of model. The effect of this field induction results in an extremely short decay time of the initial field, i.e. for an unpublished model which has a reversal period of 22 years, the initial field decreases below a physically negligible level after two or three months. The analysis in terms of this model can overcome this breakdown. To have solutions with field reversal but without decay, the characteristic tensor in the dynamo solutions must be transformed to have skew symmetry. The answer to the objection is that the elimination of the negative feedback (i.e. of the induction generated dissipation) is an analytical problem and requires the transformation of the characteristic tensor.

The second objection points out that no "positive" induction effect exists in the axisymmetric dynamo to compensate for the Ohmic loss. In the solar case the Ohmic dissipation is small, being equivalent to a decay time of 10^9 years. The compensation for the Ohmic loss is expected from a small modification of the characteristic tensor in the general, non-symmetric dynamo. It can be shown that any test of application

of the axisymmetric concept can give useful physical information on the mechanism of large scale variations in first approximation.

The transformation of the characteristic tensor to a skew symmetric form achieved in the internal field by force-free vectorial forms of the eigen-functions. A simple term in the series of the magnetic field can be written as

$$\vec{H}_n = \vec{A}_n + \frac{1}{k_n} \nabla \times \vec{A}_n ,$$

where the solenoidal vector A is defined (in the internal field) by

$$\Delta \vec{A}_n^{in} + k_n^2 \vec{A}_n^{in} = 0 .$$

In the transformation scheme for the external field the solenoidal vector - in the absence of coronal expansion - is governed by

$$\Delta \vec{A}_n^{ex} = 0 .$$

To eliminate the dissipation effect due to the Ohmic loss we start in the framework of the non-symmetric dynamo with the identical transformation

$$\nabla \times \vec{H}_n = k_n \vec{H}_n - k_n (\vec{A}_n^{ex} + \frac{1}{k_n} \Delta \vec{A}_n^{ex}) ,$$

i.e. we express \vec{H}_n as a force-free vector with an additional term symbolizing the deviation of \vec{H}_n from the force-free structure. In the external field $\Delta \vec{A}_n^{ex} = 0$ and thus, the deviation vector reduces in the present case $-k_n \vec{A}_n^{ex}$.

Substituting now \vec{H}_i and $\nabla \times \vec{H}_j$ for the characteristic tensor, we have

$$\frac{1}{k_j} \int \vec{w} \left(\vec{H}_i \times (\nabla \times \vec{H}_j) \right) dv = \int \vec{w} (\vec{H}_i \times \vec{H}_j) dv - \int \vec{w} (\vec{H}_j \times \vec{A}_j) dv .$$

The first term on the right side forms a skew tensor which permits the reversal periods of the dynamo and the zonal coefficients of the eigen-functions to be computed. The second term stands for the deviation of the characteristic tensor from the skew symmetry. The inductive effect due to this term should be able to compensate for the Ohmic dissipation if the tensorial relation

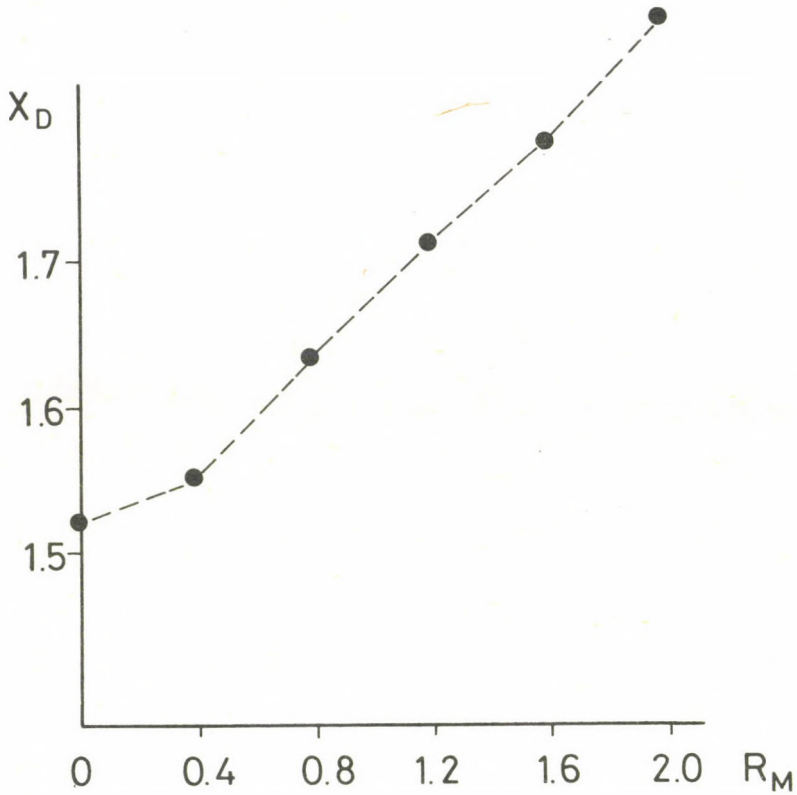


Fig. 1. The radius of the spherical boundary of the internal and external fields of the solar dynamo (dynamo radius) is larger than the optical radius. The vertical scale shows the distance from the solar center ($r_{\odot} = 1$). The Reynolds numbers on the horizontal scale are defined as the ratio of the expansion velocity and the resistivity. The diagram shows that the dynamo radius increases with the Reynolds numbers.

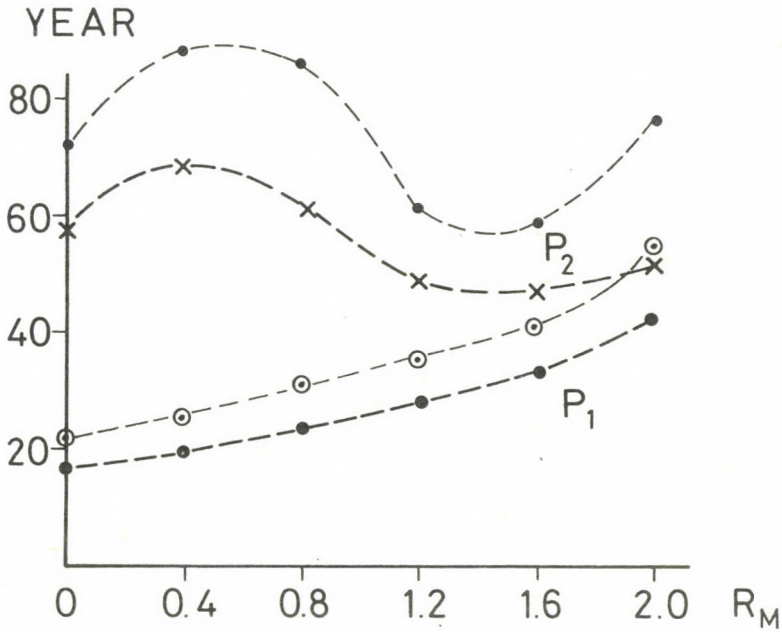


Fig.2. The variation of the shorter and the longer periods of the dynamo in terms of Reynolds numbers. The shorter period is tested by two fit values as 16 and 22 years at $R_M = 0$ and computer results are 58 and 75 years, respectively for the longer period.

$$\int w(\vec{H}_i \times \vec{A}_j) dv + \kappa \delta_{ij} k_i = 0$$

is fulfilled. This relation is equivalent to a quadratic system for the tesseral and sectorial harmonics of the eigen-functions and its solution presents the basic problem of the non-symmetric dynamo.

Computations are relatively simple for the dipole and the quadrupole. Some results and their interpretation from the point of view of solar research have been reported {1} and the thus predicted field variation is similar to the observed behaviour.

Computation by use of the axisymmetric model and the interpretation of the new results shows that in the absence of the effect of the solar wind there are two reversal periods 22 years and 75 years. In the case of increasing expansion velocity the two periods tend to approach the same value which tends to be about 55 years for both.

The 22 year period was obtained by a fit of the numerical parameters of the dynamo mechanism. There are the velocity of the internal large scale meridional current and the shearing of the differential rotation. In this paper the radius of the dynamo is applied as a new parameter and it is obtained as larger than the optical radius. The optical radius defines the surface where the law of differential rotation agrees with that observed.

Computation results are shown in Figs.1 and 2.

R e f e r e n c e s

- {1} Csada, I.K., Solar magnetic field, *Plains feux sur la physique solaire, (II.assemblée européenne de la physique solaire)* 69. Toulouse, 1978 and On the non-symmetric solar dynamo, *Solar Phys.* 74. 103, 1981
- {2} Csada, I.K., Large-scale magnetic dipole and multipole progressive waves in the photosphere, *Solar Phys.* 47. 555, 1976
- {3} Csada, I.K., Evidence for the phi-dependent rotation-oscillation of the Sun (and for the driving mechanism of the asymmetric dynamo), *Solar Phys.* 82. 439, 1983
- {4} Cowling, T.G., The present status of the dynamo theory, *Ann.Rev.Astron.Astrophys.* 19. 113, 1981

Publ. Debrecen Obs. Vol. 5

No. 5.

PAPERS ON VARIOUS OBSERVATIONAL METHODS AND RESULTS



STABILITY OF THE PHOTOMETRIC OUT-OF-ECLIPSE OBSERVATIONS
OF THE SOLAR CORONA AND VARIATIONS OF ITS INTENSITY
IN THE 21st SOLAR CYCLE

M.N. GNEVYSHCHEV, V.P. MIKHAYLUTSA

Kislovodsk Station, Pulkovo Obs., Kislovodsk

Abstract:

A comparison of the results of measurements of the intensity of the coronal line 5303 Å at the observatories at Norikura, Kislovodsk and Lomnický štít is used to determine the stability of photometric systems and cancel the effect of its variations. The graphs of the variation in the intensity of the solar corona during the 21st solar cycle are given. It is confirmed that the 11-year solar cycle consists of two maxima of activity: the first one is characterized by a simultaneous enhancement of activity in all latitudes and the second one shows up only in the equatorial zone.

СТАБИЛЬНОСТЬ ФОТОМЕТРИЧЕСКОЙ СИСТЕМЫ ВНЕЗАТМЕННЫХ НАБЛЮДЕНИЙ
СОЛНЕЧНОЙ КОРОНЫ И ВАРИАЦИИ ЕЕ ИНТЕНСИВНОСТИ В 21-м ЦИКЛЕ

М.Н. ГНЕВЫШЕВ, В.П. МИХАЙЛУЦА

ГАО ГАС, Кисловодск

Абстракт:

Путем сравнения результатов измерений интенсивности корональной линии 5303 Å на обсерваториях Норикюра, Кисловодск и Ломницкий штит определена стабильность фотометрических систем и исключено влияние ее изменений. Построены вариации интенсивности солнечной короны в течение 21-го цикла. Подтверждено, что 11-летний цикл состоит из двух максимумов активности: первого, характеризующегося одновременным усилением активности на всех широтах и второго, проявляющегося только в экваториальной зоне.

1. Introduction

The solar corona has been photographed during every total solar eclipse since 1860. However, for the 120 years the total time of the observations does not exceed one hour.

Essential progress in the physics of the solar corona began in 1930 when B.Lyot first took photographs of the solar corona at times other than at solar eclipses.

Regular observations of the solar corona in the 5302.8 Å and 6374.5 Å lines were published in the *Quarterly Bulletin on Solar Activity* by the following observatories: Pic du Midi (1947-1974), Arosa (1947-1978), Climax (1947-1966), Pic Sacramento (1953-1966), Kanzelhöhe (1948-1961). So far the observations have been carried out at Wendelstein since 1947, Mt.Norikura since 1951, Kislovodsk since 1957, Lomnický Štit since 1966.

The intensities have been given in the units of energy in the range of the spectrum within 1 Å near the measured line in the solar disc center. The measurements have been performed at a distance of about 40' from the limb in steps of 5°.

These data are used for investigations of short periodic and cyclic variations in the corona, the coronal structure and the relationships of coronal features with other solar and geophysical phenomena.

For these problems it is very important that the system of measurement of the coronal strength be stable, i.e. it should be known to what extent the observed measurement characterizes the real solar phenomena, they should be independent of instrumental and personal errors.

2.A comparison of observations

This problem can be solved through a comparison of the data of various observatories. The first comparisons were described by M.N.Gnevyshev {1},{2},{3}. Later on, such work was done by V.Letfus and J.Sýkora {4}.

Since the days when the corona can be observed are far from being numerous, it is practically impossible to have a sufficient number of common observational days, i.e. simultaneous observations at various observatories. The data of ob-

servatories may differ not only due to different photometric system, but also because the time of observation may be different, the heights of the photosphere where the measurements are made may also differ, moreover, there can be small errors in positional angles. As a result, at different observatories the observations may be made at different places of the corona with different intensities, for instance, near a coronal ray or arc.

That is why it is advisable to determine systematic differences in photometric systems not by a comparison of measurements made on common days, but by comparison of half-year averaged intensities from the data of different observatories.

For half a year at each observatory sufficient data are collected to characterize the mean intensity of the corona for that particular period. The above mentioned accidental errors are excluded by averaging, thus, only systematic differences will be present. It is important to find to what extent these differences are constant, i.e. the stability of the photometric systems.

A method like this for the comparison of the data at different observatories was proposed by M.N.Gnevyshev and adopted at the conference of the observers of the solar corona, which took place at the Pic du Midi observatory in 1967, by the majority of the observatories of the world.

A comparison of semi annual coronal intensities for each positional angle between two observatories in any combination shows a definite linear relationships between them.

It is evident that in the case of the absence of the systematic difference between the data of two stations, the regression line should pass the frame origin at the angle of 45° . Actually it happens in few cases and as a rule the line passes the frame origine at a distance a and is inclined by the angle whose tangent $b \neq 1$.

These values a and b are parameters in regression equation between the data of two observatories. a characterizes the difference in zero points of photometric systems due to

the difficulty to take the scattered light into account, and b characterizes different methods of reduction of the intensities to the absolute system. These two parameters are independent of each other and their variation with time reflects the stability of the systems.

Table 1 gives parameters a and b of regression equations for intensities of the 5302.8 Å line determined by least square method on the basis of the data of the following observatories: Norikura, Kislovodsk and Lomnický Štit for each half of the year beginning with 1973 to 1982. The r correlation coefficient is also given for the observatories compared. This coefficient is also shown in Fig.1. Solid curves refer to the 5302.8 Å line and the dashed line to the 6374.5 Å line.

It is seen from Fig.1 that the correlation coefficients are rather high in all the years except for the period of the minimum (1975-1976). This confirms the linearity and close relationship between any two observatories. During the years of the minimum, the relationship becomes less close, probably due to the fact that the measured values become as small as their errors.

Table 1 shows that the parameters a and b vary with time. Since each of them depends on the data of the two observatories to be compared it can be found at what observatory the error took place only by including the data of another observatory on the assumption that identical errors at two observatories are hardly possible.

Assuming this Kislovodsk expressions can be written using the parameters a and b from Table 1:

$$N = a_1 + b_1 K \quad \text{and} \quad L = a_2 + b_2 K$$

where N is the intensity of the corona in the system of Norikura and K of Kislovodsk, L of Lomnický Štit.

Believing that half sums of N and L are closer to true values than either of them separately we shall have:

$$\frac{N+L}{2} = a_K + b_K K \quad \text{where} \quad a_K = \frac{a_1 + a_2}{2} \quad \text{and} \quad b_K = \frac{b_1 + b_2}{2}$$

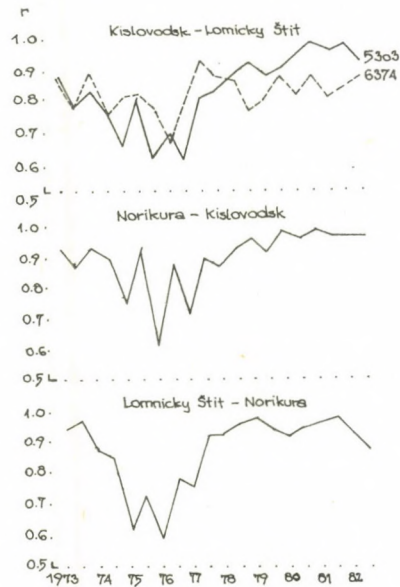


Fig. 1. Variations of the correction coefficients between the results of the intensity measurements of the coronal lines at Norikura, Kislovodsk and Lomnický Štít.

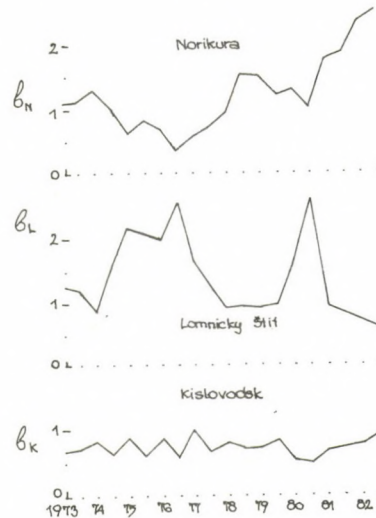


Fig. 2. Variations of the b parameter characterizing the stability of the scale of the coronal intensities.

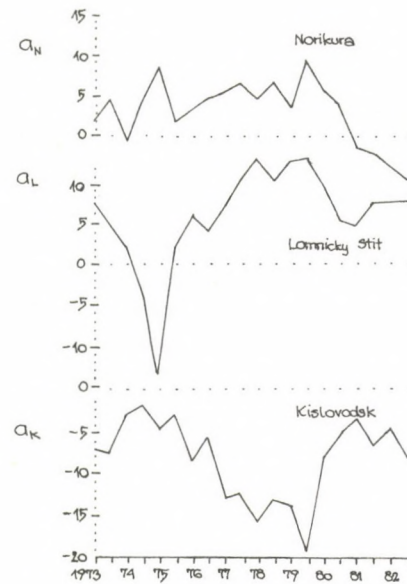


Fig. 3. Variations of the a parameter characterizing the quality of correction for the scattered light.

are parameters for reducing the Kislovodsk data to "true" values of the coronal intensities.

Similarly, we can find values of a_N and b_N for Norikura and a_L , b_L for Lomnický Štit for each half year.

Fig.2 shows the variation in the parameter b and Fig.3 parameter a for each of the observatories.

It can be seen (Fig.2) that the parameter b is most stable for Kislovodsk, i.e. all calibration parameters of coronal intensities are constant. It can be seen (Fig.3) that parameter a is most stable for Norikura. This parameter characterises the quality of estimation of the effect of the scattered light, in particular, 5302.8 Å line blending the 5302.8 Å coronal line. The stability of the b parameter is particularly important, because it is the multiplier in our formula, while a affects the intensity only additionally.

3. The variation of the coronal line 5302.8 Å intensity during the 21st cycle

Using the above method for determining parameters a_K , b_K , a_N , b_N and a_L , b_L (Figs.2,3) the "personal" intensities (determined at each observatory) can be reduced to "true" ones, i.e. free from the systematic errors and most valuable. For this reduction the data of any observatory should be multiplied by b and a should be added to the result.

Fig.4 gives the corrected intensities of 5302.8 Å line during the 21st cycle.

4. Conclusions

Using the data of at least three observatories it is possible to eliminate the systematic errors of observations and to get the most reliable results. Unfortunately there are only three observatories performing regular coronal observations.

From Fig.4 we conclude:

1) The presence of two maxima {1},{2},{3},{5} is confirmed on the data of the 21st solar cycle. The beginning of the growth of the coronal intensities during the first maximum begins at 25-30°, afterwards expanding simultaneously to the poles and

equator.

After the decay of the first maximum the other maximum begins, but at low latitudes only.

2) In the 21st solar cycle as in both the 19th and 20th, the first maximum in the circumpolar region is detected more definitely in the amplitude and location in the northern hemisphere than in the southern hemisphere. The difference between both hemispheres also lies in the fact that traces of the second maximum are seen in the southern polar latitudes that are absent in the northern latitudes.

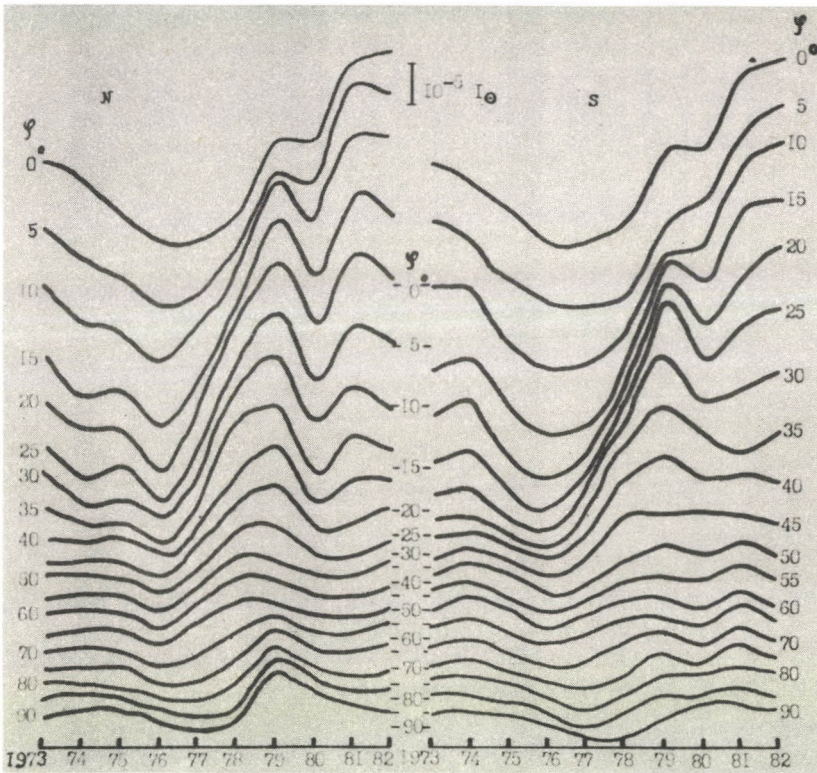


Fig. 4. Variations of the intensity of the coronal line 5303 Å during the 21st solar cycle after excluding the effect of the instability of photometric systems N - Northern hemisphere, S - Southern hemisphere, φ - heliographic latitudes; the vertical line above shows the scale of the intensity.

T A B L E 1

The parameters a and b and r -correlation coefficient in regression equations of the half-year averages of the coronal line 5302.8 Å intensities for the observatories: N - Norikura, K - Kislovodsk, L - Lomnický Stit.

Year	L = a + bN			K = a + bN			K = a + bL		
	a	b	r	a	b	r	a	b	r
1973	-3	0.87	0.94	7	1.39	0.92	13	1.51	0.88
	0	0.91	0.97	9	1.35	0.85	11	1.36	0.78
1974	-1	1.27	0.87	0	1.48	0.92	4	0.95	0.83
	5	0.66	0.84	4	1.52	0.89	1	1.66	0.77
1975	9	0.34	0.61	9	0.91	0.75	-1	1.45	0.64
	1	0.45	0.72	3	1.36	0.93	7	1.96	0.82
1976	0	0.35	0.59	7	1.15	0.61	12	1.10	0.62
	1	0.35	0.77	9	1.32	0.87	11	2.36	0.70
1977	0	0.45	0.75	11	0.80	0.71	14	1.17	0.61
	-2	0.93	0.91	15	1.58	0.89	20	1.39	0.81
1978	-5	1.34	0.92	14	1.58	0.86	23	1.04	0.83
	-2	1.38	0.95	14	1.71	0.92	20	1.11	0.88
1979	-6	1.39	0.97	13	1.65	0.95	22	1.11	0.92
	-1	1.10	0.93	21	1.29	0.90	26	1.08	0.87
1980	0	0.80	0.91	12	1.82	0.97	19	1.90	0.89
	0	0.50	0.94	8	1.47	0.95	10	2.74	0.94
1981	-3	1.59	0.95	0	1.97	0.97	7	1.17	0.97
	-2	1.79	0.97	7	1.92	0.95	11	1.03	0.95
1982	-12	2.77	0.94	-2	2.44	0.95	9	0.88	0.96
	-10	2.64	0.86	-2	2.28	0.95	12	0.72	0.91

R e f e r e n c e s

- {1} Gnevyshev, M.N., The corona and the 11-year cycle of solar activity, (in Russ.) *Astron. Zh.* 40, 401, 1963
- {2} Gnevyshev, M.N., On the 11-year cycle of solar activity, (in Russ.) *Soviet Phys. Uspekhi*, 90, 291, 1966
- {3} Gnevyshev, M.N., On the 11-years cycle of solar activity, *Solar Phys.* 1, 108, 1967
- {4} Letfus, V., Šykora, J., *Atlas of the green corona synoptic charts for the Period 1947-1976*. Bratislava 9, 1982
- {5} Gnevyshev, M.N., Essential features of the 11-year solar cycle, *Solar Phys.* 51, 175, 1977

PERIODIC VARIATIONS OF 530.3 nm CORONAL LINE

M. M I N A R O V J E C H, V. R U Š I N, M. R Y B A N S K Ý

Astron.Inst., Tatranska Lomnica

Abstract:

Periodic Doppler shift fluctuations were observed in 530.3 nm coronal line between two active regions on October 31, 1982. The oscillations have a period of 6.3 ± 0.5 min. A technique for the study of this fluctuation is also described.

ПЕРИОДИЧЕСКИЕ ИЗМЕНЕНИЯ КОРОНАЛЬНОЙ ЛИНИИ λ 530.3 нм

М. МИНАРОВЕХ, В. РУШИН, М. РЫБАНСКИЙ

Астрон.Инст., Татранска Ломница

Абстракт:

Флуктуации доплеровских скоростей наблюдались в спектральной корональной линии 530.3 нм между двумя активными областями 31-го октября 1982 г. Период пульсаций 6.3 ± 0.5 минут. Приводится методика наблюдения этих пульсаций.

Introduction

The problem of coronal heating, mass and energy transport from the underlying layers into the solar corona has not yet received a satisfactory answer (for example see {4}), and we return to it here. The study of fluctuations of different types of emission, mainly the short duration waves, could help in a better understanding of this problem.

Attempts to detect this fluctuations have been carried out for more than 20 years, but results are not uniform. In white light no short waves were detected during the total solar eclipse on June 30, 1973 {3}. As reported by Vernazza et al. {5} no short waves were detected over the disk at the transition level in *XUV*-region. From this time on all work uses spectral observations of the 530.3 nm coronal line, which were obtained with the 40 cm coronagraph at Sacramento Peak Observatory. A technique for the analysis of this spectral line was developed by Tsubaki {1}. Later he studied three parameters of the green line: the total intensity, the half width and the wavelength(λ) {6}. No periodic oscillations were detected at the first and second parameter at a standard deviation of 3.5%. The variation of Doppler shift showed a period of 300 s with an amplitude $\pm 1 \text{ km s}^{-1}$ in several places. Egan and Schneeberger {2} have found that the half width and the central intensity of the 530.3 nm central line have the period of 6.1 min., the amplitude of $2.0 \pm 1.4\%$, and are 180° out of phase with the width oscillations. No detections in the Doppler shift (velocity) were found.

Koutchmy et al. {7} detected the Doppler velocity oscillations with periods of 43 s, 80 s and 300 s with an amplitude of $\pm 2 \text{ km s}^{-1}$ for the 530.3 coronal line.

Recently Athay and White {8} confirmed the existence of 5 min type oscillations in the mid-chromosphere.

The present work deals with an attempt to detect oscillations in the wavelength of 530.3 nm coronal line. The spectra were taken with an 20 cm coronagraph at Lomnický štít Observatory. In order to undertake such an attempt, we had to im-

prove the coronagraph and equipment for the measurement of wavelength of spectral lines.

This adjustments were as follows:

- a) A photoelectric guide. It works with an accuracy greater than 0.8 arcsec in α and δ , respectively.
- b) The modification of spectrograph. A new grating permits observations with a dispersion of 0.58 nm/mm at 530.3 nm, and the instrumental resolution 0.01 nm.
- c) An automatic crystal-controlled time switch; it opens or closes the shutter at one or more predetermined times.

Observations and method of analysis

A sequence of 530.3 nm coronal emission line was obtained between two sunspot groups - Mt. Wilson 23412 (N22) and 23416 (N10) - at P;A; 76° on October 31, 1982. The sequence of 88 spectra was observed at 20 s time intervals. Exposure time was 6 s per one frame. The first one was taken at 09:59:21 UT. All observations lasted 29 min; The slit in the spectrograph was given radially to the solar limb during the sequence.

Establishment of wavelength was carried out with the Abbe comparator, where a TV camera was used instead of a microscope. Apart from this, supplementary electronic equipment was added. So we can see the direct and mirror shape of the intensity course of the spectral lines on the TV screen. An exact destination of the searched line can be obtained by the identification of the direct and mirror ones. The accuracy of measurement in this manner is of 0.003 nm. As wavelength standards we employed photospheric absorption of λ 528.1798 nm and λ 532.4191 nm Fe I lines of background. These lines are "clean" and they are not blended by any absorption line. The average value of background sky brightness was 85 millionths of the disk center brightness and changes ± 5 percent during the sequence. Measurements were made 40 arcsec above the photosphere.

Emission of 530.3 nm coronal line is blended by the 530.2314 nm absorption line. Superposition of these two lines causes a peak of emission line to shift to the longer wavelengths. This shift grows when the intensity of the background

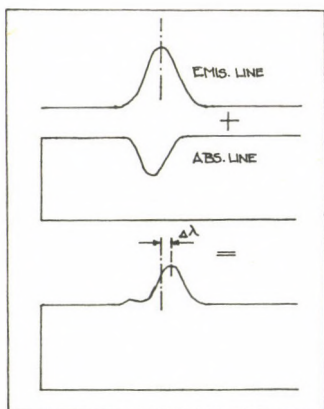


Fig. 1. A superposition of absorption and emission coronal lines in the spectrum. Other see in text.

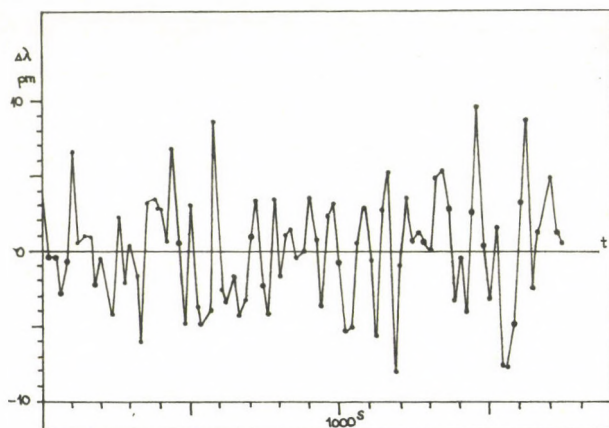


Fig. 2. Observed course of Doppler shift of the wavelength of 530.3 coronal line.

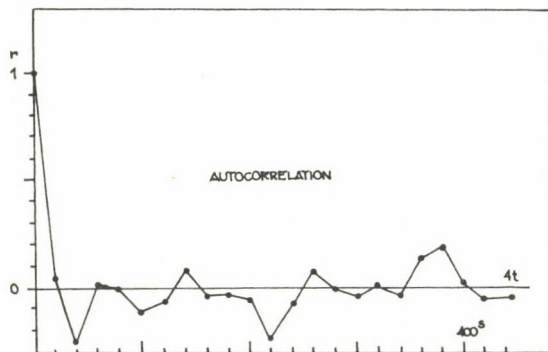


Fig. 3. An autocorrelation function of the time sequence of wavelength of 530.3 coronal line.

is greater and the intensity of emission line lower (see Fig.1).

For elimination of this influence we used the following method: the slit in the spectrograph was set to 0.03 nm, in this case both the emission and coronal lines can be expressed by a gaussian profiles and, thus, the course of spectra in the surroundings of the emission line may be expressed by the following equation:

$$i = i_o \exp\left[-\ln 2 \left(\frac{\lambda - \lambda_o}{\delta_o}\right)^2\right] + i_a \{1 - k \exp\left[-\ln 2 \left(\frac{\lambda - \lambda_1}{\delta_1}\right)^2\right]\} \quad (1),$$

where i_o = central intensity, i_a = intensity of background,
 k = relative depth of the absorption line,

λ_i = wavelength of lines, δ_i = half halfwidths of the lines

After differentiation of the equation (1) we determined numerically λ , where the course of intensity reaches a maximum (a peak of the emission line) for each frame, and, values were reduced to the average intensity of background. In our case we have $i_a = 85 \cdot 10^{-6}$, $\Delta\lambda \approx 0.0017$ nm, and the maximum reduction is 0.0006 nm.

Results and conclusion

Results obtained in this manner are given in Fig.2. The average value of the wavelength of coronal emission line is 530.2820 nm. The dispersion of values is 3.7 nm, which corresponds to radial velocity ± 2.1 km s⁻¹, and, it is in good agreement with the results of Tsubaki {6} and Koutchmy {7}. An autocorrelation function of time sequence values of the wavelength is given in Fig.3. It can be seen that if the changes are periodic, then the period is of 380 s, i.e. 6.3 min. This result is in good agreement with the period which Egan and Schneeberger {2} have established for a half width at half maximum (HWHM) intensity and for a central intensity.

We are of the opinion that periods which we can obtain from this type of observations will be various for different places in the solar corona and will be dependent on the shape of the active region, the size and orientation of coronal loops, and the intensity and orientation of magnetic field and others. Apart from this, we can observe anywhere in the spectrum

single coronal features. There are several projected generally, all in the line of sight. For this reason it will be necessary to do the observations in a single active region during a time of minimum activity of the Sun.

R e f e r e n c e s

- {1} Tsubaki, T., Line profile analysis of a coronal formation observed near a quiescent prominence: intensities, temperatures and velocity fields, *Solar Phys.* 43. 147, 1975
- {2} Egan, T.F., Schneeberger, T.J., Observations of coronal oscillations above an active region, *Solar Phys.* 64. 223, 1979
- {3} Koutchmy, S. L'étude de la couronne blanche à bord de Concorde 001 au cours de l'éclipse totale de soleil du 30 Juin 1973, *l'Astronomie*, 89. 149, 1975
- {4} Kuperus, M., Ionson, J.A., Spicer, D.S., On the theory of coronal heating mechanisms, *Ann. Rev. Astron. Astrophys.* 19. 7, 1981
- {5} Vernazza, J.E., Foukal, P.V., Huber, M.C.E., Noyes, E.W., Reeves, E.M., Schmall, E.J., Timothy, J.G., Withbroe, G.L., Time variations in extreme-ultraviolet emission lines and the problem of coronal heating, *Ap. J.* 199. L123, 1975
- {6} Tsubaki, T., Periodic oscillation found in coronal velocity fields, *Solar Phys.* 51. 121, 1977
- {7} Koutchmy, S., Zhugzhda, Yu.D., Locans, V., Short period coronal oscillations: observations and interpretation, *Astron. Astrophys.* in press
- {8} Athay, R.G., White, O.R., Chromospheric oscillations observed with OSC-8. I. Basic measurements and analytical methods, *Ap. J. Suppl.* 39. 317, 1979

ASCENT MOTIONS IN THE MONOCHROMATIC CORONA
DURING TOTAL SOLAR ECLIPSE OF JULY 31, 1981

A. B. D E L O N E, E. A. M A K A R O V A

Shternberg Astron. Inst., Moscow

J. S Ý K O R A

Astron. Inst., Tatranská Lomnicá

Abstract:

Using pictures of the monochromatic corona taken in FeXIV 5303 Å and FeX 6374 Å, spectral lines at two points of the path of totality, differing by one hour in time of observation, we were able to detect motions of some structural details.

ПОДНИМАЮЩИЕСЯ ДВИЖЕНИЯ В МОНОХРОМАТИЧЕСКОЙ КОРОНЕ
ВО ВРЕМЯ ПОЛНОГО СОЛНЕЧНОГО ЗАТМЕНИЯ 31 ИЮЛЯ 1981 Г.

А. Б. ДЕЛОНЕ, Е. А. МАКАРОВА

ГАИШ, Москва

Й. СИКОРА

Астрон. Инст., Татранска Ломница

Абстракт:

При использовании снимков монохроматической короны полученных в свете спектральных линий FeXIV Å и FeX 6374 Å в двух пунктах полосы затмения, разделенных одним часом по времени, нам удалось определить движения некоторых структур короны.

Similar to the eclipse of 1936, the solar eclipse path of totality crossed almost all the Soviet Union from the west to the east on July 31, 1981, and gave an outstanding opportunity to determine motions in the solar corona as projected into the image plane.

During the eclipse both the green line corona FeXIV 5303Å and the red line corona FeX 6374Å were observed from two points on the path of totality, differing by one hour in time. The expedition of the Astronomical Institute of the Slovak Academy of Sciences, Czechoslovakia, performed its observation near the town of Bratsk, Siberia, while the expedition of the Sternberg State Astronomical Institute, USSR, observed from Mariinskoe on the lower part of the Amur river. In Bratsk the monochromatic pictures of the corona were taken by two identical $F = 1950$ mm, $D = 120$ mm telescopes, equipped with interference filters of 2Å bandwidth for the green line and 3Å for the red line. In Mariinskoe, about one hour later, simultaneous pictures in the green and red lines were taken by a double telescope ($F = 1500$ mm) equipped with Fabry-Perot etalons (and also without them) and with interference filters of 15Å and 30Å passbands, respectively.

During the solar eclipse on July 31, 1981 the corona was most active at the west limb, where on the white light pictures (courtesy: V.I. Charugin, I.F. Nikulin and P.V. Scheglov) three coronal formations were identified as follows: $A: N20^\circ$, $B: N1^\circ$, $C: S25^\circ$ (Fig.1a). The details of these structures differ remarkably from pictures taken in white light and in green and red coronal lines. The structures are more distinctly seen in the monochromatic pictures - some are visible only in the green line, some others only in the red line. For example, a more dense region in C formation is seen at a height of about $0.2 R_\odot$ in the green line picture. At the same time, the red line radiation is practically absent in formations A and B , exist in C and is most intensive between formations B and C (for this see Fig.3 in {1}). Many structural details of the monochromatic images disappear in white light.

The green and red line pictures of the corona, obtained near Bratsk by one of the authors (J.S.), with narrow band filters are a good contrast and give a nice image of structure of the corona in those lines. Details of interest are schematically drawn in Figs.1b and 1c. As an example of identification of the details, we present Fig.2 here, which shows the green line image obtained in Bratsk, then processed by the digitalization technique with application of the procedure of increasing the local contrast. The numbering in Fig.2 is the same as in Fig.1b.

Using observations at two points, the motions in the image plane were determined by measurements of the position of some distinct details, relative to the center of the Sun. In the green line images we have chosen loop 1 and the small condensation 4 in formation C (Figs.1b and 2). In the red line images the most outstanding seemed to be curve-like features 5 and 6. The position of these details, according to filtergrams obtained in Mariinskoe, is drawn by dashed lines.

In green corona the loop 1 and the small condensation 2 on this loop moved with a velocity of about 10 km s^{-1} . The curve-like feature 3 and the small condensation 4 moved in WS direction with approximately the same velocity and they successively rose up. When determining velocity uniform motion has continuously assumed. According to the analysis of Kleczek and Topolová {2}, velocities in the order of 10 km s^{-1} are quite usual for the green corona structures or rather such velocities are not necessarily related to some eruptive processes in the corona.

Somewhat higher velocities - of about 25 km s^{-1} - have been found for the curve-like features 5 and 6 of the red line corona (Fig.1c) and, furthermore, the ascent velocity was not the same for different parts of these features. Namely, the south-west ends moved with a velocity of 11 km s^{-1} , and feature 5 successively caught feature 6. At the same time the basement of features 5 and 6 moved with higher velocity (up to 25 km s^{-1}) and it is probable that a loop at latitudes

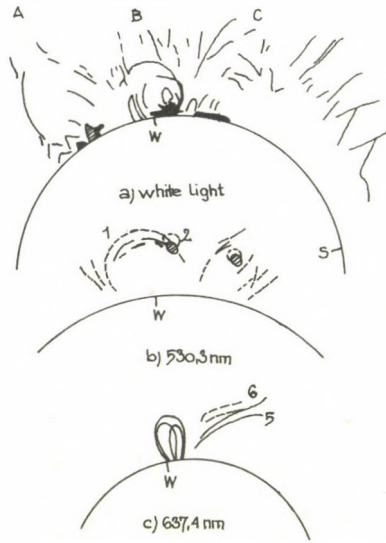


Fig. 1. Schematic drawings of the parts of a) white light corona, b) green line 5303 Å corona and c) red line 6374 Å corona, as recorded during total solar eclipse on July 31, 1981. For details see text.



Fig. 2. Green line 5303 Å image processed by digitalization technique to increase contrast of the local structural details. The same numbering as in Fig. 1b is adopted.

S11° - S25° was successively created. It is possible that this was just that loop which was somewhat later observed by a coronagraph aboard satellite P 78-1 as a transient, originating at latitude S17° {3}. If a relatively low velocity of the transient - about 50 km s^{-1} - is extrapolated backwards, then we found possible identity with a "red" loop which we observed in Mariinskoe at 0400 UT. At that time the base of the loop was at a height of $1.23 R_{\odot}$ and at a latitude of S11°. Taking the velocity of 25 km s^{-1} found by us further into account, we came to the moment of origin of the transient on the Sun's surface at 18-19 UT July 30, 1981. At that time, at the mentioned latitude, the Hale region No 17751 just set behind the west limb. Being on the solar disk this region was a source of a number of flares, though they were not of great importance. It is probable that activity of the AR also continued behind the limb. The following scheme can be imagined: the flare or an eruptive filament initiated the rising of a relatively cool plasma. This process could probably be observed in H α if located on visible Sun's disk. Ascent of a hotter plasma was observed in a 6374Å line during the solar eclipse and after that in white light at heights of more than $2.5 R_{\odot}$. It would be, of course, interesting to investigate using the data of satellites SMM and P 78-1 whether there was some other similar chronology of the events.

R e f e r e n c e s

- {1} Sýkora, J., Coronal hole as a probable source of the highest geoactivity in 1981, *this issue* 1983
- {2} Kleczek, J., Růžicková-Topolová, B., Short duration changes in green corona structures, *BAC*, 35, No.1. (in press) 1984
- {3} Fisher, R.R., Lacey, L.B., Rock, K.A., Yasukawa, E.A., Sheeley, N.R., Michels, D.J., Howard, R.A., Koomen, M.J., Bagrov, A., The solar corona on 31 July, 1981, *Solar Phys.* 83. 233. 1983

CORONAL HOLE AS A PROBABLE SOURCE OF THE HIGHEST GEOACTIVITY
IN 1981

J. S Ý K O R A

Astron.Inst., Tatranská Lomnicá

Abstract:

The last decade of July 1981 was characterized by exceedingly high geoactivity. From observations on the Sun's disk no classical source of this geoactivity, i.e. no large solar flare or some eruption of filament, was recorded. The author concludes that on the basis of the monochromatic corona observations carried out during the total solar eclipse of July 31, 1981 it is probable that a low-latitude coronal hole could act as the source of the mentioned outstanding geoactivity.

КОРОНАЛЬНАЯ ДЫРА, КАК ВОЗМОЖНЫЙ ИСТОЧНИК НАИБОЛЬШОЙ
ГЕОЭФФЕКТИВНОСТИ. В 1981 Г.

Й. СИКОРА

Астрон.Инст., Татранста Ломница

Абстракт:

Последняя декада июля 1981 года была характерна исключительно высокой геоактивностью. Из наблюдений на диске солнца не удалось отождествить ни один классический источник этой геоактивности, то есть ни одну, или несколько больших вспышек, ни одного взрывного волокна. На основании наблюдений монохроматической короны проведенных во время полного затмения солнца 31-го июля 1981 года можно было сделать заключение, что таким источником вероятно могла быть низкоширотная корональная дыра.

For some time it has been more or less clear that from the point of view of solar-terrestrial relations solar activity is not much more important than solar inactivity. Both realize themselves in complicated travel from the Sun to the Earth by the proper mechanism. In the literature covering the field of solar-terrestrial relations, a good number of cases is known when: (a) an active region on the Sun containing about 100 individual sunspots was very quiet and caused no geoactivity (such active regions were described by Sykora {1} and Ishkov et al. {2} among others), and on the contrary, (b) during evidently inactive periods on the Sun, disturbances in the Earth's magnetosphere and ionosphere were unexpectedly large.

For an example of the above affirmation we will illustrate one case of productivity of the active region which we have observed and analysed abnormal to the classical imagination. We have in mind Hale region No 17751 ($l = 337.5^\circ$, $\phi = -8.5^\circ$) and its surroundings (Fig.1). Although this AR kept its typical δ -configuration of the magnetic field for several days: the whirl chromospheric structures, changes in the magnetic flux, large horizontal gradients of the magnetic field, as well as remarkable vertical motions of the chromospheric matter were present {3},{4}, still no large manifestations of the eruptive activity were observed. No flare of an importance larger than 1 was detected; of about 60 flares only 4 were of importance 1, others were subflares.

Despite these facts, and as a result of the AR 17751 and its surroundings, transit through the Sun's central meridian (CMP date 24.2), a huge geoactivity on July 24-27, 1981, was involved. According to the K_p planetary indices it was probably the largest geoactivity in 1981 (Fig.2). Preliminary analysis of the ionospheric data {5} shows extremely high SID activity, while radio wave absorption was rather unusual - a weak response in the low ionosphere but, on the whole, expected strong responses in the upper ionosphere. A detailed analysis of the geophysical data in relation to the solar activity of the last decade of July 1981 is now in progress.

It seems that our observations of the solar corona taken in the light of the spectral lines FeXIV 5303Å and FeX 6374Å, during total solar eclipse on July 31, 1981, offer some reasonable explanation of the high geoactivity mentioned in the absence of the eruptive processes on the Sun. It is a well known fact that emission in the "green" line 5303Å is very much positively related to the activity on the Sun's surface, while, on the contrary, emission in the "red" line 6374Å is much less sensitive to the activity and is often stronger just above inactive areas of the Sun's surface. After processing the eclipse's original images by the digitalization technique and subsequent subtraction of the "inactive" component (6374Å) from the "active" component (5303Å), we have obtained Fig.3. From this figure it is evident that emission 6374Å (dark) prevails at both poles of the Sun (in fact, it probably identifies areas familiar to the polar coronal holes), but at the same time clear domination of this emission above the emission in 5303Å line, indicates a remarkable inactivity just at the time where the AR 17751 set behind the Sun's west limb.

Taking the said facts into account, we are of the opinion that the so-called low-latitude coronal hole, located in the vicinity of the AR 17751, was very probably a source of the conspicuous geophysical disturbances. Such small coronal holes are known from the Skylab period (1973-74) and it has been described (including a figure illustration) in {6} by Letfus et al. for example, where we have investigated the possibilities of identifying the coronal holes in our own green (5303Å) emission corona synoptic charts {7}. Of course, in our assumption we also have in mind the well known fact that the lifetime of the coronal holes is several months (at least weeks) and so it is quite reasonable to assume that our dark formation (if it can be identified with the coronal hole) existed and was located, together with AR 17751, on July 23 near the central meridian. Probably it is just this formation of the open magnetic field which was the source of the solar wind which caused an expressive geomagnetic storm on July 25, 1981.

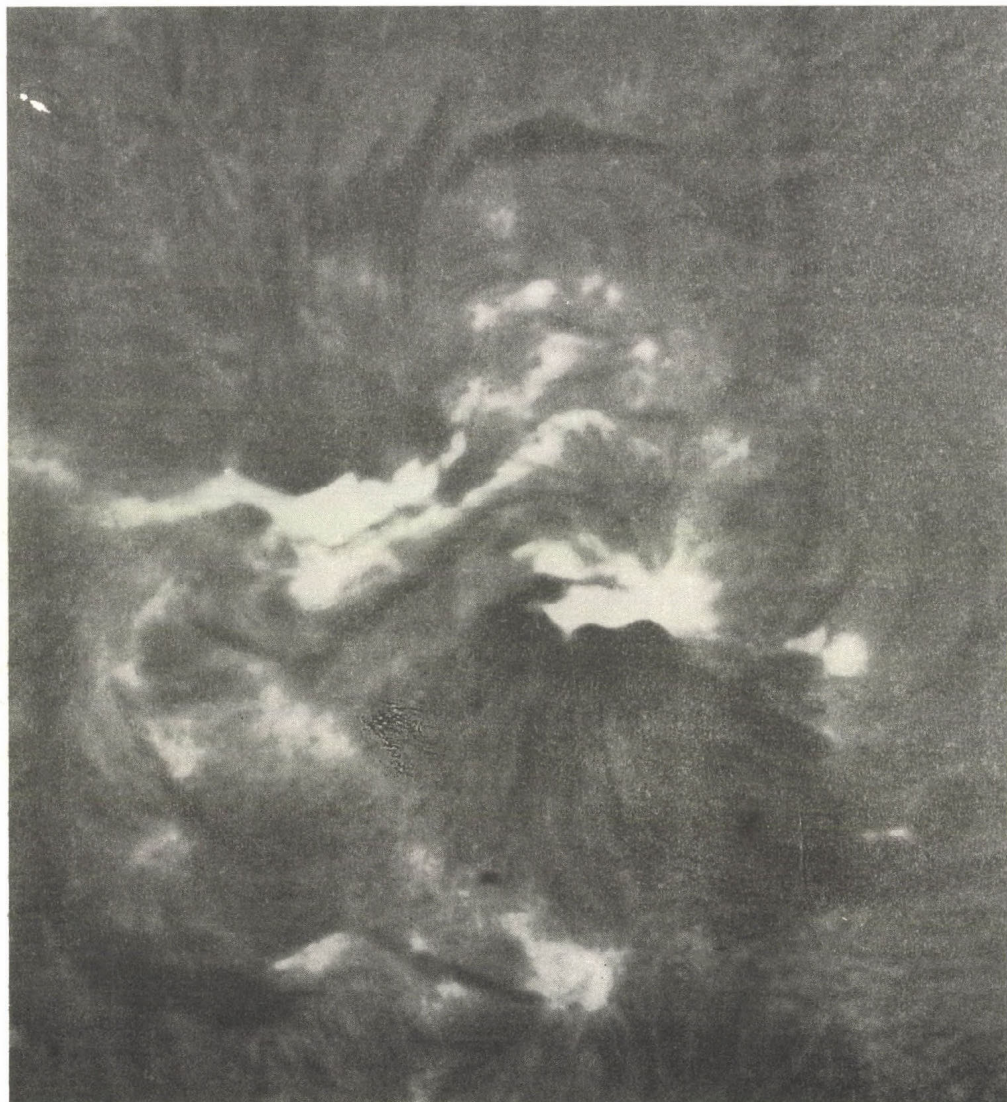


Fig. 1. Hale region No 17751 as seen in the center of the $H\alpha$ line near the central meridian of the Sun (north is above and east is to the left). Picture was taken at 20:45:39 UT, July 23, 1981 at Ottawa River Solar Observatory (Courtesy by V. Gaizauskas).

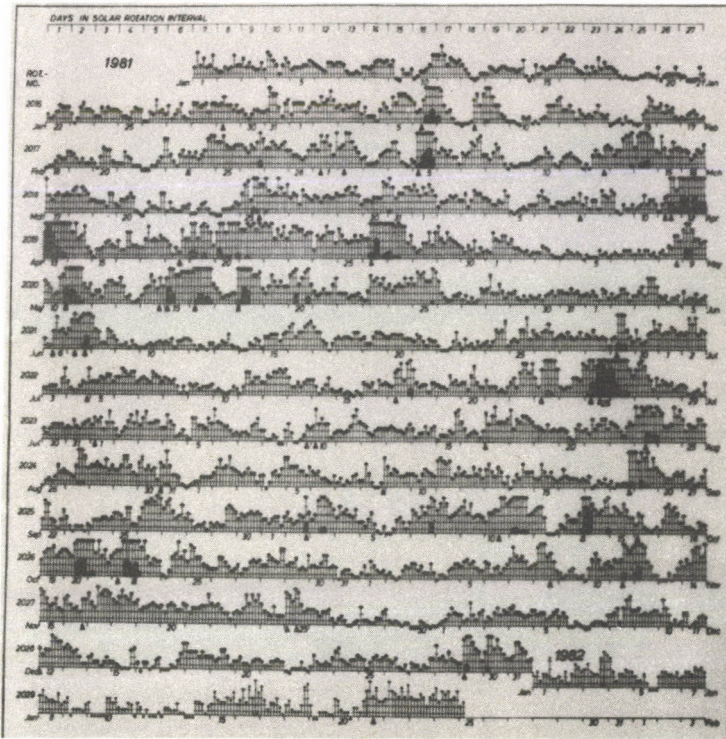


Fig. 2. Copy of the Planetary Magnetic Three-Hour-Range Indices K_p (after Bartels) as issued for 1981 by Gottingen Observatory. Interval of interest is on the right side of the central line.

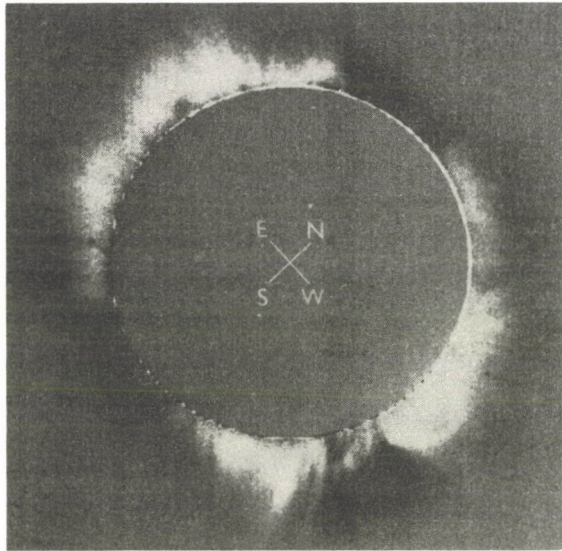


Fig. 3. The pictures taken in green 5303 Å and red 6374 Å lines (2 Å and 3 Å B-13 Baird Atomic filters were used respectively) were combined to this resulting picture by the digitalization technique. The original images were obtained by two identical 120/1950 telescopes with an exposure time of 25 seconds on high sensitive (1000 ASA) film during total solar eclipse on July 31, 1981 (Bratsk, USSR). Hypothetical coronal hole is the dark region on the west limb. For details see text.

References

- {1} Sýkora, J., Successful observation of a large but surprisingly quiet region on the Sun, *Hvar Obs. Bull.* 3, 25, 1979
- {2} Ishkov, V. N., Korobova, Z. B., Mogilevsky, E. I., Starkova, L. I., Utrobin, V. G., Evoljucija i vspyshechnaya aktivnost aktivnoj oblasti MM 15403 1978 g. (in Russ.) *Fiz.soln.akt.* 48, 1980
- {3} Ioshpa, B. A., Mogilevsky, E. I., Starkova, L. I., Utrobin, V. G., Sýkora, J., The evolution of photospheric, chromospheric and coronal magnetic fields and chromospheric structure of the powerful geoeffective active region No.325 S.D., (in Russ.) *Issl.SibIZMIR*, 62, 229, 1982
- {4} Ioshpa, B. A., Mogilevsky, E. I., Starkova, L. I., Utrobin, V. G., Sýkora, J., Development of the geoeffective sun's AR No.17751 (SGD) of July 1981, *Fiz.soln.akt.* 1983 (in Russ. in press)
- {5} Lastovicka, J., Perglerová, P., private communication
- {6} Letfus, V., Kulcár, L., Sýkora, J., On the possibility of identifying coronal holes on synoptic maps of the green corona, *IAU Symp.* 91, 49, 1980
- {7} Letfus, V., Sýkora, J., *Atlas of the green corona synoptic charts for the period 1947-1976*, VEDA, Bratislava, 1982

OBSERVATIONS AND INTERPRETATION OF A SET OF LIMB EVENTS
OF SEPTEMBER 2, 1979

J. P A C I O R E K, T. C I U R L A, B. R O M P O L T

Astron. Observatory, Wrocław

Abstract:

A number of active phenomena, that appeared above the West-limb from S37 to N15 were observed and analysed. Most of the elementary events were recorded in two limb regions. In the first one, between N02 and N05, forty recurrent surges and an active prominence were observed. In the second one, between S30 and S37, about fifty knots of matter moving down were recorded. The detailed study of all observed events suggest the existence of a physical connection between these two distant limb regions.

ИССЛЕДОВАНИЯ КОМПЛЕКСА ЛИМБОВЫХ ЯВЛЕНИЙ НАБЛЮДЕННЫХ
2 СЕНТЯБРЯ 1979 ГОДА

Я. ПАЦИОРЕК, Т. ЦЫРЛЯ, Б. РОМПОЛЬТ

Астрон.Обс.,Вроцлав

Абстракт:

В работе исследуется большой комплекс явлений, произошедших на западном лимбе между S37 и N15. Большинство явлений возникло в двух областях - в первой между N02 и N05, где наблюдалось сорок повторяющихся возвратных выбросов и активный протуберанец, и во второй - между S30 и S37, где зарегистрировано около пятидесяти опускающихся узлов светящейся материи. Подробное исследование всех наблюдавшихся явлений позволяет сделать предположение о физической взаимосвязи этих двух отдаленных областей.

1. Introduction

The exceptional features of the complex of active phenomena observed in $H\alpha$ with the Small Coronagraph of the Wrocław Observatory on 2 September 1979 have given reason of the detailed study of these phenomena. Forty recurrent small surges were observed in a four-hour period at the W-limb region N02-N05, what means that the average time interval between successive surges amounted six minutes only. According to Bruzek {2} the small surges show a tendency to recur at a rate $\sim 1/\text{hour}$, which disagrees with the mentioned short time interval. The appearance of several clouds of weakly emitting matter along a huge arch between the two distant sites of strong activity was the second interesting feature of the observed complex of events. Two hours after the strong eruptions of the active prominence, taking up a position near the base of the recurrent surges, two very small but observable expansions of a stable prominence occurred at S34. This fact was the third unusual feature of the observed set of events.

2. Observations and results of measurements

The whole complex of events was observed from 7:46 UT to 11:54 UT and recorded on 4 films (F468-471; 13 frames 7:46-7:58; 32 fr. 8:01-8:57; 38 fr. 9:01-10:18; 32 fr. 10:23-11:54). The limb region S30 - S37 was observed from 8:02 UT to 11:54 UT only. Because the film F469 has a poor quality the results for all events recorded on this film are of less value. The measurements were performed by an Ascorecord and reduced with the KSR 4100 computer.

Fig.1 shows a general schema of the observed limb events. The areas hatched mark the position of two stable prominences. The synoptic map of the Sun (Fig.2) reveals, that the limb regions N02 - N10 and S30 - S37, which at the moment of observation were close to the W-limb, are connected to two sunspot groups. The northern group, Mt. Wilson No 20835 belongs to McMath region 16239, and the second group, Mt. Wilson No 20836 to McMath region 16241. The lines of sight (LOS) marked in the map show the location of all significant limb events.

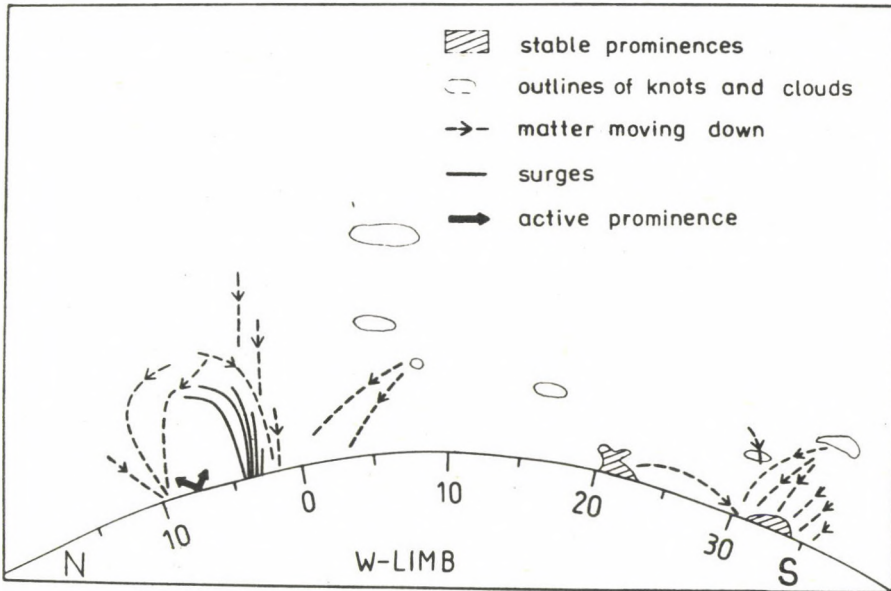


Fig.1. General schema indicating the events observed at Sun's W-limb on 2 September 1979.

In Tables 1 - 3 the results of measurements of all recurrent surges are given. Moreover, Table 1 contains one surge, which occurred a little north to the base of the recurrent surges. Table 2 contains the less accurate data. Table 3 summarizes the data of all great surges. Some parameters for all events, observed in the vicinity of the stable prominence, between S30 and S37 are presented in Table 4. In this limb region two surges occurred only and the predominant events were knots of down moving matter.

It was possible to determine the trajectories of motion, seen in the plane of the sky concerning the surges and knots recorded on the films F468, F470, and F471. These trajectories are shown in Fig.3 and 4, marked with the numbers of identification given in the first column of Table 1 and 3.

Fig.5 (A - G) shows selected frames of F470 and F471 in which one can see seven great surges marked by capital letters. Earlier these photographs were already mentioned by Rompolt{3}.

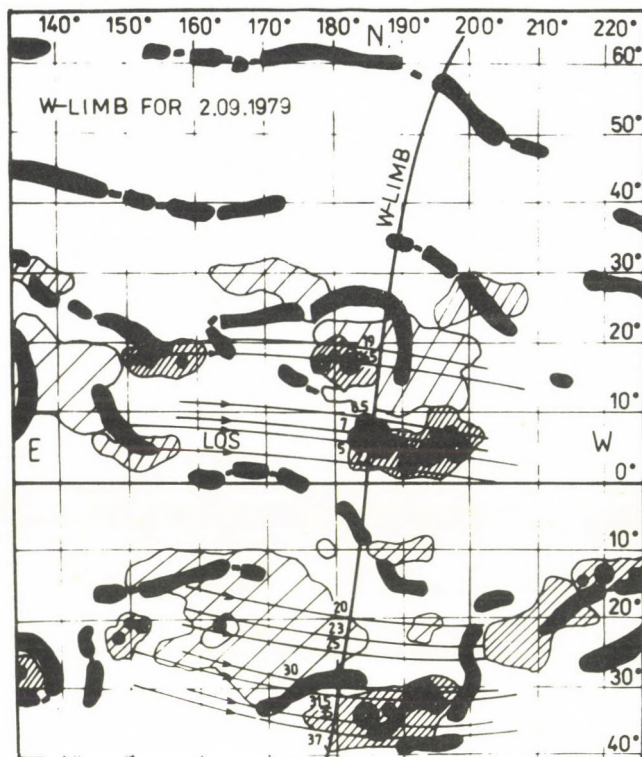


Fig. 2. Synoptic map of the Sun. The lines of sight (LOS) point to the locations of all important limb events.

Fig. 4 shows also the remnant of the active prominence, and matter moving down along a big loop. At 9:01 UT this matter was seen in a form of two arches parallel with the limb at heights $10 \cdot 10^4$ km and $9.5 \cdot 10^4$ km (the top of the big loop). Approximately for one hour these two arches were moving down to the chromosphere along the northern arm of the big loop mentioned. The elongated structures of matter, which filled the big loop present the final phase of the last strong eruption of the active prominence. The parameters of four recorded prominence expansions are given in Table 6. These expansions occurred between 7:46 UT and 8:36 UT. Two other small expansions of the stable prominence were observed at 10:18 UT and 10:39 UT. Table 7 contains the data of these expansions.

T A B L E 1

Data of the surges observed in the period 7:46 - 7:58 UT

Surge No	Limb position	Height max. 10^3 km	Time		Velocity $km\ s^{-1}$	Life time min.
			Start UT	Maximum		
1	N 02.5	35	-	0749	100	6
2	N 02.5	30	0753	0755	80	5
3	N 03	10	-	0748	-	4
4	N 03	23	0751	0755	50	5
5	N 03.5	37	-	0746	-	5
6	N 03.5	25	0756	0758	28	4
7	N 04	32	-	0751	-	10
8	N 10	65	-	0748	-	6

T A B L E 2

Data of the surges observed in the period 8:01 - 8:57 UT

Surge No	Limb position	Height max. 10^3 km	Time		Velocity $km\ s^{-1}$	Life time min.
			Start UT	Maximum		
9	N 04.5	55	0756	0802	100	7
10	N 03	20	-	0802	-	3
11	N 04	25	-	0803	-	3
12	N 02.5	25	0806	0809	100	5
13	N 03.5	20	-	0808	-	4
14	N 04	25	-	0809	-	4
15	N 04.5	40	-	0809	-	6
16	N 03	20	0811	0821	-	10
17	N 02	15	0812	0819	30	8
18	N 03.5	35	0819	0821	-	4
19	N 04	15	0819	-	-	3
20	N 03	30	-	0829	-	7
21	N 03.5	25	-	0828	-	3
22	N 04	25	-	0835	100	5
23	N 03	25	0829	0832	80	7
24	N 04	25	0834	0837	100	7
25	N 03	20	0837	0839	-	4
26	N 03	25	0842	0846	60	13
27	N 04.5	15	0842	0843	-	3
28	N 03	15	0845	0850	-	7
29	N 03	15	0847	0849	-	3
30	N 04.5	35	0851	0856	100	7
31	N 03	-	0856	-	-	3

Between these two sites of strong activity, in the limb region S01 - S20, knots and clouds of weakly emitting matter were observed. Table 5 summarizes the result of measurements.

Several knots were observed propagating from the stable prominence at S21 towards the prominence at S34 between 10:24 UT and 11:48 UT. The trajectory of this movement is indicated in Fig.1.

T A B L E 3

Data of the surges observed in the period 9:01-11:41 UT

Surge No	Limb position	Height max 10^3 km	Time		Velocity km s^{-1}	Life time min.
			Start UT	Maximum		
32	N 04	66	-	0902	-	-
33	N 04	80	0920	0929	90	28
34	N 03	25	-	0906	-	-
35	N 03	45	0924	0934	70	19
36	N 03.5	30	0923	0928	85	7
37	N 04	65	0948	1008	50	38
38	N 03	55	1028	1040	60	22
39	N 04.5	80	1030	1043	105	29
40	N 03	75	1051	1101	70	19
41	N 04	70	1112	1122	90	20

T A B L E 4

Events observed in the limb region S30 - S37

a) Surges

Surge No	Limb position	Height max. 10^3 km	Time		Velocity km s^{-1}	Life time min.
			Start UT	Maximum		
1	S 36	50	-	0802	-	17
2	S 36	50	-	0835	115	25

b) Knots observed in the period 9:06 - 11:54 UT

Limb position	Life time min.	Height of appearance 10^3 km	Number of knots	Height decrease
	3 - 42	40 - 88 16 - 39	12 6	large

c) Clouds

Time UT	Limb position	Height 10^3 km
1124	S 30 - S 32	55

T A B L E 5

Events observed in the limb region S 01 - S 20

a) Knots moving down

Appearance		Limb position		Height change 10^3 km	Life time min.
Time UT	Height 10^3 km	Initial	Final		
0901	75	S 08			
0904	50	S 06	S 04	67	60
0927	80	S 08		No change	10
1110	50	S 03.5			
1110	45	S 02.5	S 00	33	21

b) Clouds

Time UT	Limb position	Height 10^3 km
1124	S 15 - S 18	95

T A B L E 6

Expansions of the active prominence at N 07.5

T i m e			Change of top height 10^3 km	Loop of detached matter		
Start UT	Maximum UT	End UT		Time UT	Top height 10^3 km	Limb extension 10^3 km
0746	0754	0757	10	0755	20	-
0802	0808	0810	15	0809	30	30
0819	0828	0835	25	-	40	42
0836	0845	0847	25	0838	Disappearance of the loop	

T A B L E 7

Expansion of the stable prominence at S 34

T i m e			Height 10^3 km	Limb extension 10^3 km
Start UT	Maximum UT	End UT		
1018	1023	1027	5	3
1039	1118	1130	10	28

In the region N10 - N15 several micro-surges occurred but because of their very small lifetime and small maximum height their data were not included in the tables.

3. Discussion and conclusions

The result of measurements presented in the previous section allow to describe the whole evolution of the events. The complex of the phenomena begins with five small surges and the first small expansion of the active prominence. At the end of the expansion the prominence returns to its initial position. The matter detached from top of the prominence at the maximum phase of the event fills a small loop above the prominence. Each of the subsequent expansions appeared to be increasingly stronger and the detached matter filled more and more the loop lying above the prominence. The size of the loop became larger. After the fourth eruption the active prominence disappeared and the detached matter was observed at the top of a big loop at a height of 10^5 km above the limb. The comparison of Table 1 and Table 3 demonstrates, that the strength of surges increased also.

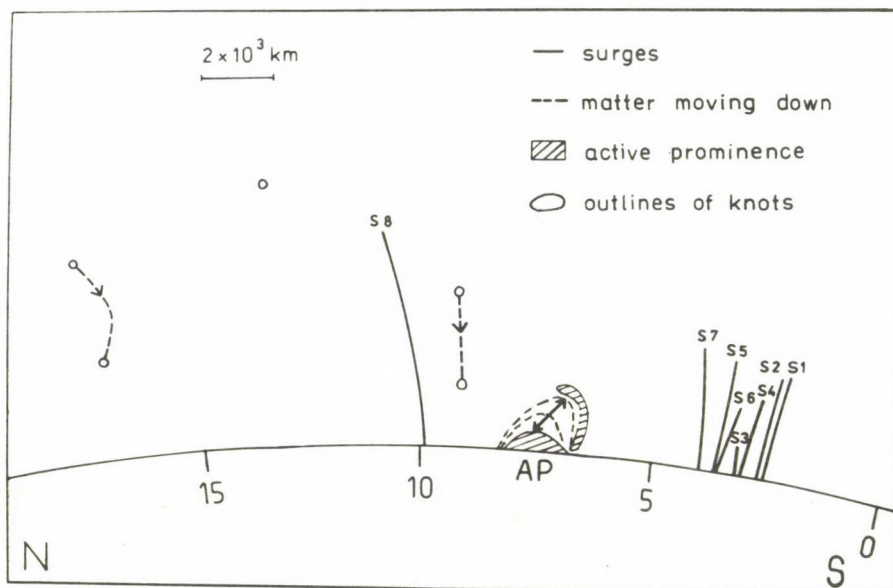


Fig. 3. Trajectories of moving matter (surges and knots) according to measurements. Period of observation 7:46 - 7:58 UT. The areas hatched show the expanding prominence. The surges trajectories are marked with numbers given in the first column of Table 1.

Near the end of the observational period very small surges appeared again (measurements impossible because of bad seeing) and the remnants of the active prominence disappeared completely.

Among the events observed near the stable prominence at S34 the knots of slowly moving matter prevailed, besides of two surges at the very beginning of observation of that prominence. The knots appeared quite high above the limb and the long lived knots were moving towards the chromosphere forming elongated structures.

The first of the two measured expansions of the stable prominence at S34 occurred about two hours after the third eruption of the active prominence at N07.5. The second expansion of this stable prominence took place two hours after the last eruption of the active prominence. The stable prominence returned to its initial size and shape.

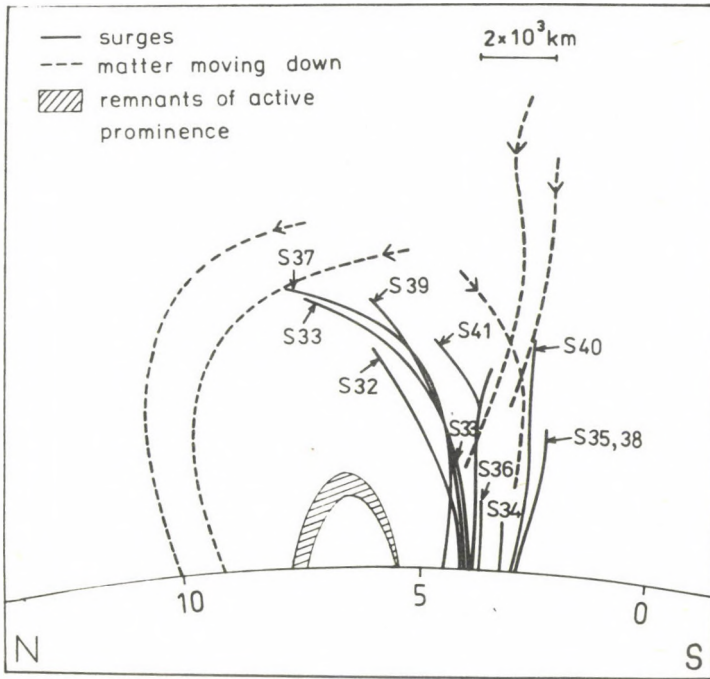


Fig.4. Trajectories of motion of surges and downward moving matter according to measurements. Period of observation 9:01-11:54 UT. The loop hatched marks the remnant of the active prominence. The trajectories of surges have the denotations given in the first column of Table 3.

During the end phase of the second expansion the clouds of weakly emitting matter appeared in the vicinity of the stable prominence, and also between the two sites of the strong activity. The location of these clouds is shown in Fig.1. The most important properties of the discussed set of events are:

- a) the strong surge activity (forty surges during four hours), the strength of which increased simultaneously with the growing strength of the prominence expansions, b) the appearance of the clouds at large heights between two distant sites of active events, and c) two small expansions of the prominence at S34, which followed the eruptions of the prominence at N07.5. These properties capable of being used as evidence that the active events observed in these distant limb regions are interconnected.

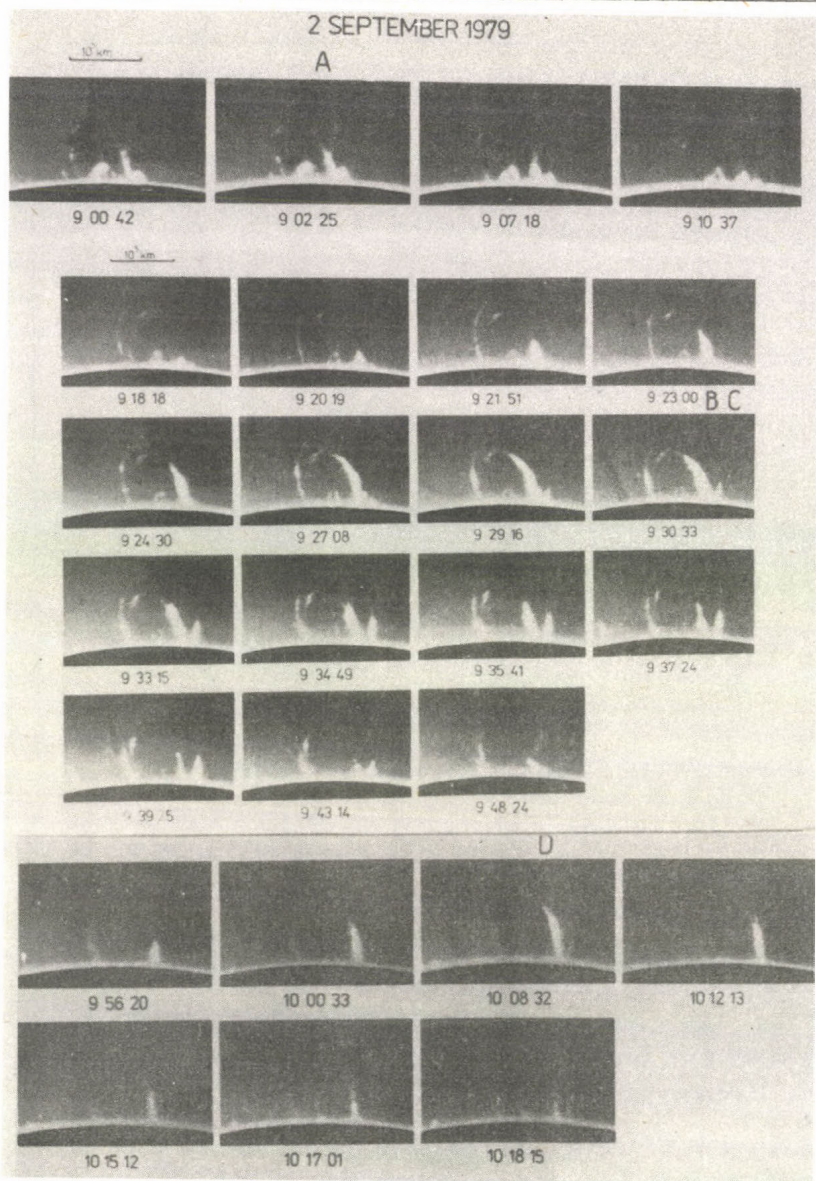
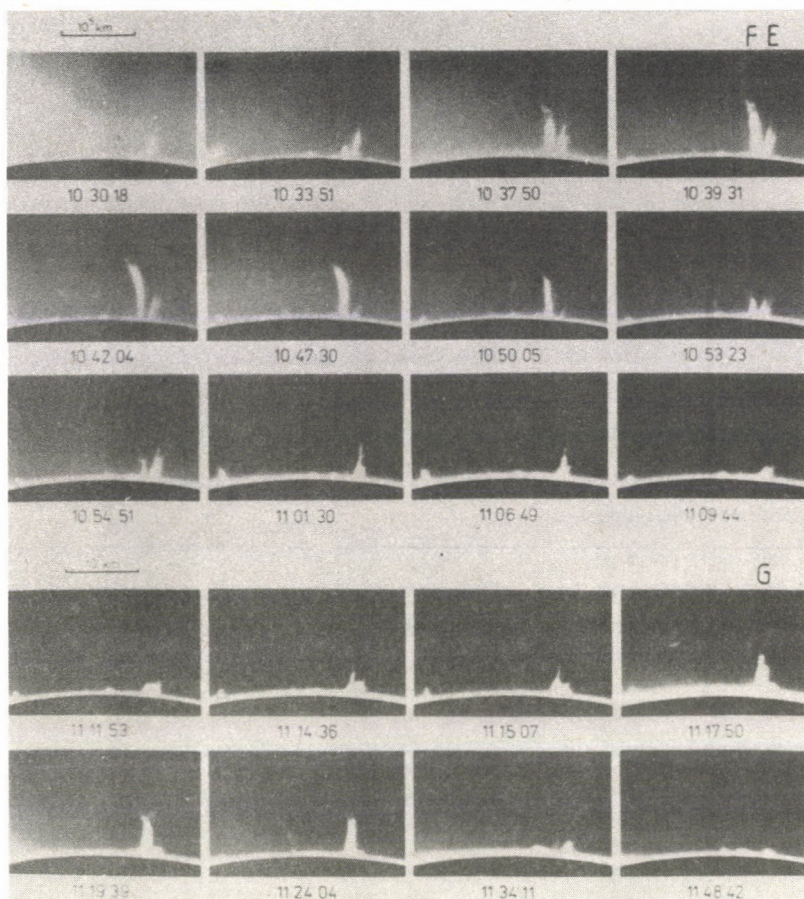


Fig.5. (A-G). Selected frames of films F470 and F471 showing several large surges. The capital letters A, B, C, D, E, F, G successively correspond to the surge nos 32, 33, 35, 37, 38, 39, 41 given in Table 3.



One may have the right to believe that some kind of a disturbance, which propagated from the site of the recurrent surges and of the active prominence towards the southern limb region resulted in the activity observed in this region as well as between these two limb regions. It is interesting to note that this supposed disturbance crossed the equator.

Rust and Švestka {5} and Rust {4} found the existence of "slowly-moving coronal disturbances" propagating with velocities under 100 km s^{-1} and extending over distances of the order of one solar radius. Among the reported properties of these disturbances there are three very interesting ones for the reason

of activity discussed in this paper: a) The disturbances start with activation of dark H α filaments. b) In many cases there are no flares associated with the filament activation, and, c) The moving disturbances themselves are not visible. Their existence was revealed only through brightening of pre-existing coronal structures. Rust and Švestka {4} reminded also of the slow wave hypothesis proposed by Bruzek{1} as an explanation of the activation of filaments at great distances from flares. Finally the very rough estimation of the velocity of the hypothetical propagating disturbance between the two distant limb regions, discussed in this paper, gives a value between 50 and 100 km s⁻¹. This value is in accordance with the one given by Rust and Švestka.

Acknowledgements

The authors wish to thank Mgr.P.Majer for his kind assistance in performing the calculations. We are indebted to the Committee of Astronomy of the Polish Academy of Sciences for financial Support.

R e f e r e n c e s

- {1} Bruzek,A., 'Die Ausbreitung von "Eruptionsstörungen"', *Z.Astrophys.*, 31, 111, 1952
- {2} Bruzek,A., Optical evidence for plasma ejections and waves in the solar corona, *IAU Symp.* 57, 323, 1974
- {3} Rompolt,B., H α limb phenomena and solar noise storms, in *Proc.4th CESRA Workshop on "Solar noise storms"* (eds.A.O.Benz, P.Zlobec), 291, 1982
- {4} Rust,D., Coronal manifestations of eruptive prominences, observations and interpretation, in *Physics of Solar Prominences* (eds.E.Jensen et al.) Proceedings, IAU Coll.No.44, 252, (Oslo) 1978
- {5} Rust,D., Švestka,Z., Slowly-moving disturbances in the X-ray corona, *Ibid.* p.276

THE CARD INDEX OF EJECTIONS OBSERVED AT THE WROCLAW OBSERVATORY

I. N. G A R C Z Y Ń S K A, P. M A J E R, B. R O M P O L T

Astron. Obs., Wroclaw

КАТАЛОГ ВЫБРОСНЫХ ПРОТУБЕРАНЦЕВ НАБЛЮДЁННЫХ ВО ВРОЦЛАВЕ

И. Н. ГАРЧИНСКАЯ, П. МАЕР, Б. РОМПОЛЬТ

Астрон. Обс., Вроцлав

The regular observations of the solar corona have been carried out at Astronomical Observatory of the Wroclaw University by means of the Small H α Coronagraph since 1966. A number of ejections of bright material (sprays, surges and eruptive prominences at the limb) have been observed. Some of these events have already been analysed, and the results were published.

Recently, a homogeneous method of treatment of the observations has been devised and a card index of strong ejections has been initiated. This method is based on measurements performed with the Ascorecord measurement system and computation done with the Odra 1305 computer.

The coordinates, trajectories and velocities of knots of the mass ejections have been calculated and placed in the card index. The locations of bright material, the inferred trajectories and the velocities are given as projections against the plane of the sky. Each event has been described carefully from the point of view of its evolution. The data of the accompanying events are taken from the *Solar-Geophysical Data* and *Solnechnye Dannye*. A set of data and information concerning each event is put in the card index and is available on request. The basic characteristics of each cataloged event are given in Table 1.

H_m - is the maximum height reached by the matter, projected on the sky plane, V_h and V_s are the maximum projected velocities of the mass ejections, perpendicular to solar limb and along the trajectory, respectively.

T A B L E 1

No	Data	Start	End	Object	Pos.	H_m	V_h	V_s
		<u>UT</u>	<u>UT</u>			$10^3 km$	$km s^{-1}$	$km s^{-1}$
1	6.07.68	<u>0717</u>	<u>0723</u>	SPR	N12-E	290	1150	-
2	6.07.68	<u>0944</u>	<u>0955</u>	SPR	N12-E	700	720	-
3	18.08.70	<u>0823</u>	<u>0829</u>	SPR	N20-W	86	970	970
4	11.09.70	<u>0816</u>	<u>0828</u>	SPR	N15-W	80	210	250
5	15.10.70	<u>0959</u>	<u>1011</u>	BSL	N15-E	48	190	320
6	7.07.71	<u>0810</u>	<u>0814</u>	EPL	S12-E	60	75	100
7	23.09.74	<u>1156</u>	<u>1207</u>	SPR	N07-W	200	500	700
8	4.07.77	<u>0857</u>	<u>0924</u>	BSL	S22-E	55	70	72
9	9.04.78	<u>0919</u>	<u>0940</u>	SPR	N38-E	73	200	290
10	24.04.78	<u>0749</u>	<u>0800</u>	SPR	N25-E	53	150	160
11	11.07.78	<u>1102</u>	<u>1105</u>	SPR	N17-E	980	1350	-
12	9.03.79	<u>1020</u>	<u>1035</u>	SPR	N16-E	115	500	900
13	10.04.79	<u>0709</u>	<u>0741</u>	BSL	N32-E	100	185	185
14	10.04.79	<u>1030</u>	<u>1245</u>	EPL	N03-E	210	270	-
15	11.04.79	<u>0836</u>	<u>0900</u>	SPR	N15-E	132	200	246
16	6.05.79	<u>1035</u>	<u>1050</u>	SPR	S23-E	63	380	380
17	8.05.79	<u>0830</u>	<u>1130</u>	EPL	S55-W	400	150	-
18	16.05.79	<u>1038</u>	<u>1042</u>	SPR	N15-W	30	230	320
19	29.05.79	<u>0851</u>	<u>0948</u>	EPL	N10-E	35	14	14
20	29.05.79	<u>1055</u>	<u>1105</u>	SPR	N10-E	215	300	310
21	27.06.79	<u>1001</u>	<u>1029</u>	EPL	S16-E	150	125	210
22	14.08.79	<u>1140</u>	<u>1216</u>	EPL	S32-E	230	270	300
23	17.08.79	<u>0905</u>	<u>0910</u>	EA	N05-E	35	70	70
24	17.08.79	<u>0920</u>	<u>0941</u>	SPR	N05-E	122	330	330
25	2.09.79	<u>0746</u>	<u>1154</u>	BSL	N05-W	82	120	120
26	13.09.79	<u>1035</u>	<u>1053</u>	SPR	N19-E	100	320	320
27	10.10.79	<u>1117</u>	<u>1123</u>	SPR	S31-W	70	360	600
28	13.04.80	<u>0834</u>	<u>0842</u>	BSL	N27-W	72	120	120
29	13.04.80	<u>0902</u>	<u>0918</u>	SPR	N03-W	100	240	330
30	13.04.80	<u>0902</u>	<u>0918</u>	BSL	N23-W	150	330	330
31	17.04.80	<u>1006</u>	<u>1021</u>	BSL	S11-E	30	38	38
32	5.05.80	<u>0912</u>	<u>1050</u>	EPL	S23-W	242	200	210
33	13.05.80	<u>0738</u>	<u>0827</u>	BSL	S26-W	57	60	60
34	16.05.80	<u>0859</u>	<u>0925</u>	SPR	N30-E	52	90	120
35	8.06.80	<u>0815</u>	<u>0904</u>	EPL	S18-E	247	170	200
36	18.08.80	<u>0953</u>	<u>1224</u>	EPL	S34-E	635	294	295
37	9.09.80	<u>1130</u>	<u>1142</u>	SPR	N13-W	62	100	160
38	20.09.80	<u>0807</u>	<u>1112</u>	EPL	S40-W	350	250	250
39	11.04.81	<u>0836</u>	<u>0945</u>	SPR	N06-W	45	75	150
40	10.05.81	<u>1211</u>	<u>1234</u>	SPR	N03-E	125	150	175
41	22.05.81	<u>0636</u>	<u>0656</u>	SPR	N16-W	165	170	250

Here: BSL - bright surge at the limb, SPR - spray, EPL - eruptive prominence at the limb, EA - eruptive arch.

Time of the "Start" and "End" of an observation is given in UT. If underlined by a full line, the real time of the start and/or the end of an event is recorded; if underlined by a broken line, an approximate time of the start and/or the end of the event is given.

FLARE GEOEFFICIENCY IN RELATION TO PHOTOSPHERIC MAGNETIC
FIELD ORIENTATION OF ACTIVE REGIONS

B. R Ů Z I Č K O V Á - T O P O L O V Á,

L. B U F K A

Astron. Inst., Ondřejov

Astron. Soc., Prague

Abstract:

The objective of this study was to investigate the geoefficiency of a set of flares which had occurred in solar cycles Nos 19 and 20, and were followed by the most severe geomagnetic storms with sudden commencements. Flares with simultaneous occurrence of type II radio bursts, observed in the years 1970-1976, were taken as comparison data. More frequent occurrence of geoeffective flares was found at the location where direction of the photospheric magnetic field was southward. Furthermore, flares occurring at the site with the dividing line between polarities oriented approximately perpendicular to the solar meridian and also flares at the site with polarity reversed against the normal bipolar distribution of photospheric magnetic field according to Hale's law display a tendency toward higher geoefficiency. Location of flares in the central zone at the solar disc is more favourable with regard to their effect on disturbing the geomagnetic field.

ГЕОЭФФЕКТИВНОСТЬ ВСПЫШЕК В СВЯЗИ С ОРИЕНТАЦИЕЙ
ФОТОСФЕРИЧЕСКИХ МАГНИТНЫХ ПОЛЕЙ АКТИВНЫХ ОБЛАСТЕЙ

Б. РУЖИЧКОВА - ТОПОЛОВА, Л. БУФКА

Астрон. Инст., Ондřejов Астрон. Общ., Прага

Абстракт:

Задачей этой работы было исследовать геоэффективность набора вспышек появляющихся в течении солнечных циклов No 19 и 20, вызывающих наиболее крупные геомагнитные бури с внезапным началом. Вспышки одновременно сопровождаемые радиовсплесками типа II из 1970-1976 гг. служили для сравнения. Более частое появление геоэффективных вспышек встречалось на местах, где направление фотосферного магнитного поля было южное. Далее вспышки на таких местах, где ориентация линий разделяющих N и S полярности была приблизительно перпендикулярна к солнечному меридиану, и тоже вспышки на местах с полярностями перевернутыми по сравнению с нормальным распределением фотосферных магнитных полей в соответствии со законом Хейла, являют тенденцию к высшей геоэффективности. Появление вспышек в центральной зоне солнечного диска кажется более пригодным из точки зрения их влияния на разрушения геомагнитного поля.

1. Introduction

The authors started out with the hypothesis that the configuration of photospheric magnetic fields affects the geoefficiency of flares. This problem has been dealt with e.g. by Pudovkin and Chertkov {5} who found that lines of force of the photospheric magnetic field oriented southward at the flare location result in enhanced geomagnetic activity, whereas if oriented northward no adequate enhancement is observed. Negative (*S*) polarity is assumed to be inward and positive (*N*) polarity outward; the direction of the photospheric magnetic field (i.e. the direction of the lines of force) is perpendicular to the line dividing the two polarities. Also Lundstedt et al. {4} found a relation between the southward orientation of the magnetic lines of force at the flare site and the solar wind velocity. This effect is the result of the different situations which occur when magnetic clouds of different orientations interact with the Earth's magnetosphere.

The objective of this study was to investigate the geoefficiency of a set of flares which had occurred in solar cycles Nos 19 and 20, and were followed by the most severe geomagnetic storms with sudden commencements (SC) in dependence on the orientation of the lines of force of the photospheric magnetic field, on the preceding polarity in the active region (AR) at the flare site, as well as the distribution of geoeffective flares in heliographic longitude on the solar disc.

2. Observation Data

The basic observation data were flares with subsequent severe geomagnetic storms as shown in the catalogue of Krajcovic and Krivský {3} for the solar cycles Nos 19 and 20. These storms had SC's and exceptionally high values of geomagnetic planetary Kp-indices ($\geq 7+$). The magnetic field data were adopted from the maps of the Mount Wilson Observatory, published in the ESSA publications *Solar-Geophysical Data*, and supplemented with data from the *Catalog of Solar Particle Events 1955-1969* {1}. The choice of events was quite limited due to the

lack of data, or due to difficult or unreliable localization of the flare in the region. The total number of cases considered was 62 (GMS).

Flares with simultaneous occurrence of type II radio bursts, observed in the years 1970-1976, were taken as comparison data. Their selection from the catalogue of Krivský and Lukáč {3} again depended on the required magnetic field data. The selected flares were divided into two groups:

a) flares suspected of being the cause of enhanced geomagnetic activity, i.e. an SC occurred or the A_p -index reached a value ≥ 25 within four days of their occurrence, or of contributing to these geomagnetic effects (Suspect); 105 cases were considered;

b) flares after which the level of geomagnetic activity defined above was not achieved (No effect); 164 cases.

We took the fact that the comparison sets, as opposed to the GMS sets, contain flares from a part of one solar cycle only into account.

3. Field direction and dividing line orientation at flare site

At the site of each flare, we determined the direction of the photospheric magnetic field relative to the projection of the Earth's axis of rotation onto the solar disc, because we are dealing with interaction with the Earth's magnetic field. By field direction we shall understand the direction of magnetic line of force which represent the lines joining the N and S polarities on the Mt. Wilson maps, perpendicular to the dividing line. We divided the flares depending on whether the field was directed to the north or south (Fig.1).

In determining the direction of the lines of force at the flare site, a rough simplification is made which may possibly introduce errors into the data. The positions of flares, although they represent extensive and complicated formations, are defined by the coordinates of their centre of gravity in $H\alpha$. Localizing the flares in magnetic field maps and determining their positions on the frequently complicated shape of

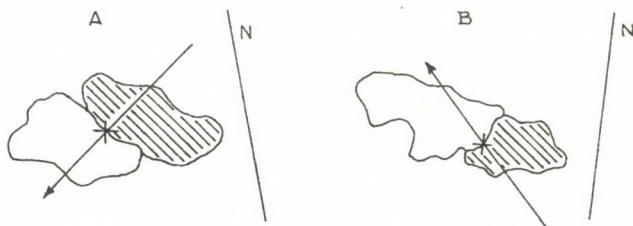


Fig. 1. Diagram for determining the direction of the photospheric magnetic field at the flare site: A - southward direction, B - northward direction. Hatched area is N polarity. The flare site is marked by a cross. Light straight line corresponds to the projection of Earth's rotation axis.

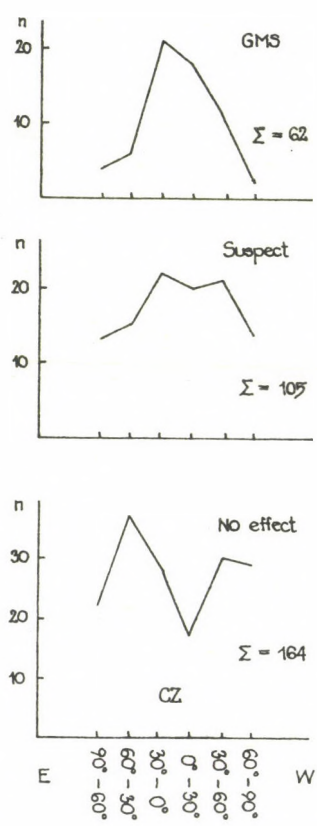


Fig. 2. Distribution of source-flares (GMS) and flares of the comparison sets (Suspect, No effect) in heliographic longitude.

T A B L E 1

	No effect	Suspect	GMS
Southward/northward ratio	0.38	0.61	1.64
Σn	54	58	37

T A B L E 2

Dividing line orientation	No effect	Suspect	GMS	100%
$\begin{matrix} N S \\ S N \end{matrix}$ and D	61%	46%	33%	137, 108, 55
$\begin{matrix} N \\ S \end{matrix}$	7%	8%	18.5%	
$\begin{matrix} S \\ N \end{matrix}$	12%	15%	18.5%	90, 66, 54
Σ	19%	13%	37%	

T A B L E 3

	No effect	Suspect	GMS
Reversed preceding polarity	26%	32%	40%
100%	54	47	43

T A B L E 4

	No effect	Suspect	GMS
Central zone	28%	40%	63%
100%	164	105	62

dividing lines was not always unambiguous. Moreover, until 1967 no systematic measurements of photospheric magnetic fields were available. The time lag between flare occurrence and the time the magnetic maps were drawn cannot be disregarded either. We know that substantial changes sometimes occur in the distribution of polarities before, during and after the flare. Consequently, we are of the opinion that there is no sense in determining the direction of the lines of force with a higher accuracy.

The ratio of the number of flares with southward field direction to the number of flares with northward field direction increases with the geoefficiency of the flares (Table 1). The table only contains the flares with which the field direction was distinctly southward or northward; naturally, cases in which no decision could be made about the direction prevailed somewhat.

In contrast to the authors referred to above, our result concerning the relation between southward field direction and geomagnetic activity is statistically proved, but the effect did not display such a large statistical predominance as we expected.

It was also found that the percentage of flares with field direction approximately perpendicular to the solar meridian (N|S and S|N orientation) and of flares distant from the line dividing the polarities (D) decreases with increasing flare geoefficiency. On contrast, the percentage of flares with field direction approximately parallel with the solar meridian, both southward and northward ($\frac{N}{S}$ and $\frac{S}{N}$ orientation), increases with geoefficiency (Table 2). The values for $\frac{N}{S}$ and $\frac{S}{N}$ in Table 2 were derived from the number of active regions regardless of the number of flares which occurred in them. They were divided depending on whether at least one Suspect flare occurred in them, or at least one GMS flare. The number of cases considered is given in the last column of the table.

Table 2 indicates that the orientation of the line dividing opposite polarities perpendicular to the solar meridian,

regardless of southward and northward field direction, is quite important for producing geoeffective flares in the active region. Consequently, even the northward field direction, provided that it makes a small angle with the meridian, does not prevent flares from affecting the geomagnetic field. This result also follows from the experience that a magnetic field configuration with the dividing line pointing against the usual orientation (by "usual" we understand slightly tilted to the meridian), indicating the complicatedness of the magnetic situation ("twist" or "shear" of the magnetic field), is always dangerous with regard to producing large, or even proton flares with geomagnetic response. Sakurai {6} found that the rotating motion of the dividing line in sunspots was related to the occurrence of mighty flares generating subcosmic and cosmic rays, namely, anticlockwise when viewed from the Earth in the northern hemisphere and clockwise in the southern hemisphere. This is due to the convective flow in subphotospheric layers which causes the lines of force to twist over the sunspot groups. Our GMS set contains mostly flares of this type.

4. Preceding polarity at the flare site

The mutual orientation of magnetic field polarities in the AR in the E-W direction, i.e. the preceding polarity at the flare site, is investigated in relation to flare geoefficiency. According to Hale's law, the preceding polarity of sunspots changes at the beginning of each solar cycle and alternates in the hemispheres.

In our three sample (No effect, Suspect, GMS) cases in the northern hemisphere predominate. This need not correspond to the normal distribution of flares on the disc. Even the comparison sets may be subject to the selection effect (occurrence of type II radio bursts). The GMS set contains flares of cycles Nos 19 and 20, the No effect and Suspect sets only those from cycle No 20. In cycle No 19, the preceding polarity in the northern hemisphere was *N*, in cycle No 20 *S*. Nevertheless, preceding *N* polarity predominates in all sets, if referred to the solar meridian. The number of cases with pre-

ceding *N* and *S* polarity become balanced if we refer the distribution to the orientation of the Earth's axis. All the cases in which no decision could be made about the preceding polarity, were eliminated from the statistics. We shall now only deal with preceding polarities referred to the solar meridian.

We considered the number of preceding polarities reversed with respect to the normal orientation according to Hale's law, at the flare site. Table 3 shows that the percentage of cases of reversed polarity increases with the geoefficiency of flares. We also tried other criteria for determining the rate of reversed polarity, e.g., AR's in which our three categories of flares occurred and their main dividing lines were considered, regardless of the flare site, or the polarities at the flare site were considered, but each AR was counted only once. We always arrived at a large difference between the reversed polarity numbers of the No effect sample, on the one hand, and the Suspect and GMS samples, on the other, which agrees with the results of Sakurai {6}.

The tendency of flares, occurring in AR's or in those parts of AR's where the polarity of the photospheric magnetic fields is reversed, to greater geoefficiency is thus proved.

5. Source-flare distribution in heliographic longitude

Pudovkin and Chertkov {5} considered the possible relation between the position of a flare on the solar disc and its geoefficiency; they came to the conclusion that the position of flares only affects the intensity of subsequent geomagnetic storms, but has no bearing on whether the flare causes or does not cause significant geomagnetic disturbances. Our material, consisting of 331 flares divided into the three samples mentioned, shows the distribution in heliographic longitude as demonstrated in Fig.2: the GMS sample has maximum flare occurrence in the central zone (CZ), $\lambda 30^{\circ}\text{E} - 30^{\circ}\text{W}$, whereas the No effect sample shows a minimum there. The Suspect flares in this heliographic longitude interval display a flat maximum. Numerically, this result is expressed by the percentage of the number of flares which occurred in the CZ for each

T A B L E 5

List of source-flares (GMS)

Date	Position		Start	Class	Date	Position		Start	Class	
	°	°				°	°			
			h	m	UT			h	m	UT
1956 Feb 23	N23	W80	3	31	3	1965 Apr 16	(N04 E20)	-	-	
1957 Jan 20	S30	W18	<11	00	3	1966 Aug 28	N21 E04	15	22	2B
Jul 3	N14	W40	7	20	3	Sep 2	N24 W56	5	42	3B
Aug 31	N25	W02	13	21	3	1967 Feb 13	N21 W10	17	49	3B
Sep 11	N13	W02	< 2	36	3	May 23	N28 E25	18	02	3B
Sep 18	N21	E08	17	22	3	Jun 3	N23 E13	2	26	1B
Sep 26	N23	E16	19	07	3	Sep 18	N16 W60	23	16	2B
1958 Feb 9	S12	W14	21	08	2+	1968 Jun 9	S14 W09	8	30	3B
Jun 4	N14	W58	<21	47	2	Oct 30	S14 W37	23	40	3B
Jul 7	N25	W07	0	20	3+	1969 Feb 1	N11 E70	21	25	1B
Aug 16	S14	W49	4	32	3	Mar 21	N20 E17	1	39	2B
Aug 22	N18	W13	14	17	3	Sep 27	N09 E02	3	50	3B
1959 May 10	N20	E47	20	55	3+	1970 Mar 7	S11 E09	1	40	2B
Jul 10	N21	E64	2	15	3+	Jul 7	S09 W13	16	54	-F
Jul 16	N16	W31	21	14	3+	Jul 22	N06 E18	19	40	-B
1960 Mar 29	N12	E31	6	50	2	Dec 11	(N10 E37)	-	-	
Apr 1	N12	W09	8	35	3	1972 Mar 5	S07 E42	(8 07	1B)	
Apr 29	N14	W21	1	07	3	May 12	N21 W48	19	28	-B
May 4	N15	W90	9	56	3	Jun 15	S10 E11	9	51	1N
May 6	S09	E08	<14	04	3	Aug 2	(N09 W17)	-	-	
Sep 3	N20	E87	0	37	3	Aug 7	N13 W37	14	49	3B
Nov 10	N29	E20	10	09	3+	Sep 11	N19 W07	10	14	1B
1961 Jul 11	S06	E32	16	15	3	Oct 28	S10 E10	18	05	-N
Jul 12	S07	E22	10	00	3+	1973 Feb 18	S09 W06	21	05	1B
Jul 15	S07	W21	15	08	2	Apr 11	S09 W10	18	38	1B
Jul 24	N18	E18	4	10	3	May 11-13	(S10 W40-60)	-	-	
Sep 28	N14	E29	22	02	3	1974 Jul 3	S15 E08	7	58	2B
Sep 20	N14	E07	< 7	06	2	Sep 13	S13 E24	14	58	2B
Sep 20	N13	W09	23	14	2	1976 Mar 23	S05 E90	8	37	-B
Oct 22	N11	E50	13	21	2	Mar 28	(S07 E28)	-	-	
Oct 28	N12	W24	< 1	35	3	Apr 30	S08 W46	20	47	1B

Coordinates in parentheses give either positions of sources which are not unambiguous in time, i.e. there were more than one flare approximately at the same location, or positions of source-regions without any known flare.

set, see Table 4.

Considering the criteria used in this paper, it seems that there exists a relation between the position of the flare on the solar disc not only with the intensity of the geomagnetic effect, but also with the occurrence of the geomagnetic response itself.

6. Conclusions

The results of this study may be summarized as follows:

1) The southward direction of the photospheric magnetic field seems to be more effective in interacting with the geomagnetic field than the northward orientation.

2) Flares occurring at the site with the dividing line between polarities oriented approximately perpendicular to the solar meridian, display larger geomagnetic effects than flares at sites where the dividing line is rather parallel with the meridian.

3) Flares which occur at a site with the polarity reversed against the normal bipolar distribution of large-scale photospheric magnetic fields display a tendency towards higher geo-efficiency.

4) The study of the distribution of flares in heliographic longitude implies that the occurrence of flares in the CZ is more favourable with regard to their effect on disturbing the geomagnetic field.

Acknowledgement

The authors wish to thank Dr. L. Krivský for his valuable comments and discussions.

R e f e r e n c e s

- {1} *Catalog of solar particle events 1955-1969* (Svestka, Z., Simon, P. eds.) *Astrophys. and Space Sci. Library Vol. 49*. D. Reidel Dordrecht 1975
- {2} Krajčovič, S., Krivský, L. Severe geomagnetic storms and their sources on the Sun, *BAC*, 33. 47, 1982
- {3} Krivský, L., Lukác, B., *Catalogue of the solar type II bursts and their source flares for the cycle No. 20. (1966-1976)* Obs. Hurbanovo, 1980
- {4} Lundstedt, H., Wilcox, J. M., Scherrer, P. M., Solar flare acceleration of solar wind: influence of active region magnetic field, *Science*, 212. 1501, 1981

- {5} Pudovkin, M.I., Chertkov, A.D., Magnetic field of the solar wind,
Solar Phys. 50. 213, 1976
- {6} Sakurai, K., Solar cosmic-ray flares and related sunspot magnetic fields
Rep. Ionos. Space Res. Japan, 21. 113, 1967

FLARES OF TYPE II AND IV RADIO BURSTS
IN MAGNETIC TYPES OF SUNSPOT GROUPS

S. K N O Š K A,

Astron. Inst., Tatranská Lomnicá

L. K Ř I V S K Ý

Astron. Inst., Ondřejov

Abstract:

The occurrence of flares was statistically processed, for those with type II and type IV radio bursts separately, in relation to the sunspot groups in which these flares took place. The period in question is cycle no. 20, 1966-1976. Zurich and magnetic classifications were taken into account. The results are given in graphs. As compared with flares accompanied by type II bursts, flares with type IV display an enhanced tendency to occur in more complex active regions in which more magnetic energy is accumulated in a small space (type δ).

ВСПЫШКИ С РАДИОВСПЛЕСКАМИ ТИПА II И IV
В ГРУППАХ СОЛНЕЧНЫХ ПЯТЕН РАЗЛИЧНЫХ МАГНИТНЫХ ТИПОВ

Ш. КНОШКА

Астрон. Инст., Татранска Ломница

Л. КРЖИВСКИЙ

Астрон. Инст., Онджейов

Абстракт:

Проведена статистическая обработка вспышек сопровождаемых радиовсплесками типа II и отдельно типом IV (которые представляют мощные извержения материи) в связи с типами групп пятен, тоже по магнетической классификации. Обработка касается цикла No 20 (1966-1976). По сравнению с вспышками с типом II, вспышки с типом IV появляются в повышенном количестве в активных областях где магнитная энергия накоплена в малом пространстве (тип δ).

Flares accompanied by type II and IV radio bursts represent shock waves and matter ejections passing through the solar corona {6} and are the most energetic manifestation of a whole series of solar activity phenomena.

The occurrence of flares was statistically processed, for those with type II and type IV radio bursts separately, in relation to the sunspot groups in which these flares took place. The period in question is cycle no. 20, 1966-1976. Zürich and magnetic classifications were taken into account.

1. Sources of data

The catalogue, published by L.Křivský and B.Lukač {3} and covering nearly the whole of cycle no. 20 (1966-1976), was used as the source of data on type II radio bursts (coronal shock wave) and flares.

As the source of data on type IV radio bursts (magnetic plasma cloud) and flares, the authors used catalogues covering the whole of solar cycle no. 20 {4},{5}.

The basic observational data for selecting sunspot groups and their Zürich classification were adopted from the Helio-graphic Maps of the Photosphere {7}. The magnetic types were determined by comparison with the daily maps published in the Solar Geophysical Data, Boulder (1966-1976), and with the magnetic classification from Mt.Wilson, given therein.

2. Occurrence of flares with type II radio bursts in relation to sunspot group types

The total number of cases $n = 354$.

Fig.1 shows the frequency matrix of flares with type II bursts for Z-types and magnetic types; the number and isolines mark the areas of enhanced occurrence: the largest accumulation occurs in $D\beta(45)$, in $E\delta(27)$ and in $H\alpha(19)$. The isolines were used for the sake of illustration and their use is not, strictly speaking, justified because of field discontinuity. A reference comparison with the occurrence of all groups processed can be made by comparing this matrix with the matrix in Fig.5.

With regard to the matrix of occurrence of flares with type IV bursts (Fig.3), there is a predominance of maxima

in the lower areas with type II flares.

The percentage occurrence of flares with type II radio bursts is shown separately for Z-types and for magnetic types of sunspot groups in Fig.2. The largest occurrence is in types D, E (20-25%) and in type β (40%). The curve in the left-hand histogram represents the reference values of types in terms of percentage calculates for the interval of heliographic longitude $\pm 70^\circ$ using all sunspot groups observed in the years 1965-1976 (i.e. from the whole of cycle no.20){2}. The reference curve of occurrences n in the right-hand histogram was derived from the processed sunspot groups (whose magnetic fields were measured) and, consequently, is not perfectly representative, particularly as regards the number of type α which is largely underestimated {1}.

It can be seen that the occurrence of flares with type II bursts corresponds to the normal observed frequency distribution of magnetic types, only the more conspicuous excess being displayed by type δ . The highest accumulation can be observed with type β (40%).

3. Occurrence of flares with type IV radio bursts in relation to sunspot group types

The total number of cases $n = 141$.

Fig.3 shows the frequency matrix of flares with type IV bursts for Z-types and for magnetic types; the number of iso-lines mark areas of increased occurrence: the largest accumulation is in E δ (22) and also in C β (16), subsidiary accumulations are in H δ (11) and H α (5). A reference comparison can be made with the occurrence of all sunspot groups processed by comparing this matrix with the matrix in Fig.5. One can see that there is a relative transfer of maxima with the type IV flares to upper positions (E δ , H δ).

As compared to the matrix of occurrence of flares with type II emissions (Fig.1), there is a conspicuous relative transfer of the maximum of the type IV's to the upper positions (E δ , H δ).

The percentage occurrence frequency of flares with type

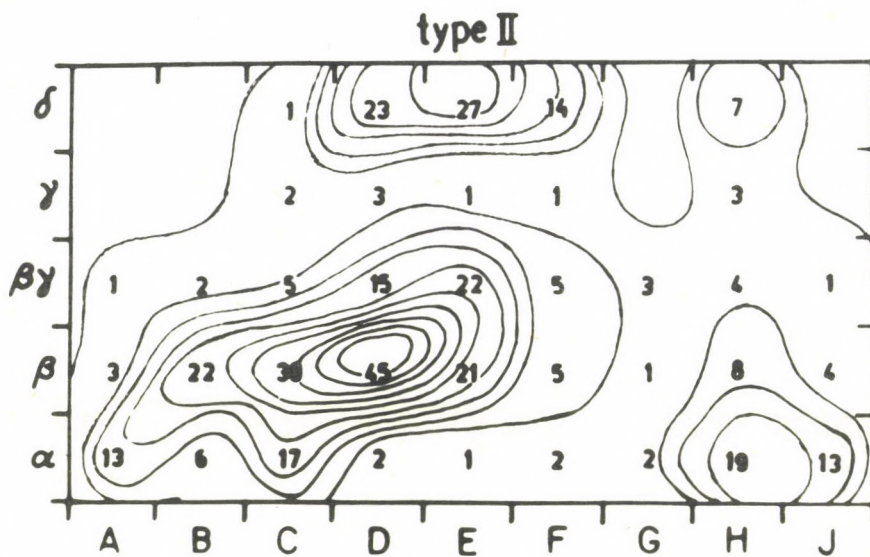


Fig.1. Matrix of occurrence frequencies of flares with type II emission according to the Z classification and magnetic types. Isolines in steps of 5. Period 1966-1976.

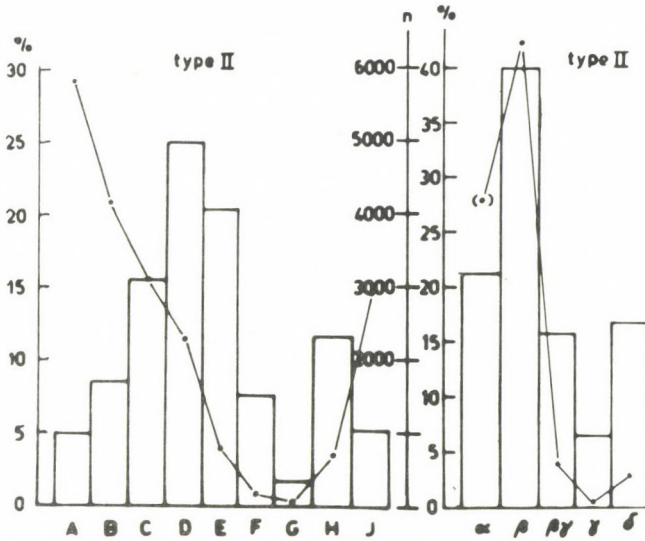


Fig. 2. Left-hand side:
 Histogram of percentage occurrence of flares with type II emission (1966-1976) in the individual sunspot types (Zurich). The curve connects the percentages of the occurrence distribution of all types of sunspot groups within the whole cycle (1965-1976).
 Right-hand side:
 Histogram of percentage occurrence of flares with type II emission (1966-1976) in the individual sunspot group types according to magnetic classification. The curve connects the numbers (n) of magnetically determined types of sunspot groups in the same cycle.

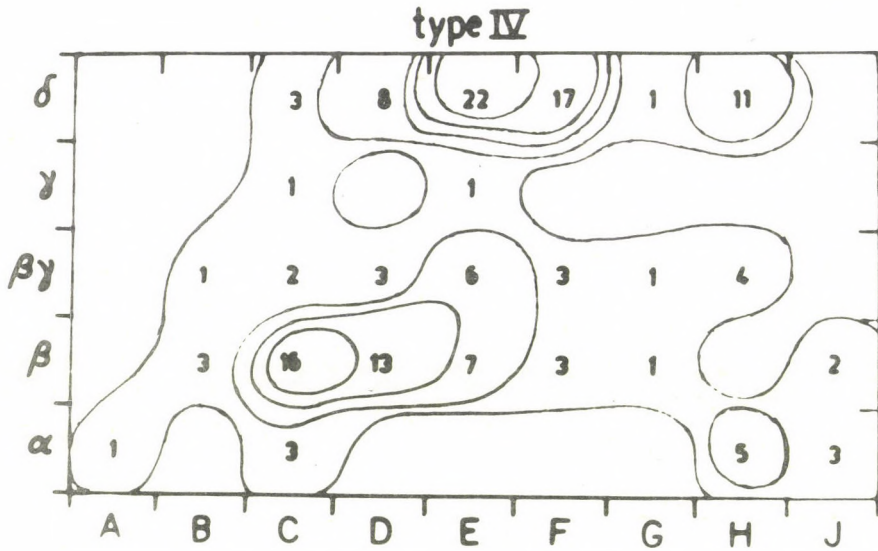


Fig.3. Matrix occurrence frequencies of flares with type IV emission according to the Z and magnetic classifications. Isolines in steps of 5. Period 1966-1976.

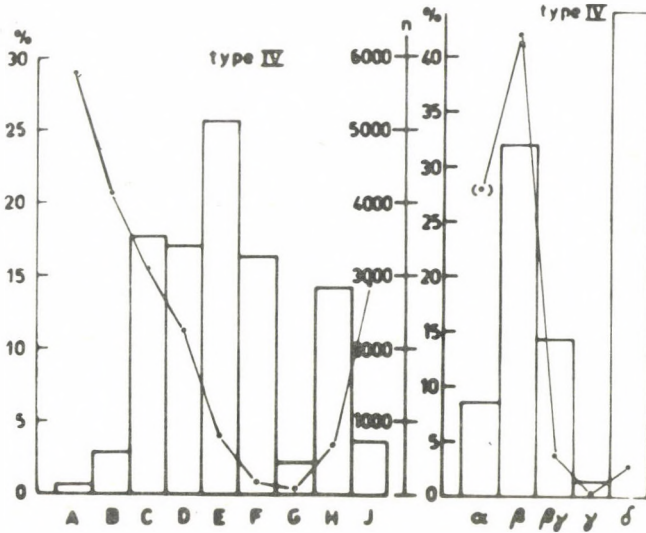


Fig.4. Left-hand side:

Histogram of percentage occurrence of flares with type IV emission (1966-1976) in the individual types of sunspots (Zurich). The curve connects the percentages of the occurrence distribution of all types of sunspot groups throughout the whole cycle (1965-1976).

Right-hand side:

Histogram of percentage occurrence of flares with type IV emission (1966-1976) in the individual sunspot group types according to the magnetic classification. The curve connects the numbers (n) of magnetically determined types of sunspot groups within the same cycle.

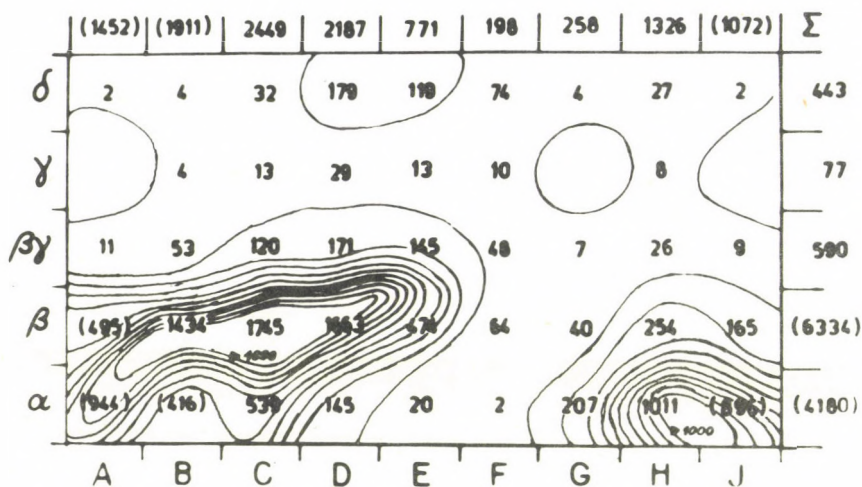


Fig. 5. Occurrence of sunspot groups by Z-type and magnetic classification for the period 1966-1976. Since only magnetically measured groups are involved, the data of small types of group are frequently lacking, the values for these groups are considerably underestimated and are in parentheses. The occurrence isolines have only been plotted up to the value 1000 in steps of 100, above that they are lacking.

IV radio emission separately for Z-types and for magnetic types of sunspot groups is shown in Fig.4. The largest occurrence accumulation is in type E (~25%) and in type δ (over 40%).

The curve in the left-hand histogram represents the reference value of occurrence in % derived from the occurrence of all types of sunspot groups (for details refer to concluding part of Section 2). The curve in the right-hand histogram represents the reference values of occurrence (n) derived from the processed sunspot groups (whose sunspot magnetic field was measured) and is, therefore, not perfectly representative, namely, the number n for type α is severely underestimated {1}.

4. Reference matrix of occurrence of all processed sunspot groups according to both classifications

Using the data in {1}, a matrix of occurrence of the Z-types and magnetic types was constructed, and the sums of the lines (magnetic types) and columns (Z-types) were calculated, see Fig.5. Since only magnetically measured sunspot groups are involved, the data pertaining to small groups of types A and B (which are however most numerous, see Fig.4) and to type α do not reflect reality within the matrix and, therefore, the sums are in parentheses to indicate this. Since magnetic measurements of small groups, mainly types A, B and J, are missing, the values pertinent to these groups show considerably underestimated occurrences (particularly if type α occurs simultaneously). Particularly unrealistic values of occurrence in the matrix are in parentheses.

For the reason given above, the matrix was constructed using occurrence frequencies and not percentages, because the latter would partially distort the correct values for type C, D, E, F, G, H and for types β , $\beta\gamma$, γ , δ . The occurrence values are underestimated with respect to reality, especially in the case of the combinations $A\alpha$, $A\beta$, $B\alpha$ and $J\alpha$, and partly in the case of $B\beta$ and $J\beta$.

5. Conclusion

The series of results presented here indicates that flares with shock waves (with type II emissions) are generated in

sunspot group types which do not display a particularly extreme accumulation of magnetic energy.

Flares associated with the emission of magnetic plasma cloud (type IV radio emissions), on the other hand, display a greater tendency to originate in more complicated active regions in which there is a larger accumulation of magnetic energy (type δ) within a small space.

R e f e r e n c e s

- {1} Knoška,S., Křivský,L., Types of sunspots, magnetic classification and flare yield in cycle No.20, *BAC*, 32, 292, 1981
- {2} Knoška,S., Křivský,L., Occurrence of types of sunspot groups in the cycle No.20, *BAC*, 1984, in press
- {3} Křivský,L., Lukač,B., Catalogue of the solar type II bursts and their source flares for the cycle No.20, *Astr.Obs.Hurbanovo*, 1980
- {4} Krüger,A., Catalogue of solar type IV radio events 1970-1976, 1980 unpublished
- {5} Krüger,A., Fürstenberg,F., Fricke,K.H., Catalogue of solar type IV radio events 1956-1969, *Suppl.Ser.Sol.Data II*, 5, (HHI),Berlin,1971
- {6} McLean,D.J., Shock waves and the ejection of matter from the Sun: radio evidence, *IAU Symp.57*, 301, 1974
- {7} Waldmeier,M., Heliographic maps of the photosphere for the years 1966-1976, *Publ.Sternwarte Zürich*, B1. 13-14, 1966-1977

THE POSITION OF FLARE SEATS IN SUNSPOT UMBRAE

V. P. M A K S I M O V

SibIZMIR, Irkutsk

Abstract:

Some morphological features of flares that cover sunspot umbrae, their possible classification and the importance of studying these events for the construction of flare models, are discussed.

ПОЛОЖЕНИЕ ОЧАГОВ ВСПЫШЕК В ТЕНЯХ СОЛНЕЧНЫХ ПЯТЕН

В. П. МАКСИМОВ

СибИЗМИР, Иркутск

Абстракт:

Обсуждаются морфологические особенности вспышек, покрывающих тени пятен, их возможная классификация и важность изучения этих событий для построения моделей вспышек.

Generally, flares occur in active regions with well-developed sunspots. According to data {1} covering the period 1956-1968, of all flares of importance ≥ 2 only seven percent occurred in regions with small sunspots or without them altogether.

Previous studies of the location of flare seats with respect to sunspots showed that the flare knots usually avoid the sunspot umbra. They are always produced outside sunspots and, once expanded, they even prefer areas of an active region devoid of sunspots {2}. Also, the motion of ribbons of large two-ribbon flares frequently ceases on the boundary of large sunspots {2},{3}.

The aforementioned is widely known and has frequently been reported, albeit without comments, in the literature. Most probably, the observable motion of flare ribbons is not the product of an actual motion of a plasma emitting in $H\alpha$ at the chromospheric level but is caused by a drain-off of plasma and high-energy particles from ever higher magnetic field lines. In such a case it might be expected that an $H\alpha$ flare is not the result of the development of some instabilities within flux tubes of magnetic fields residing in the sunspot umbra. Neither do these flux tubes serve as channels of energy transfer from the source to the chromospheric flare proper. In other words, the energy of a flare is delivered by weaker, more "ruffled" fields than those emanating from sunspot umbrae but a flare situation is created under the action of precisely these latter fields. Since flare ribbons are not observed on the outer boundary of sunspots, the source of energy release of a flare must underlie the loops that interrelate the sunspot umbrae of a given active region.

However, there is evidence that flares do indeed cover sunspot umbrae and are characterized by a variety of important features in the optical {2},{4},{5}, X-rays {2} and in the microwave range {6},{7},{8},{9},{10} as well as by the generation of low-energy cosmic rays and by proton absorption in the polar cap {11}. These features may all be summarized as

follows. Other conditions being equal, flares that cover sunspot umbrae are more powerful.

Investigations of Bumba et al. {12}, {13} showed that large flare seats located in the sunspot umbra, coincide in position with umbral gulfs and photosphere-like light bridges. These regions are intrinsically related to the convective network, and the magnetic field value there is smaller than that in the main umbra. According to {12}, the emission above the sunspot umbra avoids fields with a strength over 2000 G or somewhat higher. There also exists, however, other observational evidence for no bridges or gulfs of penumbra observable in places of flare emission in the sunspot umbra {14}.

From the foregoing it follows that the emission from the location of flare seats in the sunspot umbra may be useful in the determination of spatial structure of a flare in a complex active region and of the height location of the source of energy release in a flare. In order to carry out such investigations it is appropriate to classify the flares in sunspot umbrae. According to data from the literature it is advisable to categorize the flare distribution into the following classes.

I. Coverage of the umbra as a result of the development of large flares.

A. Full or partial coverage of the umbra by a flare ribbon, where systems of flare loops pass above the umbra in a later stage of development. An example is provided by the coverage of sunspot in the 4 August 1972 flare {15} (Fig.1,a).

B. Partial coverage of sunspot umbrae with expanding flare ribbons. Such flares occur in groups with sunspots, in close proximity to the polarity inversion line. Here the seats are often located in penumbral gulfs and photosphere-like light bridges. Examples of such flares are provided by the events of 4 August 1972 {13}, 4 July 1974 {16} and 11 July 1978 {17} (Fig.1,b).

C. Penetration of the flare into the sunspot umbra. The emission penetrates the umbra, spreading along the polarity inversion line or the filament. The seats reside in penumbral

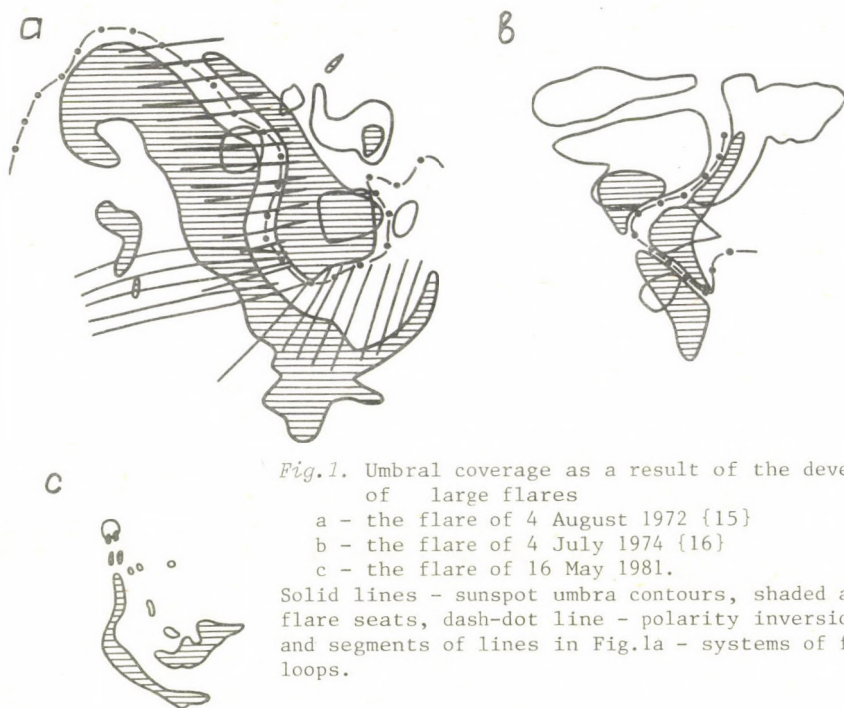


Fig.2. Flares arising in the sunspot umbra and not leaving it in the course of development.

- a - the flare of 29 June 1975
 b - the flare of 29 October 1972
 c - the flare of 1 March 1978

gulfs and photosphere-like light bridges. In contrast to *IB*, these seats do not form the main parts of flare-ribbons. Examples: flare of 6 October 1979 {18} and 16 May 1981 (Fig.1, from a picture in $H\alpha \pm 0.75 \text{ \AA}$).

II. Flares produced in the sunspot umbra and not leaving it in the course of development.

A. The flare is composed of two small ribbons. One is in the sunspot umbra and the other is in the plage area outside the sunspot {14},{19},{20},{21}. The umbra shows neither patches of opposite polarity nor umbral bridges and penumbral gulfs (Fig.2,a, from a picture taken in $H\alpha$, from {14}).

B. The flare consists of one seat in the umbra without any conjugate seat outside the umbra. The only one recorded event of such a type distinguishes itself by a long lifetime of the emission, of about 8 hr (Fig.2,b, from a picture in $H\alpha$, from {22}).

C. Seat in the sunspot umbra arising at the time of a large flare. There is no conjugate seat near the sunspot. The flare process does not preclude a separation of the seat into several parts (Fig.2,c, after a picture in $H\alpha$ from {23}).

In conclusion we will briefly discuss a possible interpretation of individual types of flare. For class *IA* the sunspots appear to have some peculiar properties, namely a large inclination of the sunspot axis to the photosphere and a weaker, diverging with height, magnetic field. Class *IC* may be explainable by a consecutive excitation of a system of small loops, unrelated to the main flare ribbons.

Class *II* events are of particular interest and they are hard to explain in terms of current flare models. At present two interpretations are available for the umbral flare, viz. as the result of emergence of MHD-solitons {19} and as the result of filament activation {21},{22},{23}. At the same time the absence in the umbra of magnetic field patches of opposite polarity, the position of the emission on boundaries of kernels, noncoincidence of seat loci in a sequence of flares occurring in the same sunspot as well as the motion of cores

prior to the flare find a natural and a consistent explanation in a model, suggested by Parker {24} and developed by Vainshtein, for energy release during an interaction of magnetic flux tubes with equidirectional longitudinal and oppositely directed azimuthal magnetic fields. In this case azimuthal magnetic fields of the tubes annihilate as a result of equilibrium loss.

Acknowledgements

The author is grateful to Dr S.A.Yazev for supplying the H α filtergrams for the flare of 16 May 1981. Thanks are also due to V.G.Mikhalkovsky for his assistance in preparing the English version of the manuscript and typing the text.

R e f e r e n c e s

- {1} Dodson,H.W.,Hedeman,E.R., Major H α flares in centers of activity with very small or no spots, *Solar Phys.*13. 401, 1970
- {2} Švestka,Z., *Solar flares*, Reidel Dordrecht, 1976
- {3} Valniček,B., Motion effects in chromospheric flares, *BAC*,12. 237, 1961
- {4} Švestka,Z.,Kopecký,M.,Blaha,M., Qualitative discussion of 244 flare spectra, *BAC*, 12. 229, 1961
- {5} Koval,A.N., The position of moustaches in a spot group relative to the magnetic field, (in Russ.) *Izv.KrAO*. 34. 278, 1965
- {6} Dodson,H.V.,Hedeman,E.R., Survey of number of flares observed during the IGY, *Astron.J.*65. 51, 1960
- {7} Martres,M.,Pick,M., Caractères propres aux éruptions chromosphériques associées à des émissions radioélectriques observées dans le domaine des longueurs d'onde métriques, *C.R.*254. 3975, 1962
- {8} Martres,M.,Pick,M., Caractères propres aux éruptions chromosphériques associées à des émissions radioélectriques, *Ann.Astrophys.*25. 293, 1962
- {9} Malville,J.M.,Smith,S.F., Type IV radiation from flares covering sunspots, *J.G.R.* 68. 3181, 1963
- {10} Hagen,J.R.,Neidig,D.F., Identification of two distinctive types of centimeter radio bursts with flare location, *Solar Phys.*18. 305, 1971
- {11} Ellison,M.A.,McKenna,S.M.P.,Reid,J.H., Cosmic ray flares, *Dunsink Obs.Publ.* 1. 51. 1961
- {12} Bumba,V.,Hejna,L., Some peculiarities in the development of the large August 1972 sunspot group, *BAC* 31. 257, 1980
- {13} Bumba,V.,Suda,J.,Ishkov,V.N., Links of H α -emission features with the underlying elements of sunspot fine structures in some flares, *BAC* 32. 286, 1981

- {14} Tang, F., Umbral flares, *Solar Phys.* 60. 119, 1978
- {15} Mogilevskij, E.I., Energetics and phenomenology of large solar flares, (in Russ.) *Fiz.soln.akt.* 3. 1980
- {16} Babin, A.N., Sunspots motion and the flare on 4 July 1974, (in Russ.) *Izv.KrAO.* 62. 142, 1980
- {17} Dezső, L., Gesztelyi, L., Kondás, L., Kovács, A., Rostás, S., Motions in the solar atmosphere associated with the white light flare of 11 July 1978, *Solar Phys.* 67. 317, 1980
- {18} Ishkov, V.N., Obashev, S.O., Chromospheric observations of the flare event on October 6, (in Russ.) *ICM-SMY Crimean Workshop*, 2. 85, 1981
- {19} Mogilevsky, E.I., Homologous H α -flares in the umbra of AR complex MM-16862-3 in May 1980, (in Russ.) *ICM-SMY Crimean Workshop*, 2. 151, 1981
- {20} Makarova, E.A., Delone, A.B., Kirjuhina, A.I., Jakunina, G.V., Shilova, N.S., Babin, A.N., Koval, A.N., Stepanyan, N.N., Golovko, A.A., Kasinsky, V.V., Some features of preflare situation in the complex HR 16862, 16863, 16864 on the 23-29 of May 1980, (in Russ.) *ICM-SMY Crimean Workshop*, 2. 162, 1981
- {21} Shilova, N.S., Babin, A.N., Delone, A.B., Kirjuhina, A.I., Makarova, E.A., Jakunina, G.V., Mamedov, S.G., Musaev, M.M., Orudjev, A.Sh., Seidov, A.G. H α umbral flares of the end of May 1980, (in Russ.) *ICM-SMY Crimean Workshop*, 2. 180, 1981
- {22} Kubota, J., Tamenaga, T., Kawaguchi, I., Kitai, R., The brightening of sunspot umbra observed on 29 October, 1972, *Solar Phys.* 38. 389, 1974
- {23} Vazquez, M., Herrera, F., An umbral brightening associated with a two-ribbon flare, *Solar Phys.* 64. 329, 1979
- {24} Parker, E.N., Rapid dissipation of magnetic fields in highly conductive fluids, *Preprint E.Fermi Institute*, Univ.Chicago, 1982

ASYMMETRY OF NON-SPLITTING SPECTRAL LINES IN SUNSPOTS

A. L U D M Á N Y

Heliophysical Observatory, Debrecen

Abstract:

Instead of the usual C-shape of the photospheric line asymmetries, an opposite tendency seems to be present in sunspot umbrae for the $\lambda 5713.896$ TiI line in most cases.

АСИММЕТРИЯ НЕРАСЩЕПЛЕННЫХ СПЕКТРАЛЬНЫХ ЛИНИЙ В СОЛНЕЧНЫХ ПЯТНАХ

А. ЛУДМАНЬ

Гелиофизическая Обсерватория, Дебрецен

Абстракт:

Вместо обычной С-формы асимметрии фраунгоферовых линий невозмущенной фотосферы, кажется, обратная тенденция поступает в тених солнечных пятен в линии $\lambda 5713.896$ TiI в большинстве случаев.

Introduction

As is widely accepted, in sunspots the convective motions are inhibited, or at least essentially altered. So such manifestation of the convection as the limb-effect is proven to be absent in sunspots on the basis of Abbe-comparator measurements made by Beckers {1}. But the convective motion field has another effect in the undisturbed photosphere: the well known C-shape of the bisector of the asymmetric lines, see e.g. Dravins {2}. On the other hand, the umbral dots have a granulation-like pattern. Obridko {3} has given more arguments in favour of the two-component model of sunspot umbrae, similar to Schröter's "Zweistrom-Modell" of the limb-effect {4}. So, the study of line-asymmetry, which is a sensible indicator of intensity- and velocity inhomogeneities, may be of importance in umbrae too.

Observations

The asymmetry of a line can be used for velocity field investigations in sunspots only if there are no disturbing circumstances, such as blending or magnetic splitting. The most complete list of $g=0$ lines is given in {5}. So far, mainly the well known $\lambda 5576.099$ FeI line has been used for this purpose, see e.g. {6}, {7}, {8}, but it is not very suitable because it is blended in sunspot umbrae. The most suitable line for asymmetry measurements in sunspots is the $\lambda 5713.896$ TiI. Its main advantages are: $g=0$, no blend, $W=5m\text{\AA}$ in the undisturbed photosphere and considerable strengthening in sunspots. This last point is rather useful, because if there were an asymmetrical line present in the surrounding photosphere, the occasional different photospheric asymmetry could disturb the measurements in the umbrae on account of scattered light.

The observational material has been collected in the Main Astronomical Observatory of the USSR Academy of Sciences in Kiev with the ACU-5 horizontal telescope. I used the spectrograph in the fourth and (later) fifth order (dispersion 2.28 and 4.02 mm/ \AA respectively). The photographic material was ORWO WO-3 or WP-3, width of spectrograph slit 50 micron, exposures ranging from 2 sec to 24 sec depending on the circumstances.

During the observations special care was taken to ensure that the slit was always across the center of the umbrae. During the photometric evaluation a slit height corresponding to 1" was chosen. After photometric calibration the instrumental profile was taken into account.

Presumably the asymmetry, if it exists at all, depends on the size and position (θ) of the spot, they have been determined on the basis of the observational material of the Debrecen Heliophysical Observatory.

Discussion

Fig.1 shows the view of two spots, and the size of one millionth of the solar hemisphere (mh) and the corresponding registered titan line profile with the bisector, the wave-

length scale is centered on the line bottom. These two spots were just on the center of the solar disc at the moment of observation. In Fig.2 the measured bisectors are plotted in different groups according to the size of the spot ($\cos\theta > 0.9$). The first group contains little spots, ($A < 8$ mh), the second contains medium size spots, ($8 \text{ mh} < A < 15 \text{ mh}$) and the third contains large spots ($A > 15 \text{ mh}$). Spots with different θ are shown in Fig.3 independently of their sizes.

It is remarkable that there is a tendency for an asymmetry opposite to that of the photospheric C-shape to develop almost independently of the size of the spot considered. This suggests that the umbral dots could be the reason for line asymmetry. It is shown by model computations that in granular patterns differing from the solar photospheric one, the sense of asymmetry of lines may be opposite to that of the solar photospheric ones, if little bright elements and larger dark intergranular lanes are present {2}. According to the available information on umbral dots {9}, they do have a geometry like this. The variability may be caused by the fact that in the relatively small sunspots a slight change in the bright dots may considerably alter the asymmetry, unlike the quiet photosphere where larger, averaged areas are always considered.

I would like to express my gratitude to the members of the Kiev Institute for their assistance and I am particularly indebted to E.A. Gurtovenko for his encouragement and help, and to S.I. Gandzha for taking the instrumental profile into account.

*

An additional note

During the discussions following the presentation of the above study, V.N. Obridko mentioned that Makita reported similar results to him (to be published) concerning the inversion of asymmetry in sunspots.

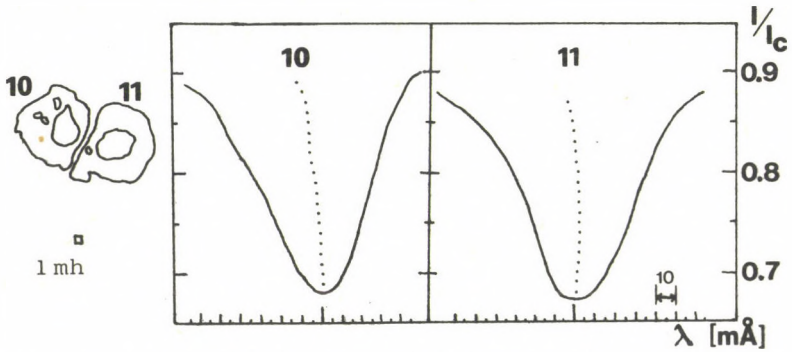


Fig. 1. The view of two sunspots with the titan line profiles with bisectors registered in the spots.

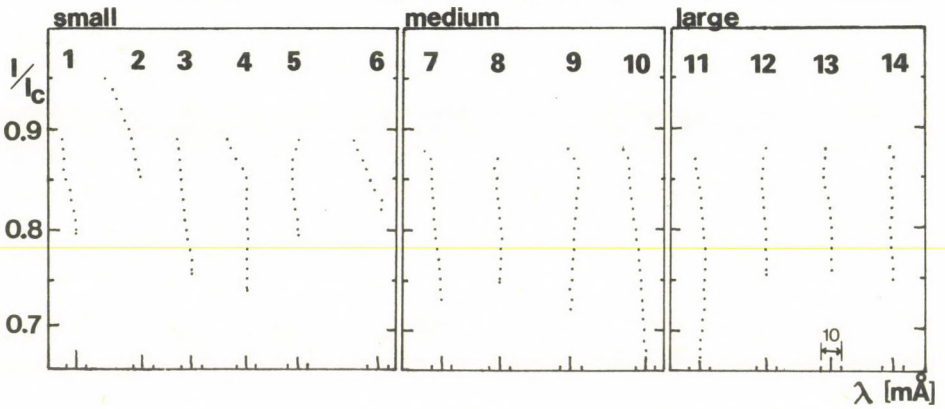


Fig. 2. Bisectors of the Ti line registered in sunspots of different sizes close to the center of the solar disc.

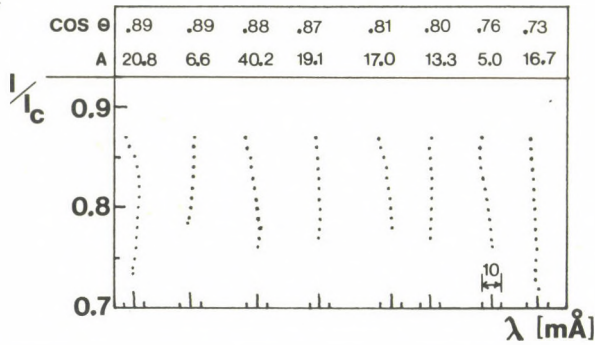


Fig. 3. Bisectors of the Ti line registered in sunspots of different sizes at different position angles.

References

- {1} Beckers, J.M., Material motions in sunspot umbrae, *Ap.J.* 213. 900, 1977
- {2} Dravins, D., Photospheric spectrum line asymmetries and wavelength shifts, *Ann.Rev.Astron.Astrophys.* 20. 61, 1982
- {3} Obridko, V.N., *Thesis*, Moscow, 1980
- {4} Sistla, G., Harvey, J.W., Fraunhofer lines without Zeeman splitting, *Solar Phys.* 12. 66, 1970
- {5} Schröter, E.H., Zur Deutung der Rotverschiebung und der Mitte-Rand-Variation der Fraunhoferlinien bei Berücksichtigung der Temperaturschwankungen der Sonnenatmosphäre, *Z.Astrophys.* 41. 141, 1957
- {6} Holmes, J., A study of sunspot velocity fields using a magnetically undisturbed line, *M.N.* 122. 301, 1961
- {7} Holmes, J., Micrometer and photometric observations of a sunspot velocity field, *M.N.* 126. 155, 1963
- {8} Koch, A., *Dissertation*, Göttingen, 1983
- {9} Bumba, V., Suda, J., Internal structure of sunspot umbrae, *BAC*, 31. 101, 1980

ОПРЕДЕЛЕНИЕ РАССЕЯННОГО СВЕТА В МАЛЫХ СОЛНЕЧНЫХ ПЯТНАХ

М. С О Б О Т К А

Астрон. Инст., Ондřejев

Абстракт:

Для правильного анализа контуров спектральных линий в солнечных пятнах необходимо определить долю α рассеянного фотосферического света. Для того можно пользоваться или приближенной формулой Мальтби, или методом введенным Цваном и Ставеландом.

Второй метод требует определение нескольких параметров дрожания и рассеяния. В случае наблюдений, проведенных на новом горизонтальном солнечном телескопе и спектрографе в Ондřejеве, вкладом рассеяния можно пренебречь. Параметры дрожания определяются по наблюдаемому фотометрическому профилю края диска. Этот профиль является сверткой истинного профиля края и соответствующей функции дрожания (т.е. взвешенной суммы двух или нескольких гауссиан с разными параметрами b_i).

Из предварительных измерений 12 спектров пятен вытекает, что значения α , полученные вышеуказанным методом, в среднем на 15 % меньше значений вычисленных при помощи приближенной формулы Мальтби.

STRAY LIGHT DETERMINATION IN SMALL SUNSPOTS

M. SOBOTKA

Astron. Inst., Ondřejov

Abstract:

Correct analysis of spectral line profiles arising from the spot requires a determination of the fraction α of photospheric stray light. To do the latter, either an approximate formula derived by Maltby, or the method introduced by Zwaan and Staveland can be used. The second method needs a determination of several blurring and scattering parameters. In the case of the observations made by a new horizontal solar telescope spectrograph in Ondřejov, the amount of scattering is negligible. The blurring parameters can be determined from an observed photometric profile of the solar limb. Such a profile is the convolution of a real limb profile and an appropriate spread function (i.e., weighted sum of two or more Gaussian profiles with various parameters b_i).

According to preliminary measurements of 12 sunspot spectra, the values of α , computed by the above method, are on average lower by a factor 0.85 as compared to those obtained from Maltby's approximate formula.

Излучение приходящее из солнечных пятен к наземному наблюдателю всегда искажается светом окружающей фотосферы вследствие рассеяния и турбулентности в атмосфере Земли. Интенсивность наблюдаемая в некоторой точке спектра тени I_u^{obs} состоит с одной стороны из интенсивности I_u излучения, которое действительно возникает в тени, и с другой стороны из некоторой части интенсивности фотосферы I_{ph} .

$$I_u^{obs} = I_u + \alpha I_{ph} \quad (1)$$

Для правильного анализа контуров спектральных линий в пятнах необходимо определить долю α рассеянного фотосферного света. К рассеянному свету особенно чувствительны спектры малых пятен с диаметром 4"-10". В настоящей работе мы будем заниматься именно этим случаем.

Коэффициент α можно определить разными методами. Один метод, например, использует линии ионизированных элементов, которые вероятно не присутствуют в тени (см. напр. {5}). Однако такие линии могут появляться в ярких точках тени и существенно искажать значения α . Наши наблюдения приводят к заключению, что в случае малых пятен этот метод является неподходящим.

В основе других методов лежит измерение хода интенсивности на краю диска Солнца. Цван {6} определил две составляющие рассеянного света: дрожание и рассеяние (в более узком смысле). Дрожание, причиной которого является главным образом атмосферная турбулентность, преобладает до расстояния около 20". Это можно выразить суммой двух двумерных распределений Гаусса

$$\varphi_b(r) = m(\pi b_1^2)^{-1} \exp(-r^2/b_1^2) + (1-m)(\pi b_2^2)^{-1} \exp(-r^2/b_2^2) \quad (2)$$

где r - радиальная координата и m, b_1, b_2 - параметры дрожания. Рассеяние в более узком смысле $|\varphi_s(r)|$ действует до расстояния нескольких минут дуги. Оно обусловлено рассеянием света на оптических поверхностях прибора, или в атмосферной дымке. Общая функция - сумма обеих составляющих:

$$\varphi(r) = (1-\epsilon)\varphi_b(r) + \epsilon\varphi_s(r). \quad (3)$$

Ее параметры можно определить по ходу интенсивности на краю солнечного диска.

Этот подход подробно разработал Ставеланд {4} и его метод широко применяется (см. напр. {1,2}). Недостатком метода является значительная трудоемкость и требования на вычислительную технику, особенно в случае большого количества наблюдательного материала.

Затруднения в определении параметров функции рассеяния из наблюдаемого хода интенсивности на краю диска можно преодолеть при помощи простого графического метода. Сначала мы обратим внимание на первую составляющую - дрожание. Параметры m, b_1, b_2 мы установим по графической записи хода интенсивности на краю диска. Для того мы применим три параметра $TG1, TG2, D$, которые можно непосредственно измерять на графике (рис.1). Измеряемые интенсивности относятся к единичной интенсивности I_0 на расстоянии $30''$ от края диска. $TG1$ - наклон прямой (1), аппроксимирующей наблюдаемый ход интенсивности в области самого большого градиента. Точка перегиба в центре этой области совпадает (с точностью $\pm 0,2''$) с истинным краем диска. $TG2$ - наклон второй прямой (2), которая прокладывается точками в области $2,8''-4,7''$ от края диска. Воспомогательный параметр D - расстояние между максимумами вторых производных хода интенсивности. Непосредственно измеряемые параметры можно присоединить к параметрам дрожания m, b_1, b_2 путем численного моделирования фотометрического профиля края диска (программа SEEING 2). Профиль является сверткой истинного хода интенсивности на краю

$$\begin{aligned} I(x) &= 0 && \text{для } x < 0 \quad (\text{вне диска}) \\ I(x) &= C + d \cdot x^a && \text{для } x \geq 0 \quad (\text{на диске}) \end{aligned} \quad (4)$$

с одномерной функцией дрожания

$$\psi_b(x) = m(\pi^{1/2} b)^{-1} \exp(-x^2/b_1^2) + (1-m)(\pi^{1/2} b_2)^{-1} \exp(-x^2/b_2^2). \quad (5)$$

Величины C, a, d характеризующие потемнение к краю можно найти в работе {4}.

Оказалось что подавляющее большинство всех случаев дрожания, которые допустимы для высококачественного наблюдения пятен,

ТАБЛИЦА 1

Параметры дрожания (M, B1, B2) и непосредственно измеряемые параметры (TG1, TG2, D).

Величина $1/(1-U) - 1$ - коэффициент применяющийся к вычислению доли α рассеянного света при заданном радиусе тени (см. формулу б).
тени (umbra) $\phi = 8.0''$ (сек. дуги)

TG1	TG2	D	M	B1	B2	$\frac{1}{1-U} - 1$	TG1	TG2	D	M	B1	B2	$\frac{1}{1-U} - 1$
1.5964	0.1092	3.1	0.9	2.0	6.0	0.088	1.2070	0.2657	4.0	0.7	2.5	6.0	0.327
1.5818	0.1063	3.1	0.9	2.0	8.0	0.104	1.1628	0.2559	3.8	0.7	2.5	8.0	0.404
1.5731	0.1024	3.1	0.9	2.0	10.0	0.113	1.1363	0.2437	3.8	0.7	2.5	10.0	0.449
1.5683	0.0989	3.1	0.9	2.0	12.0	0.119	1.1206	0.2333	3.8	0.7	2.5	12.0	0.476
1.3541	0.2150	3.8	0.9	2.5	6.0	0.154	1.0711	0.3507	4.7	0.7	3.0	6.0	0.451
1.3394	0.2117	3.8	0.9	2.5	8.0	0.173	1.0268	0.3397	4.7	0.7	3.0	8.0	0.543
1.3307	0.2077	3.8	0.9	2.5	10.0	0.183	1.0001	0.3271	4.6	0.7	3.0	10.0	0.597
1.3257	0.2042	3.8	0.9	2.5	12.0	0.189	0.9839	0.3166	4.5	0.7	3.0	12.0	0.631
1.1791	0.3217	4.6	0.9	3.0	6.0	0.276	0.9689	0.4164	5.5	0.7	3.5	6.0	0.618
1.1644	0.3181	4.5	0.9	3.0	8.0	0.299	0.9245	0.4041	5.4	0.7	3.5	8.0	0.734
1.1556	0.3139	4.5	0.9	3.0	10.0	0.311	0.8976	0.3910	5.4	0.7	3.5	10.0	0.803
1.1503	0.3104	4.5	0.9	3.0	12.0	0.319	0.8812	0.3804	5.4	0.7	3.5	12.0	0.845
1.0474	0.3834	5.4	0.9	3.5	6.0	0.445	0.8895	0.4444	6.3	0.7	4.0	6.0	0.818
1.0326	0.3797	5.4	0.9	3.5	8.0	0.474	0.8450	0.4322	6.2	0.7	4.0	8.0	0.965
1.0237	0.3756	5.3	0.9	3.5	10.0	0.490	0.8181	0.4191	6.1	0.7	4.0	10.0	1.054
1.0184	0.3721	5.3	0.9	3.5	12.0	0.500	0.8014	0.4086	6.1	0.7	4.0	12.0	1.110
0.9455	0.4396	6.1	0.9	4.0	6.0	0.653	1.2966	0.2289	3.1	0.6	2.0	6.0	0.365
0.9307	0.4355	6.1	0.9	4.0	8.0	0.692	1.2358	0.2060	3.1	0.6	2.0	8.0	0.476
0.9217	0.4311	6.1	0.9	4.0	10.0	0.713	1.2007	0.1905	3.1	0.6	2.0	10.0	0.543
0.9163	0.4276	6.1	0.9	4.0	12.0	0.726	1.1799	0.1767	3.1	0.6	2.0	12.0	0.585
1.4957	0.1452	3.1	0.8	2.0	6.0	0.167	1.1334	0.2910	4.0	0.6	2.5	6.0	0.434
1.4665	0.1395	3.1	0.8	2.0	8.0	0.205	1.0744	0.2780	3.9	0.6	2.5	8.0	0.557
1.4491	0.1318	3.1	0.8	2.0	10.0	0.227	1.0389	0.2618	3.8	0.6	2.5	10.0	0.632
1.4393	0.1248	3.1	0.8	2.0	12.0	0.240	1.0175	0.2479	3.8	0.6	2.5	12.0	0.679
1.2806	0.2403	3.8	0.8	2.5	6.0	0.235	1.0170	0.3652	4.7	0.6	3.0	6.0	0.557
1.2511	0.2338	3.8	0.8	2.5	8.0	0.278	0.9579	0.3505	4.7	0.6	3.0	8.0	0.703
1.2336	0.2257	3.8	0.8	2.5	10.0	0.303	0.9222	0.3337	4.7	0.6	3.0	10.0	0.793
1.2233	0.2187	3.8	0.8	2.5	12.0	0.317	0.9003	0.3197	4.6	0.6	3.0	12.0	0.850
1.1251	0.3362	4.7	0.8	3.0	6.0	0.358	0.9296	0.4228	5.6	0.6	3.5	6.0	0.721
1.0956	0.3289	4.6	0.8	3.0	8.0	0.410	0.8703	0.4065	5.5	0.6	3.5	8.0	0.901
1.0779	0.3205	4.5	0.8	3.0	10.0	0.440	0.8344	0.3889	5.4	0.6	3.5	10.0	1.014
1.0673	0.3135	4.5	0.8	3.0	12.0	0.458	0.8121	0.3748	5.4	0.6	3.5	12.0	1.085
1.0082	0.4099	5.4	0.8	3.5	6.0	0.527	0.8615	0.4617	6.4	0.6	4.0	6.0	0.913
0.9786	0.4018	5.4	0.8	3.5	8.0	0.594	0.8022	0.4437	6.3	0.6	4.0	8.0	1.138
0.9608	0.3930	5.4	0.8	3.5	10.0	0.632	0.7661	0.4254	6.2	0.6	4.0	10.0	1.281
0.9498	0.3685	5.4	0.8	3.5	12.0	0.655	0.7436	0.3990	6.1	0.6	4.0	12.0	1.373
0.9175	0.4420	6.2	0.8	4.0	6.0	0.732	1.1958	0.2646	3.1	0.5	2.0	6.0	0.492
0.8879	0.4338	6.1	0.8	4.0	8.0	0.818	1.1221	0.2483	3.1	0.5	2.0	8.0	0.663
0.8700	0.4251	6.1	0.8	4.0	10.0	0.868	1.0779	0.2280	3.1	0.5	2.0	10.0	0.771
0.8589	0.4181	6.1	0.8	4.0	12.0	0.899	1.0495	0.2028	3.1	0.5	2.0	12.0	0.840
1.3951	0.1813	3.1	0.7	2.0	6.0	0.258	1.0597	0.3163	4.0	0.5	2.5	6.0	0.561
1.3512	0.1727	3.1	0.7	2.0	8.0	0.327	0.9860	0.3001	4.0	0.5	2.5	8.0	0.748
1.3250	0.1611	3.1	0.7	2.0	10.0	0.367	0.9415	0.2799	3.8	0.5	2.5	10.0	0.868
1.3098	0.1507	3.1	0.7	2.0	12.0	0.391	0.9141	0.2626	3.8	0.5	2.5	12.0	0.946

TG1	TG2	D	M	B1	B2	$\frac{1}{1-U}^{-1}$	TG1	TG2	D	M	B1	B2	$\frac{1}{1-U}^{-1}$
0.9630	0.3797	4.9	0.5	3.0	6.0	0.681	0.9867	0.3557	4.1	0.4	2.5	6.0	0.711
0.8890	0.3614	4.7	0.5	3.0	8.0	0.901	0.8975	0.3221	4.0	0.4	2.5	8.0	0.993
0.8442	0.3404	4.7	0.5	3.0	10.0	1.043	0.8438	0.2980	3.9	0.4	2.5	10.0	1.184
0.8163	0.3229	4.7	0.5	3.0	12.0	1.136	0.8104	0.2773	3.8	0.4	2.5	12.0	1.314
0.8902	0.4293	5.7	0.5	3.5	6.0	0.838	0.9089	0.3942	5.0	0.4	3.0	6.0	0.826
0.8161	0.4088	5.6	0.5	3.5	8.0	1.105	0.8201	0.3722	4.8	0.4	3.0	8.0	1.150
0.7711	0.3869	5.4	0.5	3.5	10.0	1.281	0.7661	0.3470	4.7	0.4	3.0	10.0	1.375
0.7429	0.3692	5.4	0.5	3.5	12.0	1.397	0.7321	0.3260	4.7	0.4	3.0	12.0	1.529
0.8336	0.4632	6.6	0.5	4.0	6.0	1.018	0.8509	0.4357	5.9	0.4	3.5	6.0	0.973
0.7594	0.4406	6.4	0.5	4.0	8.0	1.344	0.7619	0.4112	5.7	0.4	3.5	8.0	1.356
0.7142	0.4178	6.3	0.5	4.0	10.0	1.564	0.7077	0.3849	5.6	0.4	3.5	10.0	1.629
0.6857	0.3997	6.2	0.5	4.0	12.0	1.713	0.6734	0.3636	5.4	0.4	3.5	12.0	1.819
1.0949	0.3003	3.3	0.4	2.0	6.0	0.645	0.8057	0.4646	6.8	0.4	4.0	6.0	1.136
1.0065	0.2807	3.1	0.4	2.0	8.0	0.903	0.7166	0.4376	6.6	0.4	4.0	8.0	1.594
0.9530	0.2565	3.1	0.4	2.0	10.0	1.077	0.6623	0.4102	6.4	0.4	4.0	10.0	1.928
0.9202	0.2355	3.1	0.4	2.0	12.0	1.194	0.6277	0.3884	6.3	0.4	4.0	12.0	2.165

(Единицы B1, B2, D - сек. дуги. M - относительный вес. TG1, TG2 вычислены для единичного расстояния равного 10'' и единичной интенсивности равной интенсивности излучения фотосферы на расстоянии 30'' от края диска.

ТАБЛИЦА 2

Предварительные результаты

m, b_1, b_2 - параметры дрожания, r_u - радиус тени, I_u^{obs}/I_{ph} - отношение наблюдаемых интенсивностей непрерывного спектра тени и фотосферы,

$\alpha = (1 - I_u^{obs}/I_{ph}) [1/(1-U) - 1]$ - модифицированный метод Ставеланда,

$\alpha_M = 4I_{r_u}/I_{30}$ - метод Мальтбу.

Пластика No	Дата	UT	λ nm	m	b_1	b_2	r_u	I_u^{obs}/I_{ph}	α	α_M
					"	"				
25	82, VII, 10	05:56	517.7	0.7	2.5	10	3	0.629	0.29	0.22
29	82, VII, 10	06:49	614.9	0.7	2	6	3	0.502	0.22	0.23
44	82, VII, 15	07:11	543.4	0.8	3	8	4	0.653	0.14	0.28
45	82, VII, 15	07:34	530.6	0.8	3.5	10	4	0.662	0.21	0.33
58	82, VIII, 12	07:04	517.7	0.6	2	6	3 7	0.784 0.093	0.13 0.09	0.29 0.09
67	82, VIII, 13	05:55	517.7	0.9	2.5	6	3 4	0.401 0.386	0.25 0.09	0.21 0.09
68	82, VIII, 13	07:00	543.4	0.9	2	12	3 4	0.568 0.506	0.10 0.06	0.07 0.05
69	82, VIII, 13	07:30	589.3	0.9	2	6	3 4	0.531 0.319	0.10 0.06	0.17 0.12

можно аппроксимировать 120 комбинациями параметров в пределах $2'' \bar{z}_1 \bar{z} 4''$, $6'' \bar{z}_2 \bar{z} 12''$, $0,4 \bar{z}_m \bar{z} 0,9$. Для этих случаев вычислялся ход интенсивностей на краю диска и с его помощью непосредственно измеряемые параметры TG1, TG2, D. Результаты указаны в таблице I. Пользуясь этой таблицей, мы способны найти параметры дрожания соответствующие непосредственно измеряемым параметрам TG1, TG2, D. Ошибка: определения коэффициента α вытекающая из возможной неоднозначности не превышает 6%.

Доля α рассеянного света определяется по известным параметрам дрожания при помощи метода Ставеланда {4}, который можно существенно упростить для случая малого кругообразного пятна не обладающего развитой полутенью. Для пятна с диаметром тени r_u ($2'' \bar{z}_1 \bar{z} 5''$) мы просто находим

$$\alpha = (1 - I_u^{obs} / I_{ph}) (1 / (1 - U) (1 - Z) - 1). \quad (6)$$

I_u^{obs} и I_{ph} - наблюдаемые интенсивности непрерывного спектра тени и фотосферы а функция U характеризует влияние дрожания:

$$U = m \exp(-r_u^2 / b_1^2) + (1 - m) \exp(-r_u^2 / b_2^2). \quad (7)$$

Величина Z выражает вклад рассеяния в более узком смысле. Ее можно находить напр. по интенсивностям непрерывного спектра в центре диска и в ореоле на расстоянии 1' и 5' от края диска (Ставеланд, 1972). Для большей части наблюдений полученных с помощью большого горизонтального солнечного телескопа и спектрографа (HSFA 2) в Ондражееве наблюдаемые значения Z практически постоянны и равны $0,01 \pm 0,002$. Доля ϵ рассеяния (см. формулу 3) всегда меньше 0,1. Поэтому в формуле (6) величиной Z можно пренебречь.

Мальтби опубликовал очень простой метод определения рассеянного света основанный на измерении интенсивности излучения только в двух точках - на диске, на расстоянии 30'' от края (I_{30}) и вне диска - на расстоянии совпадающем с радиусом тени (I_{r_u}) {3}.

$$\alpha = 4 I_{r_u} / I_{30}. \quad (8)$$

В таблице II приведены предварительные результаты, полученные как модифицированным методом Ставеланда, так и методом

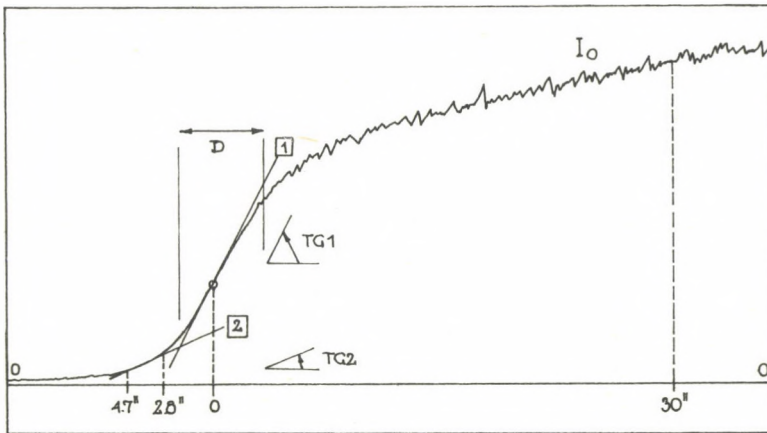


Рис. 1. Определение непосредственно измеряемых параметров из графика хода интенсивности в окрестности края диска Солнца.
 I_0 - единичная интенсивность, TG1 - наклон прямой 1, TG2 - наклон прямой 2, D - расстояние, на котором ход интенсивности мало отличается от прямой 1.

Мальтби. Пользуясь обеими методами, мы обработали 8 пластинок с 12 спектрограммами пятен в различных длинах волн. Все наблюдения проводились на горизонтальном солнечном телескопе HSFA 2 Ондражевской обсерватории.

В большей части случаев результаты полученные обеими методами очень близки друг к другу. Однако, на некоторых спектрограммах доля рассеянного света вычисленная при помощи модифицированного метода Ставеланда в сравнении с методом Мальтби недооценивается. Объяснение может заключаться в следующем: модифицированный метод Ставеланда сильно зависит от наблюдаемого отношения интенсивностей непрерывного спектра тени и фотосферы. В случае выдержек порядка 10 секунд малое пятно может в течение экспонирования под влиянием дрожания и неточности гидирования уходить с цели спектрографа. В следствие того растет наблюдаемое отношение I_u^{obs}/I_{ph} и уменьшается α (см. формулу 6). Из приведенных данных вытекает, что модифицированный метод Ставеланда дает в среднем значение α на 15% меньше по сравнению с методом Мальтбу.

Исследования, описанные в этой работе, проходят в рамках научной аспирантуры в Ленинградском государственном университете под руководством В.В. Соболева. Микрофотометрическая обработка большей части материала проводилась в Крымской астрофизической обсерватории. Автор хотел бы выразить глубокую благодарность Н.Н. Степанян за ценные советы и помощь.

Л и т е р а т у р а

- {1} Bachmann, G., Jäger, F.W., Künzel, H., Pflug, K., Staude, J., Methodical experiences regarding the measurements of solar magnetic fields at the Sonnenobservatorium Einsteinturm, *HHI-STP Rept. No. 4*, Berlin, 1975
- {2} Brahde, R., Stray light in solar observations, a method of numerical integration, *Inst. Theor. Astrophys. Blindern-Oslo, Rept. No. 41*, 1974
- {3} Maltby, P., The effect of scattered light on solar intensity observations as derived from 9 May, 1970 Mercury transit, *Solar Phys.* 18. 3, 1971
- {4} Staveland, L., Correction of solar intensity measurements for stray light, *Inst. Theor. Astrophys. Blindern-Oslo, Rept. No. 36*, 1972
- {5} Stellmacher, G., Wiehr, E., Magnetically non split lines in sunspots, *Astron. Astrophys.* 7. 432, 1970
- {6} Zwaan, C., Sunspot models, *Rech. Astron. Obs. Utrecht XII(4)*, 1, 1965

MINIMUM INSTRUMENTAL POLARIZATION AT COELOSTAT TELESCOPE

G. BACHMANN, K. PFLUG

"Einsteinturm" Solar Obs., Potsdam

Abstract:

A new vector magnetograph, now in operation, permits measurements to the amount of polarization of 0.0005 and thus demands the application of precautions with respect to the instrumental polarization caused by the mirrors of the tower telescope. Within the calibration measurements in 1982, we also carried out measurements of the instrumental polarization in the meridian position of the coelostat. In the channels for the transverse magnetic field we obtained as strong signals as from magnetic fields of 1000 G. This was the reason why, as a first precaution, we introduced the compensation by means of a tilted glass plate. With the necessary large inclination angles, however, it produced losses in brightness and image quality. Therefore, we prepared further precautions searching for optimum azimuth angles of the auxiliary coelostat mirror which provide less instrumental polarization. The results have shown that for each hour angle an auxiliary azimuth exists, where one of the three components of instrumental polarization caused by intensity crosstalk is zero. This offers the opportunity to diminish the two linear components or to eliminate the circular component, which is very difficult in any other way.

МИНИМАЛЬНАЯ ИНСТРУМЕНТАЛЬНАЯ ПОЛЯРИЗАЦИЯ НА ЦЕЛОСТАТНОМ ТЕЛЕСКОПЕ

Г. БАХМАНН, К. ПФЛУГ

Солн. Обс. "Эйнштейнтурм", Потсдам

Абстракт:

Введенный в эксплуатацию новый векторный магнитограф позволяет измерять величину поляризации света до 0.0005 и учёта инструментальной поляризации, возникающей на зеркалах целостата. В 1982 г. мы провели, одновременно с калибровочными измерениями, измерения инструментальной поляризации целостата в меридиане. В каналах для поперечного магнитного поля были получены такие сильные сигналы, какие соответствовали в магнитному полю и 1000 Г. Это явилось причиной того, что, как первая мера, была введена компенсация с помощью наклонной стеклянной пластинки. Однако, необходимые при этом большие углы наклона пластинки, особенно в полдень, приводят к потере яркости и ухудшению качества изображения. Мы подготовили дальнейшие меры напротив инструментальной поляризации путём оптимальных азимутов вспомогательного зеркала. Для каждого часового угла существует азимут, где один из трёх компонент вызванных превращением не-поляризованного света в поляризованный равен нулю. Так можно понижать линейные компоненты или устранять циркулярный компонент, что другим образом очень трудно.

1. Introduction

Polarization measurements at solar tower telescope are in general strongly disturbed by instrumental polarization originating by reflexion on the mirror surfaces. The problem has already been extensively discussed for the Einstein tower by Jäger and Oetken {1},{2}. It was shown that the mirrors produce a variable instrumental polarization depending on hour angle and declination of the Sun, and that especially weakly polarized solar radiation is strongly changed. The authors proposed to take precautions by using special analyzers and compensators, by applying differential elimination methods, and by restrictions of special azimuth angles of the coelostat. In the following we want to describe in detail the results of measurements carried out with such special azimuth angles.

2. Instrumental polarization and its compensation

As already mentioned above, in the Einstein tower the image forming system is a coelostat telescope. Because of its variable instrumental polarization it is necessary to calibrate the system telescope plus magnetograph before and after magnetic field measurements. Such calibrations are carried out using linear polarizer and quarterwave plate above the main mirror of the coelostat. Sunlight of the undisturbed disk centre provides then total polarized light of a definite polarization state. For the elimination of illumination errors we chose 16 different polarization states of the light entering the telescope. The corresponding output signals of the magnetograph are recorded on magnetic tape. For such measurements about 5 minutes are necessary.

In 1982 we got many calibrations in this way and were able to calculate, by means of the method of least mean squares, the matrix of the system telescope plus magnetograph. The results have distinctly shown the influence of temporal variations of the instrumental polarization.

The calibration measurements always included measurements without polarizing optics above the coelostat to find the contribution of the intensity to the instrumental polarization.

These measurements were carried out in the meridian position of the coelostat. In Fig.1 the results are shown. We can see that this contribution to the instrumental polarization has a maximum perpendicular to the plane of incidence of auxiliary coelostat mirror and third mirror. From morning to noon this portion grows to about 5 percent and then decreases again. The second portion in the plane 45° to the former changes the sign at noon, but has a comparable amount in the morning and the afternoon. The circularly polarized portion was always about one percent.

The results of our measurements in Fig.1 have shown that the instrumental polarization attains a value just like a transverse magnetic field of about 1000 G. In this way the determination of weak transverse magnetic fields is, in practice, impossible. Before the scanning of an active region it was, therefore, necessary to compensate for the main linear portion of the instrumental polarization by means of a glass plate which can be tilted about two axes, perpendicular to one another. Compensation of 5 percent requires, however, large inclination angles of the glass plate, resulting in a loss of brightness and image quality. Moreover, in the morning the instrumental polarization changes so quickly that the compensation only holds for about 10 minutes. Thus, the reduction of magnetic field measurements is complicated.

3. Minimization of instrumental polarization

The construction of our coelostat with the two mirrors mounted on a rotating ring with axis in the optical axis of the telescope offers the opportunity to turn the auxiliary in different azimuth angles relative to the main mirror. In this way we have a certain freedom choosing the relative angle between the planes of reflexion and thus in the amount of instrumental polarization. Corresponding to calculations the mirrors of the tower telescope produce in the meridian position, generally used until now, about 5 percent of instrumental polarization at noon and about 1 percent in the morning (hour angle -6 h). Moreover, it is shown that azimuth angles of the

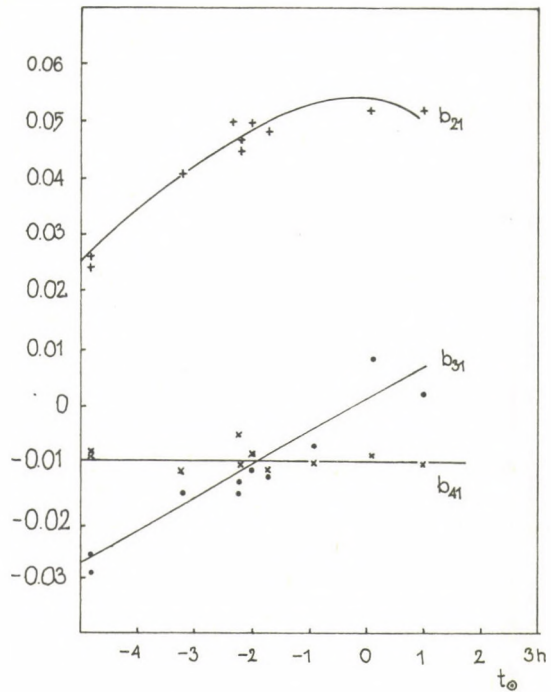


Fig. 1. Instrumental polarization transformed from unpolarized sunlight by the tower telescope for declination 20° and meridian position of the coelostat.

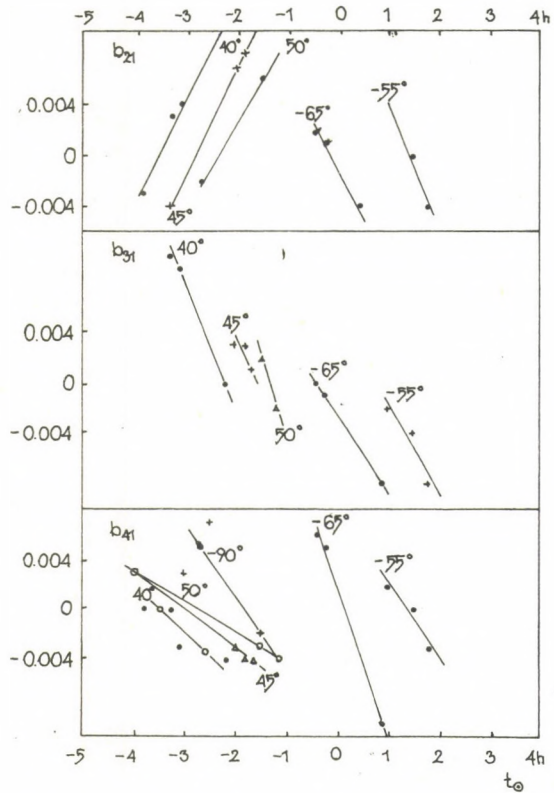


Fig. 2. The behaviour of the elements b_{21} , b_{31} and b_{41} of the system matrix at its minimum.

auxiliary different from 0° can also provide smaller instrumental polarization at noon.

The success in measuring the instrumental polarization in the meridian encouraged us also to determine it for more favourable positions of the auxiliary. On two days in September and October 1982, the azimuth angle of the auxiliary was searched for different hour angles, where the contribution of intensity to the instrumental polarization attains a minimum. For different azimuth angles the degree of polarization is measured as a function of hour angle. The Sun's declination was -2° resp. -4° .

In Fig.2, the matrix elements b_{21} , b_{31} and b_{41} presented as a function of the hour angle. One can see that they change their sign for some azimuth angles of the auxiliary, i.e. they are zero for certain hour angles. However, the zero points are not attained at the same time, therefore the total polarization is not zero, but attains amounts of about 0.001.

We suppose that for the other azimuth angles there also exist hour angles, where one of the two parameters becomes zero. We estimated these hour angles from the results shown in Fig.2 by interpolation or extrapolation. The results are presented in Fig.3. In the morning positive azimuth angles should be preferred, but later negative angles provide better results. For some combination of azimuth and hour angle we calculated b_{21} , b_{31} and b_{41} by interpolating between measurements.

For hour angles between -2 and $+2$ hours negative azimuth angles of the auxiliary furnish the smallest linear polarization. At hour angles less than -3 hours it is necessary to proceed to positive auxiliary azimuth angles.

An important problem now is the behaviour and the value of the instrumental polarization for larger declinations than 0° , because magnetic field measurements are usually carried out at declinations larger than 10° .

By applying these results we hope to attain the sensitivity of 0.0005 in our polarization measurements, which is set by the magnetograph.

The method described here is generally recommended for two-mirror system, too.

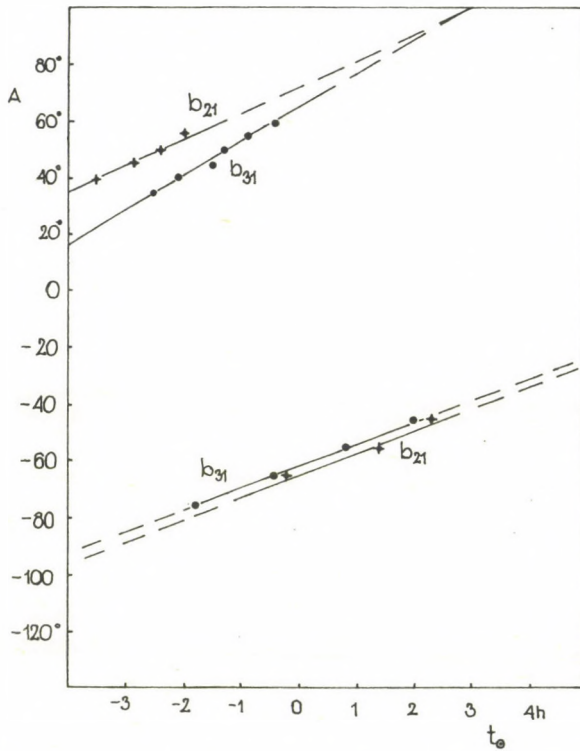


Fig.3. Combinations of auxiliary coelostat mirror azimuth and hour angle of the Sun for minimum linear instrumental polarization at the Einstein tower telescope.

References

- {1} Jäger, F.W., Oetken, L., Zur Theorie und Praxis der instrumentellen Polarisation, *Publ. Astrophys. Obs. Potsdam* No.103, 1963
- {2} Jäger, F.W., Oetken, L., Zur Theorie und Praxis der instrumentellen Polarisation II., *Publ. Astrophys. Obs. Potsdam* No.107, 1968

SYNTHESIS OF H α -PROFILES FROM FILTER TRANSMISSION FUNCTIONS

T. B A R A N Y I, A. L U D M Á N Y

Heliophysical Observatory, Debrecen

Abstract:

A method of obtaining spectral information from filtergrams is described. The transmission features of the Halle-type Lyot-filter are investigated and the process of analytical representation of H α -profiles from transmission functions is studied.

СИНТЕЗ ПРОФИЛЕЙ H α ИЗ ФУНКЦИЙ ПРОПУСКАНИЯ ФИЛЬТРА

Т. БАРАНИ, А. ЛУДМАНЬ

Гелиофизическая Обсерватория, Дебрецен

Абстракт:

Представлена методика приобретения спектральной информации из фильтрограмм. Исследованы свойства пропускания фильтра Лью типа Халлэ и разработано аналитическое представление профилей H α из функций пропускания.

Many attempts have been made to obtain spatial and spectral information on solar features simultaneously. There are two types of approach: 1./ sampling by wavelengths - the information is mainly of a spatial nature as, for instance, in the well-known velocity field-investigations in {1} and {2} where monochromatic images were made in both of the red and blue line wings and then compared; another type is the subtractive spectrograph, see e.g. {3} and {4}; moreover it is possible by tunable birefringent filters, as was shown by LaBonte B. {5}, who has built up the line profile on the basis of a series of filtergrams taken by 0.15 Å steps; 2./ spatial sampling - the information is mainly of spectral type, this is the case in the multi-slit spectrographs, see e.g. {6}.

The main dilemma is the same in all cases: it is practically impossible to achieve high spectral, spatial and temporal resolving power simultaneously. The present paper deals with the following problem: what are the principal limitations of the birefringent filters from a spectroscopic point of view, how can we build up H α -profiles from filtergram-photometry most reliably?

We used the large coronagraph-spectrograph of the Debrecen Heliophysical Observatory for the determination of the transmission function of the Halle-type Lyot-filter of the observatory. The method and results are similar to those in {7}. We illuminated the filter with a lamp of continuous spectrum and obtained the "filter-spectrum" on the spectral plate with solar reference spectrum. Then the spectra were measured with a microphotometer, the results are presented in Fig.1. It is remarkable that in the 0.5 Å mode the halfwidth of the filter profiles is about 0.4 Å, and by tuning the filter off-band, a secondary maximum appears on the other side of the H α -line.

The following dilemma in building up the H α -profile from filtergrams was encountered: on the one hand the usual 0, ± 0.5 , ± 1 Å series is not fine enough, on the other in a series by 0.1 Å steps there is a lot of overlapping and so the same spectral part is taken into account many times. Generally, much spectral information seems to be lost by the fact that the transmission function covers quite a wide spectral interval, where the incoming distribution may have considerable changes.

We think that this incident intensity distribution can be partly reconstructed if we deal not only with the photometric densities but with the transmission functions as well. For this purpose these functions have to be expressed analytically. As is well known from the theory of the Lyot-type birefringent filters, the general form of these functions is:

$$(1) \quad T(\lambda) = \prod_{j=1}^m \cos^2 \left[\pi \frac{d_j(\varepsilon - \omega)}{\lambda} \right] = \prod_{j=1}^m \cos^2 \left[\pi \frac{n_j \lambda_{H\alpha}}{\lambda} \right]$$

where j is the number of units in the filter and $d_j(\varepsilon - \omega)$ is

the optical path difference between the ordinary and extraordinary rays in the consecutive j units. We obtained the best fit with the measured profiles by using the following series of n_j parameters:

$$6272, 3136, 3136, 1568, 784$$

The resulting analytical filter profiles are plotted in Fig.2. They match the measured profiles within the accuracy of the measurement. Fig.3 shows a whole series of transmission functions shifted by 0.1 \AA steps.

We are looking for a ϕ function approaching the profile $H\alpha(\lambda)$ with the condition:

$$(2) \quad M = \int_{\lambda_1}^{\lambda_2} [H\alpha(\lambda) - \phi(\lambda)]^2 d\lambda \rightarrow \min$$

Denote by $\phi_i(\lambda)$, the different transmission profiles shifted to given λ_i wavelengths and consider the following representation:

$$(3) \quad \phi(\lambda) = \sum_{i=0}^n a_i \phi_i(\lambda)$$

so, with the (2) condition we get:

$$(4) \quad \frac{1}{2} \frac{\partial M}{\partial a_k} = \sum_{i=0}^n a_i \int_{\lambda_1}^{\lambda_2} \phi_i(\lambda) \phi_k(\lambda) d\lambda - \int_{\lambda_1}^{\lambda_2} H\alpha(\lambda) \phi_k(\lambda) d\lambda = 0$$

$k=0, \dots, n$

In words: we represent an approximation of the $H\alpha$ -profile by the linear combination (3). The a_i combining constants are determined by the inhomogeneous linear equation system (4), where the coefficients of the a_i variables are the inner products of the transmission functions and the constant members are the inner products of the transmission profiles with the $H\alpha$ -profile, these constants are the measurable intensities transmitted by the filter.

As a test, make a trial with the $0, \pm 0.5, \pm 1 \text{ \AA}$ series. Let the constants in the eq. (4) be computed values, namely the inner products of ϕ_k -s with the $H\alpha$ -profile from the {8}

solar spectrum atlas, and try to reconstruct the original line with this method. The result (for an improperly installed filter, shifted by 70 mÅ) is plotted in Fig.4. Rather ugly!

The ϕ function can be smoothed by using more ϕ_i functions (Fig.5), but the deviations from the H α still remain considerable. The main reason for this differences is the presence of the parasitic secondary maxima mentioned above. A much better fit can be achieved by diminishing the considered spectral interval. Fig.6 shows the ϕ for the (-0.8Å) - (+0.8Å) interval by a dotted (....) line, there are already deviations from the atlas-profile (----) only at the limits of the interval. The figures 7. and 8. show the reconstructions of arbitrarily constructed H α flare profiles.

The spectral resolving power has been estimated as follows: as an incident distribution we considered a pseudo delta function, a rectangular intensity distribution ($\Delta\lambda=0.01\text{Å}$, $I=1$) and tried to reconstruct it with this method. The result is shown in Fig.9. So the principal resolving power can be defined as the difference between the maximum and the first minimum (here 0.3Å).

A possible improvement in the result can be made by reconstructing the constant unity function (Fig.10). If we take the deviations of the unity function from the reconstructed one into account, the combination perfectly fits the H α -profile (Fig.6 continuous line, here only the little blend remained unaccounted for).

The constants in the eq. (4) will be determined relatively to the undisturbed intensities and so it is extremely crucial that the measured densities of the quiet chromosphere represent the real intensities. The filter central wavelength changes by its temperature, some preliminary data are given in Fig.11 for this dependence. The proper installation of the filter has to be checked photoelectrically before every observation, by shifting the transmission maximum and measuring the resulting intensity distribution. The temporal resolving power is limited by the fact that by automatic cameras a speed of about

1.4 exposure/sec can be attained, so the required 22 exposures can be made in about 16 sec.

In spite of the spectral and temporal restrictions, the above method may be recommended in such cases, when high spatial resolution is needed as, for instance, in the case of solar features, which can hardly be installed on the spectrograph slit.

We are indebted to Dr Béla Kálmán, head of Heliophysical Observatory, for his continuous interest and help in this work, and thanks are due to Dr István Mezei from the Department of Mathematical Analysis of Eötvös University, Budapest for his helpful comments.

R e f e r e n c e s

- {1} Leighton, R.B., Noyes, R.W., Simon, G.W., Velocity fields in the solar atmosphere, *Ap.J.* 135. 474, 1962
- {2} Beckers, J.M., High-resolution measurements of photosphere and sunspot velocity and magnetic fields using a narrow-band birefringent filter, *Solar Phys.* 3. 258, 1968
- {3} Mein, P., Blondel, M., A subtractive double-pass spectrograph for solar observations, *Solar Phys.* 27. 489, 1972
- {4} Mein, P., Multi-channel subtractive spectrograph and filament observations, *Solar Phys.* 54. 45, 1977
- {5} LaBonte, B.J., A measurement of the Helium D₃ profile with a birefringent filter, *Solar Phys.* 53. 369, 1977
- {6} Martin, S.F., Ramsey, H.E., Carroll, G.A., Martin, D.C., A multi-slit spectrograph and H α Doppler system, *Solar Phys.* 37. 343, 1974
- {7} Krafft, M., Spectroscopic investigation of a birefringent Lyot-filter for H α , *Solar Phys.* 5. 462, 1968
- {8} Beckers, J.M., Bridges, C.A., Gilliam, L.B., *A high resolution spectral atlas of the solar irradiance from 380 to 700 nanometers*, Sacramento Peak Observatory Project 7649, 1976

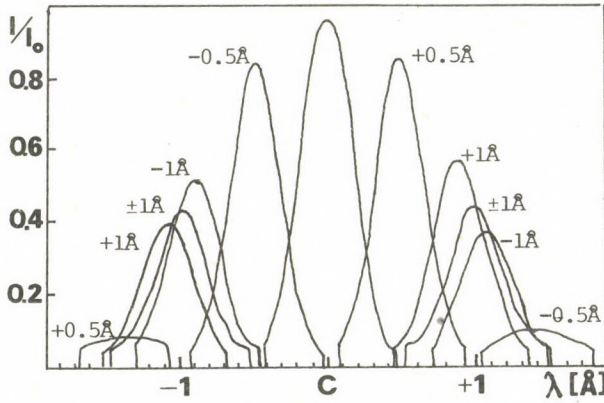


Fig. 1. Measured filter transmission functions

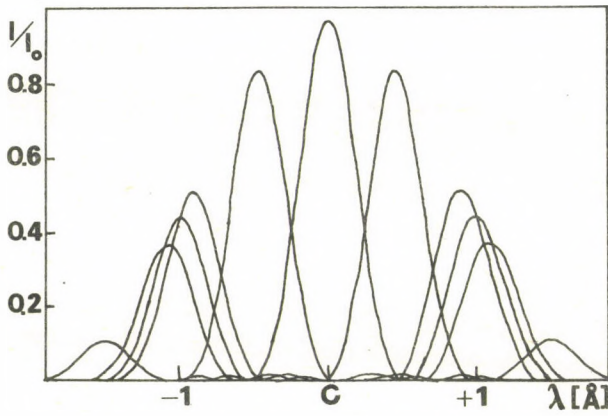
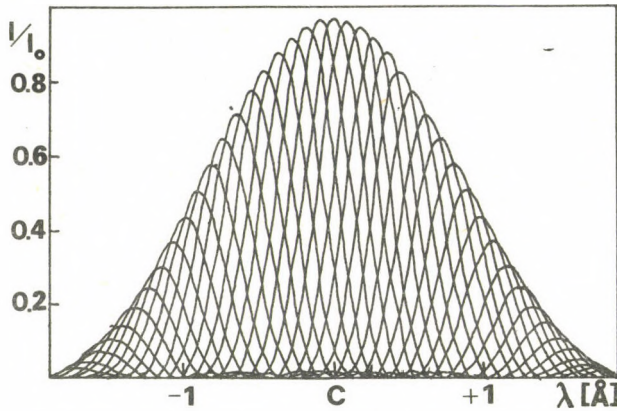


Fig. 2. Computed filter transmission functions

Fig. 3. Computed filter transmission functions by 0.1 \AA steps.

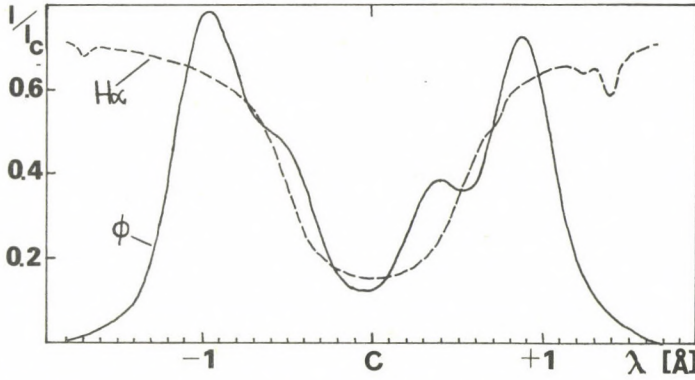


Fig.4. Reconstruction of the H α -profile from the 0, $\pm 0.5, \pm 1 \text{\AA}$ series

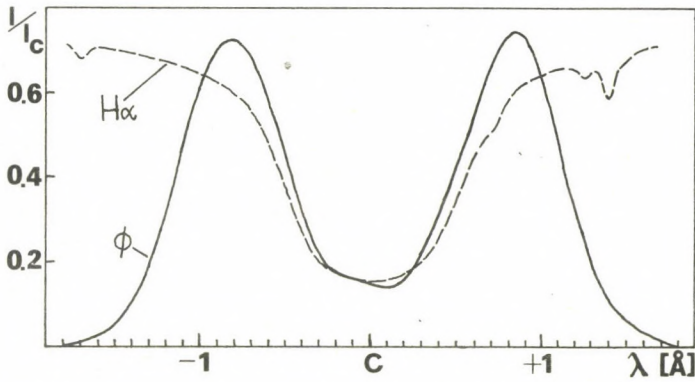


Fig.5. Reconstruction of the H α -profile from the functions shown in Fig.3.

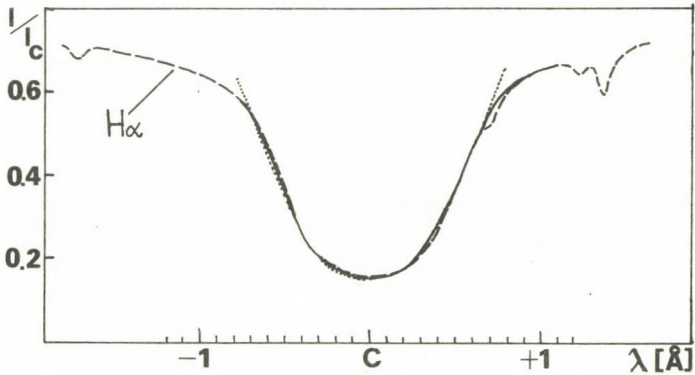


Fig.6. Reconstruction of the H α -profile from 17 functions on the restricted $-0.8 \text{\AA} - +0.8 \text{\AA}$ interval.

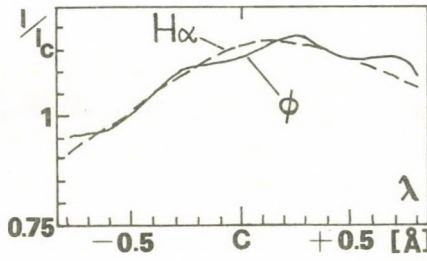
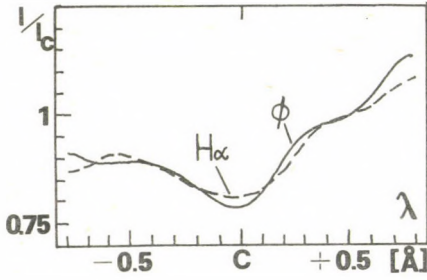


Fig. 7., 8. Reconstructions of arbitrarily constructed H α -flare profiles.

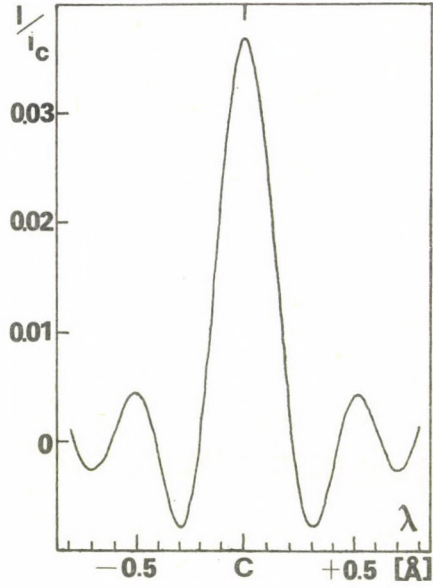


Fig. 10. To the definition of the spectral resolving power.

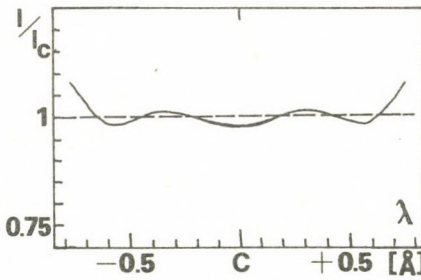


Fig. 9. Reconstruction of the constant unity function.

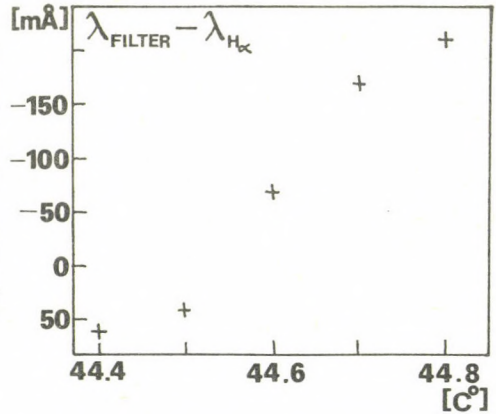


Fig. 11. Temperature dependence of the filter central wavelength.

ACTIVE REGION CHARACTERISTICS FROM TWO-FREQUENCY MAPPING
WITH A TELESCOPE TNA-1500

S.I. AVDYUSHIN[†], M.M. ALIBEGOV[†],
A.F. BOGOMOLOV[°], V.A. BUROV[†], E.I. ZAJTSEV[°],
S.P. LEONENKO[°], B.A. POPERECHEENKO[°]

[†] Inst. Appl. Geophys., Moscow

[°] Moscow Power Inst., Moscow

ХАРАКТЕРИСТИКИ АКТИВНЫХ ОБЛАСТЕЙ ПО ДАННЫМ ДВУХЧАСТОТНОГО КАРТОГРАФИРОВАНИЯ
НА РАДИОТЕЛЕСКОПЕ ТНА-1500

С.И. АВДЮШИН[†], М.М. АЛИБЕГОВ[†], А.Ф. БОГОМОЛОВ[°], В.А. БУРОВ[†],
Е.И. ЗАЙЦЕВ[°], С.П. ЛЕОНЕНКО[°], Б.А. ПОПЕРЕЧЕНКО[°]

[†] Инст. Прикл. Геофиз., Москва

[°] Моск. Энерг. Инст., Москва

Абстракт:

В работе представляются данные наблюдений активных областей No (228+229) и No 237 с 13 по 21 июля 1982 г. Рассматривается явление смены знака поляризации в этих областях и дается возможная интерпретация наблюдений. Смена знака поляризации наблюдалась практически одновременно в обеих группах: в группе No 237 до пересечения ею центрального меридиана, а в группе No (228+229) — после прохождения центрального меридиана. Смена знака начиналась несколько раньше на более короткой длине волны ($\lambda = 3,6$ см), а период смены знака был несколько короче на более длинной волне ($\lambda = 7,7$ см). Оценки высоты области взаимодействия дают величины 160 - 270 тыс. км над уровнем фотосферы. Возможная структура магнитного поля, отвечающая наблюдениям, характеризуется наклоном петель в короне и предполагает взаимодействие магнитных полей групп между собой.

The period of July 13-21, 1982 was characterized by extremely large and developed sunspot groups. Sunspot groups No. (228+229) and No. 237 were the most striking ones (the numeration is given according to Solnechnye Dannye). Sunspot groups No. (228+229) passed through the central meridian on July 15.1, and its area amounted 2700 m.h., sunspot group No. 237 passed through the central meridian on July 18.4 covering the area up to 700 m.h. Both groups are located in the northern hemisphere on latitude 10-20°. Numerous flares were registered in the groups, including rather large events.

During the mentioned period, solar radiation characteristics were observed by means of a TNA-1500 radiotelescope equipped with a 64-m parabolic antenna. HPBW makes 2.1' for the wavelength $\lambda=3.6$ cm and 4.4' for $\lambda=7.7$ cm. These wavelengths were chosen for the parallel registration in the sum channels (radiation intensity) and in the difference channel (polarization), i.e. Stokes parameters I and V were measured. The Sun mapping was carried out three times a day (at 6-7 U.T., 11-12 U.T. and at 14-15 U.T.), and in the intervals the chosen active regions were observed.

The work deals with the reversal of polarization in the active regions and the possible interpretation of the observed events.

Besides groups No. (228+229) and No. 237 within July 12-21 a number of polarized radioemission sources related to group No. 226 (northern hemisphere) and to groups No. 227 and 232 (southern hemisphere) were distinct. Group No. 226 was observed from the moment it passed the central meridian till it turned over the limb. Its polarization did not reverse, remaining positive. Group No. 227 was observed from 10°E till its turning over the limb, its polarization remaining negative. Group No. 232 was observed from 45°E till its turning over the limb. Polarization reversed from negative to positive within a day after the group crossed the central meridian. Polarization reversal in groups No. (228+229) and No. 237 took place on July 16-19, these groups being located on both sides of the central

meridian, and polarization itself having a number of peculiarities.

The possibility of polarization reversal was first pointed out in {1}, the theory of the process was worked out in {2,3}, and theoretical developments were used in estimating a number of coronal plasma parameters according to the observed polarization characteristics {4}. In recent years some studies {5,6} have been carried out in the field of individual active region modeling and coronal field estimation according to characteristics of the observed polarization reversal.

Registered emission polarization depends on source polarization and the conditions of the propagation. If one assumes that source polarization hardly changes during the observational period, polarization reversal is connected with the change of the angle of sight during the Sun's rotation. Polarization reversal can occur when while propagating the wave enters the region where the two following conditions are simultaneously fulfilled:

$$\vec{k} \times \vec{B} = 0 \quad (1)$$

$$\frac{a\omega^4}{NB^3} \left| \frac{dl}{d\alpha} \right|^{-1} = 1 \quad (2)$$

\vec{k} - wave vector

where $a \approx 3 \cdot 10^{-21}$ c.g.s.

The first condition implies the transverse wave propagation towards the direction of the magnetic field, the second points to a combination of plasma parameters (N - concentration, B - field strength and the length scale $\left| \frac{dl}{d\alpha} \right|$) which for the given frequency " ω " leads to the breach of geometrical optics approximation and to the coupling modes of waves. If (2) is valid the radioemission is linearly polarized, the degree of circular polarization being equal to "0". Naturally, at small deviations of (2) from the unit the degree of circular polarization is too small to be registered by means of our instrument with such a HPBW. The corresponding polarization chart presents the image of a depolarizing strip. The passage of this depolarizing strip connected with the direction change

→
k permits the revealing of some geometrical and physical characteristics of mode coupling region.

Within the period of July 12-16 both groups have one and the same sign of circular polarization, then, on July 16-18 depolarizing strip movement is registered in both groups, and since July 19 till turning over the limb the reversed polarization sign preserves. Figs.1-4 present polarized emission charts typical for the given period. Reversal of polarization in group No.237 took place before the group had passed the central meridian, and in group No.(228+229) after its passage through the central meridian. It is essential that polarization reversal in both groups began somewhat earlier on a shorter wavelength ($\lambda=3.6$ cm), while the period of polarization reversal was shorter on a longer wavelength ($\lambda=7.7$ cm).

The work [4] suggests formula for estimation of the distance from the source to coupling region which is determined by (1)-(2):

$$R = 0.5 l \cos \frac{Q_2 - Q_1}{2} \left\{ \operatorname{ctg} \frac{Q_2 - Q_1}{2} + \operatorname{tg} \frac{Q_2 + Q_1}{2} \right\}$$

Q_1 - angle from the central meridian corresponding to the beginning of polarization reversal;

Q_2 - angle corresponding to the end of polarization reversal;

"l" - standard dimensions of the source.

Assuming that for group No.(228+229) "l" = $10^\circ \approx 1.2 \cdot 10^{10}$ cm and for group No.237 "l" = $7.5^\circ \approx 9 \cdot 10^9$ cm and substituting observational values Q and Q for each wavelength and each group, we obtain: for group No.(228+229)

$$R_{3.6 \text{ cm}} \approx 1.9 \cdot 10^{10} \text{ cm}$$

$$R_{7.7 \text{ cm}} \approx 3.3 \cdot 10^{10} \text{ cm}$$

for group No.237

$$R_{3.6 \text{ cm}} \approx 1.9 \cdot 10^{10} \text{ cm}$$

$$R_{7.7 \text{ cm}} \approx 2.2 \cdot 10^{10} \text{ cm}$$

Let us note that the reversal of polarization was observed once, though the observational period covered the whole passage of the groups over the disk. This fact, as well as the high

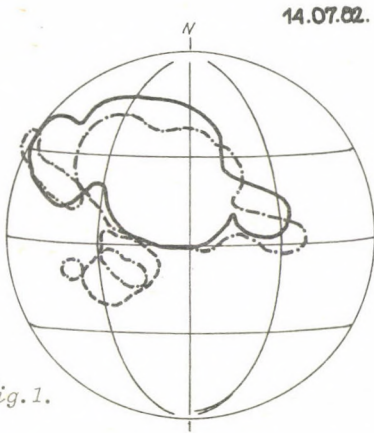


Fig. 1.

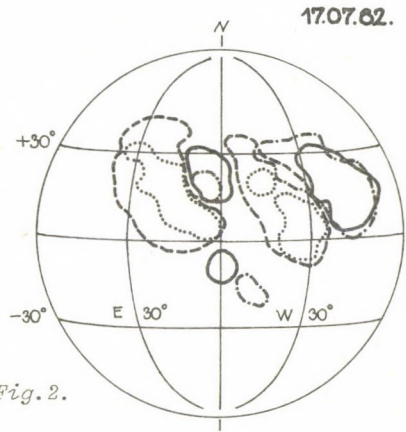


Fig. 2.



Fig. 3.

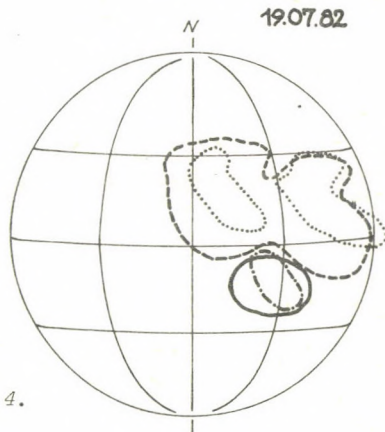


Fig. 4.

—+ } $\lambda-7.7$ -+ } $\lambda-3.6$
---+ } + }

$D=+3^\circ$

values of "R", make it possible to assume that the reversal of polarization takes place near the tops of magnetic field loops. Simultaneous polarization reversal in groups on both sides of the central meridian accounts for the fact that the loops are inclined towards each other. The good coincidence of mode coupling heights for $\lambda=3.6$ cm ($H=160$ and $175 \cdot 10^3$ km) and substantial deviation for $\lambda=7.7$ cm ($H=270$ and $200 \cdot 10^3$ km) are worth noting. Fig. 5 presents schematic magnetic field structure corresponding to observations and obtained values of "R". Each group is shown in the form of a bipolar structure. Loop inclination corresponds to the observed one, arrows with numbers show the angles at which the groups are observed on the given day. Mode coupling regions are cross-hatched. Loop inclination and field line configuration in closed regions coincide with the observations. Such configuration assumes group magnetic field interaction and possibly the formation of neutral layer. The value of the magnetic field in coupling regions was estimated according to (2) to be 5 gauss for $\lambda=7.7$ cm and ~ 10 gauss for $\lambda=3.6$ cm with the assumption that $N = 5 \cdot 10^8 + 10^9 \text{ cm}^{-3}$ and $\lambda=10^{-10}$. Evidently, propagation of such large fields for $200 \cdot 10^3$ km from the photosphere can be attributed to the existence of powerful magnetic fluxes in the active region and/or coronal currents. Note that no polarization reversal was observed in weak groups (No. 226 and 227).

Active region magnetic field interaction can lead to the transmission of information on flare processes in one active region to another. Typical transmission velocity is Alfvén velocity:

$$V_a = \frac{H}{\sqrt{4\pi\rho}} \quad \text{where } \rho - \text{plasma density.}$$

As follows from Fig. 4, $V_a \approx 10^8 \text{ cm/s}$, distance $R_0 = 7 \cdot 10^{10} \text{ cm}$, time of information transmission ~ 10 min. Indeed, a number of flares with a characteristic time interval of 5-30 min between them were observed in these groups.

In such a configuration the majority of groups is located in closed magnetic field which impedes energetic particle input.

In this respect the western part of group No. (228+229) is in a most favourable position: flux input is promoted there, the injection line being shifted eastward from the possible flare, and injected flux propagation being similar for the flares in both groups.

In conclusion it should be stressed that configuration in Fig.5 is merely a scheme which may perhaps exist in certain stages of active region development, being broken up and re-stored depending on the processes taking place in active regions.

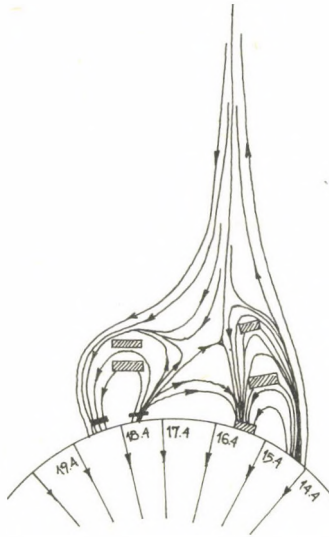


Fig.5.

References

- {1} Piddington, J.H., Minnett, H.C., Solar radio-frequency emission from localized regions at very high temperatures, *Australian J. Sci. Res. (A)* 4. 131, 1951
- {2} Cohen, M.H., Microwave polarization and coronal magnetic fields, *Ap. J.* 133. 978, 1961
- {3} Zheleznyakov, V.V., Zlotnik, E.Ya., On the polarization of radio waves, which passed through a transversal magnetic field region in the solar corona, (in Russ.) *Astron. Zh.* 40. 633, 1963

-
- {4} Peterova, N.G., On the space scales of the magnetic field of sunspots as obtained from observations of altering the polarization sense in the local sources emission, (in Russ.) *Soln. Dann.* 1975, No.3. 96.
 - {5} Bandiera, R., Diagnostic of coronal magnetic fields from microwave polarization reversal, *Astron. Astrophys.* 112. 52, 1982
 - {6} Ryabov, B., in: *Issledovanie Solntsa i krasnykh zvezd*, (in Russ.) v.16. p.40. Zinatne, Riga, 1982

OBSERVATIONS OF RAPID VARIATIONS OF THE POLARIZED AND
NON-POLARIZED RADIO EMISSION OF LOCAL SOURCES WITH THE RATAN-600
AT $\lambda = 2.3$ AND 4.5 cm BY THE "RELAY-RACE" METHOD

O.A. GOLUBCHINA,

V.N. IKHSANOVA

Spec. Astrophys. Obs., Leningrad

Pulkovo Obs., Leningrad

Abstract:

Two sets of observations have been carried out with the RATAN-600. Solar radio emission has been observed at $\lambda = 2.3$ and 4.5 cm using a new method of observations enabling Stokes parameters I and V registration every 14 minutes during several hours. Rapid variations of emission parameters were observed in flare-active regions. On the basis of the observations the authors suggest that chromospheric flares are observed in active regions whose radio emission give larger variations of emission parameters in the short-wave range of the spectrum in comparison with the long-wave range of the spectrum.

НАБЛЮДЕНИЯ БЫСТРЫХ ИЗМЕНЕНИЙ ПОЛЯРИЗОВАННОГО И НЕПОЛЯРИЗОВАННОГО
РАДИОИЗЛУЧЕНИЯ ЛОКАЛЬНЫХ ИСТОЧНИКОВ НА ВОЛНАХ 2.3 И 4.5 см
НА РАТАН-600 МЕТОДОМ "ЭСТАФЕТА"

О.А. ГОЛУБЧИНА

В.Н. ИХСАНОВА

Филиал САО, Ленинград

ГАО, Ленинград

Абстракт:

На радиотелескопе РАТАН-600 проведены две серии наблюдений радиоизлучения Солнца на волнах 2.3 и 4.5 см в новом режиме, позволяющем регистрировать параметры Стокса I и V способом прохождения через 14 минут в течение нескольких часов. Во вспышечно-активных образованиях наблюдаются быстрые изменения параметров излучения. На основе наблюдательных данных делается предположение, что хромосферные вспышки наблюдаются в активных областях, радиоизлучение которых дает более сильные вариации параметров излучения в коротковолновой части спектра по сравнению с длинноволновой.

A new method of solar radio emission observation was elaborated and used with the RATAN-600 telescope in 1980. The method was called the "relay-race" method {1}. The peculiarity of the method lies in not using all the working surface of the radio telescope, but its separate sections, which automatically join the work in such a way that the arc of the ellipse, which is the reflecting surface profile, as if it ran along a circle, i.e. a relay-race switching on each of the following reflecting elements (Fig. 1a). Thus, the relay-race method permits the carrying out of multi-fold solar drifts (passages) every 14 minutes during 10-15 hours. It is clear that the resolving power decreases. In our case it was equal to $1.1' \times 14'$ and $2.1' \times 28'$ at $\lambda = 2.3$ cm and $\lambda = 4.5$ cm respectively.

These significant observations were made at 2.3 cm in 1980 {2}. Stokes parameters I and V were recorded. On February 9 and 10 fourteen solar passages following one after the other were observed.

The new method of observation enabled us to construct a two-dimensional pattern of the radio brightness distribution on the solar disc and to determine both the heliographic coordinates of local sources (accuracy to 0.5°). The latter were found to average out over the measurements at various positional angles of solar passages (drifts) (Fig.1b).

The identification of local sources with events on the photosphere was carried out using photoheliograms of the Kislovodsk station of the Pulkovo Observatory. The coordinates of active regions were measured with the "Ascorecord" measuring machine with an accuracy of 1".

The new technique allows the making of observations for several hours, and hence the following of the migration of active regions, and the study of rapid variations of physical parameters of local sources, and the observations of the dynamics of their evolution.

As an example the local source associated with bipolar sunspot group No 69 (number from the *Solnechnye Dannye*) observed on February 9 and 10, 1980, can be given. On those days the

Fig. 1a.

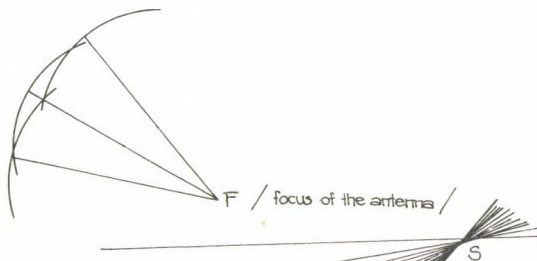


Fig. 1b.

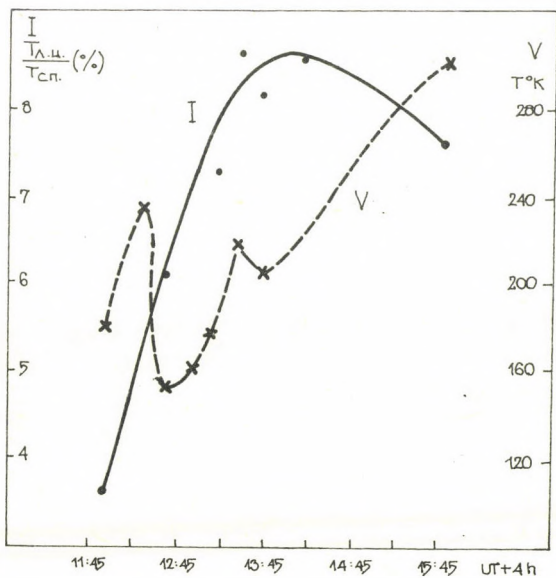
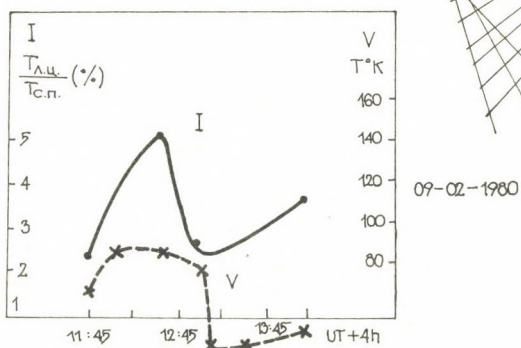


Fig. 2.

29-07-1981 No 325

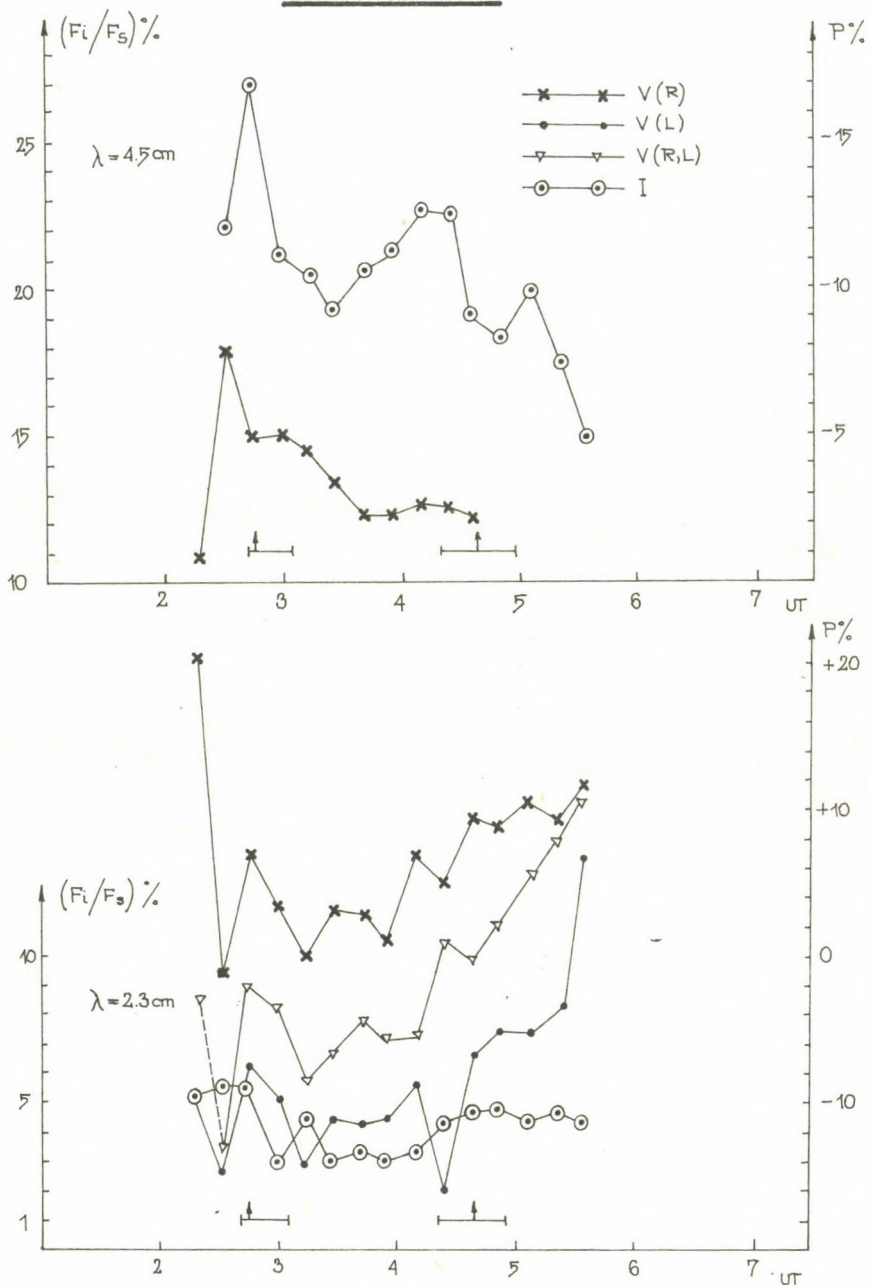


Fig. 3.

30-07-1981 No 329+332

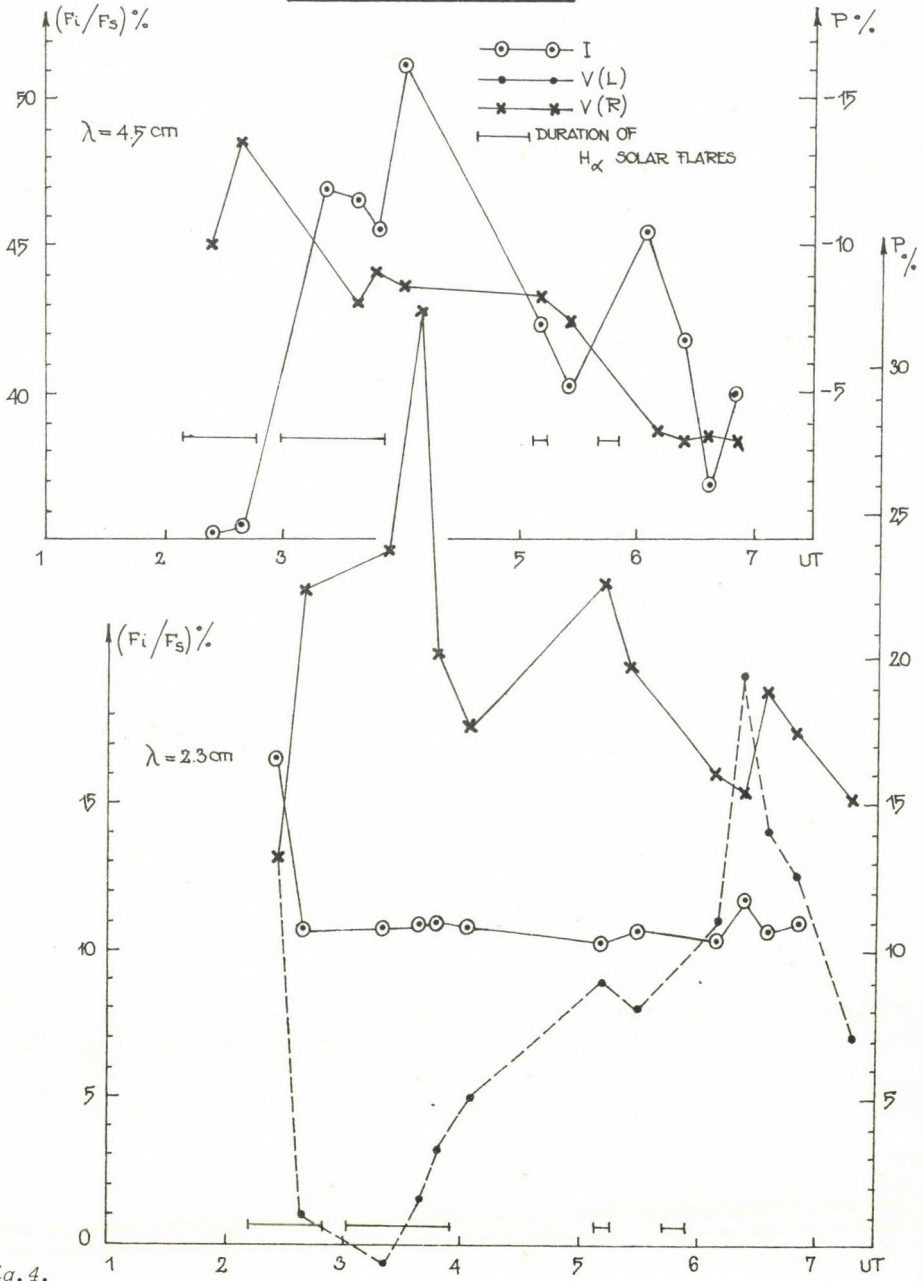


Fig. 4.

local source consisted of two parts coinciding in position with the leading and trailing sunspots. The polarized emission of the local source showed polarities in full correspondence with the polarities of separate sunspots. On February 9 and 10, 1980, the variation of the leading sunspot structure was observed. An intensive development of the corresponding local radio source was observed both in polarized and non-polarized emission (Fig.2). Fig.2 shows the variation of emission parameters of the source, connected with the leading sunspot of group No 69. On February 10, 1980, a chromospheric flare was observed in this region. It should be noted that, while the variation of Stokes parameters I and V was similar on February 9, on February 10 it was oppositely phased.

A number of sunspot groups whose local sources manifested strong time variations were observed during the series of observations in the third decade of July 1981 (the pre-eclipse period and the day of the total solar eclipse of July 31). Thus, sunspot group No 325 located on the west limb on July 30, showed radio emission fluctuations in I and V parameters at both wavelengths. The contrast of the variation at $\lambda = 2.3$ cm considerably exceeds that at $\lambda = 4.5$ cm (Fig.3). A similar pattern was observed in the sunspot group complex 329+332. That multi-centered active region was about 20° in longitude and was separated into the leading part of the S polarity and the trailing part of the N polarity. Similarly, the local source observed at $\lambda = 2.3$ cm, also had two polarities. As is seen in Fig.4 a considerable variation of emission parameters is observed at $\lambda = 2.3$ cm while at $\lambda = 4.5$ cm this variation is small in the sunspot group complex 323+332.

During the whole period of observation rapid variations of the per cent of polarization took place, which was indicative of the structural variations of the magnetic field of the source.

A number of chromospheric flares were given in the *Solar-Geophysical Data* for the same period and region whose time and duration are indicated at the bottom of Fig.4 by separate hori-

zontal lines. It is of importance that the moments of maxima of the development of the flares throughout correspond to maximum variations of radio emission parameters.

On the basis of the above examples and some additional authors' material the following suggestion is possible: Chromospheric flares are observed in active regions whose radio emission give larger variations of emission parameters in the short-wave range of the spectrum in comparison with the long-wave range of the spectrum (in particular, 2.3 cm and 4.5 cm).

R e f e r e n c e s

- {1} Golubchina, O.A., Golubchin, G.S., The relay-race method, (in Russ.)
Izv. Special Astrophys. Obs. 14. 125, 1981
- {2} Golubchina, O.A., Ikhsanova, V.N., Bogod, V.M., Golubchin, G.S.,
A two-dimensional radio image of solar local sources using the
consecutive aperture synthesis with RATAN-600, (in Russ.)
Soln. Dann. 1981 No.4. 108.

ON THE HEIGHT SCALE OF MAGNETIC FIELDS ABOVE SUNSPOTS
DERIVED FROM RATAN-600 OBSERVATIONS AND MODEL CALCULATIONS

A. KRÜGER, F. FÜRSTENBERG,

J. HILDEBRANDT

ZISTP (HHI), Berlin (GDR)

SH.B. AKHMEDOV, V.M. BOGOD, A.N. KORZHAVIN

Pulkovo Obs., Leningrad

Spec. Astrophys. Obs., Leningrad

Abstract:

Model calculations of the S-component emission have been compared with observations of the RATAN-600 telescope at the operating frequencies 7.5, 9.4, 11, 13, and 15 GHz for different active regions of the SMY and surrounding periods. The spectral variations of the flux density, degree of polarization and source diameters are used to derive the scale heights of the magnetic field in the lower solar corona. The field distribution was concluded in accordance with magnetic dipole distributions and the assumption of advanced temperature and electron density models according to most recent EUV observations and photospheric magnetic field measurements.

О ШКАЛЕ ВЫСОТ НАД СОЛНЕЧНЫМИ ПЯТНАМИ,
ПОЛУЧЕННОЙ ИЗ НАБЛЮДЕНИЙ НА РАТАН-600 И ИЗ МОДЕЛЬНЫХ РАСЧЕТОВ

А. КРЮГЕР, Ф. ФЮРСТЕНБЕРГ, Й. ХИЛЬДЕБРАНДТ

ЦИСЗФ, Берлин (ГДР)

Ш. Б. АХМЕДОВ

В. М. БОГОД, А. Н. КОРЖАВИН

ГАО, Ленинград

Филиал САО, Ленинград

Абстракт:

Модельные расчеты излучения S-компонента сравнили с наблюдениями РАТАН-600 на частотах 7.5, 9.4, 11, 13, и 15 ГГц для различных активных областей ГМС и окружающих периодов. Спектральные вариации потока излучения, степени поляризации и диаметров источников были использованы с целью определения высотных шкал магнитного поля в нижней солнечной короне. Распределение магнитного поля определено в соответствии с распределением диполя и современными моделями температуры и электронной плотности в согласии с самыми последними наблюдениями в ЭУВ диапазоне и фотосферных магнитных полей.

1. Introduction

Radio methods provide a possible access to the basic problem of deriving magnetic field parameters in the solar chromosphere and corona. The present report makes use of the conception of gyromagnetic radiation emanating from solar S-component sources in order to determine magnetic scale heights above the centre of regular sunspots by comparison of model calculations with observations by the large RATAN-600 radio telescope.

2. Method

The model used here was described by Krüger et al. {5} and first applications were described by Akhmedov et al. {1}, {2}. Now we present results using a somewhat broader material covering observations from the SMY.

The applied model calculations are essentially based on the assumption of a rotational-symmetrical source volume of gyroresonance emission permeated by the field of one pole of a magnetic dipole situated at a depth R_d below the photospheric centre of a regular sunspot (Fig.1). In this way the field is determined by two parameters B_m (this is the maximum magnetic field at the centre of the source region at the photospheric level) and the value of R_d , whereas the latter mainly influences the magnetic scale height

$$L_B = B \left(\frac{\Delta B}{\Delta z} \right)^{-1} \quad (z - \text{geometrical height}).$$

The application of dipole fields should be considered merely as a practical approximation which is less computer-time consuming than other more realistic distributions, deviating from rotational symmetry. The consistency of these results, e.g. with calculations using force-free magnetic field extrapolations of magnetograms for regions above strong sunspots and of not too large coronal heights (where loop structures may become dominating), is to be checked by investigation of individual regions (cf. {7}).

For solving the equation of radiative transfer the calculation of the emission and absorption coefficients was re-

lated to the sunspot model of Staude {8}, which is very similar to the more recent model of Lites and Skumanich {6}, using the latest measurements in the EUV-region. The extrapolation to the corona was done assuming a steep gradient and thin transition zone. (Models with finite thickness of the transition zone were also tested and discussed elsewhere (cf. {4})).

Some characteristic results of the calculations on the S-component model are shown in Fig.2, where the position of the gyroresonance layers of the radio emission at different fixed frequencies are shown in comparison with corresponding intensity profiles, the dependency of the occurrence of different gyroharmonics and different source radii on the magnetic field and the test frequency. After integration over the source region of the gyromagnetic radiation, the spectra of the radio flux density S_ν , the degree of polarization p , and the frequency distributions of the source radii R_s were obtained for different sets of the magnetic field parameters, B_m and R_d , which can now be used for the diagnostics of active regions (Figs.3a-c).

3. Observations

For the purpose of a preliminary discussion 14 cases of suitable active regions observed with the RATAN-600 radio telescope have been selected and the spectra of the quantities S_ν , p , and R_s for the five observing frequencies of the RATAN-600 in the range 7.5 - 15 GHz derived. Some examples of the measured spectral distributions are shown in Fig.4.

4. Discussion of results

As derived from a best fit of the observed and theoretical distributions of the parameters S_ν , p , and R_s the related magnetic field parameters B_m and R_d have been obtained. The results are shown in Table I. Hence it follows that the range of our results is restricted by the fact that the B_m -values (in accordance with optical observations) of the present sample vary only in the range between 2 and 3 kG (0.2 - 0.3 T). Nevertheless, the related R_d -values scatter in wider range between $1 \cdot 10^7$ and $3 \cdot 10^7$ m indicating a greater variation of magnetic scale heights than formerly expected. Most frequently, however,

T A B L E 1

Results of RATAN-600 observations

Date	$R_S(7.5 \text{ GHz})$	$S_{\nu, \max}$	R_d	B_m
	10^6 m	s.u.	10^7 m	T
24.09.77	14.2	4.2	1.5	0.3
28.01.79	9.6	1.1	2	0.2
01.05.79	12.1	4.1	1.5	0.3
01.05.79	10.4	5.2	1.5	0.3
05.10.79	6.7	0.9	1.5	0.25
23.04.80	21.4	19	3	0.25
24.04.80	26.5	16	3	0.25
25.04.80	26.5	23	2	0.3
27.05.80	> 12.3	1.4	1.5	0.3
27.05.80	> 22.2	6.9	2.5	0.3
15.07.80	6.8	1.9	1	0.25
15.07.80	14.1	1.9	1.5	0.25
12.08.80	7.0	0.05	1.5	0.2
25.11.80	~ 3.8	0.9	1	0.3

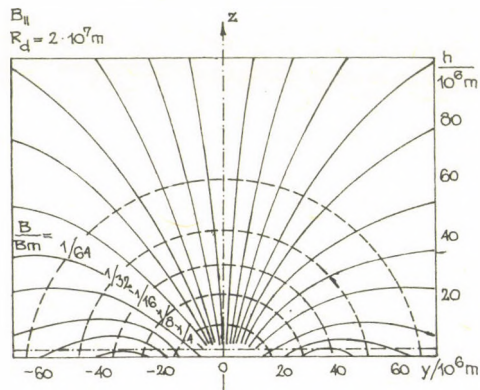


Fig. 1. Cross section of the magnetic structure of the S-component emission model

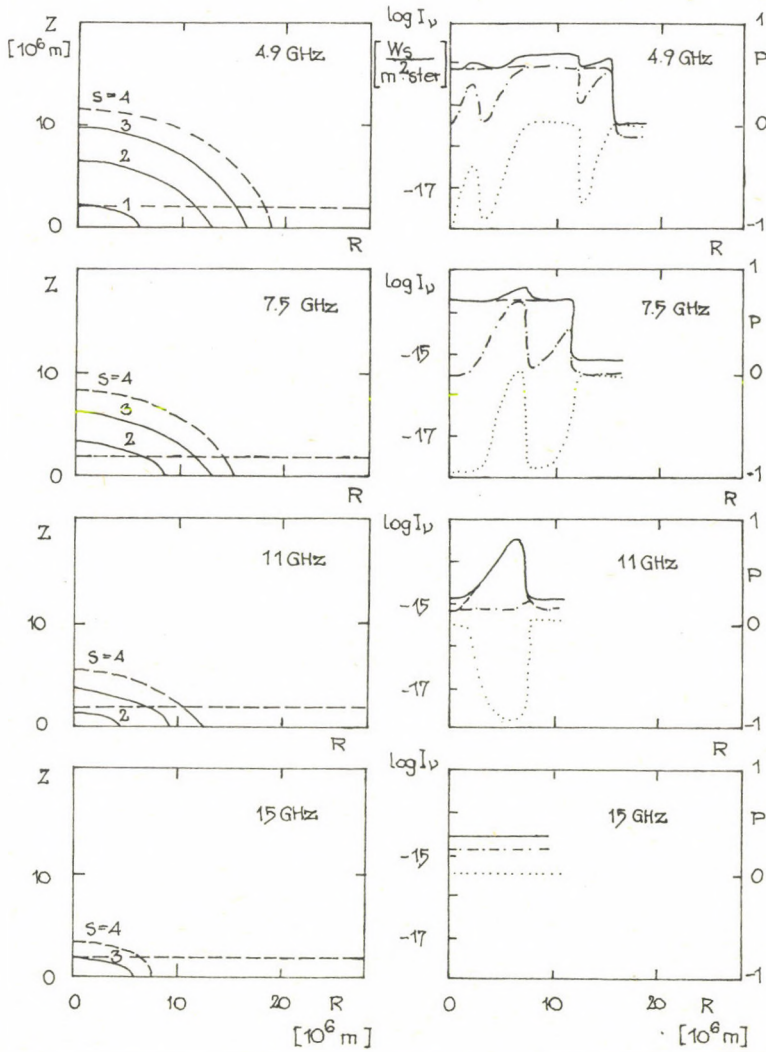


Fig.2. Position of gyro-resonance levels for $B_m = 0.25$ T, $R_d = 1.5 \cdot 10^7$ m at different frequencies; the horizontal dotted line marks the bottom of the corona (left). This is compared with e-mode (---) and o-mode (- · -) intensity profiles, the sum of both (- -), and the degree of circular polarization (. . .) (right).

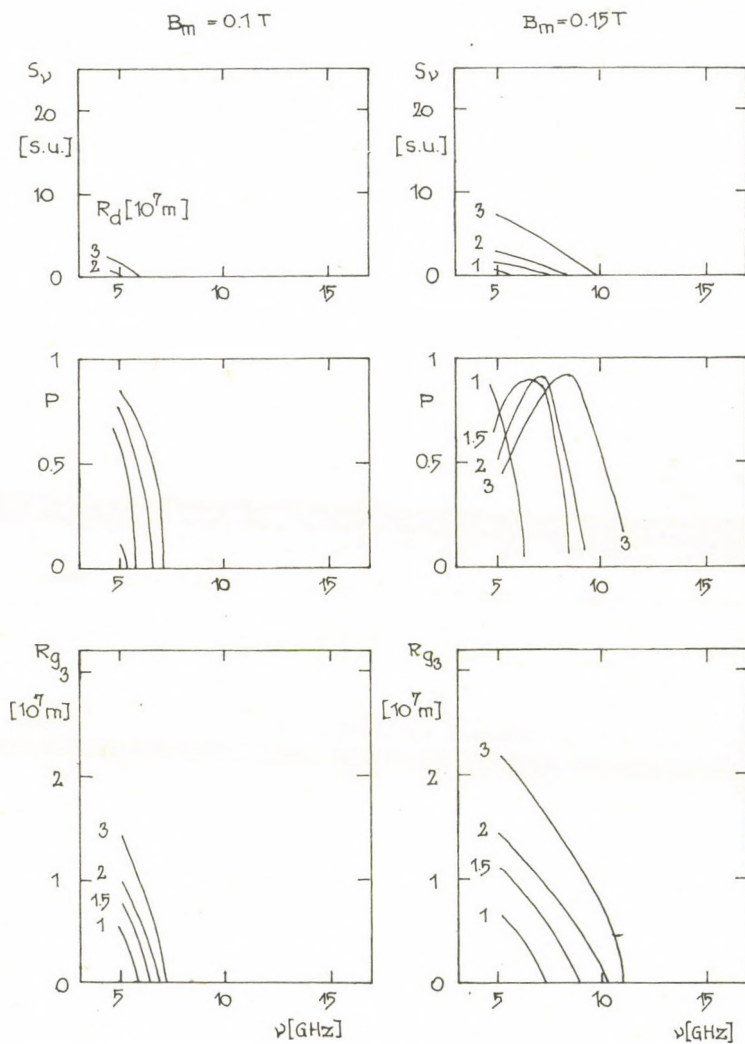


Fig. 3a.

Fig. 3a - c. Calculated spectra of the flux density S_v (top), degree of polarization p (middle), and source radius R_g of gyromagnetic emission (bottom).

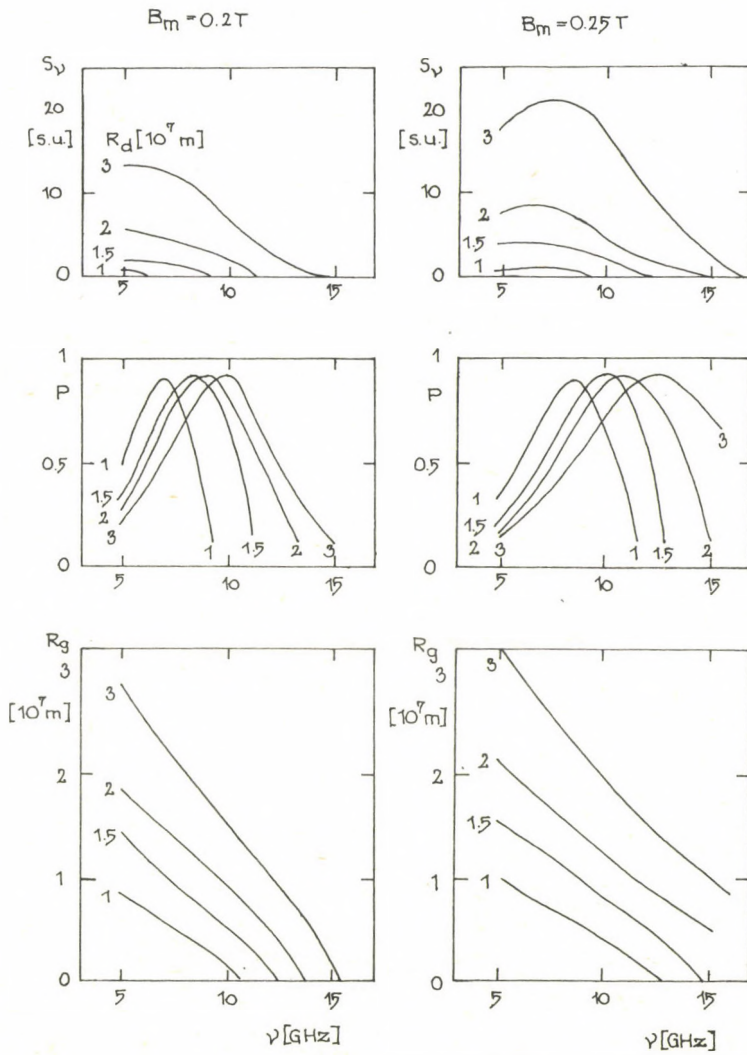


Fig.3b.

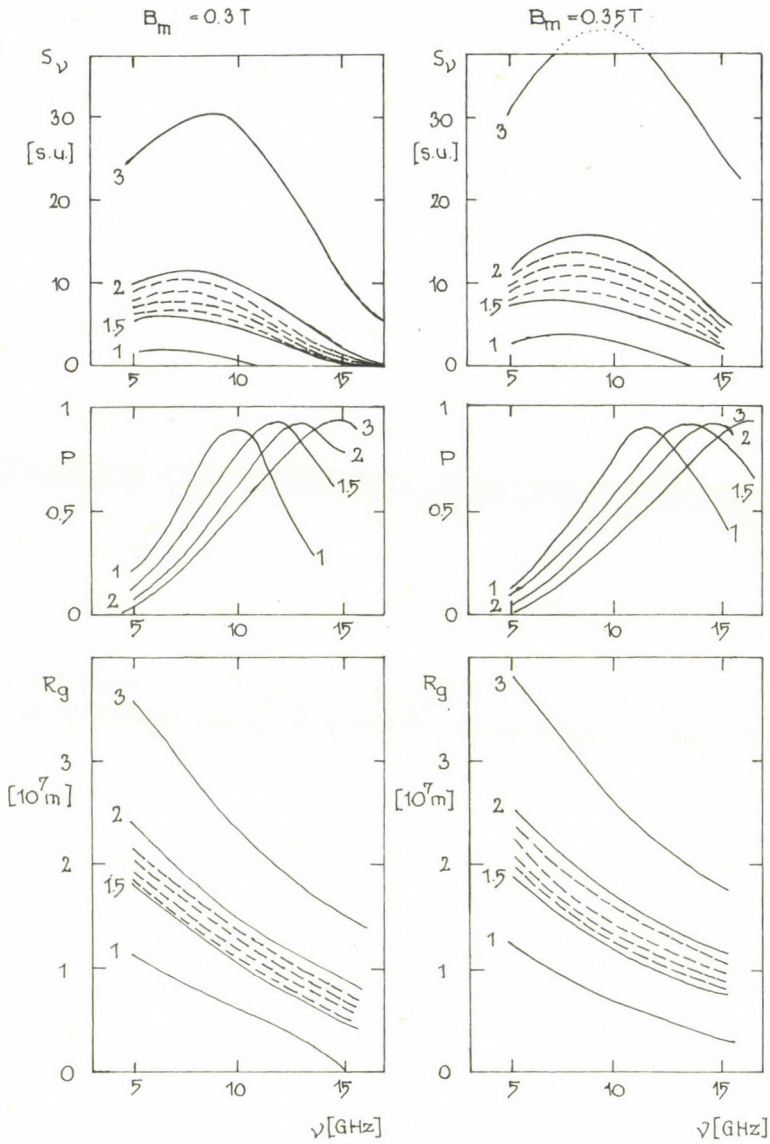


Fig. 3c.

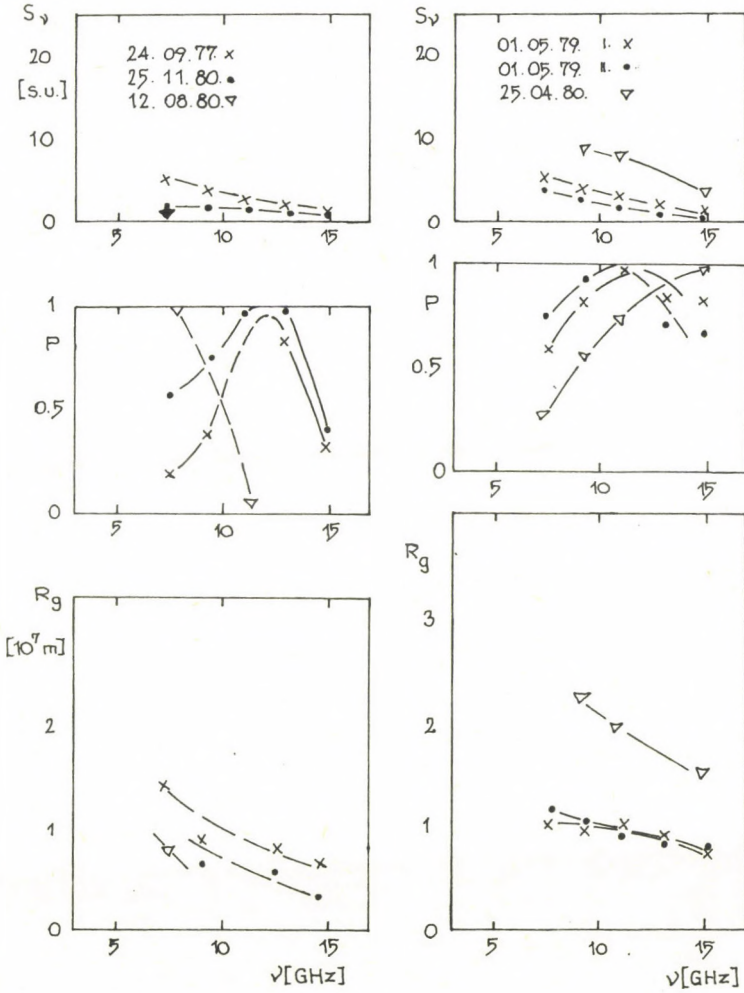


Fig.4. Examples of results of RATAN-600 observations for comparison with Fig.3.

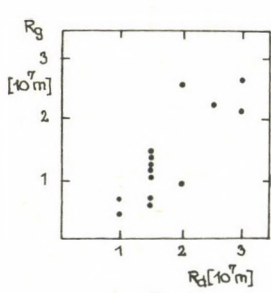


Fig. 5. Plot of derived R_d values over the source radii R_g at 7.5 GHz.

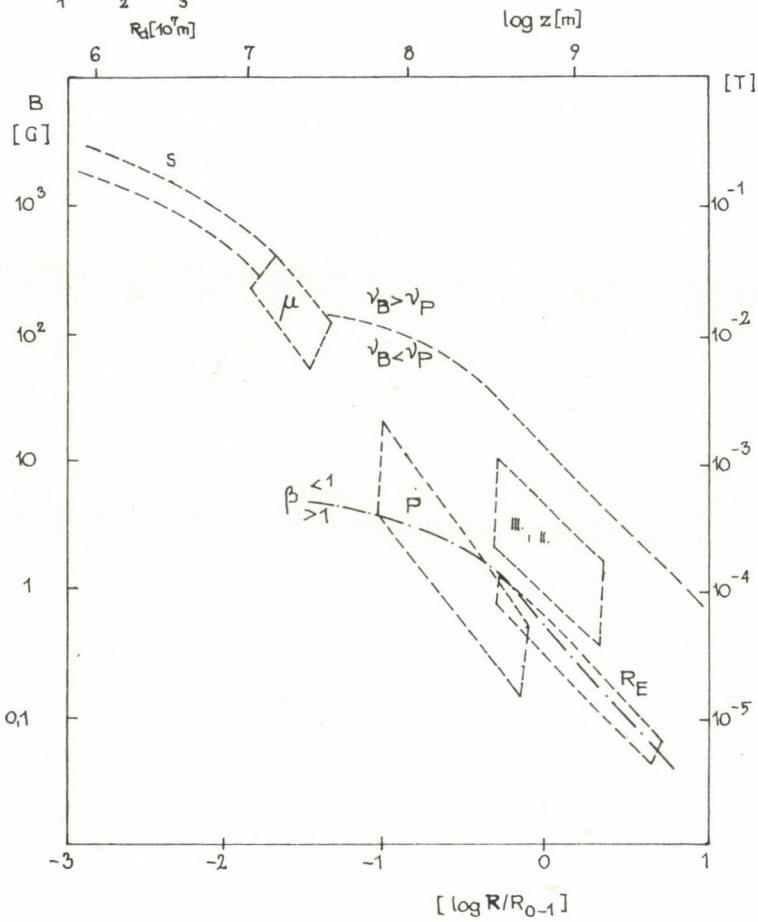


Fig. 6. Magnetic field distribution inferred from S-component observations (S) compared with other estimates compiled by Dulk and McLean {3} by application of microwave bursts (μ), potential field expansion (P), type II and type III radio bursts (II, III), and the Razin effect (RE).

we find $R_d = 1.5 \dots 2 \cdot 10^7$ m which corresponds to scale heights at $z = 10^7$ m (10 000 km) of about

$$L_B = (0.3 \dots 0.4) \cdot 10^7 \text{ m.}$$

In the frame of the discussed limited material, no dependency between B_m and R_d can be stated. But such a relationship is clearly established between R_d and R_s for a given observing frequency (cf. Fig.5).

Finally, it can be remarked that the derived height distributions of the magnetic fields are roughly within the frame of Dulk and McLean {3}, who compiled estimates of coronal magnetic fields by various radio methods. A more detailed study of these and other features of RATAN observations is in preparation.

R e f e r e n c e s

- {1} Akhmedov, Sh.B., Gelfreikh, G.B., Krüger, A., Fürstenberg, F., Hildebrandt, J., *Soln. Dann. No. 10.* 72, 1982
- {2} Akhmedov, Sh.B., Gelfreikh, G.B., Fürstenberg, F., Hildebrandt, J., Krüger, A., *Solar Phys.* 86. 1983, in press
- {3} Dulk, G.A., McLean, D.J., *Solar Phys.* 57. 279, 1978
- {4} Kaverin, N.S., Kobrin, M.M., Korshunov, A.I., Shushunov, V.V., Aurass, H., Fürstenberg, F., Hildebrandt, J., Krüger, A., Seehafer, N., *this issue* 1983
- {5} Krüger, A., Hildebrandt, J., Fürstenberg, F., Staude, J., *HHI-STP Report No. 14.* 1, 1982
- {6} Lites, B.W., Skumanich, A., *Ap. J. Suppl.* 49. 293, 1982
- {7} Seehafer, N., Hildebrandt, J., Krüger, A., Akhmedov, Sh.B., Gelfreikh, G.B., *this issue* 1983
- {8} Staude, J., *Astron. Astrophys.* 100, 284, 1981

ON THE RELATION BETWEEN SPECTRAL CHARACTERISTICS OF THE
MICROWAVE EMISSION FROM SOLAR ACTIVE REGIONS AND
PHYSICAL CONDITIONS OF THE SOLAR ATMOSPHERE

N.S. K A V E R I N, M.M. K O B R I N,
A.I. K O R S H U N O V, V.V. S H U S H U N O V

NIRFI, Gorkij

H. A U R A S S, F. F Ü R S T E N B E R G,
J. H I L D E B R A N D T, A. K R Ü G E R, N. S E E H A F E R
ZISTP (HHI), Berlin(GDR)

ЗАВИСИМОСТЬ СПЕКТРАЛЬНЫХ ХАРАКТЕРИСТИК МИКРОВОЛНОВОГО ИЗЛУЧЕНИЯ
СОЛНЕЧНЫХ АКТИВНЫХ ОБЛАСТЕЙ ОТ ФИЗИЧЕСКИХ УСЛОВИЙ
В СОЛНЕЧНОЙ АТМОСФЕРЕ

Н.С. КАВЕРИН, М.М. КОБРИН, А.И. КОРШУНОВ, В.В. ШУШУНОВ

НИРФИ, Горький

Х. АУРАС, Ф. ФЮРСТЕНБЕРГ, Й. ХИЛЬДЭБРАНДТ, А. КРЮГЕР, Н. ЗЕЕХАФЕР
ЦИСЗФ, Берлин(ГДР)

Abstract:

Spectrographic observations of the microwave emission from selected active regions were analysed and compared with S-component emission models. The observations were obtained by spectrographs of the NIRFI working in the ranges 12-8 and 7-5 GHz covering the high-frequency part of the S-component spectrum. The measurements were carried out at the RT-22 radio telescope of the FIAN Radio Astronomy Station at Pushtshino with an angular resolution of about 9 arc minutes.

The conclusions obtained mainly relate to

- *the reversal of the slope of the flux spectrum in the short cm-region by the change of the emission mechanism*
- *an excess of the observed flux spectrum at long cm-waves, which is probably due to hot loop structures, and*
- *the interpretation of the proton-flare criterion of Tanaka and Kakinuma on the basis of model calculations.*

1. Introduction

Spectral measurements of the solar microwave emission from local active regions are still quite rare in spite of the fact that spectrographic observations provide more complete information on the details of the spectrum than is obtained from observations at fixed frequencies. Based on known emission processes and extensive model calculations the spectral information can be used e.g. for the diagnostics of solar active regions and the search for new physical processes.

2. Observations

The observations used in the present study were obtained by NIRFI-radiospectrographs working in the range 5-7 and 8-12 GHz covering the high-frequency side of the spectrum of the *S*-component suitable for diagnostics of active regions up to heights of about 10 000 km and more above the photosphere. The spectrographic observations were carried out at the RT-22 radio telescope of the Radio Astronomy Station of FIAN at Pushtshino near Serpukhov. The spatial resolution ranges between 8.5' and 10' in both spectrographics bands with an average value of about 9'. This means that the details of single active regions or complexes of them are not resolved by the antenna beam. The mean error of the absolute flux determination is in the order of 20 per cent.

From a total of 16 observations the following three days have been selected for the purpose of the present study, whereas the position of the source region, not too far from the centre of the solar disk, and the complete coverage of the spectrum played a major role:

1 June, 1979	} McMath No.16046 and 16051,
2 June, 1979	
29 July, 1980	McMath No.17008 (cf.Figs.1,2,and 3).

3. Discussion

The present observations are now to be compared with calculations of *S*-component emission models. For the sake of a more general discussion possible fine structure effects of the spectra have been ignored here. Theoretical spectra of the

S-component sources assuming a rotationally symmetric magnetic (dipole) field distribution are shown in Figs.4 and 5 according to the model described by Krüger et al.{4}. The series of full and dashed spectral curves refer to gyromagnetic emission depending on two parameters, viz. the maximal magnetic field at the spot centre B_m and the scale of the magnetic field described by the assumed dipole depth R_d below the photosphere. The broken line, labeled B , is due to coulomb bremsstrahlung, its superposition with the gyromagnetic spectra is marked by dotted lines. In order to demonstrate the dependency on special model conditions, two models of different distributions of the thermodynamic plasma parameters above sunspots were used, one with a very thin transition zone to the corona, and the other (perhaps more realistic) with an extended transition layer (in our case corresponding to a conductive flux $F_C=10^4$ cgs,{1}(cf.Fig.6).

From Figs.4 and 5 it is evident that the change in the slope of the flux spectrum is due to the transition between the regions of a dominating action of the two competing emission mechanisms. The position of this transition on the frequency axis depends on both the level of gyromagnetic emission and of bremsstrahlung, i.e. on the magnetic field parameters in the gyromagnetic source region and the temperature (density distributions of the surrounding plage region governed by bremsstrahlung, as well as by the beam width of the antenna also collecting bremsstrahlung from areas outside active regions. Despite the wide range of theoretical possibilities thus arising, it seems obvious that most of the spectrographic observations, available here, show the flux minima in a narrow range between 11.5 and 12 GHz, a feature that is not exclusively represented by RATAN observations {2}. Apparently, more observations connected with model calculations adapted to individual active regions are needed for further conclusions.

Comparing theoretical and observed spectra an excess of observed radiation at frequencies smaller than 6 GHz becomes evident (Fig.7). This effect (if it is real) is not surprising and could be interpreted by higher temperatures in coronal

loop structures which have not been accounted for in the present sunspot model which already terminates at a temperature in the order of $2 \cdot 10^6$ K (cf.Fig.6).

Finally, we briefly consider the conditions of the proton flare criterion of Tanaka and Kakinuma {6} which predicts $S_{9.4} \geq 25$ s.u. and $S_{9.4} \geq S_{3.8}$ for proton active regions. In context with our model calculations, these conditions merely imply large spotgroups and large fields $B_m \gtrsim 0.3$ T together with large scale heights corresponding to $R_d > 2 \cdot 10^7$ m. Deep and thin transition layers between chromosphere and corona (and correspondingly great conductive fluxes) are in favour of the criterion, but do not seem to be necessary at all, as was argued by Jao Jin Xing {3}. High coronal temperatures are also in favour of this criterion; this feature is nicely displayed by the catalogue of Lubyshev {5}.

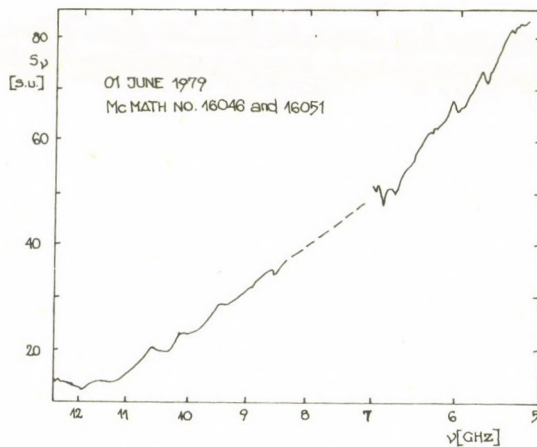


Fig.1. Radio spectrum of active regions McMath No 16046 and 16051 on June 1, 1979.

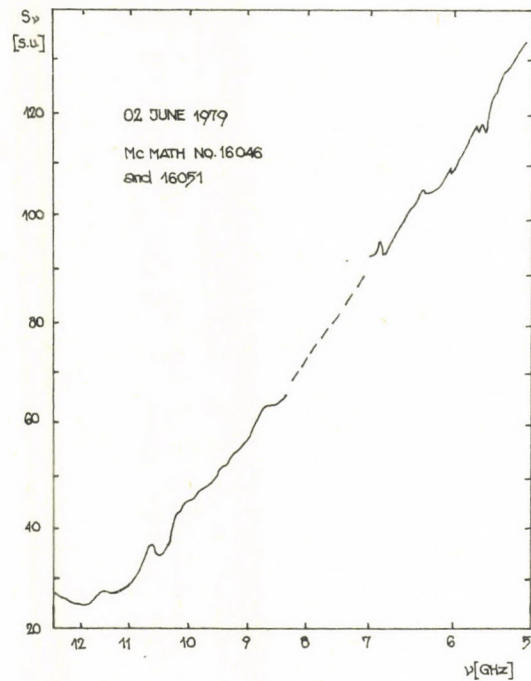


Fig. 2. Same as Fig. 1 but for June 2, 1979.

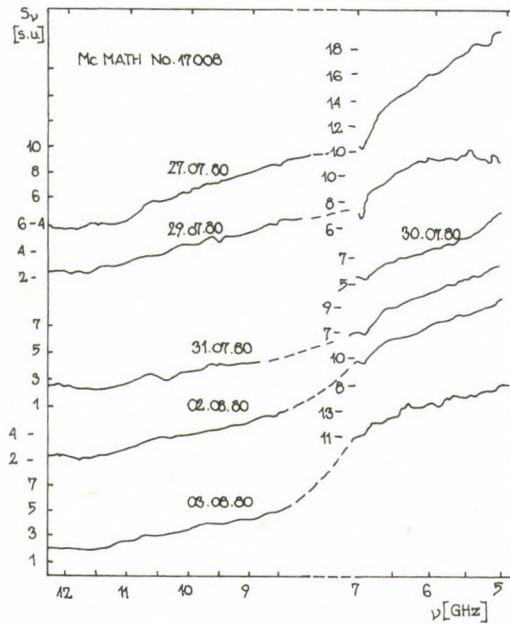


Fig. 3. Radio spectra of McMath No 17008 for different days.

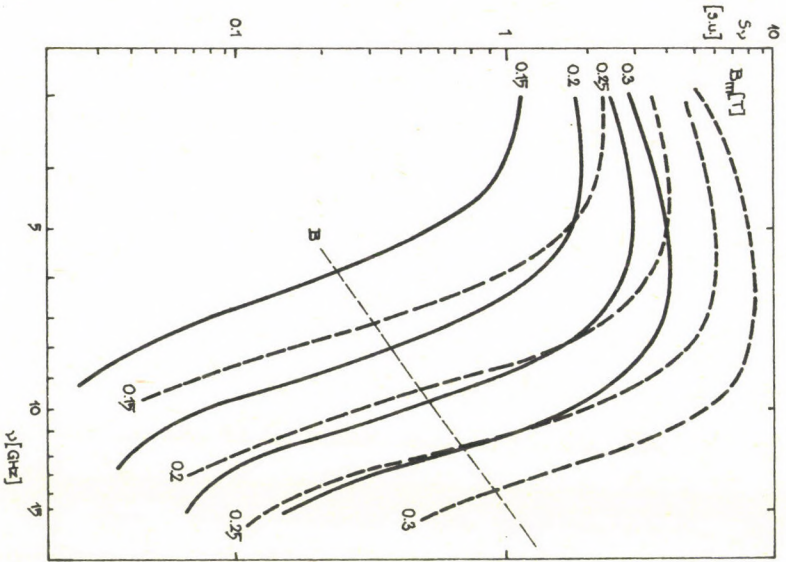


Fig.4. Calculated spectra of S-component fluxes, $F_c = 10$ cgs (Full line: $R_d = 1.5 \cdot 10^7$ m, dotted line: $R_d = 2 \cdot 10^7$ m), description cf. text.

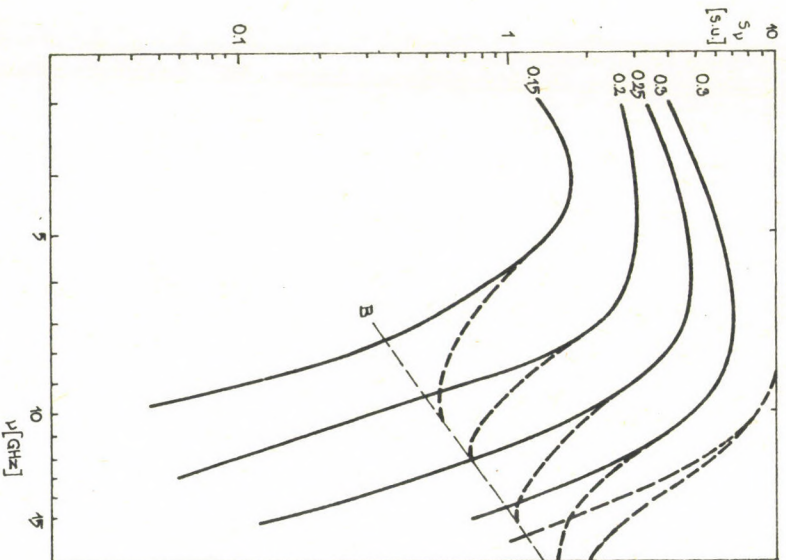


Fig.5. Same as Fig.4, but small transition layer assumed (Full line: $R_d = 1.6 \cdot 10^7$ m, dashed line: $R_d = 1.9 \cdot 10^7$ m).

637

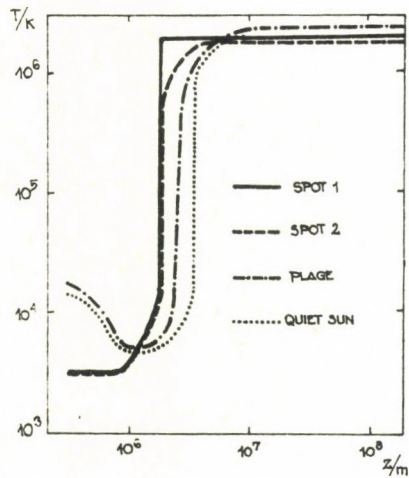


Fig. 6. Model distributions of temperature.

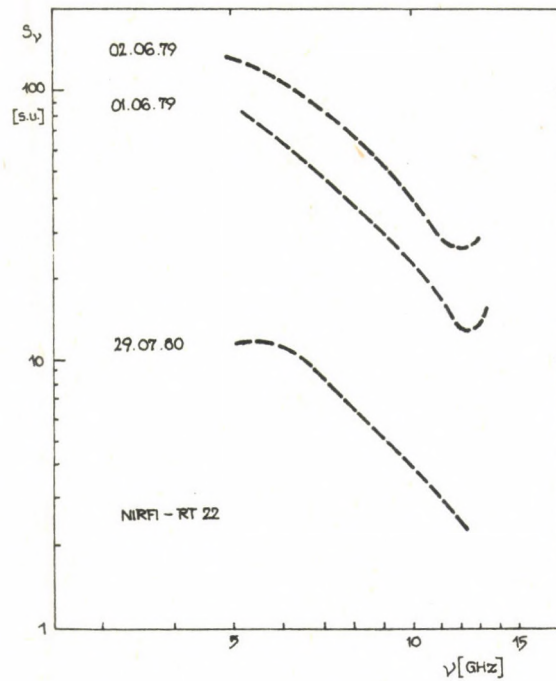


Fig. 7. Smoothed observed spectra.

R e f e r e n c e s

- {1} Alissandrakis, C.E., Kundu, M.R., Lantos, P., *Astron. Astrophys.* 82, 30, 1980
- {2} Bogod, V.M., Gelfreikh, G.B., *Solar Phys.* 67, 29, 1980
- {3} Jao Jin Xing, *Acta Astron. Sinica*, 23, 309, 1982
- {4} Krüger, A., Hildebrandt, J., Fürstenberg, F., Staude, J., *HHI-STP Report* 14, 2, 1982
- {5} Лубышев, Б.И., *Альбом расчетных спектров магнитотормозных локальных источников радиоизлучения Солнца*, АН СССР, Иркутск, 1982
- {6} Tanaka, H., Kakinuma, T., *Rep. Ionosph. Space Res. Japan*, 18, 32, 1964

EFFECTS CHARACTERIZING THE RELATIONSHIP OF RADIO BURSTS AND
PROTON FLARES BY DATA FOR 1980

S.T. AKINYAN, V.V. FOMICHEV, I.M. CHERTOK

IZMIRAN, Troitsk

H. AURASS, A. KRÜGER

ZISTP (HHI), Berlin (GDR)

Abstract:

The present paper contains the main results of a diagnostic analysis of proton events during January - October, 1980. The aims of this analysis are (i) the consideration of the radio emissions of the largest flares in a wide frequency range, (ii) the estimation of the expected parameters of proton fluxes of the order of some tens MeV on that basis, and (iii) the comparison of the obtained estimations with the data of direct measurements of the proton fluxes in the interplanetary space near the Earth. Our paper is a continuation of a series of previous papers in which the method of quantitative analysis of proton flares according to their radio emission was elaborated from data from the years 1965-1969 (cf. {1},{3},{4} and there cited literature) and applied to the events of the years 1970-1977, and 1979 {2},{5}.

ЭФФЕКТЫ ХАРАКТЕРИЗУЮЩИЕ СВЯЗЬ РАДИОВСПЛЕСКОВ И ПРОТОННЫХ ВСПЫШЕК 1980 Г.

С.Т. АКИНЯН, В.В. ФОМИЧЕВ, И.М. ЧЕРТОК

ИЗМИРАН, Троицк

Х. АУРАС, А. КРЮГЕР

ZISTP (HHI), Берлин (ГДР)

Абстракт:

В данном докладе изложены основные результаты диагностического анализа протонных событий за январь-октябрь 1980 г. Цель такого анализа - рассмотрение радиоизлучения наиболее крупных вспышек в широком диапазоне частот, оценки на этой основе ожидаемых параметров потоков протонов с энергией порядка десятков МэВ и сопоставление полученных оценок с данными прямых измерений потоков протонов в околоземном космическом пространстве. В этом смысле доклад является продолжением серии работ, в которых методика количественной диагностики протонных вспышек по радиовсплескам, разработанная по данным за 1965-1969 гг. применена к событиям 1970-1977 гг., а также 1978 и 1979 гг. Анализ протонных событий за 1980 г. представляет дополнительный интерес, поскольку это был период наиболее обширных комплексных наблюдений по программе "Год Солнечного Максимума" и для многих вспышек имеется широкий набор данных.

1. Introduction

The analysis of proton flares for 1980 bears a special interest because it covers the period of complex observations of the SMY program, thus providing rich data material for numerous events.

The scheme of the treatment of the events of 1980 was the same as for the events of the previous years which was described in detail by Akinyan et al. {2} and Avdyushin et al. {5}. The diagnostic method applied here contains two steps of the flare analysis: According to previously investigated radio burst data of a great number of cases in the first step, all those bursts 1980 were selected which are expected to be a source of a remarkable increase in the proton flux at the Earth's orbit, e.g. with intensities $I(E > 10 \text{ MeV}) \geq 1 - 5 \text{ cm}^{-2}\text{s}^{-1}\text{ster}^{-1}$. For this purpose the so-called proton flare criterion was established: It considers an estimate of a sufficiently high radio flux density (some hundreds s.u.), hard spectrum (i.e. the spectral maximum should be situated at $\nu \gtrsim 5 \text{ GHz}$), not exclusively impulsive character of the related microwave burst component (i.e. the duration at a level of 0.5 of the peak flux at the frequencies 3, 5 - 7, and 9 GHz should be $d_3 \gtrsim 3.0 - 3.5 \text{ min}$, $d_{5-7} \gtrsim 2.5 - 3 \text{ min}$, $d_9 \gtrsim 2.0 - 2.5 \text{ min}$, respectively), and also remarkable meter-wave burst components, including the spectral type II and IV bursts. In essence, a characteristic U-shaped radio spectrum is likely for proton flux associated events.

For the flares satisfying the proton flare criterion, the transition to the second step of the diagnostics can be fulfilled - the estimation of the expected proton flux parameters near the Earth, viz. the maximum intensity and time parameters for $E > 10$, > 30 , and $> 60 \text{ MeV}$. For this purpose the heliographic longitude of the flare site and information about the number and energy spectrum of the accelerated particles which are contained in the energetics (time profile) and, frequency spectrum of the associated microwave burst are taken into account, as well as data on the escape conditions of the par-

ticles from the flare region via the meter-wave components of the radio emission. Basic parameters for these estimations are the burst peak fluxes at frequencies 3, 9, and 15.4 GHz, the integral of the time profile during the increasing phase as well as the total energy of the microwave burst at 3 and 9 GHz.

In the present study, observations of proton fluxes of the satellite IMP 8 in the energy range 13.7 - 25.2, 20 - 40, and 40 - 80 MeV were used for a comparison with the calculations, taken from *Solar-Geophysical Data*. The observed intensities I_o and calculated intensities I_c refer to the text and the figures to energies $E > 10$ MeV, as far as no other remarks are given. In all our figures, where time profiles of proton fluxes are given, the scales are chosen in such a way that the proton fluxes in the ranges $E \sim 13.7-25.2$ MeV in units of $[cm^{-2}s^{-1} \times ster^{-1}MeV^{-1}]$ (left ordinate scale) correspond to the proton fluxes at $E > 10$ eV in $[cm^{-2}s^{-1}ster^{-1}]$ (right ordinate scale).

A lot of radio data were also obtained from the *Solar-Geophysical Data*. In addition, dynamic spectra and time profiles of radio bursts at fixed frequencies were used, these were taken from observations of IZMIRAN and Tremsdorf Observatory. Special data of the investigated bursts are listed in Table 1.

2. General characteristics of the investigated period

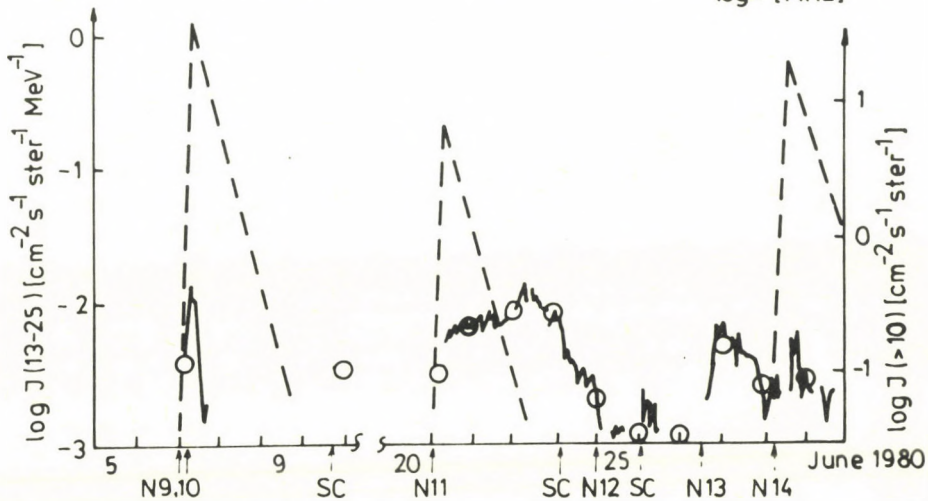
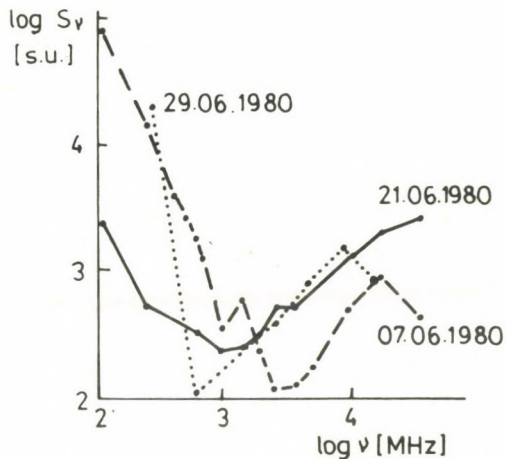
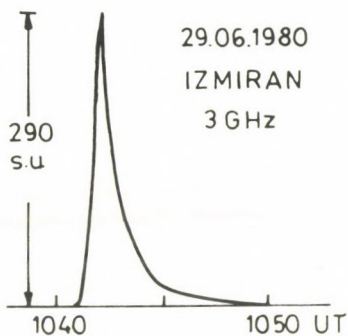
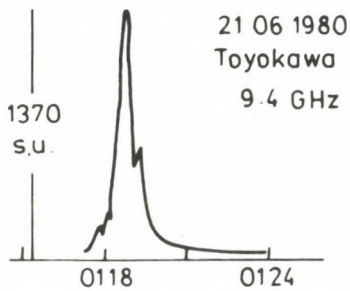
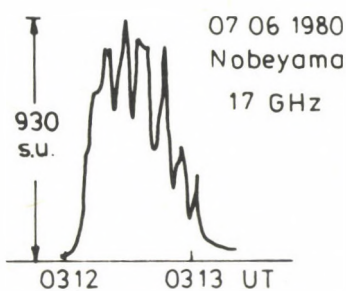
During the period January -October 1980 a total of 58 radio bursts with peak fluxes $S_\nu > 500$ s.u. at $\nu \geq 3$ GHz was recorded by world-wide observations. Among these events 26 bursts reached $S_\nu > 1000$ s.u. and hence 9 events even $S_\nu > 2000$ s.u.. The estimations, according to the method sketched above showed, however, that the corresponding flares should not be accompanied with remarkable proton flux increases: Firstly, for the majority of the events the proton flare criterion was not satisfied (mainly due to the time parameters of the radio bursts); this means that for such flares the calculated proton intensities are $I_c < 1 - 5 cm^{-2}s^{-1}ster^{-1}$. Secondly, for 8-12 flares, for which the proton flare criterion was fairly well satisfied, the calculated proton fluxes did not exceed $I_c \sim 30 cm^{-2}s^{-1}ster^{-1}$ due to the heliolongitudinal decrease

T A B L E 1

List of events in 1980

No	Date	Time UT	Flare Importance	Position	Region
1	3 Febr.	1333	1B/M3	S15 E15	2266
2	8 Febr	0906	1B/X2	N13 W80	2262
3	11 Febr.	2037	1B/M4	N13 E62	2281
4	28 Febr.	1206	1B/M4	S23 E28	2294
5	3 June	2130	1B/M7	S14 E67	2490
6	4 June	0655	1B/M6	S14 E59	"
7	4 June	0832	1N/M4	S14 E58	"
8	4 June	2301	1B/X2	S14 W69	2478
9	7 June	0118	1B/M3	N13 W72	2495
10	7 June	0313	1B/M7	N12 W74	"
11	21 June	0118	1B/X2	N19 W90	2502
12	24 June	2322	1N	S25 W14	2522
13	27 June	1616	SB/M7	S25 W64	"
14	29 June	1041	1F/M4	S27 W90	"
15	1 July	1627	1B/X2	S17 W37	2544
16	6 July	0444	SB/M2	N27 W33	2550
17	8 July	1922	SB/C2	N20 E87	2559
18	11 July	2216	2B/M5	S08 E65	2562
19	12 July	1543	1B/M3	S10 E60	"
20	17 July	0605	2N/M3	S11 E06	"
21	21 July	0256	1B/M8	S14 W60	"
22	23 July	0057	3B/M8	S19 E17	2579

Fig.1. Time profiles and radio flux spectra of events in June 1980.



in the proton fluxes, a relatively small energy content of the bursts, or not favourable escape conditions. Hereby only 3-4 cases exhibited $I_c \approx 10 \text{ cm}^{-2}\text{s}^{-1}\text{ster}^{-1}$.

The conclusion on the weakness of the proton events during the considered period as obtained from the analysis of the radio bursts is fully consistent with the direct proton flux observations in the vicinity of the Earth. This can be regarded as an important positive result, which demonstrates the effectivity of the method of quantitative proton flare diagnostics applied. Indeed, according to the IMP-8 data only 11 events exhibited proton fluxes with $I_o > 1 \text{ cm}^{-2}\text{s}^{-1}\text{ster}^{-1}$. With this, 6 cases showed $I_o < 5 \text{ cm}^{-2}\text{s}^{-1}\text{ster}^{-1}$ and of the remaining 5 events 4 exhibited $I_o < 20 \text{ cm}^{-2}\text{s}^{-1}\text{ster}^{-1}$. Only the strongest event reached an intensity of $I_o \approx 150 \text{ cm}^{-2}\text{s}^{-1}\text{ster}^{-1}$. However, as the analysis shows (cf. below) it was not associated with any distinct flare but was a corotating event. The comparison between calculated and observed parameters of the proton fluxes shows, furthermore, that in the given case only 2-3 events deviated. Hereby, it should be stressed that these, and also some other cases, less rapidly deviating between calculation and observation, correspond to a very low level of proton flux intensity.

3. Special results

Now we turn to the main effects which were detected as a result of the diagnostic analysis of the proton event in 1980.

a) Impulsive bursts

There is a great number of flares with a strong electromagnetic radiation in all spectral regions which, however, exhibit an impulsive character at centimetre waves (cf. the above mentioned quantities d_3 , d_{5-7} , d_9) and therefore do not lead to an essential increase in the proton flux. The calculation of the expected proton flux parameters can be carried out for such bursts according to our method, but in these cases the method only reveals that the proton fluxes will not exceed a given level of $I_c \approx 1 - 5 \text{ cm}^{-2}\text{s}^{-1}\text{ster}^{-1}$.

The importance of the consideration of the time para-

meters of the radio bursts, in particular their impulsive form, for the diagnostics of proton flares is clearly demonstrated by the analysis of the main events of June 1980. Here, the well known flares No 10, 11, and 14 of Table 1 are of special interest, the first two of these being connected with a γ -ray line emission, and the last one with a γ -ray continuum emission. All three flare centres were situated at the western solar hemisphere. The radio data show intense burst components with an U-shaped spectrum as characteristic of proton events, and related type II and IV bursts (for the flare No 14 type II, III, and V bursts were recorded). However, the time profiles of the radio bursts undoubtedly showed that in the given case the microwave emission (and also the soft X-ray burst) displayed an impulsive character in the sense of our method. The proton flux profile, shown in Fig.1, allow us to stress two points once more. There is, firstly, a general confirmation of the method for those flares, for which the proton flare criterion is not satisfied, in particular concerning impulsive flares. For events of this kind the proton flux should not exceed the above mentioned values and this is confirmed by the results of direct measurements. Secondly, if the impulsive character would be neglected in the first stage of the estimation of the proton efficiency in the diagnostic method, then the calculated values of the particle intensity would be found to be much higher than observed (dotted line in Fig.1 and the following figures). In this respect the situation is the same as for γ -line radiation. For impulsive flares the observed proton fluxes were found to be somewhat smaller than expected, if only the peak fluxes (and even integrated parameters) of the radio and γ -ray burst would be taken in consideration. This means that pure impulsive flares form a special class in which the connection between burst and proton flux parameters reveal a more complex character than for flares satisfying the proton flare criterion. Therefore, these events should be taken separately, already at the stage of the estimation of the proton efficiency of the flares, as was done in the present method.

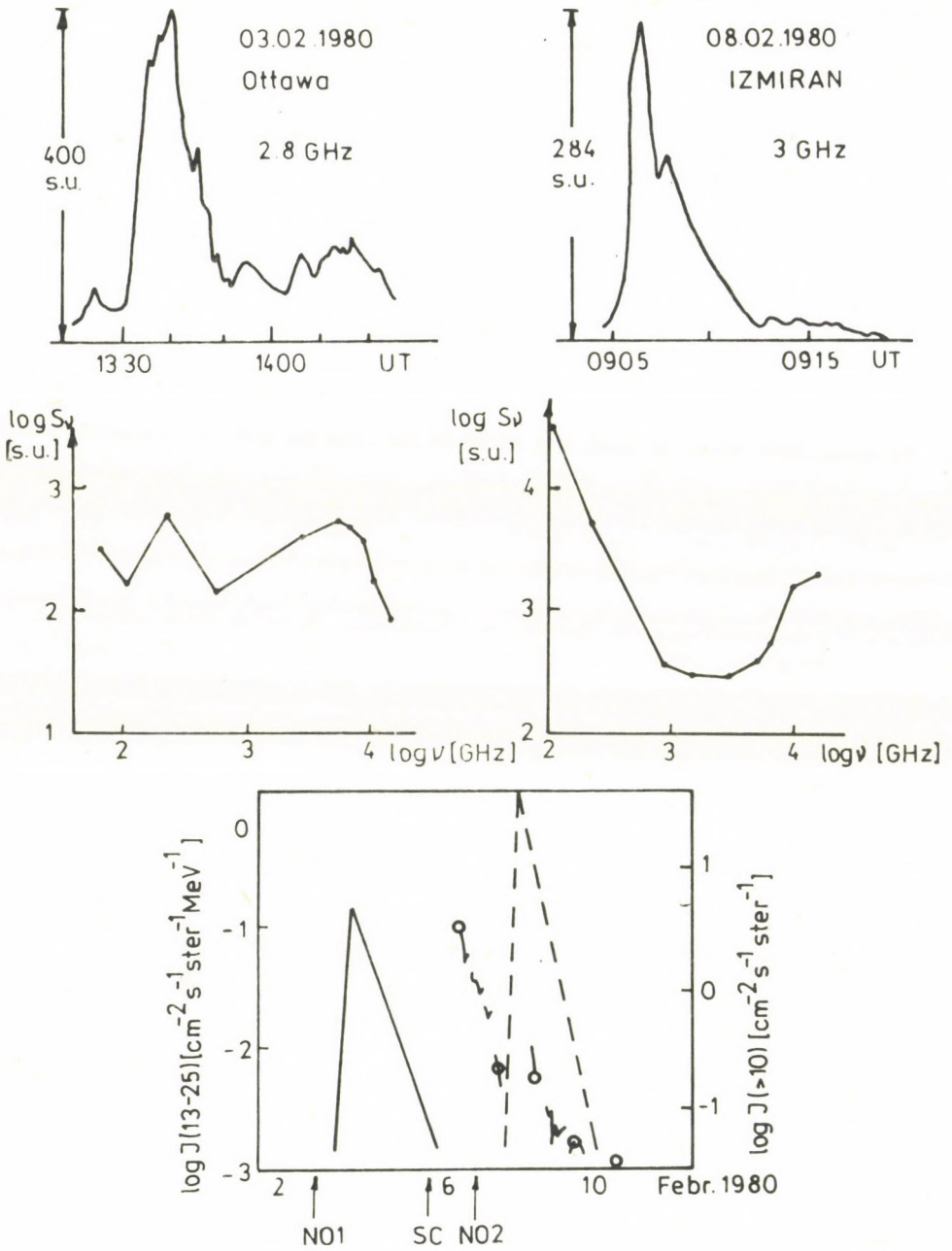


Fig.2. Time profiles and radio flux spectra of events in February 1980.

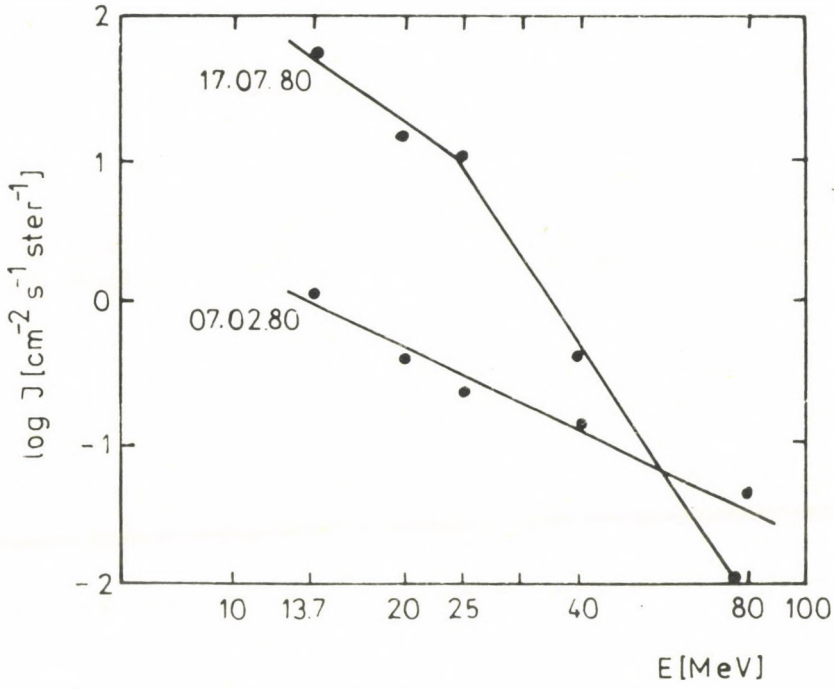


Fig.3. Selected proton flux spectra (cf. text)

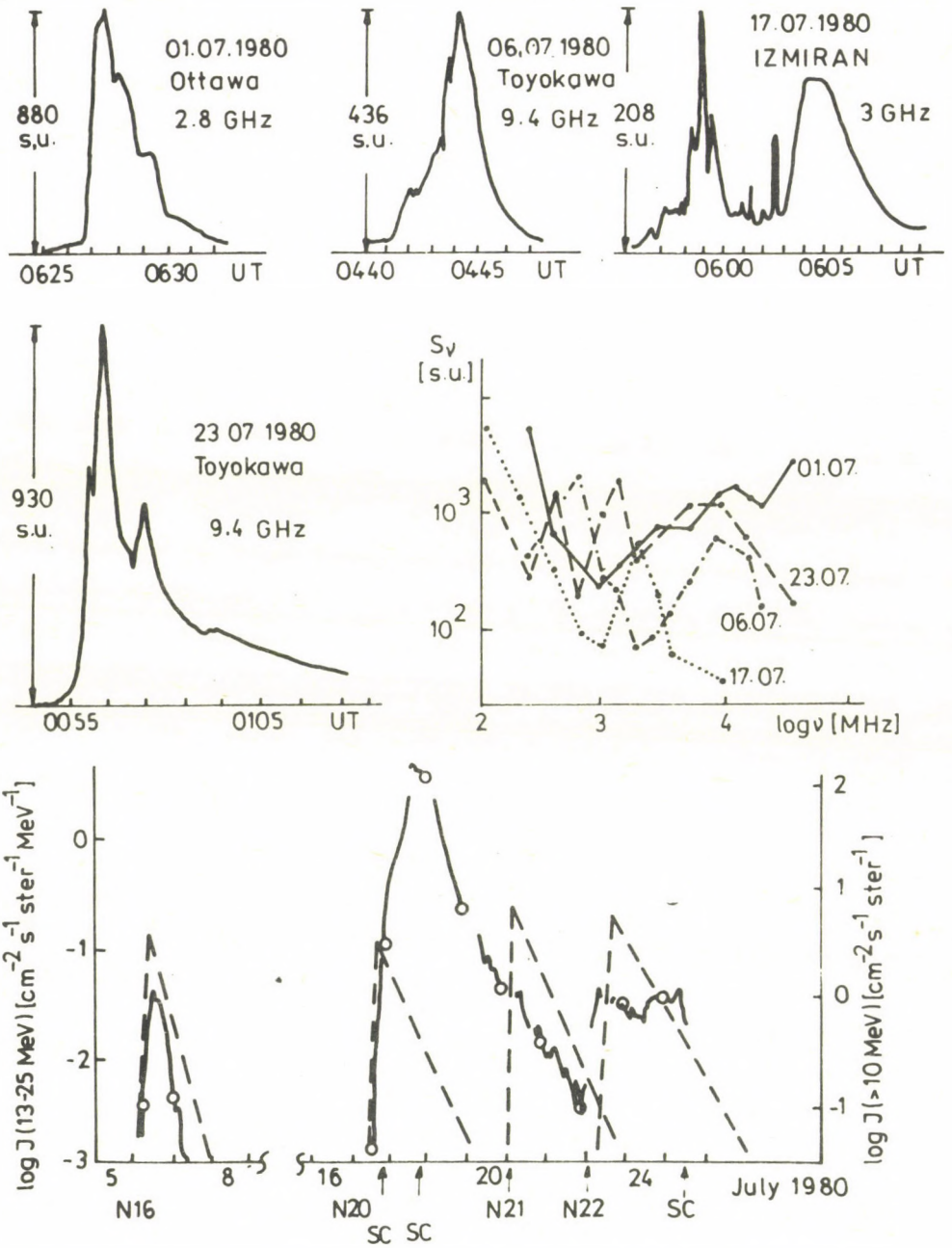


Fig.4. Time profiles and radio flux spectra of events in July 1980.

b) Anomalous retardation effect

In some cases an anomalous temporal delay of relatively weak proton fluxes took place with regard to a most probable flare association. One example of this kind is the event series of the first half of February 1980.

Among the events of this month flare No 1 exhibited proton flare characteristics. It was accompanied by a comparatively weak radio emission and according to our calculations should give an unimportant proton flux increase of $I_{\odot} \approx 4.6 \text{ cm}^{-2}\text{s}^{-1}\text{ster}^{-1}$ and a time of maximum on 2 February 07:30 UT (full line in Fig.2). From the IMP-8 observations no proton flux increase can be found on 2 February, data for 6 and 7 February are not available and beginning with 7 February, 05 UT a part of the proton flux decline was observed. According to Avdyushin et al. [5], the maximum of the proton flux increase took place on 6 February, 14 UT with an amplitude of $I_{\odot} \approx 7.7 \text{ cm}^{-2}\text{s}^{-1}\text{ster}^{-1}$.

If the observed weak proton flux increase is related to flare No 1 in this way, one can state that the proton flux intensity is near the one calculated but an anomalous strong delay in the flux maximum of about 3 days of this flare took place. Commonly such a delay is characteristic of flares located near the East limb of the Sun, but in the given case flare No 1 was observed in an active region not far from the central meridian at E15; It should be mentioned that on the day of the flare the active region No 2266 revealed a δ -configuration of the magnetic field which is usually characteristic of proton flares.

In such a situation it is necessary to look in more detail for other possible sources which could have generated the proton flux increase with the maximum on 6 February. During the two previous days the most remarkable flare occurred on 5 February, 17:27 UT (importance $1B/M3$) in the same active region No 2266. But this was a pure, impulsive microwave burst with a peak flux $S_{\nu} = 430 \text{ s.u.}$ at $\nu = 9 \text{ GHz}$ and not associated with any radio emission at meter waves. Therefore, this flare can scarcely be considered an potential source of the proton

event examined. An association with other flares during this period appears even less likely.

One should pay attention to the fact that the discussed proton flux increase took place during a geomagnetic storm with an sc on 6 February, 03:20 UT which very probably was generated by a disturbance coming to the Earth from flare No 1, with the proton flare characteristics of its radio emission. In the present case the proton energy spectrum was not as soft as can be seen from the majority of proton events associated with sc's. At the beginning of the IMP-8 observations on 7 February the spectral index was $\gamma \approx 2.0$ (Fig.3, cf. also Avdyushin et al.{5}). Such a sufficiently hard energy spectrum does not account for a reliable interpretation of the considered proton flux increase as corotational event. Nevertheless, except for the considered active region No 2266, generating flare No 1 on a favourable heliographic longitude 20-60W on February 6-7, there was another active region with a δ -configuration, No 2262, in which, on 8 February, another strong but impulsive flare No 2 originated.

The present discussion does allow us to prefer unambiguously one of the considered variants of the interpretation of the considered event, and all factors mentioned must be considered among them the connection of the proton event to flare No 1 and the subsequent anomalous delay of the particles.

An analogous situation was observed for three comparatively weak proton events on January 10-11, April 3-4, and October 13-15, 1980.

c) Corotating proton flux increase

In July 1980 a proton flux increase with remarkable intensities was observed, which mainly exhibited a corotational character.

During July a large proton flux increase was observed with the intensity $I_0 \approx 130 \text{ cm}^{-2}\text{s}^{-1}\text{ster}^{-1}$ which was not predicted by the radio data (Fig.4). The character and the parameters of this event (cf. below) exclude a connection with a behind-limb activity with high probability. Examining all

flares observed on the solar disk on the foregoing days event No 20 was the most remarkable one. However, the associated radio burst (cf. Fig.4) clearly does not satisfy the conditions of a high proton effectivity: Its peak flux at $\nu \geq 3$ GHz was $S_\nu < 300$ s.u., the spectrum had a maximum in the range 1.4-2 GHz, where the fluxes were also not very high, $S_\nu \approx 440 - 590$ s.u. at centimetric waves the flux decreases with increasing frequencies and obtains at 9 GHz only $S_\nu \approx 100$ s.u., the time profile is of impulsive nature. The meter-wave burst components were rather intense and contained a type IV burst continuum without clear type II burst connection.

The above mentioned data allow us to conclude that flare No 20 could scarcely be the main source of the considered proton flux increase.

On the other hand, one has to pay attention to the long phase of the proton flux increase and especially to the very soft energy spectrum of the protons. According to the IMP-8 data (cf. Fig.3), during the proton flux maximum a spectral index of $\nu \approx 5.2$ was observed in the energy range $E \approx 13-25$ MeV, and in the range $E > 25$ MeV the spectrum was steeper ($\gamma \approx 5.2$). The conclusion on the soft particle spectrum of this event is also confirmed by other data. According to Avdyushin et al. {3}, the spectral index was $\gamma \approx 3.6$ in the energy range $E > 5$ till $E > 40$. Further it is important to note that the beginning of the proton flux increase was near the onset time of the sc (which was on July 17, 19:36 UT) and the proton flux maximum coincides in principle with another sc observed on 16 July, 19:26 UT.

All these facts lead to the conclusion that the discussed event refers to a corotating proton flux increase connected with the active region No 2562. This region clearly dominates on the solar disk and exhibits a magnetic δ -configuration. During this period flares connected with most intense radio burst occurred, cf. in particular the events No 18-21, and also a series of flares associated with somewhat weaker microwave bursts ($S_\nu \approx$ some hundreds s.u.) but strong radiation in

the optical and soft X-ray ranges. At the time of the maximum of the proton flux the active region No 2562 was located at a favourable heliographic longitude \sim W30. It is also possible that a transport and acceleration of particles between two shock waves associated with the sc of 17 and 18 July play a certain role in the increase of the low energetic proton flux.

In this way the passage of the discussed proton event, combined with a consideration of the radio emission explains that the event was not due to any specific flare but had the character of a soft corotational proton flux increase connected with the active region No 2562.

A more detailed analysis of the events of 1980 will be published later.

R e f e r e n c e s

- {1} Akinyan, S.T., Chertok, I.M., Fomichev, V.V., *Solar-terrestrial predictions proceedings*, (Donnelly, R.F.ed.) US Dept.of Commerce, NOAA, Washington D.C., Vol.3, D-14
- {2} Akinyan, S.T., Fomichev, V.V., Chertok, I.M., *Geomagn.Aehron.* 29. 385, 1980
- {3} Akinyan, S.T., Fomichev, V.V., Chertok, I.M., *Phys.Solariterr.* 17. 135, 1981
- {4} Akinyan, S.T., Fomichev, V.V., Chertok, I.M., *XII. Leningradskij Seminar po Kosmofizike*, LFTI Leningrad, p.119. 1982 (in Russ.)
- {5} Avdyushin, S.I., Kozlovskij, V.D., Nazarova, M.N., Pereyaslova, N.K., Petrenko, I.E., Akinyan, S.T., Fomichev, V.V., Chertok, I.M., *Fiz.soln.akt.* (in Russ.) Moscow, 1980
- {6} Avdyushin, S.I., Nazarova, M.N., Pereyaslova, N.K., Petrenko, I.E., *Izv.AN SSSR, Ser.Fiz.* 46. 1754, 1982 (in Russ.)
- {7} *Solar-Geophysical Data*, Nos.426-461, 1980-1983

SPECTROGRAPHIC OBSERVATIONS OF SOLAR MICROWAVE BURSTS
IN THE 5.3 - 7.4 GHz RANGE

N.S. K A V E R I N, A.I. K O R S H U N O V,
V.V. S H U S H U N O V
NIRFI, Gorkij

H. A U R A S S, H. D E T L E F S, H. H A R T M A N N,
A. K R Ü G E R, J. K U R T H S
ZISTP (HHI), Berlin (GDR)

Abstract:

Two 5.3-7.4 GHz microwave burst spectral diagrams are shown having 20 s time resolution.

СПЕКТРОГРАФИЧЕСКИЕ НАБЛЮДЕНИЯ СОЛНЕЧНЫХ МИКРОВОЛНОВЫХ ВСПЛЕСКОВ
В ДИАПАЗОНЕ 5.3 - 7.4

Н.С. КАВЕРИН, А.И. КОРШУНОВ, В.В. ШУШУНОВ
НИРФИ, Горький

Х. АУРАС, Х. ДЕТЛЕФС, Х. ХАРТМАНН, А. КРЮГЕР, Й. КУРТС
ЦИСЗФ, Берлин (ГДР)

Абстракт:

Показаны результаты наблюдения двух микроволновых всплесков в диапазоне 5.3-7.4 ГГц со временным разрешением 20 сек.

The Gorky-type microwave spectrograph, working at Trens-dorf solar radioastronomy observatory (HHI) [1], was reconstructed to get a higher time resolution for the spectral observations. Turning from observations of the S-component and gradual bursts the aim now is to observe microwave burst spectra more generally and to include the results in burst model calculations, as discussed for instance, in [2]. Table 1 gives the technical parameters now implemented.

A critical inspection of the actual state yields that at present the achieved time resolution of 20 s is still too low for observing possible flare related drifting fronts being supposed e.g. by [3] and for a fine spectral resolution of the impulsive phase.

Nevertheless, the accuracy of the equipment and general properties of the burst emission could be checked. So, two examples of microwave burst spectral observations can be presented here - considered as the next step towards satisfactory results. Besides the spectrographic equipment, essential tools for present and future development are the fast digital recording system and the SM 4 computer of the observatory.

Illustrating the observations Fig.1 gives the time profile of the December 8, 1982 microwave burst (HHI single frequency records).

Fig.2 shows the observed spectral diagram. In the top of the figure the mean flux in the 5.3 - 7.4 GHz range is given in relative units. The spectral diagram was computed from relative spectra, where each spectrum is given as the ratio to the spectrum observed 20 s before. Further, a 3% confidence limit for spectral changes was defined. The resulting picture is given in a printer plot. Numbers denote positive changes, capital letters indicate negative changes.

Space marks no change $\pm 1\%$ ($1 \hat{=} +1 \dots +3\%$; $A \hat{=} -1 \dots -3\%$ and so on). The three abscissae columns give: the number of spectra with relative changes (constant spectra have been omitted): the absolute number of the spectra; and the time in UT. The frequency scale is given to the left of the figure.

Figs.3 and 4 give the same data for the December 9, 1982 burst. Unfortunately, due to some sensitivity scale problems, parts of the diagram are off-scale.

From an inspection of Figs.1-4 the following summary of the first observations can be given:

- 1) Broad-band spectral structures of the microwave burst development have been observed. They are mostly wider than the range of the receiver (i.e. 2.1 GHz).

8.12.1982

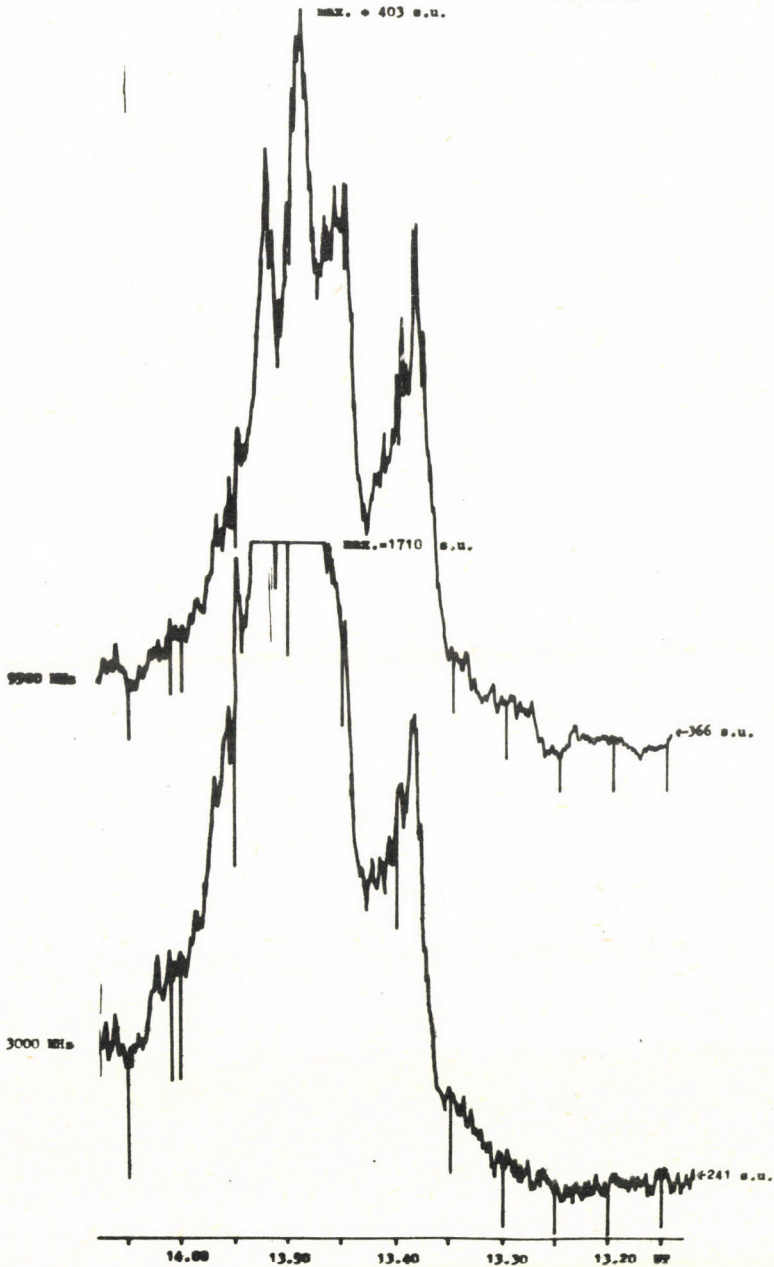


Fig.1. Single frequency records of the December 8, 1982 burst.

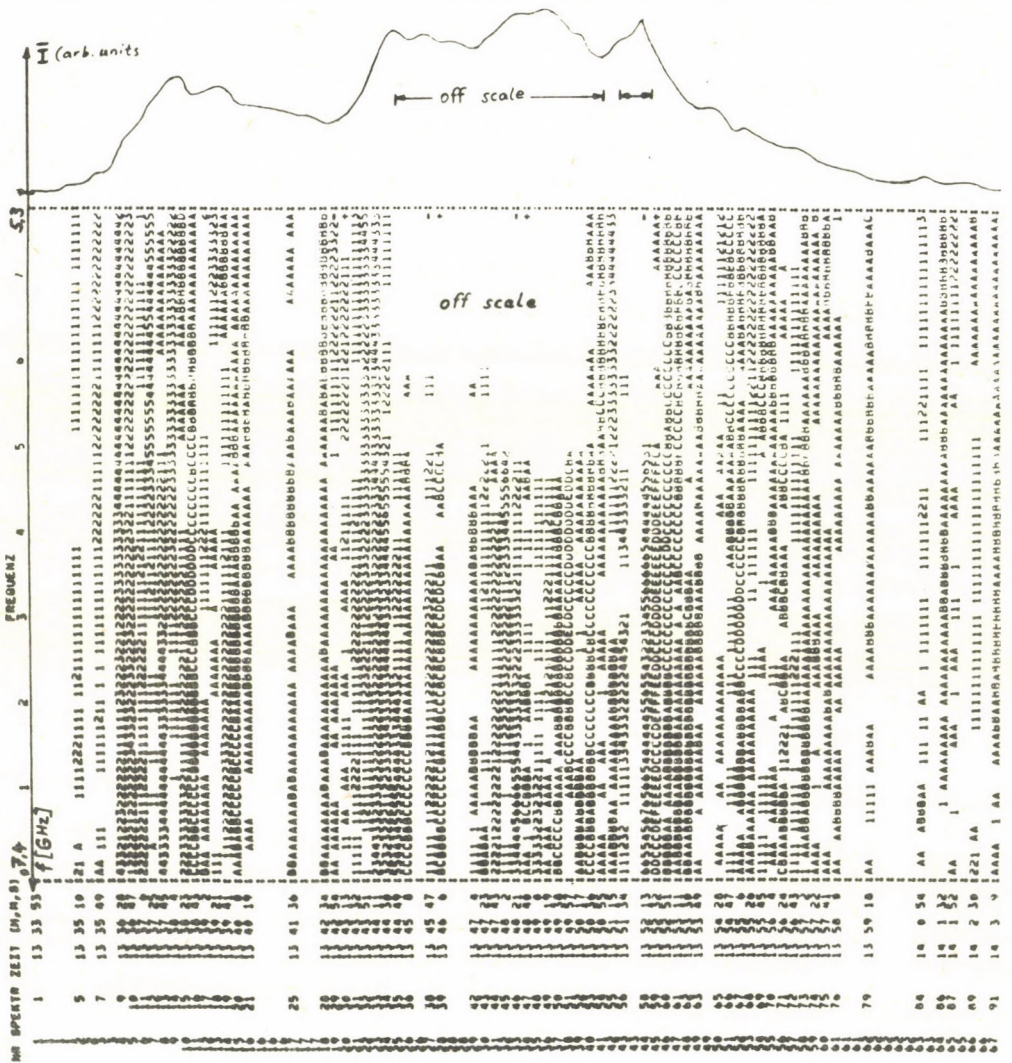


Fig. 2. Printer plot of the microwave spectral diagram of the December 8, 1982 event.

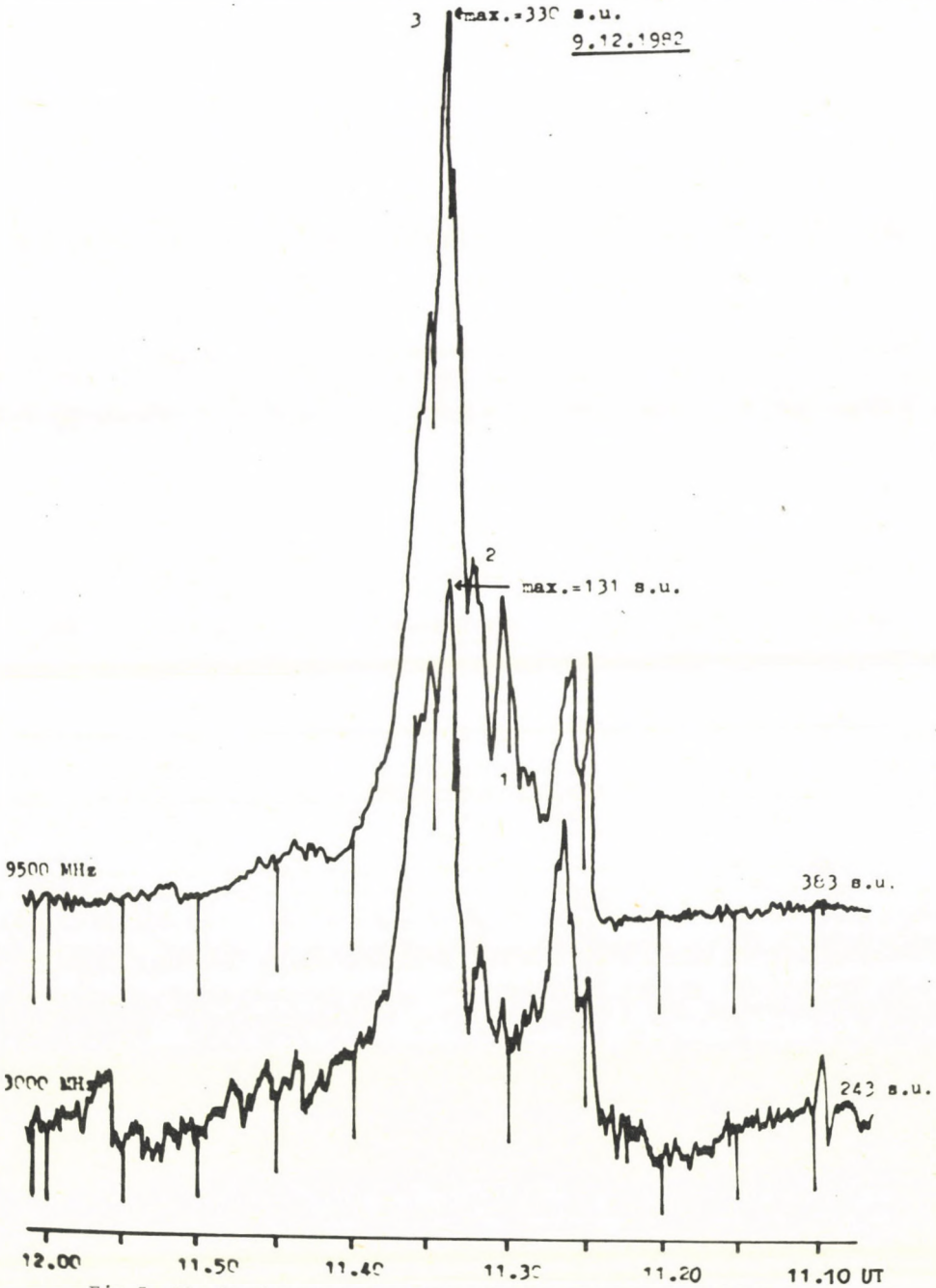


Fig.3. Single frequency records of the December 9, 1982 burst.

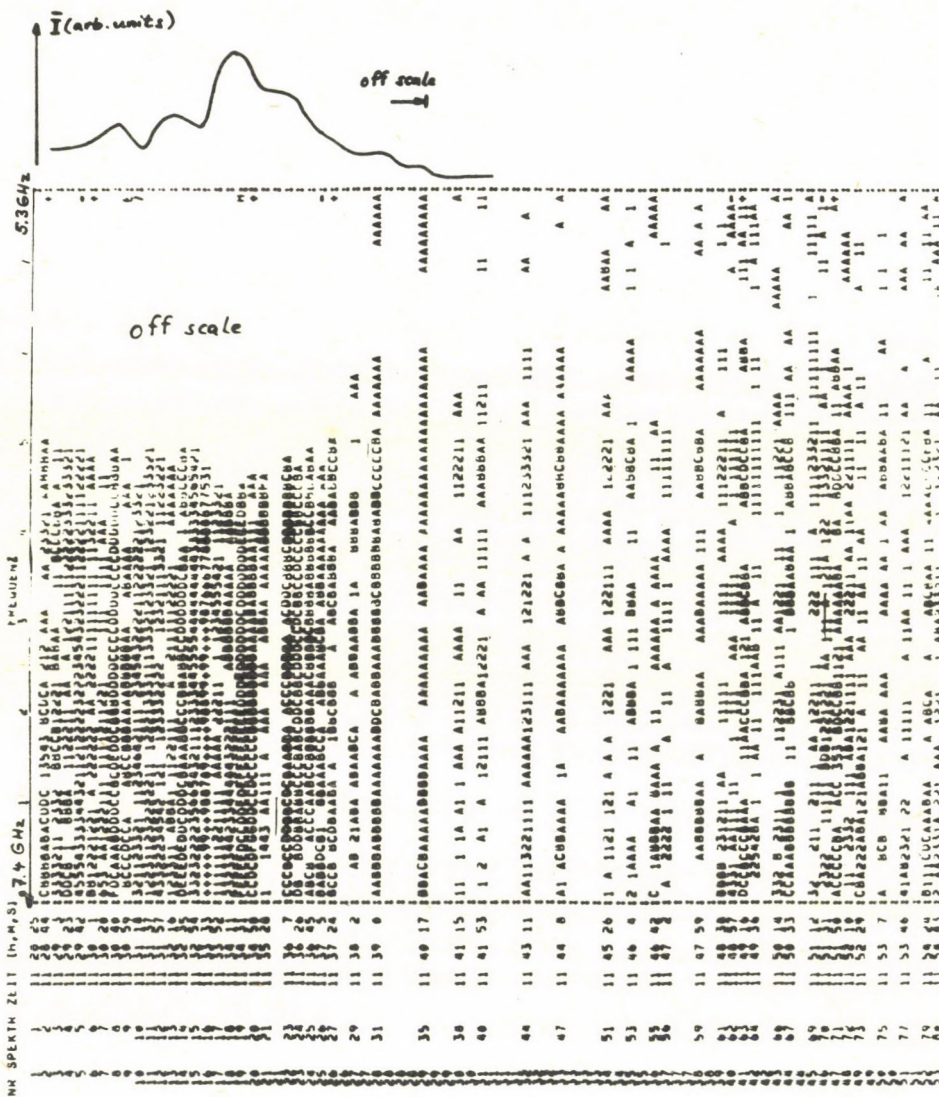


Fig. 4. Printer plot of the microwave spectral diagram of the December 9, 1982 event. The same symbols have been used as in Fig. 2.

T A B L E 1

Technical parameters of the microwave spectrograph

Frequency range, used for the burst observations	5.3 - 7.4 GHz
HF - Bandwidth	80 MHz
Sensitivity, given for the 3 possible time constants	$T_{\min} = 23.5 \text{ K (0.01 s)}$ $T_{\min} = 7.1 \text{ K (0.1 s)}$ $T_{\min} = 2.0 \text{ K (1.0 s)}$
Modulation frequency	1.58 kHz
Possible sweep periods	arbitrary in the range 10.0 - 999 s or 0.01 - 1.9 s
Actual operation mode	sweep period 20 s, 80 sample points/sweep

- 2) Some "pseudo-drift" structure during the enhancing flux intervals of the burst profile in Fig.2 is caused by the onset of individual peaks of the time profile of the burst which happens during the spectral scan with sec time scale and shorter.
- 3) The reality of spectral fine structures smaller than 500 MHz can not be checked with the given mode of observation.

R e f e r e n c e s

- {1} Aurass, H., Böhme, A., Krüger, A., Kurths, J., Paschke, J., Voigt, W., Kobrin, M.M., Korshunov, A.I., Kaverin, N.S., Shushunov, V.V., Panfilov, Yu.D., New spectrographic measurements of the S-component of solar radio emission in the 4-7 GHz range, *Phys.Solariterr.* No.12. 5, 1980
- {2} Böhme, A., Fürstenberg, F., Hildebrandt, J., Saal, O., Krüger, A., Hoyng, P., Stevens, G.A., A two-component model of impulsive microwave burst emission consistent with soft and hard X-rays, *Solar Phys.* 53. 139, 1977
- {3} Costa, J.E.R., Kaufmann, P., Mm to cm-wavelength time delays in solar burst emission and the effect of varying magnetic field, *Astron.Astrophys.* 119. 131, 1983

ABBREVIATIONS USED IN REFERENCES

- ГСМ-SMY Crimean Workshop - Solar Maximum Year, Proceedings of International Workshop, March 1981, Vol.1.,2., IZMIRAN, Sun-Earth Council, USSR Acad.Sci, Moscow, 1981*
- Иссл.СибИЗМИР (Issl.SibIZMIR) - Исследования по геомагнетизму, аэронамии и физике Солнца, СибИЗМИР АН СССР, Издат."Наука", Москва*
- Изв.КрАО. (Izv.KrAO) - Известия Крымской Астрофизической Обсерватории*
- Астрон.Ж. (Astron.Zh.) - Астрономический Журнал*
- Письма в АЖ (Pis'ma v AZh) - Письма в Астрономический Журнал*
- Солн.Данн. (Soln.Dann.) - Солнечные Данные Бюллетень*
- Физ.Солн.Акт. (Fiz.soln.akt.) - Физика солнечной активности (Physics of solar activity, generally with abstracts in English), ИЗМИРАН, Москва*
- Геомагн.Аэрон. (Geomagn.aehron.) - Геомагнетизм и аэронамия, АН СССР, Изд."Наука" Москва,*
- Солн.Зем.Физ. (Soln.Zem.Fiz.) - Солнечно-Земная Физика, Совет "Солнце-Земля", АН СССР, Москва*
- A.N. - Astronomische Nachrichten*
- BAC - Bulletin of the Astronomical Institutes of Czechoslovakia*
- HHI-STP Rept. - Akademie der Wissenschaften der DDR, Zentralinstitut für solar-terrestrische Physik (Heinrich-Herz Institut) Report, Berlin*
- Phys.Solariterr. - Physica Solariterrestris, Potsdam, Nationalkomitee für Geodäsie und Geophysik., Akademie der Wissenschaften der DDR*
- Z.Astrophys. - Zeitschrift für Astrophysik*
- M.N. - Monthly Notices of the Royal Astronomical Society*
- IAU Symp. - International Astronomical Union Symposia*
6. Electromagnetic phenomena in cosmical physics (Stockholm, Sweden) Lehnert, B. ed. Cambridge Univ.Press 1958
 22. Stellar and solar magnetic fields (Rottach-Egern, FRG) Lüst, R. ed. North-Holland Publ.Co., Amsterdam, 1965
 35. Structure and development of solar active regions (Budapest, Hungary) Kiepenheuer, K.O. ed. D.Reidel Dordrecht 1968
 43. Solar magnetic fields (Paris, France) Howard, R.ed. D.Reidel Dordrecht 1971
 56. Chromospheric fine structure (Surfer's Paradise, Queensland, Australia) Grant Athay, R. ed., D.Reidel Dordrecht 1974
 57. Coronal disturbances (Surfer's Paradise, Queensland, Australia) Newkirk, G.Jr. ed., D.Reidel Dordrecht 1974
 71. Basic mechanisms of solar activity (Prague, Czechoslovakia) Bumba, V., Kleczek, J. eds., D.Reidel Dordrecht, 1976
 91. Solar and interplanetary dynamics (Cambridge, Ma. USA) Dryer, M., Tandberg-Hanssen, E. eds., D.Reidel Dordrecht, 1980

LIST OF CONSULTATION PAPERS NOT INCLUDED IN THIS ISSUE

(The final version did not reach the editors in time
to be included in this volume.)

Г.Б.Гельфрейх (G. B. Gel'frejkh)

ЯДРА ЛОКАЛЬНЫХ ИСТОЧНИКОВ РАДИОИЗЛУЧЕНИЯ СОЛНЦА И
СТРУКТУРА МАГНИТНЫХ ПОЛЕЙ СОЛНЕЧНЫХ ПЯТЕН

В. Ромпolt

ERUPTION OF HUGE MAGNETIC SYSTEMS FROM THE SUN

J. Sylwester, B. Sylwester, R. Mewe, J. Schrijver, R. D. Bentley

DENSITY-TEMPERATURE DIAGNOSTICS OF THE FLARE PLASMA

М. Карлицкы

NARROWBAND dm-SPIKES AS INDICATION OF FLARE MASS EJECTION

М. Якимiec, L. Dezső

TESTING OF THE H α FLARE CLASSIFICATION BY MEANS OF
OBSERVATIONS IN H α WINGS AND SOFT X-RAY INTENSITIES

AN ACCOUNT OF SOME EXTRA SESSIONS OF THE CONSULTATION

I.

Formal Opening

by *M.Kopecký*, Chairman of KAPG Project 4

Respectful tribute was paid to
Gennadij Mikhailovitch Nikol'skij
and
Vladimir Alekseevitch Krat,
whose untimely deaths prevented them from attending
the Consultation.

Welcome on behalf of the Debrecen Academy Committee

by *D.Berényi*, Co-chairman of the
Physico-mathematical Special Committee
of the Debrecen Academy Committee

Opening Address

by *B.Szeidl*, Director, Astronomical Research Institute,
Hungarian Academy of Sciences

II.

L.Dezső: A Brief History of Solar Astronomy in Hungary

B.Kálmán: The Present State of Solar Physics in Debrecen

(followed by a modest reception in the Debrecen Heliophysical Observatory)

III.

L.Dezső: A review on the SMY Flare-Build-up Study Special
Workshop, held at the Big Bear Solar Observatory,
June 1983

M.Kopecký: Information on the Future of the KAPG organization

K.Pflug: The KAPG Theme 4.1 and future plans for it

N A M E I N D E X
(Authors and Participants)

- Achmedov Sh.B. 20,431,619
 Akinyan S.T. 21,639
 Alibegov M.M. 20,333,603
 Alikaeva K.V. 20,177,217
 Ambrož P. 17,145
 Antalová A. 17,93
 Aurass H. 18,185,631,639,653
 Avdyushin S.I. 20,333,603
- Bachmann G. 18,369,589
 Baranyi T. 18,595
 Bentley R.D. 17,85,662
 Bielicz E. 19
 Bogod V.M. 20,619
 Bogemolov A.F. 21,333,603
 Bouckova O. 17
 Böhme A. 18,185
 Bufka L. 17,545
 Bumba V. 17,47
 Burov V.A. 20,333,603
- Ciurla T. 19,531
 Chernov G.P. 21,193
 Chertok I.N. 21,73,193,639
 Csada I.K. 18,495
 Csepura Gy. 18
- Delone A.B. 20,517
 Dermendjiev V.N. 17,475
 Detlefs H. 18,653
 Dezső L. 2,16,18,317,662,663
- Fárnik F. 17,193
 Fomichev V.V. 21,73,193,639
 Fürstenberg F. 18,619,631
- Garczyńska I.N. 19,543
 Gel'frejkh G.B. 20,431,662
 Gerlei O. 18
 Gesztelyi L. 16,18,133
 Gnevyshev M.N. 20,503
 Golubchina O.A. 20,611
 Gopasyuk S.I. 21,249
 Grandpierre A. 18
 Grigor'ev V.M. 19,377
 Györi L. 18
- Hartmann H. 18,653
 Hildebrandt J. 18,431,619,631
 Hofmann H. 18,369
- Ikhsanova V.N. 20,611
 Ishkov V.N. 21,73,193,355
- Jakimiec J. 19,85,127
 Jakimiec M. 19,662
- Kálmán B. 2,16,18,193,207,249,663
 Karlický M. 17,193,662
 Kasinskij V.V. 19,31
 Kaverin N.S. 19,631,653
 Knoška S. 17,557
 Kobrin M.M. 19,631
 Kondás L. 18,133
 Kondrashova N.N. 20,177
 Kopecký M. 17,663
 Korobova Z.B. 21,285,341,355
 Korshunov A.I. 19,631,653
 Korzhavin A.N. 20,619
 Kovács A. 2,16,18,317
 Koval' A.N. 21,235
 Křivský L. 17,557
 Krüger A. 18,185,431,619,631,639,653
 Kuklin G.B. 19,267,389
 Kurths J. 18,653
- Leonenko S.P. 21,333,603
 Letfus V. 17
 Likin O.B. 20,193
 Locáns V. 21,451
 Lorenc M. 17
 Ludmány A. 2,18,575,595
 Lukač B. 17
- Makarova E.A. 20,517
 Maksimov V.P. 19,567
 Marik M. 18
 Markeev A.K. 21,73,193
 Mazur V.A. 19,419
 Majer P. 19,543
 Mel'nikov V.F. 19,167
 Merkulenko V.E. 19,293,463
 Mewe R. 18,85,127,662
 Mikhajlutsa V.P. 20,503
 Minarovjeh M. 17,511
 Minasyants G.S. 19,73
 Mogilevskij E.I. 21,355,409;487

- Nagy I. 18,107,207
Nefed'ev V.P. 19,167,443
Nikulin I.F. 20,217
- Obashev S.O. 19,73
Obridko V.N. 21,25
Osak B.F. 19,377
- Paciorek J. 19,531
Palamarchuk L.E. 19,293
Pap J. 18
Pflug K. 18,589,663
Pintér T. 17
Pisarenko N.F. 20,193
Podstrigach T.S. 19,167
Polupan P.N. 20,177,217
Polyakov V.I. 19,293,463
Poperechenko B.A. 21,333,603
Potapov N.N. 19,167
Prokudina V.S. 20,167
- Redyuk T.I. 20,177
Romanov V.A. 20,249
Rompolt B. 19,531,543,662
Růžičková-Topolová B. 17,545
Ryabov B.I. 21,323
Rušín V. 17,511
Rybanský M. 17,511
- Sattarov I. 21,341
Schrijver J. 18,127,662
Seehafer N. 18,117,431,631
Selivanov V.L. 19,377
Seres F. 18
Shushunov V.V. 19,631,653
Sikorski J. 19
Smol'kov G.Ya. 19,167
Sobotka M. 17,581
Spektor A.R. 21,323
Staude J. 18,369,451
Stepanov A.V. 19,419
Stepanov V.E. 19,31,389
Stepanyan N.N. 21,225,235
Sýkora J. 17,517,523
Sylwester B. 19,85,127,662
Sylwester J. 19,85,127,662
Szeidl B. 18,663
- Teplitskaya R.B. 19,267
Tlamicha A. 17,193
Tomašek P. 17
Turova I.P. 19,267
- Valniček B. 17,193
- Zajtsev E.I. 21,333,603
Zhugzhda Yu.D. 21,451

CONTENTS

PART 1

	PAGE
PREFACE	15
LIST OF PARTICIPANTS AND NON-PARTICIPANT CO-AUTHORS	17
№.1. INVITED REVIEW PAPERS	23
<i>V. N. Obridko</i> SOME TRENDS IN MODERN SOLAR PHYSICS <i>В. Н. Обридко</i> О НЕКОТОРЫХ СОВРЕМЕННЫХ ТЕНДЕНЦИЯХ В СОЛНЕЧНОЙ ФИЗИКЕ	25
<i>B. E. Stepanov, B. B. Kasinskiy</i> КРАТКИЕ ИТОГИ ИССЛЕДОВАНИЯ ВСПЫШЕК В ПЕРИОД ГСМ <i>V. E. Stepanov, V. V. Kasinskiy</i> A SHORT REVIEW OF THE INVESTIGATIONS OF SOLAR FLARES IN THE SMY	31
<i>V. Bumba</i> PROPER MOTIONS OBSERVED IN ACTIVE REGIONS <i>В. Бумба</i> СОВРЕМЕННЫЕ ДВИЖЕНИЯ НАБЛЮДАЕМЫЕ В АКТИВНЫХ ОБЛАСТЯХ	47
№.2. PAPERS RELATED TO THE SOLAR MAXIMUM YEAR PROGRAMS	71
<i>I. M. Chertok, V. V. Fomichev, V. N. Ishkov, A. K. Markeev, G. S. Minasyants, S. O. Obashev</i> RELATIONSHIP OF THE DYNAMIC EVENTS IN OPTICAL AND RADIO RANGES DURING THE FLARES OF NOVEMBER 9 AND 10, 1979 <i>И. М. Черток, В. В. Фомичев, В. Н. Ишков, А. К. Маркеев, Г. С. Минасянц, С. О. Обашев</i> СООТНОШЕНИЕ ДИНАМИЧЕСКИХ ЯВЛЕНИЙ В ОПТИЧЕСКОМ И РАДИОДИАПАЗОНАХ ВО ВРЕМЯ ВСПЫШЕК 9 И 10 НОЯБРЯ 1979 Г.	73
<i>B. Sylwester, J. Sylwester, J. Jakimiec, R. Mewe, R. D. Bentley</i> SMM FLAT CRYSTAL SPECTROMETER DATA ANALYSIS OF 7 APRIL 1980 FLARE <i>Б. Сильвестер, Я. Сильвестер, Я. Якимец, Р. Меве, Р. Д. Бентлей</i> АНАЛИЗ НАБЛЮДЕНИЙ ВСПЫШКИ ИЗ 7 АПРЕЛЯ 1980 Г ПОЛУЧЕННЫХ КРИСТАЛЛИЧЕСКИМ СПЕКТРОМЕТРОМ ИЗ БОРТА SMM	85
<i>A. Antalová</i> THE PHOTOSPHERIC DOPPLER SHIFT OBSERVED IN HALE ARS 16862 AND 16863 (MAY 22 AND 23, 1980) <i>А. Анталова</i> ФОТОСФЕРНЫЕ ЛУЧЕВЫЕ СКОРОСТИ НАБЛЮДАЕМЫЕ В АКТИВНЫХ ОБЛАСТЯХ ХЕЙЛА 16862 И 16863 (С 22 ПО 23 МАЯ 1980 Г.)	93

	PAGE
(No. 2) <i>I. Nagy</i> SUNSPOT PROPER MOTIONS IN THE WESTERN PART OF HALE REGION 16864 (MAY 25 - 29, 1980) <i>И.Надь</i> СОБСТВЕННЫЕ ДВИЖЕНИЯ СОЛНЕЧНЫХ ПЯТЕН В ЗАПАДНОЙ ЧАСТИ АКТИВНОЙ ОБЛАСТИ ХЕЙЛ № 16864 (25-29 МАЯ, 1980 Г)	107
<i>N. Seehafer</i> POSSIBLE MAGNETIC RECONNECTION IN THE SOLAR ACTIVITY COMPLEX OF MAY 1980 <i>Н.Зеехафер</i> ВОЗМОЖНОЕ МАГНИТНОЕ ПЕРЕСОЕДИНЕНИЕ В СОЛНЕЧНОМ АКТИВНОМ КОМПЛЕКСЕ МАЯ 1980 Г.	117
<i>J. Jakimiec, R. Mewe, J. Schrijver, J. Sylwester, R. Sylwester</i> TIME VARIATION OF THE DIFFERENTIAL EMISSION MEASURE OF HOT FLARE PLASMA <i>Я.Якимец, Р.Меве, Я.Шривер, Я.Силвестер, Р.Силвестер</i> ВРЕМЕННЫЕ ВАРИАЦИИ ДИФФЕРЕНЦИАЛЬНОЙ МЕРЫ ЭМИССИИ ГОРЯЧЕЙ ВСПЫШЕЧНОЙ ПЛАЗМЫ	127
<i>L. Gesztelyi, L. Kondás</i> THE DEVELOPMENT OF ACTIVITY IN HALE REGION 17098 (28 AUGUST - 8 SEPTEMBER 1980) <i>Л.Гестейи, Л.Кондас</i> РАЗВИТИЕ АКТИВНОСТИ В ОБЛАСТИ ХЕЙЛ № 17098 (28 АВГУСТА - 8 СЕНТЯБРЯ 1980 Г.)	133
<i>P. Ambrož</i> LOCATION OF SOURCES OF SOLAR NOISE STORMS' RELATIVE TO THE STRUCTURE OF EXTRAPOLATED CORONAL MAGNETIC FIELDS <i>П.Амброж</i> ПОЛОЖЕНИЕ ИСТОЧНИКОВ СОЛНЕЧНЫХ ШУМОВЫХ БУРЬ ОТНОСИТЕЛЬНО СТРУКТУРЫ ЭКСТРАПОЛИРОВАННЫХ КОРОНАЛЬНЫХ МАГНИТНЫХ ПОЛЕЙ	145
<i>V. F. Mel'nikov, V. P. Nefed'ev, T. S. Podstrigach, V. S. Prokudina, N. N. Potapov, G. Ya. Smol'kov</i> THE RADIO BURSTS OF 13 AND 16 MAY 1981 AND ASSOCIATED EVENTS IN THE RADIO BRIGHTNESS DISTRIBUTION ABOVE AN ACTIVITY COMPLEX <i>В.Ф.Мельников, В.П.Нефедьев, Т.С.Подстригач, В.С.Прокудина, Н.Н.Потапов, Г.Я.Смольков</i> ВСПЛЕСКИ РАДИОИЗЛУЧЕНИЯ 13 И 16 МАЯ 1981 Г. И СОПУТСТВУЮЩИЕ ИМ ЯВЛЕНИЯ В РАСПРЕДЕЛЕНИИ РАДИОКОСТИ НАД АКТИВНЫМ КОМПЛЕКСОМ	167
<i>K. V. Alikaeva, N. N. Kondrashova, P. N. Polupan, T. I. Reduk</i> PHOTOSPHERIC SLIPS OF FLARES FOR MAY 14, 15, 1981 IN AR 3106+3112 <i>К.В.Аликаева, Н.Н.Кондрашова, П.Н.Полупан, Т.И.Редук</i> ФОТОСФЕРНЫЕ СЛОИ ВСПЫШЕК 14 И 15 МАЯ 1981 Г. В КОМПЛЕКСЕ АР 3106+3112	177

	PAGE
(No.2) <i>H. Aurass, A. Böhme, A. Krüger</i> THE RADIO EMISSION AND ACTIVE REGION DEVELOPMENT DURING THE PERIOD OF MAY 15 - 25, 1981 <i>X. Аурас, А. Бёме, А. Крюгер</i> РАДИО ЭМИССИЯ И РАЗВИТИЕ АКТИВНЫХ ОБЛАСТЕЙ В ПЕРИОД 15 - 25 МАЯ 1981 Г.	185
<i>V.N. Ishkov, A.K. Markeev, V.V. Fomichev, G.P. Chernov, I.M. Chertok,</i> <i>O.B. Likin, N.F. Pisarenko, B. Valnišek, M. Karlický, A. Tlamiča,</i> <i>F. Fárnik, B. Kálmán</i> PECULIARITIES OF THE DEVELOPMENT OF FLARE ON MAY 16, 1981 AS OBSERVED IN OPTICAL, X-RAYS AND RADIO WAVES <i>В.Н. Ишков, А.К. Маркеев, В.В. Фомичев, Г.П. Чернов, И.М. Черток,</i> <i>О.Б. Ликин, Н.Ф. Писаренко, Б. Валничек, М. Карлицкий,</i> <i>А. Тлamiча, Ф. Фарник, Б. Калман</i> ОСОБЕННОСТИ РАЗВИТИЯ ВСПЫШКИ 16 МАЯ 1981 Г. ПО НАБЛЮДЕНИЯМ В РЕНТГЕНОВСКОМ, ОПТИЧЕСКОМ И РАДИОДИАПАЗОНАХ	193
<i>B. Kálmán, I. Nagy</i> PROPER MOTIONS IN HALE REGION 17644 (MAY 1981) AND THE MAY 16 FLARE <i>Б. Калман, И. Надь</i> СОБСТВЕННЫЕ ДВИЖЕНИЯ В ОБЛАСТИ ХЕЙЛА 17644 МАЯ 1981 Г. И ВСПЫШКА 16 МАЯ	207
<i>K.V. Alikaeva, I.F. Nikulin, P.N. Polupan</i> ИЗМЕНЕНИЕ ПРОФИЛЕЙ $H\alpha$ И $H\beta$ В ПРОЦЕССЕ ВСПЫШКИ 16 МАЯ 1981 Г. <i>K.V. Alikaeva, I.F. Nikulin, P.N. Polupan</i> VARIATION OF $H\alpha$ AND $H\beta$ PROFILES DURING 16 MAY, 1981 FLARE	217
№.3. PAPERS ON MASS MOTION AND MAGNETIC FIELDS IN SOLAR ACTIVE REGIONS	223
<i>N.N. Stepanyan</i> ФОНОВЫЕ МАГНИТНЫЕ ПОЛЯ И СОЛНЕЧНАЯ АКТИВНОСТЬ <i>N.N. Stepanyan</i> BACKGROUND MAGNETIC FIELDS AND ACTIVITY OF THE SUN	225
<i>A.N. Koval', N.N. Stepanyan</i> ИЗМЕНЕНИЕ МАГНИТНЫХ ПОЛЕЙ СОЛНЕЧНЫХ ПЯТЕН В СВЯЗИ СО ВСПЫШКАМИ <i>A.N. Koval', N.N. Stepanyan</i> VARIATIONS IN THE MAGNETIC FIELDS OF SUNSPOTS RELATED TO FLARES	235
<i>S.I. Gopasyuk, B. Kálmán, V.A. Romanov</i> CHANGES IN THE LARGE-SCALE CURRENT SYSTEMS IN THE COURSE OF THE EVOLUTION OF AN ACTIVE REGION <i>С.И. Гопасюк, Б. Калман, В.А. Романов</i> ЭВОЛЮЦИЯ КРУПНОМАСШТАБНЫХ ТОКОВЫХ СТРУКТУР ЗА ВРЕМЯ РАЗВИТИЯ АКТИВНОЙ ОБЛАСТИ	249

	PAGE
(No.3) <i>R. B. Teplitskaya, I. P. Turova, G. V. Kuklin</i> THE STUDY OF THE DYNAMIC PROCESS OF UMBRAL FLASHES <i>Р. В. Теплицкая, И. П. Турова, Г. В. Куклин</i> ИССЛЕДОВАНИЕ ДИНАМИЧЕСКОГО ПРОЦЕССА "ВСПЫШКИ В ТЕНИ"	267
<i>Z. B. Korobova</i> STUDIES OF KINEMATIC ELEMENTS IN TWO MULTICENTER SUNSPOT GROUPS <i>З. Б. Коробова</i> ИССЛЕДОВАНИЕ КИНЕМАТИЧЕСКИХ ЭЛЕМЕНТОВ В ДВУХ МНОГО- ЦЕНТРОВЫХ ГРУППАХ СОЛНЕЧНЫХ ПЯТЕН	285
<i>V. E. Merkulenko, L. E. Palamarchuk, V. I. Polyakov</i> PHASE-COHERENCE OF CHROMOSPHERIC OSCILLATIONS WITHIN AN ACTIVITY COMPLEX AND DYNAMIC PROCESSES IN A FILA- MENT DURING THE FLARES ON 6 OCTOBER 1979 <i>В. Е. Меркуленко, Л. Э. Паламарчук, В. И. Поляков</i> СИНФАЗНОСТЬ КОЛЕБАНИЙ ХРОМОСФЕРЫ В ПРЕДЕЛАХ КОМПЛЕКСА АКТИВНОСТИ И ДИНАМИЧЕСКИЕ ПРОЦЕССЫ В ВОЛОКНЕ ВО ВРЕМЯ ВСПЫШЕК 6 ОКТЯБРЯ 1979 Г.	293
<i>L. Dezső, A. Kovács</i> A NOTE ON FLARE LOOPS <i>Л. Дежэ, А. Ковач</i> ЗАМЕТКА О ВСПЫШЕЧНЫХ ПЕТЛЯХ	317
<i>B. I. Ryabov, A. R. Spektor</i> CORONAL MAGNETIC STRUCTURES RELATED TO SOLAR FLARES <i>В. И. Рябов, А. Р. Спектор</i> МАГНИТНЫЕ СТРУКТУРЫ В СОЛНЕЧНОЙ КОРОНЕ СВЯЗАННЫЕ СО ВСПЫШКАМИ	323
<i>S. I. Avdyushin, M. M. Alibegov, A. F. Bogomolov, V. A. Burov,</i> <i>E. I. Zajtsev, S. P. Leonenko, V. A. Poperechenko</i> RADIOEMISSION OF WEAK SOURCES AND MAGNETIC FIELD STRUCTURE <i>С. И. Авджишин, М. М. Алибегов, А. Ф. Богомолов, В. А. Буров,</i> <i>Е. И. Зайцев, С. П. Леоненко, В. А. Попереченко</i> РАДИОИЗЛУЧЕНИЕ СЛАБЫХ ИСТОЧНИКОВ И СТРУКТУРА МАГНИТНОГО ПОЛЯ	333
<i>I. Sattarov, Z. B. Korobova</i> ЭВОЛЮЦИЯ И ВСПЫШЕЧНАЯ АКТИВНОСТЬ БОЛЬШОЙ ГРУППЫ СОЛНЕЧНЫХ ПЯТЕН ИЮЛЯ 1982 Г. <i>I. Sattarov, Z. B. Korobova</i> DEVELOPMENT AND FLARE ACTIVITY IN THE LARGE SUNSPOT GROUP IN JULY 1982	341

	PAGE
(No. 3) <i>В.Н.Ишков, Э.Б.Коробова, Э.И.Могилевский</i> ЭВОЛЮЦИЯ СТРУКТУРЫ, СОБСТВЕННЫХ ДВИЖЕНИЙ И НЕКОТОРЫЕ ОСОБЕННОСТИ БОЛЬШИХ ВСПЫШЕК В МОЩНОЙ ВСПЫШЕЧНО- АКТИВНОЙ ОБЛАСТИ ИЮНЯ-ИЮЛЯ 1982 Г. <i>V. N. Izhkov, Z. B. Korobova, E. I. Mogilevskij</i> EVOLUTION OF STRUCTURE, PROPER MOTIONS AND SOME PECU- LIARITIES OF LARGE FLARES IN THE ACTIVE REGION OF JUNE-JULY 1982	355
<i>G. Bachmann, A. Hofmann, J. Staude</i> RESULTS OF VECTOR MAGNETOGRAPHIC MEASUREMENTS IN THE ACTIVE REGION SD 228/229 ON 15 JULY 1982 <i>Г.Бахманн, А.Хофманн, Й.Штауде</i> РЕЗУЛЬТАТЫ НАБЛЮДЕНИЙ ВЕКТОРА МАГНИТНОГО ПОЛЯ В АКТИВНОЙ ОБЛАСТИ С.Д. 228/229 15 ИЮЛЯ 1982 Г.	369
<i>V. M. Grigor'ev, B. F. Osak, V. L. Selivanov</i> DETERMINATION OF THE ACTIVE REGION MAGNETIC FIELD STRUCTURE USING VECTOR-MAGNETOGRAPHIC MEASUREMENTS <i>В.М.Григорьев, Б.Ф.Осак, В.Л.Селиванов</i> ОПРЕДЕЛЕНИЕ СТРУКТУРЫ МАГНИТНОГО ПОЛЯ АКТИВНЫХ ОБЛАСТЕЙ ПО ИЗМЕРЕНИЯМ НА ВЕКТОР-МАГНИТОГРАФЕ	377

P A R T 2

No. 4. MISCELLANEOUS PAPERS ON THEORETICAL ASPECTS OF SOLAR ACTIVITY	387
<i>Г.В.Куклин, В.Е.Степанов</i> ЗОНАЛЬНЫЕ ТЕЧЕНИЯ В СОЛНЕЧНОЙ КОРОНЕ <i>G. V. Kuklin, V. E. Stepanov</i> THE ZONAL STREAMS IN THE SOLAR CORONA	389
<i>Э.И.Могилевский</i> ПРОБЛЕМА ПЕРВИЧНОГО ИСТОЧНИКА ЭНЕРГИИ И ВЕЩЕСТВА СОЛНЕЧНЫХ ВСПЫШЕК <i>E. I. Mogilevskij</i> THE PROBLEM OF THE PRINCIPAL SOURCE OF ENERGY AND MASS OF SOLAR FLARES	409
<i>В.А.Мазур, А.В.Степанов</i> ДИНАМИКА ЭНЕРГИЧНЫХ ПРОТОНОВ В СОЛНЕЧНЫХ МАГНИТНЫХ ПЕТЛЯХ ЭФФЕКТЫ ДИСПЕРСИИ АЛЬВЕНОВСКИХ ВОЛН <i>V. A. Mazur, A. V. Stepanov</i> DYNAMICS OF ENERGETIC PROTONS ON SOLAR MAGNETIC LOOPS ALFVEN WAVE DISPERSION EFFECTS	419

	PAGE
(No. 4) <i>N. Seehafer, J. Hildebrandt, A. Krüger, Sh. Ahmedov, G. B. Gel'frejkh</i> A COMPARISON BETWEEN HIGHLY RESOLVED S-COMPONENT OBSERVATIONS AND MODEL CALCULATIONS USING FORCE-FREE MAGNETIC FIELD EXTRAPOLATIONS <i>Н. Зеехафер, Й. Хильдэбрандт, А. Крюгер, Ш. Ахмедов, Г. Б. Гельфрейх</i> СРАВНЕНИЕ НАБЛЮДЕНИЙ С-КОМПОНЕНТА С ВЫСОКИМ РАЗРЕШЕНИЕМ С МОДЕЛЬНЫМИ РАСЧЕТАМИ, ИСПОЛЬЗУЮЩИМИ БЕССИЛОВЫЕ ЭКСТРА- ПОЛЯЦИИ МАГНИТНОГО ПОЛЯ	431
<i>V. P. Nefed'ev</i> VARIATION OF CIRCULAR AND LINEAR POLARIZATION IN BURST EMISSION AS A CONSEQUENCE OF DYNAMIC PROCESSES IN THE SOLAR ATMOSPHERE <i>В. П. Неведьев</i> ИЗМЕНЕНИЕ КРУГОВОЙ И ЛИНЕЙНОЙ ПОЛЯРИЗАЦИИ В ИЗЛУЧЕНИИ ВСПЛЕСКОВ КАК СЛЕДСТВИЕ ДИНАМИЧЕСКИХ ПРОЦЕССОВ В АТМОСФЕРЕ СОЛНЦА	443
<i>Yu. D. Zhugzhda, J. Staude, V. Losāns</i> A MODEL OF THE OSCILLATIONS IN THE CHROMOSPHERE AND TRANSITION REGION ABOVE SUNSPOT UMBRAE <i>Ю. Д. Жугжда, Й. Штауде, В. Лоцанс</i> МОДЕЛЬ КОЛЕБАНИЙ В ХРОМОСФЕРЕ И ПЕРЕХОДНОМ СЛОЕ НАД ТЕНЬЮ СОЛНЕЧНЫХ ПЯТЕН	451
<i>V. E. Merkulenko, V. I. Polyakov</i> A POSSIBLE MODEL FOR GLOBAL OSCILLATIONS OF THE SUN ACCORDING TO HILL'S OBSERVATIONAL DATA <i>В. Е. Меркуленко, В. И. Поляков</i> ВОЗМОЖНАЯ МОДЕЛЬ ГЛОБАЛЬНЫХ КОЛЕБАНИЙ СОЛНЦА ПО ДАННЫМ НАБЛЮДЕНИЙ ХИЛЛА	463
<i>V. N. Dermendjiev</i> ON THE EFFECTS OF MAGNETIC ENERGY INCREASE IN THE SUNSPOT CHROMOSPHERE <i>В. Н. Дерменджиев</i> ОБ ЭФФЕКТАХ РОСТА МАГНИТНОЙ ЭНЕРГИИ В СОЛНЕЧНОЙ ХРОМОСФЕРЕ НАД ПЯТНАМИ	475
<i>Э. И. Могилевский</i> СИНЕРГИТИЧЕСКОЕ ПОНИМАНИЕ ЭВОЛЮЦИИ СТРУКТУР МАГНИТНЫХ ПОЛЕЙ НА СОЛНЦЕ <i>Е. И. Mogilevskij</i> SYNERGIC EXPLANATION OF THE EVOLUTION OF SOLAR MAGNETIC FIELD STRUCTURES	487
<i>I. K. Csada</i> NEW COMPUTATIONAL RESULTS FOR THE SOLAR DYNAMO <i>И. К. Чада</i> НЕКОТОРЫЕ ЧИСЛЕННЫЕ РЕЗУЛЬТАТЫ ДЛЯ СОЛНЕЧНОГО ДИНАМО	495

No.5. PAPERS ON VARIOUS OBSERVATIONAL METHODS AND RESULTS	501
<i>M. N. Gnevyshev, V. P. Mikhailutsa</i>	503
STABILITY OF THE PHOTOMETRIC OUT-OF-ECLIPSE OBSERVATIONS OF THE SOLAR CORONA AND VARIATIONS OF ITS INTENSITY IN THE 21th SOLAR CYCLE	
<i>М. Н. Гневтшев, В. П. Михайлуца</i>	
СТАБИЛЬНОСТЬ ФОТОМЕТРИЧЕСКОЙ СИСТЕМЫ ВНЕЗАТМЕННЫХ НАБЛЮДЕНИЙ СОЛНЕЧНОЙ КОРОНЫ И ВАРИАЦИИ ЕЕ ИНТЕНСИВНОСТИ В 21-м ЦИКЛЕ	
<i>M. Minarovjech, V. Rušin, M. Rybanskij</i>	511
PERIODIC VARIATIONS OF 530.3 nm CORONAL LINE	
<i>М. Минаровех, В. Рушин, М. Рыбанский</i>	
ПЕРИОДИЧЕСКИЕ ИЗМЕНЕНИЯ КОРОНАЛЬНОЙ ЛИНИИ $\lambda 530.3$ nm	
<i>A. B. DeLone, E. A. Makarova, J. Sykora</i>	517
ASCENT MOTIONS IN THE MONOCHROMATIC CORONA DURING TOTAL SOLAR ECLIPSE OF JULY 31, 1981	
<i>А. Б. Делоне, Е. А. Макарова, Я. Сикора</i>	
ПОДНИМАЮЩИЕСЯ ДВИЖЕНИЯ В МОНОХРОМАТИЧЕСКОЙ КОРОНЕ ВО ВРЕМЯ ПОЛНОГО СОЛНЕЧНОГО ЗАТМЕНИЯ 31 ИЮЛЯ 1981 Г.	
<i>J. Sykora</i>	523
CORONAL HOLE AS A PROBABLE SOURCE OF THE HIGHEST GEOACTIVITY IN 1981	
<i>Я. Сикора</i>	
КОРОНАЛЬНАЯ ДЫРА, КАК ВОЗМОЖНЫЙ ИСТОЧНИК НАИБОЛЬШОЙ ГЕОЭФФЕКТИВНОСТИ В 1981 Г.	
<i>J. Paciorek, T. Ciurla, B. Rompolt</i>	531
OBSERVATIONS AND INTERPRETATION OF A SET OF LIMB EVENTS OF SEPTEMBER 2, 1979	
<i>Я. Пациорек, Т. Цюрля, Б. Ромпoldt</i>	
ИССЛЕДОВАНИЯ КОМПЛЕКСА ЛИМБОВЫХ ЯВЛЕНИЙ НАБЛЮДЕННЫХ 2 СЕНТЯБРЯ 1979 ГОДА	
<i>I. N. Garczyńska, P. Majer, B. Rompolt</i>	543
THE CARD INDEX OF EJECTIONS AT THE WROCLAW OBSERVATORY	
<i>И. Н. Гарчинска, П. Маер, Б. Ромпoldt</i>	
КАТАЛОГ ВЫБРОСНЫХ ПРОТУБЕРАНЦЕВ НАБЛЮДЕННЫХ ВО ВРОЦЛАВЕ	
<i>B. Ruziřková-Topolová, L. Bufka</i>	545
FLARE GEOEFFICIENCY IN RELATION TO PHOTOSPHERIC MAGNETIC FIELD ORIENTATION OF ACTIVE REGIONS	
<i>В. Ружиřкова-Тополова, Л. Буфка</i>	
ГЕОЭФФЕКТИВНОСТЬ ВСПЫШЕК В СВЯЗИ С ОРИЕНТАЦИЕЙ ФОТОСФЕРИЧЕСКИХ МАГНИТНЫХ ПОЛЕЙ АКТИВНЫХ ОБЛАСТЕЙ	

	PAGE
(No. 5) <i>S. Knoška, L. Krivský</i> FLARES OF TYPE II AND IV RADIO BURSTS IN MAGNETIC TYPES OF SUNSPOT GROUPS <i>Ш. Knoшка, Л. Кривский</i> ВСПЫШКИ С РАДИОВСПЛЕСКАМИ ТИПА II И IV В ГРУППАХ СОЛНЕЧНЫХ ПЯТЕН РАЗЛИЧНЫХ МАГНИТНЫХ ТИПОВ	557
<i>V. P. Maksimov</i> THE POSITION OF FLARE SEATS IN SUNSPOT UMBRAE <i>В. П. Максимов</i> ПОЛОЖЕНИЕ СЧАГОВ ВСПЫШЕК В ТЕНЯХ СОЛНЕЧНЫХ ПЯТЕН	567
<i>A. Ludmány</i> ASYMMETRY OF NON-SPLITTING SPECTRAL LINES IN SUNSPOTS <i>А. Лудмань</i> АСИММЕТРИЯ НЕРАСЩЕПЛЕННЫХ СПЕКТРАЛЬНЫХ ЛИНИЙ В СОЛНЕЧНЫХ ПЯТНАХ	575
<i>M. Sobotka</i> ОПРЕДЕЛЕНИЕ РАССЕЯННОГО СВЕТА В МАЛЫХ СОЛНЕЧНЫХ ПЯТНАХ <i>M. Sobotka</i> STRAY LIGHT DETERMINATION IN SMALL SUNSPOTS	581
<i>G. Bachmann, K. Pflug</i> MINIMUM INSTRUMENTAL POLARIZATION AT COELOSTAT TELESCOPE <i>Г. Бахманн, К. Пфлуг</i> МИНИМАЛЬНАЯ ИНСТРУМЕНТАЛЬНАЯ ПОЛЯРИЗАЦИЯ НА ЦЕЛОСТАТНОМ ТЕЛЕСКОПЕ	589
<i>T. Baranyi, A. Ludmány</i> SYNTHESIS OF H α -PROFILES FROM FILTER TRANSMISSION FUNCTIONS <i>Т. Барани, А. Лудмань</i> СИНТЕЗ ПРОФИЛЕЙ H α ИЗ ФУНКЦИЙ ПРОПУСКАНИЯ ФИЛЬТРА	595
<i>S. I. Avdyushin, M. M. Alibegov, A. F. Bogomolov, V. A. Burov,</i> <i>E. N. Zajtsev, S. P. Leonenko, B. A. Poperchenko</i> ACTIVE REGION CHARACTERISTICS FROM TWO-FREQUENCY MAPPING WITH A TELESCOPE TNA-1500 <i>С. И. Авджилин, М. М. Алибегов, А. Ф. Богомолов, В. А. Буров,</i> <i>Е. И. Зайцев, С. П. Леоненко, Б. А. Поперченко</i> ХАРАКТЕРИСТИКИ АКТИВНЫХ ОБЛАСТЕЙ ПО ДАННЫМ ДВУХЧАСТОТНОГО КАРТОГРАФИРОВАНИЯ НА РАДИОТЕЛЕСКОПЕ TNA-1500	603

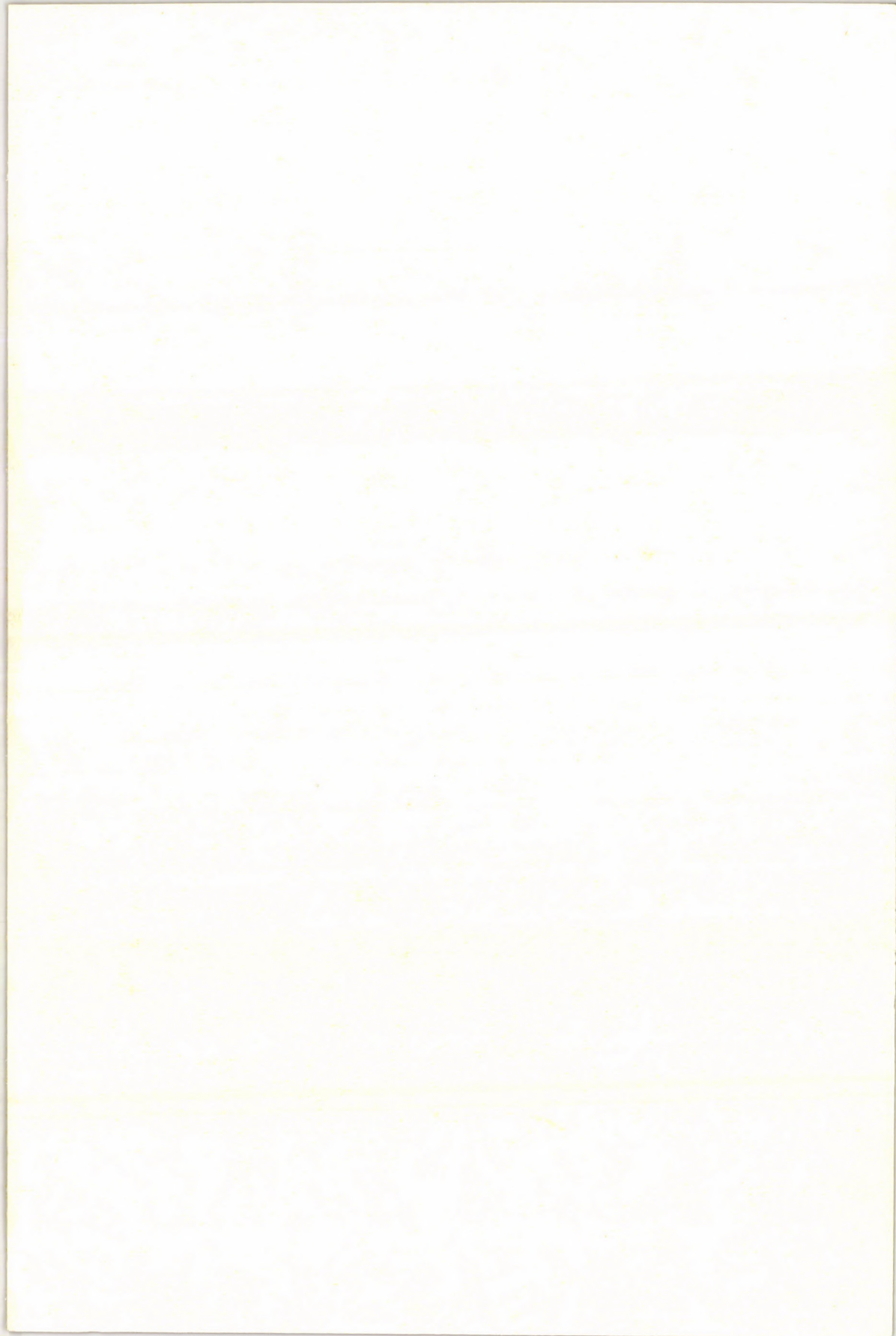
	PAGE
(No. 5) <i>O. A. Golubchina, V. N. Ikhsanova</i> OBSERVATIONS OF RAPID VARIATIONS OF THE POLARIZED AND NON-POLARIZED RADIO EMISSION OF LOCAL SOURCES WITH THE RATAN-600 AT $\lambda=2.3$ AND 4.5 cm BY THE "RELAY-RACE" METHOD <i>О. А. Голубчина, В. Н. Икханова</i> НАБЛЮДЕНИЯ БЫСТРЫХ ИЗМЕНЕНИЙ ПОЛЯРИЗОВАННОГО И НЕПОЛЯРИ- ЗОВАННОГО РАДИОИЗЛУЧЕНИЯ ЛОКАЛЬНЫХ ИСТОЧНИКОВ НА ВОЛНАХ 2.3 И 4.5 см НА РАТАН-600 МЕТОДОМ "ЭСТАФЕТА"	611
<i>A. Krüger, F. Fürstenberg, J. Hildebrandt, Sh. B. Ahmedov,</i> <i>V. M. Bogod, A. N. Korzhavin</i> ON THE HEIGHT SCALE OF MAGNETIC FIELDS ABOVE SUNSPOTS DERIVED FROM RATAN-600 OBSERVATIONS AND MODEL CAL- CULATIONS <i>А. Крюгер, Ф. Фюрстенберг, Й. Хильдебрандт, Ш. Б. Ахмедов,</i> <i>В. М. Богод, А. Н. Коржавин</i> О ШКАЛЕ ВЫСОТ НАД СОЛНЕЧНЫМИ ПЯТНАМИ, ПОЛУЧЕННОЙ ИЗ НАБЛЮДЕНИЙ НА РАТАН-600 И ИЗ МОДЕЛЬНЫХ РАСЧЕТОВ	619
<i>N. S. Kaverin, M. M. Kobrin, A. I. Korshunov, V. V. Shushunov, H. Aurass,</i> <i>F. Fürstenberg, J. Hildebrandt, A. Krüger, N. Seehafer</i> ON THE RELATION BETWEEN SPECTRAL CHARACTERISTICS OF THE MICROWAVE EMISSION FROM SOLAR ACTIVE REGIONS AND PHYSICAL CONDITIONS OF THE SOLAR ATMOSPHERE <i>Н. С. Каверин, М. М. Кобрин, А. И. Коршунов, В. В. Шушунов,</i> <i>Х. Аукас, Ф. Фюрстенберг, Й. Хильдебрандт, А. Крюгер,</i> <i>Н. Зееххафер</i> ЗАВИСИМОСТЬ СПЕКТРАЛЬНЫХ ХАРАКТЕРИСТИК МИКРОВОЛНОВОГО ИЗЛУЧЕНИЯ СОЛНЕЧНЫХ АКТИВНЫХ ОБЛАСТЕЙ ОТ ФИЗИЧЕСКИХ УСЛОВИЙ В СОЛНЕЧНОЙ АТМОСФЕРЕ	631
<i>S. T. Akinyan, V. V. Fomichev, I. M. Chertok, H. Aurass, A. Krüger</i> EFFECTS CHARACTERIZING THE RELATIONSHIP OF RADIO BURSTS AND PROTON FLARES OF 1980 <i>С. Т. Акинян, В. В. Фомичев, И. М. Черток, Х. Аукас, А. Крюгер</i> ЭФФЕКТЫ ХАРАКТЕРИЗУЮЩИЕ СВЯЗЬ РАДИОВСПЛЕСКОВ И ПРОТОННЫХ ВСПЫШЕК 1980 Г.	639
<i>N. S. Kaverin, A. I. Korshunov, V. V. Shushunov, H. Aurass, H. Detlefs,</i> <i>H. Hartmann, A. Krüger, J. Kurths</i> SPECTROGRAPHIC OBSERVATIONS OF SOLAR MICROWAVE BURSTS IN THE 5.3 - 7.4 GHz RANGE <i>Н. С. Каверин, А. И. Коршунов, В. В. Шушунов, Х. Аукас,</i> <i>Х. Детлефс, Х. Хартманн, А. Крюгер, Й. Куртс</i> СПЕКТРОГРАФИЧЕСКИЕ НАБЛЮДЕНИЯ СОЛНЕЧНЫХ МИКРОВОЛНОВЫХ ВСПЛЕСКОВ В ДИАПАЗОНЕ 5.3 - 7.4	653

	PAGE
ABBREVIATIONS USED IN REFERENCES	661
LIST OF CONSULTATION PAPERS NOT INCLUDED IN THIS VOLUME	662
AN ACCOUNT OF SOME EXTRA SESSIONS OF THE CONSULTATION	663
NAME INDEX (AUTHORS AND PARTICIPANTS)	664

Felelős kiadó: Szeidl Béla

Hozott anyagról sokszorosítva

8414467 MTA KESZ Sokszorosító, Budapest. Felelős vezető: dr. Héczey Lászlóné .



Publications of Debrecen Heliophysical Observatory

Vol.	No.		Year	Page
1	1-4	Statistical Investigations of Sunspots <i>5 et seq. follows</i>	1964	1-108
2	1-11	Proceedings of the 6th Regional Consultation on Solar Physics	1971	1-217
3	1-5	Proceedings of the Intercosmos Symposium on Solar Physics	1977	1-310
4	1-2	Sunspot Group Development <i>3 et seq. follows</i>	1980-1981	1-60
5	1-3	Proceedings of the 11th Regional Consultation on Solar Physics P a r t 1	1983	1-384
	4-5	Proceedings of the 11th Regional Consultation on Solar Physics P a r t 2	1983	385-666